



**7th INTERNATIONAL
GEOLOGICA BELGICA
MEETING 2021**

Geosciences Made in Belgium

15-17 September 2021 – AfricaMuseum Tervuren (Belgium)

Abstract book

Organizing Committee

Damien Delvaux (RMCA),
Olivier Dewitte (RMCA)
Max Fernandez-Alonso (RMCA)
Aurelia Hubert-Ferrari (ULiège)
Jan Elsen (KU Leuven)

Scientific Committee

Jean-Marc Baele (UMons)
Olivier Bolle (ULiège)
Anouk Borst (RMCA & KU Leuven)
Marc De Batist (UGent)
Augustin Dekoninck (UNamur)
Thierry De Putter (RMCA)
Stefaan Dondeyne (UGent)
Karen Fontijn (ULB)
Vanessa Heyvaert (RBINS-GSB)
François Kervyn (RMCA)
David Lagrou (VITO)
Thomas Lecocq (ROB)
Florias Mees (RMCA)
Sophie Opfergelt (UCLouvain)
Cyrille Prestianni (ULiège & RBINS)
Robert Speijer (KU Leuven)

Conference Web site: <https://geologicabelgica2021.africamuseum.be>

Partenaires



LA LIBERTÉ DE CHERCHER EN TOUTE SÉCURITÉ !

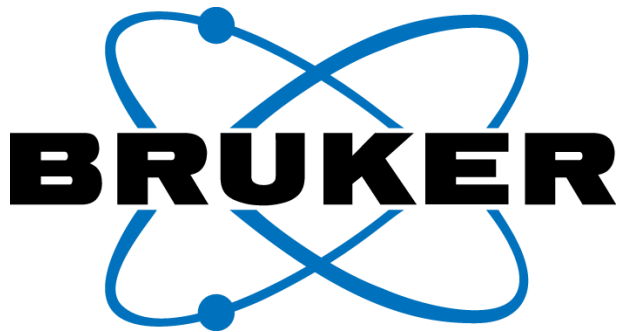


Table of Contents

Geologica Belgica Van den Broeck Medal 2021

Earthquake activity in Western Europe is typical of stable continental regions Thierry CAMELBEECK	21
--	----

Session 1- Geodynamics and Mineral Resources 23

Influence of geological structures on failure possibility around Meli area gold mine site, northwestern Tigray region, north Ethiopia Kaleab Adhena Abera ^{1,2,3} , Miruts HAGOS ² , Gebremedhin BERHANE ² , Tesfamichael GEBREYOHANNES ² , Abdelwassie HUSSEN ² and Kristine WALRAEVEENS ¹	24
Au Vein-Type Mineralisation at Escádia Grande (Portugal): A Microstructural and Geochemical Analysis Jolan ACKE ¹ , Pim KASKES ² , Philippe CLAEYS ² , Dominique JACQUES ¹ , Philippe MUCHEZ ¹	26
A long-lasting Archean deformation history in the Sangmelima terrane, NW Congo Craton, Southern Cameroon Joseph M. AKAME ^{1*} , Vinciane DEBAILLE ¹ , Thierry DE PUTTER ² , Marc POUJOL ³ , Bernhard SCHULZ ⁴ , Elson P. OLIVIERA ⁵	28
Alkaline magmatism and critical metals in Angola: Field observations and petrography of the Nejoio nepheline syenite complex Anouk BORST ^{1,2,3} , Adrian FINCH ³ , Grace NIELSON ³ , Pete SIEGFRIED ⁴ , Egidio LOPES ⁵ , Andre EUGENIO ⁵ , Aurora BAMBI ⁵	30
Carbonatitic affinity of the rare earth element (REE) mineralization at Gakara (Burundi) Florian BUYSE ^{1,2} , Stijn DEWAELE ³ , Sophie DECREÉ ⁴ , Florias MEES ⁵	32
Distribution of trace elements in the secondary minerals of Zn-Pb deposits: new results from Belgium and Moroccan willemite deposits Flavien CHOULET ¹ , Johan YANS ² , Augustin DEKONINCK ²	34
Le Sous-groupe de la Mpioka, témoins de la réactivation des failles post-Schisto-calcaire dans le fossé de la Basse-Sangha C.M.E. CIBAMBULA, TUEMA L.O., IYOLO, H.F., MUKEBA C.L., M.N.A.J. MAKUTU.	35
Characterisation and Proterozoic evolution of the granitoids of the Karagwe-Ankole belt (KAB) in Rwanda Shana DE CLERCQ ¹ , Stijn DEWAELE ¹ , Johan DE GRAVE ¹ , Frank VANHAECKE ² , Thierry DE PUTTER ³	36
Exhumation of the South Atlantic passive margin of the Democratic Republic of Congo during pre- and post- Gondwana breakup: evidence from new low-temperature thermochronology, geology and geomorphology Johan DE GRAVE ¹ , Gerben VAN RANST ¹ , Ana Carolina FONSECA ¹ , Luc TACK ² , Damien DELVAUX ² , Daniel BAUDET ² , Nicole Yaya KITAMBALA ³ , Aimée Love PAY ³	38
Petrographical, mineralogical and geochemical study of the gold mineralization at Imonga-Saramabila, Maniema, DR Congo Julie DE GROOTE ¹ , Stijn DEWAELE ¹	40

Western climate-oriented ethics and artisanal mining of cobalt in DRC: a 21stC. revival of “Potemkine villages”?	
Thierry DE PUTTER ¹ , Cristiana PANELLA ²	42
From Precambrian to Cenozoic: the manganese odyssey of Morocco	
Augustin DEKONINCK* ¹ , Gilles RUFFET ² , Jocelyn BARBARAND ³ , Yves MISSENARD ³ , Ludovic LAFFORGUE ³ , Michèle VERHAERT ¹ , Nadine MATTIELLI ⁴ , Cécile GAUTHERON ³ , Mohamed MAGOUA ⁵ , Abdellah MOUTTAQI ⁵ , Mohammed BOUABDELLAH ⁶ , Julien POOT ¹ , Johan YANS ¹	44
Experiments on silicate-carbonate liquid immiscibility in a Fe-P rich system, a premise for phoscorites formation in carbonatite complexes	
Merry DEMAUDE ¹ , Bernard CHARLIER ²	46
The geodynamic evolution of Earth viewed by the PTt record of metamorphic rocks	Camille FRANÇOIS ¹ & Vinciane DEBAILLE ² 48
Properties of refractory materials from low-cost Northern Tunisian kaolinic clays.	Oumaima GRINE ¹ , Bechir MOUSSI ¹ , Walid HAJJAJI ² , Pascal PILATE ³ , Johan YANS ⁴ , Fakher JAMOSSI ¹
	50
Tentative de décomplexification du complexe de Butare: ses extrémités NW et SE respectivement à Kalehe et Idjwi à l'Est de la RDC et à Zina-Randa et Cohoha au Nord du Burundi	
C. KALIKONE ¹ , G. FURAHA ¹ , L. KEZIMANA ¹ , C. NZOLANG ² , G. NIMPAGARITSE ³ , D. DELVAUX ³ , J. BATUMIKE ² , R. RUMANYA ² , E. MUNYALI ² , H. FAKAGE ² , D. BAUDET ³ , L. NAHIMANA ⁴ , S. DEWAELE ⁵	52
Tentative de décomplexification du complexe d’Uvira : Cas des secteurs d’Idjwi et Kalehe, Sud-Kivu/ RDC. Cartographie, pétrographie et minéralisation	
C. KALIKONE ¹ , C. NZOLANG ² , G. NIMPAGARITSE ³ , D. DELVAUX ³ , J. BATUMIKE ² , R. RUMANYA ² , E. MUNYALI ² , H. FAKAGE ² , D. BAUDET ³ , L. NAHIMANA ⁴ , S. DEWAELE ⁵	54
Tentative de décomplexification du complexe de Zina-Randa (Nord-Ouest du Burundi)	Lee Fred KEZIMANA ¹ , Louis NAHIMANA ² , Gérard NIMPAGARITSE ³ 56
Valorization of Tunisian Numidian clays (Upper Oligocene) in the manufacture of ceramic tiles	
Béchir MOUSSI ¹ , Oumaima GRINE ¹ , Walid HAJJAJI ¹ , Johan YANS ² , Mondher HACHANI ³ , Nouri HATIRA ⁴ , Joao Antonio LABRINCHA ⁵ , Fakher JAMOSSI ¹	57
Paleostress reconstruction and tectono-structural evolution of the West-Congo Orogen, in Republic Democratic of Congo and Republic of Congo	
Hardy Medry Dieu-Veill NKODIA ^{1,*} , Florent BOUDZOU MOU ^{1,2} , Timothée MIYOUNA ¹ , Damien DELVAUX ³	58
New insights from the revised geological map of the West Rwanda (Karongi-Nyamagabe-Rusizi districts)	
Alain J. NTENGE ¹ , Ariane KANYANA ¹ , Jean Claude NGARUYE ¹ , Pascal TUYISHIME ¹ , Daniel BAUDET ² , Max FERNANDEZ-ALONSO ² , Gérard NIMPAGARITSE ²	59
Controls of host rocks on weathering processes and dating of Cu-As-Pb-rich supergene deposits (Moroccan Anti-Atlas Copperbelt, Morocco)	
Michèle VERHAERT ^{1,2*} , Atman MADI ³ , Abdelaziz EL BASBAS ⁴ , Mohamed ELHARKATY ³ ,	

Abdellah OUMMOUCH³, Lahcen OUMOHOU³, Lhou MAACHA³, Benoît GRYPONPREZ¹,
Cécile GAUTHERON⁵, Johan YANS² 62

Characterization of auriferous quartz vein mineralizing fluids in the Mesoproterozoic Karagwe-Ankole belt (Byumba, Rwanda): Petrography, microthermometry and Raman spectroscopy	
Sander WOUTERS ¹ , Stijn DEWAELE ² , Philippe MUCHEZ ³	64

Session 2- Earth Surface Processes and Geohazards..... 66

Can the 12-m TanDEM-X DEM be used to accurately estimate lavaka (gully) volumes and mobilization rates? Insights from a comparative analysis with SRTM and a high resolution UAV-SfM DEM

Liesa BROSENS ^{1,2} , Benjamin CAMPFORTS ³ , Emilien ALDANA-JAGUE ⁴ , Gerard GOVERS ² , Vao Fenotiana RAZANAMAHANDRY ² , Kristof VAN OOST ⁴ , Tantely RAZAFIMBELO ⁵ , Tovonarivo RAFOLISY ⁵ , and Liesbet JACOBS ^{2,6}	67
---	----

Is there an environmental crisis in the Lake Alaotra region (Madagascar)? Insights from lavaka (gully) dynamics and floodplain sedimentation

Liesa BROSENS ^{1,2†} , Nils BROOThAERTS ^{2†} , Benjamin CAMPFORTS ³ , Liesbet JACOBS ^{2,4} , Vao Fenotiana RAZANAMAHANDRY ² , Quinten VAN MOERBEKE ² , Steven BOUILLON ² , Tantely RAZAFIMBELO ⁵ , Tovonarivo RAFOLISY ⁵ , and Gerard GOVERS ²	69
--	----

Exploring the Curve Number method to predict gully head occurrence on the continental scale of Africa.....

Sofie DE GEETER ^{1,2,3} , Matthias VANMAERCKE ² , Gert VERSTRAETEN ¹ , Jean POESEN ^{1,4}	71
--	----

Landslide and flash flood timing from satellite radar imagery in the western branch of the East African Rift.....

Axel DEIJNS ^{1,2*} , Olivier DEWITTE ¹ , Wim THIERY ² , Nicolas D'OREYE ^{3,4} , Jean-Philippe MALET ⁵ , & François KERVYN ¹	72
---	----

Application of Photogrammetry in Earth Sciences: Case Study of Lava Accumulation and Ground Deformation in an Active Volcanic Crater

Louise DELHAYE ^{1,2} , Julien BARRIÈRE ³ , Nicolas D'OREYE ^{3,4} , François KERVYN, Adrien OTH ³ , Benoît SMETS ^{1,2}	73
--	----

The LASUGEO project: monitoring LAND Subsidence caused by Groundwater exploitation through gEOdetic measurements

Xavier DEVLEESCHOUWER ¹ , Atefe CHOOPANI ^{1,2} , Aline MOREAU ² , Kristine WALRAEVENS ³ , Marc VAN CAMP ³ , Michel VAN CAMP ⁴ , Kevin GOBRON ⁴ , Alain DASSARGUES ² , Philippe ORBAN ² , Pierre-Yves DECLERCQ ¹	74
---	----

Landslide timing in the changing environments of the North Tanganyika-Kivu Rift region, Africa.....

Olivier DEWITTE ¹ , Axel DEIJNS ^{1,2} , Arthur DEPICKER ³ , Antoine DILLE ¹ , Violet KANYIGINYA ^{1,4,5} , Désiré KUBWIMANA ^{6,7} , Jean-Claude MAKI MATESSO ^{8,9} , Toussaint MUGARUKA BIBENTYO ^{1,10,11} , John SEKAJUGO ^{4,5,12}	76
---	----

Close-range remote sensing of large consecutive rockfall events from a permafrost rock face, Mattertal, Switzerland

Hanne HENDRICKX ^{1*} , Gaëlle LE ROY ² , Agnès HELMSTETTER ³ , Eric POINTNER ⁴ , Eric LAROSE ⁵ , Luc BRAILLARD ⁶ , Jan NYSSSEN ⁷ , Reynald DELALOYE ⁸ , Amaury FRANKL ⁹	78
--	----

Numerical Modeling of Volcanic Edifice Degradation: Towards an Integrated Understanding of Edifice Morphologic Evolution. Daniel O'HARA, Roos Marina Johanna van WEES, Matthieu KERVYN	80
Large landslides and ice sheets: the Patagonian lesson Tomáš PÁNEK	81
How to integrate outbreak risk issues from drainage adits from abandoned mines in land use planning: a tool for decision-makers Benedicta RONCHI, Fabian STASSEN, Jean-Pierre DREVET, Mathieu VESCHKENS	83
Reliability of citizen scientists for near-real time reporting of geohazards. An analysis of biases and accuracy for the Rwenzori Mountains, Uganda..... John SEKAJUGO ^{1,2,3} , Grace R. KAGORO ³ , Liesbet JACOBS ⁵ , Clovis KABASEKE ¹ , Esther NAMARA ¹ , Olivier DEWITTE ⁴ and Matthieu KERVYN ²	85
Analyse morpho-tectonique sur la ville de Matadi dans la province du Kongo Central (R.D.C) K.A. SEKERAVITI, H.A. IYOLO, L.O. TUEMA, C. L. MUKEBA, M.N.A.MAKUTU J., C.M.E. CIBAMBULA	86
The May 2021 Flank Eruption of Nyiragongo Volcano, Democratic Republic of Congo..... Benoît SMETS ^{1,2} , Julien BARRIÈRE ³ , Corentin CAUDRON ⁴ , Valérie CAYOL ⁵ , Oryaëlle CHEVREL ⁵ , Nicolas D'OREYE ^{3,6} , François DARCHAMDEAU ⁷ , Louise DELHAYE ^{1,2} , Dominique DERAUW ^{8,9} , Halldór GEIRSSON ¹⁰ , Raphaël GRANDIN ¹¹ , Ephrem KAMATE KALEGHETSO ^{12,13} , Célestin KASEREKA MAHINDA ¹² , Matthieu KERVYN ² , Blaise MAFUKO NYANDWI ¹⁴ , Joseph MAKUNDI ¹⁵ , Caroline MICHELLIER ¹ , Sander MOLENDIJK ¹³ , Bosco MUHINDO MUSUBAO ¹⁴ , Adalbert MUHINDO SYAVULISEMBO ¹² , Olivier NAMUR ¹³ , Ildephonse NGUOMOJA ¹⁵ , Alain Joseph NTENGE ¹⁶ , Adrien OTH ³ , Sam POPPE ^{17,18} , Sergey SAMSONOV ¹⁹ , Delphine SMITTARELLO ³ , Josué SUBIRA ^{1,12,20} , Nicolas THEYS ²¹ , Christelle WAUTHIER ²² , Mathieu YALIRE MAPENDANO ¹² , Thimm ZWIENER ^{1,2} , François KERVYN ¹	87
Remote Sensing of Geo-Hydrological Hazards in Central Africa Benoît SMETS ^{1,2} , Julien BARRIÈRE ³ , Olivier DEWITTE ¹ , Axel DEIJNS ^{1,4} , Louise, DELHAYE ^{1,2} , Arthur DEPICKER ⁵ , Dominique DERAUW ^{6,7} , Antoine DILLE ¹ , Nicolas D'OREYE ^{3,8} , Nicolas THEYS ⁹ , Thimm ZWIENER ^{1,2} , François KERVYN ¹	89
Session 3- Planetary Magmatic and Metamorphic Systems	90
The early growth of felsic continental crust revisited from Germanium/silicon versus silicon isotopic evidences Luc ANDRÉ ¹ , Laurence MONIN ^{1,2} and Axel HOFMANN ³	91
Insights on mantle melting below Osorno Volcano (Southern Volcanic Zone, Chile) Tonin BECHON ¹ , Paul FUGMANN ¹ , Olivier NAMUR ² , Billon MELVYN ¹ , Olivier BOLLE ¹ , Jacqueline VANDER AUWERA ¹	93
Timescales of crystal mush storage in the Central Southern Volcanic Zone of Chile Melvyn BILLON ¹ , Bernard CHARLIER ¹ , Olivier NAMUR ² , Jacqueline VANDER AUWERA ¹ ..	95
Experimental constraints on the internal structure of Mercury Joren CELIS ¹ , Olivier NAMUR ² , Bernard CHARLIER ³	97

Mercury and its exploration by the BepiColombo mission Bernard CHARLIER ¹ , Hadrien PIROTTE ¹ , Joren CELIS ² , Olivier NAMUR ²	98
Constraining the conditions of magmatic differentiation under Villarrica stratovolcano (Central Southern Volcanic Zone, Chile) Paul FUGMANN ¹ , Tonin BECHON ² , Olivier BOLLE ³ , Olivier NAMUR ⁴ , Jacqueline VANDER AUWERA ⁵	100
Petrology of Nyamulagira volcano, Virunga Province, DR Congo Ephrem KAMATE ^{1,2,3} , Olivier NAMUR ¹ , Sander MOLENDIJK ¹ , Jacqueline VANDER AUWERA ⁴ , Benoit SMETS ^{5,6}	102
Petrology of the Nyiragongo Volcano, DR Congo Sander MOLENDIJK ¹ , Olivier NAMUR ¹ , Paul MASON ² , Benoît SMETS ^{3,4} , Jacqueline VANDER AUWERA ⁵ , David NEAVE ⁶	103
Equilibria and trace element partitioning in silicate-metal-sulfide melts under highly reducing conditions: a key to understand the evolution of Mercury Hadrien PIROTTE ¹ , Camille CARTIER ² , Olivier NAMUR ³ , Anne POMMIER ⁴ , Bernard CHARLIER ¹	104
The response of a magmatic plumbing system to sector collapse: constraints from petrology and geochemistry at Mt. Meru, Tanzania	
Sacha RADELET ¹ , Karen FONTIJN ² , Mary KISAKA ³ , Matthieu KERVYN ⁴	106
Trace element partitioning between clinopyroxene, magnetite, ilmenite, and ferrobasaltic magmas: an experimental study Kat SHEPHERD ¹ , Olivier NAMUR ¹ , Bernard CHARLIER ²	108
Combining tourmaline crystal morphology and geochemistry to investigate disequilibrium crystallization in pegmatitic melts Laura M. VAN DER DOES ¹ , Niels HULSBOSCH ¹ , Jan ELSSEN ¹ , Philippe MUCHEZ ¹ , Mona-Liza C. SIRBESCU ²	110
Constraints on deep magmatic volatile budgets from olivine hosted melt inclusions Thomas VAN GERVE ¹ , Olivier NAMUR ¹ , Penny WIESER ² , Hector LAMADRID ³ , Niels HULSBOSCH ¹ , David NEAVE ⁴	112
Calbuco (Central Southern Volcanic Zone, Chile): petrology of a hazardous volcano	
Jacqueline VANDER AUWERA ¹ , Salvatrice MONTALBANO ¹ , Olivier NAMUR ¹⁻³ , Tonin BECHON ¹ , Pierre SCHIANO ⁴ , Jean-Luc DEVIDAL ⁴ , Olivier BOLLE ¹	114
Silicate liquid immiscibility of low-Ti and high-Ti basalts in the Emeishan Large Igneous Province, SW China	
Yi-shen ZHANG ¹ , Olivier NAMUR ¹ , Bernard CHARLIER ²	115
Petrogenesis and isotopic investigation of Pillow Lavas from the Troodos ophiolite, Cyprus: Cu and Zn isotopes Nina ZARONIKOLA ^{1*} , Vinciane DEBAILLE ¹ , Sophie DECREE ² , Ryan MATHUR ³ , Basilios TSIKOURAS ⁴ , Christodoulos HADJIGEORGIOU ⁵	116

Session 4- Geology, Man and Society 118

- Structural framework as the new fundament for international geoscientific cooperation and policy support**
Renata BARROS¹, Kris PIESENS¹, Katrijn DIRIX² 119
- Pb and Zn deportment estimation of historic mine waste by using an integrated mineralogical and geochemical approach: a case study from the Plombières mine waste (eastern Belgium)**
Srećko BEVANDIĆ¹, Rosie BLANNIN³, Alexandra Escobar GOMEZ², Jorge M. R. S. RELVAS², Alvaro PINTO², Kai BACHMANN³, Max FRENZEL³, Philippe MUCHEZ¹ 121
- Towards a dynamic and interdisciplinary assessment for the sustainable management of geological resources**
Tine COMPERNOLLE^{1,2}, Kris PIESENS², Kris WELKENHUYSEN² 123
- ‘Fossiles en Ville’: popularizing the History of Life and Earth through urban palaeontology and geology**
Julien DENAYER^{1,2}, Amandine SERVAIS², Martine VANHERCK², Thomas BEYER² & Valentin FISCHER¹ 125
- Pierre de Meuse, an exceptional Belgian historical heritage stone from the Meuse valley**
Roland DREESEN¹, Edouard POTY², Bernard MOTTEQUIN³, Jean-Marc MARION² & Julien DENAYER² 127
- Sourcing natural stone used in the architecture of stone-poor landscapes, demonstrated for northern Belgium**
Michiel DUSAR¹, Marleen DE CEUKELAIRE² 129
- 3D mapping of underground galleries from Maastricht limestone extraction in Riemst** Mike LAHAYE^{1,2}, Tim DE KOCK¹ 131
- Tectonostratigraphic evolution coupled with climate changes of the pre-Sturtian Fungurume-Mwashya platform in the Tenke-Fungurume Mining District, Democratic Republic of the Congo**
Pascal MAMBWE^{1,2}, Franck DELPOMDOR⁴, Sébastien LAVOIE³, Philippe MUKONKI³, Jacques BATUMIKE⁵, Philippe MUCHEZ¹ 132
- Seasonal variations of water-soluble heavy metals in atmospheric deposition at NE Sichuan, Central China: Natural and anthropogenic effects**
Chen-guang PAN¹, Yue-feng LIU¹, Xiao-tao PENG¹, Yu XIE¹, Hai-bo HE¹, Jing TANG¹, ZHOU Hou-yun^{1,*} 134
- Service Géologique de Wallonie : a new chapter**
D. PAS, J. DENAYER, B. DELCAMBRE, J.-M. MARION, J. MICHEL, M. SALMON, C. VANNESTE, C. 135
- Enhanced rock weathering: the overlooked hydrodynamic trap**
Kris PIESENS¹, Renata BARROS¹, Tine COMPERNOLLE¹, Sophie DECREE¹, Christian BURLET¹, Ivan JANSSENS², Sara VICCA² 136
- Characterization of metal particles in municipal solid waste incineration ashes using neural network based image analysis**
Priscilla TECK^{1,2}, Ruben SNELLINGS¹, Jan ELSSEN² 138

Geochemistry and petrography of <i>in-situ</i> flints from the type-Maastrichtian (NE Belgium and SE Netherlands): implications for flint formation processes and flint provenancing	
Hannah VAN DER GEEST ¹ , Johan VELLEKOOP ^{1,2} , Pim KASKES ² , Matthias SINNESAE ³ , John JAGT ⁴ , Patrick DEGRYSE ¹ , Philippe CLAEYS ²	140
Getting the picture of the shallow urban subsurface: a shallow subsurface model of the city of Antwerp as test case	
Tom VAN HAREN ¹ , Jef DECKERS ¹ , Roel DE KONINCK ¹ , Katrijn DIRIX ¹ , Katrien DE NIL ²	142
UNESCO Global Geopark Famenne-Ardenne, Belgium – opportunities and role for geoscientists	
Sophie VERHEYDEN ^{1,2} , Serge DELABY ^{3,4}	144
Naturally CO₂-rich water springs in Belgium evidencing complex subsurface interactions	
Kris WELKENHUYSEN ¹ , Agathe DEFOURNY ^{2,3} , Arnaud COLLIGNON ³ , Patrick JOBE ³ , Alain DASSARGUES ² , Kris PIESENS ¹ , Renata BARROS ¹	146
The Rock Garden: increasing the accessibility of geoscience skills training with a field course on campus	
Thomas WONG HEARING ¹ , Stijn DEWAELE ¹ , Stijn ALBERS ¹ , Julie DE WEIRDT ¹ , Marc DE BATIST ¹	148
Session 5- Basin Research and Sedimentology - Stratigraphy	150
Sedimentology and Microfacies assessment of Ypresian carbonate formations in the Tellian zone (NW of Tunisia)	
Imen ARFAOUI ^{1,2} , Frédéric Boulvain ¹	151
Silurian solid bitumen from Huy: evidences for a petroleum system in Belgium	
Michiel ARTS ¹ , Coralie BOSTEELS ¹ , Xavier DEVLEESCHOUWER ² , Anne-Christine DA SILVA ¹	153
Stratigraphic architecture, sedimentology and structure of the Corinth Canal (Greece)	
Basile CATERINA ¹ , Romain RUBI ² , Aurélie HUBERT-FERRARI ³	155
Les sous-groupes Schisto-calcaire et de la Mpioka dans la chaîne panafricaine West-Congo, témoins de l'évolution paléoclimatique post-Cryogénien, Province du Kongo Central, R.D. Congo	
C.M.E. CIBAMBULA ¹ , M.N.A. MAKUTU J. ¹ , C.L. MUKEBA ¹ , K.A. SEKERAVITI ¹ , H.F. IYOLO ¹ , L.O. TUEMA ¹	156
A model – proxy data comparison of mid to late Miocene paleotemperatures in western and central Europe	
Alexander CLARK ¹ , Johan VELLEKOOP ^{1,2} , Robert SPEIJER ¹	157
The French Massif Central: a witness of successive weathering periods since the Early Cretaceous in the Alpine foreland	
Augustin DEKONINCK ^{*1} , Gilles RUFFET ² , Julien BAPTISTE ³ , Robert WYNS ³ , Eric LASSEUR ³ , Jean-Yves ROIG ³ , Johan YANS ¹	159
Structure and evolution of the Congo Basin: long-lived record of tectonic and climatic events during the last Billion years	
Damien DELVAUX, Francesca MADDALONI, Magdala TESAURO, Carla BRAITENBERG	161

A 1500 years-record of North Atlantic storminess from the Shetland Islands (UK) – preliminary insights	
Max ENGEL, Katharina HESS, Tasnim PATEL, Sue DAWSON, Jan OETJEN, Andreas KOUTSODENDRIS, Polina VAKHRAMEEVA, Isa SCHÖN, Vanessa M. A. HEYVAERT	162
Stratigraphic correlations between the Brabant Massif and the Stavelot, Rocroi and Givonne inliers (Belgium), geological implications	
Alain HERBOSCH	164
Crustal and sedimentary structures of the Congo basin constrained by geophysical signatures	
Étienne KADIMA, K. ¹ , Stanislas SEBAGENZI, M.N. ¹ , Francis LUCAZEAU ² , Damien DELVAUX ³ , Christian BLANPIED ⁴	166
Lake Chala 2k: the last two millennia of environmental change in equatorial East Africa	
Inka MEYER [*] , Irina PAPADIMITRIOU ¹ , Dirk VERSCHUREN ² and Marc DE BATIST ¹	168
Frasnian–Famennian deposits of Southern Belgium: thick and complex key sections to understand the Late Frasnian extinctions and the role played by tsunamis	
Edouard POTY ¹ , Julien DENAYER ¹ , Bernard MOTTEQUIN ²	169
Etude paléoenvironnementale des roches carbonatées de la région Lufu-Toto située dans le degré carré de Mbanza Ngungu (Province du Kongo Central, R.D. Congo)	
L.O. TUEMA ¹ , C.L. MUKEBA, ¹ , C.M.E. CIBAMBULA ¹ , M.N.A.J. MAKUTU ¹ , H.M. TSHOMBE ²	171
Lake Naivasha’s response to the end of the African Humid Period	
Thijs VAN DER MEEREN ¹ , Gijs DE CORT ¹ , Christine COCQUYT ² , Lydia A. OLAKA ³ , Kazuyo TACHIKAWA ⁴ , Edouard BARD ⁴ , Priyanka KASPATHY THEVANAYAGAM ¹ , Dirk VERSCHUREN ¹	172
Correlating cross-border Cenozoic stratigraphy in the Belgian-Dutch border region: results from H3O – De Voorkempen	
Jan WALSTRA ¹ , Armin MENKOVIC ² , Jef DECKERS ³ , Frieda BOGEMANS ¹ , Michiel DUSAR ¹ , Andreas F. KRUISSELBRINK ² , Bruno MEYVIS ¹ , Dirk MUNSTERMAN ² , Bernd ROMBAUT ³ , Tamara J.M. VAN DE VEN ² , Kris WELKENHUYSEN ¹ & Ronald W. VERNES ²	174
Depositional environment and characteristics of organic matter of Namurian Shale, Namur Synclinorium and Campine Basin (Belgium and the S-Netherlands)	
Wei WEI ¹ , Ralf LITTKE ² , Rudy SWENNEN ¹	176
Uncovering earthquake doublets in a lacustrine sedimentary record	
Katleen WILS ¹ , Maxim DEPPEZ ² , Catherine KISSEL ³ , Morgan VERVOORT ¹ , Maarten VAN DAELE ¹ , Mudrik R. DARYONO ⁴ , Veerle CNUUDE ^{2,5} , Danny H. NATAWIDJAJA ⁴ , Marc DE BATIST ¹	178
Session 6- Past, Present and Future of Life on Earth	180
First occurrence of linguliformean brachiopods in the lower Tremadocian (Ordovician) of the Brabant Massif (Belgium)	
Yves CANDELA ¹ , Jean-Marc MARION ² , Thomas SERVAIS ³ , Wenhui WANG ⁴ , Mark WOLVERS ⁵ , Bernard MOTTEQUIN ⁶	181

Craniomandibular anatomy of <i>Panthera gombaszoegensis</i> from la Belle-Roche (Liège, Belgium)	
Narimane CHATAR ^{1,*} , Valentin FISCHER ¹	183
Timing and pacing of the Hangenberg Crisis (Devonian-Carboniferous Boundary) in the Chanxhe sections, Belgium	
Anne-Christine DA SILVA ¹ , Léonard FRANCK ¹ , Michiel ARTS ¹ , Julien DENAYER ^{2,3}	185
Pinaceae diversity from the Lower Cretaceous of Belgium	
Léa DE BRITO ^{1,2} , Valentin FISCHER ¹ , Cyrille PRESTIANNI ^{1,2}	187
Belgium is the best place to define the Devonian-Carboniferous Boundary	
Julien DENAYER ^{1,2} , Cyrille PRESTIANNI ^{1,3} , Bernard MOTTEQUIN ³ , Luc HANCE ⁴ & Edouard POTY ¹	188
Shelf ecosystems along the Maryland Coastal Plain prior to and during the Paleocene-Eocene Thermal Maximum	
Monika DOUBRAWA ¹ , Peter STASSEN ^{1,2} , Marci M. ROBINSON ³ , James C. ZACHOS ⁴ , Robert P. SPEIJER ¹	190
Stratigraphical context of the Pliocene right whales (Balaenidae) from the North Sea	
Guillaume DUBOYS DE LAVIGERIE ^{1,2}	192
CT-CEPH: Applying micro-CT imaging in the study of Belgian fossil nautilid cephalopods	
Stijn GOOLAERTS ^{1,2} & Bernard MOTTEQUIN ¹	194
X-ploring new tools for paleontologists: the RBINS-RMCA micro-CT lab at your service!	
Stijn GOOLAERTS ^{1,2} , Camille LOCATELLI ¹ , Jonathan BRECKO ^{1,3} , Cedric D'UDEKEM D'ACOUZ ¹ , Annelise FOLIE ¹ , Arnaud HENRARD ³ , Aurore MATHYS ^{1,3} , Erik VAN DE GEHUCHTE ¹	196
Caverne Marie-Jeanne (Belgium): How an old collection from the Royal Belgian Institute of Natural Sciences sheds new light on cave hyaenas' behaviour and adaptation	
Elodie-Laure JIMENEZ ^{1,2} & Mietje GERMONPRÉ ¹	198
Variation in long bone morphology of true seals (Mammalia, Phocidae), and its impact on understanding the fossil record	
Jacques KLASSEN ¹ , Leonard DEWAELE ^{1,2} & Valentin FISCHER ¹	199
Echolocating toothed whales (Cetacea, Odontoceti) from the Neogene of Belgium: historical studies, recent contributions and perspectives	
Olivier LAMBERT ¹	201
Mid-latitude tropical conditions during the Early Eocene Climatic Optimum: Reconstruction of a coastal paleoenvironment in the southern North Sea Basin	
Lise MARTENS ^{1,2*} , Peter STASSEN ^{1,2} , Etienne STEURBAUT ^{1,2} , Robert P. SPEIJER ¹	203
Deciphering early stages of vertebrate evolution thanks to long ignored soft-bodied fossils from the Early Devonian of Belgium	
Sébastien OLIVE ¹ , Pierre GUERIAU ² , Philippe JANVIER ³ , Bernard MOTTEQUIN	205
<i>Hirnantia</i> Fauna from the Condroz Inlier, Belgium: another case of a relict Ordovician shelly fauna in the Silurian?	
Sofia PEREIRA, Jorge COLMENAR, Jan MORTIER, Jan VANMEIRHAEGHE, Jacques VERNIERS, Petr ŠTORCH, David A.T. HARPER, Juan Carlos GUTIÉRREZ-MARCO	207

Contributions to Belgian Paleogene (plant) research: a tribute to Philippe Gerrienne	208
Thierry SMITH	
Changing life mode of <i>Campanile giganteum</i> (Lamarck, 1804) with age: Shifting habitat or food sources?	
Nick VAN HOREBEEK, Johan VELLEKOOP, Alexander J. CLARK, Robert P. SPEIJER.....	210
The mid-Maastrichtian event in the Maastrichtian-type area and its benthic foraminiferal response	
Iris VANCOPPENOLLE ¹ , Johan VELLEKOOP ^{1,2} , Monika DOUBRAWA ¹ , Pim KASKES ² , Matthias SINNESAE ^{2,3} , John JAGT ⁴ , Philippe CLAEYS ² , Robert P. SPEIJER ¹	212
Rapid biological recovery following the Cretaceous-Paleogene boundary catastrophe in the Maastrichtian type area	
Johan VELLEKOOP ^{1,2}	214
A paleoenvironmental reconstruction of the <i>Campanile giganteum</i> (Lamarck, 1804) bed (Lutetian, Paris Basin) utilizing quantitative macro- and micropaleontological data	
Anthea WILLEMS ¹ , Johan VELLEKOOP ^{1,2} , Monika DOUBRAWA ¹ , Robert P. SPEIJER ¹	216
Assessing the diversity of insects damage traces in the fossil flora of Gelinden (Limburg, Belgium)	
Raphaël ZAMBON ¹ , Cyrille PRESTIANNI ^{1,2}	218
Session 7- Karsts Investigation and Subsurface Researches	220
Radon gas in karstic environments, the case of the <i>Noû Bleû Cave</i>, Belgium	
Boris DEHANDSCHUTTER ¹ , Gauthier ROBA ²	221
Tracer tests in La Lembrée karstic system: the crucial importance of a good geological map	
Romain DELEU ¹ , Laurent BARCHY ² , Paul DE BIE ³ , Jean-Marc MARION ⁴ , Amaël POULAIN ⁵ , Gaëtan ROCHEZ ¹ , Vincent HALLET ¹	222
Karstification and associated processes of the Waulsort Formation (Furfooz, Belgium)	
Lorraine DEWAIDE ¹ , Jean-Marc BAELE ² , Vincent HALLET ³ & Rudy SWENNEN ⁴	224
RISSC: Towards a better management of cavity-related ground movements in Wallonia and Hauts-de-France Regions	
Lorraine DEWAIDE ¹ , Fanny DESCAMPS ² , Cédric LEFEBVRE ³ , Catherine PINON ⁴ & Jean-Marc WATELET ⁵	226
Sedimentary processes inside the Han-sur-Lesse Cave (Belgium)	
Olivier FONTAINE ¹ , Sabine BLOCKMANS ² , Romain DELEU ² , Vincent HALLET ² , Amaël POULAIN ³ , Gaëtan ROCHEZ ² , Jean VAN CAMPENHOUT ⁴ , Geoffrey HOUBRECHTS ⁴	228
State of knowledge on Kongo Central karst, DRC	
Pascale LAHOGUE ¹ , Ange THIJENIRA ²	230
Origin of the collapse sinkholes of the Boukadir region (Chelif-Algeria)	
Meriem Lina MOULANA ^{1&2} , Aurélie HUBERT ¹ , Mostefa GUENDOZ ² , Camille EK ¹ & Bernard COLLIGNON ³	231

Session 8- New Spectroscopic Methods in Geosciences 233

- High-resolution Raman mapping: using micro-analyses to reveal geological processes**
Fernando P. ARAUJO^{1*}, Niels HULSBOSCH^{1,2}, Philippe MUCHEZ¹ 234
- Combined Laser-Induced Breakdown Spectroscopy (LIBS) and Plasma-Induced Luminescence (PIL) for geochemical mapping and profiling of geological samples**
Jean-Marc BAELE¹, Séverine PAPIER¹, Lorraine DEWAIDE², Joris CORON¹, Anne-Christine DA SILVA³, Vincent HALLET², Rudy SWENNEN⁴ and Vincent MOTTO-ROS⁵ 236
- The ROBOMINERS LIBS spectrometer: a mining sensor prototype for autonomous in-stream, in-slurry geochemical diagnostics**
Christian BURLET¹, Giorgia STASI¹, Tobias PINKSE², Claudio ROSSI³ 238
- Unravelling the genesis of critical mineral resources by employing advanced imaging techniques**
Florian BUYSE^{1,4}, Stijn DEWAELE², Matthieu BOONE^{3,4}, Frederic VAN ASSCHE^{3,4}, Veerle CNUUDE^{1,4,5} 240
- New thermal data for the Rocroi inlier, France and Belgium, based on Raman Spectroscopy of Carbonaceous Material (RSCM)**
Corentin COBERT¹, Jean-Marc BAELE¹ and Abdeltif LAHFID² 242
- Phase identification and mapping of melt inclusions in complex mineral hosts by confocal Raman spectroscopy and multivariate data analysis**
Niels HULSBOSCH¹ and Mona SIRBESCU² 244
- Latest developments in micro-X-ray fluorescence (μ XRF) analysis in geosciences: high-resolution element mapping, digital image analysis, and quantifications**
Pim KASKES^{1,2}, Thomas DÉHAIS^{1,2}, Sietze J. DE GRAAFF^{1,2}, Steven GODERIS¹, Philippe CLAEYS¹ 246
- Recent advances in infrared spectroscopy applied to single specimen dinoflagellate cysts: methodological framework and applications**
Pjotr MEYVISCH^{1*}, Pieter Roger GURDEBEKE¹, Henk VRIELINCK², Kenneth Neil MERTENS³, Gerard VERSTEEGH⁴, Katarzyna SLIWINSKA⁵, Stephen LOUWYE¹ 248
- Geochemical imaging at hand-sample scale of Belgian Zn-Pb ores using Laser-Induced Breakdown Spectroscopy (LIBS)**
Séverine PAPIER¹, Jean-Marc BAELE¹, Hassan BOUZAHZAH², Sophie VERHEYDEN³, Christian BURLET³, Eric PIRARD², Anca CROITOR⁴, Sophie DECRÉE³, Guy FRANCESCHI⁵ and Léon DEJONGHE³ 249
- ROBOMINERS: changing the ground rules**
Giorgia STASI^{1,15}, Christian BURLET^{1,15}, Luis LOPES², Claudio ROSSI³, Stephen HENLEY⁴, Tobias PINKSE⁵, Asko RISTOLAINEN⁶, Vitor CORREIA⁷, Alicja KOT-NIEWIADOMSKA⁸, Jussi AALTONEN⁹, Michael BERNER¹⁰, Nelson CRISTO¹¹, Eva HARTAI¹², Gorazd ZIBRET¹³, Janos HORVATH¹⁴ 251
- Development of a Laser-Induced Breakdown spectrometry (LIBS) instrumentation and protocols for rapid screening of soils**
Sophie VERHEYDEN¹, Christian BURLET¹, Anca CROITOR², Jean-Marc BAELE³, Severine PAPIER³, Eric PIRARD⁴, Hassan BOUZAHZAH⁴ and Matic PUSOVNIK⁵ 253

Session 9- Polar Sciences and Ice-sheets 255

Modelling benthic methane efflux triggered by hydrate dissociation and its potential impact on ocean acidification	
Maria DE LA FUENTE ¹ , Sandra ARNDT ² , Tim MINSHULL ³ , Héctor MARIN-MORENO ⁴ ..	256
Greenland mass balance by 2200 using coupled atmospheric (MAR) and ice sheet (PISM) models	
Alison DELHASSE ¹ , Johanna BECKMANN ² and Xavier FETTWEIS ³	258
Reduction of the future Greenland ice sheet surface melt with the help of solar geoengineering	
Xavier FETTWEIS ¹ , Stefan HOFER ^{1,2} , Roland SÉFÉRIAN ³ , Charles AMORY ^{1,4} , Alison DELHASSE ¹ , Sébastien DOUTRELOUP ¹ , Christoph KITTEL ¹ , Charlotte LANG ¹ , Joris VAN BEVER ^{1,5} , Florent VEILLON ¹ , Peter IRVINE ⁶	260
Quantifying carbon transformations and fluxes at active methane seeps on the East Siberian Arctic Shelf	
Alexis GEELS ¹ , Sandra ARNDT ² , Pierre REGNIER ³ , Volker BRÜCHERT ⁴	261
Evolution of iron-organic carbon interactions during abrupt thaw in ice-rich permafrost: case study in Siberia	
Alexia GILLIOT ¹ , Arthur MONHONVAL ¹ , Justin LOUIS ¹ , Benoît PEREIRA ¹ , Aubry VANDEUREN ¹ , Loeka JONGEJANS ² , Jens STRAUSS ² , Sophie OPFERGELT ¹	262
Towards a Coupled Hydrological-Biogeochemical Model of Subglacial Environments	
Nick HAYES, Ankit PRAMANIK, Sandra ARNDT.....	264
Assessing the production and efflux of methane gas from thawing subsea permafrost on the warming Arctic shelf	
Constance LEFEBVRE ¹ , Emilia RIDOLFI ² , Maria DE LA FUENTE RUIZ ³ , Sandra ARNDT ⁴	265
Influence of thermokarst formation on manganese-organic carbon interactions in ice-rich permafrost	
Justin LOUIS ¹ , Arthur MONHONVAL ¹ , Alexia GILLIOT ¹ , Aubry VANDEUREN ¹ , Benoît PEREIRA ¹ , Loeka JONGEJANS ² , Jens STRAUSS ² , Sophie OPFERGELT ¹	266
Influence of permafrost degradation on foliar mineral element cycling upon changing subarctic tundra vegetation	
Elisabeth MAUCLET ¹ , Yannick AGNAN ¹ , Catherine HIRST ¹ , Arthur MONHONVAL ¹ , Justin LEDMAN ² , Meghan TAYLOR ² , Edward A. G. SCHUUR ² , Sophie OPFERGELT ¹	268
Seasonal dynamics of nitrous oxide in sea ice in the Central Arctic: insights from the MOSAiC Expedition	
Sofia MULLER ¹ , Katarina ABRAHAMSSON ² , Michael ANGELOPOULOS ³ , Odile CRABECK ¹ , Ellen DAMM ³ , Alessandra D'ANGELO ⁴ , François FRIPIAT ⁵ , Daiki NOMURA ⁶ , Jonathan VAN HANJA ¹ , Liyang ZHAN ⁷ , Bruno DELILLE ¹	270
Quantifying Fe-OC associations in sediment using Na-dithionite in Flow-Through Reactors (FTR)	
Silvia PLACITU ¹ , Sandra ARNDT ¹ , Steve BONNEVILLE ¹	271
Modeling methane production and emission from thawing sub - sea permafrost on the warming Arctic Shelf	
E. Ridolfi ¹ , S. Wikenskjeld ² , F. Miesner ³ , V. Brovkin ^{2,4} , P. Overduin ³ , S. Arndt ¹	273

Influence of permafrost degradation and shift in vegetation on litter and soil properties: case study in Central Alaska

Maëlle VILLANI¹, Elisabeth MAUCLET¹, Yannick AGNAN¹, Edward A. G. SCHUUR², Sophie OPFERGELT¹ 274

Session 10 - Quaternary and Anthropocene (BELQUA) 276

Preliminary results from palynological and diatoms analyses from three sites of the Medieval harbour network in the Zwin area in North of Belgium and the Netherlands: Hoeke, Mude and Aardenburg

Coralie ANDRE¹, Wim DE CLERCQ², Dante DE RUIJSSCHER², Vanessa M.A. HEYVAERT^{1,3}, Frieda BOGEMANS³, Stephen LOUWYE¹ 277

Has hydrologic connectivity been taken into account in the Lake Tana Basin (Ethiopia): a literature review on climate, hydrology and geomorphology

Anik Juli Dwi ASTUTI¹, Sofie ANNYS¹, Jan NYSSSEN¹, Stefaan DONDEYNE¹ 279

Lacustrine record of last millennia precipitation from Lake Esponja and Lake Bertrand of Northern Chilean Patagonia (72°W)

Jeanne AUBOIRON¹, Denisse ALVAREZ², Alberto ARANEDA², Pablo PEDREROS², Roberto URRUTIA² and Nathalie FAGEL³ 281

Vegetation history in the Ethiopian Highlands for the past 18000 years: a multi-proxy analysis of high altitude wetlands

Femke AUGUSTIJNS^{1,2}, Nils BROOThAERTS², Gert VERSTRAETEN² 282

Reconstructing the late Holocene sedimentary landscape of the Zwin area nearby Bruges late-medieval outpost Hoeke

Frieda BOGEMANS¹, Vanessa HEYVAERT^{1,2}, Coralie ANDRÉ², Stephen LOUWYE², Jan TRANCHET³, Wim DE CLERCQ³ 283

Changes in vegetation and sediment transfers over the last 3000 years in the catchment of Lake Alaotra, Madagascar

Nils BROOThAERTS¹, Liesa BROSENS^{1,2}, Vao Fenotiana RAZANAMAHANDRY¹, Benjamin CAMPFORTS³, Liesbet JACOBS^{1,4}, Tantely RAZAFIMBELO⁵, Tovonarivo RAFOLISY⁵, Gert VERSTRAETEN¹, Steven BOUILLON¹, Gerard GOVERS¹ 284

Metagenomics of tsunami deposits: developments and challenges from a case study on the Shetland Islands (UK)

Max ENGEL^{1,2}, Tasnim PATEL³, Anna PINT⁴, Sue DAWSON⁵, Isa SCHÖN^{3,6} & Vanessa M. A. HEYVAERT^{2,7} 286

The last millenia sedimentary record of Lago Esponja from Northern Chilean Patagonia

Nathalie FAGEL¹, Pablo PEDREROS², Denisse ALVAREZ², Isabel ISRADE ALCANTARA³, Alberto ARANEDA², Olivier NAMUR⁴, Sabine SCHMIDT⁵, Roberto URRUTIA² 288

The highest latitude waters of the Southern Ocean and glacial-interglacial change in atmospheric CO₂.....

François FRIPIAT^{1,2}, Alfredo MARTÍNEZ-GARCÍA², Frank LAMY⁴, Daniel M. SIGMAN³, and Gerald H. HAUG² 290

Spatio-temporal variation of the Omo Delta (1990-2018): what remote sensing data reveal and models explain.....

Gladys KANGI¹, Fritz KLEINSCHROTH², Jos VAN ORSHOVEN¹, Stefaan DONDEYNE³ 292

Regional sensitivity of East Asian summer monsoon to ice sheet and orbital forcing	
Anqi LYU ¹ , Qiuzhen YIN ¹ , Michel CRUCIFIX ¹ , Youbin SUN ^{2,3}	294
Paleoclimatic evolutions during the Holocene: A stalagmite $\delta^{18}\text{O}$ record from Majiaping Cave, Guizhou, China	
Ming-Qiang LIANG ^{1,2} , Hong-Chun LI [*] , Qiu-Zhen YIN ² , Horng-Sheng MII ³ , Zhi-Bang MA ⁴ , Ting-Yong LI ⁵ , Ludvig LÖWEMARK ¹	295
Topoclimate and spatio-temporal distribution of summer rain over the Ethiopian highlands ...	
Emnet NEGASH ^{1,2} , Bert VAN SCHAEYBROECK ^{3,4} , Piet TERMONIA ^{3,4} , Michiel VAN GINDERACHTER ^{3,4} , Jan NYSSSEN ¹	296
A question of time: dating Quaternary fluvial archives and landscapes.....	
Gilles RIXHON	298
Spatial variation and factors controlling sediment fluxes along the western slopes of the Peruvian Andes	
Miluska A. ROSAS ^{1,2} ; Veerle VANACKER ¹	299
Atmospheric beryllium-10 (¹⁰Be), a versatile cosmogenic nuclide to reconstruct geomagnetic strength variations, quantify paleoenvironmental processes, provide chronostratigraphic markers and date sedimentary sequences	
Quentin SIMON, Nicolas THOUVENY, Didier L. BOURLÈS	301
The response of global terrestrial vegetation to orbital forcing and CO₂ during MIS 11 and MIS 13	
Qianqian SU ¹ , Qiuzhen YIN ² , Anqi LYU ³ , Zhipeng WU ⁴	303
Anthropogenic legacy effects control sediment and organic carbon storage in temperate river floodplains	
Ward SWINNEN ¹ , Nils BROOthaerts ¹ , Gert VERSTRAETEN ¹	304
Reconstructing the spatial redox structure of anoxic oceans using a 3D ocean-based Earth system model	
Sebastiaan J. VAN DE VELDE ^{1,2} , Dominik HÜLSE ³ , Christopher T. REINHARD ⁴ , Andy RIDGWELL ³	305
Constraining the depositional history of Quaternary fluvial deposits based on grain size, geochemistry and cosmogenic radionuclides	
Nathan VANDERMAELEN ¹ , Veerle VANACKER ¹ , Marcus CHRISTL ² , Koen BEERTEN ³	306
Mineralogical and geochemical signal of the crater lake <i>La Alberca de Tacámbaro</i> in Central Mexico as an archive of precipitation over the last millennia	
Gaëlle WANLIN ¹ , Isabel ISRADE ² , Nathalie FAGEL ¹	307

Session 11-Geophysics and Seismology 309

- CO₂ gas discharge in Laacher See: visualization and mapping of accumulated gas in the water column and sedimentary infill of a caldera lake in western Germany**
Stijn ALBERS¹, Anouk VERWIMP¹, Corentin CAUDRON², Thomas VANDORPE³, and Marc DE BATIST¹ 310
- A new Hainaut coal area earthquake intensity attenuation model using 19th - 20th century shallow seismicity data**
Thierry CAMELBEECK¹, Koen VAN NOTEN^{1,*}, Thomas LECOCQ¹, Marc HENDRICKX¹ 312
- Insights from the new 3D fault model for eastern Flanders (northern Belgium)**
Jef DECKERS¹, Bernd ROMBAUT¹, Katrijn DIRIX¹, Matsen BROOThAERS¹, Timothy N. DEBACKER² 314
- BarrosRedefinition of the structural units of the Variscan Front based on the results of the Mons2012 and Hainaut2019 seismic surveys in the Hainaut (SW Belgium)**
Nicolas DUPONT¹, Olivier KAUFMANN², Jean-Marc BAELE³ 317
- Statistical imaging of the deformation over Belgium using multiple geodetic techniques**
Kevin GOBRON¹, Pierre-Yves DECLERCQ², Xavier DEVLEESCHOUWER², Michel VAN CAMP¹ 319
- Study of the eigenfrequencies of stalagmites to better understand paleoseismicity**
Aurélie MARTIN^{1,2}, Thomas LECOCQ¹, Ari LANNOY³, Yves QUINIF⁴, Sophie VERHEYDEN⁵, Serge DELABY⁶, Thierry CAMELBEECK¹, Nathalie FAGEL² 321
- The effects of Belgian crustal geology and its sedimentary cover on macroseismic intensity attenuation**
Ben NEEFS¹, Koen VAN NOTEN¹, Thierry CAMELBEECK¹ 322
- Slip tendency apply to faults systems in the Congo Basin and its surroundings: A clue to explain western central African passive margin seismicity**
Hardy Medry Dieu-Veill NKODIA^{1,*}, Timothée MIYOUNA¹, Florent BOUDZOU MOU^{1,2}, Folarin KOLAWOLE^{3,4}, Damien, DELVAUX⁵ 323
- Analyzing seismic anomalies in Carboniferous strata in the surroundings of three wells in Mol (Campine Basin, northern Belgium) by means of Amplitude Variation with Offset (AVO) analysis shows potential for deep geothermal exploration**
Bernd ROMBAUT, Jef DECKERS, Katrijn DIRIX, Matsen BROOThAERS, Ben LAENEN 324
- Geophysical well log correlations in the Quaternary deposits of the Campine area, northern Belgium**
Jan WALSTRA¹, Frieda BOGEMANS¹, Marleen DE CEUKELAIRE^{1,2}, Michiel DUSAR¹, Vanessa M.A. HEYVAERT^{1,3}, Bruno MEYVIS¹ & Kris WELKENHUYSEN¹ 327
- Towards a site-characteristic database for the Belgian permanent seismic network** Martin ZECKRA¹, Koen VAN NOTEN¹, Thomas LECOCQ¹ 328

Session 12- Geo-energy 330

12.1. Geo-energy: Opportunities and Constraints for Subsurface Uses 330

Delineation of inferred high-transmittivity zones in the Dinantian geothermal reservoir of Hainaut (SW Belgium)	
Nicolas DUPONT ¹ , Olivier KAUFMANN ² , Jean-Marc BAELE ³	331
How geomaniifestations can help in policy challenges	
Helga FERKET ¹ , Johanna VAN DAELE ¹	333
Deep Geothermal Energy Extraction, a Review on Environmental Hotspots with Focus on Geo-technical Site Conditions	
Spiros GKOUSIS ¹ , Tine COMPERNOLLE ^{1,2} , Kris WELKENHUYSEN ²	335
Influence of the heat network rollout time on the risk and profitability of a deep geothermal plant	
Bruno MEYVIS ¹ , Virginie HARCOUET-MENOU ² , Kris WELKENHUYSEN ¹	337
New geological information of the Cambrian basement obtained from geothermal exploration projects in Brussels and Walloon- and Flemish-Brabant	
Estelle PETITCLERC ¹ , Pabitra GURUNG ¹ , Pierre GERARD ² , Marc VAN CAMP ³ , Jeroen VAN DER VEKEN ⁴ , Gust VAN LYSEBETTEN ⁴ , Koen VAN NOTEN ⁵ , Kristine WALRAEVENS ³	339
Early Carboniferous limestones of southern and central Britain: preliminary assessment of deep geothermal prospectivity	
Tim PHARAOH ¹ , Darren JONES ² , Tim KEARSEY ² , Andrew NEWELL ³ , Corinna ABESSER ³ , Tom RANGLES ² , Ashley PATTON ⁴ and Rhian KENDALL ⁴	341
Fractured Lower Carboniferous carbonates of the Campine Basin (NE-Belgium) as potential geothermal reservoirs: age and origin of open carbonate veins	
Rudy SWENNEN ¹ , Eva VAN DER VOET ^{1,2} , Wei WEI ¹ and Philippe MUCHEZ ¹	343
Ranking CO₂ storage capacities and identifying their technical, economic and regulatory constraints: A review of methods and screening criteria	
Alejandra TOVAR, Kris WELKENHUYSEN, Kris PIESSENS	344
Optimal geodata centralization and disclosure as support for subsurface exploration	
Johanna VAN DAELE ¹ , Helga FERKET ¹ , Renata BARROS ²	346
Analysing CO₂ capture, transport, and storage chain options for cement industry in the LEILAC2 project	
Kris WELKENHUYSEN, Alejandra TOVAR GAVIRIA, Kris PIESSENS	348
Decision support under uncertainty for geothermal applications: case selection and concept development	
Kris WELKENHUYSEN ¹ , Tine COMPERNOLLE ^{1,2} , Olivier KAUFMANN ³ , Ben LAENEN ⁴ , Bruno MEYVIS ¹ , Kris PIESSENS ¹ , Spiros GOUSIS ² , Nicolas DUPONT ³ , Virginie HARCOUET-MENOU ⁴ , Justin POGACNIK ⁴	350

12.2. DGE Rollout, Roll-out of Deep Geothermal Energy in NW-Europe 352

- The Lower Carboniferous geothermal reservoir of the deep subsurface of North Rhine-Westphalia and its border regions: New insights from 3D mapping**
Martin ARNDT¹, Tobias FRITSCHLE¹ & Martin SALAMON¹ 353
- Deep geothermal energy in the Lower Carboniferous carbonates in the Belgian Campine Basin: current status of the Balmatt project in Mol.....**
Matsen BROOThAERS^{1*}, Virginie HARCOUËT-MENOU¹, Ben LAENEN¹, David LAGROU¹, Justin POGACNIK¹..... 354
- DGE-ROLLOUT - Promoting Deep Geothermal Energy in North-West Europe**
Tobias FRITSCHLE¹, Estelle PETITCLERC², Timme VAN MELLE³, Matsen BROOThAERS⁴, Arianna PASSAMONTI⁵, Martin ARNDT¹, Burcu TAŞDEMİR¹, Chelsea PEDERSON⁶ and Martin SALAMON¹..... 356
- Exploration for Deep Geothermal Energy at the RWE Power Plant Weisweiler, Germany**
Thomas OSWALD¹, Frank STROZYK², Tobias FRITSCHLE³, Martin SALAMON³ 357
- A Fraunhofer demonstrator on high temperature heat pump coupled with high temperature mine thermal energy storage**
Arianna PASSAMONTI¹, Matthias UTRI¹, Florian HAHN¹ 358
- Sustainability and renewability of Geothermal Energy** Timme VAN MELLE¹, Hester DIJKSTRA², Dorien DINKELMAN³ 359
- High-Temperature Medium Deep Borehole Thermal Energy Storage Pilot Plant**
Bastian WELSCH^{1,2}, Julian FORMHALS^{1,2}, Kristian BÄR¹, Lukas SEIB¹, Ingo SASS^{1,2}..... 360

Geologica Belgica Van den Broeck Medal 2021

Delivered to Thierry Camelbeeck

Ceremony and conference



Earthquake activity in Western Europe is typical of stable continental regions

Thierry CAMELBEECK

Royal Observatory of Belgium, 3 avenue circulaire, B-1180 Brussels, Belgium

Despite the real societal challenge posed by their important potential of destruction, understanding the causes of infrequent moderate and large earthquakes in tectonically stable continental regions (SCR) stays a scientific challenge. In this context, studying the historical seismicity and appraising the possible traces of large prehistorical earthquakes in the region of Western Europe between the Lower Rhine Embayment and southern North Sea greatly contributed during the last 30 years to the study of the seismicity in SCR worldwide.

Re-evaluated historical earthquake and present day seismological data show that an important part of the known seismic activity is concentrated in the Roer Valley Graben (RVG). The RVG is also the only area of Central and Western Europe where slow active faults have been identified and related to earthquake activity. However, the three largest historical earthquakes in this part of Europe with estimated magnitude around or greater than 6.0 occurred outside of the graben in 1382 (southern North Sea), 1580 (Dover Strait), and 1692 (Verviers, northern Belgian Ardenne). Therefore, most of the seismic moment release since the Middle Ages in this part of Western Europe occurred outside the RVG, despite the graben's dominance in Western European tectonic activity over the Quaternary. The Quaternary activity of the Sangatte and Hockay fault zones, which would have generated the

large (M~6.0) 1580 - Strait of Dover and 1692 - northern Belgian Ardenne earthquakes, is very elusive if it exists leading to the conclusion that such large earthquakes are very infrequent on these faults. These results support the episodic, clustered and migrating character of the seismicity in this stable continental region, which is already suggested by the observation that during the last 700 years moderate and large earthquakes always occurred at different locations.

This analysis of the long-term seismicity of this part of Europe also support the hypothesis that large earthquakes in SCR can be explained by transient perturbations of local crustal stress or fault strength because the tectonic loading on faults is very slow. By using the basic principles of frictional fault reactivation, we explain why these temporary stresses play a more fundamental role in the initiation of large earthquakes in SCR than at plate boundaries. As these disturbances in stresses can be related to natural environmental phenomena, but also to human activities, we also debate about the potential role of man-made earthquakes in SCR seismicity and seismic hazard. This discussion highlights the need to better understand the contribution of man-made earthquakes in the observed seismicity.

References

- Calais, E., Camelbeeck, T., Stein, S., Liu, M., Craig, T. (2016). **A New Paradigm for Large Earthquakes in Stable Continental Plate Interiors**. *Geophysical Research Letters*, vol. 43 (2016).
Doi:[10.1002/2016GL070815](https://doi.org/10.1002/2016GL070815).
- Camelbeeck T., Meghraoui M. (1998). Geological and geophysical evidence for large palaeoearthquakes with surface faulting in the Roer graben (northwestern Europe). *Geophysical Journal International*, 132, 347-362.
- Camelbeeck T., Alexandre P., Vanneste K., Meghraoui M. (2000). Long-term seismicity in regions of present day low seismic activity: the example of western Europe. *Soil Dynamics and Earthquake Engineering* 20, 405-414.
- Camelbeeck, T., Vanneste, K., Alexandre, P., Verbeeck, K., Petermans, T., Rosset, P., Everaerts, M., Warnant, R., Van Camp, M. (2007). **Relevance of active faulting and seismicity studies to assessments of long-term earthquake activity and maximum magnitude in intraplate northwest Europe, between the Lower Rhine Embayment and the North Sea"**. *Continental Intraplate Earthquakes: Science, Hazard, and Policy Issues: Geological Society of America, S. Stein and S. Mazzotti (eds.) vol. Special Paper 425 pp.* 193-224.
- Camelbeeck, T., Alexandre, P., Sabbe, A., Knuts, E., Garcia Moreno, D., and Lecocq, T. (2014). **The impact of earthquake activity in Western Europe from the historical and architectural heritage records, in: Intraplate Earthquakes**, *Solid Earth Geophysics*, pp. 198–230, Cambridge University Press, <https://doi.org/10.1017/CBO9781139628921.009>.
- Garcia Moreno, D., Verbeeck, K., Camelbeeck, T., De Batist, M., Oggioni, F., Zurita Hurtado, O., Versteeg, W., Jomard, H., Collier, J., Gupta, S., Trentesaux, A., Vanneste, K. (2015). **Fault activity in the epicentral area of the 1580 Dover Strait (Pas-de-Calais) earthquake (northwestern Europe)**. *Geophysical Journal International*, vol. 201 pp. 528-542 (2015). Doi:[10.1093/gji/ggv041](https://doi.org/10.1093/gji/ggv041).
- Vanneste, K., Camelbeeck, T., Verbeeck, K., Demoulin, A. (2017). **Morphotectonics and past large earthquakes in Eastern Belgium**. A. Demoulin (ed.), *Landscape and Landforms of Belgium and Luxemburg, World Geomorphological Landscapes* (2017). Doi:[10.1007/978-3-319-58239-9_13](https://doi.org/10.1007/978-3-319-58239-9_13).
- Verbeeck, K., Wouters, L., Vanneste, K., Camelbeeck, T., Vandenberghe, D., Beerten, K., Rogiers, B., Schiltz, M., Burow, C., Mees, F., De Grave, J., Vandenberghe, N. (2017). **Episodic activity of a dormant fault in tectonically stable Europe: The Rauw fault (NE Belgium)**. *Tectonophysics* (2017), Doi:[10.1016/j.tecto.2017.01.023](https://doi.org/10.1016/j.tecto.2017.01.023).

Session 1- Geodynamics and Mineral Resources

Conveners:

Johan De Grave (UGent), Stijn Dewaele (Ugent), Philippe Muchez (KU Leuven), Johan Yans (UNamur), Anouk Borst (RMCA & KU Leuven), Thierry De Putter (RMCA), Max Fernandez-Alonso (RMCA).

Invited speaker:

Camille François, Commission for the Geological Map of the World (CGMW), France (Leader IGCP project 667)

Mineral resources are at the heart of our modern societies, with high-tech technologies fuelling a fast-growing demand for commodities and rare elements or metals. The formation of ore deposits is intimately linked to major geodynamic events – magmatic activity, hydrothermal fluids circulation, vertical movements, weathering, etc. The objective of this session is to explore the various geological contexts in which ore deposits can form. Several conveners have an acknowledged expertise in Africa, and hence welcome contributions on African research topics. However, case studies from other regions are most welcome as geodynamic processes are never restricted to one specific area in the world. Contributions on the link between mineral resources exploitation and green techs or development goals are also most welcome.



Specific topics include (not exclusive): the geodynamics and mineralization of Mesoproterozoic belts in Central Africa; ore-forming process in the Neoproterozoic of Central Africa; West Congo Belt in Africa and its counterpart in SE Brazil; supergene ores; metals for a green future; secondary metal resources.

Influence of geological structures on failure possibility around Meli area gold mine site, northwestern Tigray region, north Ethiopia

Kaleab Adhena Abera^{1,2,3}, Miruts HAGOS², Gebremedhin BERHANE², Tesfamichael GEBREYOHANNES², Abdelwassie HUSSEN² and Kristine WALRAEVENS¹

¹ Laboratory for Applied Geology and Hydrogeology, Department of Geology, Ghent University, Belgium (kaleabadhena.abera@ugent.be)

² Department of Geology, School of Earth Science, Mekelle University, Ethiopia

³ Department of Geology, Faculty of Mines, Shire Campus, Aksum University, Ethiopia

Meli area is the only and very recently launched modern small-scale gold mining site in the Tigray region, Ethiopia. The gossan gold ore body of the Meli area is found as boudin structures necked into three domains (domains A, B and C). These domains are separated by a saddle morphology accompanied by sinistral strike-slip faults. Structurally controlled ore bodies are commonly complex in nature (Peters, 2001). All three domains are also intruded or crosscut by later quartz veins and the intersection of two mineralized conduits commonly results in an ore shoot (Rickard, 1902). Therefore, in addition to the existing gossan gold ore body, the younger quartz veins are also rich in gold mineralization which has its own contribution for the increment of gold concentration in the gossan area. Existing faults and fracture patterns combined with the physical properties of the host rock of the Meli gossan gold deposit present a high risk of slope failure, which has been identified as a key problem for profitable gold mining. Therefore, the main objective of this research is to evaluate rock mass characteristics and overall physical properties and geological structures of the study area.

Landsat and Spot satellite images have been used to extract fractures, faults, contacts and lithological boundaries besides to fieldwork for ground-truthing (Figure 1). Engineering geological properties of the rock mass are also evaluated based on raw data from the Ezana private mining company.

The area is generally characterized by different generations of fractures or discontinuities. The nature and intensity of the discontinuities vary from place to place (Figure 2) and total of 110 readings were taken from shear zones (SE-NW), foliations (N-S), faults and fractures of various orientations. The magnitude and intensity of the discontinuities are directly related to the degree of deformation. Metavolcanic and metasedimentary rocks host the gossan gold ore body of the area. A total of six trials of slope analysis using slope mass rating with assumed pit slope excavation angles of 60°, 45° and 30° in both directions against to the dip and parallel to the dip have been conducted. Toppling and planar failure types were found to be the main source of failure when using 60° and 45° excavation angles, while the deposit can be mined with no slope failure and are stable at an excavation angle of 30°. Generally speaking, the economics of mining operations can be improved by steepening the excavation slope in order to reduce the amount of waste excavation. Excessive slope steepening could also result in failure, leading to potential loss of life and damage to property (Singh and Singh, 1992). The natural deformation and followed geological discontinuities of the study area have already become the basic challenge for developing slope design with desired economically profitable mining.

In this work, the direct economic impact of mining operation due to structural and geotechnical properties of the rock is evaluated. The geology of the study area is characterized by intensive and repeated deformation events which results in the presence of large fractures, faults and weak rock physical properties. The investigation of cumulative rock mass characteristics and fractured rock parameters helps in identifying the natural constraints for mining at economical rate.

References

- Ezana Mining Development PLC (2014). Highlights on the Mineral Properties.
- Peters, S. G. (2001). Use of structural geology in exploration for and mining of sedimentary rock-hosted deposits. US Geological Survey Open File Report, 01–151, 1–39.
- Rickard, T.A. (1902). The formation of bonanzas in the upper parts of gold-veins: American Institute Mining Metallurgy Transactions, no. 31, p. 198–220.
- Singh, T.N. and Singh, D. P. (1992). Slope Stability Study in an Opencast Mine Over Previously Worked Seam, Int. Symp. Rock Slope, New Delhi, pp. 467-477.

Figures

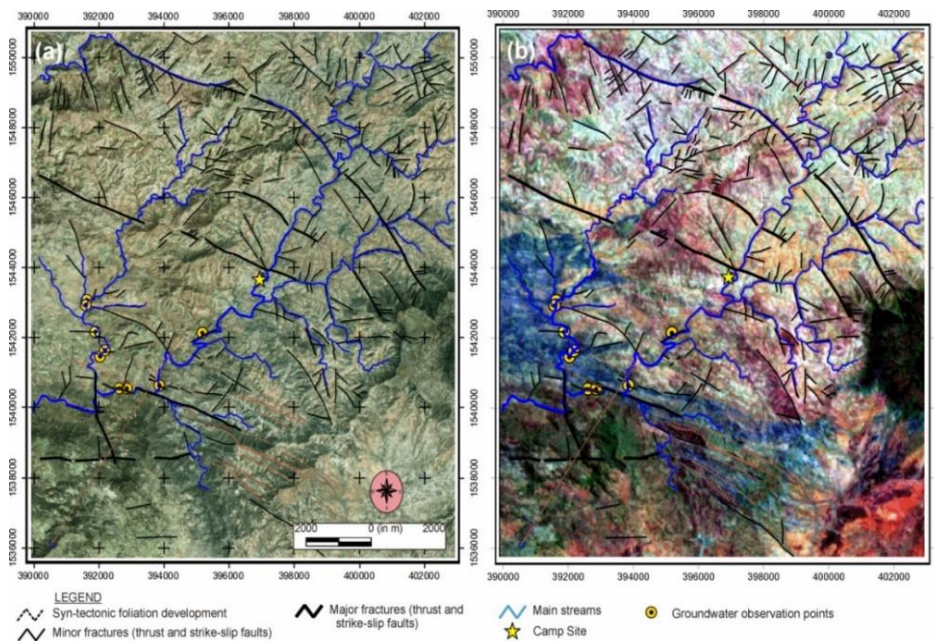


Figure. 1. a) Spot and b) Landsat satellite image interpretation of Meli (modified after Ezana, 2014).

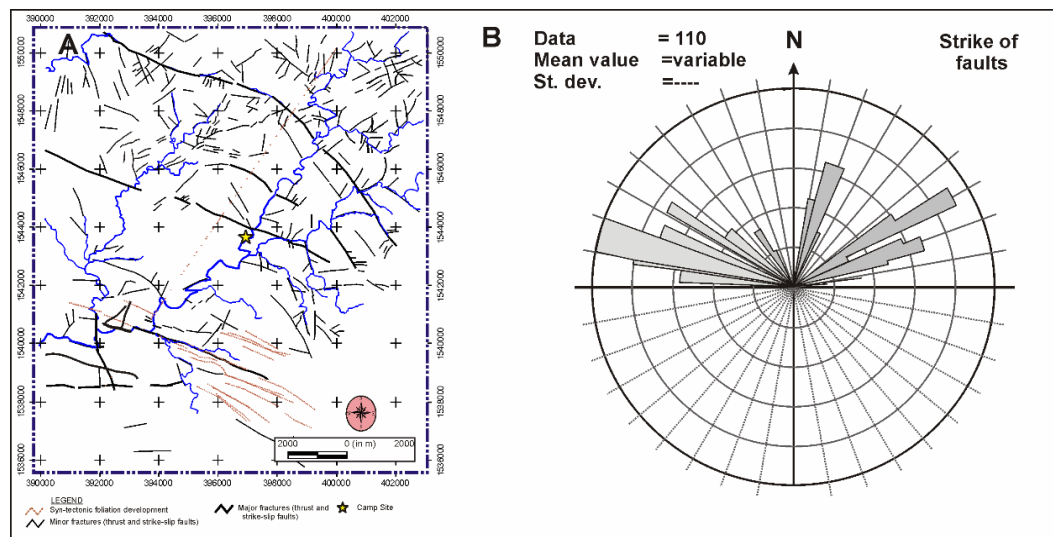


Figure. 2. Rose diagram showing the orientation of the fractures and major faults of Meli area.

Au Vein-Type Mineralisation at Escádia Grande (Portugal): A Microstructural and Geochemical Analysis

Jolan ACKE¹, Pim KASKES², Philippe CLAEYS², Dominique JACQUES¹, Philippe MUCHEZ¹

¹ KU Leuven, Department of Earth and Environmental Sciences, Celestijnenlaan 200E, B-3001 Heverlee, Belgium

² Analytical, Environmental & Geo-Chemistry Research Unit, Vrije Universiteit Brussel, Brussels, Belgium

W-Sn bearing vein-type mineralisation in the Iberian Massif shows a close structural relationship with late-Variscan tectonics and oroclinal buckling. Previous structural analyses and Rb-Sr dating have demonstrated a strong kinematic and temporal relationship between regional late-orogenic fold-related jointing and the structural emplacement of W-Sn vein-type mineralisation (Jacques et al., 2018a,b, 2021). This knowledge is of major importance in fundamental ore geology research and towards mineral exploration.

The Escádia Grande Au-bearing quartz vein system is situated in the vicinity of the world-class W-Sn Panasqueira deposit in Central Portugal. The mineralised vein systems are hosted by Neoproterozoic-Cambrian metasedimentary sequences (Meireles et al., 2013), which are affected by three main deformation stages, and are peripheral to granitic cupolas at depth. From a macrostructural point of view, the Escádia Grande and Panasqueira vein systems show a similar geometric-kinematic relationship with late-orogenic folding, i.e. emplacement took place along subhorizontal to moderately-inclined cross-fold joints, orthogonal to steep late-orogenic F3 fold axes (Jacques et al., 2018b). Despite the close temporal, spatial and kinematic relationship between the Panasqueira W-Sn and Escádia Grande Au-bearing vein systems, they appear to be characterised by a different fabric, microstructure and mineralisation style. To clarify this contrast in mineralisation, we conducted detailed microstructural and geochemical analyses.

The Escádia Grande Au-bearing quartz veins display a laminated nature due to the alternation of coarse-grained and fine-grained quartz bands with wall-rock selvages parallel to the vein wall, which were incorporated during subsequent crack-seal events. While the coarse-grained quartz represents the initial fabric formed upon sealing, the fine-grained quartz bands are interpreted as having been dynamically recrystallised by shear strain and pressure solution reactions. The microstructure in moderately-inclined and more steeply-inclined parts of the vein system varies regularly. In the moderately-inclined vein segments, wall-rock selvages display asymmetric boudinage and C'-type shear band cleavage. In the steeper vein segments, however, observed microstructures are mainly an oblique foliation defined by the quartz lattice preferred orientation in fine-grained quartz bands. These observations suggest the activity of post-sealing, normal-sense fault creep in an extensional setting.

Petrographic and μ XRF analyses indicate that Au-enrichment is present within arsenopyrite, consistently associated with pressure solution seams (stylolites) at the interface of sheared wall-rock selvages and laminations of dynamically recrystallized quartz. Pressure solution and non-coaxial creep in an extensional tectonic regime is interpreted to have passively concentrated Au (cf. Voisey et al., 2020).

Primary two-phase aqueous-carbonic fluid inclusions occur within the vein quartz. Microthermometric measurements, combined with the results from Raman spectroscopy,

demonstrate the presence of a low saline H₂O-NaCl-CO₂-CH₄-N₂ fluid with minor amounts of H₂S detected in several inclusions. This fluid composition is indicative of a metamorphic origin of the mineralising fluid (cf. Fu et al., 2014). Combining a lithostatic geothermal gradient of 40-50°C/km (Ferreira et al., 2019) with the isochores calculated from the fluid inclusion data (reflecting the P-T evolution of the fluid in equilibrium with the host rock), fluid trapping conditions are estimated at 400-450°C and 200-250 MPa. These values are consistent with P-T estimations from the Panasqueira vein system (Cathelineau et al., 2020).

The presence of minor H₂S in the fluid and abundant arsenopyrite in which Au is concentrated, indicates that destabilisation of Au(HS⁻)₂ complex during fluid-rock interaction caused Au mineralisation in locally deformed zones within the vein.

References

- Cathelineau, M. Boiron, M. Marignac, C. Dour, M. Dejean, M. Carocci, E. Truche, L. & Pinto, F, 2020. High pressure and temperatures during the early stages of tungsten deposition at Panasqueira revealed by fluid inclusions in topaz. *Ore Geology Reviews*, 126, 103741
- Cerný, P. Blevin, P.L. Cuney, M. & London, D, 2005. Granite-related ore deposits. *Economic Geology* 100th 337–370
- Ferreira, J.A. Bento dos Santos, T. Pereira, I. & Mata, J, 2019. Tectonically assisted exhumation and cooling of Variscan granites in an anatectic complex of the Central Iberian Zone, Portugal: constraints from LA-ICP-MS zircon and apatite U–Pb ages. *International Journal of Earth Sciences : Geologische Rundschau*, 108(7), 2153–2175
- Fu, B. Mernagh, T.P. Fairmaid, A.M. Phillips, D. & Kendrick, M.A, 2014. CH₄-N₂ in the Maldon gold deposit, central Victoria, Australia. *Ore Geology Reviews*, 58(C), 225–237
- Jacques, D. Muchez, P. & Sintubin, M, 2018a. Superimposed folding and W-Sn vein-type mineralisation in the Central Iberian Zone associated with late-Variscan oroclinal buckling: a structural analysis from the Regoufe área (Portugal). *Tectonophysics*, 742–743, 66–83
- Jacques, D. Vieira, R. Muchez, P. & Sintubin, M, 2018b. Transpressional folding and associated cross-fold jointing controlling the geometry of post-orogenic vein-type W-Sn mineralization: examples from Minas da Panasqueira, Portugal. *Mineralium Deposita*, 53(2), 171–194
- Jacques, D. Muchez, P. & Sintubin, M, 2021. Late- to post-Variscan tectonics and the kinematic relationship with W–Sn vein-type mineralization: evidence from Late Carboniferous intramontane basins (Porto–Sátão syncline, Variscan Iberian belt). *Journal of the Geological Society*
- Meireles, C. Sequeira, A.J. Castro, P. & Ferreira, N, 2013. New data on the lithostratigraphy of Beiras group (schist greywacke complex) in the region of góis-arganil-pampilhosa da serra (central Portugal). *Cuadernos Do Laboratorio Xeolóxico de Laxe*, 37, 105–123
- Voisey, C.R. Willis, D. Tomkins, A.G. Wilson, C.J.L. Micklethwaite, S. Salvemini, F. Bougoure, J. & Rickard, W.D.A, 2020. Aseismic refinement of orogenic gold systems. *Economic Geology and the Bulletin of the Society of Economic Geologists*, 115(1), 33–50

A long-lasting Archean deformation history in the Sangmelima terrane, NW Congo Craton, Southern Cameroon

Joseph M. AKAME^{1*}, Vinciane DEBAILLE¹, Thierry DE PUTTER², Marc POUJOL³, Bernhard SCHULZ⁴, Elson P. OLIVIERA⁵

1. *Laboratoire G-Time Géochimie Isotopique. Université Libre de Bruxelles, 50, Av. F.D. Roosevelt, CP 160/02, B-1050 Brussels, Belgium (akamejosephmartial@gmail.com; Joseph.Martial.Akame@ulb.be)*
2. *Geodynamics and Mineral Resources, Royal Museum for Central Africa (RMCA), Leuvensesteenweg 13, 3080, Tervuren, Belgium*
3. *Univ Rennes, CNRS, Géosciences Rennes - UMR 6118, F-35000 Rennes, France*
4. *TU Bergakademie Freiberg, Institute of Mineralogy, Division of Economic Geology and Petrology, Brennhaugasse 14, D, 09599, Freiberg, Saxony, Germany*
5. *Department of Geology and Natural Resources, University of Campinas-Unicamp, P.O.Box 6152, 13083-970 Campinas, Brazil*

The Sangmelima granite-greenstone belt (SGB) belongs to the Ntem Complex (NW Congo craton), and is represented by granite-gneiss terranes, granite-greenstone associations, mafic-ultramafic complexes, and mafic dyke swarms. Here, we present a new tectonic evolution model based on an aeromagnetic map, structural analysis, and geochronological data. Regional strain D1 is characterized by the development of steep foliations, steeply plunging lineations occasionally associated with vertical stretching of granitic dykes. D1 shear sense is top-to-NNE oblique normal motion, inferred from the S₁ mylonitic fabric and the finite strain suggested that the vertical flow component dominates at the regional scale compared to the horizontal motions (Akame et al., 2020b). Syn-D1 melts, mineral assemblages and microstructures indicate that D1 took place under high-grade metamorphic conditions. D2 comprises deformation associated with sinistral strike slip and granitic dyke extractions. The C₂ shear zones are locally clogged by granitic melt and epidote-chlorite-biotite mineral recrystallizations, showing that the D2 transpressive deformation occurred from ductile to brittle conditions. The basement has thus been affected by a progressive D1-D2 strains induced by the bulk EW sub-horizontal shortening associated with vertical stretching in a transpressive tectonic style (Fig.1). U–Pb zircon and U–Th–Pb EPMA monazite data from the granulites and synkinematic granites indicate that D₁ deformation took place at ca. 2840–2820 Ma, and D₂ between ca. 2760 Ma and ca. 2740 Ma, suggesting a protracted tectonic evolution (Akame et al., 2020a, 2021).

The Sangmelima greenstone belt, like most of the world's Archean greenstone belts, is a deformed zone that comprises iron-rich chemical sediments (BIFs). Soil analyses in areas of high magnetic anomaly show Fe contents of between 30-56% (Fig.2a). The analyzed BIF samples in this greenstone belt are essentially low-grade siliceous BIF with Fe content range from ~ 23 to 56 wt% Fe₂O_{3total}, and low REE content ($\sum\text{REE} = 2.5\text{--}9.3$ ppm). Positive Eu-anomaly (Eu/Eu* = 1.62–3.42) in the Post-Archean Australian Shale (PAAS)-normalized patterns (Fig.2b) and superchondritic Y/Ho value (21.66–35.71) from these BIFs suggest an oceanic hydrothermal source. Towards the south-eastern extension of the belt, the Nkout BIFs are the major deposits of iron ores of the area, with resource estimates of 1.190 million tonnes at 32.9% Fe indicated, and 1.330 million tonnes at 30.3% Fe inferred (De Waele et al., 2015).

Keywords: Archean, deformation mode, BIF, U–Pb zircon and U–Th–Pb EPMA monazite geochronology

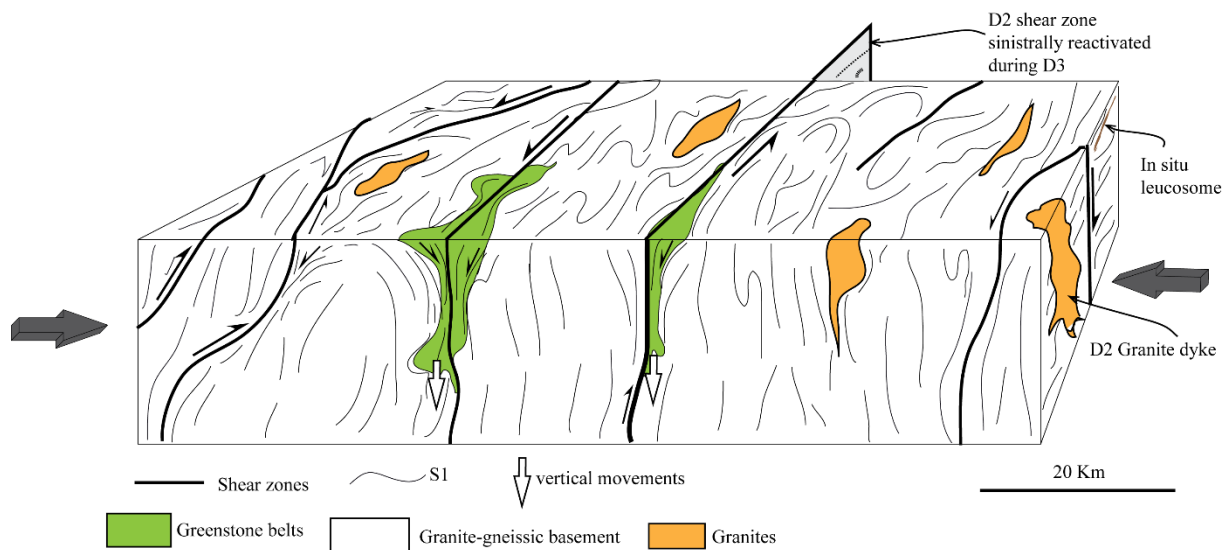


Fig. 1. Schematic 3D block diagram of the general tectonic framework of Archean Ntem Complex (Akame et al. 2020b).

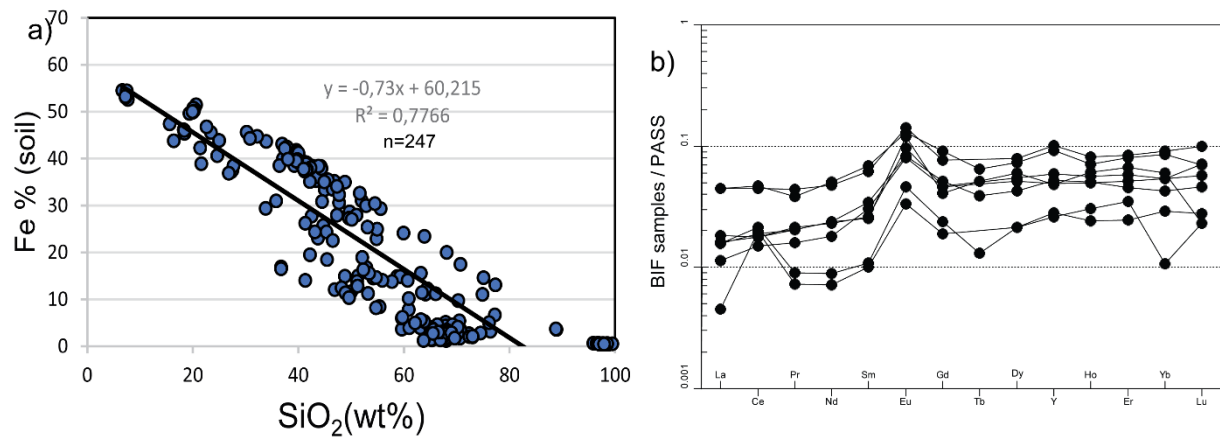


Fig.2. (a) Fe vs. SiO_2 in the soil samples of Sangmelima belt. (b) PAAS normalized fractionation diagrams for REE composition of BIFs in the SGB.

Alkaline magmatism and critical metals in Angola: Field observations and petrography of the Nejoio nepheline syenite complex

Anouk BORST^{1,2,3}, Adrian FINCH³, Grace NIELSON³, Pete SIEGFRIED⁴, Egidio LOPES⁵, Andre EUGENIO⁵, Aurora BAMBI⁵

1. Royal Museum for Central Africa, Geodynamics and Mineral Resources, Leuvensesteenweg 13, Tervuren, Belgium (anouk.borst@africamuseum.be)
2. KU Leuven, Department of Earth and Environmental Sciences, Celestijnenlaan 200E, Heverlee, Belgium (anouk.borst@kuleuven.be)
3. School of Earth and Environmental Sciences, University of St Andrews, North Street, KY16 9AL, Scotland (aaf1@st-andrews.ac.uk)
4. GeoAfrica Prospecting Services, P.O. Box 24218, Windhoek, Namibia
5. Departamento de Geologia, Universidade Agostinho Neto, Avenida 4 de Fevereiro 71, Luanda, Angola

Alkaline igneous rocks and carbonatites form important resources for technology metals such as rare earths elements (REE), Nb, Ta, Li and P. These metals appear on the European list of Critical Raw Materials 2020, due to continued growth in demand and ongoing supply concerns (European Commission, 2020). Angola hosts a series of Cretaceous to Tertiary alkaline igneous rocks and carbonatite complexes that are emplaced along a NW-SE trending structural lineament known as the Moçamedes Arch (Woolley, 2001; Comin-Chiaramonti et al. 2011). Closely associated with the opening of the Atlantic, this ‘failed rift zone’ extends into Brazil (e.g. Ponta Grossa Arch) and lies parallel to a similar rift structure in Namibia (i.e. Damara Belt) where coeval alkaline-carbonatite magmatism led to the formation of deposits with significant Nb, REE, U, Th and fluorite. The Angolan intrusives are generally less well studied although some recent work has focussed on carbonatite and associated enrichments in high field strength elements (HFSE), notably Nb and light REE. The alkaline silicate complexes, however, remain poorly studied but may exhibit favourable enrichments in the more valuable REE (Nd, Pr, Dy).

Here we present field and petrographic observations from the Nejoio (also Nendjoio) syenite complex in southern Angola and consider its economic potential. Nejoio is a small oval-shaped subvolcanic complex measuring 2 by 1.5 km (Rodrigues, 1972; 1978). It is emplaced into a Paleoproterozoic granitic-gneissic basement and dated to be 104 ± 0.8 Ma by Rb-Sr (Allsopp & Hargraves, 1985). It lies approximately 20 km to the SW of the 40 by 17 km Lutala complex which forms a prominent 1.5 km high mountain range (Serra de Neve) along the northern border of the Namibe province. Nejoio and Lutala were both reported to host transitional or agpaitic mineral assemblages (Woolley, 2001 and references therein), i.e. containing complex Na-HFSE silicate phases such as eudialyte, rosenbuschite, wöhlerite and lävenite, indicative of highly evolved peralkaline magmas. The complex comprises an inner and outer zone of intrusives, both made up of medium to coarse grained feldspathoidal syenites and separated by an intrusive breccia (Rodrigues, 1972; 1978). The complex is bound to the east by fenitised gneissic-granitic country rock, in which fenitisation is marked by the introduction of Na-pyroxene, mica and amphibole (Rodrigues, 1972). All syenites contain variable amounts of perthitic alkali feldspar, sodalite, nepheline, cancrinite, fluorite, pyrite, titanite, Na-pyroxene, Na-amphibole and various accessory phases.

The inner zone consists of various medium to coarse grained nepheline-sodalite syenites that display complex mush-mush mingling textures between mafic and felsic peralkaline magmas. Local outcrops of circular igneous layering were observed with stark contrasts in feldspar lamination between melanocratic and leucocratic bands, likely recording turbulent

magma chamber conditions with repeated injections of magma and/or crystal mush. Mingling and mixing textures were seen to intensify towards the outer margin of the inner zone. The outer zone comprises coarse-grained cancrinite-sodalite-nepheline syenites with less Na-mafic phases and thus lighter coloured than most inner zone syenites. Outer zone syenites contain variable amounts of photochromic blue sodalite (hackmanite variety), occasionally forming hexagonal prisms poikilitically enclosed in large perthitic feldspars (1-3 cm), suggesting they may have replaced early nepheline through increasing Cl and/or SO₄ activity. The syenites in the outer zone also exhibit extensive hydrothermal overprinting which replace primary aluminosilicates by hydrous or carbonate-bearing feldspathoids or zeolites, including natrolite, analcime and cancrinite, indicating extensive late-stage fluxing with H₂O and CO₂-rich fluids.

Titanite is the dominant Ti-phase and is particularly abundant in the pyroxene-rich inner zone syenites. They form euhedral lozenges or bladed crystals which can be identified as orange-yellow glassy crystals in hand sample. Zircon was also identified in some samples as large bipyramidal clusters in clay-rich float samples. Outer zone syenites locally contain pockets and crosscutting veins with radial, acicular or long-prismatic crystals of Na-Zr-Ti silicates. EDS analyses suggest these to include rosenbuschite, hiortdahlite and catapleiite. Other Ti, Zr and REE-bearing phases identified include pyrochlore (Ca(Nb,Ti)₂(O,OH₆)OH), pyrophanite (MnTiO₃) and a REE-fluorocarbonate, possibly (burbankite). The presence of these Na-HFSE silicates and REE-fluorocarbonates as late-stage overprinting or crosscutting assemblages suggests that HFSE and REE were mobile at the late-magmatic or hydrothermal stages. Veins of fluorite, pyrite and calcite are also abundant in the outer zone syenite, suggesting the presence of F, S and CO₂-rich hydrothermal fluids in the very final stages of crystallisation.

Our observations confirm that Nejoio is mildly peralkaline, dominantly containing miaskitic Zr-Ti assemblages (i.e. zircon and titanite). Transitional-agpaitic HFSE and REE-bearing minerals such as rosenbuschite and catapleiite as well as pyrochlore and fluorocarbonates crosscut and overprint the earlier miaskitic paragenesis in the outer zone syenites, suggesting that the outer zone syenites are more peralkaline and chemically evolved than the inner zone syenites. Whole rock data and mineral chemical analyses will further constrain the emplacement history and petrogenetic evolution of the Nejoio complex. A better understanding of Nejoio's geochemical evolution will allow us to draw comparisons with coeval mineralised complexes in Brazil and Namibia, and to understand better the mineral potential of Angolan alkaline complexes by placing them within the broader geodynamic context of the Parana-Angola-Etendeka magmatic province.

References:

- European Commission, 2020, EUs list of Critical Raw Materials, Final report
- Woolley, A. 2001. Alkaline rocks and carbonatites of the world. Part 3: Africa, GeolSoc, NHM London, 1-372
- Comin-Chiaramonti, P., De Min, A., Girardi, V. A. V. & Ruberti, E., 2011. Post-Paleozoic magmatism in Angola and Namibia: A review. *Volcanism and Evolution of the African Lithosphere*, 223-247
- Rodrigues, B. 1972 *Revista da Faculdade de Ciências. Universidade de Lisboa*, 17. 89-108
- Rodrigues, B. 1978. *Bol Museo e Lab Min e Geol, Faculdade de Ciências, Universidade de Lisboa*, 15 : 1-174
- Allsopp, H. & Hargraves, R. 1985. Rb-Sr ages and paleomag data for some Angolan alkaline intrusives. *Trans Geol Soc South Africa* 88, 295-299

Carbonatitic affinity of the rare earth element (REE) mineralization at Gakara (Burundi)

Florian BUYSE^{1,2}, Stijn DEWAELE³, Sophie DECREÉE⁴, Florias MEES⁵

1. Pore-Scale Processes in Geomaterials Research group (PProGResS), Department of Geology, Ghent University, Krijgslaan 281/S8, B-9000 Ghent, Belgium (florian.buyse@UGent.be)
2. Centre for X-ray Tomography (UGCT), Ghent University, Proeftuinstraat 86, B-9000 Ghent, Belgium
3. Laboratory for Mineralogy and Petrology, Department of Geology, Ghent University, Krijgslaan 281/S8, B-9000 Ghent, Belgium. (stijndg.dewaele@UGent.be)
4. Royal Belgian Institute of Natural Sciences, Rue Vautier 29, 1000 Brussels, Belgium. (sophie.decree@naturalsciences.be)
5. Royal Museum for Central Africa, Department of Geology, Leuvensesteenweg 13, 3080 Tervuren, Belgium. (florias.mees@africamuseum.be)

The rare earth element (REE) mineralization of Gakara (Burundi) was discovered in 1936 and has periodically been the subject of geological studies because of economic REE concentrations (Thoreau et al., 1958; Aderca & Van Tassel, 1971; Lehmann et al., 1994). The Neoproterozoic Gakara REE mineralization is situated in the Western Domain of the Mesoproterozoic Karagwe-Ankole belt (Tack et al., 2010) and is spatio-temporally associated with alkaline and carbonatitic magmatism along the Western Rift Valley of the East African Rift (Woolley, 2001). Despite the economic importance of this deposit, recent geological studies are largely lacking (Ntiharirizwa et al., 2018).

Using a series of mineralogical and geochemical techniques (e.g. optical microscopy, SEM-EDS, Raman spectroscopy and LA-ICP-MS), we investigated one of the present-day richest REE deposits in the world (Buyse et al., 2020). This work contributes to our further understanding of the formation history of the Gakara REE mineralization and its association with the Neoproterozoic alignment of alkaline complexes and carbonatites along the present-day Western Rift.

The mineral paragenesis of the Gakara deposit can be subdivided into 3 stages: primary ore deposition, brecciation and supergene alteration. Mineralogical and chemical evidence (e.g. comb-textured quartz, low thorium content of monazite) confirms the deposition from hydrothermal solutions in open fissures. However, evidence of fenitization processes (brecciation stage, pinkish-red cathodoluminescence of K-feldspar) and the strong enrichment of light REEs in both bastnäsite-(Ce) and monazite-(Ce) also point to a strong affinity with a carbonatitic source. Following the mineralogical-genetic classification of Mitchell (2005), the REE mineralization at Gakara qualifies as carbothermal residua derived from an unidentified potassic-suite carbonatite at depth.

Recent structural and lithological re-interpretation of geophysical data (Titley, 2020) suggests the presence of at least three large carbonatitic bodies at depth, but a direct petrogenetic relation with these carbonatitic intrusions still need some further investigations.

References

- Aderca, B.-M. & Van Tassel, R., 1971. Le gisement de terres rares de la Karonge (République du Burundi). In: Académie Royale des Sciences d'Outre-Mer, Classe des Sciences Naturelles et Médicales Mémoires, pp. 210 p.
- Buyse, F., Dewaele, S., Decrée, S. & Mees, F., 2020. Mineralogical and geochemical study of the rare earth element mineralization at Gakara (Burundi). *Ore Geology Reviews*, 124, 103659.
- Lehmann, B., Nakai, S., Höhndorf, A., Brinckmann, J., Dulski, P., Hein, U.F. & Masuda, A., 1994. REE mineralization at Gakara, Burundi: evidence for anomalous upper mantle in the western Rift Valley. *Geochim. Cosmochim. Acta* 58, 985–992.
- Mitchell, R.H., 2005. Carbonatites and carbonatites and carbonatites. *Can. Mineral.* 43, 2049–2068.
- Ntiharirizwa, S., Boulvais, P., Poujol, M., Branquet, Y., Morelli, C., Ntungwanayo, J. & Midende, G., 2018. Geology and U-Th-Pb dating of the Gakara REE deposit, Burundi. *Minerals* 8 (9), 22 n° 394.
- Tack, L., Wingate, M.T.D., De Waele, B., Meert, J., Belousova, E., Griffin, B., Tahon, A. & Fernandez-Alonso, M., 2010. The 1375 Ma “Kibaran event” in Central Africa: prominent emplacement of bimodal magmatism under extensional regime. *Precamb. Res.* 180, 63–84.
- Thoreau, J., Aderca, B.M. & Van Wambeke, L., 1958. Le gisement de terres rares de la Karonge (Urundi). *Bulletin des Séances de l'Académie Royale des Sciences d'Outre-Mer* 4, 684–715.
- Titley, M., 2020. Technical report on the Gakara REE project, Burundi. Maja Mining Limited, 120 p.
- Woolley, A.R., 2001. *Alkaline Rocks and Carbonatites of the World, Part 3: Africa*. The Geological Society, London 372 p.

Distribution of trace elements in the secondary minerals of Zn-Pb deposits: new results from Belgium and Moroccan willemite deposits

Flavien CHOLET¹, Johan YANS², Augustin DEKONINCK²

1. Chrono-Environnement UMR 6249, CNRS-Université de Bourgogne Franche-Comté, Besançon, France (flavien.choulet@univ-fcomte.fr)

2. Département de Géologie, Institute of Life, Earth and Environment, Université de Namur, Namur, Belgium (johan.yans@unamur.be, augustin.dekoninck@unamur.be)

New observations and chemical-mineralogical analyses of willemite (Zn_2SiO_4) mineralization from non-sulfide Zn-Pb deposits of La Calamine (Eastern Belgium) and Bou Arhous (Moroccan High Atlas) have been carried out. This study aims at evaluating the critical element distribution and migration, in order to establish the potential of such deposits. In both cases, willemite occurs as a variety of types that continuously formed between the protore stage (sulfides) and the late supergene stage (carbonates and hydrated phases).

Based on microscopic observations, different types of willemite may be distinguished by their shapes and zoning characteristics, supporting 1) a polyphase non-sulfide mineralisation, after the protore stage, 2) local dissolution–reprecipitation processes of willemite and 3) coprecipitation of willemite and secondary Pb minerals such as cerussite and galena. A significant change of major elements composition obtained by EPMA in the different generations of willemite is recorded. LA-ICP-MS measurements of minor and trace elements also reveal a strong variability between the various willemite types.

In the La Calamine samples, we measure abnormal high contents in P, Cd, As, Pb, Ag and Sb, the three latter ones being related to tiny galena inclusions. The Ga and In contents are very low (less than 4 ppm) or below detection limits, respectively. Significant Ge contents up to 250 ppm are observed. In the samples from Bou Arhous, willemite is variably enriched in Ge (up to 1000 ppm). Depending on the willemite generation, this substitution is positively or negatively correlated to the Zn-Pb substitution. According to the nature of zoning (sector *versus* oscillatory), the incorporation of Ge was either controlled by crystallographic factors or by the nature of the mineralizing fluids.

While, in the case of Belgium, the Ge concentrations measured in willemite are very similar to those in sphalerite (averaging 250 ppm), the Moroccan willemite are enriched compare to the primary sulfides (less than 100 ppm). This may indicate that sphalerite played a role of precursor, but an additional input of minor and trace elements by external fluids is also necessary. This conclusion is in agreement with the current models suggesting that a strict supergene origin of willemite in numerous deposits is disputable and a contribution of low temperature hydrothermal fluids for willemite precipitation should be considered.

References

- Choulet F, Richard J, Boiron M-C, Dekoninck A, Yans J. 2019. Distribution of trace elements in willemite from the Belgium non-sulphide deposits. *European Journal of Mineralogy*, 31: 983-997.
- Choulet F, Barbanson L, Buatier M, Richard J, Vennemann T, Ennaciri A, Zouhair M. 2017. Characterization and origin of low-T willemite (Zn_2SiO_4) mineralization: the case of the Bou Arhous deposit (High Atlas, Morocco). *Mineralium Deposita*, 52: 1085-1152.

Le Sous-groupe de la Mpioka, témoins de la réactivation des failles post-Schisto-calcaire dans le fossé de la Basse-Sangha

C.M.E. CIBAMBULA, TUEMA L.O., IYOLO, H.F., MUKEBA C.L., M.N.A.J. MAKUTU.

Université de Kinshasa, Fac. Sciences, Dép. Géosciences, BP.190 Kinshasa XI, R.D.C.

Dans le fossé de la Basse-Sangha, hormis les Diamictites inférieure et supérieure, la sédimentation détritique est représentée par les shales et les grès de Sansikwa et de la Petite Bembezi ainsi que par les conglomérats, les shales et les grès de la Mpioka.

L'interruption de cette sédimentation détritique par les dépôts carbonatés de la Formation des Calcaires noirs de Sekelolo et du Sous-groupe Schisto-calcaire implique les transgressions de ce fossé par les eaux salées du paléo-océan Adamastor en provenance du bassin d'Araçuaï au Brésil (Tack et al., 2001 ; Pedrosa-Soares et al., 2008). Par contre, la réinstauration des dépôts silico-clastiques de faible profondeur à mudcracks, ripple-marks, empreintes de gouttes de pluies, chips argileux du Sous-groupe de la Mpioka traduit l'abandon par la mer du domaine jusque-là submergé. De mouvements de basculement par les failles, de la surélévation orogénique et de gauchissements divers, facteurs provoquant généralement le retrait de la mer, lequel a supprimé cette accommodation marine dans le bassin en pull-apart de la Basse-Sangha.

L'analyse tectonique atteste que l'occurrence du conglomérat de Bangu-Niari situé à la base du Sous-groupe de la Mpioka résulte de l'érosion des hauts-plateaux étagés calcaires (Nicolai, 1954 ; Cibambula et al., 2013). Ceux-ci sont issus de la réactivation des failles du socle ayant affecté les calcaires sous-jacents antérieurement à la poussée orogénique Pan-africaine. Cette dernière serait responsable de l'inversion tectonique des failles normales en failles inverses de direction N153° et des uplifts de plus en plus surbaissés vers l'est (Cibambula, 2016). Les mouvements de basculement par les failles seraient donc la principale cause du retrait total de la mer et de l'affaissement du compartiment inondé ultérieurement par le lac du Sous-groupe de la Mpioka. Dans ce lac, l'espace disponible ne dépassait guère le rejet des failles bordières. Cette faible accommodation limite ainsi les roches de la Mpioka au seul plateau de Bangu, compartiment affaissé à la fois des failles normales et des failles inverses respectivement orientées N25°/53°ONO et N72°/8°SSE.

Références :

- Cibambula, C.M.E. (2016) : Le Sous-groupe de la Mpioka : un flysch de la chaîne panafricaine West Congo dans la province du Kongo Central (R.D. Congo), *Th. Doc. Inédit, Dép. Géosc., Univ. Kinshasa, 185p.*
- Cibambula, C.M.E., Makutu, M.J.A., Kanika, M. T., Mvuemba, N. F., Nzau, M.C., Mabedi, T.H., Mayombo, B.E. et Mutamba, N.R. (2013) : Dépôt de la Formation du conglomérat de Bangu-Niari et analyse morpho-géométrique des fractures dans l'avant-pays de la chaîne panafricaine West Congo : cas du secteur de Kimpese, *Rev. Cong. Sci. Nucl. Vol. N°27, (2013), 90-110.*
- Nicolai, J. (1954) : Observations sur les séries sédimentaires du Niari (Moyen-Congo) A.E.F), *Congr. Géol. Int. XIX^e Sess. Alger (1952), Fasc. XX, Ass. Serv. Géol. Afr., I, 163-173.*
- Pedrosa-Soares, A.C., Alkimim, F.F., Tack, L., Noce, C.M., Babinski, M., Silva, L.C. and Martin-Neto, M.A. (2008) : Similarities and differences between the brazilian and African counterparts of the Neoproterozoic Araçuaï-West Congo orogen. *Geological Society of London, Special Publ., v. 294, 153-172, doi : 10.1144/SP294.9.*
- Tack, L., Wingate, M.T.D., Liégeois, J.P., Fernandez-Alonso, M., Deblond, A. (2001) : Early Neoproterozoic magmatism (1000-910 Ma) of the Zadinian and Mayumbian Groups (Bas-Congo) : onset of Rodinia rifting at the western edge of the Congo craton, *Prec. Res., 110, 277-306.*

Characterisation and Proterozoic evolution of the granitoids of the Karagwe-Ankole belt (KAB) in Rwanda

Shana DE CLERCQ¹, Stijn DEWAELE¹, Johan DE GRAVE¹, Frank VANHAECKE², Thierry DE PUTTER³

1. Department of Geology, Universiteit Gent, Gent, Belgium

2. Department of Analytical chemistry, Universiteit Gent, Gent, Belgium

3. Department of Earth Sciences, Royal Museum of Central Africa, Tervuren, Belgium

The Karagwe-Ankole belt (KAB) is a poorly understood deformation belt in the Great Lakes area of Central Africa, with several hypotheses put forward considering the emplacement of the various generations of granites (Tack et al., 2010; Fernandez-Alonso et al., 2012; Koegelenberg & Kisters, 2014; Debruyne et al., 2015). The youngest generation of granites (G4; 1000 Ma) are spatially associated with Sn-W-Ta ore deposits, and are considered as the parental granites. The paragenesis of these mineral resources have been extensively scrutinised (Dewaele et al., 2016; Hulsbosch et al., 2016), but the geodynamic context and characterisation of these parental granites has been neglected. Tectonic models for the formation of this plutonic suite range from an intra-cratonic to a full-scale continent–continent collision setting (Tack et al., 2010; Debruyne et al., 2015).

Zircon U-Pb dating of several granites in the Gitarama region identified two main populations of U-Pb zircon ages in the G4 granites at 1370–1420 Ma and 950–1020 Ma (De Clercq et al., 2021). The older population is attributed to inheritance of the bimodal magmatic Kibaran event, while the younger population is ascribed to the new crystallisation. Geochemical analysis, as well as the presence of different xenocrystic zircons, implies that the younger G4 granites are derived from the recycling of older crustal rocks with a localised, heterogenous source region obtained in intra-continental setting (De Clercq et al., 2021). The Th/U ratios of the zircons of the parental granites are lower than 0.1, which would suggest a metamorphic origin for these zircons. Together with the low luminescence signal of these zircons an anatectic origin of the melt is however more plausible, implying that the parental granites could be considered more like “migmatites” formed by a low degree of partial melting, rather than by fractionation out of large magma chambers (De Clercq et al., 2021).

More regions in Rwanda will be analysed using the same methods, such as Kibuye and Akanyaru as well as more to the east, to cover the whole of Rwanda. In addition, apatite U-Pb dating will be applied to determine more recent metamorphic events in the region, to further contribute to the Proterozoic evolution of the KAB.

References

Debruyne, D., Hulsbosch, N., Van Wilderode, J., Balcaen, L., Vanhaecke, F., & Muchez, P. 2015. Regional geodynamic context for the Mesoproterozoic Kibara Belt (KIB) and the Karagwe-Ankole Belt: Evidence from geochemistry and isotopes in the KIB. *Precambrian Res.* 264, 82–97.

- De Clercq, S., Chew, D., O'Sullivan, G., De Putter, T., De Grave, J. & Dewaele, S., 2021, Characterisation and geodynamic setting of the 1 Ga granitoids of the Karagwe-Ankole belt (KAB), Rwanda. *Precambrian Res.*, 356.
- Dewaele, S., De Clercq, F., Hulsbosch, N., Piessens, K., Boyce, A., Burgess, R., Muchez, P., 2016. Genesis of the vein-type tungsten mineralisation at Nyakabingo (Rwanda) in the Karagwe-Ankole belt, Central Africa. *Mineral. Depos.* 51 (2), 283–307.
- Fernandez-Alonso, M., Cutten, H., De Waele, B., Tack, L., Tahon, A., Baudet, D., Barritt, S.D. 2012. The Mesoproterozoic Karagwe-Ankole Belt (formerly the NE Kibara Belt): The result of prolonged extensional intracratonic basin development punctuated by two short-lived far-field compressional events. *Precambrian Res.*, 216–219, 63–86.
- Hulsbosch, N., Boiron, M. C., Dewaele, S., & Muchez, P. (2016). Fluid fractionation of tungsten during granite-pegmatite differentiation and the metal source of peribatholithic W quartz veins: Evidence from the Karagwe-Ankole Belt (Rwanda). *Geochimica et Cosmochimica Acta*, 175, 299–318.
- Koegelenberg, C., & Kisters, A. F. M. (2014). Tectonic wedging, back-thrusting and basin development in the frontal parts of the Mesoproterozoic Karagwe-Ankole belt in NW Tanzania. *J. Afr. Earth Sci.*, 97, 87–98.
- Tack, L., Wingate, M.T.D., Waele, B.D., Meert, J., Belousova, E., Griffin, B., Tahon, A., Fernandez-alonso, M., 2010. The 1375 Ma “Kibaran event” in Central Africa: Prominent emplacement of bimodal magmatism under extensional regime. *Precambrian Res.* 180 (1–2), 63–84.

Exhumation of the South Atlantic passive margin of the Democratic Republic of Congo during pre- and post- Gondwana breakup: evidence from new low-temperature thermochronology, geology and geomorphology

Johan DE GRAVE¹, Gerben VAN RANST¹, Ana Carolina FONSECA¹, Luc TACK², Damien DELVAUX², Daniel BAUDET², Nicole Yaya KITAMBALA³, Aimée Love PAY³

¹ Laboratory for Mineralogy and Petrology, Department of Geology, Ghent University, Krijgslaan 281 S8, 9000, Ghent, Belgium; joan.degrave@ugent.be

² Department of Earth Sciences, Royal Museum for Central Africa, Leuvensesteenweg 13, Tervuren, Belgium

³ Centre de Recherches Géologiques et Minières, Av. de la Démocratie, Kinshasa-Gombe, Democratic Republic of the Congo

The lowermost course of the Congo River cuts through the Central African Atlantic Swell (CAAS) that encompasses the South Atlantic passive margin of the Democratic Republic of Congo (Central Africa; Figure 1). The region is underlain by litho-structural units of the Pan-African West Congo Belt, which consists of different tectono-metamorphic domains (Figure 1). The Precambrian basement is covered to the west by marine deposits of the South Atlantic Ocean and to the east by continental deposits of the Congo Basin.

In this study we aim to constrain the timing of uplift and exhumation of the CAAS by using apatite fission track (AFT) thermochronology in combination with an update of the geology and geomorphology of the region. AFT ages vary widely between 108 and 312 Ma. Short track lengths (11–12 μm) and broad, complex track length distributions however indicate mixed ages between multiple thermal events. We derive the timing of exhumation from inverse thermal history models, that show that the region experienced a first exhumation event before Gondwana breakup during the Carboniferous to Middle Jurassic. This event is probably related to compressive forces at the boundaries of Gondwana. Both rifting and subsequent opening of the South Atlantic Ocean do not seem to have had a pronounced effect on the CAAS. During the Late Cretaceous to Paleogene, a slight reheating of the basement rocks is suggested and could be due to subsidence and consequential modest reburial. A second phase of exhumation initiated around the Paleogene–Neogene and eventually emplaced the sampled rocks at surface temperatures.

The multi-phased differential denudation results from reactivation of the fault-bounded tectono-metamorphic blocks of the Precambrian basement, controlled by the combination of two systems of faults related to the Pan-African orogeny and the Cretaceous South Atlantic Ocean opening (Figure 1). Differential denudation of the region is also well-marked by independent indicators of the present-day geomorphology including distinct knick-points and steep valleys along the course of the lower Congo River, reworking of planation surfaces and associated laterite crust and contrasting karst morphology.

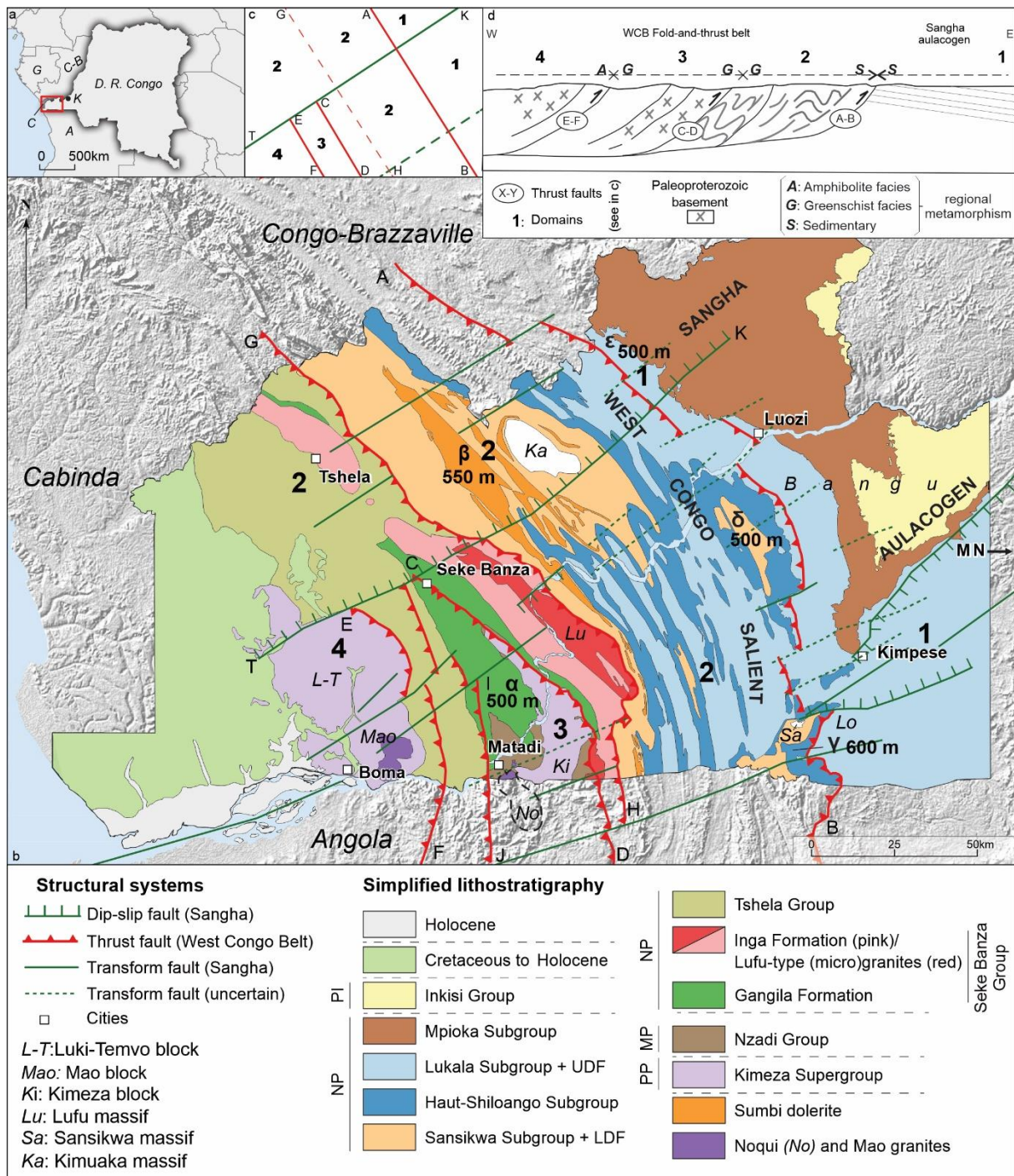


Figure 1: General setting, geology and tectonic framework of the Lower Congo study area.

Petrographical, mineralogical and geochemical study of the gold mineralization at Imonga-Saramabila, Maniema, DR Congo

Julie DE GROOTE¹, Stijn DEWAELE¹

*1. Ghent University, Department of Geology, Krijgslaan 281, S8, 9000 Ghent, Belgium
(Julie.degroote@UGent.be)*

The Karagwe-Ankole belt (KAB) in the Great Lakes area of Central Africa hosts a large metallogenic province that contains different types of mineralization. Many of these metals (e.g. Nb-Ta-W-REE-Li-Au) have been defined as critical metals that are of vital importance for a high-tech and green industry. Recent research has obtained new and valuable insight in the formation processes of Nb-Ta, Sn and W mineralization (e.g. Dewaele et al., 2016; Hulsbosch et al., 2016), but detailed knowledge on the formation processes of the Au mineralization in the Great Lakes area is largely missing (Wouters et al., 2020). Gold can be formed in a wide variety of geological settings and occurs both as magmatic-hydrothermal and hydrothermal deposits, that can be remobilized by circulating fluids and/or concentrated by hydraulic processes in sedimentary placer deposits. In this study, we focus on the Au mineralization in the Imonga-Saramabila area (Figure 1), which has been a historical centre of mineral exploitation in the Maniema province (DR Congo) between 1936 and 1958 by Cobelmin (Kazmitcheff, 1961). The deposit is well documented in the mining archives and rock collections of the Royal Museum for Central Africa (RMCA, Tervuren). This study has been performed on samples from two well-located boreholes (S1 and S3; Kazmitcheff (1961)).

The Imonga-Saramabila area consists (Figure 1) of Mesoproterozoic metasedimentary and metavolcanic rocks, belonging to the Kivu Supergroup (Fernandez-Alonso et al., 2015). The Kasese batholith and some smaller granitoid stocks are located in the immediate vicinity. The rocks in the boreholes of Imonga are predominantly mafic magmatic rocks and low-grade metamorphosed metasedimentary rocks. XRF analyses allowed to make a clear distinction between the different lithologies based on the major element content. The geological structure of the intersected rocks is apparently complex, as evidenced by the large variations of bedding angle compared to the borehole axis, the brecciated and finely folded zones and the discordant contacts that were observed. Interstratified quartz-carbonate lenses and veins are oriented N 10° E with a slope of 65°E (Kazmitcheff, 1961), which is largely parallel to the foliation. The rocks have been affected by intense metamorphism and alteration and are crosscut by different generations of fractures and fine (mm-to cm-sized) veins with as main minerals quartz, carbonate, chlorite and to a lesser extent pyrite and chalcopyrite. The alteration associated with the veins dominantly consists of chloritization, sericitization and carbonatization. Sulphides, mainly pyrite and chalcopyrite, are present in the matrix of the rocks and in the different vein generations. Gold has been identified as mineral inclusions in pyrite. The XRF analyses allowed to make a correlation between the occurrence of quartz veins and the concentration of arsenic in the investigated borehole samples. Arsenic was used as a tracer element to identify the mineralized zones as the concentration of gold was not sufficiently high to reach the detection limit of the used XRF.

The gold mineralization of Imonga-Saramabila can be classified as a typical mesothermal orogenic gold mineralization, which confirms other studies on Au-

mineralization in the KAB (e.g. Wouters et al., 2020). Based on geological observations, the Imonga-Saramabila mineralization is interpreted to be linked to the early Neoproterozoic (~980 Ma) compressional deformation event that occurred during regional convergent continent-continent collision associated with the amalgamation of the Rodinia supercontinent. Nevertheless, the exact relationship between the gold mineralization and the different magmatic, metamorphic and deformational events in Maniema and the KAB still needs more study.

References

- Dewaele, S., De Clercq, F., Hulsbosch, N., Piessens, K., Boyce, A., Burgess, R. & Muchez, P., 2016. Genesis of the vein-type tungsten mineralization at Nyakabingo (Rwanda) in the Karagwe–Ankole belt, Central Africa. *Mineralium Deposita* 51, 283-307.
- Fernandez-Alonso, M., Kampata, D., Mupande, J.F., Dewaele, S., Laghmouch, M., Baudet, D., Lahogue, P., Badosa, T., Kalenga, H., Onya, F., Mawaya, P., Mwanza, B., Mashagiro, H., Kanda-Nkula, V., Luamba, M., Mpoyi, J., Decrée, S., Lambert, A. 2015 (Ed.). *Carte Géologique de la République Démocratique du Congo au 1/2.500.000: Notice explicative*. République Démocratique du Congo, Ministère des Mines.
- Hulsbosch, N., Boiron, M.-C., Dewaele, S., Muchez, P., 2016. Fluid fractionation of tungsten during granite-pegmatite differentiation and the metal source of peribatholithic W quartz veins: Evidence from the Karagwe-Ankole Belt (Rwanda). *Geochimica et Cosmochimica Acta* 175, 299-318.
- Kazmitcheff, A., 1961. Les roches albitiques et carbonateées des sondages d’Imonga (Maniema). *Mémoires de l’Institut Géologique de l’Université de Louvain*. Tome 22, 69-96.
- Wouters, S., Hulsbosch, N., Kaskes, P., Claeys, P., Dewaele, S., Melcher, F., Onuk, P., Muchez, P., 2020. Late orogenic gold mineralization in the western domain of the Karagwe-Ankole Belt (Central Africa): Auriferous quartz veins from the Byumba deposit (Rwanda). *Ore Geology Reviews*, 125, 103666.

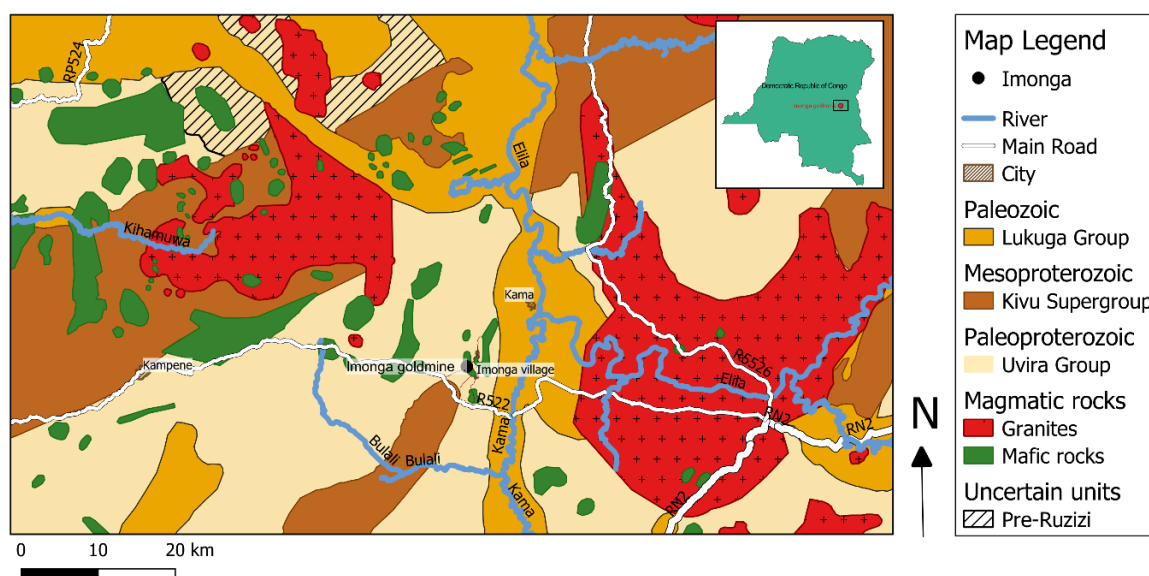


Figure 1: Geological map of the Imonga area, Maniema, DR Congo

Western climate-oriented ethics and artisanal mining of cobalt in DRC: a 21stC. revival of “Potemkine villages”?

Thierry DE PUTTER ¹, Cristiana PANELLA ²

1. Royal Museum for Central Africa, Geodynamics and Mineral Resources, Tervuren, Belgium (thierry.de.putter@africamuseum.be)
2. Royal Museum for Central Africa, Culture and Society, Tervuren, Belgium (cristiana.panella@africamuseum.be)

The story tells that Prince Grigori Potemkine, courtesan and minister of the Empress Catherine II of Russia, placed either fake houses or painted canvas panels showing cozy villages along the roads when the sovereign travelled across her Empire, in order to protect her eyes from the unpleasant view of poverty and starvation of peasants. Even though these “Potemkine Villages” are now seen as a legend forged in the 18thC., they offer a useful metaphor for the wide range of screens that prevent climate-sensitive foreigners from the unpleasant contact with social inequalities and the reality of artisanal mining of strategic minerals in Africa.

The geology of Central Africa has led to major concentrations of economic elements in very shallow, and hence accessible, geological layers. Copper has been exploited in the Katanga Copperbelt (D.R. Congo) since more than a century while cobalt has been mined later on, from the onset of WWII. Today, as a major component of lithium-ion batteries, cobalt is regarded as an important “strategic element” for Western economies (De Putter, 2019).

The artisanal and small-scale mining (ASM) of cobalt provides some 20% of DRC’s total production, which in turn accounts for 60% of world production (De Putter, 2019). In the field, 50,000 to 200,000 artisanal diggers derive a modest income (30-50 US\$/month) from the dangerous extraction of metal in narrow shafts and galleries, cut in friable weathered terranes. Studies further reveal that diggers are exposed to substantial copper, cobalt and associated trace elements, among which uranium. As these workers embody impolitic values linked to loneliness, deprivation, physical endurance and a constant bodily perception of risk, they are virtually invisible in the informal economy of cobalt. This observation is valid for several resources other than cobalt, and more generally for ASM as a whole (Jacka, 2018).

The international approach (as for instance the OECD “responsible supply chain of minerals”) provides useful “Potemkine villages” to keep these impolitic actors in a remote sphere, cut from the Western obsession for ecological cleanliness and zero greenhouse gases (GHG) emissions. Climate deontology and norms rest on an intricate bundle of fundamental inequality in trade, illegal practices, dangerous mining, forced and child labor, violence, sex abuses and drug consumption, which are commonly described in disembodied notions as social practices, trade chains, traceability and certification, etc. These concepts are fundamentally ambivalent as they altogether respond to the accepted rhetoric on ASM and simultaneously result in a total lack of empathy with the diggers, in a move to promote “planned blindness” among end-users of high-tech e-powered gadgets throughout the world.

Geology and anthropology here join to knock down some of these “Potemkine villages” and put unpleasant evidences in crude light: mineral deposits in Katanga are hosted in friable and rocky substrates which are prone to collapse and landslides; cobalt extraction in ASM takes place in deeply polluted soils and is associated with health damages. Mining intimately impacts the body, sexuality and fertility of workers (Banza *et al.*, 2009; Musa Obadia *et al.*, 2020). Uranium is the likely cause of oxidative DNA damage, especially in children, which threatens future generations and substantiate the allegation of a non-sustainable exploitation of cobalt in the ASM (Banza *et al.*, 2018). These data are widely published in scientific journals but the daily life of cobalt diggers remains largely out of the deontological landscape of the capitalist ecologic policy, as it is simply unthinkable in its body of norms.

The Western *mea culpa* on the so-called Anthropocene and global warming due to the increase of anthropic GHG emissions swiftly connects to the trendy ecologism of electric vehicles to actually underlie a deep “anthropocenic” social inequality (Chakrabarty, 2017; Panella & Little, 2021), contributing to severe pauperization and pollution in Africa. Today, as in the 18thC., poverty is regarded as an offense, described in the international scene as “illegal” and hidden from the glimpse of consumers. This complex research topic is rarely considered in geology, which tends to confine itself to the “objective” description of natural systems and mineral deposits. However, the scramble for strategic minerals and clean tech is more than just an issue of deposits and ore, and sustainability has to be more than just a preserve for rich countries. Initially a stratigraphic subdivision, the Anthropocene actually encompasses urgent economic and social issues, relevant for mankind at large. In this context, geology has to look at the world as it actually works, and bridge the gap with human and social sciences.

References

- Banza Lubaba Nkulu, C., Casas, L., Haufroid, V., De Putter, Th., Saenen, N., Kayembe Kitenge, T., Musa Obadia, P., Kyanika wa Mukoma, D., Lunda Ilunga, J.-M., Nawrot, T.S., Luboya Numbi, O., Smolders, E., Nemery, B., 2018. Sustainability of artisanal mining of cobalt in DR Congo. *Nature Sustainability*, 1, September 2018, 495-504. DOI: 10.1038/s41893-018-0139-4.
- Banza Lubaba Nkulu, C., Nawrot, T.S., Haufroid, V., Decrée, S., De Putter, Th., Smolders, E., Kabyla Ilunga, B., Luboya Numbi, O., Ilunga Ndala, A., Mutombo Mwanza, A., Nemery, B., 2009. High human exposure to cobalt and other metals in Katanga, a mining area of the Democratic Republic of Congo. *Environmental Research*, 109, 745–752.
- Chakrabarty, D., 2017. The politics of climate change is more than the politics of capitalism. *Theory, Culture & Society* 34, 25–37.
- De Putter, Th., 2019. “Cobalt means conflict” – Congolese cobalt, a critical element in lithium-ion batteries. *Bulletins des Séances de l’Académie Royale des Sciences d’Outre-Mer*, 65, 97–110.
- Jacka, J.K., 2018. The Anthropology of Mining: the social and environmental impacts of resource extraction in the Mineral Age. *Annual Review of Anthropology* 47, 61–77.
- Musa Obadia, P., Kayembe-Kitenge, T., Banza Lubaba Nkulu, C., Enzlin, P., Nemery, B., 2020. Erectile Dysfunction and Mining-Related Jobs. An Explorative Study in Lubumbashi, Democratic Republic of Congo. *Occupational and Environmental Medicine*, 77, 19–21.
- Panella, C., Little, W.E., 2021. Introduction. Risk and Hope: Daily Life Subversions of the Norm. In Panella & Little (eds), *Norms and Illegality. Intimate Ethnographies and Politics*. Lexington Books, 1–17.

From Precambrian to Cenozoic: the manganese odyssey of Morocco

Augustin DEKONINCK*¹, Gilles RUFFET², Jocelyn BARBARAND³, Yves MISSENARD³, Ludovic LAFFORGUE³, Michèle VERHAERT¹, Nadine MATTIELLI⁴, Cécile GAUTHERON³, Mohamed MAGOUA⁵, Abdellah MOUTTAQI⁵, Mohammed BOUABDELLAH⁶, Julien POOT¹, Johan YANS¹

1. Université de Namur, ILEE, Département de géologie, Belgium

(augustin.dekoninck@unamur.be) (johan.yans@unamur.be) (michele.verhaert@hotmail.com)

(julien.poot@unamur.be)

2. CNRS (CNRS/INSU) et Université de Rennes 1, Géosciences (UMR6118), France

(gruffet@univ-rennes1.fr)

3. Université Paris-Sud, GEOPS, France (jocelyn.barbarand@universite-paris-saclay.fr)

(yves.missenard@universite-paris-saclay.fr) (ludovic.lafforgue.c@gmail.com)

(cecile.gautheron@universite-paris-saclay.fr)

4. Université Libre de Bruxelles, Department of Earth and Environmental Sciences, Belgium

(nmattiel@ulb.ac.be)

5. Office National des Mines et des Hydrocarbures – Morocco (MAGOUA@onhym.com)

(mouttaqi@onhym.com)

6. Université Mohammed I^{er} Oujda, Morocco (mbouabdellah2002@yahoo.fr)

Morocco is a relevant place to study Mn deposits considering its multistage geodynamic story. In the last decades, several new studies significantly improved our understanding of various genetic types. Three main districts have been mined since the beginning of the 20th century: (i) Ouarzazate (Anti-Atlas), (ii) Bou Arfa (eastern High Atlas) and (iii) Imini-Tasdremt (High Atlas). The first and third are currently mined, accounting for the production of 80,000 tons Mn in 2018 (data from the Ministry of Energy, Mines and Sustainable Development of Morocco). The deposition of Mn spans over four main periods: Neoproterozoic, Jurassic, Upper Cretaceous and Cenozoic.

(i) The Ouarzazate deposits are vein-type and stratiform Mn-Fe orebodies (42-48% Mn) closely associated to Neoproterozoic felsic volcanic and terrigenous series (Choubert and Faure-Muret, 1973). It is the largest Mn field in Morocco (>90x60 km). Stratiform orebodies clearly improve the mining potential. The Mn-bearing assemblage includes braunite, cryptomelane, hollandite, hausmannite and pyrolusite in a hematite, goethite, barite, quartz, dolomite and calcite gangue. The formation model implies a polycyclic epithermal and epigenetic Mn accumulation during and at the final stage of the Neoproterozoic volcanic activity at ~580 Ma. Extensional tectonics of the Neoproterozoic Ouarzazate basin would be of primary order in delimiting the number and regional extension of lodes.

(ii) The Bou Arfa Mn deposit is hosted in Sinemurian dolostones, as stratabound, run-type and lenses of Mn orebodies crisscrossed by late veins hosting the high-grade pyrolusite ore (33-82% Mn). Ore formation follows a sedimentary-diagenetic model driven by three dolomitization episodes after the Sinemurian sedimentation, and an epigenetic stage similar to other MVT of the Atlas range (Lafforgue et al., 2021). The concentration of Mn in a narrow area of about 10 km² is due to the geometry of the Bou Arfa basin and its position above basement paleohighs acting as a threshold for marine inputs during transgression/regression intervals. The primary manganite-hausmannite ore was transformed into pyrolusite during burial of the Mn-rich sediments.

(iii) The Imini-Tasdremt district is the most economically important of Morocco providing the highest Mn grade (74-92% Mn) due to two stratabound pyrolusite-bearing orebodies hosted in the ~10-20 m thick Cenomanian-Turonian dolostone. A metallurgical third ore (40-48% Mn) occurs in relics of a paleosurface in the uppermost dolostone and is composed by coronadite group minerals (Dekoninck et al, 2016). Although the pyrolusite ore is restricted to the 25-30 km Imini Mn belt, the metallurgical ore has a larger extension of ~100 km and may extend across the Atlas belt (Dekoninck et al., 2020). New dating of K-Mn oxides (^{40}Ar - ^{39}Ar) and goethite (U-Th)/He dating suggest that this geometric distribution is materialized by different formation age: the upper coronadite level is late Cretaceous, whereas the pyrolusite ores are Cenozoic, indicating the importance of local processes. Goethite ages cover a period of ~40 Ma since the Turonian, involving long mineralization processes. The Atlas geodynamics played a significant role in the metallogenesis of these karst-hosted accumulations since late Cretaceous times.

References:

- Choubert, G. & Faure-Muret, A. The Precambrian iron and manganese deposits of the Anti-Atlas. in *Genesis of Precambrian iron and manganese deposits* vol. 9 115–124 (1973).
- Lafforgue, L. *et al.* Geological and geochemical constrains on the genesis of the sedimentary-hosted Bou Arfa Mn(-Fe) deposit (Eastern High Atlas, Morocco). *Ore Geology Reviews* 104094 (2021)
- Dekoninck, A. *et al.* The high-grade Imini manganese district—karst-hosted deposits of Mn oxides and oxyhydroxides. in *Mineral Deposits of North Africa* 575–594 (Springer International Publishing, 2016).
- Dekoninck, A. *et al.* Multistage genesis of the late Cretaceous manganese karst-hosted Tasdremt deposit (High Atlas, Morocco). *Mineralium Deposita* (2020)

Experiments on silicate-carbonate liquid immiscibility in a Fe-P rich system, a premise for phoscorites formation in carbonatite complexes

Merry DEMAUDE¹, Bernard CHARLIER²

1. *Petrology, Geochemistry, and Petrophysics Laboratory, Liège, Belgium*
(merry.demaude@uliege.be)
2. *Petrology, Geochemistry, and Petrophysics Laboratory, Liège, Belgium*
(b.charlier@uliege.be)

Carbonatites are magmatic rocks distributed worldwide and constitute (with their weathering products) the world first source for niobium and light rare earth elements. They may also contain economic grades of phosphate (Chakhmouradian & Zaitsev, 2012). Those carbonated rocks are often associated with Si-undersaturated alkaline magmatic rocks and locally with an iron-rich phosphate rock called phoscorite (Krasnova et al., 2004). A series of works support that immiscibility in magmas is the main differentiation process responsible for the alkaline-carbonatite-phoscorite magmas association and the differential partitioning of rare metals among them (Kjarsgaard & Hamilton, 1989; Nabyt et al., 2020). Immiscibility is suggested to be involved in the genesis of phoscorites from carbonatitic liquids (Krasnova et al., 2004; Zaitsev et al., 2014).

The objective of our project is firstly to determine the extent of immiscibility on the genesis of alkaline-carbonatite-phoscorite complexes, and secondly, to understand and parametrize the rare metals (REE and HFSE) partitioning between the immiscible liquids leading to economic concentrations. Through this project, we aim to answer a series of scientific questions regarding the composition of the parental magma, the onset conditions and compositional field of immiscibility, the enrichment processes during cooling and crystallization, and the impact of chemical composition and temperature on rare metals behavior. To reach our goals, we based our approach on new laboratory high-pressure-high-temperature experiments carried out in the piston-cylinder apparatus of the University of Liège and the centrifuging piston-cylinder at ETH Zürich. Our starting compositions represent complex systems and are inspired by previous experimental works and natural geochemical data.

One of our work hypotheses is that immiscibility occurs first between a silicate and a carbonate liquid from a Fe-P rich parental magma. After going through several changes during its evolution (temperature decrease, crystal fractionation, enrichment and compositional variation of the residual liquid, etc.), the carbonate liquid is not thermodynamically stable anymore and exsolves a phosphate liquid. The experiments we present here are focused on the silicate-carbonate immiscibility in Fe-P rich complex systems. We studied how elements, in particular P and Fe, partition during separation. We also discuss the effects of temperature and chemical composition, the links with melt structure and oxygen fugacity, and the implication for the potential genesis of phoscorites from Fe-P rich carbonate magmas.

References

- Chakhmouradian, A.R. & Zaitsev, A.N., 2012. Rare Earth mineralization in igneous rocks: sources and processes. *Elements*, 8, 347-353.
- Humphreys, W.E. & Woolley, A., 2019. A Global View of Alkaline Rocks and Carbonatites. *Goldschmidt Abstracts (2019)*, 1441.
- Kjarsgaard, B.A. & Hamilton, D.L., 1989. The genesis of carbonatites by immiscibility. *In: Carbonatites: Genesis and Evolution* (K. Bell, ed.). Chapman & Hall, London, U.K., 388-404.
- Krasnova, N.I., Petrov, T.G., Balaganskaya, E.G., Garcia, D., Moutte, J., Zaitsev, A.N. & Wall, F., 2004. Introduction to phoscorites: occurrence, composition, nomenclature and petrogenesis. *In: Phoscorites and carbonatites from mantle to mine: the key example of the Kola Alkaline Province* (A. Zaitsev and F. Wall, editors). Mineralogical Society Series, 10. Mineralogical Society, London, 43-72.
- Nabyl, Z., Massuyeau, M., Gaillard, F., Tuduri, J., Iacono-Marziano, G., Rogerie, G., Le Trong, E., Di Carlo, I., Melleton, J., Bailly, L., 2020. A window in the course of alkaline magma differentiation conducive to immiscible REE-rich carbonatites. *Geochimica et Cosmochimica Acta*, 282, 297-232.
- Zaitsev, A.N., Williams, C.T., Jeffries, T.E., Strekopytov, S., Moutte, J., Ivashchenkova, O.V., Spratt, J., Petrov, S.V., Wall, F., 2014. Rare earth elements in phoscorites and carbonatites of the Devonian Kola Alkaline Province, Russia: examples from Kovdor, Khibina, Vuoriyarvi and Turiy Mys complexes. *Ore Geology Reviews*, 61, 204-225.

The geodynamic evolution of Earth viewed by the PTt record of metamorphic rocks

Camille FRANÇOIS¹ & Vinciane DEBAILLE²

1. Commission for the Geological Map of the World, Paris, France (c.francois.geology@orange.fr)
2. ULB, Bruxelles, Belgium (vdebaille@ulb.ac.be)

One of the great puzzles of Earth's geodynamics is to determine when rigid plate tectonics (as we know it today), began on Earth and what geodynamic processes existed on early Earth. This implies to constrain the evolution of these processes over time, to know if the transition from an ancient tectonics to a modern tectonics happened quickly, by episodes or gradually, and to better understand the lithospheric dynamics in terms of burial, exhumation, and speed of processes.

Today, the tectonic regime is ruled by mobile-lid tectonics including subduction. However, the early Earth (> 2.5 Ga) - subject to a higher mantle heat flux and a thermal regime characterized by the formation of unique lithomagmatic assemblages including the emplacement of tonalite-trondjemite-granodiorite (TTG) suites - was dominated by different geodynamical processes including flat or low angle subduction (mobile-lid tectonics; *Smithies et al., 2003*) and sagduction (stagnant-lid tectonics; *MacGregor, 1951*).

The (ultra) high pressure and low temperature metamorphic rocks such as eclogites provide important clues to trace the evolution of geodynamics (*Brown & Johnson, 2018*). Nowadays these rocks are generally produced in subduction zones involving burial of a lithospheric panel in the mantle and therefore testify of plate tectonics.

The oldest eclogites, found on several continental blocks, are bracketed between 2.2 and 1.8 Ga (e.g. *Weller and St-Onge, 2017; Loose and Schenk, 2018; François et al., 2018*) and were formed during orogeneses related to the formation of the Columbia Supercontinent. Consequently, these discoveries evidence plate tectonics (but not necessary with a modern-style) at or following 2.5 Ga.

Different examples of mid to high pressure and low temperature metamorphic rocks from the Mesoarchean to the recent time - including samples from the Pilbara craton in Australia (ca. 3.3 Ga, 11 kbar/550°C; *François et al., 2014*) and from the Paleoproterozoic Kasai Block in the Democratic Republic of the Congo (ca. 2.1 Ga, 20 kbar/600°C; *François et al., 2018*) - will be presented in order to discuss the evolution of geodynamic through time based on the metamorphic rock record.

References

- Smithies, R., Champion, D. and Cassidy, K., 2003, Formation of Earth's early Archaean continental crust. *Precambrian Research*, v. 127, No. 1, pp. 89-101.
- Macgregor, A. M., 1951, Some milestones in the Precambrian of Southern Rhodesia. *The Transactions and Proceedings of the Geological Society of South Africa*, v. 54, pp. 39-50.

- Brown, M., and Johnson, T. E., 2018, Invited Centennial Article: Secular change in metamorphism and the onset of global plate tectonics. *American Mineralogist*, v. 103, pp. 181-196.
- Weller, O.M., and St-Onge, M.R., 2017, Record of modern-style plate tectonics in the Palaeoproterozoic Trans-Hudson orogeny. *Nature Geoscience*, v. 10, pp. 305–313.
- Loose, D., and Schenk, V., 2018, 2.09 Ga old eclogites in the Eburnian-Transamazonian orogen of southern Cameroon: Significance for Palaeoproterozoic plate tectonics. *Precambrian Research*, v. 304, pp. 1-11.
- François, C., Debaille, V., Paquette, J. L., Baudet, D., and Javaux, E. J., 2018, The earliest evidence for modern-style plate tectonics recorded by HP–LT metamorphism in the Paleoproterozoic of the Democratic Republic of the Congo. *Scientific reports*, v. 8, No. 1, pp. 1-10.
- François, C., Philippot, P., Rey, P. and Rubatto, D., 2014, Burial and exhumation during Archean sagduction in the east Pilbara granite greenstone terrane. *Earth and Planetary Science Letters*, v. 396, pp. 235–251.

Properties of refractory materials from low-cost Northern Tunisian kaolinitic clays

Oumaima GRINE¹, Bechir MOUSSI¹, Walid HAJAJI², Pascal PILATE³, Johan YANS⁴, Fakher JAMOSSI¹

1. *Georessources Laboratory, CERTE, Bp 273 - 8020 Soliman, Tunisia*

(moussibechir2007@gmail.com) (gr.oumaima@gmail.com) (fjamoussi@yahoo.com)

2. *Natural Water Desalination and Recovery Laboratory, CERTE, Bp 273 - 8020 Soliman, Tunisia (w.hajaji@gmail.com)*

3. *Belgian Ceramic Research Center, Avenue Gouverneur Emile Cornez 4, 7000, Mons, Belgium (p.pilate@bcrc.be)*

4. *Université de Namur, ILEE, Département de géologie – Belgium (johan.yans@unamur.be)*

The silica and alumina refractories production is not very advanced in Tunisia: factory units import expensive raw materials. It is therefore worth investigating some local kaolinitic clays as sources for silica-alumina refractories manufacturing.

We study the potential of local kaolinitic clay (24% Al₂O₃) from the Numidian Flysch Formation (Upper Oligocene) from Northern Tunisia, in silica-alumina refractories production. The X-ray Fluorescence and the X-ray Diffraction were used to identify the chemical and mineralogical composition of raw materials. The alumina content is between 20% and 35% and silica content is less than 65%, while the mineralogical composition consists mainly of kaolinite associated with illite, quartz and anatase. We added alumina-rich commercial clay (33.4 % Al₂O₃) to improve the physical and pyroscopic performances of this local kaolinitic clay.

Mixtures of various proportions of local kaolinitic clay and commercial kaolin were sintered at 1350°C during 2h, after pressing and molding using the dry way, to produce refractory dense specimens. The manufactured pellets were characterized by bulk density, open porosity, shrinkage, cold crushing strength, microstructure by scanning electron microscope (SEM) micrographs, mineralogical composition and softening under load.

The experimental data suggests that the addition of the alumina-rich clay to the main mixture enhances the softening under load from 1198°C to 1213°C, the mechanical behavior of the manufactured pellets from 36 MPa to 44 MPa, the mullite (aluminum silicate) amount from 25% to 29% and decreases the open porosity from 19.6% to 18.6%.

The obtained results are highly encouraging, but further investigation is necessary to refine this potential.

Keywords: Silica-alumina refractories, Low-cost kaolin, Refractory materials, Numidian Flysch Formation, Clays, Upper Oligocene, Tunisia.

References

Amrane, B., Ouedraogo, E., Mamen, B., Djaknoun., Mesrati, N., 2011. Experimental study of thermo-mechanical behaviour of alumina-silicat refractory materials based on mixture of Algerian kaolinitic clays. *Ceramic international*, 37, pp 3217-3227.

Chen, L., Mlfiet, A., TomJones, P., Blanpin B., Guo, M., 2015. Degradation mechanisms of alumina–silica runner refractories by carbon steel during in gotcasting process. *Ceramics international* (42)10209-10214.

- Delphine, B., 2004. Néogènes silico-alumineuses en contexte cryptokarstique de l'halloysite de Beez (Namur, Belgique) et de Aïn Khamouda (Kasserine, Tunisie). PhD Thesis, University Paris- Sud XI, France. 231pp.
- Routschka, G. (Ed.), 2004. Pocket manual—Refractory Materials: Basics, Structures and Properties. 2nd Edition Vulkan-Verlag Essen.
- Rouvier, H., 1967. Géologie de l'extrême Nord tunisien: tectoniques et paléogéographies superposées à l'extrémité orientale de la chaîne nord magrébine. Annale des Mines et de la Géologie. Office Nationale des Mines, Tunisie, p. 29.

Tentative de décomplexification du complexe de Butare: ses extrémités NW et SE respectivement à Kalehe et Idjwi à l'Est de la RDC et à Zina-Randa et Cohoha au Nord du Burundi

C. KALIKONE¹, G. FURAHA¹, L. KEZIMANA¹, C. NZOLANG², G. NIMPAGARITSE³, D. DELVAUX³, J. BATUMIKE², R. RUMANYA², E. MUNYALI², H. FAKAGE², D. BAUDET³, L. NAHIMANA⁴, S. DEWAELE⁵

1. *Ecole Doctorale de l'Université du Burundi et Université Officielle de Bukavu, Département de Géologie, kalikchrste@gmail.com, christian.kalikone@student.ub.edu.bi, furahaghislain@gmail.com; leefredk@yahoo.com*
2. *Université Officielle de Bukavu, Département de Géologie, nzolang@gmail.com, jbatumike@gmail.com; ricbindj@gmail.com; munyaliemanuel@gmail.com; hfbwanga@gmail.com*
3. *Musée Royal de l'Afrique Centrale, (gerard.nimpagaritse@africamuseum.be; damien.delvaux.de.fenffe@africamuseum.be; daniel.baudet@africamuseum.be)*
4. *Université du Burundi, Département des Sciences de la Terre, louis.nahimana@ub.edu.bi*
5. *Université de Gand, Faculté des Sciences, Département de géologie, stijndg.dewaele@ugent.be*

La chaîne Karagwe-Ankole (KAB) est une ceinture orogénique d'âge Mésoprotérozoïque s'étendant depuis l'Est de la RDC jusqu'au Sud-Ouest de l'Ouganda et au Nord-Ouest de la Tanzanie en passant par le Burundi et le Rwanda. Elle est caractérisée par des roches méta sédimentaires à méta volcanosédimentaires réparties dans deux domaines structurellement distincts, à savoir un domaine occidental (WD) reposant sur des gneiss et des migmatites paléo-protérozoïques et composé de roches sédimentaires à volcanosédimentaires méso-protérozoïques déformées métamorphosées dans les schistes verts au faciès des amphibolites. Le WD, ainsi qu'un domaine oriental (ED) reposant sur un sous-bassement archéen (Tack et al., 2010).

Dans ces formations, il est signalé des intrusions de trois générations de granitoïdes, dont un groupe de granitoïdes de type S d'âge 1375 Ma ou de type A d'âge 1205 Ma et un groupe de leucogranites d'âge moyen de 976 Ma (Tack et al. 2010; Fernandez-Alonso et al., 2012 ; Dewaele et al., 2015).

Il a été également reconnu dans cette chaîne des formations à positions stratigraphiques incertaines, comme celles constituant ce qui a été cartographié comme « complexe de Butare », du nom de son locus-typicus au Sud du Rwanda, mais qui s'étend en direction NW jusqu'au-delà de la frontière à Kalehe et Idjwi en RDC avec son appellation locale de « complexe d'Uvira, ainsi qu'en direction Sud au-delà de la frontière burundaise depuis le Nord-Ouest avec le complexe de Zina-Randa jusqu'au Nord-Est avec le complexe de Cohoha, en passant par les granites de Mwokora, Kabarore, Mparamirundi et Murehe (Baudet et al. 2019, Laghmouch et al. 2019, 2018).

La géologie des secteurs d'Idjwi et de Kalehe est constituée des roches magmatiques (leucogranites, granites à deux micas, rhyolite, basalte, aplite, gabbros, dolérite), métamorphiques (amphibolites, marbre, gneiss, micaschistes, phyllites, quartzite, schistes graphiteux) et sédimentaires (calcaire, travertin, grès). Des minéralisations de Sn, Nb-Ta, Be se trouvent dans les filons de pegmatite tandis que celles de Sn et W sont liées aux filons de

quartz et de greisen, suivant des orientations parallèles à des failles généralement NE-SW et parfois à la foliation.

Le complexe de Zina-Randa se situe au Nord-Ouest du Burundi et s'étend depuis la rivière Kagunuzi au Nord jusqu'au granite de Bubanza au Sud. Les données préliminaires de terrain montrent que ce complexe est caractérisé par de nombreuses intrusions pegmatitiques au sein des métasédiments essentiellement psammitiques et phylliteux. On remarque également plusieurs pointements de granites (leucogranites et granites à 2 micas foliés). Il renferme des zones de minéralisations, comme celle du champ pegmatitique à Sn, Nb-Ta et Li à Ndora.

Au sein du complexe de Cohoha au Nord-Est du Burundi, on observe un centre plutôt plus leucogranitique évoluant vers une zone de bordure où on trouve un mélange de lambeaux lenticulaire de métasédiments avec des granites et des pegmatites dont il ne reste parfois plus que des arènes de quartz flottant dans des restes de feldspaths kaolinisés. Alors que jusqu'à ce jour il a été seulement signalé dans la région dit « Ikibuye Cya Shyari » au Sud de Butare où il a été observé et daté, on observe dans ce mélange de bordure, à Cyumva non loin de la ville de Kirundo, des affleurements d'orthogneiss fort identiques au prototype du socle paléoproterozoïque du WD. Un échantillon en cours d'analyse géochronologique révélera bientôt son âge. Des minéralisations en Sn, Nb-Ta, W et Au se trouvent en bordure et loin de ce complexe avec une zonéogéographie allant de zones d'abord à Sn, puis Sn et Nb-Ta, W, et Au, même si le lien génétique reste à étudier.

Références

- Dewaele, S., Hulsbosch, N., Cryns, Y., Boyce, A., Burgess, R. & Muchez, Ph., 2015. Geological setting and timing of the world-class Sn, Nb-Ta and Li mineralization of Manono-Kitotolo (Katanga, Democratic Republic of Congo). *Ore Geology Reviews* 72, 373-390.
- Fernandez-Alonso, M., Cutten, H., De Waele, B., Tack, L., Tahon, A., Baudet, D., & Barrit, S. D., 2012. The Mesoproterozoic Karagwe-Ankole Belt (formerly the NE Kibara Belt): the result of prolonged extensional intracratonic basin development punctuated by two short lived far-field compressional events. *Precambrian Res.* 216-219, 63-86.
- Tack, L., Wingate, M. T. D., De Waele, B., Meert, J., Belousova, E., Griffin, A., Tahon, A. et Fernandez-Alonso, M., 2010. The 1 375 Ma 'Kibaran event' in Central Africa: prominent emplacement of bimodal magmatism under extensional regime. *Precambrian Research* 180, 63- 84.
- Baudet, D. Fernandez-Alonzo, M. Ntege, A. Ngaruye, J.-C. Kanyana, A. Tuyishimiye, P. Habiyakare, & T. Gabinema, C., 2019. Geological Map of Rwanda 1/100.000 scale series, Karongi – S3/29 NW.
- Laghmouch, M. Nimpagaritse, G. Mudende, L. Minani, M. Ndereyimana, J. Icitegetse, I. Nahimana, A. Ndarihonyoye, P. Niyongabo, J-B. Fernandez-Alonzo, M. Baudet, D. Tack, L. Kervyn, F., 2019. Carte Géologique du Burundi au 250.000ème.

Tentative de décomplexification du complexe d'Uvira : Cas des secteurs d'Idjwi et Kalehe, Sud-Kivu/ RDC. Cartographie, pétrographie et minéralisation

C. KALIKONE¹, C. NZOLANG², G. NIMPAGARITSE³, D. DELVAUX³, J. BATUMIKE², R. RUMANYA², E. MUNYALI², H. FAKAGE², D. BAUDET³, L. NAHIMANA⁴, S. DEWAELE⁵

6. *Ecole Doctorale de l'Université du Burundi et Université Officielle de Bukavu, Département de Géologie, kalikchriste@gmail.com, christian.kalikone@student.ub.edu.bi*
7. *Université Officielle de Bukavu, Département de Géologie, nzolang@gmail.com, jbatumike@gmail.com; ricbindj@gmail.com; munyaliemmanuel@gmail.com; [hf.bwanga@gmail.com](mailto:hfbwanga@gmail.com)*
8. *Musée Royal de l'Afrique Centrale, (gerard.nimpagaritse@africamuseum.be; damien.delvaux.de.fenffe@africamuseum.be; daniel.baudet@africamuseum.be)*
9. *Université du Burundi, Département des Sciences de la Terre, louis.nahimana@ub.edu.bi*
10. *Université de Gand, Faculté des Sciences, Département de géologie, minéralogie et pétrologie, stijndg.dewaele@ugent.be*

L'équivalent de complexe d'Uvira, qui serait d'âge paléoproterozoïque, affleure à Idjwi et sur une partie de Kalehe. Son prolongement Sud-Ouest (au Rwanda) constitue le complexe de Butare avec son extension SE (au Burundi) dans Mwokora, Kabarore, Kimanga et Cohoha.

Il a été signalé, dans la région des grands lacs africains, la présence de trois chaînes précambriennes dont celle du paléoproterozoïque (Ubendienne), du Mésoproterozoïque de Karagwe-Ankole Belt (KAB) au Kivu, Kibaran Belt (KIB) au Katanga et du néoproterozoïque (Panafricaine) (Tack et al. 2010; Dewaele et al., 2015). Les formations de KAB à l'Est de la RDC ont été regroupées, quant à elles, dans le Supergroupe du Kivu (Fernandez-Alonso et al., 2015). Dans ces formations, il est signalé des intrusions locales de trois générations de granitoïdes du Mésoproterozoïque. (1) Le premier groupe est caractérisé par les granitoïdes de type S d'âge 1 375 Ma (2) de type A d'âge 1 205 Ma et (3) Le second groupe est celui des leucogranites, d'âge moyen de 976 Ma (Tack et al., 2010; Fernandez-Alonso et al., 2012; Dewaele et al., 2015).

La géologie des secteurs d'Idjwi et de Kalehe est constituée des roches magmatiques (leucogranites, granites à deux micas, rhyolite, Basalte, aplite, gabbros, dolérite), métamorphiques (amphibolites, marbre, gneiss, micaschistes, phyllites, quartzite, schistes graphiteux) et sédimentaires (calcaire, travertin, grès). Dans ces régions, les minéralisations de colombo- tantalite et la cassitérite se trouvent dans les filons de pegmatite tandis que celles de cassitérite et wolframite sont liées aux filons de quartz et de greisen.

Le granite à Etain consiste en un leucogranite à muscovite (rarement à deux micas) et tourmaline. Sa paragenèse tectonothermale a été concomitante au climax métallogénique du Kibarien d'étain. Les pegmatites et veines minéralisées en Au, Sn, W, Nb, Ta, Be, phosphate, tourmaline et U l'accompagnent (Fernandez-Alonso et al., 1986; Tack et al., 1994). Ces minéralisations sont présentes à Idjwi et Kalehe et seraient aussi liées à ce type de granite.

Dans ces deux zones, les différentes failles seraient donc des zones de faiblesses pour de possibles circulations de fluides magmatiques hydrothermaux. Les structures minéralisées sont orientées parallèlement aux failles et parfois à la foliation. Ces failles présentent une orientation préférentielle de NE-SW,

La lithologie joue un rôle indispensable dans la mise en place des minéralisations. Présence de schistes graphiteux et des quartzites pourrait être le marqueur des pièges de la minéralisation de W et Sn dans ces régions.

Références bibliographiques

- Dewaele, S., Hulsbosch, N., Cryns, Y., Boyce, A., Burgess, R., Muchez, Ph., 2015. Geological setting and timing of the world-class Sn, Nb-Ta and Li mineralization of Manono-Kitotolo (Katanga, Democratic Republic of Congo). *Ore Geology Reviews* 72, 373-390.
- Fernandez-Alonso, M., Kampata, D., Mupande, J.-F., Dewaele, S., Laghmouch, M., Baudet, D., Lahogue, P., Badosa, T., Kalenga, H., Onya, F., Mawaya, P., Mwanza, B., Mashagiro, H., Kanda Nkula, V., Luamba, M., Mpoyi, J., Decree, S., Lambert, A., 2015. Carte géologique (provisoire) de la République Démocratique du Congo au 1/2.500.000, notice explicative, Ministère des mines, République Démocratique du Congo.
- Fernandez-Alonso, M., Cutten, H., De Waele, B., Tack, L., Tahon, A., Baudet, D., Barritt, S. D., 2012. The Mesoproterozoic Karagwe-Ankole Belt (formerly the NE Kibara Belt): the result of prolonged extensional intracratonic basin development punctuated by two short lived far- field compressional events. *Precambrian Research* 216-219, 63-86.
- Fernandez-Alonso, M., Lavreau, J. and Klerkx, J., 1986. Geochemistry and geochronology of the Kibaran granites in Burundi, Central Africa: implications for the Kibaran Orogeny, *Chemical Geology* 57, 217-234.
- Laghmouch, M., Kalikone, C., Ilombe, G., Ganza, G., Delvaux, D., Safari, E., Bachinyaga, J., Dewaele, S., Wazi, N., Nzolang, C., Fernandez-Alonso, M., Tack, L., Nimpagaritse, G. & Kervyn, F., 2018. Carte géologique du Kivu au 1/500 000. Musée Royal de l'Afrique Centrale, Tervuren.
- Tack, L., Liégeois, J.P., Deblond, A. et Duchesne, J.C., 1994. Kibaran A-type granitoids and mafic rocks generated by two mantle sources in a late orogenic setting (Burundi). *Precambrian Research* 68, 323-356.
- Tack, L., Wingate, M. T. D., De Waele, B., Meert, J., Belousova, E., Griffin, A., Tahon, A., Fernandez-Alonso, M., 2010. The 1 375 Ma 'Kibaran event' in Central Africa: prominent emplacement of bimodal magmatism under extensional regime. *Precambrian Research* 180, 63- 84.

Tentative de décomplexification du complexe de Zina-Randa (Nord-Ouest du Burundi)

Lee Fred KEZIMANA¹, Louis NAHIMANA², Gérard NIMPAGARITSE³

1. *Ecole Doctorale, Université du Burundi, Bujumbura, Burundi (leefredk@yahoo.com)*
2. *Département des Sciences de la Terre, Université du Burundi, Bujumbura, Burundi (louis.nahimana@ub.edu.bi)*
3. *Département des Sciences de la Terre, Musée Royal d'Afrique Centrale, Tervuren, Belgique (gerard.nimpagaritse@africamuseum.be)*

Au Nord-Ouest du Burundi, on reconnaît des complexes à position stratigraphique incertaine associés aux métasédiments mésoprotérozoïques de la chaîne Karagwe-Ankole (KAB). Ce sont des complexes tectono-métamorphiques constitués de roches intrusives essentiellement granitiques et pegmatitiques dans des niveaux de métasédiments (gneiss, métaquartzites, micaschistes, schistes) fortement déformés (Carte géologique du Burundi au 250.000ème). Ces complexes sont associés à des zones de minéralisations i.e. le champ de pegmatites lithinifères de Ndora et les pegmatites à Sn, Nb-Ta de Kabarore.

Le complexe de Zina-Randa se situe au Nord-Ouest du Burundi et s'étend depuis la rivière Kagunuzi au Nord jusqu'au granite de Bubanza au Sud. Les données préliminaires de terrain montrent que ce complexe est caractérisé par de nombreuses intrusions pegmatitiques au sein des métasédiments essentiellement psammitiques et phylliteux. On remarque également plusieurs pointements de granites (leucogranites et granites à 2 micas foliés).

Le présent travail intègre de récentes données de terrain collectées dans le complexe de Zina-Randa avec objectif de présenter une tentative de décomplexification. Un travail similaire a été réalisé du côté du complexe de Butare au Rwanda (Baudet et al., 2019).

Références

- Baudet, D. Fernandez-Alonzo, M. Ntege, A. Ngaruye, J.-C. Kanyana, A. Tuyishimiye, P. Habiyakare, & T. Gabinema, C., 2019. Geological Map of Rwanda 1/100.000 scale series, Karongi – S3/29 NW.
- Laghmouch, M. Nimpagaritse, G. Mudende, L. Minani, M. Ndereyimana, J. Icitegetse, I. Nahimana, A. Ndarihonyoye, P. Niyongabo, J-B. Fernandez-Alonzo, M. Baudet, D. Tack, L. Kervyn, F., 2019. Carte Géologique du Burundi au 250.000ème.

Valorization of Tunisian Numidian clays (Upper Oligocene) in the manufacture of ceramic tiles

Béchir MOUSSI¹, Oumaima GRINE¹, Walid HAJJAJI¹, Johan YANS², Mondher HACHANI³, Nouri HATIRA⁴, Joao Antonio LABRINCHA⁵, Fakher JAMOSSI¹

1. *Water Researches and Technologies Center (CERTE), Technopôle de BorjCedria, BP 273, Soliman, 8020, Tunisia (moussibechir2007@gmail.com) (gr.oumaima@gmail.com) (w.hajaji@gmail.com) (fjamoussi@yahoo.com)*
2. *University of Namur, ILEE, Department of Geology, Belgium (johan.yans@unamur.be)*
3. *University of Carthage Higher Institute of Environmental Science and Technology of BorjCedria, B.P. n°, 1003, 2050, Hammam Lif, Tunisia (mondher_hachani@hotmail.com)*
4. *Faculté des Sciences de Bizerte, Zarzouna, 7021, Tunisia (nhatira@gmail.com)*
5. *Materials and Ceramic Engineering Dept & CICECO, University of Aveiro, 3810-193, Aveiro, Portugal (jal@ua.pt)*

In the aim of valorization of clays in the traditional ceramics manufacture, several samples of clays were collected in the Numidian Flysch Formation (Upper Oligocene) at Tabarka and Sejnane areas (North west of Tunisia). We used the technique of dry process, which requires a mixture of powdered clay with 7% water. In order to follow the evolution of technological parameters such as shrinkage, water absorption and flexural strength, ceramic tile firing tests were carried out at temperatures varying between 1000°C and 1150°C.

The characterization of these ceramic tile products includes the determination of total shrinkage, flexural strength and water absorption. The last parameter allows us to classify the products according to the choice of the field of use. The water absorption ranges from 10 to 20%, which classifies these products in group BIII according to the international standards (ISO 13006 and EN ISO 10545-3). The obtained tiles show acceptable drying and firing shrinkage (not exceeding 3%), and bending strength (between 13 and 16 N/mm²) which are close to the required standards (EN ISO 10545-4, 15N/mm² for wall tiles).

Variation of technological parameters such as shrinkage and water absorption with the increasing of temperature reveals that optimal range of firing is 1125–1150°C for the Tabarka samples, whereas the Sejnane products might be fired at lower values (~1025°C). The Tabarka fired pieces exhibit strong brightness. These results suggest that these latter clays could be used for white products such as sanitary ware formulations while those from Sejnane ones are more appropriated for colored (red) applications.

The mineralogical composition determined by the X-ray diffraction of ceramic products shows the formation of mullite resulting from the richness in Al₂O₃, supporting their refractories properties.

Keywords: Manufacture, Ceramic, Numidian, clays, Upper Oligocene, Tunisia.

Paleostress reconstruction and tectono-structural evolution of the West-Congo Orogen, in Republic Democratic of Congo and Republic of Congo

Hardy Medry Dieu-Veill NKODIA ^{1,*}, Florent BOUDZOU MOU ^{1,2}, Timothée MIYOUNA ¹, Damien DELVAUX ³

* Corresponding author: nkodiahardy@gmail.com

¹ *Marien NGOUABI University, Faculty of Sciences and Technics, Department of Geology, Brazzaville, Republic of Congo.*

² *National Research Institute in Exact and Natural Sciences of Brazzaville, Republic of Congo*

³ *Department of Geology, Royal Museum for Central Africa, Tervuren, Belgium.*

The West-Congo Belt is a Panafrican orogen located in the African side which was part of the Araçuaí-West-Congo orogen during the assembly of Congo and Sao Francisco craton of the west Gondwana supercontinent. Over last decades, detailed structural studies have been conducted mostly in the Brazilian sides but few focused on paleostress and its significance to overall evolution of the Araçuaí-West Congo orogen. A DEM and a detail field structural analysis of the foreland and the front of the hinterland were carried out in order to produce a structural map of the West Congo orogen. The paleostress and kinematic analysis of the West Congo belt conducted has showed 28 stage stress tensors. All these stages constituted long period of deformation from the Neoproterozoic until present day probably. From 28 stress stages we come to the evidence that the West Congo belt has experienced an oblique convergence expressed in progressive deformation by two major stages of deformation. The first stage of deformation is NNE-SSW to NE-SW oriented compressional to strike-slip regime that resulted in the development of major conjugate NW-SE dextral strike-slip brittle and NE-SW to ESE-WSE brittle-ductile shear zones and WNW-ESE to NW-SE folds, and the second that stage that is a E-W compressional to strike-slip regime, this stage reactivated earlier shear zones in reverse kinematics N-S to NE-W fold. This suggest that during the development of the Araçuaí-West Congo the Congo craton rotated clockwise, this rotation could be forced by collision of the West African, eastern Saharan cratons in the north. This also confirms that the Araçuaí is a forced orogen.

New insights from the revised geological map of the West Rwanda (Karongi-Nyamagabe-Rusizi districts)

Alain J. NTENGE¹, Ariane KANYANA¹, Jean Claude NGARUYE¹, Pascal TUYISHIME¹, Daniel BAUDET², Max FERNANDEZ-ALONSO², Gérard NIMPAGARITSE²

(1) Rwanda Mines, Petroleum and Gas Board, Kigali, Rwanda,
alainjoseph.ntenge@rmb.gov.rw

(2) Royal Museum for Central Africa, Tervuren, Belgium

Rwanda is dominantly occupied by metasedimentary rocks of the Mesoproterozoic domain regionally known as Karagwe Ankole Belt (ex - Kibaran), which belong to the Akanyaru Supergroup. These have undergone some tectono-metamorphic phases and were affected by different events of magmatic rocks intrusions. The studied area is generally made up of low to medium grade metamorphic Akanyaru sediments and of a high metamorphic Butare complex. Structurally, the region has numerous faults and folds trending NNW.

A new geological mapping campaign has been launched in 2018 under a project between RMB and RMCA financially supported by the Belgium Cooperation Agency (ENABEL). This project produced some insightful information that allowed to propose an updated new geological map for the 1/100.000 scale Kibuye (Karongi) sheet.

Along a N-S section of the area, it is noticed that the upper levels of the Akanyaru stratigraphy alternate with lower parts in the centre before appearing back in the South; which clearly defines a regional antiformal setting.

This geometry allowed to detail the lowest, less well known levels of the Akanyaru Supergroup: mainly here the Kaduha Formation, but also more important basement gneisses and migmatites. It was also possible to observe magmatic bodies usually present in the heart of anticlinal structures. Mostly granites and some gabbro, this association possibly represents the bimodal magmatism event which has been described in the literature for the Karagwe Ankole Belt.

A closer observation in sediments shows lenticular paths of feldspar of different size formed during metasomatism. It was noticed that the affected zone is mainly in the lower part of the stratigraphy (Nyungwe and Kaduha formations). Similarly, some gneiss were intruded by magmatic venues creating “exomigmatites”. This feldspar-alteration is mainly occurring in the heart of the anticlinorium.

Finally, the conglomerates from Nyamasheke (Karamba formation), can now be confirmed to be Neoproterozoic diamictites and are probably correlated to the diamictites found in the Itombwe Supergroup in the D. R. Congo, across lake Kivu.

Geological Map of Rwanda
1/100,000 scale series



Republic of Rwanda



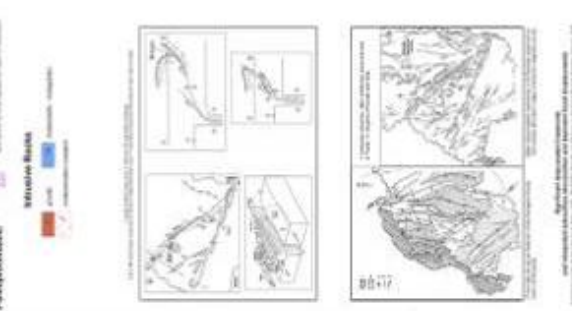
Repubulika y'u Rwanda

KARONGI - S3/29 NW

TRANSFER OF GEO-DATA AND KNOWLEDGE IN SUPPORT OF A GIMCS AT RMB
A COOPERATION ACTIVITY BETWEEN THE RWANDA MINES, PETROLEUM AND GAS BOARD (RMB), KIGALI, RWANDA
AND THE ROYAL MUSEUM FOR CENTRAL AFRICA (RMCA), Tervuren, Belgium
#17 FRAME OF THE 2017-2023 SUSTAINABLE DEVELOPMENT OF MINING IN RWANDA (SDMI) PROGRAMME



Category	Legend	Number
Geological	Quaternary	1
	Neoproterozoic	2
Mesoproterozoic	Alusino	3
	Synorogin	4
Paleoproterozoic	Archaean	5
	Archaean	6



Geological Units

- Quaternary
- Neoproterozoic
- Mesoproterozoic
- Paleoproterozoic

Topographic Profile

Profile line: Karongi - S3/29 NW

Scale: 1:100,000

Projection: UTM Zone 36S

Datum: WGS 1984

Units: Meter

Scale: 1:100,000

Projection: UTM Zone 36S

Datum: WGS 1984

Units: Meter

Unravel the rate of pyrite oxidation under weathering conditions: an experimental approach

Julien POOT 1, Alexandre FELTEN 2, Guillaume LEPECHEUR 1, Pierre LOUETTE 2, Augustin DEKONINCK 1, Johan YANS 1

1. *Department of Geology, Institute of Life-Earth-Environment (ILEE), University of Namur, Rue de Bruxelles 61, 5000 Namur, Belgium (julien.poot@unamur.be; augustin.dekoninck@unamur.be; johan.yans@unamur.be)*
2. *Department of Physics, Synthesis, Irradiation and Analysis of Materials (SIAM), University of Namur, Rue de Bruxelles 61, 5000 Namur, Belgium (alexandre.felten@unamur.be; pierre.louette@unamur.be)*

Pyrite is one of the most common sulfides on Earth. It occurs in various geological settings, in sedimentary rocks and hydrothermal deposits, including many polymetallic sulfides ore deposits. The oxidation of pyrite can lead to environmental issues due to acid mine drainage but also extraction difficulties requiring specific mining processes (Holmes et al., 2000; Sun et al., 2015).

For this study, pyrite samples were collected from the Hautrage Clay Formation (Upper Barremian to Basal Aptian) in the Hautrage quarry (Mons Basin, Belgium). In these clayey rocks, pyrite has remained protected from direct atmospheric conditions and can be considered as "fresh".

The main objective of this work is to determine the oxidation rate of pyrite. To do this, different experiments are made on carefully selected samples of Hautrage pyrite: (i) open air exposure, (ii) underwater and (iii) drip exposure to tridistilled water. XPS (X-Ray Photoelectron Spectroscopy) analyses are further carried out at different time steps on the surface and at depth of the samples to decipher the extent of the oxidation zone (more than five thousand hours of experiment). The first results show an oxidation depth close to 1 micrometer for drip exposure pyrite over a 6 months period. This value is half for air exposure, whereas pyrite under water shows only a very slight oxidation. An experiment was also conducted to determine the impact of pyrite oxidation on the acidity of meteoric fluids. Pyrite are put underwater for a given time (lab temperature between 20 and 25°C) with regular pH measurements. It appears that the pH of the water stabilizes around 2 after 6 months of experiment. A small fraction of Hautrage clays is also added in some flasks in order to measure the buffering capacity of these clays.

At a human scale, this oxidation depth seems low, but can be responsible for many environmental (aquatic life or aquifers) and construction-related issues (stability, cracks in walls, heaved floors, ...) that could take place over decades. At a geological scale, by extrapolating the results obtained, a few tens of thousands of years would be sufficient to fully oxidize the pyrite and then form secondary mineralization.

References

- Holmes, P. R., & Crundwell, F. K., 2000. The kinetics of the oxidation of pyrite by ferric ions and dissolved oxygen: An electrochemical study. *Geochimica et Cosmochimica Acta*, 64(2), 263–274.
- Sun, H., Chen, M., Zou, L., Shu, R., & Ruan, R., 2015. Study of the kinetics of pyrite oxidation under controlled redox potential. *Hydrometallurgy*, 155, 13–19.

Controls of host rocks on weathering processes and dating of Cu-As-Pb-rich supergene deposits (Moroccan Anti-Atlas Copperbelt, Morocco)

Michèle VERHAERT^{1,2*}, Atman MADI³, Abdelaziz EL BASBAS⁴, Mohamed ELHARKATY³, Abdellah OUMMOUCH³, Lahcen OUMOHOUS³, Lhou MAACHA³, Benoît GRYMOPREZ¹, Cécile GAUTHERON⁵, Johan YANS²

1. *Centre Terre et Pierre, Chaussée d'Antoine 55, 7500 Tournai, Belgium. (Michele.Verhaert@ctp.be; Benoit.Grymonprez@ctp.be)*
2. *Department of Geology, University of Namur, Institute of Life, Earth, and Environment, ILEE, Rue de Bruxelles 61, 5000 Namur, Belgium. (johan.yans@unamur.be)*
3. *Managem Group, BP 5199, 20100 Casablanca, Morocco. (a.madi@managemgroup.com; m.elharkaty@managemgroup.com; A.OUMMOUCH@managemgroup.com; L.OUMOHOUS@managemgroup.com; L.MAACHA@managemgroup.com)*
4. *Département des Sciences de la Terre, Ecole Nationale Supérieure des Mines de Rabat, Avenue Ahmed Cherkaoui, BP 753, Agdal, 10000 Rabat, Morocco. (abdelazizbasbas@gmail.com)*
5. *GEOPS, University Paris-Saclay, 91405 Orsay, France. (cecile.gautheron@u-psud.fr)*

The Tazalaght and Agoujgal Cu-As deposits, hosted by Neoproterozoic to Cambrian formations in the Moroccan Anti-Atlas, are exploited by the mining company Managem for their copper and silver ores.

As many other deposits in this area (e.g. Tizert), these primary sulfide deposits underwent significant weathering leading to the development of supergene profiles and to the formation of various secondary ores. Both deposits present secondary copper ores that were formed through quite similar processes, despite some mineralogical and chemical variations highlighting the influence of host rocks on weathering. Their shared special feature is the presence of Cu-Pb arsenates and vanadates.

At the Tazalaght's deposit, weathering led to the development of four mineralogical zones clearly distinguished in each vertical cross-section of the deposit, from base to top: the hypogene sulfide zone (chalcopyrite, pyrite, tennantite), the large cementation zone hosting secondary sulfides (bornite, chalcocite), the oxidized zone (malachite, azurite, olivenite, chenevixite), and the leached zone (goethite, hematite). Scarce Co-sulfides and Co-arsenates complement the sequence. These mineral associations are also identified at Agoujgal, but are less spatially confined. While the cementation zone is reduced in size, in comparison with Tazalaght, the oxidized zone is much more extended and diversified. Three mineralogical processes are distinguished at Agoujgal: (1) the replacement of hypogene sulfides (chalcopyrite, pyrite, tennantite, galena) by small volumes of supergene sulfides (chalcocite) in the cementation zone; (2) the large-scale formation of oxidized minerals (malachite, olivenite, conichalcite, yukonite, cerussite, anglesite, osarizawaite, plumbojarosite, beaverite, phosphohedyphane, mimetite, mottramite, calcio-duftite, ...) in a more oxidizing and neutral environment; and (3) the precipitation of late phases (hematite, goethite, mottramite) in the gossan.

Single hand specimens collected at both sites enabled the description of a boxwork texture derived from tennantite. These textures, which record the transition from the fresh ore, to the cementation zone, the oxidation zone, and finally to the gossan, are useful tools reflecting the evolution of fluid-rock interactions with time.

The difference between the secondary assemblages of both deposits clearly demonstrates the influence of the host rocks on supergene processes and neoformations. At Tazalaght, the mineralization is hosted by quartzitic host rocks that were obviously not able to

neutralize fast enough the fluids acidity, which jeopardized the development of the oxidized mineralization. The scarcity of carbonate rocks limited the formation of Ca-bearing oxidized phases, and in particular of Ca-arsenates (conichalcite, yukonite), which are, at the contrary, ubiquitous at Agoujgal. At the latter deposit, the large amount of dolomitic host rocks must have enabled the quick buffering of the fluids acidity, as attested by the almost total absence of secondary sulfides and the omnipresence of carbonates. The particularly broad set of Cu- and Pb-carbonates, arsenates, sulfates, phosphates, vanadates and oxides reflects the circulation of fluids of complex composition and the physical-chemical evolution of the mineralizing fluids, in relation with pH and Eh fluctuations.

Goethite specimens, collected at both sites, have been the subject of (U-Th-Sm)/He dating, which is a particularly suitable method to refine our knowledge about the formation of supergene deposits. Agoujgal goethite samples provided ages ranging from Middle Miocene to Late Pleistocene, while Tazalaght samples seem much older, with Late Cretaceous to Late Eocene ages. These ages may be related to uplift phases already defined in the Atlas (Leprêtre et al., 2015; Gouiza et al., 2017). Therefore, it is suggested that the formation of such oxides, and, generally speaking, of such supergene mineralization, could ensue from, and be driven by, long-wave exhumation processes.

References

- Gouiza, M., Charton, R., Bertotti, G., Andriessen, P., & Storms, J., 2017. Post-Variscan evolution of the Anti-Atlas belt of Morocco constrained from low-temperature geochronology. *International Journal of Earth Sciences*, 106, 593–616.
- Leprêtre R., Missenard Y., Saint-Bezar B., Barbarand J., Delpech G., Yans J., Dekoninck A. & Saddiqi O., 2015. The three main steps of the Marrakech High Atlas building in Morocco: Structural evidences from the southern foreland, Imini area. *Journal of African Earth Sciences*, 109, 177–194.

Characterization of auriferous quartz vein mineralizing fluids in the Mesoproterozoic Karagwe-Ankole belt (Byumba, Rwanda): Petrography, microthermometry and Raman spectroscopy

Sander WOUTERS¹, Stijn DEWAELE², Philippe MUCHEZ³

1. KU Leuven, Department of Earth and Environmental Sciences, Celestijnenlaan 200E, B-3001 Leuven, Belgium (sander.wouters@kuleuven.be)

2. Ghent University, Department of Geology, Krijgslaan 281, S8, 9000 Ghent, Belgium (stijndg.dewaele@ugent.be)

3. KU Leuven, Department of Earth and Environmental Sciences, Celestijnenlaan 200E, B-3001 Leuven, Belgium (philippe.muchez@kuleuven.be)

Mineral deposit research in the Central African Mesoproterozoic Karagwe-Ankole belt (KAB) has known a recent increase of interest. The KAB metallogenic province is well known for hosting different types of magmatic-hydrothermal rare metal (Nb, Ta, Sn, W) and gold deposits (Fernandez-Alonso et al., 2012; Pohl & Günther, 1991). Despite the resurgence of new research, numerous open questions concerning the genesis of the gold deposits in the area remain (Pohl et al., 2013). Central African orogenic gold mineralization has been linked to fold-and-thrust belt formation and associated shear zones (Brinckmann et al., 2001; Pohl et al., 2013). A genetic link between the auriferous quartz veins and magmatic-hydrothermal fluids from the early-Neoproterozoic post compressional magmatism (G4 granites) is however still under discussion. The characterization of the quartz vein mineralizing fluids at Byumba (Rwanda) can provide answers to these open questions. In the research presented, fluid inclusions from the different quartz vein generations at the Byumba mineralization were studied by petrography, microthermometry and Raman spectroscopy. The structural setting, insight in the mineralization age and the petrographic and geochemical (μ XRF) characterization of the gold occurrence at Byumba has been published by Wouters et al. (2020). The Byumba deposit shows distinct phases of folding and shear deformation of the metasediments. Three main phases of quartz veining are reported (pre-(V1), syn-(V2) and post-folding(V3)). Post-folding chlorite-rich quartz veins (V3) host the primary gold mineralization, mainly in the form of sub-micron gold.

Petrography of the fluid inclusions within the different Byumba quartz vein generations identified three main fluid types and shows the presence of numerous leaked/decrepitated inclusions in all vein types. Type I are primary H₂O-CO₂-X fluid inclusions which consist of an aqueous and a liquid carbonic phase (Lw-Lc) and other gasses (X). Type II fluid inclusions are also primary with a CO₂-H₂O-X composition and are dominantly carbonic liquid with a rim of H₂O (Lc-Lw). Aqueous fluid inclusions (Lw-V) found inside secondary trails are categorized as Type III and have not been studied further due to their small size. Fluid inclusions inside V1 quartz veins and V3 quartz veins are compositionally similar, but V1 veins contain more secondary trails and smaller inclusion sizes. Syn-folding V2 quartz vein inclusions were not suited for further microthermometric analysis due to the fact that they are too small to be measured or have leaked/decrepitated. Auriferous V3 quartz veins show large cloudy clusters of primary inclusions crosscut by small secondary trails.

Microthermometric measurements of primary fluid inclusions of Type I and II generated similar data in the pre- and post-folding quartz veins. Both Type I and Type II inclusions show average melting temperatures of CO₂ (T_{mCO₂}) between -61.0 °C and -59.0 °C, with a slightly higher average for Type I inclusions. Such temperatures are indicative for the presence of other gasses (N₂ and CH₄) inside the carbonic phases which is confirmed by

subsequent Raman spectroscopy. For Type I fluid inclusions it was often impossible to observe the formation of frozen CO₂ because it was (almost) completely consumed in clathrate formation. Both primary fluid types show a large variability in homogenization of the carbonic phase (Th_{CO2}), even within a single assemblage. Th_{CO2} lies mostly between 3.5 °C and 9.5 °C. Clathrate melting temperatures (T_{mCLATH}) of fluid Type I are mostly between 8.5 °C and 10.5 °C while the dominant range of Type II T_{mCLATH} is higher, i.e. mostly between 10.5 °C and 11.0 °C. Raman spectroscopy peak area assessment allows the calculation of the gaseous compositions. Fluid Type I gaseous composition range on average from 2%-5% N₂ and 3%-6% CH₄, while Type II ranges on average from 3%-7% N₂ and 4%-10% CH₄.

The primary fluid present in the post-folding auriferous quartz generation has a H₂O-CO₂-CH₄-N₂ composition, which is interpreted to be of a metamorphic origin (Goldfarb & Groves, 2015) and typical for orogenic gold type mineralization (Groves et al., 2003). However, in a next step a more detailed analysis of the major and trace element composition of the inclusions will be performed to determine the possible influence/mixing of this metamorphic fluid with other likely fluid types such as magmatic-hydrothermal fluids.

References

- Brinckmann, J. Lehmann, B. Hein, U. Höhndorf, A. Musallam, K. Weiser, T. & Timm, F, 2001. *La Géologie et la Minéralisation Primaire de l' Or de la Chaîne Kibarienne, Nord-Ouest du Burundi, Afrique Orientale*: Stuttgart. Schweizerbart Science Publishers, Germany, pp. 195.
- Fernandez-Alonso, M. Cutten, H. De Waele, B. Tack, L. Tahon, A. Baudet, D. & Barritt, S. D, 2012. The Mesoproterozoic Karagwe-Ankole Belt (formerly the NE Kibara Belt): The result of prolonged extensional intracratonic basin development punctuated by two short-lived far-field compressional events. *Precambrian Research*, 216–219, 63–86.
- Goldfarb, R. J. & Groves, D. I, 2015. Orogenic gold: Common or evolving fluid and metal sources through time. *Lithos*, 233, 2–26.
- Groves, D. I. Goldfarb, R. J. Robert, F. & Hart, C. J. R, 2003. Gold Deposits in Metamorphic Belts: Overview of Current Understanding, Outstanding Problems, Future Research, and Exploration Significance. *Economic Geology*, 98(1), 1–29.
- Pohl, W. & Günther, M. A, 1991. The origin of Kibaran (late Mid-Proterozoic) tin, tungsten and gold quartz vein deposits in Central Africa: a fluid inclusions study. *Mineralium Deposita*, 26, 51–59.
- Pohl, W. L. Biryabarema, M. & Lehmann, B, 2013. Early Neoproterozoic rare metal (Sn, Ta, W) and gold metallogeny of the Central Africa Region: a review. *Applied Earth Science*, 122, 66–82.
- Wouters, S. Hulsbosch, N. Kaskes, P. Claeys, P. Dewaele, S. Melcher, F. & Muechez, P, 2020. Late orogenic gold mineralization in the western domain of the Karagwe- Ankole Belt (Central Africa): Auriferous quartz veins from the Byumba deposit (Rwanda). *Ore Geology Reviews*, 125, doi: 10.1016/j.oregeorev.2020.103666

Session 2- Earth Surface Processes and Geohazards

Conveners :

François Fripiat (ULB) ; Xavier Devleeschouwer (RBINS-GSB);
Steven Goderis (VUB); Matthieu Kervyn (VUB) ; Matthias
Vanmaercke (ULiège); Olivier Dewitte (RMCA) ; François Kervyn,
(RMCA)

Invited speaker:

Tomáš Pánek, Dept. of Physical Geography and Geoecology,
University of Ostrava, Czech Republic

The Earth's ever-changing surface is shaped by processes that govern its evolution over all temporal and spatial scales. These processes frequently act in interactions, leading to physical, chemical and biological changes. Geohazards are processes associated with sudden environmental changes. They often result in loss of life and socio-economic impacts. This session welcomes contribution in the broad fields of geomorphology and geohazards.



Specific topics include (not exclusive): fluvial, aeolian and coastal sediment transport; hillslope mass movements and soil erosion; surface manifestation of volcanisms and tectonism; weathering and pedogenesis, modelling and theoretical and quantitative geomorphology; geological records of Earth surface processes in relation to environmental change; impacts of past, current and future environmental change upon Earth surface processes; relationship between Earth surface processes, hazard, risk, and management.

Can the 12-m TanDEM-X DEM be used to accurately estimate lavaka (gully) volumes and mobilization rates? Insights from a comparative analysis with SRTM and a high resolution UAV-SfM DEM

Liesa BROSENS^{1,2}, Benjamin CAMPFORTS³, Emilien ALDANA-JAGUE⁴, Gerard GOVERS², Vao Fenotiana RAZANAMAHANDRY², Kristof VAN OOST⁴, Tantely RAZAFIMBELO⁵, Tovonarivo RAFOLISY⁵, and Liesbet JACOBS^{2,6}

¹ *Research Foundation Flanders (FWO), Brussels, Belgium (liesa.brosens@kuleuven.be).*

² *Department of Earth and Environmental Sciences, KU Leuven, Leuven, Belgium*

³ *Institute for Arctic and Alpine Research, University of Colorado at Boulder, Boulder, CO*

⁴ *Earth and Life Institute, Georges Lemaitre Centre for Earth and Climate Research, Université Catholique de Louvain, Louvain-la-Neuve, Belgium*

⁵ *Laboratoire des Radio Isotopes, Université d'Antananarivo, Antananarivo, Madagascar*

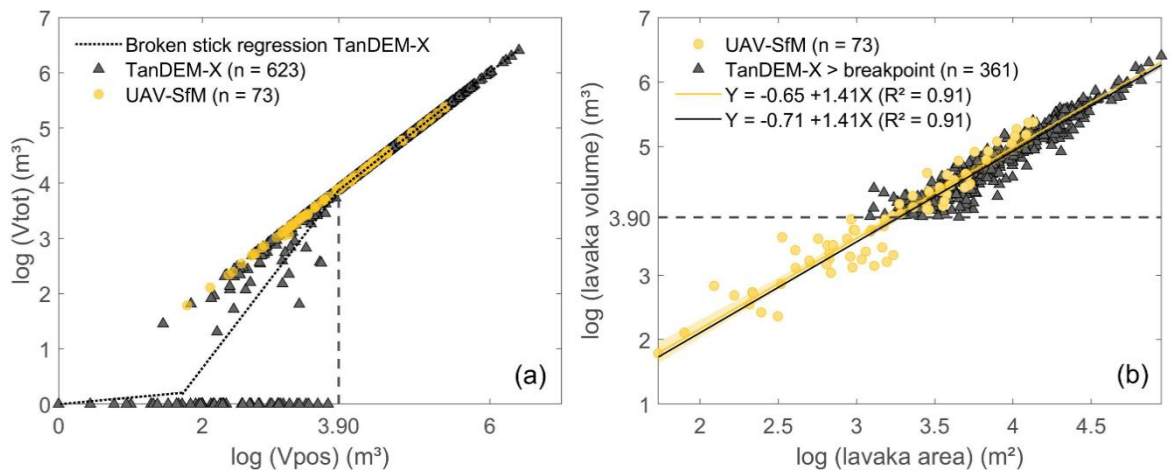
⁶ *Ecosystem & Landscape Dynamics, Institute for Biodiversity and Ecosystem Dynamics, University of Amsterdam, Amsterdam, Netherlands*

Over the past decades more and more advanced technology has become available for the assessment of surface topography: SfM (structure-from-motion) algorithms applied to UAV (unmanned aerial vehicle) imagery now allow centimeter-scale resolution, thereby revolutionizing the way we study earth-surface processes. Obtaining these high resolution DEMs, however, still requires substantial fieldwork and is spatially limited due to the nature of the technology. On the other hand, TanDEM-X is an interferometric SAR mission of the Deutsche Zentrum für Luft-und Raumfahrt with near-global coverage at 12 m resolution, and while being less detailed than UAV-SfM DEMs it is a major step forward in comparison to the 30 m SRTM DEM.

Here, we evaluated the performance of the TanDEM-X 12 m DEM to i) estimate gully volumes, ii) establish an area-volume (A-V) relationship, and iii) determine mobilization rates, through comparison with a high resolution (0.2 m) UAV-SfM DEM and lower resolution (30 m) SRTM DEM. We did this for six study areas in the lake Alaotra region (central Madagascar) where lavaka (gullies) are omnipresent and surface changes over the period 1949-2010s for 699 lavaka are available. SRTM derived volumes were systematically underestimated, indicating that the SRTM DEM is too coarse to accurately estimate volumes of geomorphic features at the lavaka-scale (100 - 100 000 m²). Lavaka volumes obtained from TanDEM-X were similar to UAV-SfM-volumes for the largest features, whereas smaller features were generally underestimated.

To deal with this bias we introduce a breakpoint analysis to eliminate volume reconstructions that suffer from processing errors as evidenced by significant fractions of negative volumes. This elimination allowed the establishment of an area-volume relationship for the TanDEM-X data that lies within the bounds of the uncertainty of the UAV-SfM A-V relationship. Our calibrated area-volume relationship enabled us to obtain large-scale lavaka mobilization rates ranging between 18 ± 6 and 289 ± 125 ton ha⁻¹ yr⁻¹ and were underestimated by ca. 15% by TanDEM-X. With this study we demonstrate the potential of the global TanDEM-X 12m DEM to estimate volumes of gully-shaped features at the lavaka-scale (100 - 100 000 m²), where the proposed breakpoint-method can be applied without requiring the availability of a higher resolution DEM.

Figure



(a) A broken stick regression (dotted black line) is fitted through the log-transformed positive (V_{pos}) and total (V_{tot}) volumes obtained from the TanDEM-X DEM. The automatically identified breakpoint is located at $\log(V_{\text{pos}}) = 3.90$ m³. (b) Linear area-volume relationships fitted through the log-transformed lavaka area and volume data for the full UAV-SfM dataset and TanDEM-X volumes exceeding the identified breakpoint ($\log(V_{\text{pos}}) > 3.9$). Shaded areas indicate the 95% confidence intervals of the fitted relationships.

Is there an environmental crisis in the Lake Alaotra region (Madagascar)? Insights from lavaka (gully) dynamics and floodplain sedimentation

Liesa BROSENS^{1,2†}, Nils BROOTHAERTS^{2†}, Benjamin CAMPFORTS³, Liesbet JACOBS^{2,4},
Vao Fenotiana RAZANAMAHANDRY², Quinten VAN MOERBEKE², Steven BOUILLON²,
Tantely RAZAFIMBELO⁵, Tovonarivo RAFOLISY⁵, and Gerard GOVERS²

¹ *Research Foundation Flanders (FWO), Brussels, Belgium (liesa.brosens@kuleuven.be).*

² *Department of Earth and Environmental Sciences, KU Leuven, Leuven, Belgium
(nils.broothaerts@kuleuven.be)*

³ *Institute for Arctic and Alpine Research, University of Colorado at Boulder, Boulder, CO*

⁴ *Ecosystem & Landscape Dynamics, Institute for Biodiversity and Ecosystem Dynamics,
University of Amsterdam, Amsterdam, Netherlands*

⁵ *Laboratoire des Radio Isotopes, Université d'Antananarivo, Antananarivo, Madagascar*

[†] *These authors contributed equally to this work*

The Malagasy highlands are scattered with large inverse teardrop-shaped gullies called lavaka, which are by many considered as the prime indication of a currently ongoing human-induced environmental crisis (Dewar 2014, Klein 2002). Yet, lavaka are known to have existed long before human arrival and account for the majority of the long-term sediment input into the highland rivers and floodplains (Mietton *et al* 2005, Cox *et al* 2009, Wells and Andriamihaja 1993). The role of anthropogenic disturbances in their formation therefore remains highly debated.

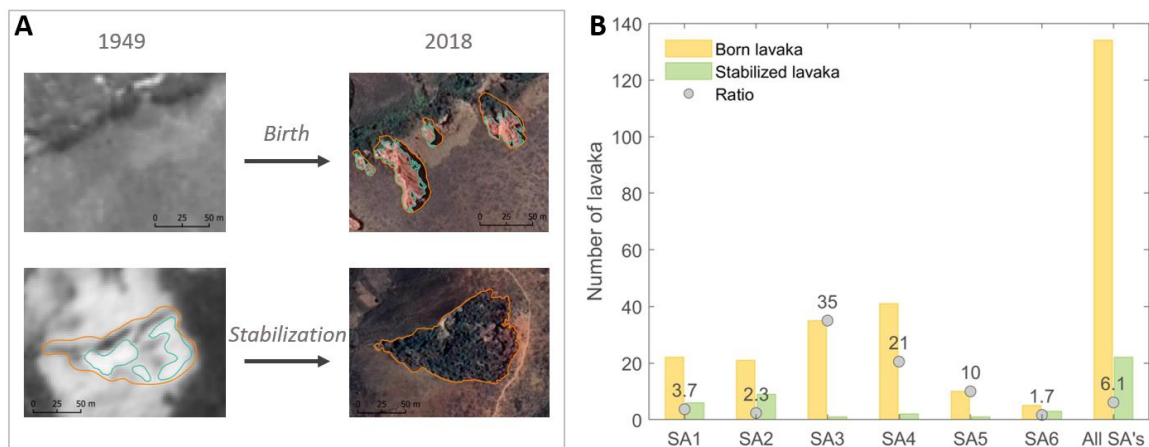
Here, we assess the dynamics of 699 lavaka from 1949 to the 2010s in the Lake Alaotra region (central highlands) by using historical aerial pictures and present day satellite imagery. An overall birth to stabilization ratio of 6.1 indicates a rapidly growing lavaka population in our study areas. Observed lavaka growth, birth and stabilization rates allowed us to calculate a mean lavaka population age of 410 ± 40 years, and estimate that the disequilibrium started at 870 ± 430 cal. BP. Floodplain sedimentation data were obtained from 5 coring transects on two of the main inflowing rivers of the lake. Baseline sedimentation rates over the past 20 000 years are low and ca. 1 mm yr^{-1} up to ca. 1000 cal. BP. From then onwards floodplain sedimentation starts to increase, peaking over the past 400 years with rates up to $10\text{-}30 \text{ mm yr}^{-1}$. The majority of river and floodplain sediments are lavaka-derived (Cox *et al.* 2009), thereby independently confirming this time frame of increased lavaka activity. In order to link the evolution of environmental pressure with lavaka population dynamics we formulated a temporally explicit lavaka population model, where different environmental pressure scenarios were evaluated. Modelling outcomes indicate that a strong recent increase in environmental pressure over the last centuries is needed to attain current disequilibrium levels.

While the onset of increased lavaka activity around 1000 cal. BP can be linked to both the start of a climatic drying trend (Li *et al* 2020) and the introduction of cattle and permanent human settlements in the area (Douglass *et al* 2019, Godfrey *et al* 2019), the recent acceleration cannot be explained by climatic changes alone and seems to be linked to increased anthropogenic pressure on the environment related to increasing human and cattle populations. With this study we show the potential of an integrated multiple source data-modelling approach, where demographic concepts are applied to geomorphic features, allowing to link their evolution with past (anthropogenic) environmental changes.

References

- Cox R, Bierman P, Jungers M C and Rakotondrazafy A F M 2009 Erosion rates and sediment sources in Madagascar inferred from ^{10}Be analysis of lavaka, slope, and river sediment *J. Geol.* 117 363–76
- Dewar R E 2014 Early human settlers and their impact on Madagascar’s landscapes *Conservation and Environmental Management in Madagascar* ed I R Scales (Routledge) pp 44–64
- Douglass K, Hixon S, Wright H T, Godfrey L R, Crowley B E, Manjakahery B, Rasolondrainy T, Crossland Z and Radimilahy C 2019 A critical review of radiocarbon dates clarifies the human settlement of Madagascar *Quat. Sci. Rev.* 221 105878
- Godfrey L R, Scroton N, Crowley B E, Burns S J, Sutherland M R, Pérez V R, Faina P, McGee D and Ranivoharimanana L 2019 A new interpretation of Madagascar’s megafaunal decline: The “Subsistence Shift Hypothesis” *J. Hum. Evol.* 130 126–40
- Klein J 2002 Deforestation in the Madagascar Highlands - Established “truth” and scientific uncertainty *GeoJournal* 56 191–9
- Li H, Sinha A, André A A, Spötl C, Vonhof H B, Meunier A, Kathayat G, Duan P and Voarintsoa N R G 2020 A multimillennial climatic context for the megafaunal extinctions in Madagascar and Mascarene Islands *Sci. Adv.* 6 eabb2459
- Mietton M, Leprun J-C, Andrianaivoarivony R, Dubar M, Erismann J, Beiner M, Bonnier F, Grisori E, Rafanomezana J-P and Grandjean P 2005 Ancienneté et vitesse d’érosion des lavaka à Madagascar *Actes des Journées Sci. du réseau Eros. GCES l’AUF* 87–94
- Wells N A and Andriamihaja B 1993 The initiation and growth of gullies in Madagascar: are humans to blame? *Geomorphology* 8 1–46

Figure



A) Example of new lavaka being born (top) and stabilizing (bottom) over the period 1949-2018. Orange polygons indicate the lavaka extent, blue ones the bare surface area. B) Amount of newly born and stabilized lavaka and their ratio for each study area (SA) for the longest available time period (1949-2010s for SA1-5 and 1969-2010s for SA6).

Exploring the Curve Number method to predict gully head occurrence on the continental scale of Africa

Sofie DE GEETER^{1,2,3}, Matthias VANMAERCKE², Gert VERSTRAETEN¹, Jean POESEN^{1,4}

¹*KU Leuven, Division of Geography and Tourism, Department of Earth and Environmental Sciences, Celestijnenlaan 200E, 3001 Heverlee, Belgium (sofie.degeeter@kuleuven.be)*

²*University of Liège, Department of Geography, Clos Mercator 3, 4000 Liège, Belgium*

³*Research Foundation Flanders – FWO, Brussels, Belgium*

⁴*Maria-Curie Skłodowska University, Faculty of Earth Sciences and Spatial Management, Krasnicka 2D, 20-718, Lublin, Poland*

Gully erosion is an important land degradation process, threatening soil and water resources worldwide. However, in contrast to sheet and rill erosion, our ability to simulate and predict gully erosion remains limited, especially at the continental scale. Nevertheless, such models are essential for the development of suitable land management strategies, but also to better quantify the role of gully erosion in continental sediment budgets. We aim to bridge this gap by developing a first spatially explicit and process-oriented model that simulates average gully erosion rates at the continental scale of Africa.

We are developing a model that predicts the likelihood of gully head occurrence by means of the Curve Number (CN) method. This model will allow to simulate the spatial patterns of gully density at high resolution (30m) based on the physical principles that control the gully erosion process by using GIS and spatial data sources that are available at the continental scale. To calibrate and validate this model, we make use of an extensive database of 44 000 gully heads mapped over 1680 sites that are randomly distributed across Africa. The exact location of all gully heads was manually mapped by trained experts, using high resolution optical imagery available in Google Earth. This allows to extract very detailed information at the level of the gully head, such as the local slope and the area draining to the gully.

Based on an explorative analysis on a subset of this dataset we found that the CN method does not directly allow to make reliable predictions on gully head occurrence within a pixel. Although land use and land cover seem to play an important role (with gully heads being clearly located in erosion-prone land use classes), the hydrological soil groups (HSGs) based on soil texture do not provide a clear relation between soils with high runoff risk and gully occurrence. A potential cause for this is likely that compensating soil effects occur: i.e. HSGs that produce low runoff volumes may be characterized by a lower soil cohesion, making them nonetheless prone to gullying. This may then cause the combination of HSG and land use to be an insignificant predictor of gully occurrence. Also uncertainties on the input data likely play an important role in this.

Overall, our results indicate that modelling gully densities using a process-oriented and spatially explicit method offers opportunities to better quantify this important land degradation process at the global scale. Nevertheless, a key challenge lies in accurately quantifying the importance of soil characteristics and especially in better understanding their relative contribution to runoff production and soil cohesion.

Landslide and flash flood timing from satellite radar imagery in the western branch of the East African Rift

Axel DEIJNS^{1,2*}, Olivier DEWITTE¹, Wim THIERY², Nicolas D'OREYE^{3,4}, Jean-Philippe MALET⁵, & François KERVYN¹

¹ *Department of Earth Sciences, Royal Museum for Central Africa, 3080 Tervuren, Belgium*

² *Department of Hydrology and Hydraulic Engineering, Earth System Science, Vrije Universiteit Brussel, 1050 Elsene, Belgium*

³ *Department of Geophysics/Astrophysics, National Museum of Natural History, 2160 Walferdange, Luxembourg*

⁴ *European for Geodynamics and Seismology, 7256 Walferdange, Luxembourg*

⁵ *École et Observatoire des Sciences de la Terre, Institut de Physique du Globe de Strasbourg, Centre National de la Recherche Scientifique, University of Strasbourg, UMR 7516 Strasbourg Cedex, France*

*Corresponding Author. Email: axel.deijns@africamuseum.be

Geomorphic hazards such as landslides and flash floods (hereafter called GH) often result from a combination of complex interacting physical and anthropogenic processes across multiple spatial and temporal scales. In many instances, GH occur very quickly, sometimes in a matter of a few hours occasionally leading to catastrophic impact on human lives. Given that they are mostly related to common meteorological events, GH frequently co-occur and interact, leading to more severe impacts. The tropics are environments where GH are under-researched while, in the meantime, GH disproportionately impact these regions. In addition, GH frequency and/or risks in the tropics are expected to increase in the future in response to increasing demographic pressure, climate change and land use/cover changes. To understand the role of climate and landscape (topographic and land use/cover) in controlling the spatio-temporal distribution of GH in the context of environmental change, establishing a regional-scale inventory of GH events that are localised accurately in space and time is essential. In this study we focus on the accurate detection of GH timing using remote sensing. The tropics are frequently cloud covered and an accurate characterization of the timing of GH at a regional scale can only be achieved through the use of Synthetic Aperture Radar (SAR) due to its cloud penetrating capabilities. The objective here is to present the methodology and results of our research on the use of SAR amplitude and phase coherence data to accurately estimate the timing of landslide and flash flood events with a multi-temporal change analysis approach. The method is applied on four case studies located in tropical Africa, more specifically, in the western branch of the East African Rift. Copernicus Sentinel 1 (SAR imagery) is the key satellite product used, which next to being open access, offers a very good trade-off between frequency of acquisition and spatial resolution. The actual timing of the events (as a means for validating the estimations from the methodology) is captured using information from three citizen observer networks and high temporal resolution optical imagery. The results show that both amplitude and phase coherence can provide valuable information for event timing detection. Estimated event timing from phase coherence time series ranges from a couple of days to a one month difference. Estimated timing using a derivative of the amplitude ranges from a couple of days to a maximum of 2,5 months difference. This research is one of the first to show the capabilities of radar remote sensing to constrain the timing of GH events with an accuracy much higher than what can be obtained from optical imagery in cloud-covered environments. These methodological results have the potential to be implemented in cloud-based computing platforms to improve GH detection tools at regional scales, which in turn helps to establish unprecedented inventories of GH processes in changing environments like the East African Rift.

Application of Photogrammetry in Earth Sciences: Case Study of Lava Accumulation and Ground Deformation in an Active Volcanic Crater

Louise DELHAYE^{1,2}, Julien BARRIÈRE³, Nicolas D'OREYE^{3,4}, François KERVYN, Adrien OTH³, Benoît SMETS^{1,2}

¹ *Natural Hazards Service, Dpt. Of Earth Sciences, Royal Museum for Central Africa, Tervuren, Belgium*

² *Cartography and GIS Research Group, Dpt. of Geography, Vrije Universiteit Brussel, Brussels, Belgium*

³ *European Centre for Geodynamics and Seismology, Walferdange, Luxembourg*

⁴ *Dpt. of Geophysics/Astrophysics, National Museum of Natural History, Walferdange, Luxembourg*

SfM photogrammetry is a technique that provides useful products for geoscientists, which include 3D point clouds, digital elevation models (DEMs) and mosaics of orthophotos (i.e., orthomosaics). It is increasingly used in Earth sciences for its ability to measure 3D geological or geomorphological structures, topographic changes and, sometimes, ground surface deformation, in an efficient and relatively low-cost way. When used in time series, photogrammetric products are efficient to study into details geohazards associated with, e.g., landslides, volcanoes, coastal erosion, etc. To produce time series of photogrammetric products, co-registration is important to allow a proper comparison between each periods of image acquisition, or epochs. Co-aligning all the epochs during image matching (i.e., multi-epoch alignment) is amongst the recommended best practices. However, this technique shows limitations when the epochs are not similar, i.e., not composed of images acquired with a relatively similar viewing geometry, with the same camera or type of camera. In this work, we produce a time-series of dense point clouds and DEMs of the summit crater of Nyiragongo volcano, in order to test the best way to co-align epochs made of highly different image acquisitions and derive accurate measurements on the summit eruptive activity. Our results highlight that, if multi-epoch co-alignment works well for homogeneous time-series, it is actually more complex when the image datasets are acquired with varying types of equipment, in harsh volcanic environment. Depending on the time series, selecting other options for co-registration may provide similar or better results than with the multi-epoch co-alignment. In the case of Nyiragongo crater, co-aligning the images of each epochs on a reference epoch that is, first, independently processed provide the best co-registration result. This option also has the advantage of allowing the co-alignment of newly acquired epochs without the need to reprocess the entire time-series each time. In terms of measurements, the photogrammetric products allowed us to derive accurate volume estimates of the lava accumulated in the summit crater between 2002 and 2018. These lava volume estimates correlate with those derived from satellite remote sensing. By comparing the 2013 and 2014 epochs, ground subsidence was also accurately measured on the bottom of the crater around the lava lake. All the measured changes and the mapping performed using the photogrammetric time series provide key information to better understand the dynamics of the Nyiragongo lava lake and the rate of lava accumulation in the main crater.

The LASUGEO project: monitoring LAND Subsidence caused by Groundwater exploitation through gEOdetic measurements

Xavier DEVLEESCHOUWER¹, Atefe CHOOPANI^{1,2}, Aline MOREAU², Kristine WALRAEVENS³, Marc VAN CAMP³, Michel VAN CAMP⁴, Kevin GOBRON⁴, Alain DASSARGUES², Philippe ORBAN², Pierre-Yves DECLERCQ¹

1. *Royal Belgian Institute of Natural Sciences, Geological Survey of Belgium, Rue Vautier 29, 1000 Brussels, Belgium* (xdevleeschouwer@naturalsciences.be ; achoopani@naturalsciences.be ; pydeclercq@naturalsciences.be)
2. *Liège University, Hydrogeology & Environmental Geology, Urban & Environmental Engineering, allée de la Découverte 9, 4000 Liège, Belgium* (aline.moreau@uliege.be ; alain.dassargues@uliege.be ; p.orban@uliege.be)
3. *Gent University, Department of Geology, Krijgslaan 281, S8, 9000 Gent, Belgium* (kristine.walraevens@ugent.be ; marc.vancamp@ugent.be)
4. *Royal Observatory of Belgium, Avenue Circulaire, 3, 1180 Brussels, Belgium* (michel.vancamp@seismologie.be ; kevin.gobron@oma.be)

In the last decades, rapid urbanization, global climate change and uncontrolled anthropogenic transformations of the territory caused a relevant increase in geo-hazards events with huge economic and social consequences. The dramatic increase of these events with environmental degradation highlights the importance of improving ground monitoring and natural resources management with a continuous exchange of knowledge between the scientific community and authorities in charge of environmental risk management. Since the late 1990s, SAR (Synthetic Aperture Radar) data allow measuring slow-moving ground deformations. In the last decades, the use of spaceborne InSAR (Interferometric SAR) has increased significantly thanks to the availability of large-area coverage, millimetre precision, high spatial/temporal data resolution and good cost-benefit. For the last 3 decades, the development of Multi-Temporal Interferometric SAR techniques (MT-InSAR), commonly grouped into PSI-like (Persistent Scatterers Interferometry) and SBAS-like (Small Baseline Subset) algorithms, has changed the way radar images can be exploited for geohazard monitoring (natural gas extraction, mining activities, groundwater overexploitation, karst or landslides processes, etc.). Most of the subsidence bowls mapped by the PSI technique in Belgium have been related to strong fluctuations of an aquifer implying at the surface ground deformations (Declercq et al., 2017; 2021). Besides, the recent dry years are related to ground stability problems in large areas of Flanders. Land subsidence poses significant problems. The most affected regions lie on compressible loose sediments. Any change in the piezometric heads modifies the pore pressure, which may induce consolidation if the geological formations are compressible. Geomechanical aspects are fully coupled to groundwater flow equations. If groundwater levels and pressures are restored, a partial rebound (uplift) corresponding to the elastic part of the geological formations is observed. Consolidation and elastic rebound processes occur in confined and unconfined conditions. The most sensitive parts of the concerned aquifers contain clay, loam or peat lenses but consolidation may occur mostly in the underlying and overlying layers that are often less permeable and more compressible than the aquifer itself. In this case, it is largely a delayed process occurring as far as the pore pressure variation slowly propagates in the low permeability (aquitard) layers. We propose to confront the results of the PSInSAR technique data with hydrogeological groundwater models and two other geodetic techniques: GNSS and gravimetry. LASUGEO

focuses on ground deformations in different areas in Belgium: the deep aquifer system of western Flanders, the Tertiary aquifer system in Central Flanders, the Antwerp area, the Leuven area and the Brussels Region.

The possible groundwater overexploitation needs to be established through a transient hydrogeological model considering all the stress factors applied to the aquifers. The estimated compaction in the subsiding bowls will be compared with 1D geomechanical model results. The latter will be performed using geotechnical effective stresses as deduced from the pore pressure distribution from the hydrogeological model (Dassargues et al., 1989). These different steps will be done by the partners of the LASUGEO project that are involved in the different case study areas.

References

- Dassargues, A. Schroeder, C. and X.L. Li, X. L., 1993. Applying the Lagamine model to compute land subsidence in Shanghai. *Bulletin of Engineering Geology and the Environment*, 47, 13-26.
- Declercq, P.-Y. Walstra, J. Gérard, P. Pirard, E. Perissin, D. & Devleeschouwer, X., 2017. Subsidence related to groundwater pumping for breweries in Merchtem are (Belgium) highlighted by Persistent Scatterer Interferometry. *International Journal of Applied Earth Observations and Geoinformation*, 63, 178–185.
- Declercq, P.-Y. Gérard, P. Pirard, E. Walstra, J. & Devleeschouwer, X., 2021. Long-Term Subsidence Monitoring of the Alluvial Plain of the Scheldt River in Antwerp (Belgium) Using Radar Interferometry. *Remote Sensing* 13/6: 1160.

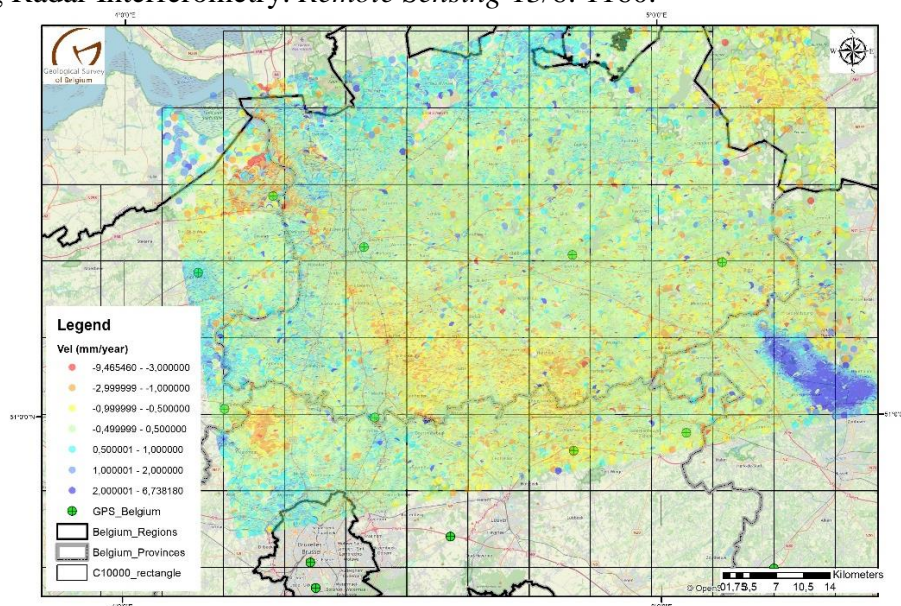


Figure. PSInSAR data showing the average LOS velocities (in mm/year) from Sentinel-1A ascending scenes (2016-2020) covering a large area in Flanders (between Brussels and Antwerp). Red colours indicate land subsidence areas while the blue colours indicate uplifting ground deformations. Green circles are the GNSS stations located in that area.

Landslide timing in the changing environments of the North Tanganyika-Kivu Rift region, Africa

Olivier DEWITTE ¹, Axel DEIJNS ^{1,2}, Arthur DEPICKER ³, Antoine DILLE ¹, Violet KANYIGINYA ^{1,4,5}, Désiré KUBWIMANA ^{6,7}, Jean-Claude MAKI MATESO ^{8,9}, Toussaint MUGARUKA BIBENTYO ^{1,10,11}, John SEKAJUGO ^{4,5,12}

1. *Department of Earth Sciences, Royal Museum for Central Africa, Tervuren, Belgium*
(*olivier.dewitte@africamuseum.be, axel.deijns@africamuseum.be, antoine.dille@gmail.com, violet.kanyiginya@vub.ac.be, toussaint.mugarukabibentyo@UGent.be*)
2. *Department of Hydrology and Hydraulic Engineering, Vrije Universiteit Brussel, Brussels, Belgium*
3. *Department of Earth and Environmental Sciences, KU Leuven, Leuven, Belgium*
(*arthur.depicker@kuleuven.be*)
4. *Department of Geography, Vrije Universiteit Brussel, Brussels, Belgium*
(*sekajugo@gmail.com*)
5. *Mbarara University of Science and Technology, Department of Environment and Livelihoods Support Systems, Mbarara, Uganda*
6. *Department of Earth Sciences, University of Burundi, Bujumbura, Burundi*
(*desire.kubwimana@ub.edu.bi*)
7. *Department of Earth Sciences, Mohammed V University, Rabat, Morocco*
8. *Department of Geophysics, Centre de Recherche en Sciences Naturelles, Lwiro, DR Congo*
(*makigeo2013@gmail.com*)
9. *Earth and Life Institute, Université catholique de Louvain, Louvain-la-Neuve, Belgium*
10. *Department of Geology, Université Officielle de Bukavu, Bukavu, DR Congo*
11. *Department of Geology, Ghent University, Ghent, Belgium*
12. *Mountains of the Moon University, School of Agriculture and Environmental Sciences, Fort Portal, Uganda*

Understanding when landslides occur and how they evolve is fundamental to grasp the dynamics of the landscapes and anticipate the dangers they can offer up. However, knowledge on the timing of the landslides remains overlooked in large parts of the world. This is particularly the case in regions where infrastructures are weak or absent and data scarcity is common. Many populated regions of the tropics stand out as such places, despite being affected by high and increasing landslide impacts. There, persistent cloud cover, rapid natural vegetation regeneration, cultivation practices and deep weathering further challenge the harvest of timing information. We present key findings on the characterisation of the timing of the landslides in the North Tanganyika-Kivu Rift region in Africa, a changing tropical environment lacking baseline studies where population density is high and on the rise. From an inventory of more than 15000 landslides with various timing accuracy (from daily to thousands of years), we identify causes and triggers of the slope instabilities in a context of important human-induced landscape changes. The interaction between uplift associated with the continental rifting in the region and fluvial incision, deforestation, and urban growth are key elements that are considered in our analysis. This is achieved through a holistic approach that combines fieldwork, optical and SAR/InSAR satellite remote sensing, time-series analysis, UAS image acquisition, historical photograph processing, citizen science and geomorphic marker understanding.

References

- Depicker, A., Govers, G., Jacobs, L., Campforts, B., Uwihirwe, J., Dewitte, O., 2021. Interactions between deforestation, landscape rejuvenation, and shallow landslides in the North Tanganyika – Kivu Rift region, Africa. *Earth Surface Dynamics* 9, 445–462.
- Dewitte, O., Dille, A., Depicker, A., Kubwimana, D., Maki Mateso, J.C., Mugaruka Bibentyo, T., Uwihirwe, J., Monsieurs, E., 2021. Constraining landslide timing in a data-scarce context: from recent to very old processes in the tropical environment of the North Tanganyika-Kivu Rift region. *Landslides* 18, 161–177.
- Dille, A., Kervyn, F., Handwerger, A.L., d'Oreye, N., Derauw, D., Mugaruka Bibentyo, T., Samsonov, S., Malet, J.-P., Kervyn, M., Dewitte, O., 2021. When image correlation is needed: unravelling the complex dynamics of a slow-moving landslide in the tropics with dense radar and optical time series. *Remote Sensing of Environment* 258, 112402.
- Dille, A., Kervyn, F., Mugaruka Bibentyo, T., Delvaux, D., Bamulezi Ganza, G., Ilombe Mawe, G., Kalikone Buzera, C., Safari Makito, E., Moeyersons, J., Monsieurs, E., Nzolang, C., Smets, B., Kervyn, M., Dewitte, O., 2019. Causes and triggers of deep-seated hillslope instability in the tropics – insights from a 60-year record of Ikoma landslide (DR Congo). *Geomorphology* 345, 106835.
- Jacobs, L., Kabaseke, C., Bwambale, B., Katutu, R., Dewitte, O., Mertens, K., Maes, J., Kervyn, M., 2019. The geo-observer network: A proof of concept on participatory sensing of disasters in a remote setting. *Science of the Total Environment* 670, 245–261.
- Kubwimana, D., Ait Brahim, L., Nkurunziza, P., Dille, A., Depicker, A., Nahimana, L., Abdelouafi, A., Dewitte, O., 2021. Characteristics and Distribution of Landslides in the Populated Hillslopes of Bujumbura, Burundi. *Geosciences* 11, 259.
- Monsieurs, E., Jacobs, L., Michellier, C., Basimike Tchangaboba, J., Bamulezi Ganza, G., Kervyn, F., Maki Mateso, J.-C., Mugaruka Bibentyo, T., Kalikone Buzera, C., Nahimana, L., Ndayisenga, A., Nkurunziza, P., Thiery, W., Demoulin, A., Kervyn, M., Dewitte, O., 2018. Landslide inventory for hazard assessment in a data-poor context: a regional-scale approach in a tropical African environment. *Landslides* 15, 2195–2209.

Close-range remote sensing of large consecutive rockfall events from a permafrost rock face, Mattertal, Switzerland

Hanne HENDRICKX ^{1*}, Gaëlle LE ROY ², Agnès HELMSTETTER ³, Eric POINTNER ⁴, Eric LAROSE ⁵, Luc BRAILLARD ⁶, Jan NYSSSEN ⁷, Reynald DELALOYE ⁸, Amaury FRANKL ⁹

¹ Department of Geography, Ghent University, Belgium (hanne.hendrickx@ugent.be)

² Univ. Grenoble Alpes, Univ. Savoie Mont Blanc, CNRS, IRD, Univ. Gustave Eiffel, ISTERre, Grenoble, France / Géolithe, Crolles, France (gaelle.le-roy@univ-grenoble-alpes.fr)

³ Univ. Grenoble Alpes, Univ. Savoie Mont Blanc, CNRS, IRD, Univ. Gustave Eiffel, ISTERre, Grenoble, France (agnes.helmstetter@univ-grenoble-alpes.fr)

⁴ Rovina & Partner AG, Visp, Switzerland (eric.pointner@rpgeol.ch)

⁵ Univ. Grenoble Alpes, Univ. Savoie Mont Blanc, CNRS, IRD, Univ. Gustave Eiffel, ISTERre, Grenoble, France (eric.larose@univ-grenoble-alpes.fr)

⁶ Department of Geosciences, University of Fribourg, Switzerland (luc.brillard@unifr.ch)

⁷ Department of Geography, Ghent University, Belgium (jan.nyssen@ugent.be)

⁸ Department of Geosciences, University of Fribourg, Switzerland (reynald.delaloye@unifr.ch)

⁹ Department of Geography, Ghent University, Belgium & INRAE, AMAP, IRD, CIRAD, CNRS, University Montpellier, Montpellier, France (amaury.frankl@ugent.be)

Rockfall is a major geomorphic process in high mountains situated in cold climates. While primarily controlled by lithology and orientation of geological structures, changes in precipitation and temperature caused by climate change is expected to alter the magnitude and frequency of rockfall events. As temperature increases, the strength of ice-filled joints is reduced. Permafrost degradation has therefore been related to an increase in rockfall events over the last three decades in European Alps, exposing communities to natural hazards.

To increase our understanding of rockfall events and its preconditions, we monitored the rockfall activity at the Grosse Grabe rock face (2700 m a.s.l., Mattertal, Western Swiss Alps) in a timespan of four years (2017-2020). Due to the study sites inaccessibility, we used a combination of several close-range remote sensing techniques to study morphologic and morphometric changes. The monitoring of the rock face started in 2011 with a fixed automatic camera taking photographs every hour, originally in place for the monitoring of nearby rock glaciers. This makes the presented dataset unique since data collection started before any major rockfall event. After detection of the first rockfall activity since the start of the observations, more detailed Terrestrial Laser scanning (TLS) and Uncrewed Aerial Vehicle (UAV) surveys were performed. This allowed to quantify pre-failure displacement, rockfall location and volume. A complete dataset of all individual rockfall events, including exact timing and estimated volumes, could then be established using seismic data from a nearby rock glacier study site.

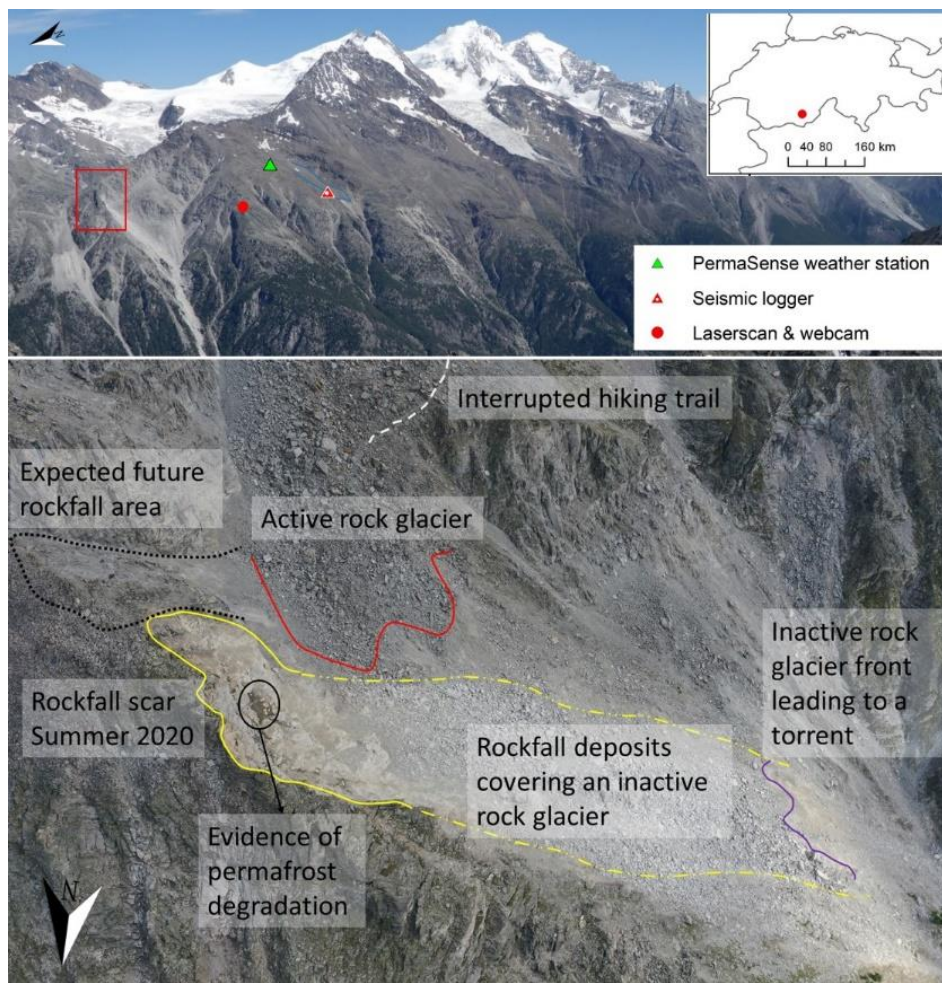
In total 339 rockfall events were observed, including 11 larger events above 5000 m³, depositing more than 200 000 m³ of debris. The highly fractured gneiss lithology is viewed as the main precondition for the observed magnitude and frequency of the rockfall events, while permafrost degradation is viewed as a triggering factor, believed to be responsible for the observed outward displacement of the rock face during summer. The largest rockfall events ($\geq 5000 \text{ m}^3$) were precluded by warmer periods and systematically exposed ice in the clefts. Its exposure caused follow-up rockfall events due to thermal adjustment and unloading. Measured pre-failure displacement indicates that further rockfall events will still take place.

Due to the specific timing and location of the large rock fall events, the deposits will remain stationary, posing no real threat to downslope communities at present.

References

- Davies, M. C. R., Hamza, O. & Harris, C (2001). The effect of rise in mean annual temperature on the stability of rock slopes containing ice-filled discontinuities. *Permafr. Periglac. Process.* 12, 137–144.
- Fischer, L., Purves, R. S., Huggel, C., Noetzli, J. & Haeberli, W. (2012) On the influence of topographic, geological and cryospheric factors on rock avalanches and rockfalls in high-mountain areas. *Nat. Hazards Earth Syst. Sci.* 12, 241–254
- Gruber, S. & Haeberli, W. (2007) Permafrost in steep bedrock slopes and its temperatures-related destabilization following climate change. *J. Geophys. Res. Earth Surf.* 112, F02S18
- Hasler, A., Gruber, S. & Beutel, J. (2012) Kinematics of steep bedrock permafrost. *J. Geophys. Res. Earth Surf.* 117
- Hendrickx, H., Le Roy, G., Helmstetter, A., Pointner, E., Larose, E., Braillard, L., Nyssen, J., Delaloye, R., Frankl, A. (Submitted) A high resolution record of a disintegrating permafrost rock face, Matternal, Switzerland. *Earth Surf. Proc. Land.*
- Ravanel, L., Magnin, F. & Deline, P. (2017) Impacts of the 2003 and 2015 summer heatwaves on permafrost-affected rock-walls in the Mont Blanc massif. *Sci. Total Environ.* 609, 132–143

Figure



Numerical Modeling of Volcanic Edifice Degradation: Towards an Integrated Understanding of Edifice Morphologic Evolution

Daniel O'HARA, Roos Marina Johanna van WEES, Matthieu KERVYN

*Department of Geography, Vrije Universiteit Brussel, Brussels, Belgium
(daniel.ohara@vub.be)*

Volcanic edifices represent a set of dynamic landforms whose morphology encodes the long-term (thousands to millions of years) interaction between construction and erosion. Short-term (years to decades) volcanic processes cumulatively build topography through both subsurface intrusions of shallow magma bodies and surface-mantling of lava flows and tephra deposits. Over longer timescales, these processes compete with climate-based erosive processes that incise and degrade landforms, generating a variety of edifice morphologies.

Despite the relevance of disentangling edifice morphologic histories to better discern a region's volcanic record and assess potential hazards, studies related to volcanic landform evolution have been limited. Multiple studies have analyzed a variety of edifice types (e.g., cinder cones, shields, and stratovolcanoes), generating a set of morphometrics that distinguish degrees of edifice degradation on both global- and arc-scales. However, how these metrics relate to the morphologic evolution of edifices has been restricted to small-scale cinder cones within select environments.

Numerical landscape evolution modeling remains one of the most efficient methods to analyze and understand landform development. By combining equations that approximate hillslope erosion and river channel incision with drivers of landscape evolution (e.g., surface uplift, changing lithology, gradational precipitation) within a numerical environment, previous studies have had success in distinguishing the processes that govern landscape morphology and reconstructing past topography within tectonic settings.

Here, we present our analysis of edifice degradation history using landscape evolution models. Starting with idealized stratovolcano shapes, we test the impact of changing lithology, precipitation, and growth rate on edifice morphology over 100 kyr timescales. With these models, we determine a set of morphometrics that describes the evolution of erosion throughout an edifice's lifespan. Furthermore, we derive a series of nondimensional parameters that distinguishes the processes that govern edifice shapes. Finally, we compare the results of our numerical models to satellite data of real edifices to analyze the competition of processes and resulting landform evolution within a natural environment.

Large landslides and ice sheets: the Patagonian lesson

Tomáš PÁNEK

Department of Physical Geography and Geoecology, Faculty of Science, University of Ostrava, Chittussiho 10, Ostrava 710 00, Czech Republic (tomas.panek@osu.cz)

The current deglaciation of alpine and polar regions requires an understanding of the temporal and spatial aspects of slope instability. However, to date, only a few inventories have focused on systematic mapping of large populations of landslides over extensive deglaciated areas, such as ice sheets (e.g. Crosta et al., 2013). To reveal the factors influencing large scale paraglacial landslide distribution, we performed landslide inventory for the unprecedentedly large area (~305,000 km²) within the Last Glacial Maximum (LGM; ~35 ka) limits of the Patagonian Ice Sheet (PIS). Patagonia is a unique natural laboratory for research on paraglacial landslides. The territory was covered in the Pleistocene by one of the world's largest ice sheets and available paleoenvironmental data provides excellent background information for assessing the spatial pattern of the slope response to post-LGM ice retreat (Davies et al., 2020).

We mapped footprints of all large landslides (≥ 1 km²) within the PIS region defined by Davies et al. (2020) using GeoEye-1 satellite images (Maxar dataset from ESRI™ World Imagery service) and TanDEM-X digital elevation model. To obtain chronological information about landslides, GIS analyses were supplemented by field morphostratigraphical research and OSL and radiocarbon dating of selected landslides (Pánek et al., 2018, 2020; Schönfeldt et al., 2020). Of the 1,475 mapped large landslides, more than one-third concentrate in a 10-km-wide zone along the eastern LGM margin of PIS while they are almost absent in the Patagonian Andes. This distribution of mass movements in Patagonia is peculiar compared to other tectonically active glaciated orogens (such as Southern Alps of New Zealand or Himalayas): large landslides are relatively scarce here, and they are concentrated in the driest and topographically least exposed part of the mountain range. Despite the extreme values of postglacial isostatic uplift (up to 39 mm yr⁻¹; Dietrich et al., 2010), large landslides do not overlap with the fastest uplifted area, and they are almost absent in the vicinity of major faults such as Liquiñe-Ofqui and Magallanes-Fagnano strike-slip faults (Pánek et al., 2021).

The chronology of the largest landslides and rock avalanches along the eastern foothills of the Patagonian Andes followed the deglaciation pattern. Rotational slides and spreads affecting the margins of volcanic plateaus have been active since deglaciation ~35 ka ago and their activity has continued in the last 5 ka (Schönfeldt et al., 2020). On the other hand, the largest catastrophic rock avalanches with volume >1 km³ probably occurred mainly during the short transitional period after deglaciation, and many of them descended into glacial meltwater lakes (Pánek et al., 2018, 2020).

We conclude that 1) lithology rather than topography controls distribution of large landslides in the Patagonia, 2) highest parts of Patagonian Andes lacks major landslides due to occurrence of hard rocks and the existence of “matured” glacial topography related to very long (~6 Ma) glaciation (much more than other world orogens) with glacial valleys well adapted to efficient ice discharge, and 3) eastern margin of PIS has been affected by large landslides due to spatial coincidence of a large mass of remaining weak rocks, presence of the long-term oscillating ice sheet front in the last ~35 ka, and draw-downing glacial lakes. Lesson from the Patagonian Andes shows that the presence of hard rocks can prevent origin of large landslides in paraglacial landscapes, especially if the terrain has been indurated by long-term repeated glaciations. In such areas, large landslides can be expected mainly along

the glacial forefield, where glacial erosion has not been so effective, and the area is covered by unconsolidated glacial sediments.

References

- Crosta, G., Frattini, P. & Agliardi, F., 2013. Deep seated gravitational slope deformations in the European Alps. *Tectonophysics* 605, 13-33.
- Davies, B.J., Darvill, Ch.M., Lovell, H., Bendle, J.M., Dowdeswell, J.A., Fabel, D., García, J.L., Geiger, Al., Glasser, N.F., Gheorghiu, D.M., Harrison, S., Hein, A.S., Kaplan, M.R., Martin, J.R.V., Mendelova, M., Palmer, A., Pelto, M., Rodés, Á., Sagredo, E.A., Smedley, R.K., Smellie, J.L. & Thorndycraft, V.R., 2020. The evolution of the Patagonian Ice Sheet from 35 ka to the present day (PATICE). *Earth-Science Reviews* 204, 103152.
- Dietrich, R., Ivins, E.R., Casassa, G., Lange, H., Wendt, J. & Fritschke, M., 2010. Rapid crustal uplift in Patagonia due to enhanced ice loss. *Earth and Planetary Science Letters* 289, 22-29.
- Pánek, T., Korup, O., Lenart, J., Hradecký, J. & Břežný, M., 2018. Giant landslides in the foreland of the Patagonian Ice Sheet. *Quaternary Science Reviews* 194, 39-54.
- Pánek, T., Schönfeldt, E., Winocur, D., Břežný, M., Šilhán, K., Chalupa, V. & Korup, O., 2020. Moraines and marls: Giant landslides of the Lago Pueyrredon valley in Patagonia, Argentina. *Quaternary Science Reviews* 248, 106598.
- Pánek, T., Břežný, M., Winocur, D., Kilnar, J., 2021. Complex causes of landslides after ice sheet retreat: post-LGM mass movements in the Northern Patagonian Icefield region. *Science of the Total Environment* 758, 143684.
- Schönfeldt, E., Pánek, T., Winocur, D., Šilhán, K. & Korup, O., 2020. Postglacial Patagonian mass movement: From rotational slides and spreads to earthflows. *Geomorphology* 367, 107316.

How to integrate outbreak risk issues from drainage adits from abandoned mines in land use planning: a tool for decision-makers

Benedicta RONCHI, Fabian STASSEN, Jean-Pierre DREVET, Mathieu VESCHKENS

ISSeP, Institut Scientifique de Service Public, Liège, Belgium (b.ronchi@issep.be; f.stassen@issep.be; drevet.jp@issep.be; m.veschkens@issep.be)

Mining activities can affect the environment decennia after extraction activities stopped. Once extraction activities stopped, flooding of the abandoned mines (i.e. ground water rebound) starts until the mine water surface equilibrates with the regional ground water surface or reaches a point of discharge, e.g. a drainage adit. Consequently, outbreak, flooding and/or stability problems can occur in the surrounding area (Wolkersdorfer, 2008). Mining risk management is thus an important issue to ensure public safety where extraction activities were intense during several centuries, e.g. in Wallonia (Pacyna and Salmon, 2012). Following the observation of an increasing number of problems at these poorly known drainage adits, the Walloon Mining Authority decided to draw up a prevention plan covering all drainage adits in Wallonia. This plan initially consists of making an inventory of the dewatering galleries, prioritising them according to outbreak hazards, and finally defining the potentially impacted areas. The methods are applied on a regional scale, over the entire inventory with automated tools when possible.

Mapping the galleries consists of georeferencing old mining maps and vectorising each gallery with its localisation uncertainties. In 2021, the inventory covers more than 420 galleries in the districts of Namur and Liège. In order to apprehend the outbreak hazard, no robust statistical analysis could be carried out as only few poorly documented incidents were recorded in the archives. A method of prioritising galleries according to criticality scores has been developed. Since only cartographical data are available over the whole inventory, four parameters influencing outbreak hazard has been selected:

- the maximum hydrostatic pressure was calculated by the difference between the maximum elevation of the relief at the gallery and the topographic level of the gallery exit;
- the length of the gallery was used to approximate the void volume or the volume of water that can potentially accumulate and easily be released within the gallery;
- the number of shafts potentially connected to the gallery were used as a proxy to estimate the size of the workings around the gallery;
- the distance between the mine outlet and a watercourse to assess the ease of water discharge.

The values of parameter were classified into scores (between 0 and 3 for increasing hazard) according to criteria selected from the literature and the distribution of these values for a sample of the gallery inventory. Different scenarios (i.e. 2 to 4 parameters, different weights) were tested in order to determine the sensitivity of the parameters. The final method (Table 1) was selected and validated by a committee of experts, by comparing the scores of known galleries where an incident had occurred in the past. In order to be able to easily apply the method each year to the latest galleries added to the inventory, the method was automated with the Model Builder function of ArcGis.

Table 1: Scoring criteria and weights for each parameter considered in the 'water outbreak' hazard analysis.

Score	0	1	2	3	Weight
Hydraulic pressure	0	>0	>10	>20	0.3
Gallery length	>0	>100	>200	>500	0.3
Number of shafts	0	>0	>5	>10	<u>0.1</u>
Distance to the nearest watercourse	<25	>25	>500m	>1000m	0.3

To delineate the area impacted by a water outbreak, one must delineate the drainage basin whose water source is the gallery outlet. Since no automatic technique allows indicating a point as a water source to delimit a flow basin, a stepwise approach has been proposed. Firstly, the watershed including the gallery outlet is delineated with the "Hydrology" package of the ArcGIS program. However this watershed covers areas located upstream from the gallery outlet. Moreover different hazard levels can be variable depending on the water level (Franck, 2018). As a first try, a waterlevel of 20cm is simulated for each gallery outlet. This allows to delineate the basin covered by 20cm of water.

Future work will include the completion of the inventory and fine-tuning the hazard assessing methods. Indeed, the scores of the parameters were determined on the basis of the mine workings of the Liège district. It will be important to validate this parameterization on the whole inventory, once it is completed. The water level heights to be used to delimit the flooding zones still need to be validated by the committee of experts and the method will have to be applied on a large number of galleries to validate its feasibility on the entire inventory.

We acknowledge SPW ARNE for financing this study and the technical committee (i.e. S. Roquet, J-M. Bamboneyho, L. Funcken, D. Pacyna, E. Lheureux, Prof. A. Dassargues) for their advice.

References

- Wolkersdorfer, C., 2008. Water Management at Abandoned Flooded Underground Mines: Fundamentals, Tracer Tests, Modelling, Water Treatment, Springer, 465 p.
- Pacyna, D. and Salmon, M., 2012. Mining risk management in Wallonia (Belgium): The WebGIS tools in the service of prevention. GESRIM 2012 Colloque "La gestion des rejets miniers et l'après mine".
- Franck C., Salmon R., Didier C., Paquette C. & Pokryszka Z., 2018. Guide Evaluation des aléas miniers. Rapport INERIS DRS-19-178745-02411A <https://www.ineris.fr/en/post-mining-hazard-evaluation-and-mapping-france> dernièrement consulté le 13 février 2020

Reliability of citizen scientists for near-real time reporting of geohazards. An analysis of biases and accuracy for the Rwenzori Mountains, Uganda

John SEKAJUGO^{1,2,3}, Grace R. KAGORO³, Liesbet JACOBS⁵, Clovis KABASEKE¹, Esther NAMARA¹, Olivier DEWITTE⁴ and Matthieu KERVYN²

¹*Mountains of the Moon University, School of Agriculture and Environmental Sciences, Fort Portal, Uganda (sekajugo@gmail.com)*

²*Vrije Universiteit Brussel, Department of Geography, Brussels, Belgium (Matthieu.Kervyn.De.Meerendre@vub.be)*

³*Mbarara University of Science and Technology, Department of Biology, Mbarara, Uganda (kgraceug2002@must.ac.ug)*

⁴*Royal Museum for Central Africa, Department of Earth Sciences, Tervuren, Belgium (Olivier.Dewitte@africamuseum.be)*

⁵*KU Leuven, Division of Geography and Tourism, Leuven, Belgium (Liesbet.jacobs@kuleuven.be)*

Documenting the occurrence of natural hazards and their impacts in near-real time is important for understanding the vulnerability levels and building resilience. However, recording frequent but low impact events that are spatially and temporally scattered is challenging. This challenge is even greater in rural areas of developing countries such as Uganda, where limited IT facilities prevent dissemination of information through social media. Here we analyse an inventory of geohazards (landslides and floods) reported by a network of citizen scientists in the Rwenzori Mountains, Uganda. This network of citizen (geo-) observers was established in February 2017 and was trained to collect temporally explicit geo-referenced information on geohazards and their impacts using smartphone technology. Since then, over 1300 hazard occurrences have been reported. We here assess the accuracy and potential biases affecting this citizen-science inventory and discuss the characteristics of the geo-observers and the of hazard events that might affect the reporting. We compare the geo-observer-based records with two independent inventories collected through systematic field mapping and PlanetScope satellite imagery mapping, focusing on landslide and flash flood events for the period between May 2019 and May 2020. Of the 221 landslide and 52 flash floods reported by geo-observers, 98.6% and 100% were respectively validated by fieldwork, suggesting a very low rate of false positive. In contrast, out of the 817 landslide and 116 flash flood occurrences mapped on satellite imagery, only 57% and 82% were confirmed as true positive by field work, respectively. The level of false negative (real events not reported) is however larger for geo-observer's data (about 45%) compared with the satellite imagery (about 29%). The amount and frequency of reporting depend both on geo-observer and hazard specific features. The older the geo-observer and the lesser he/she is engaged in off-farm employment (private business or formal employment), the higher are the chances of reporting. On the other hand, the more impactful the hazard is, the higher are the chances of it being publicized to be known and reported by a specific geo-observer. In addition, the further the event is from the geo-observer's residence and the community access routes, the higher are the chances that such an occurrence will not be reported. While satellite imagery mapping provides an opportunity to record geohazard occurrences even in extremely inaccessible places, small landslides are often missed while shallow ones can easily be confused with freshly cleared vegetation for crop planting. Depending on the topography of the area and the weather conditions, it can take several days to weeks before a cloud-free satellite image of a place can be obtained. Geo-observers hence provide an added value for documenting in near real time geo-referenced information for spatially spread but frequent hazards, something difficult to achieve with systematic field work or satellite imagery mapping.

Analyse morpho-tectonique sur la ville de Matadi dans la province du Kongo Central (R.D.C)

K.A. SEKERAVITI, H.A. IYOLO, L.O. TUEMA, C. L. MUKEBA, M.N.A.MAKUTU J.,
C.M.E. CIBAMBULA

*Université de Kinshasa, Faculté des Sciences, Dép. des Géosciences, B.P.190 Kinshasa XI
RDC*

Localisé entièrement dans la flexure formée par la chaîne West Congo dans son segment central (Tack et al., 2001 ; Cibambula, 2016), le relief moutonné de la ville de Matadi, perceptible également sur la rive droite du fleuve Congo, se traduit par des interfluves plus ou moins parallèles à l'écoulement du fleuve Congo de direction N132°. Ces interfluves sont entrecoupés en collines séparées les unes des autres par des vallées dissymétriques et à versants inclinés soit vers l'amont, soit vers l'aval des talwegs. Ce relief est également caractérisé par une succession des vallées rectilignes profondes ou non de direction N124° parallèles à l'écoulement de la rivière Mpozo. Cette diversité morphologique peut-elle être liée aux variations lithologiques, à leur dureté, à leur altérabilité climatique ou à leurs déformations tectoniques ?

D'après le levé géologique, toutes ces formes de relief affectent indistinctement aussi bien les schistes fissiles plus ou moins tendres de la Formation de Palabala que les roches dures de formations des métaquartzites de Matadi, du granite de Noqui et des metabasaltes de Gangila (Makutu et al., 2004). Les collines s'imbriquant partiellement, constituent les compartiments surélevés de failles inverses parallèles et conjuguées de direction N125°/16°SO et N159°/12°NE (Aubouin et al., 1979). Les versants de vallées entre ces collines sont abrupts en bordure des compartiments surélevés et en pente douce sur la bordure du compartiment affaissé dans le prolongement des plans de failles. Les vallées entre les interfluves orientées N44°E de même que celles parallèles à la rivière Mpozo de direction N170° résultent de l'altération très avancée des différents blocs de failles de Riedel contenues dans les zones d'endommagements de failles décrochantes parallèles à celles longées par le fleuve Congo et la rivière Mpozo.

Références:

- Aubouin, J., Brousse, R. et Lehman, J.P., (1979) : *Précis de géologie, tome 3 : Tectonique, tectonophysique, morphologie*, Dunod Université, 800p.
- Cibambula, C.M.E, (2016) : Le Sous-Groupe de la Mpioka : un flysch de la chaîne panafricaine West Congo dans le Kongo Central (R.D.Congo), *Th. de Doct. Inédit. Dép. Géosc. Unikin. 185p.*
- Makutu, M.N., Kanika, M., Bwanga, N., Nguangu, K. and Mpoyi, K., (2004) : Pétrologie et géochimie des roches magmatiques du complexe alcalin de Noqui (Bas-Congo, République Démocratique du Congo). *Bulletin du Centre de Recherches Géologiques et Minières*, 5 (1), 28-39.
- Tack, L., Wingate, M.T.D., Liégeois, J.P., Fernandez-Alonso, M., Deblond, A. (2001) : Early Neoproterozoic magmatism (1000-910 Ma) of the Zadinian and Mayumbian Groups (Bas-Congo) : onset of Rodinia rifting at the western edge of the Congo craton, *Prec. Res.*, 110, 277-306.

The May 2021 Flank Eruption of Nyiragongo Volcano, Democratic Republic of Congo

Benoît SMETS ^{1,2}, Julien BARRIÈRE ³, Corentin CAUDRON ⁴, Valérie CAYOL ⁵, Oryaëlle CHEVREL ⁵, Nicolas D'OREYE ^{3,6}, François DARCHAMDEAU ⁷, Louise DELHAYE ^{1,2}, Dominique DERAUW ^{8,9}, Halldór GEIRSSON ¹⁰, Raphaël GRANDIN ¹¹, Ephrem KAMATE KALEGHETSO ^{12,13}, Célestin KASEREKA MAHINDA ¹², Matthieu KERVYN ², Blaise MAFUKO NYANDWI ¹⁴, Joseph MAKUNDI ¹⁵, Caroline MICHELLIER ¹, Sander MOLENDIJK ¹³, Bosco MUHINDO MUSUBAO ¹⁴, Adalbert MUHINDO SYAVULISEMBO ¹², Olivier NAMUR ¹³, Ildephonse NGUOMOJA ¹⁵, Alain Joseph NTENGE ¹⁶, Adrien OTH ³, Sam POPPE ^{17,18}, Sergey SAMSONOV ¹⁹, Delphine SMITTARELLO ³, Josué SUBIRA ^{1,12,20}, Nicolas THEYS ²¹, Christelle WAUTHIER ²², Mathieu YALIRE MAPENDANO ¹², Thimm ZWIENER ^{1,2}, François KERVYN ¹

1. Natural Hazards Unit, Department of Earth Sciences, Royal Museum for Central Africa, Tervuren, Belgium (benoit.smets@africamuseum.be)
2. Department of Geography, Vrije Universiteit Brussel, Belgium (benoit.smets@vub.be)
3. European Center for Geodynamics and Seismology, Walferdange, Luxembourg
4. Institut des Sciences de la Terre de Grenoble, Chambéry, France
5. Laboratoire Magmas et Volcans, Université Clermont-Auvergne, Clermont-Ferrand, France
6. Department of Geophysics/Astrophysics, National Museum of Natural History, Walferdange, Luxembourg
7. ContourGlobal/Kivu watt Ltd, Kibuye, Rwanda
8. Centre Spatial de Liège, Liège, Belgium
9. Instituto de Investigación en Paleobiología y Geología, Universidad Nacional de Río Negro, General Roca, Argentina
10. Faculty of Earth Sciences, University of Iceland, Reykjavik, Iceland
11. Institut de Physique du Globe de Paris, Paris, France
12. Goma Volcano Observatory, Goma, D.R. Congo
13. Department of Earth and Environmental Sciences, Katholieke Universiteit Leuven, Leuven, Belgium
14. Department of Geology, University of Goma, Goma, D.R.Congo
15. Civil Protection – North Kivu Division, Goma, D.R.Congo
16. Rwanda Mines, Petroleum and Gas Board (RMB), Kigali, Rwanda
17. Université Libre de Bruxelles, Bruxelles, Belgium
18. Mars Exploration Laboratory, Space Research Centre PAS, Warsaw, Poland
19. Canada Center for Mapping and Earth Observation, National Resources Canada, Ottawa, Canada
20. Department of Geography, University of Liège, Liège, Belgium
21. Royal Belgian Institute for Space Aeronomy, Brussels, Belgium
22. Dpt. of Geosciences & Institute for Computational and Data Sciences, Pennsylvania State University, State College, U.S.A.

On 22nd May 2021, the Nyiragongo volcano (North Kivu, D.R. Congo) erupted without any warning, destroying buildings and infrastructures nearby and within the city of Goma. The flank eruption lasted only few hours, but was followed by a seismic crisis indicative of magma movement beneath Goma and Lake Kivu, which raised the possibility of a worst-case scenario that could have included lava erupting within the city (> 1 million inhabitants) and/or an eruption under Lake Kivu potentially leading to a lethal limnic eruption. In this work, we provide a description of the volcanic and

magmatic crisis based on the observations and data made and analyzed by the Goma Volcano Observatory (GVO) and the international group of scientists that assisted the GVO during this crisis. Through monitoring data, field surveys and remote sensing observations, we describe the unique characteristics of this eruption, highlight the differences and similarities with the two previous eruptions of 1977 and 2002, and provide an assessment of the impact made by the lava flows on the nearby population and infrastructures.

Remote Sensing of Geo-Hydrological Hazards in Central Africa

Benoît SMETS^{1,2}, Julien BARRIÈRE³, Olivier DEWITTE¹, Axel DEIJNS^{1,4}, Louise, DELHAYE^{1,2}, Arthur DEPICKER⁵, Dominique DERAUW^{6,7}, Antoine DILLE¹, Nicolas D'OREYE^{3,8}, Nicolas THEYS⁹, Thimm ZWIENER^{1,2}, François KERVYN¹

1. Natural Hazards Unit, Dpt. of Earth Sciences, Royal Museum for Central Africa, Tervuren, Belgium (benoit.smets@africamuseum.be)
2. Dpt. of Geography, Vrije Universiteit Brussel, Brussels, Belgium (benoit.smets@vub.be)
3. European Center for Geodynamics and Seismology, Walferdange, Luxembourg
4. Hydrology and Hydraulic Engineering, Vrije Universiteit Brussel, Brussels, Belgium
5. Dpt. of Earth and Environmental Sciences, Katholieke Universiteit Leuven, Leuven, Belgium
6. Centre Spatial de Liège, Liège, Belgium
7. Instituto de Investigación en Paleobiología y Geología, Universidad Nacional de Río Negro, General Roca, Argentina
8. Dpt. of Geophysics/Astrophysics, National Museum of Natural History, Walferdange, Luxembourg
9. Royal Belgian Institute for Space Aeronomy, Brussels, Belgium

Earth Observation (EO) using remote sensing (RS) has become a major tool for the study, monitoring, prevention and management of geo-hydrological hazards and associated disasters. Complementary to ground information, satellite-, aerial- and drone-based sensors help to get observations and measurements at different spatial and temporal scales, and sometimes in difficult-to-access areas, providing key intel for decision-making and field action. Geo-hydrological hazards encompass numerous different physical phenomena, e.g., volcanic activity, landslides, (flash) floods, earthquakes, etc. These natural processes, which are sometimes altered by anthropogenic activities, can be sporadic events that occur at various spatial and temporal scales, with possible interactions between them. It is therefore no surprise that their study through RS tends to challenge the existing techniques. During the past decade, new series of sensors and platforms have become real game-changers for the study of geo-hydrological hazards, thanks to both high-temporal and high-spatial resolution at the same time, and/or more sensitive sensors with a better signal-to-noise ratio. In addition, free access to remote sensing data for scientific research is an increasing trend, which promotes the use of EO, the processing of image time-series and the development of new methods.

In many regions, especially in developing countries, RS is the only solution to get quantitative measurements of the processes at play. In the present work, we show different and, sometimes, innovative RS approaches used to study geohydrological hazards in Central Africa. Different types of images are exploited: multispectral, radar, drone-based acquisitions, historical aerial photographs. The velocity of slow-moving landslides is measured using InSAR time-series methods, as well as with pixel-offset tracking techniques on both optical and radar images. The evolution of landslide risk is studied over several decades thanks to the combination of satellite imagery and historical aerial photographs. Difficult to access active craters and landslides are modelled in 3D thanks to SfM photogrammetry. The dynamics of the eruptive activity in active craters is studied by combining methods exploiting Sentinel-1, -2, -3 and -5P satellite images to measure, for the same time periods, the ground deformation, topographic changes, thermal radiations and gas emissions. Landslides and (flash) flood events are detected thanks to the specific properties of radar satellite images. Thanks to upcoming new images and sensors, new capabilities in terms of image fusion and recent developments in terms of cloud computing and machine learning, new perspectives and evolutions remain numerous.

Session 3- Planetary Magmatic and Metamorphic Systems

Conveners:

Jacqueline Vander Auwera (ULiège) ; Olivier Namur(KU Leuven)

Igneous activity has affected all planets. On Earth, the compositional variability of magmas is large and depends on the nature of the source, the conditions of partial melting as well as the on the effects of magmatic differentiation processes, such as crystal fractionation, mixing, assimilation or immiscibility. Basalts appear to be common to all rocky bodies but the abundance of highly evolved felsic magmas seems to be a characteristic of our planet.



Metamorphism will modify the rocks from their original igneous state. In most extraterrestrial bodies, fragmentation due to impacts is the main form of metamorphism but thermal and hydrothermal metamorphism has also been recognized in meteorites. On Earth, the dynamic evolution of the lithosphere is preserved in the metamorphic rock record that encompass a large variety of processes ranging from thermal to regional scale metamorphism.

This session will highlight research on case studies of magmatic differentiation starting from the formation of the solar system and meteorites, the partial melting of the upper mantle and lower crust, up to the formation of upper crustal melts. We welcome contributions in integrated metamorphic petrology and its application to the Earth lithosphere and rocky bodies.

The early growth of felsic continental crust revisited from Germanium/silicon *versus* silicon isotopic evidences

Luc ANDRÉ¹, Laurence MONIN^{1,2} and Axel HOFMANN³

¹ Tervuren, Belgium (luc.andre@africamuseum.be)

² Louvain, Belgium (laurence.monin@uclouvain.be)

³ Johannesburg, South Africa (ahofmann@uj.ac.za)

The recent discovery of heavy Si isotopic components in both high-Na Tonalite-Trondhjemite-Granodiorite (TTG) and High-K Granite-Monzonite-Syenite (GMS) components of the early continental growth (André et al., 2019; Deng et al., 2019) requires that a notable seawater-derived silica-rich component had been added in their respective protoliths. Here we use Ge/Si ratio as a complementary tracer to $\delta^{30}\text{Si}$ in order to delineate the exact role of modal quartz and silicified basalts from the Archean seafloor among the primary controls of the early appearance of felsic melts on Earth. We have approached the question by (1) specifying the Ge/Si signatures of various Archean and post-Archean rock types by compiling the Ge-SiO₂ data stored within the georock database; (2) coupling Ge/Si investigation to silicon isotopes on a large selection of silicified and unsilicified altered mafic and ultramafic greenstones, felsic volcanics, TTG and GMS granitoids and TTG's mineral separates from the Barberton Greenstone Belt (BGB) from South Africa.

The georock compilation demonstrates that Archean TTGs and granites display much lower Ge/Si ($1,09\pm 0,07$ and $0,99\pm 0,06\mu\text{mol/mol}$, respectively) than post-Archean adakites, granites, tonalites and granodiorites (with average Ge/Si in the range of 1,64 to $1,85\mu\text{mol/mol}$). This reveals the strengths of Ge as a proxy to Archean rock-forming processes. This result is thoroughly corroborated by the Ge/Si ratios we report on the pre-cratonic BGB 3,5Ga Theespruit felsic metavolcanics, 3,5-3,2Ga TTGs and 3,2-3,1Ga GMSs which all exhibit low values ($0,61\pm 0,19$; $0,92\pm 0,17$; $1,05\pm 0,19\mu\text{mol/mol}$, respectively).

Based on their low TTG-like Ge/Si, pre-cratonic GMSs are dismissed as being derived from melting of both TTG and metasedimentary sources. In contrast our finding means that both TTGs and GMSs originated from similar Ge-depleted sources. We find that such low Ge/Si ratios, coupled to heavy Si isotopic signatures ($-0,14\text{‰} < \delta^{30}\text{Si} < +0,27\text{‰}$) are also a characteristic feature of altered mafic and ultramafic BGB greenstones, especially at the interface between the silicified ($0,2 < \text{Ge/Si} < 1,2\mu\text{mol/mol}$) and unsilicified ($1,8 < \text{Ge/Si} < 3,1\mu\text{mol/mol}$) portions of the transformed Archean seafloor. From there we infer that both Na-rich and K-rich Archean felsic melts can derive from a unique class of protoliths: Ge-depleted metabasalts containing significant modal proportion of a supracrustal quartz generated by the silicification of the Eo-Paleoarchean basaltic seafloors. The pre-cratonic transition from Na-rich to K-rich felsic melts is assumed to be connected to the gradual incoming of potassium as a key element associated to the seafloor alteration (Lieu and He, 2021). In contrast, post-cratonic younger (3,07-2,69Ga) granites have higher Ge/Si ($1,81\pm 0,33\mu\text{mol/mol}$) and can be generated through the reworking of a TTG-like basement,

by incongruent melting of biotite and hornblende ($1,79 < \text{Ge/Si} < 2,49 \mu\text{mol/mol}$) leaving an oligoclase-rich ($0,64 < \text{Ge/Si} < 0,72$) residue.

Our finding has two major issues in terms of the evolution of the early Earth. First, considering the large volume of Paleoarchean TTGs and GMSs, these silicifications would have been quantitatively abundant at the Eo-Paleoarchean seafloor with a potential substantial feedback on the seawater composition. By removing most major cations from the ultramafic-mafic seafloors, these silicifications would be a major feeding source of Na, Mg, Ca, Fe and P to the Archean ocean. Hence this silicification pathway might be the missing Na-Mg inputs to the primitive ocean which is sought to improve the conceptual framework of the early Earth seawater composition (e.g., Albarède et al., 2020). Second, by showing that the Earth has moved from a prevalent Ge-depleted felsic crust in early-middle Archean to a widespread Ge-enriched post-Archean crust, we actually emphasize the importance of late Archean intra-crustal reworking and/or crust-mantle recycling events in the evolution of the Earth continental crust. It might be the sign that a vigorous continental crust recycling like the “early Earth mode of plate tectonics (sensu Korenaga, 2021)” prevailed until the Mesoarchean before it was superseded by a more standard kind of plate tectonics and crustal growth about three billion years ago.

References

- Albarède, F., Thibona, F., Blichert-Toft, J., and Tsikos, A. 2020. Chemical archeoceanography. *Chem. Geol.*, 548, 119625
- André, L., Abraham, K., Hofmann, A., Monin, L., Kleinhanns, I.C., Foley, S., 2019. Early continental crust generated by reworking of basalts variably silicified by seawater. *Nat. Geosci.* 12 (9), 769-773.
- Deng, Z.B., Chaussidon, M., Guitreau, M., Puchtel, I.S., Dauphas, N., Moynier, F., 2019. An oceanic subduction origin for Archaean granitoids revealed by silicon isotopes. *Nat. Geosci.* 12 (9), 774-777.
- Korenaga, J., 2021. Hadean geodynamics and the nature of early continental crust. *Precambrian Res.* 359, 106178.
- Lieu, C.-T. and He, Y.-S., 2021. Rise of major subaerial landmasses about 3,0 to 2,7 billion years ago. *Geoch. Persp. Let.*, 18,1-5.

Insights on mantle melting below Osorno Volcano (Southern Volcanic Zone, Chile)

Tonin BECHON¹, Paul FUGMANN¹, Olivier NAMUR², Billon MELVYN¹, Olivier BOLLE¹, Jacqueline VANDER AUWERA¹

¹ University of Liège, Liège, Belgium (ULG) – tonin.bechon@uliege.be

² Katholieke Universiteit Leuven, Leuven, Belgium (KUL)

Knowing the extent of mantle wedge melting below volcanic arcs is critical to improve magma genesis models. During the last decades, experimental petrology provided significant data and ready to be used models to retrieve the melting conditions producing primary magmas (Mg# >0.7, Ni > 150ppm, Cr > 1000 ppm after Baker et al. (1994) and Grove et al. (2012)). The Central Southern Volcanic zone (CSVZ, southern Chile) of the Andean arc lies on a thin continental crust (50-30 km : Tassara and Echaurren, 2012) and is crosscut by a major transcrustal fault (LOFZ : Cembrano and Lara, 2009) which speed up magma ascent. As a consequence, (near-) primary magmas have been sampled in the area avoiding the blurring of its original characteristics by deep (MASH) (Hildreth and Moorbath, 1988) to shallower (differentiation) magmatic processes. Osorno is one of the CSVZ volcano that possess the most primitive recorded rocks (Mg# =0.72, MgO: 10.23-10.53 wt%, Cr: 584-745 ppm, Ni: 171-179 ppm, Fo# of olivines up to Fo₈₉) in the area. Using lherzolite melting experiments (Hirose and Kushiro, 1993) as well as numerical (Lee *et al.*, 2009), empirical (Wood, 2004) and chemical models (Kelley *et al.*, 2006) together with modal batch melting equations (Hickey-Vargas *et al.*, 2016a, 2016b), we retrieved temperature, pressure, mantle water content and mantle melting rate (F) below Osorno. Temperatures range from 1303 to 1327 °C, pressures from 10.5 to 13.6 kbar (around MOHO depth, ca. 35-44 km), mantle water content from 0.08 to 0.33 wt% and F from 0.12 to 0.22. The uncertainty on F values reflects the difficulty to precisely estimate this parameter. However, this range allows better constraining geophysical models. Values estimated using a global arc numerical model (Turner *et al.*, 2016; F ≈ 0.11 at ca. 60 km and T≈1100°C, mantle H₂O =0.6 wt%) or using Arc basalt simulator, isotopes and trace elements (Jacques *et al.*, 2014; F = 1.6-5.5, P=19 kbar, T = 1240°C) vary significantly from our data emphasizing the remaining gap of knowledge of the mantle melting conditions. Our results nonetheless agree with those calculated at La Picada (Vander Auwera *et al.*, 2019) or southwards (Watt *et al.*, 2013; Weller and Stern, 2018) in the southern SVZ.

References:

- Baker, M. B., Grove, T. L. & Price, R. (1994). Primitive basalts and andesites from the Mt. Shasta region, N. California: products of varying melt fraction and water content. *Contributions to Mineralogy and Petrology* 118, 111–129.
- Cembrano, J. & Lara, L. (2009). The link between volcanism and tectonics in the southern volcanic zone of the Chilean Andes: A review. *Tectonophysics* 471, 96–113.
- Grove, T. L., Till, C. B. & Krawczynski, M. J. (2012). The Role of H₂O in Subduction Zone Magmatism. *Annual Review of Earth and Planetary Sciences* 40, 413–439.

- Hickey-Vargas, R., Holbik, S., Tormey, D., Frey, F. A. & Moreno Roa, H. (2016a). Basaltic rocks from the Andean Southern Volcanic Zone: Insights from the comparison of along-strike and small-scale geochemical variations and their sources. *Lithos* 258–259, 115–132.
- Hickey-Vargas, R., Sun, M. & Holbik, S. (2016b). Geochemistry of basalts from small eruptive centers near Villarrica stratovolcano, Chile: Evidence for lithospheric mantle components in continental arc magmas. *Geochimica et Cosmochimica Acta* 185, 358–382.
- Hildreth, W. & Moorbath, S. (1988). Crustal contributions to arc magmatism in the Andes of Central Chile. *Contributions to Mineralogy and Petrology* 98, 455–489.
- Hirose, K. & Kushiro, I. (1993). Partial melting of dry peridotites at high pressures: Determination of compositions of melts segregated from peridotite using aggregates of diamond. *Earth and Planetary Science Letters* 114, 477–489.
- Jacques, G., Hoernle, K., Gill, J., Wehrmann, H., Bindeman, I. & Lara, L. E. (2014). Geochemical variations in the Central Southern Volcanic Zone, Chile (38–43°S): The role of fluids in generating arc magmas. *Chemical Geology* 371, 27–45.
- Kelley, K. A., Plank, T., Grove, T. L., Stolper, E. M., Newman, S. & Hauri, E. (2006). Mantle melting as a function of water content beneath back-arc basins. *Journal of Geophysical Research: Solid Earth* 111.
- Lee, C.-T. A., Luffi, P., Plank, T., Dalton, H. & Leeman, W. P. (2009). Constraints on the depths and temperatures of basaltic magma generation on Earth and other terrestrial planets using new thermobarometers for mafic magmas. *Earth and Planetary Science Letters* 279, 20–33.
- Tassara, A. & Echaurren, A. (2012). Anatomy of the Andean subduction zone: three-dimensional density model upgraded and compared against global-scale models. *Geophysical Journal International* 189, 161–168.
- Turner, S. J., Langmuir, C. H., Katz, R. F., Dungan, M. A. & Escrig, S. (2016). Parental arc magma compositions dominantly controlled by mantle-wedge thermal structure. *Nature Geoscience* 9, 772–776.
- Vander Auwera, J., Namur, O., Dutrieux, A., Wilkinson, C. M., Ganerød, M., Coumont, V. & Bolle, O. (2019). Mantle Melting and Magmatic Processes Under La Picada Stratovolcano (CSVZ, Chile). *Journal of Petrology* 60, 907–944.
- Watt, S. F. L., Pyle, D. M., Mather, T. A. & Naranjo, J. A. (2013). Arc magma compositions controlled by linked thermal and chemical gradients above the subducting slab. *Geophysical Research Letters* 40, 2550–2556.
- Weller, D. J. & Stern, C. R. (2018). Along-strike variability of primitive magmas (major and volatile elements) inferred from olivine-hosted melt inclusions, southernmost Andean Southern Volcanic Zone, Chile. *Lithos* 296–299, 233–244.
- Wood, B. J. (2004). Melting of fertile peridotite with variable amounts of H₂O. *Washington DC American Geophysical Union Geophysical Monograph Series* 150, 69–80.

Timescales of crystal mush storage in the Central Southern Volcanic Zone of Chile

Melvyn BILLON¹, Bernard CHARLIER¹, Olivier NAMUR², Jacqueline VANDER AUWERA¹

1. Université de Liège, Liège, Belgique (melvyn.billon@uliege.be)
2. KULeuven, Louvain, Belgique (olivier.namur@kuleuven.be)

During the last few decades, there has been an important change in paradigm in igneous petrology from the classic concept of a large melt-dominated magma chamber to a storage reservoir that is dominated by crystal mush where the crystals form a framework in which melt is distributed [1]. During eruption, these crystals may be unlocked from the mush and transported as individual macrocrysts or glomerocrysts.

Time is a fundamental parameter in geology and particularly in volcanology where volcanic hazard must be assessed. If the process of rising magma from the surface reservoir is relatively fast [2], the process of crystal mush storing can take from centuries to thousands of years [3].

The project focuses on constraining the timescales (t) of crystal growth (G) in the main storage region of several volcanoes (Osorno, Calbuco, Villarica, La Picada) of the Central Southern Volcanic Zone of the Andean arc (CSVZ) (Chile). These timescales will be obtained by combining experimentally determined growth rates of plagioclase, the main macrocryst in the studied volcanoes, and detailed plagioclase crystal size distributions (CSD, [4, 5]). Experiments of plagioclase crystallization are performed on a natural basaltic andesite sample (from Osorno) that is representative of the CSVZ and more generally of arc magmatism. We particularly study the effect of melt composition and H₂O content, an important parameter in subduction zone magmatism, on the growth rate of plagioclase. Cooling experiments at different rates (1°C/h, 3°C/h, ...) are run at 1 atm (anhydrous) and 2 kbar (hydrous) and at an oxygen fugacity close to NNO. These conditions are constrained by results from our extensive petrological database on these volcanoes. The various experimental charges obtained are then polished, observed by different processes (SEM, Probe, tomography), and texture is analyzed by segmentation with different software (GIMP, ImageJ), so as to compare the shape and growth of the crystals according to the conditions.

Plagioclase crystal size distributions are acquired on a selection of samples from the different volcanoes. Crystal size data obtained from high quality BSE images are then quantified with the software package *ImageJ* freeware to calculate the CSD plots. Using our data on growth rates (G) and the slope of these plots ($-1/Gt$) will enable us to extract information about the duration [6, Figure 1] of crystal growth (t).

References

- [1] Cashman, K., R. Sparks and J. Blundy, 2017, Vertically extensive and unstable magmatic systems: A unified view of igneous processes. *Science*, 355.
- [2] Morgan, D., et al., 2004, Time scales of crystal residence and magma chamber volume from modelling of diffusion profiles in phenocrysts: Vesuvius 1944. *Earth and Planetary Science Letters*, 2004, 222: 933-946.

- [3] Reubi, O., S.R. Scott, and K.W.W. Sims, 2017, Evidence of Young Crystal Ages in Andesitic Magmas from a Hyperactive Arc Volcano, Volcan de Colima, Mexico. *Journal of Petrology*, 58(2): 261-276.
- [4] Cashman, K.V. and B. Marsh, 1988, Crystal size distribution (CSD) in rocks and the kinetics and dynamics of crystallization. *Contributions to Mineralogy and Petrology*, 99: 292-305.
- [5] Marsh, B. 1988, Crystal size distribution (CSD) in rocks and the kinetics and dynamics of crystallization. *Contributions to Mineralogy and Petrology*, 99: 277-291.
- [6] Higgins, 1996, Magma dynamics beneath Kamani volcano, Thera, Greece, as revealed by crystal size and shape measurements. *M. Journal of Volcanology and Geothermal Research*, 70: 37-48.

Figure

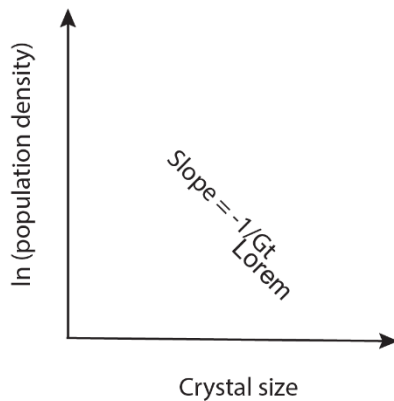


Figure 1: The crystal size distribution of a phase in the magma storage region is a straight line on graph of ln (population density) against size.

Experimental constraints on the internal structure of Mercury

Joren CELIS¹, Olivier NAMUR², Bernard CHARLIER³

1. KU Leuven, Leuven, Belgium (*joren.celis@kuleuven.be*)

2. KU Leuven, Leuven, Belgium (*olivier.namur@kuleuven.be*)

3. ULiège, Liège, Belgium (*b.charlier@uliege.be*)

Mercury is the smallest terrestrial planet of our solar system and, in comparison to other planets, is characterized by a very large metal/silicate ratio. Understanding the formation of this planet requires constraints on primordial differentiation processes. As such, finding equations of the liquidus and solidus of the mantle is crucial to properly model the structure of the mantle as a function of mantle composition and pressure.

The parent composition of Mercury is thought to be similar to enstatite chondrites (Nittler et al., 2011). The MESSENGER spacecraft (NASA) measured unusually high amounts of sulphur (up to 4 wt% S) in basaltic lavas on the surface of Mercury, which is significantly higher than those of any basaltic composition on other terrestrial planets (Namur et al., 2016). The combination of low iron content, high sulphur and high sodium contents is expected to have a significant effect on the solidus and liquidus curves of Mercury.

The objectives of the project are to precisely constrain the crystallization sequence of the Mercurian magma ocean and to determine phase equilibria during melting of mantle cumulates. Experiments will be performed using presses and furnaces at high temperature (>1000 °C) and for pressures relevant to the Mercury's mantle (1 bar to 60 kbar). Theoretical models and experimental data will allow interpreting the processes of mantle differentiation of Mercury, as well as to determine the potential mantle source of the basalts observed at the planet's surface.

A couple of starting compositions were based on enstatite chondrites, where the silicon content was adapted based on the core-mantle ratio of Mercury and the likely Si content of Mercury's core (Cartier et al., 2020). A third composition was derived from an Earth-like composition with an increased sodium content, matching estimates of Mercury's mantle. Thermodynamic diagrams were obtained with Thermocalc and pMelts.

Piston-cylinder press and multi-anvil press experiments are currently being conducted on the three compositions, both sulphur-free and sulphur-bearing. The glasses produced during these experiments will be analysed with an electron probe micro-analyser. The results of these analyses will then be compared with the results of the thermodynamic models to gain a better insight into the crystallisation of Mercury's magma ocean and better constrain early differentiation processes of the planet.

References

- Cartier, C., Namur, O., Nittler, L. R., Weider, S. Z., Crapster-Pregont, E., Vorburger, A., Franck, E. A., & Charlier, B. (2020). No FeS layer in Mercury? Evidence from Ti/Al measured by MESSENGER. *Earth and Planetary Science Letters*, 534, 116108.1
- Namur, O., Charlier, B., Holtz, F., Cartier, C., & McCammon, C. (2016). Sulfur solubility in reduced mafic silicate melts: Implications for the speciation and distribution of sulfur on Mercury. *Earth and Planetary Science Letters*, 448, 102–114.
- Nittler, L. R., Starr, R. D., Weider, S. Z., McCoy, T. J., Boynton, W. V., Ebel, D. S., Ernst, C. M., Evans, L. G., Goldsten, J. O., Hamara, D. K., Lawrence, D. J., McNutt, R. L., Schlemm, C. E., Solomon, S. C., & Sprague, A. L. (2011). The major-element composition of Mercury's surface from MESSENGER X-ray spectrometry. *Science*, 333(6051), 1847–1850.

Mercury and its exploration by the BepiColombo mission

Bernard CHARLIER¹, Hadrien PIROTTE¹, Joren CELIS², Olivier NAMUR²

1. *Département de Géologie, Université de Liège, 4000 Sart Tilman, Belgium
(b.charlier@uliege.be)*

2. *Department of Earth and Environmental Sciences, KU Leuven, 3001 Leuven, Belgium*

Unique physical and chemical characteristics of planet Mercury have been revealed by measurements from NASA's MESSENGER spacecraft. The closest planet to our Sun is made up of a large metallic core that is partially liquid, a thin mantle thought to be formed by solidification of a silicate magma ocean, and a relatively thick secondary crust produced by partial melting of the mantle followed by volcanic eruptions. Mercury is thus a unique terrestrial planet with its small size and its large metal/silicate ratio. However, the origin of this metal-rich body and the conditions of accretion remain elusive. Metal enrichment has been proposed to originate either from primordial processes in the solar nebula or from a giant impact that stripped most of the silicate portion of a larger planet leaving Mercury as we know it today (Figure 1).

In this presentation, we discuss the evolutionary paths and processes that connect Mercury's present-day characteristics to its potential building blocks. Our methodology involves the use of high-temperature and low- to high-pressure experiments on silicate, metallic and sulfide melts in order to constrain equilibria between the metallic core and the silicate portion of Mercury, during crystallization of the silicate magma ocean, and between the solid mantle and its melting products. We specifically study the role of highly reducing conditions on phase stability and element behavior (lithophile, siderophile or chalcophile) during equilibration of immiscible silicate-metal-sulfide melts and their crystallization upon cooling. We benefit from data obtained by the MESSENGER spacecraft to get insights on compositions representative for surface lavas on Mercury and their inferred mantle sources.

Our projects also aim at preparing the ESA/JAXA (Europe/Japan) BepiColombo mission that en route to Mercury (arrival in 2025). The two spacecrafts will deliver new data on the planet and its magnetosphere and will contribute to our understanding of the formation and evolution of the planet. Studying Mercury provides a unique opportunity to broaden our knowledge of the formation and evolution of terrestrial planets, including Earth and exoplanets.

References

Charlier B, Namur O (2019). The origin and differentiation of planet Mercury. *Elements* 15: 9-14.

Figure

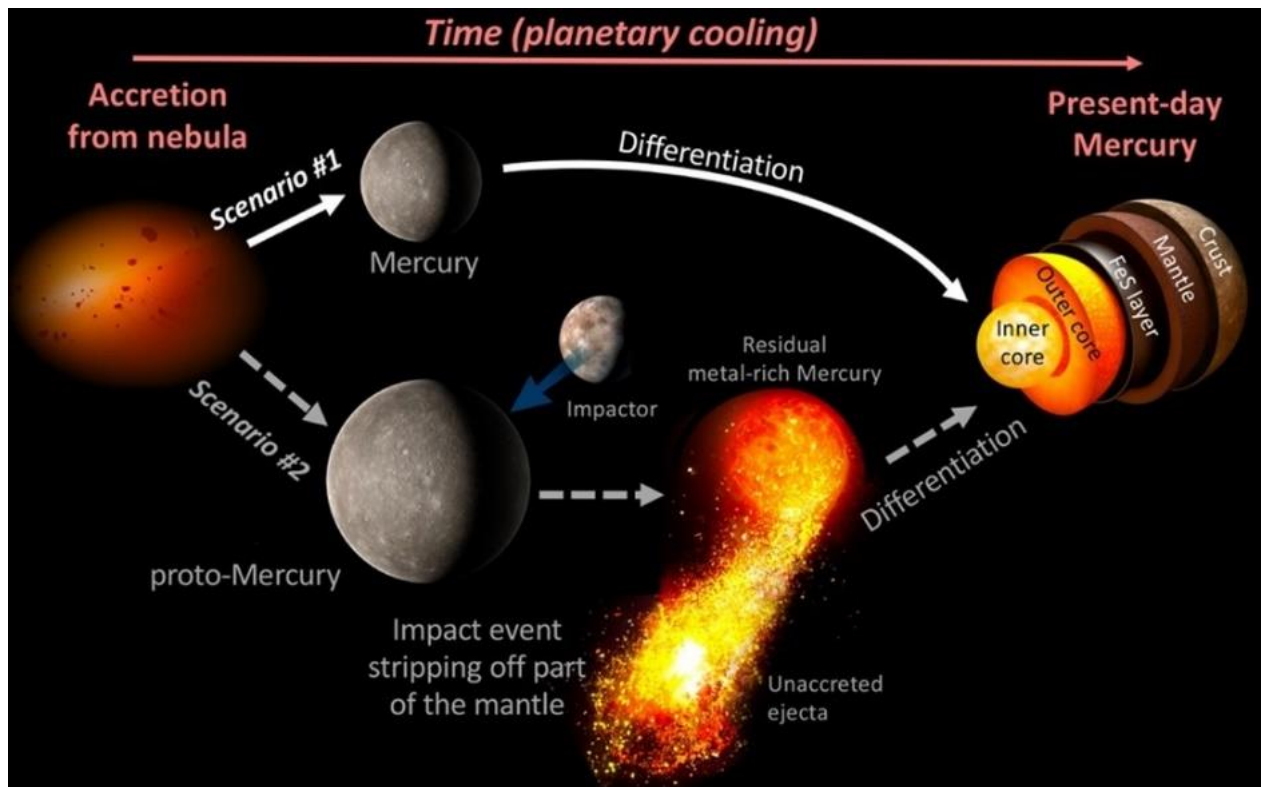


Figure 1: Plausible evolutionary pathways of Mercury, from the accretion of its building blocks to its present-day state. Scenario #1 considers primary metal-enrichment followed by internal differentiation, but might be challenged by Scenario #2, involving an impact-related reduction in size. After Charlier and Namur (2019)

Constraining the conditions of magmatic differentiation under Villarrica stratovolcano (Central Southern Volcanic Zone, Chile)

Paul FUGMANN¹, Tonin BECHON², Olivier BOLLE³, Olivier NAMUR⁴, Jacqueline VANDER AUWERA⁵

1. *University of Liège, Department of Geology, Liège, Belgium (p.fugmann@uliege.be)*
2. *University of Liège, Department of Geology, Liège, Belgium (tonin.bechon@uliege.be)*
3. *University of Liège, Department of Geology, Liège, Belgium (olivier.bolle@uliege.be)*
4. *University of Leuven, Department of Earth and Environmental Sciences, Leuven, Belgium (olivier.namur@kuleuven.be)*
5. *University of Liège, Department of Geology, Liège, Belgium (jvdauwera@uliege.be)*

The Villarrica stratovolcano (39.3°S, 71.6°W) in Chile is one of the most active volcanoes within the Central Southern Volcanic Zone (CSVZ). There, a thin crust (~ 35 km; Hickey-Vargas et al., 2016) and a major dextral transpressional structure, the Liquiñe-Ofqui fault zone (LOFZ; Cembrano et al. 1996, 2000; Lange et al., 2008), favor rapid magma ascent from the mantle wedge to the surface. Villarrica has been constantly degassing since the mid 80's through an open conduit, filled by a summit lava lake. Recent petrological data acquired on volcanoes of the CSVZ (e.g. Calbuco, La Picada, Osorno, Villarrica) indeed indicate, that most of the differentiation takes place in shallow reservoirs at about 0.2 to 0.3 GPa. However, for Villarrica, Morgado et al. (2015, 2017) implied an additional deep reservoir at ~0.8 GPa. Reservoirs at that corresponding depth (~35 km, MOHO) are more characteristic for the CSVZ monogenetic small eruptive centers (SECs).

The aim of this study is to precisely quantify several parameters (P, T, fO_2 , wt. % H₂O) for the Villarrica system. Knowing details about melting- and storage processes is necessary to further constrain ascent rates in an apparently highly permeable magmatic system, regarding the high frequency of its eruptions. They are around ten times higher than at the nearby and compositionally close Osorno volcano. Both systems are majorly composed of basaltic andesites to basaltic lavas and pyroclasts with less andesitic lavas and minor dacitic to rhyodacitic domes (e.g. Hickey-Vargas et al., 1989; López-Escobar et al., 1992). For that, a series of samples were collected from different units of Villarrica (lavas, pyroclasts) and at SECs that surround Villarrica (Los Nevados, Chaillupén, San Jorge).

Our whole-rock geochemical data, combined with published analyses, define a single differentiation trend that shares characteristics of tholeiitic and calc-alkaline series. This trend extends from ~50 to ~71 wt.% SiO₂ with Mg# up to 62 and a compositional “Daly” gap between ~58 to ~62 wt.% SiO₂. A second gap exists between ~65 to ~70 wt.% SiO₂. Most near-primary basalts occur at the proximate San Jorge SEC (Mg# 69, SiO₂ 50.6, MgO 9.5 wt.%). Mass balance modelling, thermodynamic simulations using *r-MELTS*, detailed mineral compositional data (plagioclase, olivine, clinopyroxene, Fe-Ti oxides) together with a collection of geothermobarometers suggest fractional crystallization as a major differentiation process in shallow reservoirs (0.1 to 0.4 GPa, ~1250 to 900 °C), with fO_2 between NNO and QFM and estimated H₂O contents from 1.0 to 1.9 % (e.g. Mandler et al., 2014) using San Jorge data as starting compositions.

References

- Cembrano, J., Hervé, F., Lavenu, A., 1996. The Liquiñe Ofqui fault zone: a long-lived intra-arc fault system in southern Chile. *Tectonophysics* 259, 55–66.
- Cembrano, J., Schermer, E., Lavenu, A., Sanhueza, A., 2000. Contrasting nature of deformation along an intra-arc shear zone, the Liquiñe-Ofqui fault zone, southern Chilean Andes. *Tectonophysics* 319, 129–149.
- Hickey-Vargas, R., Holbik, S., Tormey, D., Frey, F. A., Moreno Roa, H., 2016. Basaltic rocks from the Andean Southern Volcanic Zone: Insights from the comparison of along-strike and small-scale geochemical variations and their sources. *Lithos* 258–259, 115–132.
- Lange, D., Cembrano, J., Rietbrock, A., Haberland, C., Dahm, T., Bataille, K., 2008. First seismic record for intra-arc strike-slip tectonics along the Liquiñe-Ofqui fault zone at the obliquely convergent plate margin of the southern Andes. *Tectonophysics* 455, 14–24.
- López-Escobar, L., Parada, M., Moreno, H., Frey, F., Hickey-Vargas, R., 1992. A contribution to the petrogenesis of Osorno and Calbuco volcanoes, Southern Andes (41°00'–41°30'S): comparative study. *Revista Geológica de Chile* 19 (2), 211–226.
- Mandler, B. E., Donnelly-Nolan, J. M., Grove, T. L., 2014. Straddling the tholeiitic/calc-alkaline transition: The effects of modest amounts of water on magmatic differentiation at Newberry volcano, Oregon. *Contributions to Mineralogy and Petrology* 168, 1–25.
- Morgado, E., Parada, M. A., Contreras, C., Castruccio, A., Gutiérrez, F., McGee, L. E., 2015. Contrasting records from mantle to surface of Holocene lavas of two nearby arc volcanic complexes: Caburgua-Huelemolle Small Eruptive Centers and Villarrica Volcano, South-ern Chile. *Journal of Volcanology and Geothermal Research* 306, 1–16.
- Morgado, E., Parada, M. A., Morgan, D. J., Gutiérrez, F., Castruccio, A., Contreras, C., 2017. Transient shallow reservoirs beneath small eruptive centres: Constraints from Mg-Fe interdiffusion in olivine. *Journal of Volcanology and Geothermal Research* 347, 327–336.

Petrology of Nyamulagira volcano, Virunga Province, DR Congo

Ephrem KAMATE^{1,2,3}, Olivier NAMUR¹, Sander MOLENDIJK¹, Jacqueline VANDER AUWERA⁴, Benoit SMETS^{5,6}

1. *Department of Earth and Environmental Sciences, KU Leuven, Leuven, Belgium, kamatekaleghetso.ephrem@kuleuven.be*
2. *Observatoire Volcanologique de Goma, Goma, D.R. Congo*
3. *Université de Goma, Goma, D.R. Congo*
4. *Department of Geology, University of Liege, Belgium*
5. *Natural Hazards Service, Department of Earth Sciences, Royal Museum for Central Africa, Tervuren, Belgium*
6. *Cartography and GIS Research Group, Department of Geography, Vrije Universiteit Brussel, Brussels, Belgium*

The East African Rift (EAR) is an extensive continental rift system, forming as a result of a major mantle upwelling, known as the African Superplume. Volcanism in the Western Branch of the rift occurs in four provinces: Toro-Ankole, Virunga, South Kivu, and Rungwe volcanic fields. The Virunga Volcanic Province (VVP), is situated between the two half-graben basins of Lake Edward and Lake Kivu. Eruptions in this province started during the Miocene, around 11 Ma, and volcanic activity in the region has been continuous ever since. The magmatism in VVP is characterized by unusual highly alkaline, silica-undersaturated, mafic volcanism with clear geochemical variations across the volcanic field. Eight main volcanoes are located in the VVP, including the currently active volcanoes of Nyamuragira and Nyiragongo. Nyamulagira erupts very regularly (~ every 2-3 years) whereas for Nyiragongo only three eruptions are documented: January 1977, January 2002 and May 2021. Several eruptions prior to 1977 are undated.

Nyamulagira and Nyiragongo are real threats to the densely populated city of Goma and its surroundings. The scientific knowledge about the petrology of Nyamulagira is highly limited, in part due to the complexities associated with sample collection in the politically unstable region. However, a better understanding of sub-volcanic processes is essential to adequately monitoring the activity of the volcano and to predicting realistic paths for future eruptions. In this PhD project, we propose a research plan combining (1) a petrological study of historic lavas of Nyamulagira to assess the conditions of magma formation beneath the volcano; (2) the use of photogrammetric and remote sensing techniques to estimate the volumes of individual eruptive events; and (3) a detailed rheological modelling of the properties of Nyamulagira's lavas to estimate the probability of lava flow inundation of inhabited areas.

Petrology of the Nyiragongo Volcano, DR Congo

Sander MOLENDIJK¹, Olivier NAMUR¹, Paul MASON², Benoît SMETS^{3,4}, Jacqueline VANDER AUWERA⁵, David NEAVE⁶

1. *KU Leuven, Belgium* (sander.molendijk@kuleuven.be)
2. *Utrecht University, The Netherlands* (p.mason@uu.nl)
3. *Royal Museum for Central Africa, Belgium* (benoit.smets@africamuseum.be)
4. *Vrije Universiteit Brussel, Belgium*
5. *University of Liège, Belgium* (jvdauwera@uliege.be)
6. *University of Manchester, United Kingdom* (david.neave@manchester.ac.uk)

The Nyiragongo volcano is one of the most alkali-rich magmatic systems on the planet, currently characterized by the presence of a persistent lava lake in the summit crater which hosts silica-undersaturated ($\text{SiO}_2 < 40$ wt.%), low viscosity lavas with a significantly elevated alkali content ($\text{Na}_2\text{O} + \text{K}_2\text{O} > 10$ wt.%).

In order to better understand this exotic magmatic system, we present a set of 244 samples of the Nyiragongo volcano, collected during a field expedition in 2017. Lithologies range from primitive picrites (Mg# 82) erupted from parasitic cones to a variety of highly evolved nephelinites, leucitites, and melilitites erupted from the main edifice as recently as 2016.

Extensive mineralogical characterisation in terms of major and trace element geochemistry is presented for the full lithological diversity of Nyiragongo, revealing a compositional range in olivine from forsteritic (Fo = 91) to Ca-rich (Fo \approx 2, 31 wt.% CaO). Similarly, clinopyroxene crystals cover a compositional range from Mg# = 89 to Mg# = 2. Melilite is dominantly alumo-åkermanitic, with only minor compositional variation driven by Ca-Na substitution; it also hosts substantial Sr and Ba.

Trace element patterns indicate significant enrichment (up to 100 times E-MORB concentrations) of LREE and LILE increasing with fractionation, coinciding with relative depletions in HFSE.

Primitive olivine trace element compositions and associated melt-inclusion compositions will be discussed in order to identify the significant chemical disparity between parasitic cone- and main-crater products, and shed light on the mantle sources from which they are derived.

Equilibria and trace element partitioning in silicate-metal-sulfide melts under highly reducing conditions: a key to understand the evolution of Mercury

Hadrien PIROTTE¹, Camille CARTIER², Olivier NAMUR³, Anne POMMIER⁴, Bernard CHARLIER¹

1. *Department of Geology, University of Liège, 4000 Sart Tilman, Belgium (hadrien.pirotte@uliege.be; b.charlier@uliege.be)*

2. *Centre de Recherches Pétrographiques et Géochimiques, 54501 Vandoeuvre-lès-Nancy, France (camille.cartier@univ-lorraine.fr)*

3. *Department of Earth and Environmental Sciences, KU Leuven, Leuven, 3001, Belgium (olivier.namur@kuleuven.be)*

4. *Scripps Institution of Oceanography, UC San Diego, La Jolla, CA 92093, USA (pommier@ucsd.edu)*

Mercury has a large partially liquid metallic core (~80% of the planet radius, Hauck et al., 2013; Rivoldini & Van Holst, 2013; Margot et al., 2018 and references therein), a thin mantle and a thick crust (10% of the silicate part, Padovan et al., 2015). The planet may also host a FeS layer at the core-mantle interface (Malavergne et al., 2010; Hauck et al., 2013). Magmatic rocks at its surface are rich in sulfur (up to 4wt%) and poor in FeO (<1wt%) (Nittler et al., 2011), which implies that the planet formed under very reducing conditions (McCubbin et al., 2012; Zolotov et al., 2013). While MESSENGER's orbital mission to Mercury gave us great insights on the planet's interior and surface composition, experimental work is still needed to better constrain phase equilibria under the unique highly reducing conditions and the behavior and partitioning of major and trace elements under those conditions. The role of sulfur (and thus, sulfides) is moreover fundamental in the distribution of many trace and minor elements in the different reservoirs (silicate, core, and the hypothetical FeS layer; Wohlers & Wood, 2015).

Here we present the results of phase equilibrium experiments using piston-cylinder and internally heated pressured vessel on synthetic powder representative of Mercury's bulk silicate composition. The starting materials consisted of mixed pure oxides doped in a large number of trace and minor elements. FeS, CaS and S were added to reach sulfur saturation in the silicate melt, as well as Fe-Si in some experiments to form some metal melts. The experiments were performed at pressures relevant to the silicate part of Mercury (1 – 30kbar) and at high temperatures (1500°C to 1700°C). Redox conditions were highly reducing, with oxygen fugacity in our experiments ranging from IW-2 to IW-8 (with IW being the iron-wüstite buffer). The reducing conditions were obtained by changing the $\text{Si}_{\text{metal}}/\text{SiO}_2$ ratio in the starting material without changing the total Si content of the powder. The retrieved quenched products present three types of melts; a metal one (Fe-Si), a sulfide one (FeS) and a silicate one, as well as some MgS and (Mg,Fe,Ca)S grains. The major and minor compositions of the different phases were analyzed using EPMA, and trace element content were measured using LA-ICP-MS.

We show that under reducing conditions, all elements have increased chalcophile and siderophile behaviors. All transition metals (except groups 3 and 4) are strongly chalcophile

and siderophile under these reducing conditions. Lanthanides and thorium stay lithophile, but uranium becomes chalcophile at very low oxygen fugacity. We also present the first partitioning data between silicate melts and MgS and (Mg,Fe,Ca)S.

Our results are implemented into a model of element distribution in the planet and compared with surface compositional data, using different scenarios for Mercury's evolution, specifically by changing bulk S content of the planet. In particular, our model focuses on the volatile budget of the planet by using partitioning data for U, Th and K, which have a similar behavior (these elements are incompatible during silicate differentiation) but present different volatilities (U and Th are refractory, while K is volatile).

References

- Hauck, S.A., Margot, J.-L., Solomon, S.C., Phillips, R.J., Johnson, C.L., Lemoine, F.G., Mazarico, E., McCoy, T.J., Padovan, S., Peale, S.J., Perry, M.E., Smith, D.E. and Zuber, M.T., 2013. The curious case of Mercury's internal structure. *Journal of Geophysical Research: Planets* 118, 1204-1220.
- Malavergne, V., Toplis, M.J., Berthet, S. and Jones, J., 2010. Highly reducing conditions during core formation on Mercury: Implications for internal structure and the origin of a magnetic field. *Icarus* 206, 199-209.
- Margot, J.L., Hauck, S.A.I., Mazarico, E., Padovan, S. and Peale, S.J., 2018. Mercury's internal structure, in: Solomon, S.C., Nittler, L.R., Anderson, B.J. (Eds.), *Mercury: The View after MESSENGER*. Cambridge University Press, pp. 85-113.
- McCubbin, F.M., Riner, M.A., Vander Kaaden, K.E. and Burkemper, L.K., 2012. Is Mercury a volatile-rich planet? *Geophysical Research Letters* 39, L09202.
- Nittler, L.R., Starr, R.D., Weider, S.Z., McCoy, T.J., Boynton, W.V., Ebel, D.S., Ernst, C.M., Evans, L.G., Goldsten, J.O., Hamara, D.K., Lawrence, D.J., McNutt, R.L., Schlemm, C.E., Solomon, S.C. and Sprague, A.L., 2011. The major-element composition of Mercury's surface from MESSENGER x-ray spectrometry. *Science* 333, 1847-1850.
- Padovan, S., Wieczorek, M.A., Margot, J.-L., Tosi, N. and Solomon, S.C., 2015. Thickness of the crust of Mercury from geoid-to-topography ratios. *Geophysical Research Letters* 42, 1029-1038.
- Rivoldini, A. and Van Hoolst, T., 2013. The interior structure of Mercury constrained by the low-degree gravity field and the rotation of Mercury. *Earth and Planetary Science Letters* 377-378, 62-72.
- Wohlars, A. and Wood, B.J., 2015. A Mercury-like component of early Earth yields uranium in the core and high mantle ^{142}Nd . *Nature* 520, 337-340.
- Zolotov, M.Y., Sprague, A.L., Hauck, S.A., Nittler, L.R., Solomon, S.C. and Weider, S.Z., 2013. The redox state, FeO content, and origin of sulfur-rich magmas on Mercury. *Journal of Geophysical Research: Planets* 118, 138-146.

The response of a magmatic plumbing system to sector collapse: constraints from petrology and geochemistry at Mt. Meru, Tanzania

Sacha RADELET¹, Karen FONTIJN², Mary KISAKA³, Matthieu KERVYN⁴

¹*Université Libre de Bruxelles, Brussels, Belgium (sacha.radelet@ulb.be)*

²*Université Libre de Bruxelles, Brussels, Belgium (karen.fontijn@ulb.be)*

³*Vrije Universiteit Brussel, Brussels, Belgium & University of Dodoma, Dodoma, Tanzania (mary.john.kisaka@vub.be)*

⁴*Vrije Universiteit Brussel, Brussels, Belgium (makervyn@vub.be)*

Mt. Meru is a 4565m high active stratovolcano (the fifth highest peak in Africa), with its most recent eruptive activity dating back to 1910 CE. The volcano is situated at the border between Tanzania and Kenya in the Arusha region, in the eastern branch of the East African Rift system. Next to the main stratovolcano edifice, Mt Meru is accompanied by two smaller volcanic centers, Little Meru on the northern flank and Meru West on the western flank, as well as many small cones, domes and maars around its flanks (Roberts, 2002). Meru was the stage of large-scale explosive activity, with at least 3 moderate-to-major explosive eruptions of phonolite magma in the last 40.000 years, i.e. MXP1, MXP2 and MXP3 (Kisaka et al., in review). Meru is marked on its eastern flank by a prominent horseshoe-shaped scar that is the result of an early Holocene sector collapse event and associated with a debris avalanche deposit. The volume of this deposit is estimated at $20 \pm 2 \text{ km}^3$ (Delcamp et al., 2017). Older, poorly mapped or dated debris avalanche deposits have also been recognized (Delcamp et al., 2016). Post-collapse activity is restricted to within the summit scar and comprises a lava dome, an ash cone and lava flows.

We investigate the pre- and post-collapse magmatic differentiation trends at Mt. Meru using petrography, major and trace element, and Sr isotope geochemical data, using a set of existing (Roberts, 2002; Kisaka, in preparation) and new data. We test the hypothesis that a major sector collapse would have a significant influence on the magmatic plumbing system and hence composition of erupted magmas (Watt, 2019). We present all data in a stratigraphic sequence to highlight pre- and post-collapse signatures in magmatic composition and differentiation. Observations suggest fractional crystallization to be the dominant magmatic differentiation process; however crustal assimilation is evident in some of the larger pre-collapse deposits representing the most evolved compositions erupted. Post-collapse magmas are not significantly different from pre-collapse magmas suggesting the crustal plumbing system may have remained largely unaffected by Meru's most recent sector collapse.

References

- Delcamp, A., Kervyn, M., Benbakkar, M., Kwelwa, S., & Peter, D. (2017). Large volcanic landslide and debris avalanche deposit at Meru, Tanzania. *Landslides*, 14(3), 833-847. <https://doi.org/10.1007/s10346-016-0757-8>
- Kisaka, M., Fontijn, K., Shemsanga, C., Tomašek, I., Gaduputi, S., Debaille, V., Delcamp, A., Kervyn, M. (in review). *The Late Quaternary Eruptive History of Meru Volcano, Northern Tanzania*. Journal of Volcanology and Geothermal Research.
- Roberts, M. A. (2002). *The Geochemical and Volcanological Evolution of the Mt. Meru Region, Northern Tanzania*. PhD Thesis, University of Cambridge.
- Delcamp, A., Delvaux, D., Kwelwa, S., Macheyeke, A., & Kervyn, M. (2016). Sector collapse events at volcanoes in the North Tanzanian divergence zone and their implications for regional tectonics.

Bulletin of the Geological Society of America, 128(1–2), 169–186.

<https://doi.org/10.1130/B31119.1>

Watt, S. F. L. (2019). The evolution of volcanic systems following sector collapse. *Journal of Volcanology and Geothermal Research*, (xxxx).

<https://doi.org/10.1016/j.jvolgeores.2019.05.012>

Kisaka, M.J. (in preparation). The eruption history of Meru volcano and its spatio-temporal relation with fluoride contamination in Arusha region, Tanzania. *PhD Thesis*, Vrije Universiteit Brussel.

Trace element partitioning between clinopyroxene, magnetite, ilmenite, and ferrobasaltic magmas: an experimental study

Kat SHEPHERD¹, Olivier NAMUR¹, Bernard CHARLIER²

¹ Department of Earth and Environmental Sciences, KU Leuven, 3000 Leuven, Belgium
(kat.shepherd@kuleuven.be; olivier.namur@kuleuven.be)

² Department of Geology, University of Liège, 4000 Sart Tilman, Belgium
(b.charlier@uliege.be)

Mineral-melt trace element partition coefficients in clinopyroxene and iron-titanium oxide phases have been determined experimentally from synthetic ferrobasaltic bulk compositions. Experiments were performed at a constant temperature (1080°C) and pressure (1 atm) over a range of oxygen fugacity (fO_2) conditions (QFM -2.1 to QFM +1.95; QFM = quartz-fayalite-magnetite equilibrium). Calculated partition coefficients indicate that the transition metals Ti, Zn, Co, Ni, V and Cr are moderately to highly compatible in Fe-Ti oxides, while other elements (REE, HFSE) are incompatible. In clinopyroxene, transition metals such as V, Sc, Cr and Ni are the most compatible elements.

Partition coefficients for divalent cations in clinopyroxene, Ti-magnetite and ilmenite are found to be controlled by the degree of polymerisation of the coexisting melt (NBO/T); a clear trend of increasing partition coefficient with decreasing NBO/T is observed for all phases. For trivalent cations including REE, fO_2 is the dominant control on trace element partitioning; coefficients are significantly higher at increasing fO_2 .

Multivalent cations such as Cr, Fe, Ti and V have important implications for understanding the redox state of a magma (Papike et al. 2005; Mallman and O'Neill 2009). Vanadium in particular can occur as V^{2+} , V^{3+} , V^{4+} or V^{5+} , covering the entire range of redox conditions on the terrestrial planets; this lends itself to the applicability of V as a universal redox indicator (Toplis and Corgne 2002; Mallman and O'Neill 2009). In our experiments, we infer that V^{3+} and V^{4+} are the dominant valence states, determined by application of the lattice strain model (Blundy and Wood 1994). Vanadium in the Fe-Ti oxides correlates positively with the TiO_2 content of each phase. Vanadium in magnetite correlates positively with ulvöspinel content, while V in ilmenite is inversely correlated with hematite content.

Economically important concentrations of elements such as vanadium are often associated with ilmenite and magnetite in Fe-rich cumulates and layered intrusions, e.g. Bushveld and Skaergaard (Balan et al. 2006; Charlier et al. 2015). Simple partitioning models, experimentally derived using a non-linear least squares routine, are presented to effectively predict partition coefficients of multivalent cations such as vanadium. This information may be used to assess under which redox conditions an economically viable concentration of vanadium may be found.

References

- Balan, E. De Villiers, JPR. Eeckhout, SG. Glatzel, P. Toplis, M.J. Fritsch, E. Allard, T. Galoisy, L. & Calas, G. 2006. The oxidation state of vanadium in titanomagnetite from layered basic intrusions. *American Mineralogist*, 91, 953–956.
- Blundy, J. & Wood, B. 1994. Prediction of crystal-melt partition coefficients from elastic moduli. *Nature*, 372, 452–454.

- Charlier, B. Namur, O. Bolle, O. Latypov, R. & Duchesne, J.C. 2015. Fe-Ti-V-P ore deposits associated with Proterozoic massif-type anorthosites and related rocks. *Earth-Science Reviews*, 141, 56–81.
- Mallmann, G. & O'Neill, H.S.C. 2009. The Crystal/Melt Partitioning of V during Mantle Melting as a Function of Oxygen Fugacity Compared with some other Elements (Al, P, Ca, Sc, Ti, Cr, Fe, Ga, Y, Zr and Nb). *Journal of Petrology*, 50, 1765–1794.
- McBirney, A.R. 1998. The Skaergaard Layered Series. Part VI. Included Trace Elements. *Journal of Petrology*, 39, 255–276.
- Papike, J.J. Karner, J.M. & Shearer, C.K. 2005. Comparative planetary mineralogy: Valence state partitioning of Cr, Fe, Ti, and V among crystallographic sites in olivine, pyroxene, and spinel from planetary basalts. *American Mineralogist*, 90, 277–290.
- Toplis, M.J. & Corgne, A. 2002. An experimental study of element partitioning between magnetite, clinopyroxene and iron-bearing silicate liquids with particular emphasis on vanadium. *Contributions to Mineralogy and Petrology*, 144, 22–37.

Combining tourmaline crystal morphology and geochemistry to investigate disequilibrium crystallization in pegmatitic melts

Laura M. VAN DER DOES¹, Niels HULSBOSCH¹, Jan ELSSEN¹, Philippe MUCHEZ¹,
Mona-Liza C. SIRBESCU²

1. *KU Leuven, Department of Earth and Environmental Sciences, 3001 Leuven, Belgium (laura.vanderdoes@kuleuven.be)*
2. *Central Michigan University, Department of Earth and Atmospheric Science, Mount Pleasant, Michigan 48859, USA*

Pegmatite dykes are characterized by coarse grain-sizes and anisotropic mineral textures, such as unidirectional solidification textures (UST), skeletal crystals and graphic intergrowths between minerals. These textures are interpreted as an effect of disequilibrium crystallization forced by large liquidus undercooling (Simmons and Webber, 2008), with nucleation and growth rate mainly controlling the morphology (Sirbescu et al., 2017). Disequilibrium crystallization in natural systems is poorly understood, as most relevant studies are based on experimental studies. Contrasting models of crystallization of pegmatitic melt involve an exsolved aqueous fluid with a major influence on formation of pegmatitic textures (Jahns and Burnham, 1969, Hulsbosch et al., 2016, Hulsbosch and Muchez, 2020); the coexistence of up to three immiscible fluids (Veksler et al., 2002); and crystallization of a single-phase, hydrous melt through constitutional zone refining and compositionally-modified boundary layers developing around the rapidly growing crystals (London, 2005). Tourmaline group minerals are good petrogenetic indicators due to their broad chemical variability and stability range (van Hinsberg et al., 2011). Here we explore tourmaline geochemistry in relation to its crystal morphology to understand the processes that led to liquidus undercooling and disequilibrium crystallization of a pegmatitic melt.

The Emmons Pegmatite (Oxford County, Maine, USA), a relatively thin, internally-zoned dyke with sharp contacts with the host rock (Falster et al., 2019), was selected for this study. Elongated, tapered prisms of schorl-group tourmaline were collected from the border-zone UST assemblage. Inwards, in the wall-zone, tourmaline becomes progressively coarser and more skeletal. Subhedral crystals of several dm's in length are surrounded by quartz-tourmaline intergrowths (QTI's). Geochemical variations among different crystal morphologies were examined through detailed petrography and major and minor element contents in tourmaline using EMPA. Petrographically, the tourmalines can be divided into four different morphology types: 1) elongated, euhedral prismatic tourmaline, 2) central tourmaline as the root of QTI's, 3) second tier tourmalines radiating from the end of the central tourmalines, and 4) skeletal QTI's. Type 1 tourmaline nucleates directly on contact with the host rock, in the border zone, and extends <5 cm in length (Fig. 1). Types 2, 3, and 4 found in the wall zone form up to 50 cm long, optically-coherent QTI assemblages (Fig. 1). In transmitted light, most crystals are strongly zoned with pink-purple cores and brown rims.

Major and minor element contents vary between samples, with increasing distance from the contact with the host rock. Mg decreases from 0.77 to 0.13 apfu, whereas Fe, Mn and Zn increase from 1.59 to 2.06 apfu, 0.01 to 0.05 apfu and 0.005 to 0.029 apfu, respectively. Additionally, certain elements vary from core to rim of single crystals in a direction perpendicular to the *c*-axis. For instance, Ti averages 0.018 apfu in the cores and 0.036 apfu in rims and Na averages 0.56 apfu in the cores and 0.65 apfu in rims. The variations among Type 2, 3 and 4 tourmalines within single QTI's, occur on mm to cm scale and are therefore unlikely to be linked to the bulk evolution of the pegmatite melt.

Instead, we suggest that the chemical variations result from the formation of a boundary layer around the first formed tourmaline. This boundary layer becomes progressively depleted in tourmaline components (mainly B) but enriched in silica causing tourmaline crystallization to pause, and quartz grains to form and dominate towards the edges of the QTI. As boundary layers develop, they become increasingly enriched in fluxing network modifiers (H₂O, F, P, B, Li), causing a prolonged delay in nucleation followed by accelerated crystal growth, when crystallization restarts (Simmons and Webber, 2008; Nabelek et al., 2010). The rapid, disequilibrium growth within the fluxed, silica-saturated boundary layer leads to the crystallization of coarser tourmaline in the wall-zone competing with quartz and forming the skeletal QTI morphology instead of an elongated, prismatic morphology in the border-zone.

References

- Falster, A. U., Simmons, W. B., Webber, K. L., Dallaire, D. A., Nizamoff, J. W. & Sprague, R. A. 2019. The Emmons Pegmatite, Greenwood, Oxford County, Maine. *Rocks & Minerals*, 94, 498-519.
- Hulsbosch, N., Boiron, M.-C., Dewaele, S. & Muchez, Ph., 2016. Fluid fractionation of tungsten during granite-pegmatite differentiation and the metal source of peribatholithic W quartz veins: Evidence from the Karagwe-Ankole Belt (Rwanda). *Geochimica et Cosmochimica Acta*, 175, 299-318.
- Hulsbosch, N. and Muchez, Ph., 2020. Tracing fluid saturation during pegmatite differentiation by studying the fluid inclusion evolution and multiphase cassiterite mineralization of the Gatumba pegmatite dyke system (NW Rwanda). *Lithos*, 354-355, 105285.
- Jahns, R. H. & Burnham, C. W., 1969. Experimental Studies of Pegmatite Genesis: I. A Model for the Derivation and Crystallization of granitic pegmatites. *Bulletin of the Society of Economic Geologists*, 64, 843-864.
- London, D., 2005. Granitic pegmatites: an assessment of current concept and directions for the future. *Lithos*, 80, 281-303.
- Nabelek, P. I., Whittington, A. G. & Sirbescu, M.-L. C. 2010. The role of H₂O in rapid emplacement and crystallization of granite pegmatites: resolving the paradox of large crystals in highly undercooled melts. *Contrib Mineral Petrol*, 160, 313-325.
- Simmons, W. B. & Webber, K. L., 2008. Pegmatite genesis: state of the art. *Eur. J. Mineral.*, 20, 421-438.
- Sirbescu, M.-L. C., Schmidt, D., Veksler, I. V., Whittington, A. G. and Wilke, M. (2017). Experimental Crystallization of Undercooled Felsic Liquids: Generation of Pegmatitic Texture. *Journal of Petrology*, 58, 539-568.
- van Hinsberg, V. J., Henry, D. J. & Dutrow, B. L., 2011. Tourmaline as a Petrologic Forensic Mineral: A Unique Recorder of Its Geologic Past. *Elements*, 7, 237-332.
- Veksler, I. V., Thomas, R. & Schmidt, C., 2002. Experimental evidence of three coexisting immiscible fluids in synthetic granitic pegmatite. *American Mineralogist*, 87, 775-779.

Figure 1

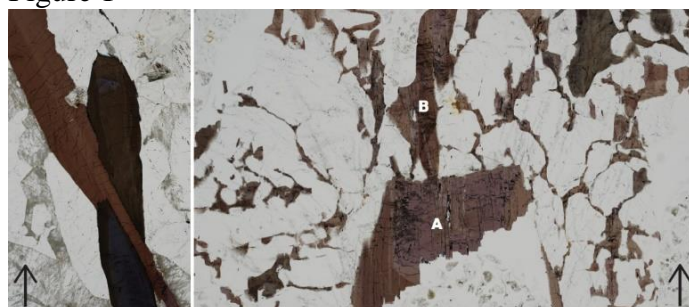


Figure 1 Elongated, euhedral prismatic tourmaline (left) and QTI (right) with the central tourmaline (A), second tier (B) and skeletal tourmaline (not annotated). Black arrows show growth direction. Image is approx. 8 cm x 5 cm.

Constraints on deep magmatic volatile budgets from olivine hosted melt inclusions

Thomas VAN GERVE¹, Olivier NAMUR¹, Penny WIESER², Hector LAMADRID³, Niels HULSBOSCH¹, David NEAVE⁴

1. KU Leuven, Leuven, Belgium (thomas.vangerve@kuleuven.be, , olivier.namur@kuleuven.be, niels.hulsbosch@kuleuven.be)

2. Oregon State University, Corvallis, US (wieserp@oregonstate.edu)

3. University of Missouri, Columbia, US (lamadridh@missouri.edu)

4. University of Manchester, Manchester, UK (david.neave@manchester.ac.uk)

Physical properties of magmas are strongly influenced by their volatile contents (Giordano & Dingwell, 2003). Due to their pressure dependent solubility volatiles are however largely lost from erupted lavas (Degruyter *et al.*, 2019). As a result, magma degassing plays a significant role in volcanic eruption styles (Tait *et al.*, 1989). Olivine, a phase commonly found in mafic magmas, often contains small glassy inclusions that form when droplets of silicate liquid are trapped by crystals at depth in the crust. These melt inclusions provide a unique way to analyse near-primary volatile abundances in magmas. This not only allows for important constraints on the dynamics of (deep) magmatic processes, but also on the pressures of melt inclusion formation (Métrich & Wallace, 2008; Colman *et al.*, 2015; Bennett *et al.*, 2019) and consequently depths of magma storage in volcanic plumbing systems.

Still, even glassy inclusions often do not preserve the original composition of melts trapped at depth, especially for volatile components. During ascent inclusions can partially crystallise, diffusion of elements in or out of the inclusion can take place (Hartley *et al.*, 2015) and vapour bubbles may form as the host crystal and melt shrink by different amounts (Moore *et al.*, 2015; Wieser *et al.*, 2020). Crystalline and vapour phases potentially host the majority of the total CO₂ budget of inclusions (Schiavi *et al.*, 2020; Wieser *et al.*, 2020). To reconstruct volatile contents of primary magmas rigorous constraints are therefore needed on both chemical composition and volumetric proportion of all phases present in the inclusion. Here we established a routine where high-resolution 3D scanning techniques are combined with in-situ chemical data to accurately reconstruct CO₂ and H₂O concentrations of deep magmas. It is a four-step process where 1) vapour bubble CO₂ density is calculated from Raman spectroscopy, 2) volumes of hydrous and/or carbonic crystalline phases are estimated from 3D Raman maps, 3) inclusion and bubble volumes are calculated from CT scans and 4) glass and crystal major, trace and volatile composition is measured in-situ by electron microprobe, Raman, LA-ICP-MS and SIMS.

Our approach is illustrated with olivine hosted melt inclusions from basaltic eruptions on the island of Pico, Azores. The vast majority of inclusions observed here have vapour bubbles and close to 40% include carbonate micro-crystals on the bubble walls. CO₂ vapour densities are high, clustering around 0.20 g.cm⁻¹. High concentrations of volatiles are in line with current theories that propose melting of a hydrous mantle as the formation mechanism for the Azores (Métrich *et al.*, 2014).

References

- Bennett, E. N., Jenner, F. E., Millet, M.-A., Cashman, K. V. & Lissenberg, C. J. (2019). Deep roots for mid-ocean-ridge volcanoes revealed by plagioclase-hosted melt inclusions. *Nature* 252.
- Colman, A., Sinton, J. M. & Wanless, V. D. (2015). Constraints from melt inclusions on depths of magma residence at intermediate magma supply along the Galápagos Spreading Center. *Earth and Planetary Science Letters* 412, 122–131.
- Degruyter, W., Parmigiani, A., Huber, C. & Bachmann, O. (2019). How do volatiles escape their shallow magmatic hearth? *Phil. Trans. R. Soc. A* 377.
- Giordano, D. & Dingwell, D. B. (2003). Viscosity of hydrous Etna basalt: Implications for Plinian-style basaltic eruptions. *Bulletin of Volcanology*. Springer 65, 8–14.
- Hartley, M. E., Neave, D., Maclennan, J., Edmonds, M. & Thordarson, T. (2015). Diffusive over-hydration of olivine-hosted melt inclusions. *Earth and Planetary Science Letters*. Elsevier 425, 168–178.
- Métrich, N. & Wallace, P. J. (2008). Volatile abundances in Basaltic Magmas and their degassing Paths tracked by Melt Inclusions. *Reviews in Mineralogy & Geochemistry* 69, 363–402.
- Métrich, N., Zanon, V., Créon, L., Hildenbrand, A., Moreira, M. & Marques, F. O. (2014). Is the ‘Azores Hotspot’ a Wetspot? Insights from the Geochemistry of Fluid and Melt Inclusions in Olivine of Pico Basalts. *Journal of Petrology* 55, 377–393.
- Moore, L. R., Gazel, E., Tuohy, R., Lloyd, A. S., Esposito, R., Steele-MacInnis, M., Hauri, E. H., Wallace, P. J., Plank, T. & Bodnar, R. J. (2015). Bubbles matter: An assessment of the contribution of vapor bubbles to melt inclusion volatile budgets. *American Mineralogist* 100, 806–823.
- Schiavi, F., Bolfan-Casanova, N., Buso, R., Laumonier, M., Laporte, D., Medjoubi, K., Venugopal, S., Gómez-Ulla, A., Cluzel, N. & Hardiagon, M. (2020). Quantifying magmatic volatiles by Raman microtomography of glass inclusion-hosted bubbles. *Geochemical Perspectives Letters* 16, 17–24.
- Tait, S., Jaupart, C. & Vergnolle, S. (1989). Pressure, gas content and eruption periodicity of a shallow, crystallising magma chamber. *Earth and Planetary Science Letters*. Elsevier 92, 107–123.
- Wieser, P. E., Lamadrid, H. M., Maclennan, J., Edmonds, M., Matthews, S., Jenner, F. E., Gansecki, C., Trusdell, F. & Lee, R. L. (2020). Reconstructing Magma Storage Depths for the 2018 Kilauean Eruption from Melt inclusion CO₂ Contents: The Importance of Vapor Bubbles. *Geochemistry, Geophysics, Geosystems*.

Calbuco (Central Southern Volcanic Zone, Chile): petrology of a hazardous volcano

Jacqueline VANDER AUWERA¹, Salvatrice MONTALBANO¹, Olivier NAMUR¹⁻³, Tonin BECHON¹, Pierre SCHIANO⁴, Jean-Luc DEVIDAL⁴, Olivier BOLLE¹

1. *Université de Liège, Département de géologie, B-4000 Liège (Belgium), jvdauwera@uliege.be*
2. *Leibniz Universität Hannover, Institute of Mineralogy, D-30167 Hannover (Germany)*
3. *University of Leuven, Department of Earth and Environmental Sciences, B-3001 Leuven (Belgium), olivier.namur@kuleuven.be*
4. *Laboratoire Magmas et Volcans, Université Clermont Auvergne, Clermont-Ferrand (France), j.l.devidal@opgc.univ-bpclermont.fr, pierre.schiano@uca.fr*

Calbuco is one of the three most dangerous volcanoes in Chile (Andean Southern Volcanic Zone (SVZ)). Its recurrent explosive eruptions threaten a rapidly expanding touristic and economic region as witnessed by the recent 2015 sub-Plinian eruption that occurred nearly without warning and caused significant damage to the local communities. Several parameters that are crucial for improving volcanic hazard assessment such as the depth of magma storage, the composition, including volatiles, of erupted magmas that dictates viscosity and thus potential explosivity, and reconstruction of the magma plumbing system can be derived from petrological data. Calbuco is also distinguished by amphibole-bearing assemblages that contrast with the anhydrous parageneses of most Central SVZ volcanoes. Here, a detailed petrological model of the magmatic system beneath Calbuco is proposed. Geochemical data acquired on a hundred samples collected in the four units of the volcano display no secular compositional change suggesting a steady magmatic system since ~300 ka. The parent magma is a tholeiitic Al₂O₃-rich (20 wt. %) basalt (Mg# = 0.59) that initiated a differentiation trend straddling the tholeiitic/calc-alkaline fields and displaying a narrow compositional Daly gap. The higher H₂O content of the basalt (3-3.5 wt. % H₂O at 50 wt. % SiO₂) compared to neighboring volcanoes resulted in amphibole crystallization. This characteristic is interpreted as inherited from the primary mantle melt and possibly results from a lower degree of partial melting induced by the mantle wedge thermal structure. Although macrocrysts are not all in chemical equilibrium with their host rocks and were thus presumably unlocked from the zoned crystal mush and transported in the carrier melt, the whole-rock trend overlap both experimental liquid lines of descent and the chemical trend of calculated melts in equilibrium with amphibole (AEMs). These contradictory observations can be reconciled if minerals are transported in near cotectic proportions. The AEMs overlap the Daly gap revealing that the missing liquid compositions were present in the storage region. Geothermobarometers all indicate that the chemical diversity from basalt to dacite was acquired at a shallow depth (210-460 MPa). We suggest that differentiation from the primary magma to the parental basalt took place either in the same storage region or at the MOHO.

Silicate liquid immiscibility of low-Ti and high-Ti basalts in the Emeishan Large Igneous Province, SW China

Yi-shen ZHANG¹, Olivier NAMUR¹, Bernard CHARLIER²

1. Department of Earth and Environmental Sciences, KU Leuven, 3000 Leuven, Belgium

(yishen.zhang@kuleuven.be, olivier.namur@kuleuven.be)

2. Department of Geology, University of Liège, 4000 Sart Tilman, Belgium (b.charlier@uliege.be)

Mafic-ultramafic layered intrusions in Large Igneous Provinces (LIP) commonly host world-class Fe-Ti-V oxides ore deposits. In order to understand processes responsible for the formation of Fe-Ti-V ores, we have conducted a stepwise experimental approach to reproduce fractional crystallization of high-Ti and low-Ti basalts. In particular, we tested whether these melts could develop silicate liquid immiscibility during cooling and fractionation, a process commonly suggested as the origin of the Fe-Ti oxides in Emeishan LIP (Zhou et al., 2005; 2013). We also investigated the role of fO_2 in the development of immiscibility and the saturation and relative stability field of ilmenite and magnetite.

Synthetic high-Ti (FeO_{tot} = 12.12 wt.%, TiO₂ = 2.28 wt.%) and low-Ti (FeO_{tot} = 10.61 wt.%, TiO₂ = 0.97 wt.%) picritic starting compositions were selected from a compiled database of Emeishan lavas. Experiments were carried out in one-atmosphere gas-mixing furnace (CO-CO₂ gas mixtures) from 1330 to 1040°C under the QFM (quartz-fayalite-magnetite) and QFM+2 buffers. The crystallization sequences of high-Ti and low-Ti magmas are olivine + spinel + augite + plagioclase ± pigeonite ± magnetite ± ilmenite ± whitlockite ± tridymite at both fO_2 . Liquid immiscibility started at 1040°C in both high-Ti and low-Ti magmas at QFM and QFM+2. Fe-rich globules (ferrobasalt) developed in the Si-rich melts (rhyolite) and nucleated on plagioclase, magnetite, and pyroxene.

Our study suggests that both high-Ti and low-Ti magmas can reach a two-liquid field. Immiscibility also developed during Fe and Ti depletion. High fO_2 triggers early crystallization of Fe-Ti oxides but does not hamper the development of immiscibility in the Emeishan LIP. We consider dual origins of Fe-Ti ores in the Emeishan LIP: Fe-Ti oxides could form from the Fe-rich melts segregated from immiscibility and/or early Fe-Ti oxides accumulation during fractionation.

References

Zhou, M-F. Robinson, P. Leshner, M. Keays, R. Zhang, C-J. & Maplas, J, 2005. Geochemistry, Petrogenesis and Metallogensis of the Panzihua Gabbroic Layered Intrusion and Associated Fe-Ti-V Oxide Deposits, Sichuan Province, SW China. *J. Petrol.*, 46, 2253–2280.

Zhou, M-F. Chen, WT. Wang, CY. Prevec, SA. Liu, PP. Howarth, GH, 2013. Two stages of immiscible liquid separation in the formation of Panzihua-type Fe-Ti-V oxide deposits, SW China. *Geosci. Front.*, 4, 481–502.

Petrogenesis and isotopic investigation of Pillow Lavas from the Troodos ophiolite, Cyprus: Cu and Zn isotopes

Nina ZARONIKOLA^{1*}, Vinciane DEBAILLE¹, Sophie DECREE², Ryan MATHUR³, Basilios TSIKOURAS⁴, Christodoulos HADJIGEORGIOU⁵

1. *Laboratoire G-Time, Universite Libre de Bruxelles, Brussels, Belgium*
(*nina.zaronikola@ulb.be*), (*vinciane.debaille@ulb.be*)

2. *Royal Belgian Institute of Natural Sciences, B-1000 Brussels, Belgium*
(*sdecree@naturalsciences.be*)

3. *Juniata College, 1700 Moore Street, Huntingdon, Pennsylvania 16652, USA*
(*MATHURR@juniata.edu*)

4. *Geosciences Programme, Faculty of Science, Universiti Brunei Darussalam, Jalan Tungku Link, BE1410, Bandar Seri Begawan, Brunei Darussalam* (*Basilios.tsikouras@ubd.edu.bn*)

5. *Geological Survey Department, 1 Lefkonos Street, 2064 Strovolos, Lefkosia, Cyprus*
(*chadjigeorgiou@gsd.moa.gov.cy*)

*Corresponding author.

Ophiolites represent relic fragments of oceanic crust and upper mantle, which were obducted into continental margins (Gass, 1968). A complete ophiolitic sequence, usually consists, from bottom to top of upper mantle peridotites, layered ultramafic-mafic rocks, layered to isotropic gabbros, sheeted dikes, extrusive rocks and sediments (Dilek and Furnes, 2009). The extrusive sequence of an ophiolitic complex includes the pillow lavas sequence, which is derived from underwater eruptions (Abdioğlu Yazar, 2018). Notably, in the Troodos ophiolite (Cyprus), the pillow lava sequence, subdivided in Lower Pillow Lavas (LPL) and Upper Pillow Lavas (UPL), host the Cyprus-type Volcanogenic Massive Sulfide (VMS) ore deposits (Hannington et al., 1998; Adamides, 2010 a,b; Martin et al., 2020). The UPL are usually basaltic to picritic in composition, while the LPL are basaltic-andesitic (Robinson and Malpas, 1990). As the mafic-type deposits of the Troodos ophiolite are found in the UPL and LPL, the latter play a key role in fluid circulation, metals source and enrichment investigations, as well as to describe metal precipitation conditions in hydrothermal systems and then secondary alteration.

In this study, in order to give a holistic overview of Cu enrichment in the pillow lava units, we present major element, trace element, Cu and Zn isotopes data of the Pillow Lava Series from the Troodos ophiolite from Agrokipia, Kambia and Troulli mines. The studied pillow lavas present Cu isotopic values between $-1.24 \pm 0.04\text{‰}$ and $+1.32 \pm 0.02\text{‰}$ (with an exception one sample enriched in pyrites with significant heavier Cu fractionation $+4.81 \pm 0.06\text{‰}$). Zinc isotopes fractionation range between $-0.69 \pm 0.01\text{‰}$ to $+0.43 \pm 0.02\text{‰}$. We discuss the petrogenesis of both UPL and LPL, as well as the Cu and Zn isotopes fractionation for the first time in the extrusive sequence of the ophiolite, aiming to investigate the behavior of Cu and Zn isotopes fractionation in low temperature alteration processes, derived from hydrothermal fluid interaction seen in host rocks for Cyprus-type VMS deposits of the Troodos ophiolite.

References:

- Abdioğlu Yazar, Emel, 2018. Alteration mineralogy, mineral chemistry and stable isotope geochemistry of the Eocene pillow lavas from the Trabzon area, NE Turkey. *Journal of African Earth Sciences*, 138(), 149–166.
- Adamides, N. G., 2010a. Mafic-dominated volcanogenic sulphide deposits in the Troodos ophiolite, Cyprus part 1-the deposits of the Solea graben. *Transactions of the Institutions of Mining and Metallurgy, Section B: Applied Earth Science*, 119(2), 65–77.
- Adamides, N., 2010b. Mafic-dominated volcanogenic sulphide deposits in the Troodos ophiolite, Cyprus Part 2- a review of genetic models and guides for exploration. *Appl. Earth Sci.* 119, 193–204.
- Dilek, Y. and Furnes, H., 2009. Structure and geochemistry of Tethyan ophiolites and their petrogenesis in subduction rollback systems. *Lithos* 113 (1), 1–20.
- Gass, I. G., 1968. Is the Troodos massif of Cyprus a fragment of Mesozoic oceanic floor? *Nature* 220, 39-42.
- Hannington, M. D., Galley, A. G., Herzig, P. M. and Petersen, S. 1998. Comparison of the TAG mound and stockwork complex with Cyprus-type massive sulphide deposits, *Proceedings of the Ocean Drilling Program, Scientific results*, 158, 389–415.
- Martin, A. J., Keith, M., Parvaz, D. B., Mcdonald, I., Boyce, A. J., Mcfall, K. A., ... Nürnberg, U. E.-. (2020). Effects of magmatic volatile influx in mafic VMS hydrothermal systems: Evidence from the Troodos ophiolite, Cyprus. *Chemical Geology*, 531,119325.
- Robinson, P.T., Malpas, J., 1990. The Troodos ophiolite of Cyprus: new perspectives on its origin and emplacement. In: Malpas, J., Moores, E.M., Panayiotou, A., Xenophontos, C. (Eds.), *Ophiolites, Oceanic Crustal Analogues, Proceedings of the Symposium “Troodos 1987”*. The Geological Survey Department, Nicosia, Cyprus, pp. 13–26.

Session 4- Geology, Man and Society

Conveners:

Jan Elsen (KU Leuven), Nuno Da Silva (UBLG), Michiel Dusar (RBINS-GSB), Eric Goemaere (RBINS-GSB)

Invited speaker:

Gilles Rixhon, Faculté de géographie et d'aménagement and Ecole Nationale du Génie de l'Eau et de l'Environnement, University of Strasbourg, France

In this section Belgium's rich geological heritage is depicted in its impact on landscapes and its provision of the mineral base of the built environment, past and present. The link between the geological substrate and cultural heritage were created and maintained by many generations of inhabitants with profound knowledge of their environment, but this link seems to be broken today. Much of the traditional knowledge has been lost on where to find and how to use local mineral resources or on the hazards related to former exploitations or land use.



Geoscientists have become essential partners to archeologists, historians, architects, city planners, tourist agencies ... in reconstructing these links, but also to quarry operators, construction companies for providing sound bases for efficient and ecological extraction and use of the subsurface materials. The geological diversity of Belgium's landscapes is gradually becoming acknowledged as a valuable resource for education and tourism and integrated into global protection and management schemes.

Structural framework as the new fundament for international geoscientific cooperation and policy support

Renata BARROS ¹, Kris PIESSENS ¹, Katrijn DIRIX²

¹ Geological Survey of Belgium, Royal Belgian Institute of Natural Sciences, Brussels, Belgium
(Renata.Barros@naturalsciences.be)

² VITO, Boeretang 200, Mol, Belgium (Katrijn.dirix@vito.be)

The transition towards a clean and low carbon energy system in Europe will increasingly rely on the use of the subsurface. Communicating the potential and limitations of subsurface resources and applications remains challenging. This is partly because the subsurface is not part of the world people experience, leaving them without reference frame to understand impacts or consequences. A second element is that the geological context of a specific area is very abstract, three dimensional, and hence difficult to correctly and intuitively disclose using traditional geological maps or models.

The GeoConnect^{3d} project is finalising the development and testing of a new type of information system that can be used for various geo-applications, decision-making, and subsurface spatial planning. This is being accomplished through the innovative structural framework model, which reorganises, contextualises, and adds value to geological data. The model is primarily focused on geological limits, or broadly planar structures that separate a given geological unit from its neighbouring units. It also includes geomanifestations, highlighting any distinct local expression of ongoing or past geological processes. These manifestations, or anomalies, often point to specific geologic conditions and therefore can be important sources of information to improve geological understanding of an area and its subsurface (see Van Daele et al., this volume, Rombaut et al., this volume).

Geological information in this model is composed of spatial data at different scales, with a one-to-one link between geometries and their specific attributes (including uncertainties), and of semantic data, categorised conceptually and/or linked using generic SKOS hierarchical schemes. Concepts and geometries are linked by a one-to-many relationship. The combination of these elements subsequently results in a multi-scale, harmonised and robust model. In spite of its sound technical basis, consultation is highly intuitive. The underlying vocabulary is of high scientific standard and linked to INSPIRE and GeoSciML schemes, but can also automatically, both visually and semantically, be simplified to be understood by non-experts.

The structural framework-geomanifestations methodology has now been applied to different areas in Europe. The focus on geological limits brings various advantages, such as displaying geological information in an explicit, and therefore more understandable way, and simplifying harmonisation efforts in large-scale geological structures crossing national borders originating from models of different scale and resolution. The link between spatial and semantic data is key in adding conceptual definitions and interpretations to geometries, and provides a very thorough consistency test for present-day regional understanding of geology. As a framework, other geological maps and models can be mapped to it by identifying common limits, such as faults, unconformities, etc, allowing to bring together non-harmonised maps in a meaningful way.

The model demonstrates it is possible to gather existing geological data into a harmonised and robust knowledge system. We consider this as the way forward towards pan-European integration and harmonisation of geological information. Moreover, we identify the great potential of the structural framework model as a toolbox to communicate geosciences

beyond our specialised community. Making geological information available to all stakeholders involved is an important step to support subsurface spatial planning to move forward towards a clean energy transition. .

This project has received funding from the European Union's Horizon 2020 research and innovation programme under grant agreement No 731166.

References

Van Daele, J., Ferket, H. & Barros, R. Optimal geodata centralization and disclosure as support for subsurface exploration. Geologica Belgica Conference, 2021.

Rombaut, B., Deckers, J., Dirix, K. Broothaers, M., Laenen, B. Analyzing seismic anomalies in Carboniferous strata in the surroundings of three wells in Mol (Campine Basin, northern Belgium) by means of Amplitude Variation with Offset (AVO) analysis and its potential for deep geothermal exploration. Geologica Belgica Conference, 2021.

Figure

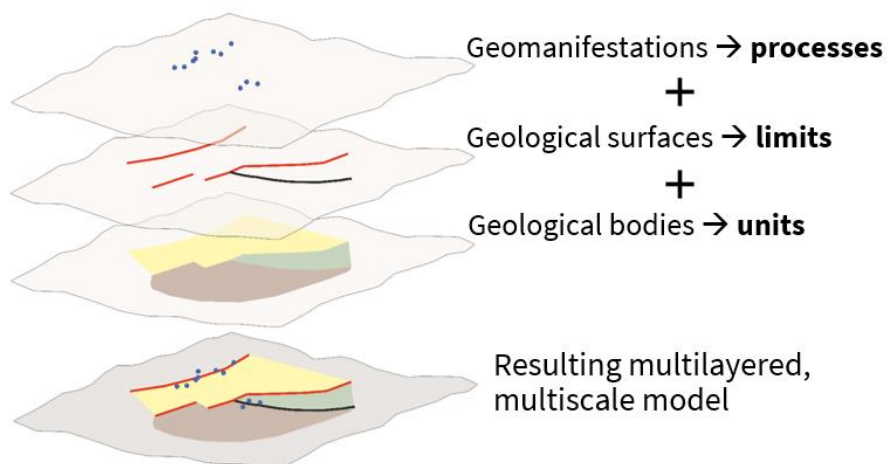


Fig. 1: Schematic representation of the structural framework model: a new approach to disclose the state of geoscientific knowledge.

Pb and Zn deportment estimation of historic mine waste by using an integrated mineralogical and geochemical approach: a case study from the Plombières mine waste (eastern Belgium)

Srećko BEVANDIĆ¹, Rosie BLANNIN³, Alexandra Escobar GOMEZ², Jorge M. R. S. RELVAS², Alvaro PINTO², Kai BACHMANN³, Max FRENZEL³, Philippe MUCHEZ¹

¹ KU Leuven, Department of Earth and Environmental Sciences, 3001 Leuven, Belgium (sreko.bevandi@kuleuven.be; philippe.muchez@kuleuven.be)

² Instituto Dom Luiz, Faculdade de Ciências, Universidade de Lisboa, 1749-016 Lisbon, Portugal (agescobar@fc.ul.pt; jrelvas@fc.ul.pt; ampinto@fc.ul.pt)

³ Helmholtz-Zentrum Dresden-Rossendorf, Institute Freiberg for Resource Technology, 09599 Freiberg, Germany (blanni70@hzdr.de; k.bachmann@hzdr.de; m.frenzel@hzdr.de)

Due to the variability and complex nature of mine waste materials, it is vital to understand their mineralogical properties, before starting with any tests that could lead to potential re-use. Mine waste materials, especially historic ones, are being nowadays considered as a secondary raw materials. This is closely related to the lack of mineral processing technology in the past (Evans, 2016). For the re-processing of mine wastes to be economically feasible it is important to maximise metal recovery. To achieve this, an in-depth mineralogical analysis is a prerequisite (Frenzel et al., 2019).

This study investigates the mineralogy and geochemical speciation of different types of mine waste material from the Plombières mining site (eastern Belgium), focussing on the ancient tailing pond. The tailings pond covers a minimum surface area of 8000 m², with 4 main types of material, i.e. soil, metallurgical waste, brown and yellow tailings (Bevandić et al., 2021). The soil has developed on the metallurgical waste and it is also considered as mine waste material (Bevandić et al., 2021). For this study, a combination of scanning electron microscope (SEM) based Mineral Liberation Analyser (MLA) and electron probe microanalysis (EPMA) was used for sample characterisation. The focus was on the distribution and location of the metals Pb and Zn within the mine wastes. Therefore, all the Pb and Zn phases were identified and their abundance quantified by MLA. In order to quantify the deportment of Pb and Zn, the chemistry of the minerals and amorphous material (e.g. slags) was determined by EPMA.

This integrated approach revealed that the major hosts of Pb are Pb-oxides, anglesite and pyrometallurgical slags. For zinc, the major hosts are slags and the minerals fraipontite and bannisterite. The deportments of Pb and Zn strongly depend on the type of the mine waste. In the soils, slags are the major host of Pb, followed by anglesite. For metallurgical waste, the Pb is mainly present in Pb oxides and slags. In brown tailings, the major host of Pb are Pb-oxides, followed by anglesite and slags. In yellow tailings, all Pb is hosted in the slags. In all 4 types of the mine waste, Zn is mainly hosted in slags, followed by either fraiponite (soil and metallurgical waste) or bannisterite (brown and yellow tailings).

References

1. Evans, K., 2016. The History, Challenges, and New Developments in the Management and Use of Bauxite Residue. *J. Sustain. Metall.* 2, 316-331.
2. Frenzel, M., Bachmann, K., Carvalho, J.R.S. et al., 2019. The geometallurgical assessment of by-products geochemical proxies for the complex mineralogical department of indium at Neves-Corvo, Portugal. *Miner Deposita* 54, 959–982.
3. Bevandić, S., Blannin, R., Vander Auwera, J., Delmelle, N., Caterina, D., Nguyen, F. & Muchez, P., 2021. Geochemical and Mineralogical Characterisation of Historic Zn–Pb Mine Waste, Plombières, East Belgium. *Minerals* 2021, 11, 28.

Towards a dynamic and interdisciplinary assessment for the sustainable management of geological resources

Tine COMPERNOLLE^{1,2}, Kris PIESENS², Kris WELKENHUYSEN²

1. University of Antwerp, Department of Engineering Management, Prinsstraat 13, 2000 Brussels, Belgium

2. Geological Survey of Belgium – Royal Belgian Institute of Natural Sciences, Jennerstraat 13, 1000 Brussels, Belgium

Like ecosystems, the subsurface can be considered as a geosystem, providing multiple services and a variety of activities take place at varying depths (Gray et al., 2013). Subsurface pore space is a valuable commodity, fixed geographically but potentially subject to multiple uses over time. The strategic importance of the subsurface can vary with time, as witnessed in the growth of unconventional oil/gas extraction, or of increased interest in geothermal resources and requirement for CO₂ storage space to mitigate climate change. It is therefore useful to consider pore space as a strategic asset that is likely to have potential future uses and where direct and indirect interactions need to be assessed and prioritized (Field et al., 2018). Because the number of known and suitable geological formations is limited and because the subsurface is a complex and interlinked system, competition between subsurface uses is already taking place and is likely to increase. Additionally, subsurface activities will leave geochemical, geomechanical, geohydraulic and geothermal imprints. Past activities have left imprints that dictate current subsurface utilizations, and present subsurface activities will leave imprints that will dictate the options for future subsurface utilization (Michael et al., 2016). One activity could prohibit the adoption of another activity and even though different subsurface activities could be operating simultaneously, their operations will influence each other.

Based on an extensive literature review, we present a conceptual framework that reveals the relationships and interactions between different subsurface activities and their associated above-ground impacts. We use this framework to identify existing knowledge gaps and to propose a future research agenda.

We find that there is no common understanding about what ‘sustainable subsurface management’ actually involves. Current sustainability indicator frameworks fall short in recognizing that the demand for the geological resource at hand could change in time and that specific geological volumes might need to be conserved for future usages such as the disposal of nuclear waste or CO₂ storage.

To assess the sustainability of interacting subsurface activities and to determine the threshold values that must be met to respect the sustainability criteria, a set of compatible and advanced hydrogeological, environmental, and socio-economic models need to be developed first. Existing (hydro)geological models are tailored to a specific type of subsurface activity and these reservoir models do not provide knowledge about the dynamic interaction effects between multiple subsurface activities. A high-level generalized workflow framework as proposed by Michael et al. (2016) is useful to explore potential interacting activities. To progress into site-specific evaluations, a more detailed characterization of interference effects between subsurface activities is required. We need flexible, loosely coupled and dynamic hydrogeological models that are sensitive to each other and capable to quantify the impacts of a changing hydrogeological context on other activities, covering wide time scales while being practical to solve.

In order to reconcile geological resource conservation with changing demands on geological resource use, it is essential that the geological and the above-ground ecological,

socio-cultural and economic values of the geological resource can be fully taken into account in planning and decision making. However, there exist no methodological decision support framework for subsurface planning that accounts for both the plurality of values as well as their dynamic nature. Within the field of Ecological Economics, it has long been recognized that resource conflicts cannot be settled by attempts to commensurate the plurality of values by the use of monetary measures that assign the settlement of conflicts to markets or to cost-benefit analysis. Multi-criteria decision analysis (MCDA) is considered more appropriate to evaluate alternatives under incommensurability of values. It is a methodology to structure complex problems in matrix form, with alternatives on one axis and evaluation criteria on the other. The matrix can consist of qualitative, quantitative or both types of information and can be applied for macro, micro and project evaluation (Pirgmaier & Urhammer, 2015).

Within the field of Economics and Operations Research, the real options theory is considered to be more appropriate than cost benefit analysis to account for impact dynamics and managerial flexibility. It is recognized that the flexibility of waiting with a development and the flexibility to adopt adaptive measures have value and should be integrated in economic decision support methods (Dixit & Pindyck, 2012). However, current real options approaches do not account for a plurality of values to determine an optimal time to invest or to value flexibility. Therefore, we need a methodological framework that on the one hand accounts for a plurality of values and on the other hand recognizes that subsurface developments are made in consecutive steps, to deal with uncertainty, acknowledging possible adaptations in time.

The identified knowledge gaps can only be filled in by adopting an interdisciplinary approach and by forming interinstitutional collaborations. By working on mutual topics and integrating discipline-specific methodologies, scientific cross-overs can be realized. Such an interdisciplinary research team then develops integrated models through an iterative process in which side-by-side analyses evolve and adjust, connect and become a single model that provides joint research conclusions. Furthermore, such cross-overs should not be limited to Geology and Environmental Economics. Driven by the multifaceted research challenges, a network of bridges that connect multiple research topics, methods, and disciplines can be build. Also, the interaction with society is important. Not only to deal with values and normative judgements but also to develop analyses and solutions for practical problems and to feed results back to practical actions.

References

- Gray, M., Gordon, J.E., & Brown, E.J., 2013. Geodiversity and the ecosystem approach: the contribution of geoscience in delivering integrated environmental management. *Proceedings of the Geologists' Association*, 124, 4, 659-673.
- Field, B., Barton, B., Funnell, R., Higgs, K., Nicol, A., & Seebeck, H., 2018. Managing potential interactions of subsurface resources. *Proceedings of the Institution of Mechanical Engineers, Part A: Journal of Power and Energy*, 232, 1, 6-11.
- Michael, K., Whittaker, S., Varma, S., Bekele, E., Langhi, L., Hodgkinson, J., & Harris, B., 2016. Framework for the assessment of interaction between CO₂ geological storage and other sedimentary basin resources. Royal Society of Chemistry.
- Pirgmaier, E., & Urhammer, E., 2015. Value pluralism and incommensurability in Ecological Economics. *Thor Heyerdahl Summer School in Environmental Governance*, 3, 1-15. http://www.nmbu.no/sites/default/files/pdfattachments/thss_volume_3_0.pdf
- Dixit, R.K., & Pindyck, R.S., 2012. *Investment under Uncertainty*. Princeton: Princeton University Press.

‘Fossiles en Ville’: popularizing the History of Life and Earth through urban palaeontology and geology

Julien DENAYER^{1,2}, Amandine SERVAIS², Martine VANHERCK², Thomas BEYER² & Valentin FISCHER¹

1. *Evolution & Diversity Lab, Université de Liège, Allée du Six-Août, B18, Sart Tilman, B4000 Liège, Belgium, julien.denayer@uliege.be, v.fischer@uliege.be,*
2. *Réjouissciences, Université de Liège, Quai Van Beneden, 11, B4020 Liège, Belgium, amandine.servais@uliege.be, martine.vanherck@uliege.be, thomas.beyer@uliege.be*

Despite the obvious public interest for palaeontology, the fossils are usually poorly known. Belgium suffers from a double issue: the non-valorisation of its incredible geoh heritage and the lack of popularisation of this subject to a wide audience. This fact is even more unfortunate knowing that fossils are numerous and diverse in the building stones everywhere around us. Whereas palaeontologists could easily spot numbers of fossils in a stone wall, most people do not see anything or even consider the fossils as stains or imperfections within the stones. The project ‘Fossiles en Ville’ (‘Fossils in the City’) aims to cure these issues in a simple way by making the fossils visible, understandable and accessible freely through several media. Moreover, the fossils are a ludic way of arousing the interest for the History of Life and Earth, and promoting the other Earth sciences such as sedimentology, evolution, climatology and palaeogeography.

‘Fossiles en Ville’ is designed as 1-2 km-long walks in the center of cities and towns, connecting 15-20 fossils spotted on the walls of public buildings, pavement, statues, staircases, etc., and provides explanations on each fossil (taxonomy, age, environment, geographic origin of the stone) as well as pictures of the organism. In October 2019, three tours and their explanations were set up in the centre of Liège as a test phase and were made available on the online platform and mobile application ‘Cirkwi’. In July 2020, the project entered a second phase with the edition of booklets in collaboration with Réjouissciences (Science Popularisation Department at the University of Liège). Each booklet, designed as a road-book, covers one single tour and provides information on all spotted fossils. A second booklet covers theoretical questions (what are the fossils? how do they form? why are there so many fossils in towns? what is the geological time scale? what the fossils can tell about climates of the past and palaeogeography?); a second one is a simplified identification key to help recognising the most common fossils in sections; and the third one is a kids activity booklet designed for 7-12 years children. Special guided tours were organised in Liège for the Journées wallonnes du Patrimoine (Heritage Day) with more than 100 participants and >250 consultations on ‘Cirkwi’ for self-guided tours. The project also led to the organisation of indoor and outdoor palaeontology-centered activities for children during holiday times with Art&Fact asbl in Liège.

The project ‘Fossiles en Ville’ demonstrated the interest of the public for local, free and accessible activities, adapted for non-scientific public and in particular to children. The number of tours increased progressively with now 15 available tours and booklets in Liège, Namur, Mons, Huy, Gembloux, Dinant, Couvin and Marche-en-Famenne* whereas other tours are under development. The online equivalents on ‘Cirkwi’** record, on average, 200 consultations per month with peaks up to 500 consultations during holiday times.

In 2020, 'Fossiles en Ville' was granted the Wernaers Award of the FNRS for its new concept of popularisation of palaeontology and geology through a multi-platform project. Besides the tours available on 'Cirkwi', a new dedicated mobile application is currently developed. It will eventually make accessible all the tours either through the choice a destination or by scanning QR codes positionned on public buildings near interesting fossils. The QR codes will automatically open a webpage summarizing information on the fossils and proposing a guide to the next fossil on the tour.

In conclusion, 'Fossiles en Ville' is a project aiming to shed light on the numerous fossils that can be spotted in urban context and to provide scientific, though adapted, knowledge to a broad public and therefore to arouse interest for Earth Sciences. Moreover, it also has an interest for Earth scientists as it gathers a lot of characteristic and less characteristic fossils useful to identify the building stones in historical or modern buildings.

References

*https://www.rejouisciences.uliege.be/cms/c_11988615/fr/des-fossiles-en-ville

**<https://cutt.ly/UnqC6gn>

Pierre de Meuse, an exceptional Belgian historical heritage stone from the Meuse valley

Roland DREESEN¹, Edouard POTY², Bernard MOTTEQUIN³, Jean-Marc MARION² & Julien DENAYER²

1. *Belgian Geological Survey, Brussels, Belgium* (roland.dreesen@telenet.be)
2. *Université de Liège, Liège, Belgium* (E.Poty@uliege.be, jmmarion@uliege.be, julien.denayer@uliege.be)
3. *Royal Belgian Institute of Natural Sciences, Brussels, Belgium* (bmottequin@naturalsciences.be)

Among the many Belgian historical heritage stones, the Viséan (lower Carboniferous) ‘Pierre de Meuse’ or Meuse Limestone is certainly one of the most important and famous building and decorative stones. It is also known as ‘Pierre bleue de Namur’ or ‘Naamse steen’. The ‘Pierre de Meuse’ shares the overarching name ‘pierre bleue’ (blue stone or ‘blauwe steen’) with two other famous Belgian calcareous building stones, the ‘Pierre de Tournai’ and the ‘Petit Granit’, both fossiliferous limestones and well-known building stones of lower Carboniferous age. The ‘Pierre de Meuse’ *sensu stricto* is a limestone of middle Viséan age (Livian; Lives Formation) that is particularly well exposed and well accessible in the Meuse valley, downstream of the city of Namur. We here restrict the definition of the ‘Pierre de Meuse’, excluding several other Carboniferous limestones also extracted in the Meuse valley and its tributaries, because they belong to different lithostratigraphic units and were used in different ways at different times (e.g. ‘Pierre de Vinalmont’ and ‘Pierre de Longpré’). The analysis of a significant quantity of ‘Pierre de Meuse’ in historical buildings reveals that only particular beds within the Haut-le-Wastia and Corphalie members of the Lives Formation were quarried as building and decorative stone in the vicinity of Namur.

The Romans were first to make a wide use of this limestone, both as a building stone and a decorative stone within the capital, agglomerations, rural settlements and villas of the *civitas Tungrorum*. Moreover, they have even exported this particular stone to Roman settlements in neighboring *civitates* (Heerlen, Trier, Xanten, Echternach, Vichten, Colijnsplaat). Furthermore, during Medieval times it has become the real hallmark of Romanesque religious and public buildings, funerary monuments, floor tiles and tombstone, especially in the Principality of Liège. Later on, its distribution has spread towards the north (The Netherlands) and the south (N-France). Due to the presence of a nice subhorizontal bedding and a regular bed thickness, a regular spacing of joints and the proximity of a river, the ‘Pierre de Meuse’ was preferentially extracted in the vicinity of the city of Namur, whereas the Meuse represented its main transport means since Antiquity through the Middle Ages.

Detailed *in situ* investigations of numerous historical monuments allowed to define five distinct macroscopic lithofacies within the ‘Pierre de Meuse’. All these varieties have been successively used as building and/or decorative stone, but during different time intervals. Their main macroscopic and microscopic (palaeontological and petrographical) characteristics will be briefly presented, as well as their characteristic carbonate microfacies and index fossils. Some of the finest and most famous Belgian black marbles, the ‘Marbre noir de Namur’ (Black marble of Namur), is a particular thinly-bedded, black-colored micritic limestone belonging to the Corphalie Member of the Lives Formation. Its unique chroma and quality have been appreciated at least since Roman times. Most famous are the medieval baptismal fonts and the incised tombstones manufactured in ‘Pierre de Meuse’, whereas

particular architectural trends in the Meuse valley are dominated by the use of this stone, such as the Mosan gothic and Mosan renaissance styles.

Not much is known about the earliest (Roman) extraction, probably because of younger quarrying activities that destroyed all former traces. However, a number of abandoned historical quarries (both underground and open-air) still exist, most of which are located in the direct vicinity of Namur. Some of these have now become important biotopes and/or geosites, whereas others represent popular speleological attraction sites. The 'Pierre de Meuse' is particularly rich in invertebrate fossils (corals, brachiopods, gastropods) as well as in sedimentary structures (laminated stromatolites, oncolites). The latter fossil assemblages and structures can be simply recognised and allow to easily identify the 'Pierre de Meuse' in historical context.

Sourcing natural stone used in the architecture of stone-poor landscapes, demonstrated for northern Belgium

Michiel DUSAR ¹, Marleen DE CEUKELAIRE ²

1. Royal Belgian Institute of Natural Sciences Geological Survey of Belgium, Brussels & Faninbel bvba, Wechelderzande, BE (mdusar@naturalsciences.be)

2. Royal Belgian Institute of Natural Sciences Scientific Heritage Service & Geological Survey of Belgium, Brussels, BE (mdeceukelaire@naturalsciences.be)

In contrast to southern Belgium (Wallonia), where Paleozoic rocks are well exposed and clear links exist to the local building industry, northern Belgium (Flanders) consists of generally unconsolidated strata, practically devoid of exposure. Despite this apparent difference in geological landscape, practically all cohesive rocks occurring in the Flemish subsurface have been quarried for local use as building stone in the past. Visibility or knowledge on former extraction sites is nearly inexistent but historic buildings constitute a good proxy, replacing the quarries and outcrops as source material on local geodiversity.

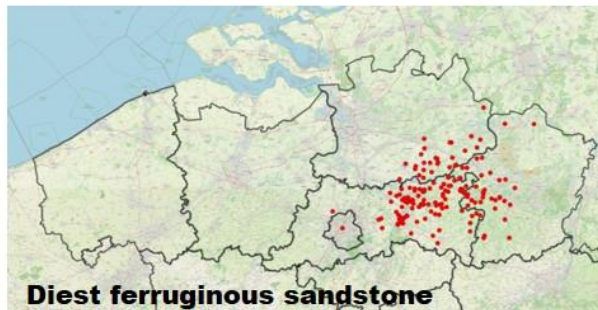
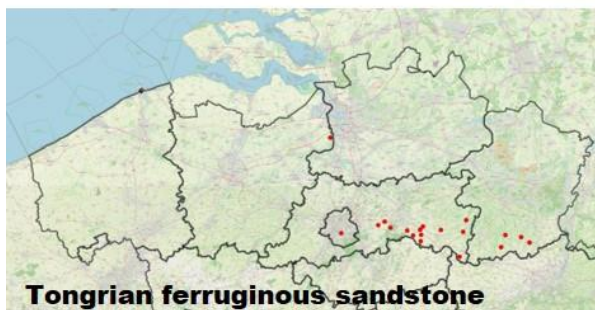
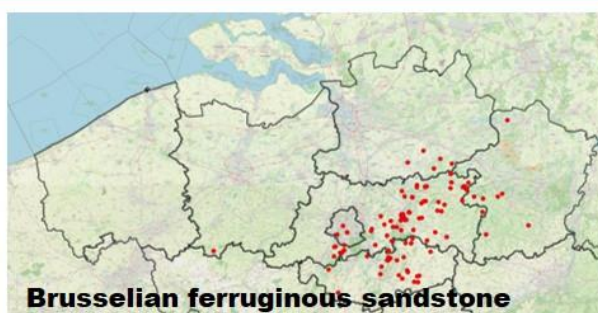
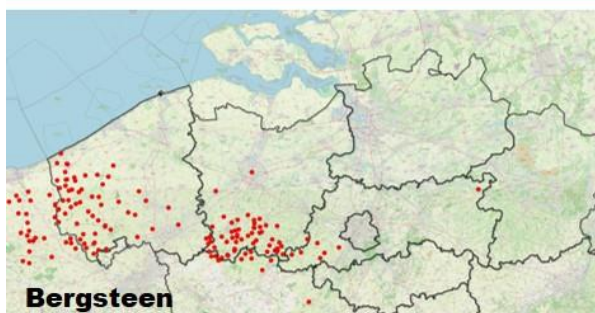
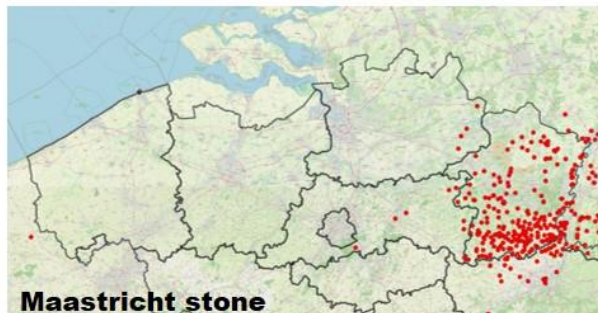
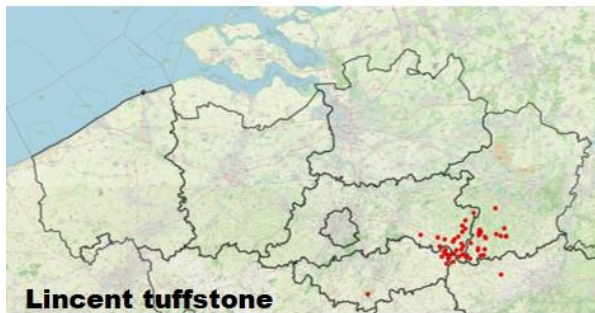
Although use of natural building stones and their replacement stones depend on various factors such as availability, technology, transport and fashion, the geographic distribution of stone types in historic buildings remains clearly related to their exploitation areas: cultural diversity follows geodiversity. Stone types only occasionally used as building material are not recorded far beyond the area of their natural occurrence, whereas stone types of more commercial value extend from stone-rich to stone-poor areas, mostly going downriver. This system prevailed during the entire building history from the 11th till the 20th century and is actually (partly) maintained in accordance with the restauration principles.

A georeferenced database of natural stone records from monuments and other buildings is an essential instrument to follow-up on historical stone use. Such a database has been elaborated at the Geological Survey of Belgium after the pioneering work in the province of Limburg (Dreesen et al., revised edition 2019). It is focused on stone-poor northern Belgium but covers also surrounding areas for a better grasp on the effective realm of the different stone types. Although it is a permanent work in progress, anno May 2021 the database contains nearly 18 000 records on natural stone occurrence in Flanders and Brussels, allowing confidence for this part of the country in the observed natural stone variability and their geographical spreading from extraction sites to the buildings. This is illustrated for some well-known Maastrichtian to Eocene limestones and Eocene to Miocene ferruginous sandstones of local origin (Fig.).

References

Dreesen, R.; Dusar, M.; Doperé, F., 2019. Atlas Natuursteen in Limburgse gebouwen. Provinciaal Natuurcentrum, Genk, 352 p.

De Ceukelaire, M., 2021. RBINS Collection of Geology – Monuments. <https://collections.naturalsciences.be/ssh-geology/monuments> (version May 2021).



Occurrence maps for the principal indigenous light-coloured limestones ('witstenen') above, and ferruginous sandstone ('ijzerzandstenen') below the separation line in monuments, considered representative for their distribution area in Flanders and Brussels regions. Names according to common use.

3D mapping of underground galleries from Maastricht limestone extraction in Riemst

Mike LAHAYE ^{1,2}, Tim DE KOCK ¹

1. *Antwerp Cultural Heritage Sciences (ARCHES), University of Antwerp, Mutsaardstraat 31, Antwerpen, Belgium (Tim.DeKock@uantwerpen.be)*

2. *Municipality of Riemst, Maastrichtersteenweg 2b, 3770 Riemst, Belgium (Mike.Lahaye@riemst.be)*

The underground limestone quarries in the southeastern part of the Limburg province (Belgium) have been used for limestone extraction, storage, shelter, and cultivation of mushrooms. Many geological features can be distinguished and observed in these Cretaceous limestone gallery systems (Willems and Rodet, 2018) This multifunctional and frequent use has left many traces in the landscape above and underground and the quarries are inherent part of the local culture as they are still being used.

The underground extraction of limestone started in the Late Middle Ages and continues to this day. The multifunctional use and long duration has left many traces of inscriptions, drawings, and quarrying techniques. Since a few years the cultural values of the underground quarries are valued, as some underground quarries are protected as an archaeological site or protected landscape (de Haan and Lahaye, 2018).

The present-day stewardship of the quarries is confronted with many challenges (Lahaye, 2017). Relatively limited information is known about the underground limestone quarries in the municipality of Riemst, such as their exact location relative to the surface, infrastructure, and buildings. In order to inspect and monitor stability problems an exact location is necessary. Various underground quarries have already been prone to collapse resulting in possible unknown areas which may still be intact but cannot be mapped.

By conducting fieldwork, 3D measurements, and researching archives, a more profound knowledge and new insights are obtained about the underground quarries. The underground galleries are mapped using a mobile 3D laserscanner (Geoslam RT). Unknown galleries are identified and based on the obtained 3D data, decisions are made on further inspection or gallery stabilization. This 3D data is also valuable in documenting the archaeological and geological features, and can be used to describe the means of extraction, as well its consequences on the landscape (Lahaye, 2020).

References

- de Haan, A. and Lahaye, M.F.A., 2018. Grote Berg Zussen - Inventarisatie en waardering van de mergelgroeve. Onderzoeksrapporten Agentschap Onroerend Erfgoed nr. 100.
- Lahaye, M.F.A., 2017. Op Losse groeven - ondergronds mergelerfgoed en stabiliteitsproblemen in Riemst. In: Ruimte volume 9 nr. 34.
- Lahaye, M.F.A., 2020. 3D laserscanning van ondergrondse mergelgroeven. In: SOK Mededelingen nr. 74 (Natuurhistorisch Genootschap Limburg), p. 34-52. 2/2
- Willems, L. and Rodet, J., 2018. Karst and Underground Landscapes in the Cretaceous Chalk and Calcarene of the Belgian-Dutch Border – The Montagne Saint-Pierre. In: A. Demoulin (ed.), *Landscapes and Landforms of Belgium and Luxembourg*, World Geomorphological Landscapes. Springer International Publishing AG, p. 177-192. DOI 10.1007/978-3-319-58239-9_11.

Tectonostratigraphic evolution coupled with climate changes of the pre-Sturtian Fungurume-Mwashya platform in the Tenke-Fungurume Mining District, Democratic Republic of the Congo

Pascal MAMBWE^{1,2}, Franck DELPOMDOR⁴, Sébastien LAVOIE³, Philippe MUKONKI³, Jacques BATUMIKE⁵, Philippe MUCHEZ¹

1. *KU Leuven, Department of Earth & Environmental Sciences, Celestijnenlaan 200E, B-3001 Leuven, Belgium*

(pascal.mambwematanda@kuleuven.be, philippe.mucchez@kuleuven.be)

2. *University of Lubumbashi, Department of Geology, B.P. 1850 Lubumbashi, Democratic Republic of Congo.*

3. *CMOC Mining USA Ltd., 2600 N Central Av., Phoenix, AZ 85004-3032, United States of America (geologue@sebastienlavoie.com).*

4. *Illinois State Geological Survey, University of Illinois at Urbana-Champaign, 615 E Peabody Dr, Champaign, IL 61820, United States of America (fdelpomd@illinois.edu)*

5. *Macquarie University, ARC Centre of excellence for Core to Crust Fluid Systems (CCFS) and GEMOC, NSW 2109 Sydney, Australia (jbatumike@gmail.com)*

A tectonostratigraphic model is here proposed for the Fungurume-Mwashya platform succession at Tenke Fungurume Mining District (TFMD), south-east Democratic Republic of Congo. TFMD in the Katanga Copperbelt hosts the stratiform to stratabound Cu-Co mineralization. Sedimentary slumping and the generation of mass flows were principally controlled by tectonic activity during the initial rifting of the intracratonic Nguba Rift-Basin, around ~760-740 Ma. At least three tectonostratigraphic sequences recorded the tectonic reorganization between the Congo Craton and the Tanzanian block. One of them, which has been recognized at the base of the Mwashya Subgroup, has recently been coupled with the ~760-740 Kaigas glacial event. It is characterized by a backstepping to shallowing-upward sequence capped by an erosion surface at the top of the Kansuki Formation. This sequence begins by deposition of the periglacial polygenetic conglomerate, the lateral stratigraphic equivalent of the Mwashya Conglomerate, and the post-glacial cap carbonate sequence of the Kamoya Formation (Fig.1).

The Fungurume-Mwashya succession was deposited in a protected coastal lagoon adjacent to a tidal flat environment which was protected from the open sea by a barrier shoal (Cailteux et al., 2007; Mambwe et al., 2019). The platform was then flooded by fluvio-deltaic siliciclastics in the aftermath of the Sturtian glacial event. This is evidenced by the diamictitic facies of the Mwale Formation. Large amount of hematite within the matrix of the polygenic conglomerate recorded a remobilization of ferrous iron in bottom waters from the ~765-745 volcanic activity, which was oxidized by the mixing of layers of the stratified seawater at the onset of the Kaigas deglaciation. This bottom-water mixing was probably controlled by local fault-controlled uplift that generated subaqueous mass movements. The overlying cap carbonate sequence successively comprises an ~100 m-thick deepening-upward transgressive to shallowing-upward carbonate succession that was marked by deposition of oolites on the barrier platform top. It was followed by the development of lagoonal and tidal flat sediments during a sea-level highstand. This study concludes that the cycles of deposition in the Fungurume-Mwashya platform succession were driven by regional tectonics, superimposed upon the ~750-720 Ma Kaigas and ~717–660 Ma Sturtian glacial intervals (Mambwe et al., 2020).

References

- Cailteux, J.L.H., Kampunzu, A.B. & Lerouge, C., 2007. The Neoproterozoic Mwashya-Kansuki sedimentary rock succession in the central African Copperbelt, its Cu–Co mineralization, and regional correlations. *Gondwana Research*, 11, 414–431.
- Lefebvre, J.J., 1978. Le Groupe de Mwashya. Megacyclothème terminal du Roan (Shaba, Zaïre sud-oriental). Approche lithostratigraphique et étude de l'environnement sédimentaire. *Annales de la Société Géologique de Belgique*, 101, 209- 225.
- Mambwe, M.P., Lavoie, S., Delvaux, D. & Batumike, J.M., 2019. Soft sediment deformation structures in the Neoproterozoic Kansuki formation (Katanga Supergroup, Democratic Republic of the Congo): Evidence for deposition in a tectonically active carbonate platform. *Journal of African Earth Science*, 150, 86-95.
- Mambwe, P., Delpomdor, F., Lavoie, S., Mukonki, Ph., Batumike, J. & Muchez, Ph., 2020. Sedimentary evolution and stratigraphy of the ~765–740 Ma Kansuki-Mwashya platform succession in the Tenke-Fungurume Mining District, Democratic Republic of the Congo. *Geologica Belgica*, 23, 1-2, 69-85.

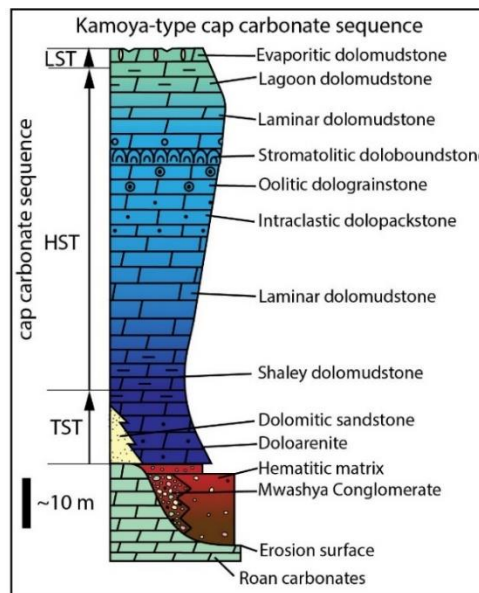


Figure 1: Idealized Kamoya cap carbonate sequence at Tenke-Fungurume Mining District

Seasonal variations of water-soluble heavy metals in atmospheric deposition at NE Sichuan, Central China: Natural and anthropogenic effects

Chen-guang PAN¹, Yue-feng LIU¹, Xiao-tao PENG¹, Yu XIE¹, Hai-bo HE¹, Jing TANG¹, ZHOU Hou-yun^{1,*}

1. School of Geographical Science, South China Normal University, Guangzhou 510631, China

Geochemical study of atmospheric deposition is important for explanation of the geochemical behavior of elements in the epigenetic environment. However, previous studies largely focused on cities or areas strongly affected by industrial activities. In this study, the NE Sichuan Province, a remote area receiving little influence from industrial activities, was selected to investigate water-soluble heavy metals (such as Cr, Co, Ni, Cu, Zn, Ga, As, Cd and Pb) in the atmospheric depositions collected from in August 2011 to July 2014. The results indicated that Zn had the deposition flux with an annual average of $158\mu\text{g}\cdot(10^2\text{ cm}^2\cdot\text{a})^{-1}$, while Ga had the smallest one with an annual average of $0.06\mu\text{g}\cdot(10^2\text{ cm}^2\cdot\text{a})^{-1}$, 4 orders of magnitude lower than that of the Zn. The deposition flux of heavy metals at NE Sichuan was lower than those obtained at cities and towns or in areas affected by industrial activities. In general, Co and Ni showed higher in the winter and spring seasons which might be related to the atmospheric dust activities in these seasons. Ga, Pb, Cr, Cd, Zn and As displayed higher deposition fluxes in the summer season, which might be due to increased precipitation as well as more tourist activities in this season. The local road reconstruction in December 2012-September 2013 led to a significant increase in the deposition flux of heavy metals.

Service Géologique de Wallonie : a new chapter

D. PAS, J. DENAYER, B. DELCAMBRE, J.-M. MARION, J. MICHEL, M. SALMON, C. VANNESTE, C.

Service géologique de Wallonie - Service public de Wallonie : Agriculture, Ressources naturelles et Environnement, Avenue Prince de Liège 15 - 5100 Jambes
(damien.pas@spw.wallonie.be)

In 2013, the Walloon regional government decided to create, within the “Service Public de Wallonie - Agriculture, Ressources naturelles et Environnement (SPWARNE)”, a new department aiming to enlarge the missions of the “Cellule Sous-sol/Géologie” and to allow the emergence of a regional geological survey – the “Service géologique de Wallonie (SGW)”. Beside the geological mapping and the development of an underground natural resources database, the geological survey also operates as a backup and provides expertise for the other departments of the SPW (e.g., geotechnics, urbanism, archaeology, hydrogeology and mine monitoring) and for scientific institutions. All in all, the background work of the SGW helps the planification of infrastructure projects and provides technical assistance on the investments to be made to secure or upgrade the infrastructures, both in the public and private sectors.

The main goal of the SGW focuses on the geological mapping and on increasing the general knowledge of the underground. As the mapping phase of Wallonia at the scale of 1/25000 has been successfully achieved, we now entered a phase of continuous update of the published maps. This aims to combine published data with newly collected ones (e.g. from public works, drilling database, new outcrops, LIDAR numerical field model, etc.) ultimately allowing to refine the lithostratigraphy, the geological structure and adjust the geological contours to match new concepts.

The outcrop database and new maps are available online on the Geological Map of Wallonia, viewer as fully accessible layers. The associated geodatabases are yet available for most of the territory and are constantly updated and supplemented. Thematic maps focusing on mineral resources, superficial formations, swelling clay issues, etc. are also in development. The large amount of data gathered during the last 30+ years allows to revise the lithostratigraphy and therefore, to provide a new stratigraphic scale. The continuous mapping and active collaborations with neighboring’s geological surveys insure the homogenization of the maps on both sides of the boundaries. Ongoing collaboration with the Geologischer Dienst NordrheinWestphalen (GDNRW) for the mapping of the Stavelot-Venn Massif and its couverture is a promising example.

Beside the geological mapping and related matters, the SGW is building and updating a database of the natural underground resources covering the territory (metallic, nonmetallic and energy raw materials, etc). This is developed to answer the need of a strategic plan of sustainable development and to help the decision makers. This inventory aims to be available online as a query layer and is connected to a complete database.

The “*Cahiers de Géologie de la Wallonie*” is the digital publication of the SGW that aims to provide a new support for the diffusion of new geological data and updated maps of Wallonia (<http://geologie.wallonie.be>). Note that the publication is open to any contribution dealing with the geology of the Walloon territory. Besides this new journal, a newsletter will be published to diffuse news and agenda of the activities organized by the survey (including meetings and fieldtrips) or any other institution dealing with earth sciences. Promoting the geology by creating new attractive media is also one of the cornerstones of the SGW aiming to popularize the Earth sciences to a wide public.

Enhanced rock weathering: the overlooked hydrodynamic trap

Kris PIESSENS¹, Renata BARROS¹, Tine COMPERNOLLE¹, Sophie DECREE¹, Christian BURLET¹, Ivan JANSSENS², Sara VICCA²

¹ Geological Survey of Belgium, Royal Belgian Institute of Natural Sciences, Brussels, Belgium
(Kris.Piessens@naturalsciences.be)

² University of Antwerp, Department of Biology, Global Change Ecology

Enhanced rock weathering (ERW) is a technique proposed to remove large amounts of CO₂ from the atmosphere (*i.e.* a negative emission technology) in which finely fragmented silicate rocks such as basalts (ground basalt) are distributed over agricultural or other land plots. The weathering process involves trapping CO₂ but will also typically ameliorate soil properties (pH, soil moisture retention, cation exchange capacity, availability of Si), and can therefore be expected to positively affect plant and microbiological activity. This technique has been proposed in different modified forms over the past decades. In its current format, mainly its potential for near global application (e.g. Beerling et al. 2020) is stressed, and its acceptance is helped by the positive reception by e.g. nature organisations that already apply it as a technique for ecological restoration.

Two main and largely separated processes result in trapping of CO₂. The first is precipitation of carbonates, often as nodules, in the soil. The second is increased CO₂ solubility in groundwater and eventually ocean water due to an increase of the pH value, referred to as the pH-trap.

Most of the pH-trapping schemes are built on the assumption that CO₂ is dissolved in infiltrating and shallow ground water, then discharged into surface water and consecutively transported to the seas and oceans. In that reservoir CO₂ is expected to remain dissolved for centuries and possibly up to ten thousands of years, depending on surfacing times of deep oceanic currents.

Another pathway that is systematically overlooked is that of groundwater fluxes that recharge deeper groundwater bodies. Depending on the regional geology, a significant fraction of infiltrating water will engage in deeper and long-term migration. For Belgium, the contribution of hydrodynamic trapping, depending on the hydrogeological setting, could be any part of the 15 to 25% of precipitation that infiltrates. Once infiltrating water enters these cycles, it will not come into contact with the atmosphere for possibly fifty thousand years.

In this model, the long-term impact of ERW as a climate mitigation measure rests on a good understanding of the larger hydrogeological context, which encompasses infiltration and the deeper aquifers. Deep aquifers, as well as the migration paths towards them, are strictly isolated and residence times are much longer than for oceans. Recharge areas for deeper aquifer systems may therefore become preferential sites for ERW application, becoming an additional evaluation factor for siting ERW locations that is currently based on surface factors alone.

References

Beerling, D. J., Kantzas, E. P., Lomas, M. R., Wade, P., Eufrazio, R. M., Renforth, P., Sarkar, B., Andrews, M. G., James, R. H., Pearce, C. R., Mercure, J., Pollitt, H., Holden, P. B., & Edwards, N. R. (2020). Potential for large-scale CO₂ removal via enhanced rock weathering with croplands. *Nature*, 583(July), 242–248. <https://doi.org/10.1038/s41586-020-2448-9>

Figure

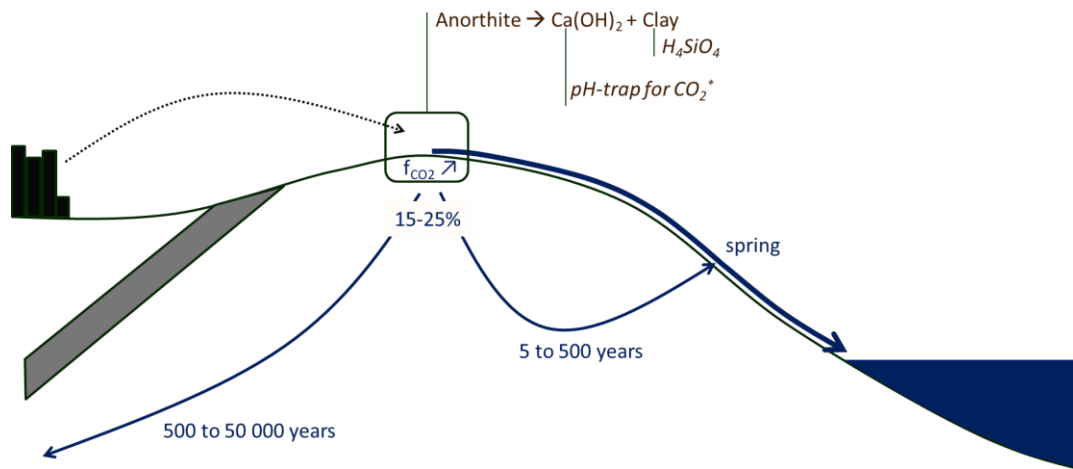


Figure 1: Conceptual summary of the transport routes from quarry to field application, and from there of CO₂ that becomes pH-trapped in water from precipitation.

Characterization of metal particles in municipal solid waste incineration ashes using neural network based image analysis

Priscilla TECK^{1,2}, Ruben SNELLINGS¹, Jan ELSSEN²

1. VITO, Sustainable Materials, Boeretang 200, 2400 Mol, Belgium (e-mail: priscilla.teck@vito.be, ruben.snellings@vito.be)

2. KU Leuven, Department of Earth and Environmental Sciences, Celestijnenlaan 200 E, 3001 Heverlee, Belgium (e-mail: jan.elsen@kuleuven.be)

Municipal solid waste incineration ashes are the residue of the incineration of municipal solid waste and consists of a complex intermixed and entangled assemblage of metallic and mineral particles together with some non-combusted organics. In Europe in 2017, 19 million tonnes of bottom ashes was produced. Typically bottom ashes consist of 80-85% mineral fraction, 10-12% of metals and 2-5% non-ferrous metals of which 2/3 is aluminum (CEWEP, 2016). The metallic fraction coarser than 2 mm in particle size can be recovered on site with magnetic separation and eddy current separation. The residual part of the coarse fraction is then left ageing so the ashes are stable and can be used in e.g. road construction. The fraction < 2 mm is separated in a sand fraction (0.1-2 mm) and a sludge fraction (<0.1 mm). The sludge fraction is landfilled without stabilization and the sand fraction is applied in the covering layers of landfills. (Vandecasteele et al., 2007). This fraction can be up to 30-40% of the total bottom ashes and therefore this landfilled fraction leads to important losses in potentially valuable resources. This research will focus on the characterization fraction of the bottom ash which is below 2 mm.

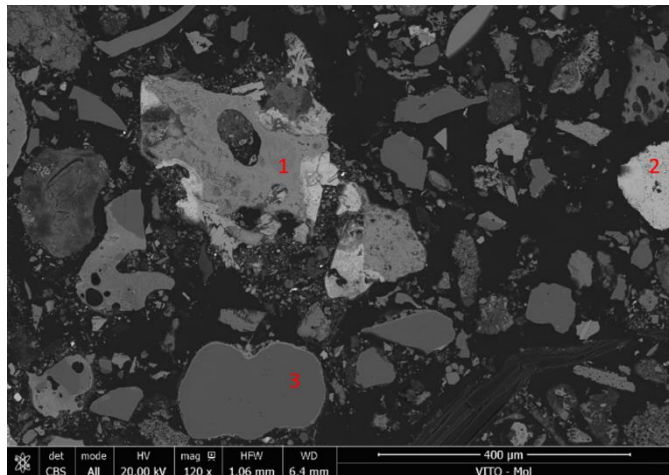
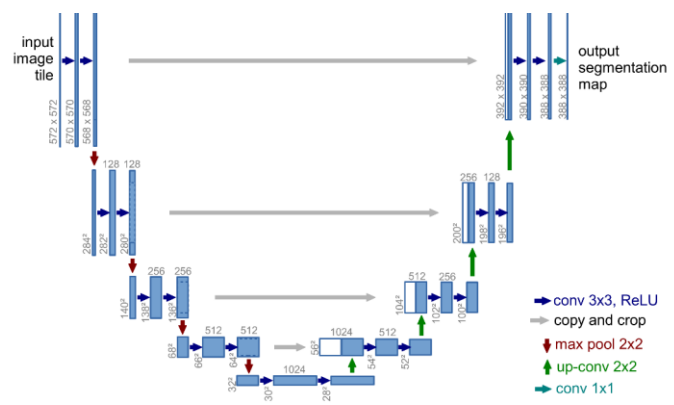


Figure 2: BSE image bottom ash. Particle 1 is a Zn metal – Calcium compound particle, Particle 2 a steel particle and particle 3 a mineral particle.

The aim of this case study is to check how much of the metallic fraction contained in the fine fraction can be recovered by innovative magnetic and density separation techniques. In order to do so, samples will be examined by electron microscopy and image analysis will be applied in order to extract the percentage and type of metals before and after the separation treatments. Figure 1 shows a back-scattered electron microscopy image of the bottom ash fine fraction. For the image segmentation procedure, a U-net will be used instead



of a classical image analysis procedure. Classically, images are segmented applying a combination of filters, thresholds, morphological operators etc. These are very powerful tools to segment images where there is a large difference in contrast/brightness between different phases. When this is not the case, developing a reliable and accurate segmentation procedure can be quite hard. In order to find a procedure to segment a large amount of images, often, a lot of trial and error is necessary. Further, anyone developing such a procedure will come to a different routine, depending on their knowledge and expertise. By using the U-net, we try to overcome some of these issues. The U-net (developed by Ronneberger et al., 2015, Figure 2) is a type of convolutional neural network architecture that can be trained for fast and accurately segmenting of images. Training is performed by supervised learning, the model is presented a number of example input images and their respective output images (ground truth). Based on these, the model will try to find the underlying structure in the data and will, in the end, be able to segment new images. This has the advantage that only a fraction of the image set has to be segmented using classical image analysis and the other images can then be segmented all at once, once the model is trained. Further, a U-net model can also learn to recognize particles based on their shape or texture.

The study includes 3 types of incineration ashes: two ash fractions from a MSWI grate furnace, i.e. a fine bottom ash fraction (63 μm - 2 mm) and a filter cake fraction resulting from a washing step of the same bottom ashes (<63 μm); and one ash material from a MSWI fluidized bed furnace, i.e. a mix of boiler ash and fly ash (<63 μm). The incineration ashes are subsequently treated by innovative magnetic and density separation techniques.

From the samples before and after the treatments, polished sections are prepared according to Bouzahzah et al. (2015) in order avoid internal particle settlement. Images are acquired on a *FEI FEG Nova NanoSEM 450*. *The image analysis is carried out mainly on BSE images, supplemented with EDX mappings where necessary.*

The results are cross-checked against the bulk chemical composition of the samples and additionally provide data on the content, type and size distribution of the metals of interest before and after treatment. As such, it is shown how this new, neural network based image analysis routine, can assist in the development of new resource recovery schemes for MSWI ashes.

Bouzahzah, H., Benzaazoua, M., Mermillod-Blondin, R., & Pirard, E., 2015, August. A novel procedure for polished section preparation for automated mineralogy avoiding internal particle settlement. In Proceedings of the 12th International Congress for Applied Mineralogy (ICAM), Istanbul, Turkey (pp. 10-12).

CEWEP, 2016. Bottom ash fact sheet. Available online: <https://www.cewep.eu/bottom-ash-factsheet/> (accessed on 31 May 2021)

Ronneberger, O., Fischer, P., & Brox, T., 2015, October. U-net: Convolutional networks for biomedical image segmentation. In International Conference on Medical image computing and computer-assisted intervention (pp. 234-241). Springer, Cham.

Vandecasteele, C., Wauters, G., Arickx, S., Jaspers, M., & Van Gerven, T., 2007. Integrated municipal solid waste treatment using a grate furnace incinerator: The Indaver case. *Waste Management*, 27(10), 1366-1375.

Geochemistry and petrography of *in-situ* flints from the type-Maastrichtian (NE Belgium and SE Netherlands): implications for flint formation processes and flint provenancing

Hannah VAN DER GEEST¹, Johan VELLEKOOP^{1,2}, Pim KASKES², Matthias SINNESAELE³, John JAGT⁴, Patrick DEGRYSE¹, Philippe CLAEYS²

¹Department of Earth and Environmental Sciences, Division Geology, KU Leuven, Celestijnenlaan 200E, 3001 Leuven, Belgium

²Department of Chemistry, Analytical, Environmental and Geo-Chemistry, Vrije Universiteit Brussel, Pleinlaan 2, 1050 Brussels, Belgium

³Department of Earth Sciences, Mountjoy Site, Durham University, South Road, Durham DH1 3LE, UK

⁴Natuurhistorisch Museum Maastricht, De Bosquetplein 6-7, 6211 KJ Maastricht, the Netherlands

The chalk deposits of the type-Maastrichtian, in the SE Netherlands and NE Belgium (Liège-Limburg region) are characterized by abundant flint layers. Since prehistoric times, flints from this region have been used as raw materials for tool making (Rademakers, 1998). While the formation, cyclicity and lithostratigraphy of flint layers from the type-Maastrichtian have been previously studied (Zijlstra, 1987; Felder and Bosch, 1998), their stratigraphic, lateral and internal geochemical and petrological variability are still poorly constrained, posing challenges for tracing the provenance of flint tools. Therefore, in the context of the Maastrichtian Geoheritage Project, we have analysed *in-situ* flint samples macroscopically, microscopically and with micro-X-ray fluorescence (μ XRF). The flint samples were collected from a 50-m-thick interval from the Upper Cretaceous Gulpen Formation at the Hallembaye quarry (BE) and the former ENCI quarry (NL). In contrast to averaged outcomes of bulk or portable X-ray fluorescence techniques commonly used for provenance studies of flints in geoarchaeology (e.g. Hughes et al., 2010), the use of μ XRF has the advantage of offering insights into the internal variability and heterogeneity of flints, by displaying relative distributions of major and trace elements within flint samples (Kaskes et al., 2021).

Our results (Figure 1) show that flint nodules from the Gulpen Formation can be subdivided based on composition. Flint layers in the middle part of this formation (Vijlen Member) consist of a massive siliceous matrix and display a heterogeneous distribution of elements such as Ca, S, K, Fe, Rb and Sr. Flint layers from the overlying Lixhe 1-3 members consist of a crystalline quartz matrix and have a more homogeneous distribution of chemical elements. The transition between the two types of flints is accompanied by an increase in the degree of silicification. Stratigraphically through the Hallembaye quarry, this increase seems to be related to a decrease in the Al-content of the surrounding chalk succession, which can be regarded as a proxy for clay content associated with varying terrigenous input into the carbonate system (Vellekoop et al., in prep.). The occurrence of the different flint types can thus be related to the varying chalk geochemistry. The geochemical data show that the flints from the Campanian (Zeven Wegen Member) correspond to the Campanian flints from the Mons Basin (Fiers, 2020). This suggests different oceanic conditions during the deposition of flints in the Campanian and the Maastrichtian. The observed heterogeneity and variability within the flint nodules can thus not only provide insights into the complex formation processes of flints, but it might also be useful for the geochemical provenancing of flint artefacts.

References

- Felder, W.M. & Bosch, P.W., 1998. Geologie van de St. Pietersberg bij Maastricht. Grondboor & Hamer, 52(3), 53-64.
- Fiers, G., 2020. The characteristics and alteration of flint: a multi-methodological approach and significance for archaeological research. Ghent University.
- Kaskes, P., Déhais, T., de Graaff, S. J., Goderis, S., & Claeys, P., 2021. Micro-X-ray fluorescence (μ XRF) analysis of proximal impactites: High-resolution element mapping, digital image analysis and quantifications. In W. U. Reimold & C. Koeberl (Eds.), Large Meteorite Impacts and Planetary Evolution VI: Geological Society of America Special Paper 550 (pp. 1–36). The Geological Society of America.
- Hughes, R., Högborg, A., & Olausson, D., 2010. Sourcing Flint from Sweden and Denmark: A Pilot Study Employing Non-Destructive Energy Dispersive X-ray Fluorescence Spectrometry. Journal of Nordic Archaeological Science, 17, 15–25.
- Rademakers, P. C. M. (Ed.), 1998. *de Prehistorische Vuursteenmijnen van Ryckholt - St. Geertruid*. Nederlandse Geologische Vereniging afd. Limburg.
- Vellekoop, J., Kaskes, P., Sinnesael, M., Dehais, T., Huygh, J., Jagt, J., Speijer, R. P., & Claeys, P. A new age model and chemostratigraphic framework for the Maastrichtian type area (southeastern Netherlands, northeastern Belgium). (*In prep.*).
- Zijlstra, H.J.P., 1987. Early diagenetic silica precipitation, in relation to redox boundaries and bacterial metabolism, in Late Cretaceous chalk of the Maastrichtian type locality. Geologie En Mijnbouw, 66(4), 343-355.

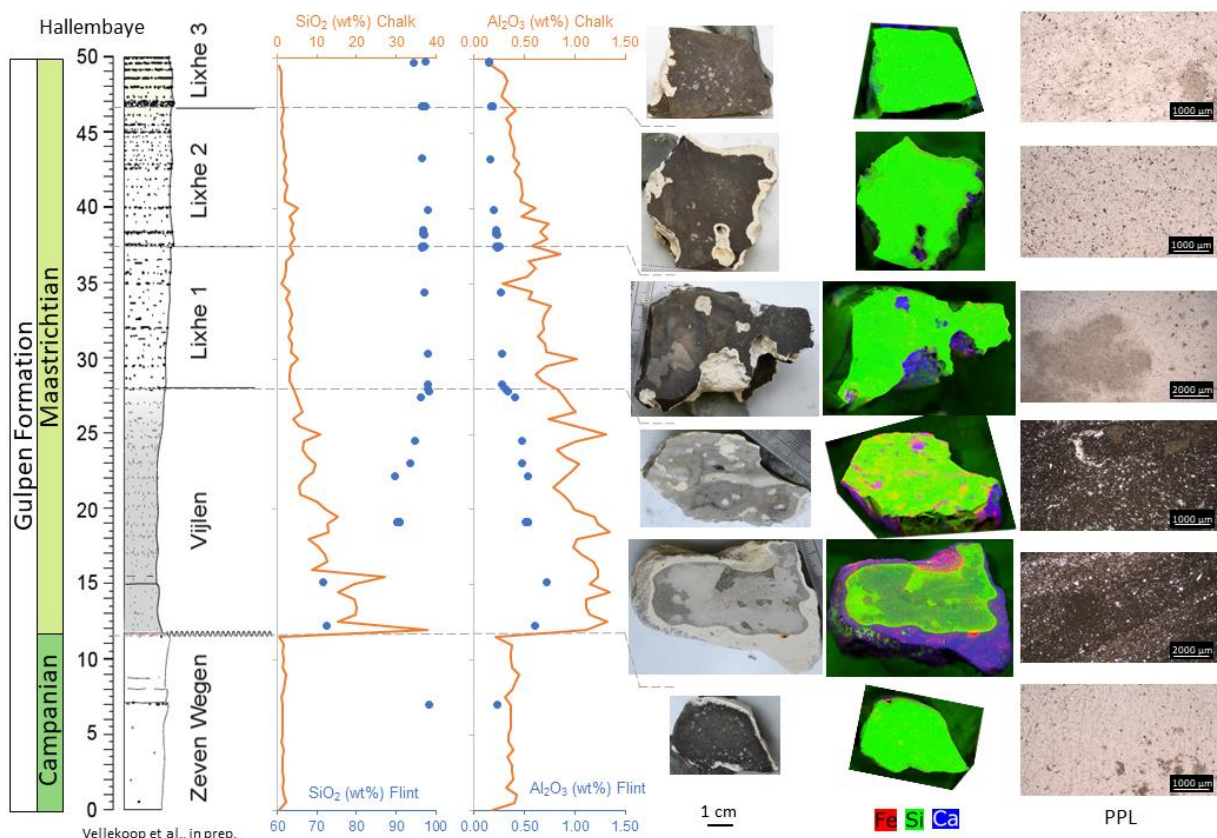


Figure 1: Stratigraphic profile through the Hallembaye Quarry (BE) with from left to right: stratigraphic plots of flint data (semi-quantitative) in blue and surrounding chalk data (fully quantitative) in orange (Vellekoop et al., in prep.) for SiO_2 and Al_2O_3 ; photographs of polished sections per member; corresponding μ XRF maps of polished sections; microphotographs in PPL of corresponding thin sections.

Getting the picture of the shallow urban subsurface: a shallow subsurface model of the city of Antwerp as test case

Tom VAN HAREN¹, Jef DECKERS¹, Roel DE KONINCK¹, Katrijn DIRIX¹, Katrien DE NIL²

1. VITO NV, Mol, Belgium (tom.vanharen@vito.be)
2. Flemish Planning Agency for the Environment and Spatial Development - Department Environment, Brussels, Belgium (katrien.denil@vlaanderen.be)

The subsurface represents a precious and multifunctional resource for cities which requires careful planning and sensitive management in accordance with its potential and its value for society. It offers both many opportunities and threats for topics like groundwater management, climate adaptation, subsidence and reuse of materials. In order to grasp and locate these opportunities, a good detailed picture of the shallow subsurface is necessary. Therefore the Bureau for Environment and Spatial Development of the Flemish Government (VPO) commissioned VITO a test case by creating a detailed 3D layer cake and voxel model of the urban area of Antwerp and parts of its harbour (see figure 1).

The inventory includes geological point data (boreholes and cone penetration tests (CPTs) from [DOV](#)), soil, geological and geomechanical maps and models, topographic GIS data, BIM data and literature. After quality checks the boreholes and CPTs were geologically (re)interpreted for the Quaternary to lower Oligocene lithostratigraphic units in the area. A systematic interpretation of CPTs was new compared to previous geological 3D models of the area (Matthijs et al., 2014; Deckers et al., 2019). It helped to provide more detail and having cross validation of nearby boreholes interpretations. The interpreted lithostratigraphic units were modelled into 3D layers by means of ArcGIS© software and were filled in with lithological parameters to create a voxel model. For this purpose, lithological information from borehole descriptions was modelled in 3D in between the lithostratigraphic boundaries using python scripting and software Rockworks©. Finally, also ranges of glauconite content for the different lithostratigraphic units were added as additional voxel information.

The modelling process resulted in a shallow urban subsurface model representing 17 lithostratigraphic units, starting from the Anthropocene to the lower Oligocene Boom Formation (see figure 1). The voxel model contains cell based information about the spatial lithological variety and lithostratigraphic depending glauconite ranges. The XYZ-resolution of the voxel model is 25x25x0.5m. On one hand the layer modelling process resulted in new lithostratigraphic insights such as mapped gullies at the base of the erosive lower Pliocene Kattendijk Formation, a detailed base of the Quaternary strata, locating Early Holocene paleo meanders of the river Scheldt, mapping the thickness of the thick peat layer present in the Rotselaar Member of the Arenberg Formation, modelling old dyke failures, etc. New insights on the Neogene deposits were already published by Deckers & Louwye (2020), Deckers et al. (2020) and the data points were included in the DOV reference sets of De Nil et al. (2020) in the geological journal *Geologica Belgica* for the special volume of Neogene 2020. On the

other hand the voxel model resulted in insights such as the location of soft sediments in Quaternary deposits, the location of high concentrations of coarse sand in the Eeklo Formation, variation in glauconite content between Neogene formations, etc. The model will be published on [DOV](#) in the coming months, which allows external users to consult the model and its underlying data.

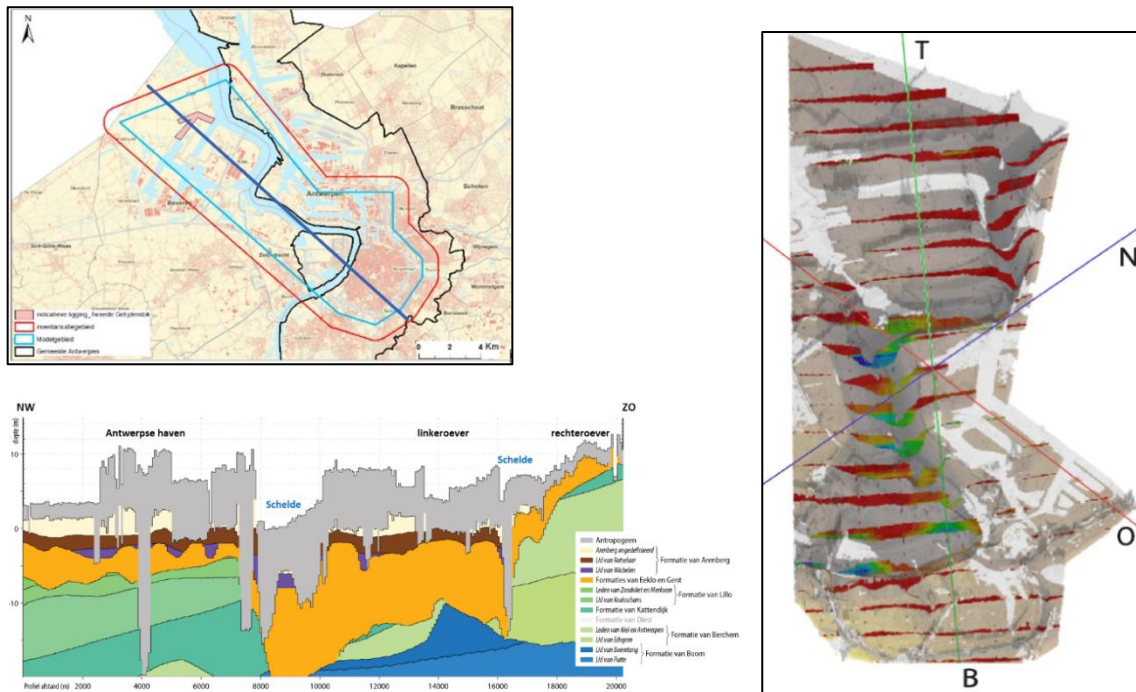


Figure 1: Illustrations showing the model area (upper left), a NW-SE profile through the lithostratigraphic layer model (lower left) and profiles cutting the voxelmodel (right) illustrating concentrations of coarse sand (lowest and highest concentrations resp. in red and blue) in the Formation of Eeklo.

REFERENCES

- Deckers, J., De Koninck, R., Bos, S., Broothaers, M., Dirix, K., Hamsch, L., Lagrou, D., Lanckacker, T., Matthijs, J., Rombaut, B., Van Baelen, K. & Van Haren, T., 2019. Geologisch (G3Dv3) en hydrogeologisch (H3D) 3D-lagenmodel van Vlaanderen. Studie uitgevoerd in opdracht van het Vlaams Planbureau voor Omgeving, departement Omgeving en de Vlaamse Milieumaatschappij. VITO, Mol, VITO-rapport, 2018/RMA/R/1569.
- Deckers, J. & Louwye, S., 2020. The architecture of the Kattendijk Formation and the implications on the early Pliocene depositional evolution of the southern margin of the North Sea Basin. *Geologica Belgica*, 23/3–4, 323-331.
- Deckers, J., Louwye, S. & Goolaerts, S., 2020. The internal division of the Pliocene Lillo Formation: correlation between Cone Penetration Tests and lithostratigraphic type sections. *Geologica Belgica*, 23(3-4), 333-343.
- De Nil, K., De Ceukelaire, M. & Van Damme, M., 2020. A reference dataset for the Neogene lithostratigraphy in Flanders, Belgium. *Geologica Belgica*, 23/3–4, 413-427.
- Matthijs, J., Lanckacker, T., De Koninck, R., Deckers, J., Lagrou, D. & Broothaers, M., 2013. Geologisch 3D lagenmodel van Vlaanderen en het Brussels Hoofdstedelijk Gewest - versie 2, G3Dv2. Studie uitgevoerd door VITO in opdracht van de Vlaamse overheid, Departement Leefmilieu, Natuur en Energie, Afdeling Land en Bodembescherming, Ondergrond, Natuurlijke Rijkdommen, VITO-rapport, 2013/R/ETE/43.

UNESCO Global Geopark Famenne-Ardenne, Belgium – opportunities and role for geoscientists

Sophie VERHEYDEN^{1,2}, Serge DELABY^{3,4}.

1. *Royal Belgian Institute of Natural Sciences – RBINS, Belgium*
(*sophie.verheyden@naturalsciences.be*)
2. *Earth Sciences - University of Lille, France*
3. *UNESCO Global Geopark Famenne-Ardenne,*
(*serge.delaby@geoparkfamenneardenne.be*)
4. *Dép. Sciences de la Terre - Université Libre de Bruxelles (ULB), Belgium.*

UNESCO Global Geoparks (UGG) are defined as ‘single, unified geographical areas where sites and landscapes of international geological significance are managed with a holistic concept of protection, education and sustainable development.’ (UNESCO website, 2021). UGGs need to be managed by a legal organisation and financed structurally. The presence of 1 full-time equivalent geoscientist in the organisation is mandatory. UGGs are one of the three UNESCO areas, besides Man&Biosphere reserves and World Heritage sites. UGGs represent an efficient tool to (1) increase the awareness of geological heritage and geosciences in general and of the related need of geological knowledge & research, (2) create a wide platform for the dissemination of research results and for citizen science application.

‘Famenne-Ardenne’ is the first UNESCO Global Geopark in Belgium. The geopark was initiated by geoscientists and introduced successfully thanks to the collaboration between geoscientists (RBINS, U-Mons, U-Namur), actors of the touristic sector (Attraction & Tourisme, asbl., local ‘Maisons du Tourisme’, the Commission Wallonne de l’Étude et de la Protection des Sites Souterrains (CWE PSS) and local policymakers. The geopark area is about 1000km² for ~70000 inhabitants. It is situated in eight localities: Beauraing, Wellin, Rochefort, Tellin, Marche-en-Famenne, Nassogne, Hotton and Durbuy (Verheyden et al., 2016; 2020). The international value of the geopark relates to the close interactions between karstic phenomena and Humans. The region is known for its historical karst research. Moreover, several stratotypes are present in and around the geopark. Since the obtention of the label in 2018, several geotrails, educational activities, quarry-revalorization projects were finalized or started.

The role of geoscientists is to supply the scientific base and re-frame if or where necessary the general functioning of the geopark to keep the geopark in the ‘spirit’ of the UNESCO prescriptions. Geoscientists help the geopark to protect and increase the knowledge and protection of the geopark’s geohéritage, and have a role



Figure 4: Karstified limestone & speleothem door-decoration on a house of Han-sur-Lesse, Belgium. The picture is ~1m large.

to play in the international scientific networking.

Since this first UGG label in Belgium, awareness on the related geoscientific, touristic, political, international prestige or spatial management potential increased. UNESCO Flanders, together with several administrations dealing with spatial management and/or environment created an interactive website and are dealing with a global strategy for spatial planning. UNESCO tools, since fostering sustainable development and awareness of earth sciences, including climate change, can possibly be considered in the Paris objectives and could therefore be used by local administrations. Further potential for UGGs exists in Belgium. In Flanders, several new projects are upcoming such as the Schelde-Delta aspiring UGG, a Flanders-Wallonia-Dutch-German collaborative project in the chalk region of eastern-Belgium, including the former Pb-Zn extraction area. In Wallonia, the region around Mons for example, despite the low political support leading to the failure of a previous demand for a UNESCO label, is a target area to create a new UGG because of timely well-developed geological topics such as coal, geothermal energy and iguanodons but also because there would be a potential of important touristic and economic development. Since awareness is raising, it would be opportune for the area and for geosciences in Belgium, in general, to renew the demand for the UGG label in close agreement with UNESCO guidelines. Other potential regions are those known for historical coticule and slate industry in south-eastern Belgium (Goemaere et al., 2020) and/or the Meuse Valley, to increase the visibility of their geological heritage and its societal value.

We can conclude that UNESCO Global Geoparks are a solid tool to increase awareness on the high societal value of geological deposits and research. These areas are a unique opportunity to disseminate research results towards a wider audience. The Geopark and related geoheritage issues still offer high potential for development in Belgium.

References

- Goemaere, E., Blicq, A., Coen-Aubert, M., Cuvelier, J., Dejonghe, L., De Wever, P., Fronteau, G., Hallet, V., Mottequin, B. & Quinif Y., 2020. Le géopatrimoine du Massif ardennais In : Le Massif ardennais. Un jeune massif ancien. Chapitre 3 : Un riche patrimoine. Géochronique, SGF et BRGM Ed.,154 (juin 2020), pp 56-60.
- UNESCO website 2021. <http://www.unesco.org/new/en/natural-sciences/environment/earth-sciences/unesco-global-geoparks/frequently-asked-questions/what-is-a-unesco-global-geopark/>
- Verheyden, S., Quinif, Y., Delaby, S., Hallet, V., Petit, A. & Vankeerberghen, M., 2016. The Calestienne Lesse&Lomme Geopark – A first step to a structured valorisation of the karstic heritage in Belgium. In Cornée A., Egoroff G., De Wever P., Lalanne A., and Durenthon F., (Eds) Actes du colloque International "Les inventaires du Géopatrimoine" 22-26 Septembre 2015, Toulouse. Mémoire hors-série de la Société géologique de France 16, 368p. : 331-343.
- Verheyden, S., Quinif, Y., Thys, G., Delaby, S., Hallet, V., Petit, A., Vankeerberghen, S. & Vankeerberghen M., 2020. Le Geopark Famenne-Ardenne, premier géoparc mondial UNESCO en Belgique. In Commission Wallonne d'Etude et de Protection des Sites Souterrains, 2020. Atlas du Karst Wallon, Bassin de l'Ourthe Calestienne. SPW-Editions Atlas – Environnement. 560pp: 66-69.

Naturally CO₂-rich water springs in Belgium evidencing complex subsurface interactions

Kris WELKENHUYSEN¹, Agathe DEFOURNY^{2,3}, Arnaud COLLIGNON³, Patrick JOBE³, Alain DASSARGUES², Kris PIESSENS¹, Renata BARROS¹

1. Royal Belgian Institute of Natural Sciences – Geological Survey of Belgium, Jennerstraat 13, 1000 Brussels, Belgium (kris.welkenhuysen@naturalsciences.be)

2. University of Liège, Hydrogeology, Urban and Environmental Engineering, Quartier Polytech 1, Allée de la Découverte, 9, Bât. B52 - Sart Tilman 4000 Liège, Belgium

3. Spadel S.A., Water resource department, Rue Auguste Laporte 34, B-4900 Spa, Belgium

Numerous naturally CO₂-rich mineral water springs, locally called ‘pouhons’, occur in southeast Belgium. These are oversaturated in CO₂ (up to 4g/L) and have attracted economic, touristic and scientific interest for centuries. Water sources occur within Palaeozoic rocks of the Rhenohercynian deformation zone, a fold-and-thrust belt at the north of the Variscan orogeny in central Europe. Many occurrences are concentrated in the Cambro-Ordovician Stavelot-Venn massif. A widely accepted model, supported by H-O isotopic signatures, is that sources are primarily fed by meteoric water, which infiltrates through Quaternary sediments, then reaching Lower Palaeozoic rocks to meet the mineral and CO₂ source at unknown depth.

Different ideas for the origin of CO₂ are grouped in two main hypotheses: a) generation by dissolution of carbonate rocks and/or nodules, and b) volcanic degassing related to the neighbouring Eifel area in Germany. These well-known interpretations are mostly based on geochemical studies that are dispersed and poorly accessible. These have now been gathered in the light of new sampling campaigns, allowing to revisit and compare the views of earlier authors. We also for the first time include the geotectonic setting of the region.

Carbonate rocks in the region are represented by Lower Carboniferous and Middle Devonian limestones. Depending on the assumed structural evolution for this foreland fold-and-thrust belt, these may occur at >2 km depth below the Stavelot-Venn massif. Carbonate nodules are present in other formations, but their limited volume is unlikely to originate high and long-lived quantities of CO₂. Springs enriched in CO₂ are also common in the volcanic Eifel area, with presence of mantle CO₂ well established. The supposed extension of the Eifel plume would allow for a magmatic CO₂ source below the Stavelot-Venn massif from degassing of the plume (>50 km deep), or of an unknown shallower magmatic reservoir. Available stable and noble isotopes point to a mixed carbonate-magmatic origin.

If considering the presence of limestones at depth, meteoric water should infiltrate at least 2 km. Known deep-rooted faults are thought to act as preferential groundwater pathways. However, such deep circulation is incompatible with the low temperatures of springs (~10°C), unless the ascent is slow enough to fully dissipate heat prior to resurfacing. Another possibility is that meteoric water does not infiltrate as deep, with CO₂ being transported upwards to meet groundwaters at shallower depths. The presence of CO₂ surface leaks, locally called ‘mofettes’, could be evidence of such relatively shallow availability of CO₂.

The evaluation of existing hypotheses highlights complex subsurface processes that involve water infiltration, CO₂ assimilation and water resurfacing in southeast Belgium (Figure 1). As such, this review is an important guide for the newly launched sampling campaigns.

Acknowledgements

This work is part of two research projects: GeoConnect^{3d}-GeoERA that has received funding by the European Union's Horizon 2020 research and innovation programme under grant agreement number 731166, and ROSEAU project, as part of the Walloon program «Doctorat en Entreprise», co-funded by the SPW Région Wallonne of Belgium and the company Bru-Chevron S.A. (Spadel group), under grant number 7984.

References

Barros, R., Defourny, A., Collignon, A., Jobé, P., Dassargues, A., Piessens, K. & Welkenhuysen, K., 2021. A review of the geology and origin of CO₂ in mineral water springs in east Belgium. *Geologica Belgica*, 24 (1-2), p.17-31. <https://doi.org/10.20341/gb.2020.023>

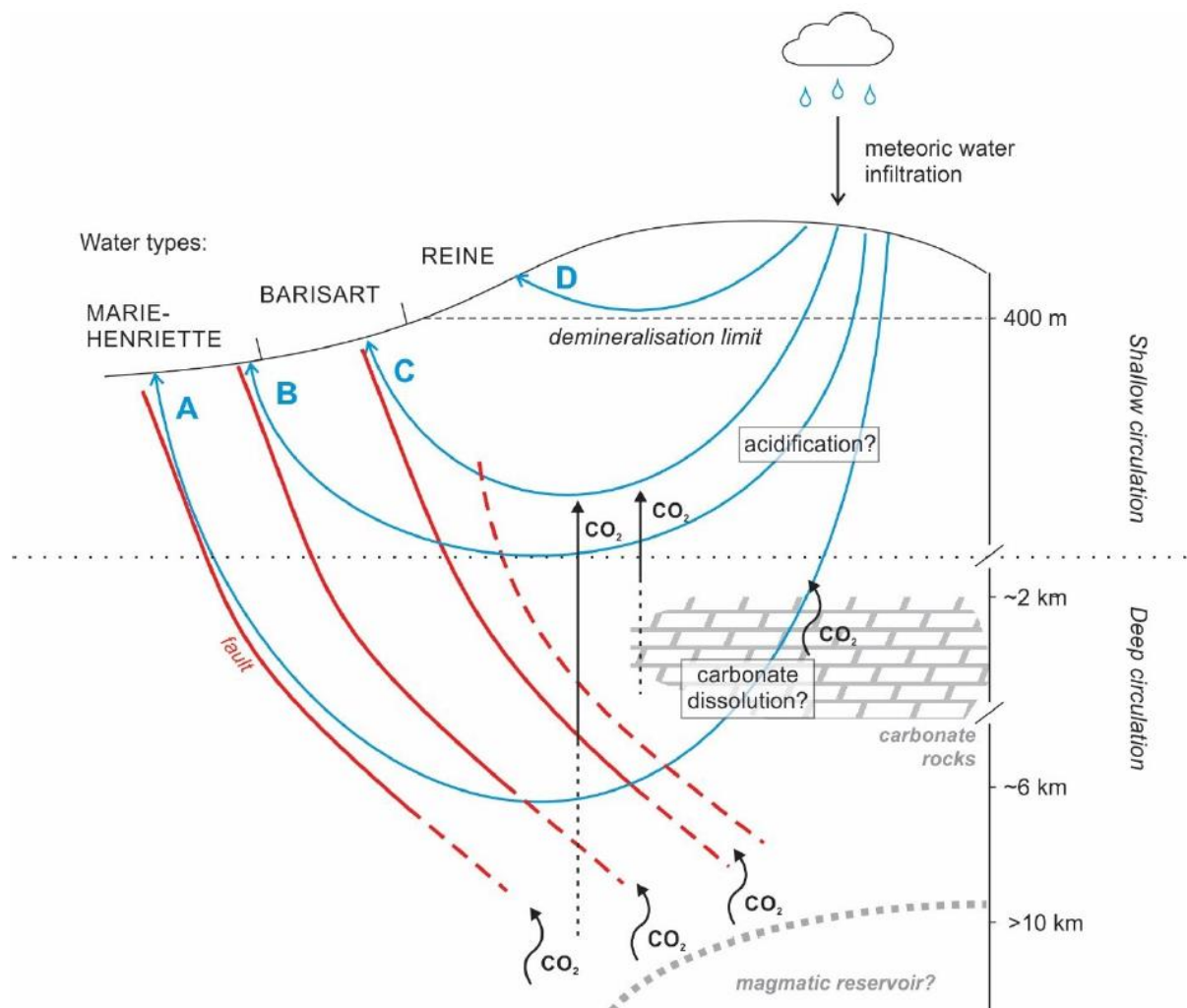


Figure 1. Schematic cross section in the Spa region. Possible deep circulation (A) and shallow circulation (B) paths for pouhon waters are represented. C and D represent possible water circulation paths for Barisart and Reine waters, respectively (Barros et al., 2021). Pouhons are the local name for naturally CO₂-rich mineral water springs.

The Rock Garden: increasing the accessibility of geoscience skills training with a field course on campus

Thomas WONG HEARING¹, Stijn DEWAELE¹, Stijn ALBERS¹, Julie DE WEIRDT¹, Marc DE BATIST¹.

1. Geology Department, Ghent University, Ghent, Belgium (thomas.wonghearing@ugent.be; stjindg.dewaele@ugent.be; stijn.albers@UGent.be; judweird.deweirdt@UGent.be; marc.debatist@UGent.be)

The Rock Garden is a newly developed resource for training geological field skills on campus at Ghent University. Developing specific field skills is an integral component of most geoscience degree programmes and is typically concentrated into whole-day excursions and longer residential field courses. Such field courses can have exceptional educational value, drawing together multiple strands of classroom theory and practical laboratory learning in the dynamic environment of student-led discovery in tackling real-world geoscience questions. However, field courses are expensive and time-intensive to run, and are consequently relatively infrequent over the course of a degree programme. From a student perspective, the infrequency of field courses means that key skills may not be practiced for long periods and students may lose confidence in applying these skills in the field. More fundamentally, long and especially residential field courses can raise multiple barriers to accessing geoscience degree programmes, from physical accessibility concerns to financial barriers either from direct course costs or from being away from home and work for long periods of time (e.g. Stokes *et al.*, 2019; Giles *et al.* 2020). In 2019, we identified a need to bolster student confidence in practical geoscience skills and to increase the accessibility of field skills training in our degree programmes. When the coronavirus pandemic began in 2020, the need to be able to deliver field skills training locally became more pronounced.

Most key geological field skills, including orienteering, lithology identification, and measuring and recording structural data, coalesce around the mapping of outcrops and structures. We therefore decided to develop a training resource based on a geological mapping exercise. We reverse-engineered an outcrop plan by combining a hypothetical geological map and cross-sections with the available areas on campus. The availability of campus space constrained the maximum extent of possible outcrop areas, and we consequently aimed for an exercise comparable to mapping inland areas with limited exposure. Having produced an idealised geological map and identified usable outcrop areas, we sourced a variety of large rock samples from local building stone and quarry companies. Working with the University's Directie Gebouwen en Facilitair Beheer, we prepared the ground on Campus De Sterre and installed the rocks, aiming to match the strikes and dips as closely as possible to the original plan. Following installation, the area was re-mapped and both the rocks and the plan were adjusted to produce an interpretable distribution of geological outcrops and matching geological map.

We have already used the Rock Garden as a partial replacement for undergraduate geological mapping training in mitigation of coronavirus restrictions on travel. The quality of student mapping work was comparable to that expected from a 'real-world' field course. Moreover, student enthusiasm for the Rock Garden was extremely high, concerning practice as well as objectives. However, we do not consider the Rock Garden as a substitute for existing field courses. Instead, it is a way to teach essential field skills in a more controlled environment where accessibility barriers can be minimised and students can become familiar

with some of the exigencies of field work. Recently, there has been debate over the inclusivity of making field work a mandatory component of a geoscience degree, and indeed many graduates will not need to use the field skills they develop during a geoscience degree. However, accessibility issues should not be a barrier to learning key field skills and to developing an understanding of the methods and uncertainties inherent in geoscience field work. A campus-based resource like the Rock Garden provides one method for addressing accessibility and student confidence issues in field skills training and development.

References

Giles, S., Jackson, C. & Stephen, N., 2020. Barriers to fieldwork in undergraduate geoscience degrees. *Nature Reviews Earth & Environment*, 1, 77–78.

Stokes, A., Feig, A.D., Atchison, C.L. & Gilley, B., 2019. Making geoscience fieldwork inclusive and accessible for students with disabilities. *Geosphere*, 15, 1809–1825.

Figure



Figure 5. Installation of Rock Garden blocks on Campus De Sterre.

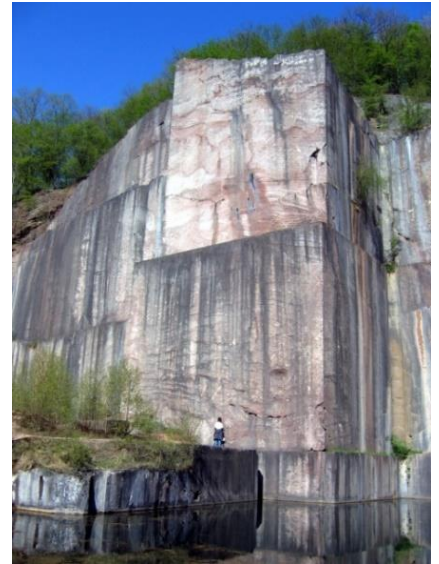
Session 5- Basin Research and Sedimentology - Stratigraphy

Conveners:

Vanessa Heyvaert (RBINS-GSB); Noel Vandenberghe (KU Leuven), Anne Christine da Silva (ULiège), Marc De Batist (UGent), Gert Jan Weltje (KU Leuven), Damien Delvaux (RMCA)

This session supports any submission related to basin research and sedimentology and stratigraphy. This includes all types of sedimentary settings (marine, continental, deep, shallow, clastics, carbonate), oriented towards basin scale or more local studies. We also welcome research associated with techniques and technologies in sedimentary and stratigraphy research.

Specific topics include (not exclusive): the East African Rift; the Congo Basin; the sedimentological imprint of natural hazards.



Sedimentology and Microfacies assessment of Ypresian carbonate formations in the Tellian zone (NW of Tunisia)

Imen ARFAOUI^{1,2}, Frédéric Boulvain¹

1. Laboratoire de Pétrologie sédimentaire, B20, Université de Liège, Sart Tilman, 4000 Liège, Belgium (fboulvain@uliege.be) (Imen.Arfaoui@uliege.be)

2. UR3G: Research Unit Geosystems, Georesources and Geoenvironments, Faculty of Science of Gabes, Cité Erriadh 6072 Zrig, Gabes, Tunisia

The Eocene layer is known for its tectonic complexity, inherited from the Mesozoic-Cenozoic geodynamic evolution (Bishop 1988). A structural instability affected the south Tethyan area. Specifically, the North Tunisian margin shows NE-SW topographic highs and lows (Rouvier 1977; Ben Ayed 1986; Rigane et al. 1994).

The paleo-depressions were characterized by the proliferation of planktonic foraminifera (Bou Dabbous Formation – source rock). Simultaneously, benthic foraminifera-rich limestones were deposited on the flanks and tops of the shoals (El Garia Formation - reservoir), where nummulites are the most common, like all around the Mediterranean basin during the Eocene period. (P. F. Burolet 1956; P. Burolet 1973; Jauzein 1967; Vincent Perthuisot 1978; V Perthuisot 1981; Zargouni and Abbes 1987; Aoudjehane et al. 1992; Adil 1993; Belayouni et al. 2012).

The sedimentology and sequence stratigraphy of three outcrops were studied, and extensively sampled for petrographic, mineralogical, and geochemical analysis. The study area covers the Tellian zone, NW of Tunisia. Two of the outcrops (OK and AG sections) belong to the Kasseb tectonic Unit, and the TS section belongs to the Adissa tectonic Unit. Those layers correspond to the lower Eocene succession, which is part of the Metlaoui Group (P. F. Burolet 1956).

Seven microfacies (MF1- MF7), ranging from the outer to the inner ramp environment, were recognized. The distal ones correspond to Globigerina-rich mudstones and wacke- to packstones. Locally, organic matter (OK section) filled stylolites/ fissures and oil seeps on the field were observed during the sampling process. The studied outcrops sections show a progressive coarsening up, leading to the nummulites-rich pack- to grainstones microfacies, detected in the uppermost part of El Garia Formation (MF6 - MF7 in AG section).

The lithological description of the studied succession shows an alternation of massive carbonates and marly limestones. Based on lithology and thickness variation of the beds' doublets and their facies and fabrics, three lithostratigraphic units were defined.

The first two units recorded a transgressive sequence characterized by m to dm limestones alternating with cm-thick carbonate beds, containing planktonic foraminifera-rich facies on the top of a glauconite-rich interval (MF1, MF2, MF3, and MF4). The upper unit is characterized by nummulithoclastic packstones associated with some phosphate, glauconite grains, and radiolarians (MF5), and nummulitic packstones to grainstones (MF6, MF7). Those microfacies are interpreted as an outer ramp that corresponds to a regressive sequence.

According to the previous work on the Ypresian sections in the North of Tunisia, and the current studied sections, the sedimentological correlations show a deepening up and thickening upwards in a NSW-NNE direction.

References

- Adil, S. 1993. 'Dynamique Du Trias Dans Le Nord de La Tunisie: Bassins En Relais Multiples de Décrochement, Magmatisme et Implications Minières'. Doctorat de Spécialité, Université de Tunis.
- Aoudjehane, Mohamed, Azzedine Bouzenoune, Henri Rouvier, and Jacques Thibieroz. 1992. 'Halocinèse et Dispositifs d'extrusion de Trias Dans l'Atlas Saharien Oriental (NE Algérien)'. *Géologie Méditerranéenne* 19 (4): 273–86.
- Belayouni, Habib, Francesco Guerrera, Manuel Martín Martín, and Francisco Serrano. 2012. 'Stratigraphic Update of the Cenozoic Sub-Numidian Formations of the Tunisian Tell (North Africa): Tectonic/Sedimentary Evolution and Correlations along the Maghrebian Chain'. *Journal of African Earth Sciences* 64: 48–64.
- Ben Ayed, Noureddine. 1986. 'Evolution Tectonique de l'avant-Pays de La Chaîne Alpine de Tunisie Du Début Du Mésozoïque à l'Actuel'.
- Bishop, William F. 1988. 'Petroleum Geology of East-Central Tunisia'. *AAPG Bulletin* 72 (9): 1033–58.
- Burollet, PF. 1973. 'Importance Des Fractures Salifères Dans La Tectonique Tunisienne (Importance of Salt Fractures in Tunisian Tectonics)'. *Mines Geol Ann Tunisia* 26: 111–20.
- Burollet, Pierre Félix. 1956. 'Contribution à l'étude Stratigraphique de La Tunisie Centrale'. *Ann. Mines Géol.* 18: 350.
- Jauzein, André. 1967. Contribution à l'étude Géologique Des Confins de La Dorsale Tunisienne (Tunisie Septentrionale). République tunisienne, Secrétariat d'état au plan et à l'économie nationale
- Perthuisot, V. 1981. 'Diapirism in Northern Tunisia'. *Journal of Structural Geology* 3 (3): 231–35.
- Perthuisot, Vincent. 1978. 'Dynamique et Pétrogenèse Des Extrusions Triasiques En Tunisie Septentrionale'.
- Rigane, ADEL, CLAUDE Gourmelen, PAUL Broquet, and RENÊ Truillet. 1994. 'Originalité Des Phénomènes Tectoniques Syn-Sédimentaires Fini-Yprésiens En Tunisie Centro-Septentrionale (Région de Kairouan)'. *Bulletin de La Société Géologique de France* 165 (1): 27–35.
- Rouvier, H. 1977. 'Géologie de l'Extrême-Nord Tunisien: Tectoniques et Paléogéographies Superposées à l'extrémité Orientale de La Chaîne Nord-Maghrebine'. These Doctorat Es Sc., Univ. Pierre et Marie Curie.
- Zargouni, F, and CH Abbes. 1987. 'Zonation Structurale de La Tunisie'. *Rev Sciences Des La Terre INRS* 6: 63–69.

Silurian solid bitumen from Huy: evidences for a petroleum system in Belgium

Michiel ARTS¹, Coralie BOSTEELS¹, Xavier DEVLEESCHOUWER², Anne-Christine DA SILVA¹

1. *Université de Liège, Liège, Belgium (Michiel.arts@uliege.be)*
2. *Royal Belgian Institute of Natural Sciences, Geological Survey of Belgium, Brussels, Belgium*

The discovery of a bitumen bed within the Silurian Bonne Esperance Formation near the city of Huy (Belgium) is the first clear evidence for a petroleum system in Belgium. The studied section near the city of Huy (Belgium) is part of a larger structural unit called the Condroz inlier. This structural unit is a wedge of Ordovician to Silurian aged marine sediments which was thrust up along the Midi detachment fault during the Hercynian orogeny and forming the Ardennes Massif (Adams & Vandenberghe, 1999). To understand the geological processes involved in the formation of the bitumen bed, the Bonne Esperance Formation was logged and 82 samples were collected for XRF chemostratigraphy, five samples were collected (Figure 1, pictures 1-5) for biostratigraphic purposes and one sample was taken from the bitumen itself. ICP-MS, TOC, Rock-Eval pyrolysis and Gamma-ray measurements are underway to quantify the source rock potential of the Bonne Esperance Formation. Preliminary XRF measurements already show that especially the lower part of the Bonne Esperance Formation is enriched in elements linked to anoxic conditions/enrichment of organic material, which indicates that the Bonne Esperance Formation itself is the likely candidate source rock for the bitumen. The sample from the bed which includes the bitumen has already been tested to confirm the nature of the bitumen material. The sample was crushed and heated in a vial and the released hydrocarbons were then ignited with a flame (Figure 1, picture 6C). The First occurrence of the graptolites of the Family Monograptidae was used to pinpoint the location of the Ordovician-Silurian boundary (Akidograptus Ascensus zone at sample 4) (Maletz, 2017). Given the current results and the ongoing analyses a picture emerges of the Silurian of the Condroz inlier as being Belgium's first and to date only petroleum system.

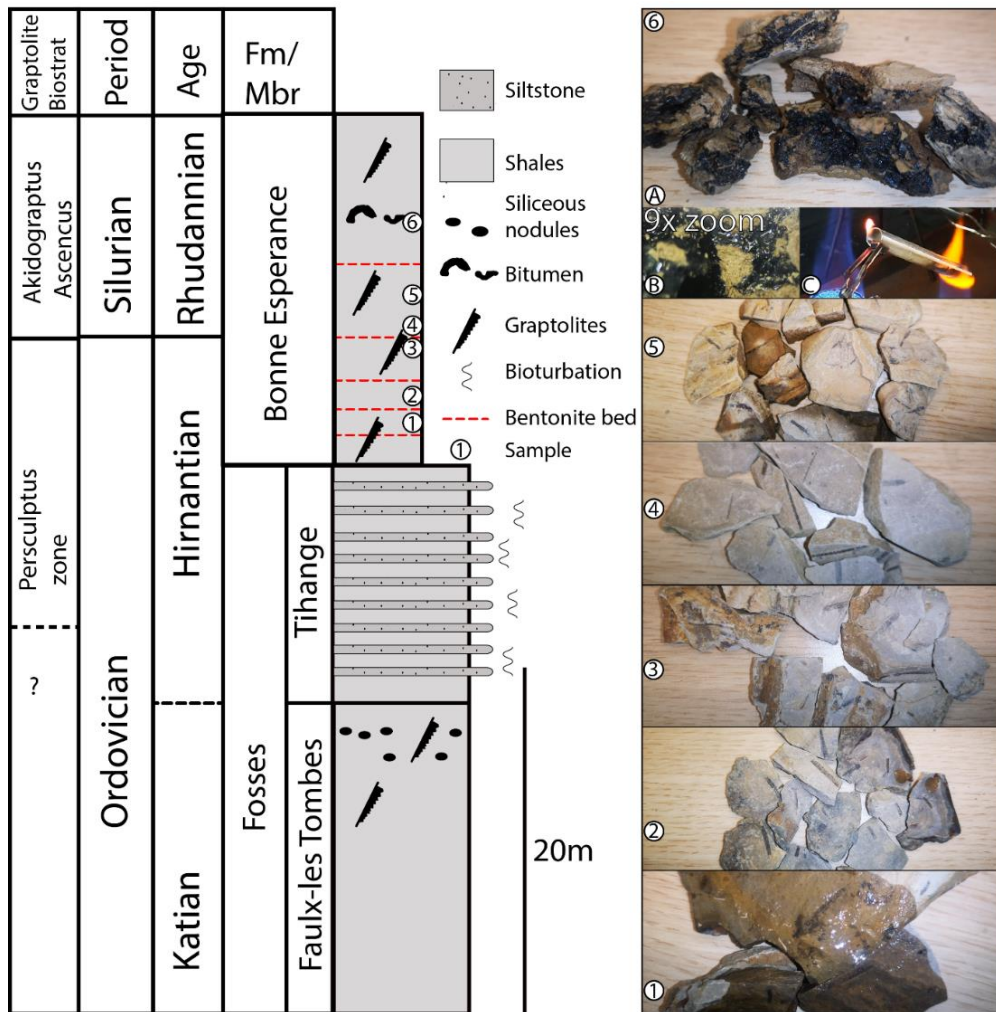


Figure 1 Stratigraphy of the section at Rue Bonne Esperance Huy (modified after (Mottequin & Marion, 2012) and pictures of 6 samples. Pictures 1-5 are graptolite samples while sample 6 shows samples of bitumen. 6c shows a Bunsen burner test. The yellow flame at the end of the test tube indicates that the sample contains hydrocarbons.

References

Adams, R., & Vandenberghe, N. (1999). The Meuse section across the Condroz-Ardennes (Belgium) based on a predeformational sediment wedge. *Tectonophysics*, 309(1–4), 179–195.
[https://doi.org/10.1016/S0040-1951\(99\)00138-9](https://doi.org/10.1016/S0040-1951(99)00138-9)

Maletz, J. (2017). Graptolite Paleobiology. *Graptolite Paleobiology*.
<https://doi.org/10.1002/9781118515624>

Mottequin, B., & Marion, J. (2012). *Notice explicative de la carte géologique Huy-Nandrin 48/3-4* (p. 84).

Stratigraphic architecture, sedimentology and structure of the Corinth Canal (Greece)

Basile CATERINA ¹, Romain RUBI ², Aurélie HUBERT-FERRARI ³

1. *ULiège, Liège, Belgium (basile.caterina@student.uliege.be)*

2. *ULiège, Liège, Belgium (romain.rubi@uliege.be)*

3. *ULiège, Liège, Belgium (aurelia.ferrari@uliege.be)*

The man-made Corinth Canal connects the Aegean Sea with the Corinth Gulf while displaying high steep walls allowing to study the sedimentological structure of this canal. This canal is supposed to be the former strait which connected the gulf with the Aegean Sea. Therefore, the canal could be used as analogue to study tidal straits once its stratigraphic architecture, sedimentology and structure are defined. To do so, we used field observations associated with a 3D model done by drone imaging. With these data we observed a central horst, located at the central part of the canal and an associated graben called Isthmia. The top and NW parts of the canal section consist of a min. 20 m thick unit of conglomeratic tidal dune bedded deposits. These deposits are evidenced by the presence of asymmetrical herringbones, tidal dune bedded features and cross-stratification. These deposits may then totally propose a new paleostratigraphic interpretation for the Corinth Canal but also complete the “classical” tidal strait depositional model. In the regional context, such deposits confirm the probable connection between the Aegean Sea and the Corinth Gulf at ~300 ka. This connection faded due to the regional uplift and the activation of the major Kalamaki-Isthmia fault.

Les sous-groupes Schisto-calcaire et de la Mpioka dans la chaîne panafricaine West-Congo, témoins de l'évolution paléoclimatique post-Cryogénien, Province du Kongo Central, R.D. Congo

C.M.E. CIBAMBULA¹, M.N.A. MAKUTU J.¹, C.L. MUKEBA¹, K.A. SEKERAVITI¹, H.F. IYOLO¹, L.O. TUEMA¹

¹Université de Kinshasa, Fac. des Sciences, Dép. Géosciences, B.P.190, Kinshasa XI, R.D.C

L'évolution climatique du Cryogénien (850 à 635 Ma) est très particulière, à cause du plus grand nombre d'épisodes glaciaires. Parmi ces derniers, la glaciation du Marinoen est enregistrée par la Diamictite supérieure du Kongo Central. Les dépôts des carbonates consécutifs à cet épisode glaciaire témoignent des changements climatiques qui s'en sont suivis. Les climats étant les moteurs de la sédimentation tant au niveau de la production des particules que du transport et de la mise en place de celles-ci, la question est de savoir lesquels ont régi cette variation des dépôts post-marinoens ?

Dans le Groupe Ouest-Congolien, la Formation de la Diamictite supérieure est surmontée du Sous-groupe Schisto-calcaire sous-jacent lui-même aux dépôts conglomératiques de Bangu-Niari et grés-argileux de la Basse- et de la Haute-Mpioka. Tout comme la lithologie qui varie progressivement de bas en haut, les climats changent aussi régulièrement lors de la sédimentation. Par la présence des évaporites et des biohermes à *Collenia* et à *Cryptozoon* dans les formations de Kwilu et de Lukunga, le Sous-groupe Schisto-calcaire s'est déposé sous un climat chaud et aride développé à l'Ediacarien d'après les travaux de Playford et Cockbain (1976) au pool d'Hamlin sur la côte Ouest de l'Australie. Les creux à remplissage plus grossier que les grains du substratum, les structures clast- à matrix-supported et la nature de ses clastes modérément mal classés dans des grands volumes d'argiles et de silt indiquent que le conglomérat de Bangu-Niari s'est développé dans un paléomilieu périglaciaire au cours du Terreneuvien selon les travaux d'Eyles et al. (2004) et de Tohver, E. et al. (2006). Le litage granoclassé et répété de shales des formations de la Basse- et de la Haute-Mpioka d'âge Cambro-Ordovicien (Cibambula, 2016) rappelle celui des rythmites varvaires des lacs d'environnement périglaciaire tel qu'interprété par Olausson et Olsson (1969) sur une carotte provenant du Golfe d'Aden. Ces différentes caractéristiques montrent qu'après le Snowball marinoen (Hoffman, 1998), le mégacraton du Congo-Sao Francisco a subi successivement un climat tropical sec et un climat tempéré des régions proglaciaires.

Références :

- Cibambula, C.M.E. (2016) : Le Sous-groupe de la Mpioka : un flysch de la chaîne Panafricaine West Congo dans la Province du Kongo Central (R.D. Congo), *Th. Doc. Inédit, Dép. Géosc., Univ. Kinshasa*, 185p.
- Eyles, N. et Januszczak, N. (2004) : 'Zipper-rift' : a tectonic model for Neoproterozoic glaciations during the breakup of Rodinia after 750Ma. *Earth Sci. Rev.* 65, 1-73.
- Hoffman, P. F., Kaufman, A. J., Halverson, G. P., Scharg, D. P. (1998) : A Neoproterozoic Snowball Earth. *Sci.* 281, 1342-1346.
- Olausson, E. et Olsson, I.U. (1969) : Varve stratigraphy in a core from Gulf of Aden, *Palaeogeogr. Palaeoclim. Palaeoecol.* 6. 87-103.
- Playford, P.E. et Cockbain, A.E. (1976) : Modern algal stromatolites at Hamlin pool, a hypersaline barred basin in Shark Bay, western Australia in M.R. Walter (Ed.), *Stromatolites. Developments in Sedimentology*, 20, Elsevier, 389-411.
- Tohver, E., D'Agrella-Filho, M.S., Trindade, R.I.F. (2006) : paleomagnetic record of Africa and South America for 1200-500 Ma interval, and evaluation Rodinia and Gondwana assemblies, *Prec. Research* 147, 193-222.

A model – proxy data comparison of mid to late Miocene paleotemperatures in western and central Europe

Alexander CLARK¹, Johan VELLEKOOP^{1,2}, Robert SPEIJER¹

1. Department of Earth and Environmental Sciences, KU Leuven, Celestijnenlaan 200E, 3001 Heverlee, Belgium

2. Analytical, Environmental and Geochemistry Research Group, Vrije Universiteit Brussel, Pleinlaan 2, B-1050, Brussels, Belgium

To be able to tackle the problems an ever-warming climate presents, insights into what the future will bring are needed. Climate models, such as ECHAM5 and HadCM3L, are a way of predicting what the climate will look like (Henrot et al. 2017). Most of these models simulate, among others, global, seasonal, sea and surface air temperatures. In order to evaluate and improve the accuracy of these climate models, model data needs to be validated with proxy data. Climate models predict that temperatures within the next century will approximate those of the Langhian, Serravallian and Tortonian (mid Miocene, ~15.9 to ~7.2 Ma). To test how well the climate models are able to reconstruct mid-Miocene temperatures for western and central Europe, a model-proxy data comparison is made, with published proxy data, including paleobotanical and $\delta^{18}\text{O}$ data, from these three time intervals, focussing on the Atlantic coast and Central Paratethys.

Three variables were used for comparison; mean winter, annual and summer temperatures, MWT, MAT and MST respectively. From these variables, the mean annual range in temperature (MART) is used for comparison, shown in Figure 1. The Coexistence Approach (CA) is used for the paleobotanical record (Utescher et al. 2017) and the empirically derived temperature-oxygen isotope fractionation relationship for calcite or aragonite is used for the $\delta^{18}\text{O}$ data (Harzhauser et al. 2011; Briard et al. 2020), with $\delta^{18}\text{O}_{\text{sw}}$ estimated by comparing recorded proxy data to estimated minimum sea temperatures and clumped isotopes. For comparison the simulated paleotemperatures are compiled from numerous climate models, including ECHAM5, HadCM3L, Planet Simulator, FOAM-LMDZ4, MPI-ESM, CESM1.0 and CCSM3.0 (Bradshaw et al. 2012; Henrot et al. 2017; Frigola et al. 2018). These climate models assume pCO_2 values of 500-560, 200, 280 ppmv for the Langhian, Serravallian and Tortonian, respectively.

In the Langhian, the warmest age of the Miocene, there is no systematic offset between the model and proxy paleotemperature data. The model MART is generally higher, except for a few localities around the relatively extreme northern and southern latitudes. A similar outcome is also found for the Serravallian age. Even for localities relatively close to each other, such as for the eastern North Sea or the Central Paratethys, the differences in MART are larger than the MART itself. For the Tortonian, the coolest of the three studied time intervals, a similar picture is found although there is a higher variability in MART between the studied localities.

As shown in this initial model-proxy data comparison for the mid Miocene, there is no uniform or systematic offset or difference between proxy and model paleotemperatures. Even between neighbouring localities for one period there can be differences between model and proxy data. Therefore the need for more proxy data studies is highlighted in order to further improve the climate model simulations of the mid Miocene.

References

C.D., Bradshaw. D.J., Lunt. R., Flecker. U., Salzmann. M.J., Pound. A.M., Haywood. & J.T., Eronen, 2012. The relative roles of CO_2 and palaeogeography in determining late

Miocene climate: results from a terrestrial model–data comparison. *Climate of the Past*, 8(4), 1257-1285.

J., Briard. E., Pucéat. E., Vennin. M., Daëron. V., Chavagnac. R., Jaillet. D., Merle. & M., de Raféllis, 2020. Seawater paleotemperature and paleosalinity evolution in neritic environments of the Mediterranean margin: Insights from isotope analysis of bivalve shells. *Palaeogeography, Palaeoclimatology, Palaeoecology*, 543, 109582.

A., Frigola. M., Prange. & M., Schulz, 2018. Boundary conditions for the middle Miocene climate transition (MMCT v1. 0). *Geoscientific Model Development*, 11(4), 1607-1626.

M., Harzhauser. W.E., Piller. S., Müllegger. P., Grunert. & A., Micheels, 2011 Changing seasonality patterns in Central Europe from Miocene Climate Optimum to Miocene Climate Transition deduced from the *Crassostrea* isotope archive. *Glob. Plan. Change*, 76, 77-84.

A.J., Henrot. T., Utescher. B., Erdei. M., Dury. N., Hamon. G., Ramstein. M., Krapp. N., Herold. A., Goldner. E., Favre. & G., Munhoven, 2017. Middle Miocene climate and vegetation models and their validation with proxy data. *Palaeogeography, Palaeoclimatology, Palaeoecology*, 467, 95-119.

T., Utescher. A., Dreist. A.J., Henrot. T., Hickler. Y.S.C., Liu. V., Mosbrugger. F.T., Portmann. & U., Salzmann, 2017. Continental climate gradients in North America and Western Eurasia before and after the closure of the Central American Seaway. *Earth and Planetary Science Letters*, 472, 120-130.

Figure

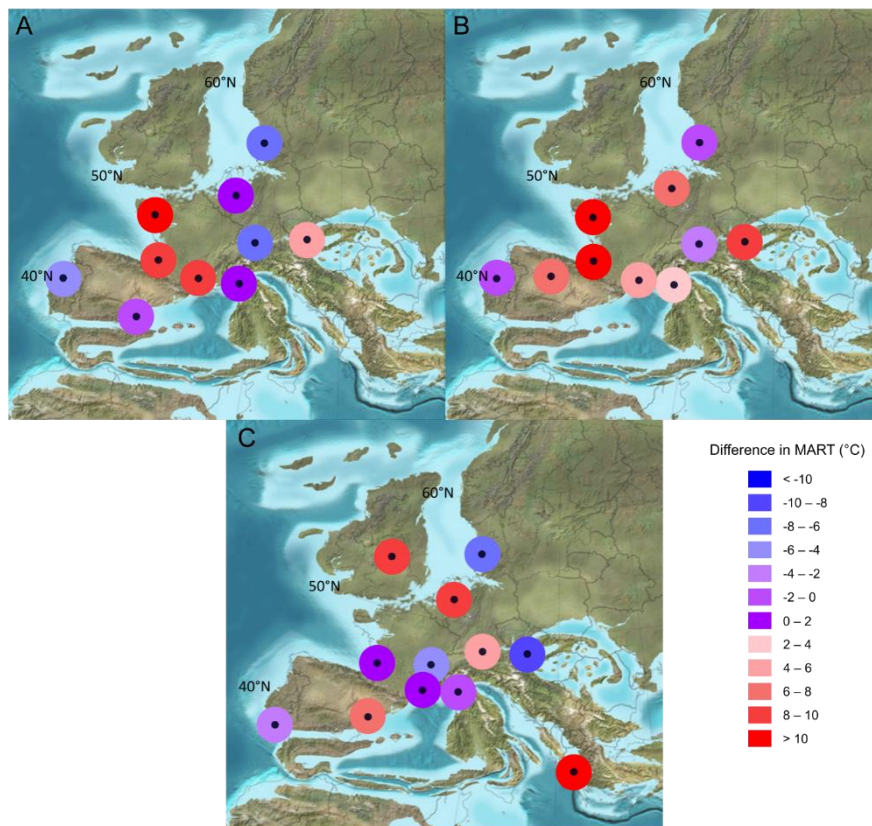


Figure 1. Paleogeographic maps highlighting the differences between model and proxy MART data for the A) Langhian, B) Serravallian and C) Tortonian periods.

The French Massif Central: a witness of successive weathering periods since the Early Cretaceous in the Alpine foreland

Augustin DEKONINCK^{*1}, Gilles RUFFET², Julien BAPTISTE³, Robert WYNS³, Eric LASSEUR³, Jean-Yves ROIG³, Johan YANS¹

1. *Université de Namur, ILEE, Département de géologie – Belgium*
(augustin.dekoninck@unamur.be)(johan.yans@unamur.be)

2. *CNRS (CNRS/INSU) et Université de Rennes 1, Géosciences (UMR6118) – France*
(gilles.ruffet@univ-rennes1.fr)

3. *Bureau de Recherches Géologiques et Minières (BRGM) – France*
(j.baptiste@brgm.fr)(e.lasseur@brgm.fr)(jy.roig@brgm.fr)(r.wyns@free.fr)

Many European uplands have remained topographic highs for protracted periods of weathering during the Mesozoic and Cenozoic. The long-term elevation position as low relief of these massifs acted as a source for adjacent sedimentary basins, their weathering playing a major role in the production of sediments available for erosion. Weathering profiles on these uplands are mostly incomplete/truncated since weathering products have often been washed away during repeated periods of erosions, leading to patchworks of remaining weathered rocks. In order to better address the events that have shaped these source areas, a complementary approach of both the source (upland) and sink (sedimentary basin) areas is crucial, but the record in the hinterland often remains partial due to lack of dating material and incomplete sequence.

The study presented here after is part of the BRGM-TOTAL *Source-to-Sink* project and aims at identifying key periods of exposure of the Massif Central (France). We used the combination of a careful petrogenesis and ⁴⁰Ar/³⁹Ar dating of K-bearing Mn oxides (coronadite group and romanèchite). The French Massif Central hosts several Mn occurrences sporadically mined until the first half of the 20th Century. We have targeted five of these sites that contain dating minerals: (1) “Nontronais” (Haute-Dordogne; Mn-Fe; south-west), (2) Villerembert (Montagne Noire; Mn; south), (3) Vieussan (Montagne Noire; Mn; south), (4) Auxilhac (Lozère; Mn-Fe; south), and (5) Romanèche (Mn-F-Ba; east). The combined petrography, mineralogy and geochemistry of these Mn ores show that Mn deposits 1, 2 and 3 belong to a weathering crust model (“laterite”), sampling site 4 follows a karst-hosted model whereas sampling site 5 follows an epithermal model. In any of these cases, the dated K-Mn oxides were formed at the end of the weathering paragenetic sequence, except maybe for Romanèche which encompasses epithermal formation. This and their oxidizing precipitation environment support a formation under surface or sub-surface conditions. Therefore, their ages are instructive of periods of meteoric waters circulation under near-surface conditions. For the first time in these areas, the ⁴⁰Ar/³⁹Ar ages define at least four weathering periods: (i) Albian and older, (ii) Campanian, (iii) Oligocene-Early Miocene and (iv) Late Miocene to Quaternary. The French Massif Central is a key place in the West European landscape that better constrain the long-term evolution of weathering that has affected basement rocks and their cover. The Early Cretaceous period is well known in Western Europe for having provided various and thick weathering products (bauxite, kaolin, siderolithic). The Campanian

age fits well with the first slow Pyrenean compression that exposed the Montagne Noire (south Massif Central), whereas Oligocene-Quaternary weathering events correspond to widespread weathering phases and compressional phases of the Alpine and Pyrenees. The lack of any Eocene period in the age record might be due to erosional conditions that overcome weathering, as it corresponds to the paroxysmal phase of the Pyrenean compression and strong siliciclastic discharge from the Massif Central to the Aquitaine and Paris basins.

This work is funded and carried out in the framework of the BRGM-TOTAL project Source-to-Sink.

Structure and evolution of the Congo Basin: long-lived record of tectonic and climatic events during the last Billion years

Damien DELVAUX ¹, Francesca MADDALONI ², Magdala TESAURO ³, Carla BRAITENBERG ⁴

*1: Royal Museum for Central Africa, Dept. Earth Sciences, Tervuren, Belgium
(damien.delvaux@africamuseum.be)*

2: University of Trieste, Department of Mathematics and Geoscience, Trieste, Italy

3: University of Utrecht, Department of Geosciences, the Netherlands

The Congo Basin is a remarkable intracontinental sag basin developed in the middle of the African continent since the late Mesoproterozoic. A recent investigation combining all the available data from various geological and geophysical exploration campaigns allowed producing a new view of its sedimentary and tectonic evolution since its onset as a failed rift system at about 1.06 GA (Delvaux et al., 2021). We propose a revised seismostratigraphic model based on a detailed interpretation of about 1600 km of seismic profiles, borehole and outcrop data. We produced depth maps for the prominent reflectors and thickness maps for the seismostratigraphic units that highlight the three-dimensional evolution of the CB trough time. It recorded the deposition history of up to one billion years of sediments above a metamorphic basement. It registered several global glacial events in a geodynamic setting evolving from the end of the Rodinia amalgamation to the Gondwana assembly and breakup while drifting over the South Pole and terminating at the Equator. Its early history parallels the evolution of the Mesoproterozoic-Neoproterozoic Kibaride belts of Central Africa. Surrounded by Pan-African orogenic belts in the late Neoproterozoic to Cambrian, it was affected by far-field deformations and associated vertical movements that left a prominent tectonic unconformity coeval with well-expressed Pan-African unconformities elsewhere in Gondwana. During the late Paleozoic to early Mesozoic, sedimentation occurred in the context of the Gondwanide orogeny along the southern margin of Gondwana. It induced locally intense tectonic reactivation and general vertical movements, leading to the development of a second basin-scale unconformity at the base of the Jurassic).

References

Delvaux, D., Maddaloni, F., Tesauro, M., Braitenberg, C., 2021. The Congo Basin: Stratigraphy and subsurface structure defined by regional seismic reflection, refraction and well data. *Global and Planetary Change* 198, 103407. doi: 10.1016/j.gloplacha.2020.103407.

A 1500 years-record of North Atlantic storminess from the Shetland Islands (UK) – preliminary insights

Max ENGEL^{1,2}, Katharina HESS¹, Tasnim PATEL³, Sue DAWSON⁴, Jan OETJEN⁵,
Andreas KOUTSODENDRIS⁶, Polina VAKHRAMEEVA⁶, Isa SCHÖN^{3,7} & Vanessa M. A.
HEYVAERT^{2,8}

1. *Heidelberg University, Institute of Geography, Im Neuenheimer Feld 348, 69120 Heidelberg, Germany (max.engel@uni-heidelberg.de; katharina.hess@stud.uni-heidelberg.de)*
2. *Royal Belgian Institute of Natural Sciences, OD Earth and History of Life, Geological Survey of Belgium, Jennerstraat 10, 1000 Brussels, Belgium (mengel@naturalsciences.be; vanessa.heyvaert@naturalsciences.be)*
3. *Royal Belgian Institute of Natural Sciences, OD Nature, ATECO, Freshwater Biology, Vautierstraat 29, 1000 Brussels, Belgium (tpatel@naturalsciences.be; ischoen@naturalsciences.be)*
4. *University of Dundee, Department of Geography, Tower Building, Nethergate, Dundee DD1, UK (s.dawson@dundee.ac.uk)*
5. *RWTH Aachen University, Institute of Hydraulic Engineering and Water Resources Management, Mies-van-der-Rohe-Str. 17, 52074 Aachen, Germany (oetjen@iww.rwth-aachen.de)*
6. *Heidelberg University, Institute of Earth Sciences, Im Neuenheimer Feld 234, 69120 Heidelberg, Germany (andreas.koutsodendris@geow.uni-heidelberg.de; polina.vakhrameeva@geow.uni-heidelberg.de)*
7. *University of Hasselt, Research Group Zoology, Campus Diepenbeek, 3590 Diepenbeek, Belgium*
8. *Ghent University, Department of Geology, Krijgslaan 281, 9000 Ghent, Belgium*

Severe storms and their extreme waves and surges pose a major hazard to the coasts of northwestern Europe. For assessing future risks that may arise from storm surges and assessing the question whether storm activity has increased in recent decades, high-resolution records of North Atlantic (NA) storminess are required. However, this information is generally limited to instrumental weather data or historical documentation from the last few centuries. Long-term patterns of storm frequency and intensity require proxy records from sedimentary or geomorphic archives (e.g. May et al. 2013). Since the most severe storms passing over Europe originate in the NA, the Shetland Islands are a prime location to search for long-term records. The present study aims at a better understanding of (i) the longer-term recurrence pattern of extreme storm events on the Shetland Islands beyond the instrumental and historical record, (ii) the parameters driving extra-tropical storms in the wider region as well as (iii) the role and variability of the North Atlantic Oscillation (NAO).

The present study investigates sediments from the small, shallow freshwater lake Flugarth (depth ca. 3 m) on Mainland, which is separated from the ocean by a low sand and gravel barrier. Three sediment cores (up to 90 cm-long) were retrieved to trace the variability of storm overwash and cover the past c. 1500 years based on a Bayesian AMS-¹⁴C age model, that is currently being refined by ¹³⁷Cs dating and tephrostratigraphy. Potential overwash layers are assumed to create thin sand layers as a contrast to dark, organic-rich background sedimentation and identified by a multi-proxy study, including laser diffraction-based grain-size analysis, magnetic susceptibility, bulk density, total organic carbon (TOC), and high-resolution XRF core scanning. The study of micro-sedimentary patterns in thin sections as well as a palynological analysis (pollen, dinoflagellate cysts) are in progress. So far, neither

the coastal source sediments nor the different layers in the core revealed any carbonate microfossils (e.g. foraminifera, ostracods). Historical documentation of NA storm events and their tracks covering most of the Modern Era (e.g. Lamb, 1991) is used to calibrate the sedimentary record of this study. The intensity of the sedimentary archive and the critical threshold height of a combined storm surge and wave setup required for overwash sediment deposition in the lake is assessed using a hydrodynamic model in DELFT3D-Flow.

The bright sand layers are clearly revealed by increased magnetic susceptibility, bulk density and grain size, while the background sedimentation shows elevated TOC and S/Ti ratios. The Si/Ti ratio is associated with increased biogenic silica, i.e. diatoms, which may benefit from nutrient-rich salty water (Balascio et al., 2011) caused by overwash events. The Ca/Fe ratio is generally low related to a lack of Ca in the catchment geology and the adjacent beach, but shows a remarkable increase between 18–32 cm, where the concentration of clastic sand layers is low. Higher values of the Mn/Fe ratio, that predominantly occur in the upper parts of the core, indicate oxic conditions and may relate to increased lake mixing as a result of higher wind velocity (Davies et al., 2015); significant sea level-controlled lake-level fluctuations can be excluded for the last 1500 years (Bondevik et al., 2005). Based on the current age model, the Medieval Warm Period (MWP, c. AD 950–1250) shows a relatively high concentration of intercalated sand layers. The first part of the Little Ice Age (LIA, ca. AD 1400–1850), in contrast, reflects low connectivity between the lake and sea, with only little sand input, while after c. AD 1700, a sudden increase of storm overwash can be inferred.

As data generation and analysis are still in progress, the results presented here have to be considered as preliminary. However, the higher concentration of overwash sand during the MWP coincides with an intensified NAO at that time, which is inferred from speleothem records and is known to drive westerly wind intensity. In contrast, subsequent low overwash activity in the core is in phase with a negative NAO during the early LIA (Baker et al., 2015). Thus, first results seem to confirm a link of storm intensity to NAO in the Shetlands and indicate that the present record may provide a high-resolution archive of regional storminess. Storm variability inferred from this record may inform future strategies of coping with coastal hazards in the NA realm under scenarios of climatic changes.

References

- Baker, A., Hellstrom, J.C., Kelly, B.F.J., Mariethoz, G. & Trouet, V., 2015. A composite annual-resolution stalagmite record of North Atlantic climate over the last three millennia. *Scientific Reports*, 5, 10307.
- Balascio, N.L., Zhang, Z., Bradley, R.S., Perren, B., Dahl, S.O. & Bakke, J., 2011. A multi-proxy approach to assessing isolation basin stratigraphy from the Lofoten Islands, Norway. *Quaternary Research*, 75, 288–300.
- Bondevik, S., Mangerud, J., Dawson, S., Dawson, A. & Lohne, Ø., 2005. Evidence for three North Sea tsunamis at the Shetland Islands between 8000 and 1500 years ago. *Quaternary Science Reviews*, 24, 1757–1775.
- Davies, S.J., Lamb, H.F. & Roberts, S.J., 2015. Micro-XRF core scanning in palaeolimnology: recent developments. In: Croudace, I.W. & Rothwell, R.G. (eds), *Micro-XRF Studies of Sediment Cores*. Springer, Dordrecht, 189–226.
- Lamb, H.H., 1991. *Historic storms of the North Sea, British Isles and Northwest Europe*. Cambridge, Cambridge University Press
- May, S.M., Engel, M., Brill, D., Squire, P., Scheffers, A. & Kelletat, D., 2013. Coastal hazards from tropical cyclones and extratropical winter storms based on Holocene storm chronologies. In Finkl, C. (ed), *Coastal Hazards*. Springer, Dordrecht, 557–585.

Age Ma	Series	Global Stages	Brabant M. formations	Trilobite graptolite zonation	Acrit. Zone Vanguestaine	Stavelot Inlier formations	Rocroi Inlier formations	Givonne Inlier formations						
ORDOVICIAN	LATE ORDO. 458.2	SANDBIAN	ITTRE Fm.	<i>C. bicornis</i> <i>N. gracilis</i> <i>H. terestiusculus</i> <i>D. murchinsoni</i>	Zone 9 Zone 8 Zone 7 Zone 6 Zone 5 Zone 4b Zone 3 Zone 2 Zone 1 Zone 0	hiatus	hiatus		MEGASEQUENCE 2					
	MIDDLE ORDOVICIAN	DARRIWILIAN	RIGENEE Fm.	<i>D. artus</i>										
			469.4	TRIBOTTE AB. VILLERS						<i>A. cucullus</i> <i>I. gibberulus</i> <i>I. v. victorizae</i> <i>E. simulans</i> <i>B. varicosus</i> <i>T. phyllograptus</i>	BIHAIN Fm. (Sm3)	Vieux Moulin de Thilay Fm. (Sm3)		
	LOWER ORDOVICIAN	FLOIAN	hiatus	<i>A. murrayi</i>						OTTRE Fm. (Sm2)				
		477	TREMADO-CIAN	CHEVLI-PONT Fm.						<i>R. f. anglica</i> <i>R. f. parabola</i> <i>R. praeparabola</i> Acerocarina <i>Peltura</i> Protopeltura Leptoplastus Parabolina <i>Olenus</i>	JALHAY Fm. (Sm1)	hiatus		
	487	FURONGIAN	STAGE 10 491	MOUSTY Fm.						Zone 6	LA GLEIZE Fm. (Rv5)	PETITE-COMMUNE Fm. (Rv4)	Sedimentary record is ongoing but undated	MEGASEQUENCE 1
	497		JIANGSHANIAN 494							Zone cf. 6	(Rv4)			
	CAMBRIAN	Former Upper Camb.	PAIBIAN	JODOIGNE Fm.						Zone cf. 5	LA VENNE Fm. (Rv3)	ANCHAMPS Fm. (Rv3)	Unnamed Fm. (Rv3)	
			500.5							GUZHANGIAN 500.5	Zone 4b	(Rv2)	La ROCHE à 7 HEURES (Rv2)	Unnamed Fm. (Rv2)
		Former Middle Camb.	DRUMIAN 504.5	WULIUAN						OISQUERCQ Fm.	Zone 3	WANNE Fm. (Rv1)	ROCHER de l'UF (Rv1)	Unnamed Fm. (Rv1)
509			DRUMIAN 504.5		Zone 2									
SERIE 2		STAGE 4 514.5	TUBIZE Fm. <i>Ol.</i>	BLANMONT Fm.	Zone 1	BELLEVAUX Fm. (Dv2)	QUATRE FILS AYMON Fm. (Dv2)	The Devillian Group is not exposed						
					Zone 0				HOURT Fm. (Dv1)	LONGUE-HAIE Fm. (Dv1)				
520	521	STAGE 3												
529	TERRENEUVIAN	STAGE 2												

Fig. 2: Synthetic stratigraphic correlations between the Brabant Massif and the 3 main inliers of the Ardenne (Stavelot-Venn, Rocroi, Givonne) from the upper Terreneuvian to the Middle Ordovician. In the middle, informal Vanguestaine zones are correlated with trilobite and graptolite zones (Peng et al., 2020; Goldman et al., 2020). The formation name given by Beugnies (1960) at Givonne are invalidated by Vanguestaine and Léonards (2005). Dotted line: less precise boundary between formations. Megasequence 2 is in grey color. *Rh.* = *Rhabdinopora*; *Ol.* = *Oldhamia*.

Beugnies, A., 1960. Le Massif cambrien de Givonne. ASGB, 83, M1-40.

Goldman, D., Sadler, P.M., Leslie, S.A., 2020. The Ordovician Period, *In*: Gradstein, F.M., Ogg, J.G., Schmitz, M.D., Ogg, G.M (Eds) The concise Geologic Time Scale. Cambridge University press, vol. 2, 631-694.

Herbosch, A., Boulvain, F., submitted 2021. Chapter 8.1 The Ardenne *In* "Geology of the Central European Variscides and its Avalonian-Cadomian precursors" Linnemann U. (Ed.). Herbosch, A., Liégeois, J.P., Gärtner, A., Hofmann, M., Linnemann, U., 2020. The Stavelot-Venn Massif (Ardenne, Belgium), a rift shoulder basin ripped off the West African craton: cartography, stratigraphy, sedimentology, new U-Pb on zircon ages, geochemistry and Nd isotopes evidence. Earth-Sciences Reviews, 203, 1031-1042.

Peng, S.C., Babcock, L.E., Ahlberg, P., 2020. Chapter 19 The Cambrian Period *In*: Gradstein F.M., Ogg, J.G., Schmitz, M.D., Ogg, G.M. (Eds.) The Geologic Time Scale 2020. Cambridge University press, 565-629.

Vanguestaine, M., 1992. Biostratigraphie par acritarches du Cambro-Ordovicien de Belgique et des régions limitrophes: synthèses et perspectives d'avenir. ASGB, 115, 1–18.

Vanguestaine, M., Léonard, R., 2005. New biostratigraphic and chronostratigraphic data from the Sautou Formation and adjacent strata (Cambrian, Givonne Inlier, Revin Group, N France) and some lithostratigraphic and tectonic implications. Geologica Belgica, 8, 131-144.

Crustal and sedimentary structures of the Congo basin constrained by geophysical signatures

Étienne KADIMA, K. ¹, Stanislas SEBAGENZI, M.N. ¹, Francis LUCAZEAU ², Damien DELVAUX ³, Christian BLANPIED ⁴

1. *Unilu, Laboratoire de Géophysique et Dynamique de la lithosphère, B.P. 1825 Lubumbashi, RD Congo*
2. *Dynamique des Fluides Géologiques, Institut de Physique du Globe de Paris/Sorbonne Paris, UMR CNRS 7154, 1, rue Jussieu, 75005 Paris, France*
3. *Geodynamic and Mineral Ressources Royal Museum for Central Africa, Tervuren, Belgium*
4. *Total Exploration & Production, Paris La Défense*

The Congo Basin (CB) is a distinctive large sub-circular long-term sedimentation area in Central Africa. It consists of a thick sedimentary package, 9 km deep or more, overlying a mosaic of Precambrian blocks amalgamated during successive Proterozoic tectonic events. The CB's thick and large sedimentary cover would hide its complex subsurface structure, i.e. the unexplored Precambrian blocks and their probable connection, the underlying structure of explored blocks and the possible crustal as well as its sedimentary deformations.

Outcrops scarcity coupled with dense forest and a thick cover of recent sediments allow more importance to be given to the geophysical approach for various geological work undertaken in this basin. A first campaign geophysics, including seismic measurements (refraction and reflection), gravimetric and magnetic 1950s conducted by the "Union for the geological study of the Congolese Basin" (Evrard, 1957, 1900; Jones et al., 1960)) was followed by a reflection seismic survey of 2900 km of high resolution undertaken by the "Compagnie Generale de Geophysique (CCG)" and the "Sismograph Seismic Limited (SSL)" on behalf of Texaco and Exxon (Daly et al. (1991, 1992). The crossed interpretations of these various geophysical data have been presented in several rich scientific publications but uncertainties and controversies still remain especially on the subsurface structure of this large basin and the nature of its sedimentary deformations.

Using seismic, gravity and isostasy constraints, we interpret lateral change of the sedimentary cover and its crustal structure and highlight the basin's subsurface architecture. While the extent and location of the main structure defined in this basin, the Kiri Shoal, are known, debates about its nature and the process of its formation remain. New geophysical constraints shed light on this important structure by which various sub-basins and shoals are defined.

Gravity stripping facilitated the removal of sediment's effect and residual data set thus obtained allows mapping the crustal architecture concealed by the sediment. Choosing an Airy-Heiskanen model of compensation, we obtained an isostatic anomaly map of the CB area in which relevant patterns reflect different structures beneath the basin. This map shows that the CB is dominated by large overcompensated zones separated in the center by two thin and elongated undercompensated zones.

The overcompensated area, equivalent to thick continental crust zone, correlates with low residual gravity (less than -30 mGal), and the undercompensated area, corresponding to the thin continental crust zone of the basin, correlate with high residual gravity anomaly zones (up to + 80 mGal).

A combined interpretation of old reflection and refraction seismic data guide to a definition of plausible connection lines between the known and explored Precambrian blocks (The Archean to Paleo-Proterozoic Kasai-Angola shield in the southern side and the Meso-

Proterozoic Kibaran belt to the eastern) and the Congo Central Craton (CCC) hidden by recent sediments. Our interpretation highlights also the existence, in the southwestern margin of the basin, of a half-graben like structure stretch E-W and filled with the Karoo, Mesozoic to recent sediments.

These results confirm the complex structure of the CB, the lack of knowledge about its geology, and more specifically its subsurface structure, and the value of undertaking additional work to learn more about it.

References

- Evrard, P. (1957) Les recherches géophysiques et géologiques et les travaux de sondage dans la Cuvette congolaise. Acad. Roy.Sci. Coloniale., Sc.Techn. Bruxelles,VII(1), 62pp.
- Evrard, P. (1960) Sismique. (Résultats scientifiques des missions du Syndicat pour l'étude géologique et minière de Cuvette congolaise). Ann. Mus. Roy. Afrique centrale, Tervuren (Belgique), série in- 8, Sci. geol., 33, 87p.
- Jones, L., Mathieu, P.L. and Strenger, H. (1960) Gravimétrie: Les résultats scientifiques des missions du syndicat pour l'étude géologique et minière de la Cuvette Congolaise et travaux connexes. Ann. Mus. Roy. Congo belge, Tervuren (Belgique), serie in- 8, Sci. geol., 36, 46pp.
- Daly, M.C., Lawrence, S.R., Diemu-Thiband, K. and Matouana, B. (1992) Tectonic evolution of the Cuvette Centrale, Zaire. J. Geol. Soc. Lond., 149, 539-546.
- Daly, M.C., Lawrence, S.R., Kimun'a, D. and Binga, M. (1991) Late Paleozoic deformation in central Africa: a result of distant collision? Nature, 350, 605-607.

Lake Chala 2k: the last two millennia of environmental change in equatorial East Africa

Inka MEYER^{1*}, Irina PAPADIMITRIOU¹, Dirk VERSCHUREN² and Marc DE BATIST¹

¹ Renard Centre of Marine Geology, Department of Geology, Ghent University, Krijgslaan 281 s.8, B-9000 Gent, Belgium

² Limnology unit, Department of Biology, Ghent University, Ledeganckstraat 35, B-9000 Gent, BELGIUM

*Corresponding author: Inka.Meyer@UGent.be

In order to disentangle natural climate variability from anthropogenically caused variations, environmental reconstructions of the past 2000 years have gained renewed scientific interest during the last ~20 years. Whereas climatic and environmental changes during this period, such as the Medieval Climate Anomaly (MCA) and the Little Ice Age (LIA) are fairly well expressed in Western Europe and the North Atlantic area, knowledge about equivalent changes in African climate and environment (e.g. changes in temperature and precipitation, monsoonal activity and resulting vegetation feedbacks) can be much improved. Here we present new results from Lake Chala, a crater lake in equatorial East Africa, based on sedimentary grain-size distributions. Notwithstanding the relatively minor clastic mineral component, we are able to discriminate between different aeolian and fluvial sources of terrigenous material, and to reconstruct temporal trends in their contribution to the sediment. This can be linked to both local environmental dynamics and changes in the large-scale monsoonal systems over the East African landmass. Our findings point to arid conditions during the MCA and humid conditions during the LIA, in support of regional hydroclimate history as reconstructed from other moisture-balance proxies. The results of this study form an important piece of the puzzle to better understand past changes in African environments, which is a key aspect in the debate about future climate change in one of the most climate-sensitive regions on the planet.

Frasnian–Famennian deposits of Southern Belgium: thick and complex key sections to understand the Late Frasnian extinctions and the role played by tsunamis

Edouard POTY¹, Julien DENAYER¹, Bernard MOTTEQUIN²

1. *Evolution & Diversity Lab, Université de Liège, Liège, Belgium (e.poty@uliege.be, julien.denayer@uliege.be)*

2. *O.D. Earth and History of Life, Royal Belgian Institute of Natural Sciences, Brussels, Belgium (bmottequin@naturalsciences.be)*

The Late Frasnian mass extinction, mainly recorded among invertebrate marine faunas, is traditionally considered as one of the ‘Big Five’ of the Phanerozoic, even if the crisis known as the Hangenberg Crisis at the Devonian–Carboniferous boundary was probably more significant than previously thought. The Late Frasnian extinctions are usually considered to be linked with two black anoxic shale–limestone horizons (the lower Kellwasser (LKW) and the upper Kellwasser (UKW)), and they were subsequently named the Kellwasser events. However, most of the research dedicated to the Late Frasnian events and the Frasnian–Famennian boundary in Western Europe is focused on deep-setting sections where the sedimentary record is extremely reduced (some metres in thickness), giving clear-cut, but very simplified, geochemical data and conodont records. Usually, these sections are not condensed, but just very lacunar, and therefore very smoothed, contrary to their contemporaneous equivalents from ramp and platform settings, which are considerably thicker and more complex.

The Southern Belgian Basin (SBB) offers a unique opportunity to detail not only the timing and the aftermath of the late Frasnian extinctions on shallow-water biota (mainly brachiopods and corals), but also to document the evolution of the carbonate platform and buildups during the Middle Frasnian, and their decrease related to the Frasnian crises. The sequence stratigraphy of the Middle and Upper Frasnian was revised recently by Mottequin & Poty (2016) and allowed to establish that the development of the buildups was clearly correlated with third-order sequences. During the Middle Frasnian, the onset and vertical growth of the three successive levels of reefs (Arche, Boverie and Lion members) correspond to the transgressive system tract (TST) of the third-order sequences. During the high-stand (HST) and the falling-stage system tracts (FSST), their vertical growth decreased, and they evolved to progradant carbonate platforms, 1–3 km wide and up to 140 m thick (including the biohermal core) as is the case of the sequence observed in Frasnies-les-Couvin (*carrière du Nord*), in which boundstones are replaced by packstone–grainstones, then by shallow-water and intertidal mudstones (FSST). Note that there is no evidence for the development of atolls rimmed by stromatoporoïd–coral barriers as suggested previously.

During the onset of the transgression of the Late Frasnian ‘Aisemont sequence’ (the first of the two recognized Late Frasnian sequences), when TST deposits reached the top of the ‘Lion’ reef–platform or invaded the northern carbonate platform (top of Philippeville–Lustin formations), they were not different from the previous TST deposits which covered the ‘Arche’ and ‘Boverie’ reefs–platforms. They were characterized by shaly limestones, mostly with crinoids, tabulate and numerous rugose corals (mainly ‘*Hexagonaria*’), which usually were the basement for the growing of a bioherm. But very quickly, ‘*Hexagonaria*’ colonies died, as the associated tabulate (e.g. thamnoporids) and rugose (e.g. fasciculate disphyllids) corals, and were replaced by frechastreïd–phillipsastraëid colonies that were previously unknown from the basin. Some of them developed directly on the ‘*Hexagonaria*’ colonies. The major change observed in the coral fauna was probably related to a decrease in the

atmospheric oxygen rate as suggested, among others, by the occurrence of brachiopods adapted to poorly oxygenated environments (e.g. Mottequin & Poty, 2016). This event locally marks the onset of the Late Frasnian crises and the end of the previous carbonate platform and that of the Middle Frasnian-type reefs which never recovered. In the distal areas, reddish microbial mudmounds ('Petit-Mont'-type buildups), grew during the TST and the HST of this first Late Frasnian ('Aisemont') sequence. They are smaller than the previous buildups, reaching up to 300 m in width and 80 m in thickness. Their growth was essentially vertical and there is no marked progradation during the HST. During the FSST of the 'Aisemont sequence', shallow-water mudstones and stromatolites developed on their top, then their emersion stopped their development.

On the proximal previous carbonate 'Philippeville–Lustin' platform, the 'Aisemont' TST was also characterized by the replacement of a '*Hexagonaria*-type fauna' by a 'frechastreid–phillipsastraetid' coral and associated fauna. But quickly, black dysoxic to anoxic greenish-black shales invaded all the platform. They are correlated with the LKW and correspond to the maximum flooding zone of the sequence (Poty & Chevalier, 2007). The LKW had strictly no effect on the distribution of corals and brachiopods, as stated by Poty & Chevalier (2007), except that the latter are locally absent during the development of these dysoxic–anoxic facies. Therefore, there is no extinction at all correlated with this event, contrary to what is claimed in studies dedicated to 'condensed' sections.

During the ultimate Late Frasnian sequence ('Lambermont sequence') the extension of anoxic–dysoxic facies prevented the development of large buildups, and only 1 to 2 m-wide micro-mudmounds have so far been recorded in the Philippeville Anticlinorium (Mottequin & Poty, 2016).

It is worthwhile to remind here that black dysoxic–anoxic shales (Matagne Formation) have developed from the base of the Upper *Palmatolepis rhenana* conodont Zone in the most distal and deepest parts of the SBB, regardless of what can be observed in the other areas.

The UKW is responsible for the last Frasnian extinctions. It is widespread in the SBB and developed even in places where anoxic shales were previously absent since the LKW. Everywhere, the UKW rests on a 0.15 to 1 m-thick set of limestone beds with shaly intercalations. These limestone levels clearly can be due to a series of tsunamis (Poty et al., 2014; Mottequin & Poty, 2016) that triggered the input of anoxic–dysoxic waters in previously more or less oxygenated environments, killing most of the rest of benthic faunas. Isochronous levels related to tsunamites are known worldwide and probably triggered the last and definitive step of the Late Frasnian extinctions. Therefore, the final Frasnian extinction is most probably related to both a series of tsunamis, possibly of tectonic origin, and the resulting widespread of dysoxic–anoxic waters into areas that were already depleted in oxygen.

References

- Mottequin, B. & Poty, E. 2016. Kellwasser horizons, sea-level changes and brachiopod-coral crises during the late Frasnian in the Namur-Dinant Basin (southern Belgium): a synopsis. Geological Society, London, Special Publications, 423, 235–250.
- Poty, E. & Chevalier, E. 2007. Late Frasnian phillipsastreid biostromes in Belgium. Geological Society, London, Special Publication, 275, 143–161.
- Poty, E., Denayer, J. & Mottequin, B. 2014. Tsunamis triggered the Late Frasnian Kellwasser extinction event. In: Cerdeño, E. (ed.) The History of Life: A View from the Southern Hemisphere. Abstract Volume of the 4th International Palaeontological Congress, September 28–October 3, CCT-CONICET, Mendoza, Argentina. International Palaeontological Association, Lawrence, KS, 598.

Etude paléoenvironnementale des roches carbonatées de la région Lufu-Toto située dans le degré carré de Mbanza Ngungu (Province du Kongo Central, R.D. Congo)

L.O. TUEMA ¹, C.L. MUKEBA, ¹, C.M.E. CIBAMBULA ¹, M.N.A.J. MAKUTU ¹, H.M. TSHOMBE ²

¹Université de Kinshasa, Faculté des Sciences, Dép. des Géosciences, BP 190, Kinshasa XI RDC

²Centre de Recherche Géologique et Minière (CRGM), BP 898, Kinshasa-Gombe, RDC

Située dans la plaine Schisto-calcaire au SO du petit plateau de Mbanza-Ngungu, la région de Lufu-Toto est comprise entre 14° 37' et 14° 48' de longitude Est et 5° 24' et 5° 35' de latitude Sud. Elle renferme essentiellement des roches du niveau C4a constituant, un cortège de bas niveau marin caractérisé par un important apport silico-clastique dans le bassin Ouest-congolien. Ces roches du niveau 4a sont sus-jacentes aux calcaires du niveau C3b2 appartenant aux dépôts de haut niveau marin. Elles sont, du point de vue paléoenvironnemental, similaires aux faciès de rampe à lagon évaporitique de la côte des Pirates. Ces variations eustatiques devant conduire à des migrations spatio-temporelles des milieux, quels sont les marqueurs environnementaux enregistrés lors du dépôt des roches du niveau C4a ?

L'étude paléoenvironnementale réalisée dans la région de Lufu-Toto témoigne que ces roches sont réparties dans quatre zones des faciès. La première zone des faciès est caractérisée par les marnes gris vert à litage lenticulaire de marais maritimes, les marnes mauves à litage planaire de flat boueux et les shales dolomitiques d'étang salant. La deuxième zone des faciès est caractérisée par les marnes gréseuses de flat mixte. La combinaison de ces deux zones avec les criques tidales traduites par les marnes mauves à litage oblique est typique d'une côte macrotidale, adjacente au lagon restreint à biolithite, calcaire mudstone et dolomie grise si l'on se réfère aux travaux de Nichols (2009), et que Selley (1996) qualifie autrement de « complexe côtier-lagonaire ».

Références:

Nichols, G. (2009) : *Sedimentology and stratigraphy*. 2nd ed., Wiley-Blackwell, Oxford, U.K., 418p.

Selley, R.C., 1996, Ancient sedimentary environments and their sub-surface diagnosis : *Chapman and Hall publications (4th ed.)*, 300 pp.

Lake Naivasha's response to the end of the African Humid Period

Thijs VAN DER MEEREN¹, Gijls DE CORT¹, Christine COCQUYT², Lydia A. OLAKA³, Kazuyo TACHIKAWA⁴, Edouard BARD⁴, Priyanka KASPATHY THEVANAYAGAM¹, Dirk VERSCHUREN¹

1. Limnology Unit – Department of Biology – Ghent University, Ghent, Belgium

(thijs.vandermeeren@ugent.be, gijls.decort@ugent.be,

priyanka.kaspathythevanayagam@UGent.be, dirk.verschuren@ugent.be)

2. Meise Botanical Garden, Meise, Belgium (christine.cocquyt@plantentuinmeise.be)

3. University of Nairobi, Nairobi, Kenya (lydiaolaka@uonbi.ac.ke)

4. Aix Marseille Université, CEREGE, Aix-en-Provence, France (kazuyo@cerege.fr, bard@cerege.fr)

Lake Naivasha is a vital regional freshwater resource in the central rift valley of Kenya, located at 1884 m. above sea level. It is also recognized as a classic amplifier lake (Trauth et al. 2010), where lake level (and surface area) responds dramatically to climate variability because of the important contribution of river inflow to lake water balance. During the African Humid Period (ca. 14800 to 5500 year ago), Lake Naivasha's surface level is estimated to have been ca. 80 m higher than today, establishing a southward overflow (Richardson & Richardson 1972; Bergner et al. 2003). It has been demonstrated that also climatic variation in the last ca 1650 years induced major hydrological shifts, including salinity crises and associated reshuffling of the aquatic ecosystem (Verschuren et al. 2001, Van der Meeren et al. 2019). Preservation of a continuous sedimentary archive in such a dynamic environmental setting is only possible because of the protected depositional environment present in the submerged Crescent Island Crater basin (Verschuren 1999). We here present the first results of a new sedimentary sequence recovered from this basin in 2020, and representing the last 7000 years of climate and environmental history.

Our proxy data (sediment composition based on loss-on-ignition and x-ray fluorescence) indicate that Lake Naivasha was already in a shrinking phase 7000 years ago, and experienced episodes of pronounced hydrological closure around 5900, 4000 and 3400 years ago. Around 3000 years ago, a brief but prominent low-stand initiated the high responsiveness of the Lake Naivasha system to decadal-scale variations in moisture balance, similar to that documented in the last 1650 years.

Our high-resolution paleohydrological record really improves understanding of Lake Naivasha's response to the progressively deteriorating water balance associated with the shift from the African Humid Period towards the drier Late-Holocene period. We show that the timing of the major lake-level regression at Lake Naivasha, associated with the loss of its southward overflow, predates the commonly accepted end of the East African Humid Period ('EAHP', Tierney et al. 2011) around 5000 years ago (Tierney & deMenocal 2013), as well as the most pronounced lake-level regression at the more northerly situated rift-valley lakes Suguta and Turkana (Bloszies et al. 2015). We suggest that different hydrological sensitivity among these lake basins to shifts in precipitation and temperature-controlled evaporation may explain some of the observed differences, besides a different balance between westerly (Atlantic) and easterly (Indian Ocean) contributions to local rainfall.

References

- Bergner, A.G., Trauth, M.H. & Bookhagen, B, 2003. Paleoprecipitation estimates for the Lake Naivasha basin (Kenya) during the last 175 ky using a lake-balance model. *Global and Planetary Change*, 36, 117-136.
- Bloszies, C., Forman, S.L. & Wright, D.K, 2015. Water level history for Lake Turkana, Kenya in the past 15,000 years and a variable transition from the African Humid Period to Holocene aridity. *Global and Planetary Change*, 132, 64-76.
- Richardson, J.L. & Richardson, A.E, 1972. History of an African rift lake and its climatic implications. *Ecological monographs*, 42, 499-534.
- Tierney, J.E., Lewis, S.C., Cook, B.I., LeGrande, A.N., & Schmidt, G.A, 2011. Model, proxy and isotopic perspectives on the East African Humid Period. *Earth and Planetary Science Letters*, 307, 103-112.
- Tierney, J.E. & deMenocal, P.B, 2013. Abrupt shifts in Horn of Africa hydroclimate since the Last Glacial Maximum. *Science*, 342, 843-846.
- Trauth, M.H., Maslin, M.A., Deino, A.L., Junginger, A., Lesoloyia, M., Odada, E.O., Olago, D.O., Olaka, L.A., Strecker, M.R. & Tiedemann, R, 2010. Human evolution in a variable environment: the amplifier lakes of Eastern Africa. *Quaternary Science Reviews*, 29, 2981-2988.
- Van der Meeren, T., Ito, E., Laird, K.R., Cumming, B.F. & Verschuren, D, 2019. Ecohydrological evolution of Lake Naivasha (central Rift Valley, Kenya) during the past 1650 years, as recorded by ostracod assemblages and stable-isotope geochemistry. *Quaternary Science Reviews*, 223, 105906.
- Verschuren, D, 1999. Sedimentation controls on the preservation and time resolution of climate-proxy records from shallow fluctuating lakes. *Quaternary Science Reviews*, 18, 821-837.
- Verschuren, D, 2001. Reconstructing fluctuations of a shallow East African lake during the past 1800 yrs from sediment stratigraphy in a submerged crater basin. *Journal of Paleolimnology*, 25, 297-311.

Correlating cross-border Cenozoic stratigraphy in the Belgian-Dutch border region: results from H3O – De Voorkempen

Jan WALSTRA¹, Armin MENKOVIC², Jef DECKERS³, Frieda BOGEMANS¹, Michiel DUSAR¹, Andreas F. KRUISSELBRINK², Bruno MEYVIS¹, Dirk MUNSTERMAN², Bernd ROMBAUT³, Tamara J.M. VAN DE VEN², Kris WELKENHUYSEN¹ & Ronald W. VERNES²

1. Royal Belgian Institute of Natural Sciences – Geological Survey of Belgium, Brussels, Belgium (jan.walstra@naturalsciences.be)
2. TNO – Geological Survey of the Netherlands, Utrecht, The Netherlands (ronald.vernes@tno.nl)
3. VITO – Flemish Institute of Technological Research, Mol, Belgium (jef.deckers@vito.be)

The sustainable use and management of natural resources in border regions require unambiguous geological information from neighbouring countries. However, the available data often lack compatibility and the same level of detail across borders. Aim of the Belgian-Dutch H3O projects is to produce seamless, cross-border, 3D geological and hydrogeological models of the Cenozoic deposits across the border between Belgium and The Netherlands. “H3O – De Voorkempen” is the third consecutive project, focusing on the Noorderkempen (Flanders) and the western part of Noord-Brabant (The Netherlands). The project started in 2020 and the final results will be delivered in 2023.

A crucial step in any cross-border geological modelling task is to establish the correlation between lithostratigraphic units on both sides of the border. In this project, the correlation is initially based on the available knowledge of regional lithostratigraphy (including chronology, depositional environment, sedimentological characteristics) and then further fine-tuned based on the interpretation of high-quality boreholes, geophysical well logs and seismic lines that cover the main geological complexities and cross the international border. The correlations are graphically presented in a chrono-lithostratigraphic correlation chart and cross-section profiles.

The established correlation scheme will be used as a base for converting or reinterpreting the available data. In the final stage, the harmonized datasets will be used to create a geometrically and stratigraphically consistent 3D model of “De Voorkempen”. The result will be a state-of-the-art reference for the subsurface structure of the project area, which can be used as a base for scientific research and cross-border management of natural resources.

The Belgian-Dutch H3O projects are carried out by a partnership between TNO – Geological Survey of the Netherlands, VITO and RBINS – Geological Survey of Belgium, with support from the Flemish Bureau for Environment and Spatial Development (VPO), Flanders Environment Agency (VMM), Province of Noord-Brabant and drinking water company Brabant Water. The geological models are/will be available in the public domain via the online data portals of DOV (Database of the Subsoil in Flanders) and DINOloket (Data and Information on the Dutch Subsurface). For the technical reports of previous H3O projects, see Deckers *et al.*, 2014 and Vernes *et al.*, 2018.

References

Deckers, J., Vernes, R.W., Dabekaussen, W., Den Dulk, M., Doornenbal, J.C., Duser, M., Hummelman, H.J., Matthijs, J., Menkovic, A., Reindersma, R.N., Walstra, J.,

Westerhoff, W.E. & Witmans, N., 2014. Geologisch en hydrogeologisch 3D model van het Cenozoïcum van de Roerdalslenk in Zuidoost-Nederland en Vlaanderen (H3O-Roerdalslenk). VITO/TNO report, Mol/Utrecht, 208 pp. (incl. 8 appendices).

Vernes, R.W., Dekkers, J., Bakker, M., Bogemans, F., De Ceukelaire, M., Doornenbal, J., den Dulk, M., Duser M., Van Haren, T., Heyvaert, V., Kiden, P., Kruisselbrink, A., Lanckacker, T., Menkovic, A., Meyvis, B., Munsterman, D., Reindersma, R., Rombaut, B., ten Veen, J., van de Ven, T., Walstra, J. & Witmans N., 2018. Geologisch en hydrogeologisch 3D model van het Cenozoïcum van de Belgisch-Nederlandse grensstreek van Midden-Brabant / De Kempen (H3O – De Kempen). TNO/VITO/KBIN-BGD report, Utrecht/Mol/Brussel, 109 pp. (+8 appendices).

Depositional environment and characteristics of organic matter of Namurian Shale, Namur Synclinorium and Campine Basin (Belgium and the S-Netherlands)

Wei WEI¹, Ralf LITTKE², Rudy SWENNEN¹

1. *KU Leuven, Department of Earth & Environmental Sciences, Geology, Celestijnenlaan 200E, B-3001 Heverlee, Belgium (wei.wei@kuleuven.be) (rudy.swennen@kuleuven.be)*

2. *Institute of Geology and Geochemistry of Petroleum and Coal, Energy and Mineral Resources Group, RWTH Aachen University, 52056 Aachen, Germany (ralf.littke@emr.rwth-aachen.de)*

During the last decade organic-rich shales (mudstones, siliceous mudstones and marlstones) gained scientific interest as unconventional petroleum reservoir and source rocks. The main shale gas target in the Northwest European Carboniferous Basin (NWECEB) is the Namurian basinal shale which belongs to the Mississippian shale play that occurs in the UK, France, Belgium, the Netherlands, Germany, Poland and Ukraine. A series of studies have been conducted on these shales, including the Bowland Shale in the UK, Epen Formation with Geverik Member in the Netherlands and the Upper Alum Shale in Germany (Kombrink, 2008; Doornenbal and Stevenson, 2010; Uffmann et al., 2012; Ghazwani et al., 2018; Emmings et al., 2020). Geological characteristics like geochemistry and mineralogy, depositional environment, provenance and preservation status of organic matter as well as reservoir quality of Namurian basinal shale have been addressed at these locations. Similar data are sparse in Belgium which leads to difficulties in evaluating its shale gas potential. Namurian basinal shale in Belgium is assigned to Namurian A age which is distributed in the Namur Synclinorium and Campine Basin. In order to infer the depositional environment and the characteristics of organic matter of Namurian basinal shale in Belgium and neighboring areas, samples from five locations have been collected and thin section petrography (including optical microscopy, cathodoluminescence), X-ray diffraction, X-ray fluorescence, total organic carbon, total nitrogen, stable isotope analysis, organic petrography and Rock-Eval pyrolysis have been carried out. The major objectives of this investigation are to (1) define and describe the lithofacies and depositional setting of Namurian A mudstone, (2) describe the type, thermal maturity and enrichment mechanism of organic matter, (3) discuss shale gas potential of Namurian A mudstone.

Sedimentological, petrographic and geochemical analyses at multiple scales from these five sampling locations allowed to distinguish eleven lithofacies. These sediments were deposited through various processes, including low density turbidity currents, low to moderate strength cohesive debris flows as well as hemipelagic and pelagic suspension settling. Namurian A mudstone in the Namur Synclinorium and Campine Basin consists of an organic-rich mudstone succession that was deposited in a distal shelf-slope-basin floor setting below storm wave base within the Variscan foredeep zone. Namurian A mudstone in the Namur Synclinorium was deposited more specifically in a restricted shallow water foreland basin environment which had poor connection with the Paleo-Tethys ocean while deposition occurred in a shallow water foreland basin with good circulation with the Paleo-Tethys ocean in the Campine Basin. Four major provenances are responsible for Namurian A mudstone, including detrital minerals from Variscan orogeny and London-Brabant Massif, calcareous bioclasts from nearby basinal highs, *in situ* fauna from the slope settings as well as hemipelagic and pelagic suspension settling.

Namurian A mudstone in the study area is overmature (vitrinite reflectance V_{Ro} 1.9 to 3.5%). Solid bitumen, vitrinite and inertinite dominate the organic assemblage in Namurian A

mudstone while the liptinite maceral group is missing in all samples. This is explained by the fact that liptinites comprising Type I/II kerogen almost completely convert to hydrocarbons and a residue (solid bitumen) and therefore they are not present in high maturity shale gas reservoirs (Hackley, 2017). Organic carbon isotope results, organic petrology and sedimentological data indicate that the original, immature Namurian source rock contained both terrestrial organic and marine organic matter, but in different percentages at different locations. The origin of marine organic matter can be linked to phytoplankton and microorganisms while terrestrial organic matter relates to continental plants. Mechanism of organic matter enrichment includes several factors. Lithofacies with high TOC deposited commonly in the environment with relative high primary marine productivity, good preservation conditions, relative high deposition rate and dominated marine organic matter while lithofacies with low TOC deposited in the environment with decreasing primary marine productivity, less good preservation conditions with more oxygenated water, siliclastic and carbonate dilution, relative low deposition rate, increasing terrestrial organic matter.

Rock-Eval pyrolysis indicates that S₂ values (ranging from 0.1 mg HC/g to 2.2 mg HC/g, averaging 0.5 mg HC/g) are low at all locations which indicates homogeneous and low remaining hydrocarbon generating potential in Namurian A mudstone. According to burial and thermal history modelling results, rapid deposition occurred during the Pennsylvanian. During this rapid subsidence period, the base of the Namurian A Formation was buried to a depth between 3500 to 4000 m when the highest burial temperatures (roughly 200 to 230°C) were reached. Namurian A mudstone became overmature during this period and extensive hydrocarbon generation took place. Loss of generated gas has occurred during uplift and pressure decrease afterwards.

References

- Doornenbal, H., and Stevenson, A., 2010. Petroleum geological atlas of the Southern Permian Basin area. EAGE.
- Emmings, J. F., Davies, S. J., Vane, C. H., Moss-Hayes, V., & Stephenson, M. H., 2020. From marine bands to hybrid flows: Sedimentology of a Mississippian black shale. *Sedimentology*, 67(1), 261-304.
- Ghazwani, A., Littke, R., Gaus, G., & Hartkopf-Fröder, C., 2018. Assessment of unconventional shale gas potential of organic-rich Mississippian and Lower Pennsylvanian sediments in western Germany. *International Journal of Coal Geology*, 198, 29-47.
- Hackley, P. C., 2017. Application of organic petrology in high maturity shale gas systems. Bentham Science Publishers, Vol.1, 205-235.
- Kombrink, H., 2008. The Carboniferous of the Netherlands and surrounding areas; a basin analysis. *Geologica Ultraiectina* (294). Department Aardwetenschappen.
- Uffmann, A. K., Littke, R., & Rippen, D., 2012. Mineralogy and geochemistry of Mississippian and Lower Pennsylvanian black shales at the northern margin of the Variscan Mountain Belt (Germany and Belgium). *International Journal of Coal Geology*, 103, 92-108.

Uncovering earthquake doublets in a lacustrine sedimentary record

Katleen WILS¹, Maxim DEPRESZ², Catherine KISSEL³, Morgan VERVOORT¹, Maarten VAN DAELE¹, Mudrik R. DARYONO⁴, Veerle CNUDDÉ^{2,5}, Danny H. NATAWIDJAJA⁴, Marc DE BATIST¹

1. Renard Centre of Marine Geology, Department of Geology, Ghent University, Ghent, Belgium (katleen.wils@ugent.be)
2. PProGRess/UGCT, Department of Geology, Ghent University, Ghent, Belgium
3. Laboratoire des Sciences du Climat et de l'Environnement, Université Paris-Saclay, Gif-sur-Yvette, France
4. Research Center for Geotechnology, Indonesian Institute of Sciences, Bandung, Indonesia
5. Environmental Hydrogeology, Department of Earth Sciences, Utrecht University, Utrecht, The Netherlands

Two successive earthquakes with similarly high magnitudes on nearby fault segments separated by no more than a few hours' time are considered to form an earthquake doublet. Such doublets have been described in historical archives around the world (e.g. Lay and Kanamori, 1980; Lin et al., 2008), but their identification in paleoseismic records remains ambiguous. This has major implications for seismic hazard assessments based on those records, as inferred major paleo-earthquakes could also have resulted from separate, consecutive earthquakes. Moreover, our limited knowledge on the occurrence of earthquake sequences inhibits identification of potential common fault behaviour, which could result in significant mitigation of the risk associated to an imminent second shock. Identification of earthquake doublets in paleoseismic records is thus of crucial importance. The continuous sedimentation records provided by lacustrine settings have great potential to record closely-timed earthquakes in the form of multi-pulsed seismo-turbidites (e.g. Van Daele et al., 2015; Migeon et al., 2017). However, such multi-pulsed character could also originate from synchronously-generated turbidity currents in multiple locations by the same earthquake. To distinguish those from turbidity currents generated separately as a result of individual earthquakes, identification of flow directions and thus source areas is required. The most compelling argument for the occurrence of an earthquake doublet is then formed by the delayed arrival of turbidity currents originating from the same source location.

To determine whether lacustrine paleoseismic records are indeed capable of revealing earthquake doublets, we performed a detailed analysis of a multi-pulsed turbidite identified in the sedimentary infill of Lake Singkarak, located in West Sumatra. This turbidite has been attributed to an earthquake doublet that occurred in March 2007 (Wils et al., 2021), consisting of two $M_w > 6$ earthquakes on adjacent fault segments of the Sumatran Fault, separated by no more than 2 hours (Daryono et al., 2012). Considering that elongated grains tend to align according to the dominant flow direction (e.g. Paris et al., 2010), we developed a new methodology that analyses the geographical orientation of grains present within each turbidite pulse to determine its source area. For this purpose, we combine high-resolution X-ray computed tomography with paleomagnetic measurements. Application to the 2007 seismo-turbidite in Lake Singkarak reveals the presence of similar source areas in two intervals of turbidity current amalgamation, clearly offset in time. To rule out potential confounding processes such as seiching or slope failures in absence of a second external trigger, grain-size analysis was additionally used. This confirmed that each earthquake in the 2007 West Sumatra doublet triggered separate turbidity currents in the lake. In this way, we provide the first unmistakable sedimentary evidence of an earthquake doublet, underscoring the

invaluable sensitivity of lacustrine paleoseismic records. Moreover, the outlined methodology is highly promising to analyse previously-described multi-pulsed lacustrine turbidites and reveal the occurrence of, up to now, unknown prehistoric earthquake doublets.

References

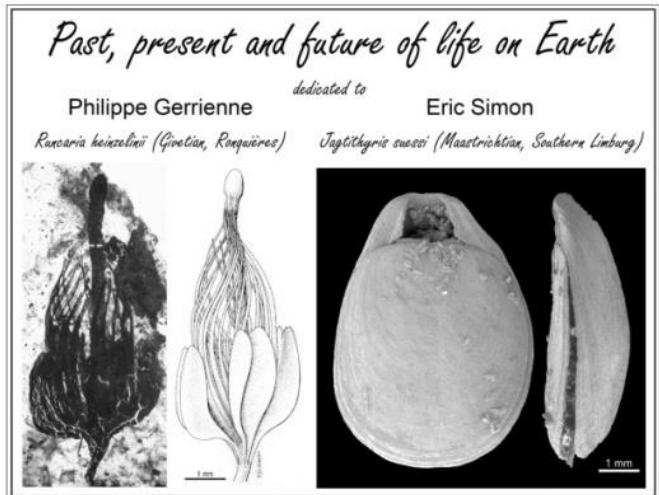
- Daryono, M. R., Natawidjaja, D. H. & Sieh, K., 2012, Twin-surface ruptures of the March 2007 $M > 6$ earthquake doublet on the Sumatran Fault: *Bulletin of the Seismological Society of America*, 102, 2356-2367.
- Lay, T. & Kanamori, H., 1980, Earthquake doublets in the Solomon Islands: *Physics of the Earth and Planetary Interiors*, 21, 283-304.
- Lin, C.-H., Yeh, Y.-H., Ando, M., Chen, K.-J., Chang, T.-M. & Pu, H.-C., 2008, Earthquake doublet sequences: Evidence of static triggering in the strong convergent zones of Taiwan: *Terrestrial, Atmospheric and Oceanic Sciences*, 19, 589-594.
- Migeon, S., Garibaldi, C., Ratzov, G., Schmidt, S., Collot, J. Y., Zaragosi, S. & Texier, L., 2017, Earthquake-triggered deposits in the subduction trench of the north Ecuador/south Colombia margin and their implication for paleoseismology: *Marine Geology*, 384, 47-62.
- Paris, R., Fournier, J., Poizot, E., Etienne, S., Morin, J., Lavigne, F. & Wassmer, P., 2010, Boulder and fine sediment transport and deposition by the 2004 tsunami in Lhok Nga (western Banda Aceh, Sumatra, Indonesia): A coupled offshore–onshore model: *Marine Geology*, 268, 43-54.
- Van Daele, M., Moernaut, J., Doom, L., Boes, E., Fontijn, K., Heirman, K., Vandoorne, W., Hebbeln, D., Pino, M., Urrutia, R., Brümmer, R., De Batist, M. & Trofimovs, J., 2015, A comparison of the sedimentary records of the 1960 and 2010 great Chilean earthquakes in 17 lakes: Implications for quantitative lacustrine palaeoseismology: *Sedimentology*, 62, 466-1496.
- Wils, K., Daryono, M. R., Praet, N., Santoso, A. B., Dianto, A., Schmidt, S., Vervoort, M., Huang, J. S., Kusmanto, E., Suandhi, P. A., Natawidjaja, D. H. & De Batist, M., 2021, The sediments of Lake Singkarak and Lake Maninjau in West Sumatra reveal their earthquake, volcanic and rainfall history: *Sedimentary Geology*, 416, 105863.

Session 6- Past, Present and Future of Life on Earth

Conveners:

Julien Denayer (ULiège), Valentin Fisher (ULiège), Stephen Louwye (UGent), Cyrille Prestianni (ULiège & RBINS), Thierry Smith (RBINS), Robert Speijer (KU Leuven)

For this session we invite contributions from the entire spectrum of palaeontology. We aim at establishing an interesting mix of new developments in palaeontology, representative of the various research groups and lines of research "made in Belgium". Accordingly, the scope will range from micropalaeontology to macropalaeontology, from systematics to stratigraphy, from ecology to evolution, from climate to CT-scanning, and from dinosaur digs to nanofossil oozes.



This session will be dedicated to Philippe Gerrienne and Eric Simon, two good colleagues that left us in recent years.

First occurrence of linguliformean brachiopods in the lower Tremadocian (Ordovician) of the Brabant Massif (Belgium)

Yves CANDELA¹, Jean-Marc MARION², Thomas SERVAIS³, Wenhui WANG⁴, Mark WOLVERS⁵, Bernard MOTTEQUIN⁶

1. *Department of Natural Sciences, National Museums Scotland, Edinburgh, United Kingdom*
(y.candela@nms.ac.uk)
2. *Service géologique de Wallonie, Service public de Wallonie, Direction générale opérationnelle Agriculture, Ressources naturelles et Environnement, Jambes, Belgium*
(jeanmarc.marion@spw.wallonie.be)
3. *CNRS, Université de Lille, Lille, France* (thomas.servais@univ-lille.fr)
4. *Key Laboratory of Metallogenic Prediction of Nonferrous Metals and Geological Environment Monitoring, Ministry of Education, School of Geosciences and Info-Physics, Central South University, Changsha, PR China* (whwang@csu.edu.cn)
5. *Brunel 19, 3641VG Mijdrecht, The Netherlands* (markwolvers@msn.com)
6. *O.D. Earth and History of Life, Royal Belgian Institute of Natural Sciences, Brussels, Belgium* (bmottequin@naturalsciences.be)

Contrary to the well-exposed Devonian–Mississippian succession, Cambrian–Silurian of Belgium is generally poor in brachiopods. Few Upper Ordovician lithostratigraphic units, such as the Huet Formation in the Brabant Massif (e.g. Malaise, 1873), have yielded rich brachiopod faunas. Only one brachiopod occurrence was documented so far in the Cambrian (Wanne Formation) of the Stavelot–Venn Massif (Vanguetaine & Rushton, 1979) whereas the Silurian, mostly represented by graptolitic shaly facies, is almost devoid of brachiopods although the Přídolí transgressive cover contains abundant but poorly diverse brachiopod faunas (e.g. Godefroid, 1995; Mottequin, 2019). Up to now, only Schmidt & Geukens (1959) have briefly discussed the occurrence of Tremadocian brachiopods found on both sides of the Belgian–German border within the Stavelot–Venn Massif (Jalhay Formation).

The lowermost Ordovician remained undiscovered in the Brabant Massif until the studies of Lecompte (1948, 1949), who recorded the presence of graptolitic horizons (see Wang & Servais' (2015) discussion) and scarce trilobite specimens in the Thyle Valley, demonstrating the presence of Tremadocian rocks. Since these studies no new macrofossil faunas have been described from the Lower Ordovician until the recent, quite fortuitous discovery of brachiopods within the Chevlipont Formation (Ottignies Group), in the close vicinity of the ruins of the Villers-la-Ville Abbey (Candela et al., in press).

The brachiopod assemblage collected from the Chevlipont Formation is neither abundant nor diverse. Eighteen samples were collected totalling over 100 specimens, some of which cannot be fully identified due to their poor preservation. In increasing abundance, the assemblage is composed of *Broeggeria* cf. *salteri* (70% of the total amount of specimens identified), *Thysanotos* sp. (29%) and *Rosobolus?* sp. (1%). The brachiopods are not associated to graptolites and trilobites although these were reported by Lecompte (1949) in the investigated area.

The scarcity of the shelly faunas observed within the thick lithostratigraphic succession recognized in the Brabant Massif, which ranges from the upper Terreneuvian to the lower Tremadocian (525–482 Ma), is mostly due to the palaeoenvironmental conditions. Indeed, the succession comprises clastic, mostly pelagic and turbiditic sediments deposited in an embayment of a large rift that developed on the western Gondwana margin (Linnemann et al., 2012) in continuation with the Pan-African orogen.

The presence of this low diversity assemblage of linguliformean brachiopods in a peri-Gondwanan terrane, is typical of lowermost Ordovician brachiopod assemblages that have an origin in the Cambrian. Popov et al. (2013) suggested that the radiation and dispersion of lineages, which survived the severe crisis of linguliformean brachiopods experienced during the late Furongian to early Tremadocian, clearly controlled the biogeographic distribution of this group in the Ordovician.

References

- Candela, Y., Marion, J.-M., Servais, T., Wang Wenhui, Wolvers, M. & Mottequin, in press. New linguliformean brachiopods from the lower Tremadocian (Ordovician) of the Brabant Massif, Belgium, with comments on contemporaneous faunas from the Stavelot–Venn Massif. *Rivista Italiana di Paleontologia e Stratigrafia*.
- Godefroid, J., 1995. *Dayia shirleyi* Alvarez & Rachebœuf, 1986, un brachiopode silurien dans les ‘Schistes de Mondrepuis’ à Muno (sud de la Belgique). *Bulletin de l’Institut royal des Sciences naturelles de Belgique, Sciences de la Terre*, 65, 269-272.
- Lecompte, M., 1948. Existence du Trémadocien dans le Massif du Brabant. *Bulletin de l’Académie royale de Belgique, Classe des Sciences*, 34, 5e série, 677-687.
- Lecompte, M., 1949. Découverte de nouveaux gîtes à *Dictyonema* dans le Trémadocien du Massif du Brabant. *Bulletin de l’Institut royal des Sciences naturelles de Belgique*, 25(45): 1-8.
- Linnemann, U., Herbosch, A., Liégeois, J.-P., Pin, C., Gärtner, A. & Hofmann, M., 2012. The Cambrian to Devonian odyssey of the Brabant Massif within Avalonia: A review with new zircon ages, geochemistry, Sm-Nd isotopes, stratigraphy and palaeogeography. *Earth-Science Reviews*, 112, 126-154.
- Malaise, C., 1873. Description du terrain silurien du centre de la Belgique. *Mémoires Couronnés et Mémoires des Savants Étrangers, publiés par l’Académie royale des Sciences, des Lettres et des Beaux-Arts de Belgique*, 37, 1-122.
- Mottequin, B., 2019. An annotated catalogue of types of Silurian–Devonian brachiopod species from southern Belgium and northern France in the Royal Belgian Institute of Natural Sciences (1870–1945), with notes on those curated in other Belgian and foreign institutions. *Geologica Belgica*, 22, 47-89.
- Popov, L.E., Holmer, L.E., Bassett, M.G., Ghobadi Pour, M. & Percival, I.G., 2013. Biogeography of Ordovician linguliform and craniiform brachiopods. *Geological Society, London, Memoirs*, 38, 117-126.
- Schmidt, W. & Geukens, F., 1959. Nouveaux gîtes à Brachiopodes dans le Salmien inférieur du Massif de Stavelot. *Bulletin de la Société belge de Géologie, de Paléontologie et d’Hydrologie*, 67(2), 159-161.
- Vanguetstaine, M. & Rushton, A., 1979. Découverte d’un brachiopode inarticulé, *Acrothele* cf. *bergeroni* Walcott, dans le Revinien inférieur de Trois-Ponts, Cambrien du Massif de Stavelot, Belgique. *Annales de la Société géologique de Belgique*, 102, 295-301.
- Wang Wenhui & Servais, T., 2015. A re-investigation of the *Rhabdinopora flabelliformis* fauna from the early Tremadocian ‘*Dictyonema*’ Shale in Belgium. *Geologica Belgica*, 18, 66-77.

Craniomandibular anatomy of *Panthera gombaszoegensis* from la Belle-Roche (Liège, Belgium)

Narimane CHATAR^{1,*}, Valentin FISCHER¹

¹ Evolution and Diversity Dynamics Lab, Université de Liège, Belgium

* Corresponding author: narimane.chatar@uliege.be

All big cats, i.e. the clade Pantherinae, have always attracted attention but the jaguar (*Panthera onca*) has truly marked the cultural heritage of the whole South American continent (Sunquist & Sunquist, 2002). The jaguar is a heavy and powerful animal with the most powerful bite and the strongest canine within extant felines (Gonyea, 1976; Van Valkenburgh & Ruff, 1987; Werdelin, 1983). Researchers have tried to find a corresponding species in the fossil assemblages of Eurasia. Often called “European jaguar” or “Eurasian jaguar”, *Panthera gombaszoegensis* was a medium to large pantherine that went extinct approximately 350,000 years ago and is considered as the ancestor of the extant jaguar (O’Regan & Turner, 2004).

While it was first regarded as proper pantherine species (Kretzoi, 1938b) it was quickly re-attributed as a subspecies of the living jaguar, *Panthera onca* (Hemmer, 1971). Its taxonomic attribution remains debated as some authors still regard this taxa as a species on its own (Argant & Argant, 2011; Jiangzuo & Liu, 2020; Marciszak, 2014; Reynolds, 2013; Stimpson et al., 2015) while others maintain that the differences between *P. gombaszoegensis* and the living jaguar were not significant (Hankó, 2007; Hemmer et al., 2001, 2010; Mol et al., 2011). The scarce material of *P. gombaszoegensis* made it difficult to solve this taxonomic debate as the species was created solely based on isolated teeth by Kretzoi (1938b) and almost all material ever described is dental material. Nevertheless, some undescribed material of *P. gombaszoegensis* from “La Belle-Roche” in Belgium could shed a new light on this obscure taxon. The skull ULg-PA-BR-II-81-146 is relatively complete and is almost three dimensionally preserved and we hereby provide the first comparative description of the craniomandibular anatomy of this taxon. This skull also shows that *P. gombaszoegensis* varies from *P. onca* in various points such as having less rounded skull, a less marked lambdoidal crest, a slightly more protruding mastoid processes in dorsal view or a ventrally directed jugular process. The skull ULg-PA-BR-II-81-146 is also much larger than any extant jaguar showing a clear size reduction in the jaguar lineage. This suggests that the species *P. gombaszoegensis* is taxonomically and possibly ecologically distinct from *P. onca*.

Argant, A., & Argant, J. (2011). The Panthera Gombaszoegensis story: The contribution of the château breccia (Saône-Et-Loire, Burgundy, France). *Quaternaire, Supplement*, 4, 247–269.

Gonyea, W. J. (1976). Adaptive differences in the body proportions of large felids. *Acta Anatomica*, 96(1), 81–96. <https://doi.org/10.1159/000144663>

Hankó, P. E. (2007). A revision of three Pleistocene subspecies of Panthera, based on mandible and teeth remains, stored in Hungarian collections. *Fragmenta Palaeontologica Hungarica*, 24–25, 25–43.

Hemmer, H. (1971). zur Charakterisierung und stratigraphischen Bedeutung von Panthera gombaszoegensis (kretzoi, 1938). *Neues Jahrbuch Für Geologie Und Paläontologie Monatshefte*, 12, 701–711.

Hemmer, H., Kahlke, R.-D., & Vekua, A. K. (2001). The Jaguar - Panthera onca gombaszoegensis (Kretzoi, 1938) (Carnivora: Felidae) in the late lower pleistocene of Akhalkalaki (south Georgia; Transcaucasia) and its evolutionary and ecological significance. *Geobios*, 34(4), 475–486. [https://doi.org/10.1016/s0016-6995\(01\)80011-5](https://doi.org/10.1016/s0016-6995(01)80011-5)

Hemmer, Helmut, Kahlke, R. D., & Vekua, A. K. (2010). Panthera onca georgica ssp. nov. from the Early Pleistocene of Dmanisi (Republic of Georgia) and the phylogeography of jaguars (Mammalia, Carnivora, Felidae). *Neues Jahrbuch Für Geologie Und Paläontologie* -

Abhandlungen, 257(1), 115–127. <https://doi.org/10.1127/0077-7749/2010/0067>

Jiangzuo, Q., & Liu, J. (2020). First record of the Eurasian jaguar in southern Asia and a review of dental differences between pantherine cats. *Journal of Quaternary Science*, 35(6), 817–830. <https://doi.org/10.1002/jqs.3222>

Kretzoi, M. (1938a). Die Raubtiere von Gombaszög nebst einer Übersicht der Gesamtfaua. *Geologic Paleontology*, 31, 88–157.

Kretzoi, M. (1938b). Die Raubtiere von Gombaszög nebst einer Übersicht der Gesamtfaua. *Annales Musei Nationalis Hungarici, Pars Mineralogica, Geologica, Palaeontologica*, 31, 88–157.

Marciszak, A. (2014). Presence of panthera gombaszogensis (Kretzoi, 1938) in the late middle pleistocene of biśnik cave, Poland, with an overview of Eurasian jaguar size variability. *Quaternary International*, 326–327, 105–113. <https://doi.org/10.1016/j.quaint.2013.12.029>

Mol, D., Logchem, W. Van, & Vos, J. De. (2011). New record of the European jaguar , Panthera onca gombaszogensis (Kretzoi , 1938), from the Plio-Pleistocene of Langenboom (The Netherlands). *Cainozoic Research*, 8(1–2), 35–40.

O'Regan, H. J., & Turner, A. (2004). Biostratigraphic and palaeoecological implications of new fossil felid material from the Plio-Pleistocene site of Tegelen, The Netherlands. *Palaeontology*, 47(5), 1181–1193. <https://doi.org/10.1111/j.0031-0239.2004.00400.x>

Reynolds, B. (2013). Determiners, Feline Marsupials, and the Category-Function Distinction: A Critique of ELT Grammars. *TESL Canada Journal*, 30(2), 1. <https://doi.org/10.18806/tesl.v30i2.1138>

Stimpson, C. M., Breeze, P. S., Clark-Balzan, L., Groucutt, H. S., Jennings, R., Parton, A., Scerri, E., White, T. S., & Petraglia, M. D. (2015). Stratified Pleistocene vertebrates with a new record of a jaguar-sized pantherine (Panthera cf. gombaszogensis) from northern Saudi Arabia. *Quaternary International*, 382, 168–180. <https://doi.org/10.1016/j.quaint.2014.09.049>

Sunquist, M., & Sunquist, F. (2002). *Wild cats of the world*. The University of Chicago Press.

Valkenburgh, B. Van, & Ruff, C. B. (1987). Canine tooth strength and killing behaviour in large carnivores. *Journal of Zoology*, 212(3), 379–397. <https://doi.org/10.1111/j.1469-7998.1987.tb02910.x>

Werdelin, L. (1983). Morphological patterns in the skulls of cats. *Biological Journal of the Linnean Society*, 19(4), 375–391. <https://doi.org/10.1111/j.1095-8312.1983.tb00793.x>

Timing and pacing of the Hangenberg Crisis (Devonian-Carboniferous Boundary) in the Chanxhe sections, Belgium

Anne-Christine DA SILVA¹, Léonard FRANCK¹, Michiel ARTS¹, Julien DENAYER^{2,3}

1. *Geology, Faculty of Sciences, University of Liège, Belgium (ac.dasilva@uliege.be)*

2. *Evolution & Diversity Dynamics Lab, University of Liège, Belgium*

3. *Service Géologique de Wallonie, Service Public de Wallonie, Namur, Belgium (julien.denayer@spw.wallonie.be)*

The Hangenberg Crisis, at the Devonian–Carboniferous Boundary, severely affected the marine realm. The crisis is characterised by several events associated with change in the sedimentation and biotic extinctions and turnovers. The Hangenberg Black Shale event that recorded the extinction peak in the pelagic realm corresponds to a widespread development of oceanic anoxia and/or dysoxia. The Hangenberg Shale event record minor turnovers. The Hangenberg Sandstone event is associated with an extinction of neritic fauna in shallow-water settings, including the final demise of several classical Devonian faunas (stromatoporoids, quasiendothyrid foraminifers, placoderms, etc.). The succession of event is nowadays explained by a combination of sea level fluctuations (third order transgressive sequence, out-of-sequence regression) and global climatic changes (end of the Famennian glaciation and global warming during the Strunian, rapid cooling triggering the regression associated to the Hangenberg Sandstone event). Through the identification of Milankovitch cycles in the Chanxhe section, we aim at getting a better understanding of the timing of the different events of the Hangenberg Crisis in shallow-water settings. The sedimentary record of the interval of interest at Chanxhe is composed of alternating decimetre-thick carbonate beds with shaly siltstones, corresponding to the upper part of the Comblain-au-Pont Formation. The equivalent of the Hangenberg Black Shale is recorded by two dark shaly intervals separated by a carbonate bed. The dark character and the occurrence of pelecypods and smooth-shelled ostracodes, are pointing to dysoxia (Denayer et al., 2019). Above these dark horizons, the sedimentation is again dominated by neritic crinoidal packstone-grainstone tempestites. The Hangenberg Sandstone event in Chanxhe corresponds to a 20 cm-thick horizon of coarse-grained crinoidal and bioclastic grainstone containing detrital quartz grains (Denayer et al., 2020). It probably resulted from a short-term regression which is interpreted as associated with a rapid cooling. The termination of this regressive event, bracketed by biostratigraphy (spores and conodonts), has been proposed as the new criterium to define the Devonian-Carboniferous Boundary.

The studied section, prior the Hangenberg Crisis, displays a clear cyclicity, with the carbonate-siliciclastic alternations (~0.8 m) bundled into larger cycles (~5 m) and separated by intervals dominated by the shaly facies. These 5 metre-thick limestone/shale alternations are in a preliminary interpretation associated with short eccentricity (100 kyr, Fig.1). Samples have been collected along the record every 10 cm and each sample was measured by the portable X-Ray Fluorescence device (Tracer 5, Bruker), allowing to provide elemental evolution through the record. Spectral analysis is applied on a selection of elements and on the facies evolution, to identify the main cyclicity in the record and to confirm or not the preliminary interpretations.

References

- Denayer, J., Prestianni, C., Mottequin, B., Poty, E., 2019. Field trip A1: The Uppermost Devonian and Lower Carboniferous in the type area of Southern Belgium. 19th International Congress on the Carboniferous and Permian, Cologne 2019. Kölner Forum für Geologie und Paläontologie 24, 5–41.
- Denayer, J., Prestianni, C., Mottequin, B., Hance, L., & Poty, E., 2020. The Devonian–Carboniferous boundary in Belgium and surrounding areas. *Palaeobiodiversity and Palaeoenvironments*, 101/2, 313-356.



Figure 1 Chanxhe I section showing the alternation of shales and carbonates in the Strunian Comblain-au-Pont Formation, with preliminary cyclostratigraphic interpretation.

Pinaceae diversity from the Lower Cretaceous of Belgium

Léa DE BRITO^{1,2}, Valentin FISCHER¹, Cyrille PRESTIANNI^{1,2}

1. *Evolution & Diversity Dynamics Lab, UR Geology, Université de Liège, Belgium*
(l.debrito@uliege.be, v.fischer@uliege.be, cyrille.prestianni@uliege.be)

2. *Royal Belgian Institute of Natural Sciences, Brussels, Belgium*

The expansion of Pinaceae during the Cretaceous is exemplified by the numerous ovulate cone taxa found in Western Europe and North America. The Belgian Wealden facies deposits (Barremian-Albian, 125.0–100.5 My) have delivered hundreds of exceptionally well-preserved, yet isolated, pinaceous ovulate cones; these cones were placed by convention in form-genera (Alvin, 1953; Alvin, 1957; Alvin, 1960). A total of 10 species has been described in Belgium, representing about 33% of the known fossil cone species of this period. However, the validity of these taxa is questionable as their intra- and interspecific variabilities have never been studied. Moreover, quantifying the expansion of Pinaceae in terms of morphospace occupation is desirable, in order to reveal the dynamics of this important radiation.

We use so-called traditional (length measurements and counts) and geometric (landmarks and semi-landmarks) morphometry to quantify the shape of the extensive sample of Cretaceous cones of Belgium, as well as a thorough sample of extant forms. Based on analyses of modern and fossil samples, we also propose a model to predict the number of specimens needed to most of the morphological variation. We used ordination methods, PCA and NMDS on morphometrics data to recreate the morphospace occupation and test for species delineation. We observe that the morphological disparity isn't higher in fossil species than in present-day species. The very high morphological variability is confirmed for the current definition of *Pityostrobus andraei* and support this splitting of two distinct morphotypes (De Brito and Prestianni, 2021) as distinct species. This work demonstrates that a reassessment, with quantitative methods, of the ovulate cone species described in the 20th century is finally revealing the diversity of early Pinaceae and the shape of their radiation.

References

- Alvin K.L., 1953. Three abietaceous cones from the Wealden of Belgium. *Mémoires de l'Institut Royal des Sciences naturelle de Belgique*, 125, 1-42.
- Alvin K.L., 1957. On the two cones *Pseudoaraucaria heeri* (Coemans) nov. comb. and *Pityostrobus villerotensis* nov. sp. from the Wealden of Belgium. *Mémoires de l'Institut royal des Sciences naturelles de Belgique*, 135, 1-27.
- Alvin K.L., 1960. Further conifers of the Pinaceae from the Wealden formation of Belgium. *Mémoires de l'Institut royal des Sciences naturelles de Belgique*, 146,1-39.
- De Brito L. & Prestianni, C., 2021. *Pityostrobus andraei* (Pinaceae) from the Barremian (Lower Cretaceous) of Belgium: A Morphometric Revision. *International Journal of Plant Sciences*, 182, 174-184.

Belgium is the best place to define the Devonian-Carboniferous Boundary

Julien DENAYER^{1,2}, Cyrille PRESTIANNI^{1,3}, Bernard MOTTEQUIN³, Luc HANCE⁴ & Edouard POTY¹

1. *Evolution & Diversity Lab, Université de Liège, Allée du Six-Août, B18, Sart Tilman, B4000 Liège, Belgium* (julien.denayer@uliege.be, e.poty@uliege.be, cyrille.prestinani@uliege.be)
2. *Service Géologique de Wallonie, Service Public de Wallonie, Namur, Belgium*
3. *O.D. Earth and History of Life, Institut royal des Sciences naturelles de Belgique, rue Vautier 29, B1000 Brussels, Belgium* (cyrille.prestianni@naturalsciences.be, bmottequin@naturalsciences.be)
4. *Consult'Hance, rue de la Chapelle, 50, 5340 Gesves, Belgium* (hanceluc@gmail.com)

The Devonian-Carboniferous Boundary (DCB) was the first chronostratigraphic boundary to be officially and globally defined in 1935. It was soon acknowledged that the definition was not suitable, and 50 years of discussions were necessary before an agreement on the definition was reached. The DCB therefore was placed at the first appearance of the conodont *Siphonodella sulcata* in the stratotype section 'La Serre E' in S France. Once again, many specialists agreed that both the definition and the chosen stratotype were not sustainable due to taxonomic issues about siphonodellids, because the first occurrence of the marker was found in older strata (Kaiser 2009) and because the French stratotype was included within a sequence of reworked sediments. Hence, in 2016 the Working Group on the DCB suggested to revise the definition and collegially proposed a new criterium: the end of the reworking caused by the Hangenberg Sandstone regressive event concomitant to the end of the extinction phase, close to the first entry of the conodont *Protognathodus kockeli*. This depositional event bracketed by biostratigraphy being chosen, it was then tested in various settings in sections worldwide and proven to be working in many cases.

The DCB is associated with a major extinction event caused by a rapid but short-lasting change in deposition and eustasy called Hangenberg event that extends all along the latest Devonian (Strunian) and earliest Carboniferous (basal Hastarian) with several extinction phases in the pelagic realm but a single short-time extinction event in the neritic and continental realms. This extinction occurred during a period of biotic recovery that followed the Kellwasser event and covers the whole Famennian stage. The Strunian recovery most probably happened during a phase of climatic amelioration at the end of the Famennian and to a transgression that produced a switch from coastal siliciclastic to proximal mixed deposits with a progressive increase of the carbonate content. Hence, the Comblain-au-Pont and lower Hastière Formations are regarded as the transgressive system tract of a 3rd-order sequence. The middle member of the Hastière Fm is interpreted as the highstand system tract and is capped by an erosion surface corresponding to the sequence boundary. This 3rd-order sequence boundary can be traced within the Basin, but also outside, as far as South China (Poty, 2016). Superimposed to the 3rd-order sequences are well marked orbitally-forced precession cycles (wet-dry climate alterations) of c. 18.6 ka, appearing as irregular c. 40 cm-thick couplets of limestone and calcareous shale beds (Poty, 2016).

The Hangenberg Black Shale event is locally recorded as dark shale that likely spread on the shelf and marks the maximum flooding surface of sequence 1. Before and after this event, carbonate facies rich in benthic macro- and micro-fauna continued to develop, with no significant change in the marine biota. The Hangenberg Sandstone event, recorded as a sandstone bed in pelagic sections, is variously recorded at the base of the Hastière Fm, either as a sandy siltstone bed in proximal sections, or as a horizon with limestone clasts in more distal ones. The Hangenberg Sandstone event beds occur sharply in the stratigraphic record and does not correspond to the long sea-level fall of a 3rd-order sequence boundary but interpreted as a short out-of-sequence event (Poty, 2016).

The revision of the stratigraphic distribution of major fossil groups led to the demonstration of a continuous biostratigraphic succession of foraminifers and palynomorphs with no obvious hiatus in neritic settings. The variable development of some micropalaeontological zones that were often described as evidence for depositional hiatuses are nowadays regarded as complex eco-biostratigraphical interaction with the environment. The LN palynozone has been demonstrated to be an ecozone based on occurrence of strongly environment-related markers and consequently included in the LE zone (Prestianni et al. 2016). In Belgium, it is only recorded in a thin horizon within the Hangenberg Sandstone equivalent (Denayer et al. 2020). The DFZ8 foraminifer zone is re-interpreted as a facies-related variation of the basal Tournaisian MFZ1 (Denayer et al. 2020) and is clearly post-Hangenberg Sandstone event after contemporaneous fauna (rugose corals, conodonts) and correlated by sequence stratigraphy above the DCB.

The base of the Carboniferous is marked by extinctions of Devonian taxa, concomitantly with the end of the reworking produced by the Hangenberg Sandstone event just below the entry of the conodont *P. kockeli*. It is also coincident with the boundary between the foraminifer zones DFZ7-MFZ1 and palynozones LE-VI and coral zones RC0-RC1, which all see the extinction of Devonian taxa. After the short-lasting regressive phase of the Hangenberg Sandstone event, normal settings returned with the deposition of the Hastière Fm. Hence the Hangenberg Sandstone event is proposed as the most natural Devonian-Carboniferous Boundary.

Recent reviews of deep-water – ‘condensed’, in fact very lacunar – sections, coupled with unsolvable issues concerning the taxonomy – not mentioning palaeobiology – of conodonts demonstrated their strong limitation for defining global stratotypes. As suggested by many authors (e.g. Lucas 2020), the use of single palaeontological marker should be abandoned. Therefore, the definition of the DCB by several biotic and abiotic markers along a biostratigraphically-constrained timeline is potentially the best solution.

The applicability of such a timeline-based definition was demonstrated during the 19th International Congress on Carboniferous and Permian and approved by the Working Group on the Devonian-Carboniferous Boundary of the Subcommittee on the Carboniferous Stratigraphy. The search for a stratotypic section for the DCB is ongoing and Belgium has excellent candidate sections to propose. Thanks to decades of detailed research on sedimentology, macro- and micro-palaeontology, and very fine stratigraphic correlations within the Basin, sections such as Anseremme, Gendron-Celles, Spontin and Chanxhe are among the best documented worldwide and display all the markers established by the new criterium. Recent holistic revision of biostratigraphy, together with ongoing geochemical and cyclostratigraphic analyses make the Belgian sections the best candidates for the Global Stratigraphic Section and Point for the Devonian-Carboniferous Boundary.

References

- Denayer, J., Prestianni, C., Mottequin, B. et al. The Devonian–Carboniferous boundary in Belgium and surrounding areas. *Palaeobiology and Palaeoenvironment*, 101/2, 313-356.
- Kaiser, S.I., 2009. The Devonian/Carboniferous boundary stratotype section (La Serre, France) revisited. *Newsletters on Stratigraphy*, 43, 195-205.
- Lucas, S., 2020. Rethinking the Carboniferous Chronostratigraphic scale. *Newsletters on Stratigraphy*, 54/3, 257-274.
- Poty, E., 2016. The Dinantian succession of Belgium and surrounding areas: the classical area refined. *Geologica Belgica*, 19, 177-200.
- Prestianni, C., Sautois, M., & Denayer, J., 2016. Disrupted continental environments around the Devonian–Carboniferous Boundary: introduction of the tener event. *Geologica Belgica*, 19, 135-145.

Shelf ecosystems along the Maryland Coastal Plain prior to and during the Paleocene-Eocene Thermal Maximum

Monika DOUBRAWA¹, Peter STASSEN^{1,2}, Marci M. ROBINSON³, James C. ZACHOS⁴, Robert P. SPEIJER¹

1. Department of Earth and Environmental Sciences, KU Leuven, 3000, Leuven, Belgium (monika.doubrawa@kuleuven.be, robert.speijer@kuleuven.be, peter.stassen@kuleuven.be)
2. OD Earth and History of Life, Royal Belgian Institute of Natural Sciences, 1000, Brussels, Belgium
3. US Geological Survey, Florence Bascom Geoscience Center, 20192, Reston, Virginia, USA (mmrobinson@usgs.gov)
4. Earth and Planetary Sciences, University of California-Santa Cruz, 95064, Santa Cruz, California, USA (jzachos@ucsc.edu)

During the early Paleogene, Earth's climate was under the influence of a long-term warming trend that was punctuated by short-term, global warming events, with the Paleocene-Eocene Thermal Maximum (PETM) being the most pronounced (Westerhold et al., 2020). The PETM is globally characterized by negative stable isotope excursions ($\delta^{18}\text{O}$ and $\delta^{13}\text{C}$) in both marine and terrestrial sediments. In the subsurface of the US Atlantic Coastal Plain, the PETM is additionally marked by the widespread distribution of fine-grained sediments, contrasting with the sediment-starved shelf setting during the Paleocene. Isotopic data from that area show additional small, but distinct, $\delta^{13}\text{C}$ and $\delta^{11}\text{B}$ excursions in a more clay-rich interval just below the base of the PETM, coined as the “pre-onset excursion” (POE) (Lyons et al., 2019; Babila et al., submitted). Its relationship with the PETM is still undetermined, but it may indicate that the latest Paleocene climate was not as stable as previously assumed and experienced a more gradual or stepwise change towards the PETM in association with an enigmatic disturbance in the carbon cycle.

In this study we focus on the South Dover Bridge (SDB) core in Maryland, where the POE is best expressed in the geochemical record, and the Paleocene-Eocene (P-E) transition is stratigraphically constrained by calcareous nannoplankton and stable carbon isotope data (Self-Trail et al., 2012). In addition, the SDB site is presumed to be situated in a middle to outer neritic marine setting near the paleo-Potomac River outflow system thus providing insight into variations in the regional hydrological cycle. We generated a high-resolution benthic foraminiferal, stable isotope, trace-metal and grain size record to disentangle the environmental changes leading up to and throughout the PETM. The dominant mid-shelf benthic foraminiferal assemblage indicates a shift from well-oxygenated, continuously oligo- to mesotrophic bottom water conditions during the late Paleocene to an environment under the increasing river influence. The POE is marked by modest ocean warming ($<2-3^\circ\text{C}$) associated with minor, but important changes in the assemblages, with a group of taxa (e.g. *Pseudovigerina triangularis*, *Cibicidoides alleni*) strongly decreasing in relative numbers and the appearance of planktic excursion taxa, normally only found within the PETM (Robinson and Spivey, 2019). At the PETM onset, and subsequent warming of $3-4^\circ\text{C}$ during the main PETM, an input of kaolinitic clay points towards major shifts in the hydrological regime. Benthic foraminiferal diversity decreases as more stress-resistant taxa (e.g. *Pulsiphonina prima*, *Anomalinoides acutus*, *Pseudovigerina wilcoxensis*) become dominant and planktic foraminifera become abundant, similar to the observation at other sites from this coastal plain (Stassen et al. 2012). This indicates periodically dysoxic bottom water caused by river-induced stratification of the water column. The PETM recovery phase marks a return to high food levels, decreased river influence and higher oxygen levels, as indicated by the

relative decrease of more stress-resistant taxa, the steady increase of e.g. *Bulimina virginiana* and the reappearance of *Paralabamina lunata*. The topmost part of the recovery phase is truncated by a regional unconformity.

Additionally, we place the record in a depth-transect across the paleoshelf and correlate it with sites from New Jersey in order to evaluate stratigraphic completeness and regional variations in sediment accumulation during the PETM. This exercise shows that the SDB core is expanded and presents an excellent record of the P-E transition. The high sedimentation rate at this site, resulting from increased fluvial input, enables a detailed record of the peak warming during the PETM. To conclude, we show that changes in the marine environment started during the POE, hinting to an environmental trigger gradually building up, until the system was suddenly perturbed at the onset of the PETM. This scenario is not compatible with an extraterrestrial impact triggering the PETM onset, but better fits a longer-term process, like episodic volcanic outgassing.

References

- Babila, T. L., Penman, D. E., Standish, C. D., Doubrava M., Bralower, T. J., Robinson, M. M., Self-Trail, J. M., Speijer, R. P., Stassen P, Foster G. L. & Zachos, J. C., submitted. Surface ocean warming and acidification driven by rapid carbon release precedes Paleocene-Eocene Thermal Maximum.
- Lyons, S. L., Baczynski, A. A., Babila, T. L., Bralower, T. J., Hajek, et al., 2019. Palaeocene–Eocene Thermal Maximum prolonged by fossil carbon oxidation. *Nature Geoscience* 12(1), 54.
- Robinson, M. M. & Spivey, W. E., 2019. Environmental and Geomorphological Changes on the Eastern North American Continental Shelf Across the Paleocene-Eocene Boundary. *Paleoceanography and Paleoclimatology* 34(4), 715–732.
- Stassen, P., Thomas, E. & Speijer, R. P., 2012. Integrated stratigraphy of the Paleocene-Eocene thermal maximum in the New Jersey Coastal Plain: Toward understanding the effects of global warming in a shelf environment, *Paleoceanography* 27, 1–17.
- Self-Trail, J. M., Powars, D. S., Watkins, D. K. & Wandless, G. A., 2012. Calcareous nannofossil assemblage changes across the Paleocene–Eocene Thermal Maximum: Evidence from a shelf setting. *Marine Micropaleontology*, 92–93, 61-80.
- Westerhold, T., Marwan, N., Drury, A. J., Liebrand, D., Agnini, C., Anagnostou, et. al., 2020. An astronomically dated record of Earth’s climate and its predictability over the last 66 million years. *Science*, 369, 1383–1387.

Stratigraphical context of the Pliocene right whales (Balaenidae) from the North Sea

Guillaume DUBOYS DE LAVIGERIE ^{1,2}

1. Institut royal des Sciences naturelles de Belgique, D.O. Terre et Histoire de la Vie, Brussels, Belgium, (gduboydelavigerie@naturalsciences.be)

2. Evolution & Diversity Dynamics Lab, Université de Liège, 14 Allée du 6 Août, 4000 Liège, Belgium

Baleen whales (Mysticeti) are the largest mammals that ever lived; nowadays they are represented by fourteen species located within four families (Balaenidae, Balaenopteridae, Eschrichtiidae and Cetotheriidae). The evolutionary history of baleen whales can be traced back to the late Eocene, and the extant families diverged from each other during the Miocene. Balaenids (right whales) appear in the fossil record of Patagonia around 20 Ma ago with the species *Morenocetus parvus*. Despite that early record, until the late Miocene only one species was described, *Peripolocetus vexilifer* (16-15 Ma). However, many fossils of this family were described from latest Miocene to Pliocene deposits around the world. Nowadays, the family Balaenidae includes two genera (*Balaena* and *Eubalaena*) and four species (the bowhead *Balaena mysticetus* and three right whales *Eubalaena* spp.), that are all quite morphologically similar, with common traits such as an arched rostrum, a large head, long baleen plates, high lower lips, and a finless back.

The fossil record of balaenids from the Pliocene of the southern part of the North Sea stands out for its diversity. Five species were described based on specimens discovered in the area of Antwerp (north of Belgium): *Antwerpibalaena liberatlas*, *Balaenella brachyrhinus*, *Eubalaena ianitrix*, *Balaenula balaenopsis* and *Balaenotus insignis*. Adding to this rich North Sea record, a few species are known from the Pliocene of other places of the world (for example *Achaebalaena dosanko* from Japan, *Balaenula astensis* and *Balaena montalionis* from Italy). New balaenid specimens keep being discovered in the Antwerp area, such as the type material of the recently described *A. liberatlas*, further highlighting a high diversity of fossil balaenids in the southern North Sea. However, some more work is needed to better understand the stratigraphical context of earlier finds. Indeed, the syntypes of *Balaenula balaenopsis* and *Balaenotus insignis* were described in the late 19th century by paleontologist Pierre-Joseph Van Beneden and the descriptions and stratigraphical information provided in these early works are now outdated and need to be reassessed.

Looking deeper into the stratigraphical issues, in his 1878 paper Van Beneden provided limited information about the geographical context of *Balaenotus insignis* and *Balaenula balaenopsis*: that the specimens were found near Stuyvenberg, close to Antwerp. Thanks to the work done by De Meuter et al. (1976) on local geological sections and stratigraphical work done by De Schepper et al. (2009), we can correlate the available geographical data with stratigraphic units present at the place. With this method, it was recently concluded that the syntypes of both *B. insignis* and *B. balaenopsis* most likely originate from the lower Pliocene Kattendijk Formation, although it cannot be completely excluded that they could originate from the reworked Lillo Formation. This second hypothesis appears less likely because in the discovery area, this unit is very thin (only a few centimeters thick). Based on dinoflagellate cyst assemblages, these fossils are most likely to be dated from the Zanclean (in an interval of 5-4.4 Ma for the Kattendijk Formation).

The other fossil balaenids were also found in sandy deposit near Antwerp, but were described more recently, within an updated stratigraphical context. The holotype of

Antwerpibalaena liberatlas was discovered in the base of the Oorderen Sands Member of the Lillo Formation, with a Pliocene age (between 3.21 and 2.76 Ma). The holotype of *Eubalaena ianatrix* was found in the Kruisschans Sands Member of the Lillo Formation, which deposited in the same time interval. The last balaenid species from the Belgian Pliocene is *Balaenella brachyrhynchus*; its holotype was found in the Kattendijk Formation, meaning that it is older than the holotypes of both *Eubalaena ianatrix* and *Antwerpibalaena liberatlas*, and possibly approximately contemporary to the syntypes of *Balaenotus insignis* and *Balaenula balaenopsis*.

The balaenid fossil record from the Belgian Pliocene thus reveals a moderately high diversity (as compared to other fossil balaenid localities worldwide) during a relatively short time interval. The next steps of the revision of the North Sea balaenids will be to reassess the anatomy, systematics, phylogeny, and stratigraphic context for specimens described during the 19th century, providing further insight into this unique sample. By doing this, a better understanding of the whole family Balaenidae could be obtained, including a closer look at evolutionary trends such as convergence toward gigantism and the evolution of the forelimb and other postcranial elements. Still, many balaenid specimens from the Belgian Pliocene are very incomplete, and additional species (and more complete specimens from previously described species) could still be found in the region of Antwerp, as hinted by the presence of more fragmentary remains, particularly a broad morphological range of earbones (periotics and tympanic bullae). The construction of new buildings in that area and the resulting access to temporary outcrops will most likely lead to new discoveries that will help gaining a better understanding of the evolution of this highly specialized family of skim-feeding baleen whales.

References

- De Meuter, F. J. C., Wouters, K. & Ringele, A. 1976. Lithostratigraphy of Miocene Sediments from Temporary Outcrops in the Antwerp City Area. Ministère des Affaires Economiques, Administration des Mines, Service Géologique de Belgique, 42 pp.
- De Schepper, S., Head, M. J. & Louwye, S. 2009. Pliocene dinoflagellate cyst stratigraphy, palaeoecology and sequence stratigraphy of the Tunnel-Canal Dock, Belgium. *Geological Magazine*, 146, 92–112
- Van Beneden, P. J. 1878. Description Des Ossements Fossiles Des Environs d'Anvers: Texte, Cétacés, Genres *Balaenula*, *Balaena* et *Balaenotus*; Hayez, 82 pp.

CT-CEPH: Applying micro-CT imaging in the study of Belgian fossil nautilid cephalopods

Stijn GOOLAERTS ^{1,2} & Bernard MOTTEQUIN ¹

1. *OD Earth & History of Life, Royal Belgian Institute of Natural Sciences, Brussels, Belgium*
(stijn.goolaerts@naturalsciences.be; bmottequin@naturalsciences.be)

2. *Scientific Service of Heritage, Royal Belgian Institute of Natural Sciences, Brussels, Belgium*

Brain project in Pillar II Heritage science B2/191/P2/CT-CEPH, nicknamed CT-CEPH, and funded by the Belgian Science Policy Office (BESLPO), is presented. The project will take a fresh look at Devonian, Early Carboniferous and latest Cretaceous to Paleogene nautilid cephalopods (Fig. 1) from Belgium, trying to further document major steps in nautilid evolution by CT scanning of the type collections of the Royal Belgian Institute of Natural Sciences (RBINS) and Royal Museum for Central Africa (RMCA).

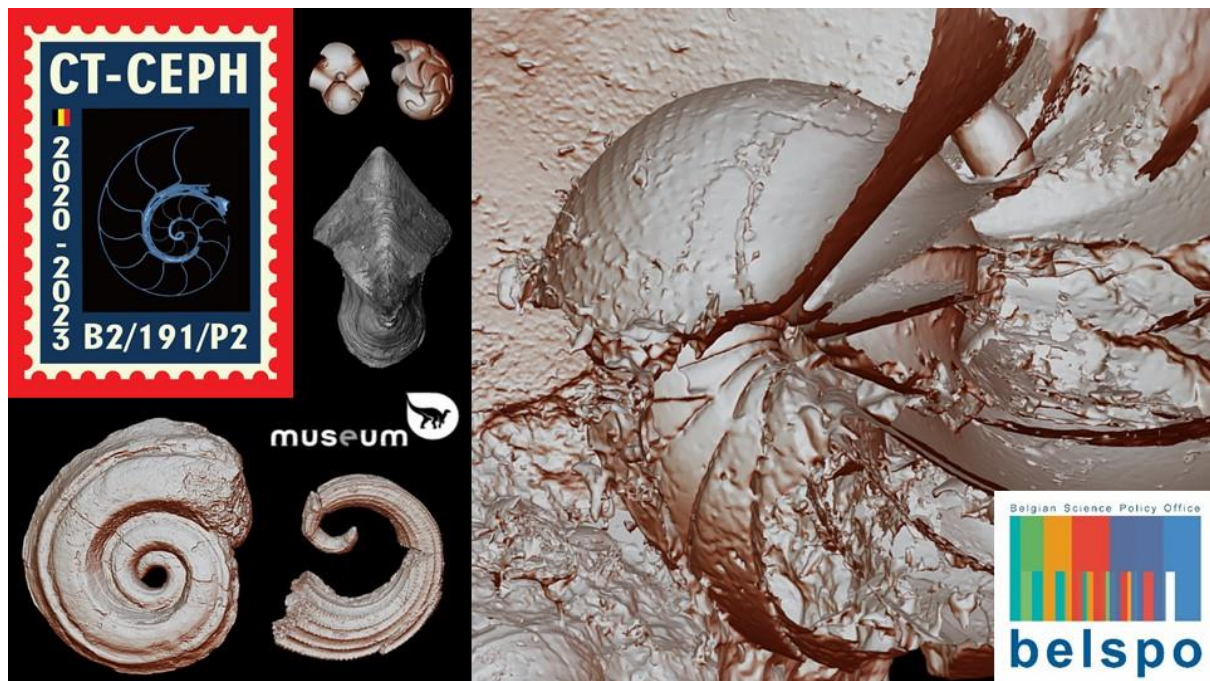


Figure 1. Collage of screenshots of various 3D-models and volume renderings of fossils of Belgian Early Carboniferous, Late Cretaceous and Paleogene nautilid cephalopods, supplemented with the logos of the project, the RBINS and Belspo.

Cephalopods (Class Cephalopoda, Phylum Mollusca) are amongst the most diverse, intelligent, and rapidly evolving marine invertebrates that have explored a multitude of evolutionary pathways since their entry point more than 500 My ago. Their invention of a chambered shell providing an energy-efficient way to migrate up and down the water column, makes them stand out from all other mollusks. It is especially the internal organization of this complex three-dimensional buoyancy mechanism that allows to document major steps in their evolution, making from X-ray computed tomography an extremely powerful method in the study of fossil Cephalopoda. It allows for correct and detailed measurements of typical shell parameters, as well as for the exploitation of new and/or previously underexplored and (partly) hidden parameters.

The project aims at gaining better insights in the complex evolutionary history of the Nautilida (Subclass Nautilia), the lineage leading up to the single surviving stock of externally shelled cephalopods alive today, extant *Nautilus*. It focuses on Devonian, Early Carboniferous and latest Cretaceous to Paleogene time slices of nautilid history, during which major steps in their evolution took place and which are not fully understood, and for which RBINS and RMCA collections hold a large number of important specimens. It will exploit on (1) the ongoing mass-accumulation of CT scanning data of RBINS & RMCA type specimens currently taking place (in the scope of the DIGIT & DiSSCo-Fed projects), and (2) the knowledge and expertise of the RBINS. It also aims to make a major contribution to the scientific valorization of the collections of the federal scientific institutions by executing innovative research.

The latest information about the project is available via the following links: <https://www.naturalsciences.be/en/science/do/94/scientific-research/research-projects/project/21138> and <https://twitter.com/ctceph>

X-ploring new tools for paleontologists: the RBINS-RMCA micro-CT lab at your service!

Stijn GOOLAERTS ^{1,2}, Camille LOCATELLI ¹, Jonathan BRECKO ^{1,3}, Cedric D'UDEKEM D'ACQZ ¹, Annelise FOLIE ¹, Arnaud HENRARD ³, Aurore MATHYS ^{1,3}, Erik VAN DE GEHUCHTE¹

1. Scientific Service of Heritage, Royal Belgian Institute of Natural Sciences, Brussels, Belgium (stijn.goolaerts@naturalsciences.be; clocatelli@naturalsciences.be; jbrecko@naturalsciences.be; cdudekem@naturalsciences.be; afolie@naturalsciences.be; amathys@naturalsciences.be evandeguchte@naturalsciences.be)

2. OD Earth & History of Life, Royal Belgian Institute of Natural Sciences, Brussels, Belgium

3. Department of Biology, Royal Museum for Central Africa, Tervuren, Belgium (arnaud.henrard@africamuseum.be)

X-ray computed tomography (CT-) scanning is revolutionizing the study of extinct organisms. Its non-invasive and non-destructive character makes it currently by far the most potent method to allow fossils to be studied in three dimensions and with unprecedented detail. More importantly, and differing from other 3D techniques, CT-scanning looks through and inside objects, revealing hidden structures and characters. Recent innovations in the field of CT-scanning allow obtaining details up to a few micrometers in resolution, and higher quality images of relatively dense materials, like fossils, even when wholly encased in hard sediment (Keklikoglou et al., 2019).

In 2016, the Royal Belgian Institute of Natural Sciences (RBINS) acquired two high-end X-ray CT machines: the micro-CT RX EasyTom and the nano-CT XRE-Tescan UniTom. Both scanners are currently nearly full time in use to help accomplishing the gigantic task of the digitization of the RBINS and Royal Museum for Central Africa (RMCA) type collections, the aim of two multi-year Belspo funded projects, DiSSCo-Fed (2018-2023) and DIGIT-4 (2019-2024). With about 300.000 types and 48.000.000 general specimens, 46.000 and 3.000.000 respectively in their paleontology collections, the results of nearly two centuries of intensive collecting and research, these two Belgian Federal Scientific Institutions (FSI's) are major players in the European framework of scientific research infrastructures for natural history. Digitizing this large number of types, spread across almost the entire Tree of Life, and exhibiting an entire array of differing taphonomies, results in a steadily growing expertise of the RBINS-RMCA micro-CT lab (Brecko et al., 2018). While the newly acquired infrastructure and ongoing digitization projects are primarily oriented towards the digitization of type and figured specimens, these also offer great opportunities for researchers and teachers in various disciplines of paleontology.

Targeting on researchers interested in incorporating micro-CT as a technique in their research projects, the current digitization workflow of the RBINS-RMCA micro-CT lab will be presented. While micro-CT offers many advantages, there are also pitfalls and limitations that need to be considered. Based on our expertise, and illustrated by some of our scanning results, important constraints that may block the pathway between your expectations and perfect micro-CT-imaging results that can be fully incorporated into research projects will be presented. Possible effects of some of the most important parameters that may influence the quality of the output, and thus can increase the signal to noise ratio (SNR) will be reviewed, such as the size and shape of the specimen to be scanned, the density of its matrix the specimen is made of or encased in, the presence of certain minerals (e.g. pyrite) and how these may be distributed inside the specimen (e.g. finely disseminated, dense masses or crystals), the best possible resolution in relation to the specimen and preferred output, the time

needed to scan a specimen, the choice between machines to be used and their limits and different possible scan settings (e.g. beam power, filters...). Post-processing parameters to be considered are the size of the image stack output (will the computer be able to handle the amount of Gigabytes?), the time needed to render and segment regions of interest and optimize 3D-models, and which format suits best to visualize and export the data (renderings, meshes, videos, virtual sections...). While segmentation may be a time-consuming task, new developments like the incorporation of artificial intelligence (e.g. the Deep Learning function in Dragonfly ORS) offer great potential to reduce the workload in complex segmentation.

Many researchers are also teachers. The reason why they may also be particularly interested in the 3D models of the already digitized types that are available on the Virtual Collections platforms of the RBINS (<http://virtualcollections.naturalsciences.be/>) and RMCA (<https://virtualcol.africamuseum.be/>). While 3D models are not intended to replace physical specimens, they may become significant teaching aids in both the physical and virtual classroom. In addition, the presence of a steadily growing number of 3D-models and animations of extant animals that are also added to these Virtual Collections, would allow teachers to connect fossils (in general incomplete) with extant (more complete) relatives.

Last but not least, while the focus of this communication is largely on micro-CT, some of the many other new techniques that are being tested, used and improved will be highlighted (see e.g. Brecko & Mathys, 2020; Brecko et al., 2014, 2016, 2018; Mathys et al., 2013, 2019 for some examples). Interested in our work, expertise, techniques, equipment, or scans-on-demand? Please do not hesitate to reach out!

References

- Brecko, J., Lefevre, U., Locatelli, C., Van de Gehuchte, E., Van Noten, K., Mathys, A., De Ceukelaire, M., Dekoninck, W., Folie, A., Pauwels, O., Samyn, Y., Meirte, D., Vandenspiegel, D. & Semal, P. 2018. Rediscovering the museum's treasures: μ CT digitisation of the type collection. Poster presented at 6th annual Tomography for Scientific Advancement (ToScA) symposium, Warwick, England, 10-12 Sept 2018.
- Brecko, J. & Mathys, A., 2020. Handbook of best practice and standards for 2D+ and 3D imaging of natural history collections. *European Journal of Taxonomy*, 623, 1-115.
- Brecko, J., Mathys, A., Dekoninck, W., De Ceukelaire, M., Vandenspiegel, D. & Semal, P., 2016. Revealing Invisible Beauty, Ultra Detailed: The Influence of Low-Cost UV Exposure on Natural History Specimens in 2D+ Digitization. *PLoS One* 11(8):e0161572.
- Brecko, J., Mathys, A., Dekoninck, W., Leponce, M., Vandenspiegel, D. & Semal, P., 2014. Focus stacking: Comparing commercial top-end set-ups with a semi-automatic low budget approach. A possible solution for mass digitization of type specimens. *Zookeys*, 464, 1-23.
- Keklikoglou, K., Faulwetter, S., Chatzinikolaou, E., Wils, P., Brecko, J., Kvaček, J., Metscher, B. & Arvanitidis, C. 2019. Micro-computed tomography for natural history specimens: a handbook of best practice protocols. *European Journal of Taxonomy*, 522, 1-55.
- Mathys, A., Semal, P., Brecko, J. & Van den Spiegel, D., 2019. Improving 3D photogrammetry models through spectral imaging: Tooth enamel as a case study. *PLoS One*, 14(8): e0220949.
- Mathys, A., Brecko, J., Di Modica, K., Abrams, G., Bonjean, D. & Semal, P., 2013. Agora 3D. Low cost 3D imaging: a first look for field archaeology. *Notae Praehistoricae*, 33/2013, 33-42.

Caverne Marie-Jeanne (Belgium): How an old collection from the Royal Belgian Institute of Natural Sciences sheds new light on cave hyaenas' behaviour and adaptation

Elodie-Laure JIMENEZ^{1,2} & Mietje GERMONPRÉ¹

1. Royal Belgian Institute of Natural Sciences, Belgium (eljimenez@naturalsciences.be; mgermonpre@naturalsciences.be)
2. University of Aberdeen, Scotland

In Belgium, the Pleistocene was characterised by a subarctic environment with highly fluctuating conditions. Species had to adapt to the diverse landforms the region had to offer. The Ardennes uplands served as migration corridors and ecological hub where many species could find resources. The calcareous reliefs and the impressive karstic and cave systems in southern Belgium also offered countless shelters for large predators - humans and large carnivores alike.

Many Pleistocene cave sites and sedimentary sequences have been discovered in this area since the first explorers Ph-Ch. Schmerling and É. Dupont excavated the filling deposits of the vast limestone system in the 19th century. The numerous palaeontological and anthropogenic vestiges that were recovered from these early explorations clearly demonstrate the attractiveness of the region during the last glaciation of the Pleistocene. However, if cave bears and cave hyaenas were the most predominant predator species in this region alongside with Neanderthals and Anatomically Modern Humans, little is known about their respective behaviours amongst the predator guild and how they occupied and shared this territory.

Caverne Marie-Jeanne is one of the many palaeontological collections that are housed at the Royal Belgian Institute of Natural Sciences. Despite being excavated in the 1940's, the assemblage is very well documented (stratified deposits, collection of the fine fraction, etc) which allows advanced faunal analyses. Our in-depth reassessment of the faunal material from Level 4 has highlighted the presence of a hyaena "natal den", where the remains of more than 200 hyaena cubs were identified. The contextual data suggest that these remains accumulated in a relative short period of time, suggesting a high mortality rate and a possible reduced genetic fitness in *Crocota* around this time period. In any way, the exceptional number of cubs in this level makes this den truly unique and sheds new light on cave hyaenas' reproductive behaviour, territory management and local adaptation. Backed-up with extant literature references on modern *Crocota* species and ongoing isotopic studies, the rediscovery of Caverne Marie-Jeanne material helps us further our knowledge of cave hyaena ethology and understand how apex predators of the Pleistocene adapted to local northern environments.

Figure

Figure 6 - Skeleton of one of the cave hyaena cubs discovered at Caverne Marie-Jeanne (photo: RBINS).



Variation in long bone morphology of true seals (Mammalia, Phocidae), and its impact on understanding the fossil record

Jacques KLASSEN¹, Leonard DEWAELE^{1,2} & Valentin FISCHER¹

1. *Evolution and Diversity Dynamics Lab, Université de Liège, Liège, Belgium*
(jacques.klassen@student.uliege.be; ldewaele@uliege.be; v.fischer@uliege.be)
2. *Directorate Earth and History of Life, Royal Belgian Institute of Natural Sciences, Brussels, Belgium* (ldewaele@naturalsciences.be)

Today, the semi-aquatic clade of Pinnipedia is represented by three extant families: Odobenidae (the walrus), Otariidae (fur seals and sea lions), and Phocidae (true seals). The latter, i.e. the clade Phocidae, is morphologically the most diverse family. Indeed, regarding their size, extant phocids range from slightly over one meter (genus *Pusa*) to over six meters (*Mirounga leonina*, southern elephant seal). In addition, as for other pinnipeds, phocids have a marked sexual dimorphism, which is most easily visible in the size difference between males and females. This size difference is most remarkable in elephant seals (genus *Mirounga*) in which the females are approximately half the length of males.

Historically, long bones, or appendicular bones, and primarily the humerus and the femur, have been considered to be diagnostic for phocid seal identification. As such, humeri and femora have often been used as type specimens for extinct phocid taxa. In total, over twenty extinct species of seals are represented by either an isolated humerus or an isolated femur as type specimen. These taxa are primarily taxa described from the Neogene of the North Atlantic realm and Parathetys, and the state of preservation of these type specimens varies largely. Also, consequently, morphological phylogenetic analyses have relied (too?) heavily on humeri and femora, as they are the only fossil remains consistently found in variable conditions for many known extinct species (e.g.: Van Beneden, 1877). However, recent preliminary studies start to question whether the variation of morphological features of long bones are truly diagnostic: can isolated long bones be used as type specimens for species identification? Are these differences significant enough, allowing to build phylogenetic tree heavily relying on characteristics of long bones? Or is interspecific morphological variation obscured by intraspecific variation, due to intense sexual dimorphism in some species and geographical distribution among different populations of the same species? Despite this, to date, only very few published studies focussed on a quantitative assessment of intra- and interspecific bone morphology in phocids (Churchill & Uhen, 2019). Furthermore, morphological variation between both subfamilies of Phocidae, the “northern” Phocinae and the “southern” Monachinae, has long been described qualitatively but only preliminarily treated in quantitative studies.

Whereas the limited number of previous studies either used few, simple measurements and/or 2D data of small datasets, a large and comprehensive study capturing intraspecific and interspecific morphological variation in three dimensions has been lacking. Thus, this study aims to quantitatively analyse the significance of morphological variations for the current phocid’s phylogeny using 3D morphometry. To do so, a 3D Procrustes morphometric analysis followed by a Principal Component Analysis (PCA) followed by a Discriminant Function

Analysis (DFA) has been performed on 101 humeri and 78 femora 3D models sampling respectively from 18 and 16 phocid species. This biological sample includes the extant *Cystophora cristata*, *Erignathus barbatus*, *Halichoerus grypus*, *Histiophoca fasciata*, *Hydrurga leptonyx*, *Leptonychotes weddellii*, *Lobodon carcinophaga*, *Mirounga angustirostris*, *Monachus monachus*, *Monachus schauinslandi*, *Ommatophoca rossii*, *Pagophilus groenlandicus*, *Phoca vitulina concolor* & *richardii*, and the extinct *Callophoca obscura*, *Leptophoca* sp., *Phocanella pumila*, *Pliophoca* sp., *Prophoca* sp. and *Sarmatonectes sintsovi*. To capture the 3D morphology of the long bones, 17 fixed landmarks and 29 curves (188 semi landmarks) have been selected on the humeri as well as 14 fixed landmarks and 25 curves (140 semi landmarks) for the femora.

The intraspecific variation of long bones morphology in extant species is thus compared with the interspecific variation among extant and extinct species. The resulting PCAs' morphospaces seem to sort more or less at the subfamily level while the DFA seems to better sort the taxa into the subfamilies suggested by previous studies, but most genera appear poorly defined. Thus, the morphological variation of long bones in phocids suggests that humeri and femora might be diagnostic enough to differentiate between subfamilies (Phocinae and Monachinae) as well as some genera within each subfamily. However, other characters from other bones than humeri and femora are needed to differentiate all the genera. As such, isolated long bones perhaps should not be used as type specimens based only on their morphology. However, the fact that genera can still be separated on the basis of isolated humeri and femora to a limited extent, indicates that the existing fossil record of Phocidae with isolated long bones as type specimen cannot be disregarded altogether and special care is needed when reassessing these records on a species-by-species base.

References

- Churchill, M. & Uhen, M. D. (2019). Taxonomic implications of morphometric analysis of earless seal limb bones. *Acta Palaeontologica Polonica*, 64(2), 213–230.
<https://doi.org/10.4202/app.00607.2019>
- Van Beneden, P.-J. (1877). Description des ossements fossiles des environs d'Anvers, première partie: Pinnipèdes ou Amphithériens. *Annales Du Musée Royal d'Histoire Naturelle de Belgique*, 1, 1–88.

Echolocating toothed whales (Cetacea, Odontoceti) from the Neogene of Belgium: historical studies, recent contributions and perspectives

Olivier LAMBERT¹

1. Institut royal des Sciences naturelles de Belgique, D.O. Terre et Histoire de la Vie, Brussels, Belgium (olambert@naturalsciences.be)

Odontocetes, the echolocating toothed whales, represent the largest group of modern marine mammals, with at least 75 extant species allocated to 10 families, including sperm whales (Kogiidae and Physeteridae, in the superfamily Physeteroidea), beaked whales (Ziphiidae), several monogeneric families of strictly freshwater to coastal dolphins (Iniidae, Platanistidae, Pontoporiidae, and the recently extinct Lipotidae), porpoises (Phocoenidae), the family of the beluga and narwhal (Monodontidae), and true dolphins (Delphinidae). Whereas the origin of Odontoceti can be traced back to the Eocene-Oligocene transition, most modern families of this cetacean suborder only appear during the Miocene, with further radiation events occurring during the Pliocene. Their Neogene fossil record is thus critical to understand the evolutionary history of extant odontocete faunas. Over the past 160 years, marine deposits from the Neogene of the southern North Sea Basin in northern Belgium (and especially the area of Antwerp) yielded rich marine mammal faunas, now curated at the Royal Belgian Institute of Natural Sciences (RBINS) and including a relatively high number of odontocete species. Historical studies by P.-J. Van Beneden, B. du Bus, and O. Abel during the second part of the nineteenth and beginning of the twentieth centuries led to the description of a large number of extinct odontocete species. However, part of these taxa was defined based on type specimens with a low diagnostic value. Furthermore, the stratigraphic context of these early finds was generally poorly resolved, partly due to the complex geometry of Neogene marine deposits in northern Belgium and the lack of information about the precise locality and horizon for many specimens.

Together with the systematic and taxonomic reassessment of historic finds and biostratigraphic analyses of associated sediment samples, new fossil discoveries (often by citizen scientists and fossil collectors) in the different lithological units of the Belgian Neogene allowed for an improved understanding of local Miocene and Pliocene odontocete assemblages.

Though often lacking some stratigraphic resolution, the records from the lower to middle Miocene Berchem Formation include members of two extinct families: the heterodont Squalodontidae (genus *Squalodon*) and the hyper-longirostrine Eurhinodelphinidae (several species in the genera *Eurhinodelphis*, *Schizodelphis* and *Xiphiacetus*). In addition, another hyper-longirostrine dolphin from the Berchem Formation has been referred to the extinct subfamily Pomatodelphininae, in the family Platanistidae (nowadays only retaining the South-East Asian river dolphin *Platanista*). Several physeteroids were recovered from the Berchem Formation, including the stem physeteroid *Eudelphis mortezelensis* and the physeterids *Placoziphius duboisi* (from the Edegem Sands Member) and *Orycterocetus crocodilinus*. Probably originating from the Antwerpen Sands Member, the diminutive species *Thalassocetus antwerpiensis* was previously referred to the Kogiidae (pygmy and dwarf sperm whales), but has been recently revised as a physeterid. This unit also yielded some of the geologically oldest beaked whales worldwide, in the genera *Archaeoziphius*, *Beneziphius*, and possibly *Aporotus*. Finally, the diversity of early delphinidans ('kentriodontids') from the Berchem Formation is most likely considerably under-estimated, with only one species from the genus *Kentriodon* and, more tentatively from a stratigraphic viewpoint, the diminutive species *Pithanodelphis cornutus* being currently recorded, a low number that contrasts with other Miocene localities of the North Atlantic realm.

The upper Miocene Diest Formation yielded a somewhat less disparate assemblage, with another record of the sperm whale *Thalassocetus*, several beaked whales, some of them known from many skulls (at least species of the genera *Choneziphius* and *Ziphirostrum*), and possibly a small pontoporiid dolphin (*Protophocaena minima*, to be confirmed with in situ finds). Recent discoveries in the lower part of the Diest Formation indicated the survival of one eurhinodelphinid species, *Xiphiacetus cristatus*, during the Tortonian, a phenomenon that appears to be restricted to the North Sea Basin.

Contrasting with its richer assemblage of mysticetes (baleen whales), the lower Pliocene Kattendijk Formation only yielded an unnamed monodontid (with cranial remains displaying shark bite marks), the phocoenid *Brabocetus gigaseorum* (the earliest named porpoise outside the Pacific realm) and the delphinid *Pliodelphis doelensis* (the earliest named true dolphin for the North Sea Basin). In addition, dinoflagellate cysts associated to crania of the beaked whale *Mesoplodon posti* suggest that this species also originates in the Kattendijk Formation, providing a calibration point for the early radiation of this species-rich extant ziphiid genus.

From younger deposits of the uppermost lower to upper Pliocene Kruisschans Sands Member of the Lillo Formation, up to now only one odontocete was named, the porpoise

Septemtriocetus bosselaersi.

Recent finds in the Antwerp area and the reappraisal of the historical collection at the RBINS underscored the interest of the Belgian odontocete faunas to (1) investigate the emergence, radiation, and extinction of various clades, (2) tackle palaeobiogeography-related questions, more specifically the faunal similarities with the Atlantic Coastal Plain, along the east coast of USA, and (3) focus on palaeobiological questions, for example through tooth wear and dental damage on physeteroid teeth and bone microstructure and osteohistological analyses on beaked whale rostra.

More fragmentary specimens (e.g. isolated ear bones) and comparisons with coeval, richer fossil localities from the North Atlantic realm and Mediterranean suggest that much remains to be discovered about the odontocetes from the Neogene of northern Belgium. The future construction of large buildings, parking lots, docks, and tunnels in the area of Antwerp will give access to temporary outcrops that should provide new opportunities to improve our knowledge of the Miocene and Pliocene evolutionary history of echolocating toothed whales in the North Sea.

Mid-latitude tropical conditions during the Early Eocene Climatic Optimum: Reconstruction of a coastal paleoenvironment in the southern North Sea Basin

Lise MARTENS^{1, 2*}, Peter STASSEN^{1, 2}, Etienne STEURBAUT^{1, 2}, Robert P. SPEIJER¹

¹Department of Earth and Environmental Sciences, KU Leuven, Celestijnenlaan 200E, B-3001 Heverlee, Belgium (lise.martens@kuleuven.be, peter.stassen@kuleuven.be, robert.speijer@kuleuven.be,)

²Directorate Earth and History of Life, Royal Belgian Institute of Natural Sciences, Vautierstraat 29, B-1000 Brussels, Belgium (etienne.steurbaut@naturalsciences.be)

The early Eocene is characterized by a long-term climate warming toward the Early Eocene Climatic Optimum (EECO), accompanied by a northward shift of tropical conditions. During this warm period, shallow marine conditions prevailed in Belgium as recorded by the fine sands of the Egem Member (Mbr.) of the Hyon Formation. These sands are well-exposed in the Ampe quarry and contain abundant well-preserved, large nummulites. Here, we present a high-resolution reconstruction of nearshore marine conditions by use of grain size data, stable isotope data (foraminifera and otoliths) and elemental geochemistry (nummulites). Previous paleotemperature reconstructions in this region have been based on the $\delta^{18}\text{O}$ of fish otoliths (Vanhove et al., 2011 and 2012), indicating mean annual shallow sea temperatures around 25-35°C during the EECO. However, the otolith $\delta^{18}\text{O}$ record shows a wide range of variation within one sample layer, which is partially due to species-specific $\delta^{18}\text{O}$ fractionation and dissimilar living conditions (ontogenetic effects). Additionally, when converting the otolith $\delta^{18}\text{O}$ value to a paleotemperature estimate, the regional Eocene $\delta^{18}\text{O}$ value of the seawater ($\delta^{18}\text{O}_{\text{sw}}$) has to be assumed (e.g., -1.0 ‰; Vanhove et al., 2011), raising concerns about the validity of this record. By combining new nummulite-based paleotemperature record (Mg/Ca paleothermometry, see Martens et al., 2019) with the $\delta^{18}\text{O}$ signal of *Cibicidoides proprius*, a small benthic foraminifera, subtle variations in the $\delta^{18}\text{O}_{\text{sw}}$ values can be reconstructed, allowing a re-interpretation of otolith-based paleotemperature data and enable a high-resolution paleoenvironmental reconstruction of this shallow marine setting.

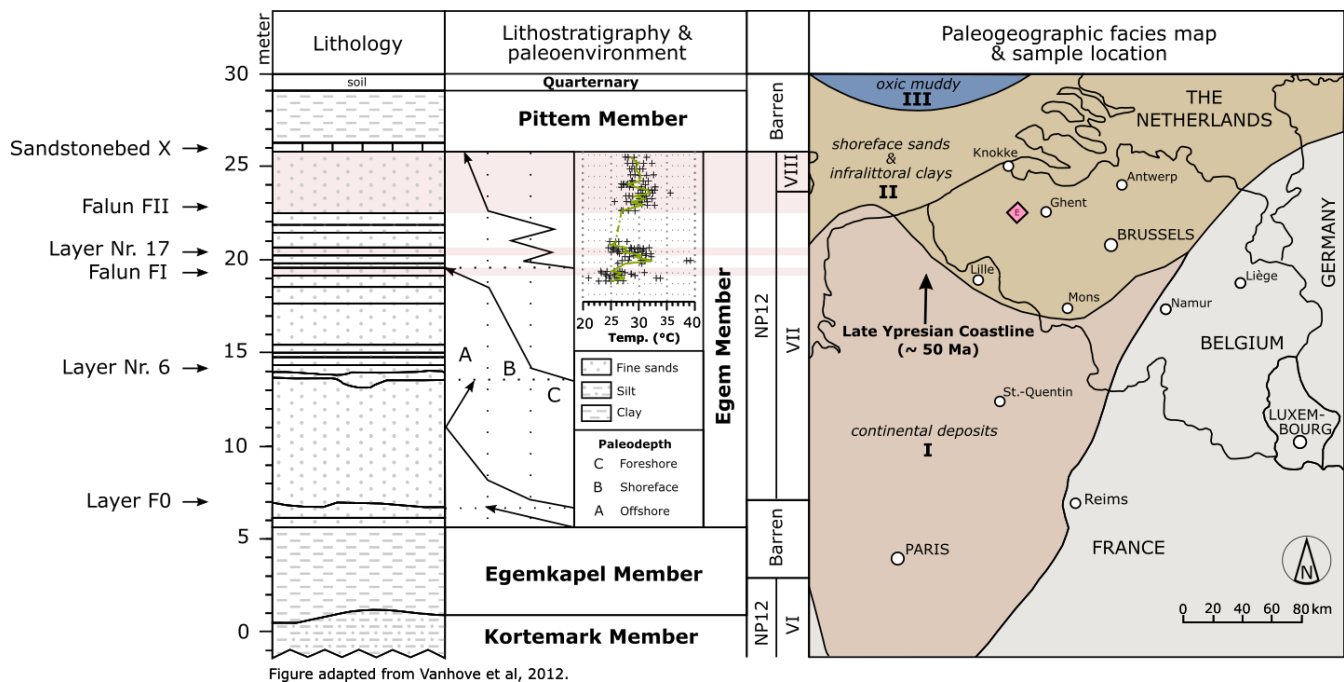
Nummulites are sessile larger benthic foraminifera, which do not fractionate their Mg/Ca, and the resulting paleotemperature record is not directly dependent on the $\delta^{18}\text{O}$ estimates of the seawater. Within the Egem Mbr, *Nummulites aquitanicus* first appear within layer F0, near the base of the Egem Mbr., together with oysters and solitary corals. The oysters remain abundant within the overlying sand layers, with the corals recurring in the succeeding beds. Nummulites re-occur throughout the middle to upper part of the member and are highest in abundance in the poorly sorted layers FI and FII, and within the laminated silty sands of layer nr. 17 (figure). Their absence within the lower part might be due to a differing salinity or too shallow paleodepths as the highest abundancies occur in layers FI and FII, which coincide with deeper offshore conditions. The nummulites from the middle part of the Egem Mbr. record an paleotemperature of 25 °C (averaged mean annual temperatures), which increases to 28 °C as recorded by the nummulites from the silty sands of layer Nr. 17. Near the top of the Egem Mbr (FII), a maximum average temperature of 30 °C is reached.

In conclusion, when using nummulite geochemistry as a paleotemperature proxy, we solve certain problems of the otolith-based method and document a paleotemperature rise of ± 5 °C. Our data show that during the EECO the southern North Sea Basin was a warm, tropical marine environment with the annual average temperature seawater ranging between 25 to 30 °C. These temperature data are in line with previous evidence for a weakened Eocene equator-to-mid-latitude gradient (Evans et al., 2018) and allow snapshots of the paleoenvironmental and climate evolution on a regional scale.

References

- Evans, D., Sagoo, N., Renema, W., Cotton, L.J., Müller, W., Todd, J.A., Saraswati, P.K., Stassen, P., Ziegler, M., Pearson, P.N., Valdes P.J. & Affek, H.P., 2018. Eocene greenhouse climate revealed by coupled clumped isotope-Mg/Ca thermometry. *Proceedings of the National Academy of Sciences*, 115, 1174-1179.
- Martens L., Stassen, P., Steurbaut, E., Speijer, R., 2019. Geochemistry of *Nummulites* as a proxy for early Eocene paleotemperature evolution in the southern North Sea Basin. *Geologica Belgica*, 22(1-2), 93-94.
- Vanhove, D., Stassen, P., Speijer, R., & Steurbaut, E., 2011. Assessing paleotemperature and seasonality during the early Eocene climatic optimum (EECO) in the Belgian Basin by means of fish otolith stable O and C isotopes. *Geologica Belgica*, 14(3-4), 143-157.
- Vanhove, D., Stassen, P., Speijer, R., Claeys, P., & Steurbaut, E., 2012. Intra- and intertaxon stable O and C isotope variability of fossil fish otoliths: an early Eocene test case. *Austrian Journal of Earth Sciences*, 105(1), 200-207.

Figure



Deciphering early stages of vertebrate evolution thanks to long ignored soft-bodied fossils from the Early Devonian of Belgium

Sébastien OLIVE ¹, Pierre GUERIAU ², Philippe JANVIER ³, Bernard MOTTEQUIN ¹

1. Royal Belgian Institute of Natural Sciences, Brussels, Belgium

(sebastien.olive@naturalsciences.be, bernard.mottequin@naturalsciences.be)

2. Institut photonique d'analyse non destructive des matériaux anciens, Gif-sur-Yvette, France

(pierre.gueriau@unil.ch)

3. Muséum national d'Histoire naturelle, Paris, France (philippe.janvier@mnhn.fr)

The evolutionary history of vertebrates began, at the latest, during the early Cambrian (c. 520 Ma) with the first occurrence of elongated and laterally flattened soft-bodied organisms known as chordates, possessing a notochord (the forerunner of the vertebral column) but devoid of backbone and jaw. Vertebrates subsequently underwent major anatomical changes, such as the acquisition of a vertebral column, development of a skull, formation of jaws, and adaptations to terrestrial life. The VERTIGO project is a Belspo-funded project (Brain project B2/202/P1/VERTIGO) that started in March 2021 and preliminary results will be given during this talk. This project focuses on two of the major steps of the evolutive history of vertebrates, namely (i) the evolution of early soft-bodied chordates and (ii) the radiation of a group of early vertebrates (euphaneropids).

Early chordate and early vertebrate fossils provide our only direct information on the origin of vertebrates and on how their distinctive body plan evolved. Unfortunately, the fossil record of early chordates and part of the early vertebrates (i.e. euphaneropids, in the scope of this project) is extremely scarce as these organisms mostly consist of decay-prone soft parts (e.g. integument and muscles) that are usually degraded and lost prior to fossilisation, making the interpretation of their anatomy highly challenging (Sansom et al., 2010). As a result, the affinities of soft-bodied fossils of purported chordates, such as *Metaspriggina* or *Pikaia*, remain highly debated. A broad range of phylogenetic affinities has been proposed for each taxon, and little consensus has been reached. The myomeral arrangement, as well as the presence of a notochord, a dorsal nerve chord, a pharynx and an endostyle are all characters pivotal in the debate of the chordate origin, but they first need to be clearly identified.

Euphaneropids ('naked anaspids') are a group of early jawless vertebrates. Because they are generally preserved as imprints, the same issues of preservation and interpretation of morphological characters occur. Euphaneropids are the group that first demonstrated the presence of (i) gill filaments enclosed by gill pouches (Janvier et al., 2006), (ii) paired anal fins (Sansom et al., 2013) and pelvic fins (Chevrinais et al., 2018), and (iii) an intromittent organ in vertebrates (Chevrinais et al., 2018). Consequently, and in spite of its scarcity in the fossil record and the usual poor preservation of the fossils, this group of jawless vertebrates is crucial for our understanding of early vertebrate evolution.

Although early stages of vertebrate evolution are regularly clarified by new finds of fossils, serious gaps remain in our understanding of the modalities and the timing of the character acquisitions. To overcome these issues, the VERTIGO project focuses on the study of new findings of putative early chordates and early vertebrates (euphaneropids) from the Lower Devonian of Belgium. It is crucial to retrieve as much anatomical details as possible from these unique specimens for systematic, phylogenetic and evolutionary purposes. In this aim, state-of-the-art imaging and spectroscopy techniques allowing new sources of morphological contrasts and a spatial resolution of their (bio)chemistry are used: band-pass emission macroscopy and Synchrotron-based micro-X-ray

fluorescence major-to-trace elemental mapping. They will allow to (i) test the early chordate assignment of the Belgian soft-bodied fossils – if their early chordate assignment is confirmed, these exceptional findings would broadly extend the stratigraphic range of these animals and these hitherto unknown fossils could provide pivotal new insights into our understanding of chordate evolution; (ii) study precisely the Belgian euphaneropids that, given the importance of this group and the recent advances they permitted for our understanding of vertebrate evolution, require a lot of consideration.

References

- Chevrinais, M. Johanson, Z. Trinajstić, K. Long, J. Morel, C. Renaud, C.B. & Cloutier, R., 2018. Evolution of vertebrate postcranial complexity: axial skeleton regionalization and paired appendages in a Devonian jawless fish. *Palaeontology*, 61, 949-961.
- Janvier, P. Desbiens, S. Willett, J.A. & Arsenault, M., 2006. Lamprey-like gills in a gnathostome-related Devonian jawless vertebrate. *Nature*, 440, 1183-1185.
- Sansom, R.S. Gabbott, S.E. & Purnell, M.A., 2010. Non-random decay of chordate characters causes bias in fossil interpretation. *Nature*, 463, 797-800.
- Sansom, R.S. Gabbott, S.E. & Purnell, M.A., 2013. Unusual anal fin in a Devonian jawless vertebrate reveals complex origins of paired appendages. *Biology Letters*, 9, 20130002.

***Hirnantia* Fauna from the Condroz Inlier, Belgium: another case of a relict Ordovician shelly fauna in the Silurian?**

Sofia PEREIRA ¹, Jorge COLMENAR ², Jan MORTIER ³, Jan VANMEIRHAEGHE ³, Jacques VERNIERS ³, Petr ŠTORCH ⁴, David A.T. HARPER ⁵, Juan Carlos GUTIÉRREZ-MARCO ⁶

1. *Centro de Geociências, Universidade de Coimbra, Coimbra, Portugal*
(ardi_eu@hotmail.com)
2. *Instituto Geológico y Minero de España, Madrid, Spain*
(jorgecolmenarlallena@gmail.com)
3. *Department of Geology, Ghent University, Krijgslaan, 281/S8, Belgium*
(jan.vanmeirhaeghe@wienerberger.com; janlmortier@gmail.com;
jacques.verniers@ugent.be)
4. *Institute of Geology AS CR, Praha, Czech Republic* (storch@gli.cas.cz)
5. *Palaeoecosystems Group, Department of Earth Sciences, Durham University, Durham, UK*
(david.harper@durham.ac.uk)
6. *Instituto de Geociencias (CSIC, UCM) and Área de Paleontología GEODESPAL, Facultad de Ciencias Geológicas, Universidad Complutense de Madrid, Madrid, Spain*
(jcgrapto@ucm.es)

The end-Ordovician mass extinction, linked to a major glaciation, led to profound changes in Hirnantian-Rhuddanian biotas (Ordovician-Silurian transition). The *Hirnantia* Fauna, the first of two Hirnantian survival brachiopod-dominated communities, characterizes the lower-middle Hirnantian deposits globally, and mapping its distribution is essential to understand how the extinction occurred. In this presentation, we describe, illustrate, and discuss the first reported macro-fossiliferous *Hirnantia* Fauna assemblage from Belgium, occurring in the Tihange Member of the Fosses Formation at Tihange (Huy), within the Central Condroz Inlier.

Six fossiliferous beds have yielded a low-diversity brachiopod-dominated association. Besides the brachiopods (*Eostropheodonta hirnantensis*, *Plectothyrella crassicosta*, *Hirnantia* sp. and *Trucizetina?* sp.), one trilobite (*Mucronaspis* sp.), four pelmatozoans (*Xenocrinus* sp., *Cyclocharax* (col.) *paucicrenulatus*, *Conspectocrinus* (col.) *celticus* and *Pentagonocyclicus* (col.) sp.), three graptolites (*Cystograptus ancestralis*, *Normalograptus normalis* and ?*Metabolograptus* sp.), together with indeterminate machaeridians and bryozoans are also identified.

The graptolite assemblage indicates the *Akidograptus ascensus* - *Parakidograptus acuminatus* Biozone, indicating an early Rhuddanian (earliest Silurian) age, and thus, an unexpected late occurrence of a typical *Hirnantia* Fauna. This Belgian association may represent an additional example of a relict *Hirnantia* Fauna in the Silurian, sharing characteristics with the only other known example, from Rhuddanian rocks at Yewdale Beck (Lake District, England), although reworking has not been completely ruled out.

The survival of these Hirnantian taxa into the Silurian might be linked to delayed post-glacial effects of rising temperature and sea-level, which may have favoured the establishment of refugia in these two particular regions that were palaeogeographically close during the Late Ordovician-early Silurian.

(Paper accepted for Journal of Paleontology)

Contributions to Belgian Paleogene (plant) research: a tribute to Philippe Gerrienne

Thierry SMITH

Royal Belgian Institute of Natural sciences, Directorate Earth and History of Life, Brussels, Belgium (thierry.smith@naturalsciences.be)

The paleobotanist Philippe Gerrienne was internationally renowned for his work on early land plants. His research career was however not limited to the study of Devonian floras. He also actively contributed to the progress of Belgian Wealdian (Early Cretaceous), early Paleogene and Quaternary research. In this framework, Philippe's interest for Paleogene plants already appeared when he helped to sort Stockmans' paleobotanical collections of the Royal Belgian institute of Natural Sciences (RBINS) during a civil service he did between 1987 and 1989. In the old conservatoires, he discovered hundreds of silicified trunks and branches from the "upper Landenian" (early Eocene) of Belgium, which were collected in 1970 in the area of Hoegaarden during the construction of the Brussels-Liège highway (E40-A3).

From 1994, the RBINS developed new research activities in early Paleogene Belgian sites. At this occasion, fossil plants discovered next to vertebrates from the warm earliest Eocene at Dormaal were studied in collaboration with the Royal Museum for Central Africa, which owns an excellent xylotheque of tropical woods (Doutrelepon et al., 1997). This first step allowed in 1999, after several preliminary works, to start a partnership with the University of Liège (ULiège) and the University of Mons (UMons) through a F.R.F.C.-I.C. (FNRS) project, leaded by Muriel Fairon-Demaret (ULg), on the "Reconstruction of the terrestrial ecosystems in Belgium during the Palaeocene-Eocene transition, 50-60 million years ago". During three years (1999-2002), numerous fieldworks in Belgium and research activities in labs were realized, including a first database of more than 600 hundreds fossil wood specimens.

In this overview, I summarize the main accomplishments that have been done in the field. At Péruwelz, we found a silicified trunk fragment of a new arborescent Ericaceae in the marine Thanetian (Upper Paleocene), which was named *Agaristoxylon garennicum* (Gerrienne et al., 1999). The paleoenvironment of Dormaal was reconstructed based on fruits and seeds from the Paleocene Eocene Thermal Maximum (Fairon-Demaret & Smith, 2002). The most successful work was probably the study of the in situ monospecific *Glyptostroboxylon* forest of Overlaar at Hoegaarden (Fairon-Demaret et al., 2003). This warm Everglades-like paleoenvironment attracted the Belgian media and finally led to the construction of the geopark of Hoegaarden.

In 2004, Philippe described the Givetian (middle Devonian) seed precursor *Runcaria heinzelinii* Stockmans, 1968 from Ronquières, Belgium (Gerrienne et al., 2004). The rediscovery of the 385-million-year-old basal seed plant and, the same year, the retirement of his close colleague Muriel Fairon-Demaret focused definitively his interest on the Paleozoic.

References

Doutrelepont, H., Smith, T., Damblon, F., Smith, R. & Beeckman, H., 1997. Un bois silicifié de peuplier de la transition Paléocène-Eocène de Dormaal, Belgique. Bulletin de l'Institut royal des Sciences naturelles de Belgique, 67, 183-188.

Fairon-Demaret, M. & Smith, T., 2002. Fruits and seeds from the Tienen Formation at Dormaal, Paleocene-Eocene transition in eastern Belgium. Review of Palaeobotany and Palynology, 122, 47-62.

Fairon-Demaret, M., Steurbaut, E., Damblon, F., Dupuis, C., Smith, T. & Gerrienne, P., 2003. The in situ Glyptostroboxylon forest of Hoegaarden (Belgium) at the Initial Eocene Thermal Maximum (55 Ma). Review of Palaeobotany and Palynology, 126, 103-129.

Gerrienne, P., Beeckman, H., Damblon, F., Doutrelepont, H., Fairon-Demaret, M. & Smith, T., 1999. Agaristoxylon garennicum Gerrienne et al., gen. et sp. nov., an arborescent Ericaceae from the Belgian Upper Paleocene: palaeoenvironmental implications. Review of Palaeobotany and Palynology, 104, 299-307.

Gerrienne, P., Meyer-Berthaud, B., Fairon-Demaret, M., Streef, M. & Steemans, P., 2004. Runcaria, a Middle Devonian Seed Plant Precursor. Science, 306, 856-858.



Figure Philippe Gerrienne (in the middle) with two volunteers at the early Oligocene vertebrate site of Boutersem during the construction of the Brussels-Liège TGV railway in September 1999.

Changing life mode of *Campanile giganteum* (Lamarck, 1804) with age: Shifting habitat or food sources?

Nick VAN HOREBEEK¹, Johan VELLEKOOP^{1,2}, Alexander J. CLARK¹, Robert P. SPEIJER¹

1. Department of Earth and Environmental Sciences, KU Leuven, Celestijnenlaan 200E, B3001 Heverlee, Belgium (nick.vanhorebeek@student.kuleuven.be, johan.vellekoop@kuleuven.be, alexanderjohannes.clark@student.kuleuven.be, robert.speijer@kuleuven.be)

2. Analytical & Environmental Geo-Chemistry (AMGC), Vrije Universiteit Brussel, Pleinlaan 2, B-1050, Brussels, Belgium

The Eocene gastropod *Campanile giganteum* combines a large size with very high growth rates (600 mm/year) along the helix. This combination enables retrieval of stable isotopic profiles with a resolution of days to weeks (de Winter et al., 2020). To correctly interpret these results, an accurate assessment of the life conditions of this giant gastropod is important. Whereas there were numerous species of the family Campanilidae during the Eocene, there is only one extant species, *Campanile symbolicum* (Iredale, 1917), and only few studies have been performed on its life and habitat.

To gain a better understanding of the ecology, habitat and life mode of *Campanile giganteum*, we have generated a stable carbonate carbon isotope ($\delta^{13}\text{C}$) record on a specimen with a length of 283 cm along its helix, from the Lutetian of Fleury-la-Rivière (France). The age model of this specimen is based on its stable oxygen isotope profile (Van Horebeek et al., 2021). Even though stable carbon isotopes in biogenic carbonates are complex, a $\delta^{13}\text{C}$ record can provide insights in changes in habitat or food sources through the life of these animals. The carbon-isotopic composition of mollusc shell carbonate is largely controlled by the CO_2 present in the extrapallial fluid, in the space between the outer space between the outer epithelium and the shell. The CO_2 extrapallial fluid is derived from respired CO_2 and dissolved inorganic carbon (DIC) of ambient seawater. According to McConnaughey & Gillikin (2008), the CO_2 in marine invertebrates is mainly dependent on ambient DIC with only 10% coming from respired CO_2 .

The stable carbon isotope record of the specimen used in this study (Fig 1) varies between -2.75‰ and $+2.41\text{‰}$ with an average of -0.29‰ and a total range of 5.22‰ . The specimen shows a shift from mainly positive $\delta^{13}\text{C}$ values to mainly negative $\delta^{13}\text{C}$ values at about the age of two years. There are multiple possible explanations as to why this shift is present. The change from mainly positive $\delta^{13}\text{C}$ values to negative $\delta^{13}\text{C}$ values could be caused by a migration to a habitat with a DIC that has different $\delta^{13}\text{C}$ values, such as a migration from a lagoonal setting to a more open marine setting, or a shifting diet, causing large variations in $\delta^{13}\text{C}$ values of the respired CO_2 .

References

de Winter, N.J., Vellekoop J., Clark A. J., Stassen, P., Speijer, R. P. & Claeys, P. (2020). The giant marine gastropod *Campanile giganteum* (Lamarck, 1804) as a high-resolution archive of seasonality in the Eocene greenhouse world. *Geochemistry, Geophysics, Geosystems*, 21, 4.

Judd, E., Wilkinson, B., & Ivany, L. (2018). The life and time of clams: Derivation of intra-annual growth rates from high-resolution oxygen isotope profiles. *Paleogeography, Palaeoclimatology, Palaeoecology*, 490, 70-83.

McConnaughey, T., & Gillikin, D. (2008). Carbon isotopes in mollusk shell carbonates. *Geo-Marine Letters*, 28(5-6), 287-299.

Van Horebeek, N., Vellekoop, J., Clark, A. J., de Winter, N. J., Stroobandt, Y., and Speijer, R. P.: A stable oxygen isotope record of weather-timescale variability in the Eocene greenhouse world, using the giant marine gastropod *Campanile giganteum*, EGU General Assembly 2021, online, 19–30 Apr 2021, EGU21-3268, <https://doi.org/10.5194/egusphere-egu21-3268>, 2021.

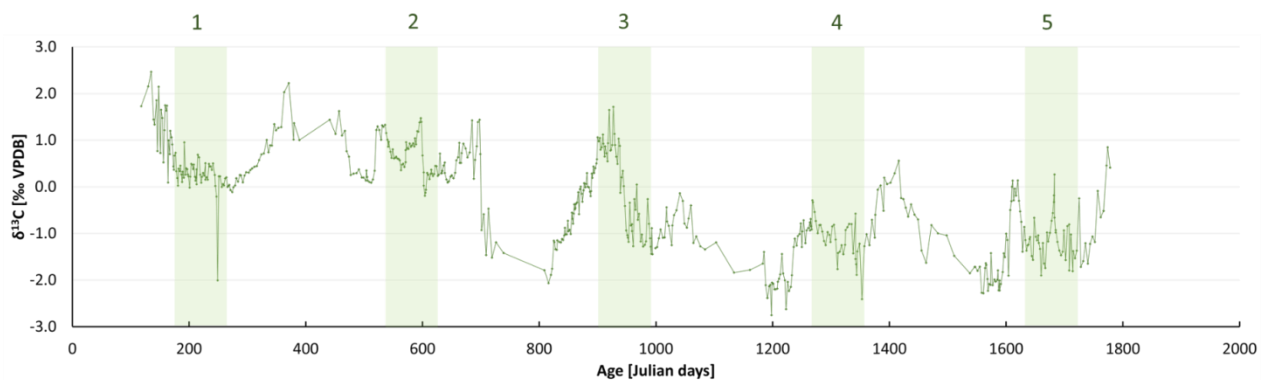


Figure 1: $\delta^{13}C$ values during the life of the studied specimen given by Julian dates. Summers are indicated in green with numbers indicating the age of the specimen. A blue line represents a $\delta^{13}C$ value of 0.00‰. Age values are obtained with the age model of Judd et al., 2018.

The mid-Maastrichtian event in the Maastrichtian-type area and its benthic foraminiferal response

Iris VANCOPPENOLLE¹, Johan VELLEKOOP^{1,2}, Monika DOUBRAWA¹, Pim KASKES², Matthias SINNESAE^{2,3}, John JAGT⁴, Philippe CLAEYS², Robert P. SPEIJER¹

1. Department of Earth and Environmental Sciences, Division Geology, KU Leuven, Celestijnenlaan 200E, B-3001, Leuven, Belgium (iris.vancoppenolle@student.kuleuven.be, johan.vellekoop@kuleuven.be, monika.doubrawa@kuleuven.be, robert.speijer@kuleuven.be)
2. Department of Chemistry, Analytical, Environmental and Geo-Chemistry, Vrije Universiteit Brussel, Pleinlaan 2, B1050, Brussels, Belgium (pim.kaskes@vub.be, phclaeys@vub.be)
3. Department of Earth Sciences, Mountjoy Site, Durham University, South Road, Durham DH1 3LE, UK (matthias.sinnesael@durham.ac.uk)
4. Natural History Museum Maastricht, De Bosquetplein 7, 6211 KJ, Maastricht, the Netherlands (john.jagt@maastricht.nl)

The mid-Maastrichtian event (MME), ~69 Ma, represents a global negative $\delta^{13}\text{C}$ excursion which appears to coincide with the extinction of inoceramid bivalves and latitudinal migration of planktonic foraminifera (Frank et al., 2005; Huber et al., 2008). While the actual extinction of inoceramids was diachronous across the globe, the decline of this important marine fossil group is generally linked to environmental changes across the mid-Maastrichtian interval. The MME is potentially related to changes in oceanic circulation, but the true mechanisms causing this event and its relation to the inoceramid extinction are not well understood. While the MME, and associated decline of inoceramids, has been recorded from a variety of deep-sea sites (Voigt et al., 2012 and references therein), little is known about the MME signature in shallow epicontinental environments.

Recently, the MME has been recorded for the first time from the type-Maastrichtian, in the Maastricht-Liège region (The Netherlands and Belgium), in newly generated bulk carbonate carbon isotope records (Vellekoop et al., *in prep.*). These records come from the Hallembaye quarry (NE Belgium) and former ENCI quarry (SE Netherlands), which are approximately 8 km apart. The carbonate succession was deposited in a shallow subtropical sea during the Late Cretaceous. We generated species-specific stable carbon and oxygen isotope records and high-resolution benthic foraminiferal assemblage data across the MME interval at these two quarries, in order to unravel biotic and environmental expressions of the MME in the Maastrichtian type area. This was done using the high-resolution sample set acquired in the context of the Maastrichtian Geoheritage Project (Vellekoop et al., *in prep.*).

The MME does not seem to have had a large impact on the benthic environment in the type-Maastrichtian epicontinental environment, as highlighted in Figure 1. Strong fluctuations in benthic foraminiferal number (BFN, per gram of dry sediment) during the MME indicate fluctuations in organic matter flux. However, the high and nearly constant species evenness (E) shows that neither oxygen nor organic matter flux were limited during the event. Remarkably, in the Hallembaye quarry the otherwise rare endobenthic species *Cuneus trigona* reaches a peak abundance of 33% at the onset of the MME, which can be explained by a change in either quantity or quality of the organic matter reaching the seafloor. This peak is not yet found in the ENCI quarry, which might be due to the low (2 m) sampling resolution.

The species-specific benthic foraminiferal $\delta^{13}\text{C}$ values are consistently higher than the bulk $\delta^{13}\text{C}$ values (dominated by calcareous nannoplankton). This inverted $\delta^{13}\text{C}$ gradient may suggest that the Maastrichtian chalk sea was characterized by enhanced oxygen minimum zones in the water column. The inverted gradient appears to decrease during the MME, which suggests that the oxygen minimum zone was weaker during the MME, hinting towards changes in productivity or ocean circulation during the event.

References

- Frank, T. D., Thomas, D. J., Leckie, R. M., Arthur, M. A., Bown, P. R., Jones, K., & Lees, J. A., 2005. The Maastrichtian record from Shatsky Rise (northwest Pacific): A tropical perspective on global ecological and oceanographic changes. *Paleoceanography*, 20(1), PA1008.
- Huber, B. T., MacLeod, K. G., & Tur, N. A., 2008. Chronostratigraphic framework for Upper Campanian-Maastrichtian sediments on the Blake Nose (subtropical North Atlantic). *The Journal of Foraminiferal Research*, 38(2), 162–182.
- Voigt, S., Gale, A. S., Jung, C., & Jenkyns, H. C., 2012. Global correlation of Upper Campanian-Maastrichtian successions using carbon-isotope stratigraphy: development of a new Maastrichtian timescale. *Newsletters on Stratigraphy*, 45(1), 25.

Figure

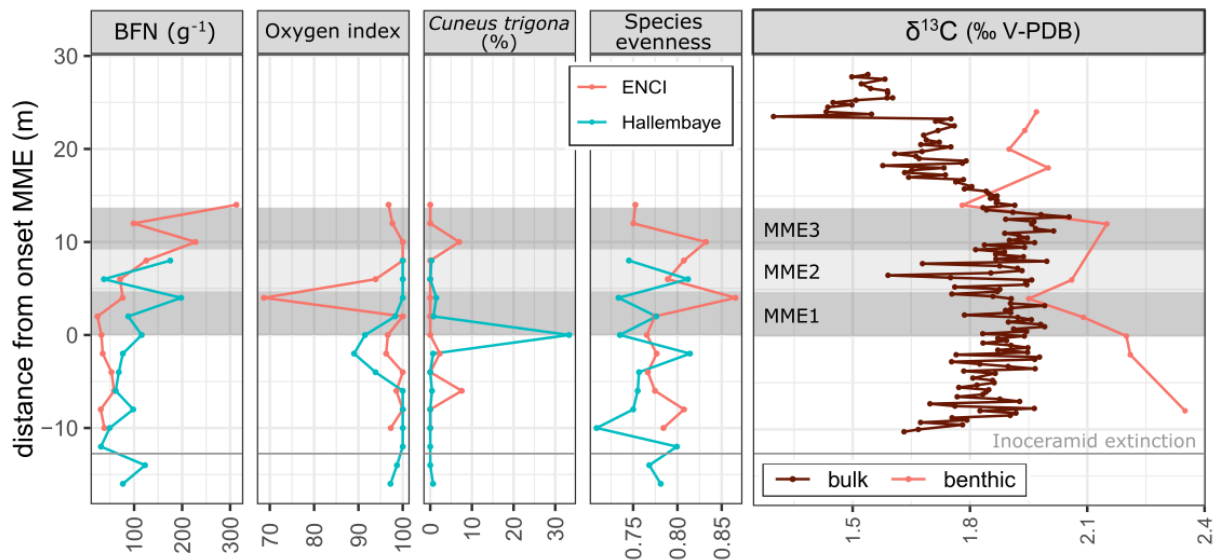


Figure 1: summary of the most important data from both the ENCI and Hallembaye quarry

Rapid biological recovery following the Cretaceous-Paleogene boundary catastrophe in the Maastrichtian type area

Johan VELLEKOOP^{1,2}

1. *Analytical, Environmental and Geo-Chemistry (AMGC), Vrije Universiteit Brussel, Brussels, Belgium*

2. *Division of Geology, Department of Earth & Environmental Sciences, KU Leuven, Leuven, Belgium; johan.vellekoop@kuleuven.be*

Present-day marine biotas are increasingly subject to anthropogenically-forced extinctions. The study of the global mass extinction event at the Cretaceous-Paleogene (K-Pg) boundary can aid in our understanding of the patterns of selective extinction and survival and the dynamics of ecosystem recovery. Outcrops in the Maastrichtian type region (The Netherlands, Belgium) comprise an expanded K-Pg boundary succession, presenting a unique opportunity to study marine ecosystem recovery within the first thousands of years following the Chicxulub impact (Smit and Brinkhuis, 1996; Vellekoop et al., 2020). Here, the palynological, micro- and macropaleontological record of this unique succession is studied and reevaluated. Ecosystem changes across the K-Pg boundary in this region are rather limited, showing a general shift from epibenthic filter feeders to shallow-endobenthic deposit feeders. The fauna of the lowermost Paleocene still has many 'Maastrichtian' characteristics, a biological assemblage that survived the first hundreds to thousands of years into the earliest Paleocene. The shallow-marine oligotrophic carbonate sea of the Maastrichtian type area was inhabited by starvation-resistant, low nutrient-adapted taxa, that were seemingly less affected by the short-lived detrimental conditions of the K-Pg boundary catastrophe, such as darkness, cooling, food-starvation, ocean acidification, resulting in relatively high survival rates. The high survival rate allowed for a fast recolonization and rapid recovery of marine faunas in the Maastrichtian type area.

References

- Smit, J. & Brinkhuis, H., 1996. The Geulhemmerberg Cretaceous/Tertiary boundary section (Maastrichtian type area, SE Netherlands); summary of results and a scenario of events. *Geologie en Mijnbouw* 75, 283-293.
- Vellekoop, J., Van Tilborgh, K.H., Van Knippenberg, P., Jagt, J.W.M., Stassen, P., Goolaerts, S. & Speijer, R.P., 2020. Type-Maastrichtian gastropod faunas show rapid ecosystem recovery following the Cretaceous-Palaeogene boundary catastrophe. *Palaeontology* 63, 2, 349-367.

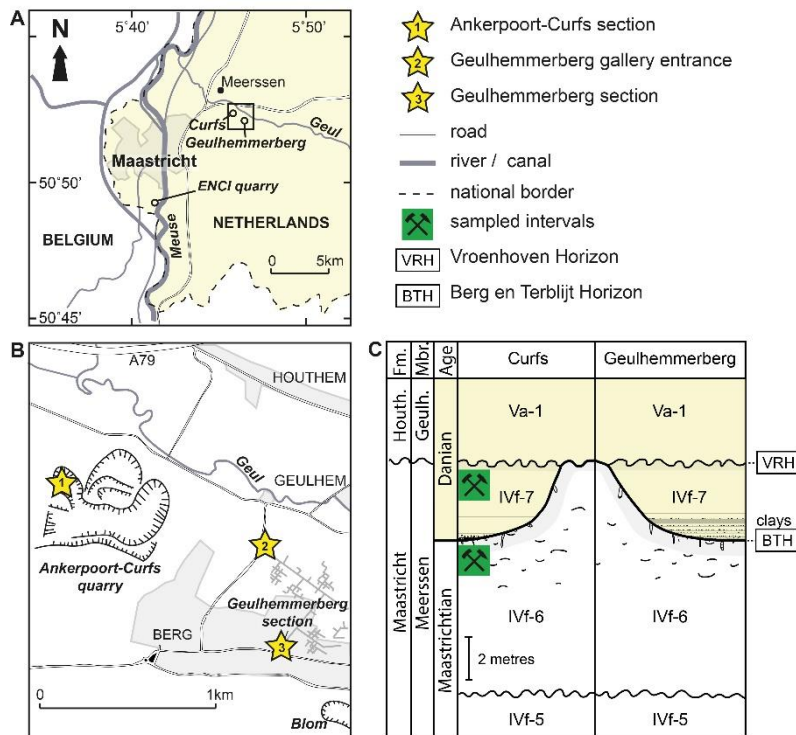


Figure 1: A) map of the Maastricht area (SE Netherlands, NE Belgium), showing the localities referred to in the text; the boxed area is shown in B. B) detailed map of the Geulhem area, with the former Ankerpoort-Curfs quarry and the adjacent Geulhemmerberg K/Pg boundary sections in subterranean galleries. C) schematic stratigraphical context of the former Ankerpoort-Curfs quarry and adjacent Geulhemmerberg K/Pg boundary sections (note: vertical exaggeration is 10x). Adapted after Vellekoop et al., 2020.

A paleoenvironmental reconstruction of the *Campanile giganteum* (Lamarck, 1804) bed (Lutetian, Paris Basin) utilizing quantitative macro- and micropaleontological data

Anthea WILLEMS¹, Johan VELLEKOOP^{1,2}, Monika DOUBRAWA¹, Robert P. SPEIJER¹

1. Department of Earth and Environmental Sciences, KU Leuven, Celestijnenlaan 200E, B- 3001 Heverlee, Belgium (anthea.willems@student.kuleuven.be, johan.vellekoop@kuleuven.be, monika.doubrawa@kuleuven.be, robert.speijer@kuleuven.be)

2. Analytical & Environmental Geo-Chemistry (AMGC), Vrije Universiteit Brussel, Pleinlaan 2, B-1050, Brussels, Belgium.

Campanile giganteum (Lamarck, 1804) is an extraordinary gastropod occurring in Lutetian (~45 Ma) deposits. The largest specimens of *C. giganteum* are almost one meter long and with growth rates surpassing 600 mm/year along their helix, these giant snails have some of the highest known growth rates among gastropods (de Winter et al., 2020). They are abundantly present in the Paris Basin (France), specifically in the Banc à Verrains, also known as ‘the *Campanile* bed’, which is part of the Calcaire Grossier Formation (Dominici & Zuschin, 2016). Finding several specimens of *C. giganteum* within one square meter is not unusual. *Campanile* specimens can also be found in regions outside the Paris Basin, such as the Hampshire Basin. However, the number of specimens in these regions is not as high as in the Banc à Verrains. To this day, it is not clear why this species occurred in such high abundance in the Lutetian deposits of the Paris Basin. Therefore, the aim of this study was to reveal the preferred habitat of *C. giganteum*. We reconstructed the paleoenvironment of the Banc à Verrains utilizing quantitative macro- and micro-paleontological data.

A sample of 308 g was taken from the original matrix of a *C. giganteum* specimen from the Banc à Verrains in Fleury-la-Rivière. Foraminiferal and non-foraminiferal components were counted and identified to genus or species level in five different fractions ranging from 63 µm to >1 mm (fig. 1). The diversity and abundance of various taxa indicates the presence of two disparate paleoenvironments. The foraminiferal assemblage is dominated by porcelaneous species of the miliolid suborder, suggesting hypersaline lagoonal conditions. The non-foraminiferal components mainly consist of turritellid gastropods in the largest fraction and broken bryozoan pieces, sponge spicules and sea urchin needles in the smaller fractions, indicating a normal marine, high-nutrient environment with deltaic influences (Molenaar & Martinius, 1996; Dominici & Kowalke, 2007). Furthermore, the large number of epifaunal grazers, such as Cerithiidae species, suggests a shallow marine seagrass environment (max. 20 m deep). Based on this seemingly contradictory information, we suggest that deposition of the Banc à Verrains took place at 10-20 m depth where the giant *Campanile* snails lived in seagrass meadows. The finer particles with numerous miliolids were likely derived from a nearby superhaline lagoon from which sediment was swept into the slightly deeper and more offshore part of the basin during storms.

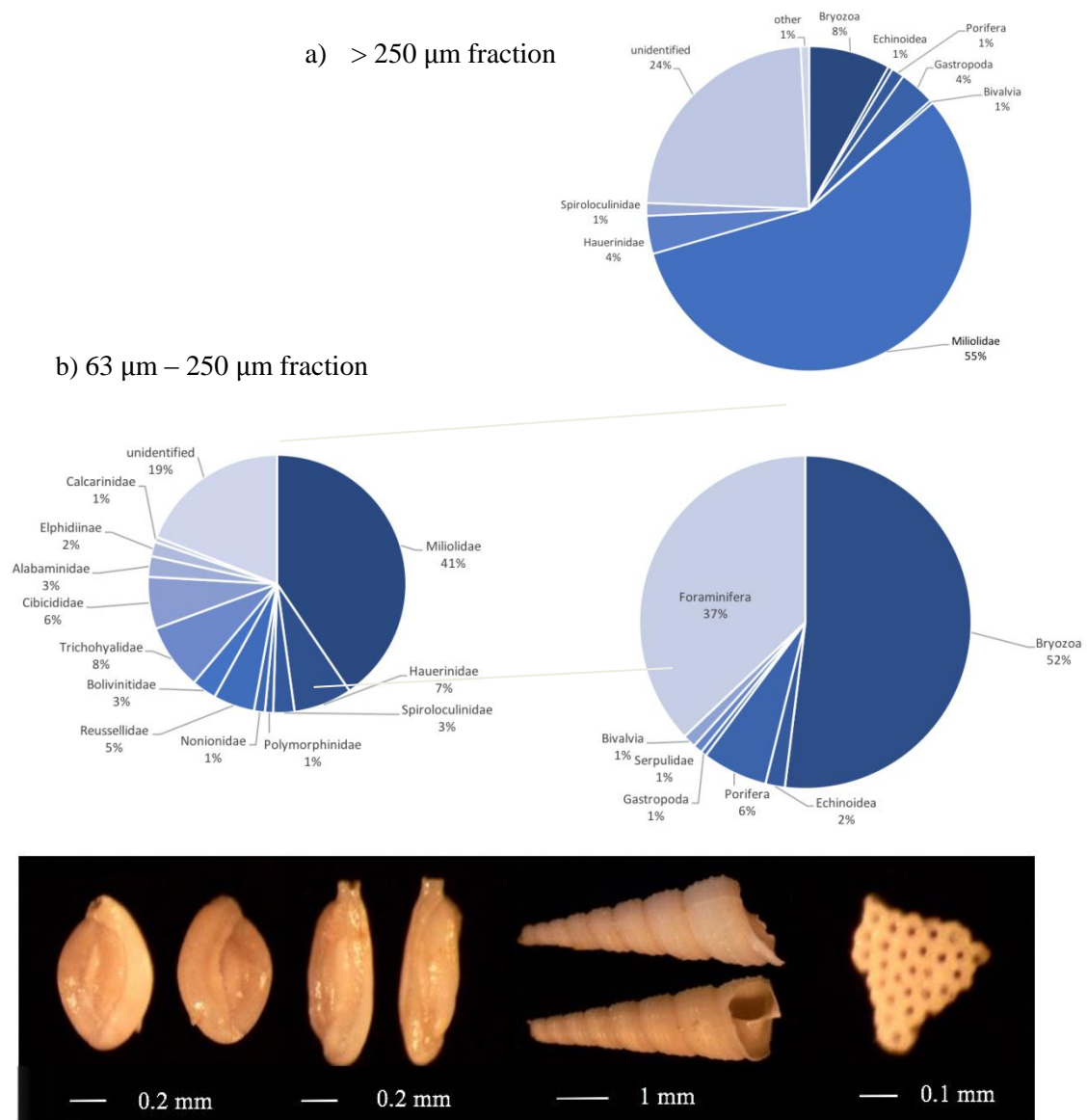


Figure 1: Relative contributions of the different classes of non-foraminiferal components and foraminiferal families in (a) the > 250 μm fraction and (b) the 63 μm – 250 μm fraction. c) from left to right: 2 miliolid specimens, 1 turrnellid specimen, 1 bryozoan fragment.

References

- de Winter, N.J., Vellekoop J., Clark A. J., Stassen, P., Speijer, R. P. & Claeys, P. (2020). The giant marine gastropod *Campanile giganteum* (Lamarck, 1804) as a high-resolution archive of seasonality in the Eocene greenhouse world. *Geochemistry, Geophysics, Geosystems*, 21, 4.
- Dominici, S. & Kowalke, T. (2007). Depositional dynamics and the record of ecosystem stability: Early Eocene faunal gradients in the Pyrenean foreland, Spain. *Palaios*, 22, 268-284.
- Dominici, S. & Zuschin, M. (2016). Paleocommunities, diversity and sea-level change from middle Eocene shell beds of the Paris Basin. *Journal of the Geological Society*. 173, 889-900.
- Molenaar, N. & Martinius, A.W. (1996). Fossiliferous intervals and sequence boundaries in shallow marine, fan-deltaic deposits (Early Eocene, southern Pyrenees, Spain). *Palaeogeography, Palaeoclimatology, Palaeoecology*, 121, 147-168.

Assessing the diversity of insects damage traces in the fossil flora of Gelinden (Limburg, Belgium)

Raphaël ZAMBON¹, Cyrille PRESTIANNI^{1,2}

1. Evolution and Diversity Dynamics Lab, Université de Liège, Liège, Belgium

(raphael.zambon@student.uliege.be, cyrille.prestianni@uliege.be)

2. OD Earth and Life Directory, Royal Belgian Institute of Natural Sciences, Bruxelles, Belgium (cprestiani@naturalsciences.be)

Plants and insects are two of the most important clades of multicellular organisms, both in terms of diversity and in abundance. They are relatively ancient groups, appearing in the Late Ordovician according to molecular clocks (Sanderson et al., 2004, Misof et al., 2014). Indeed, it is the colonisation of the continents by the plants that allowed the insects to develop on land (Labandeira, 2005). Therefore, these two groups have shared a long history of coevolution, developing a wide diversity of complex interactions, whose oldest examples are described as early as the Late Silurian (Labandeira, 2006). These interactions range from mutualist relations, such as pollination, to more predatory forms, such as herbivory and parasitism. The latter can be particularly evident in the fossil record thanks to the traces they left on the host plants, which are often more abundant, older and more informative than the remains of their perpetrator (Labandeira, 2007).

The study of these interactions in the fossil record is of great importance, as it not only gives us a better understanding of the evolution of such relations, through time and space (Labandeira, 1998, 2006), but also provides us with crucial information on the mechanics of these associations, which are still relevant in present time (Liu et al., 2015). Indeed, interactions are at the direct basis of the food chain, of the associated ecosystems (Labandeira, 2006). The study of their evolution through time notable allows to understand the reaction of such interactions to environmental change (Wilf & Labandeira, 1999).

The Palaeocene is a particularly interesting period from this point of view, as it directly follows the cataclysmic event of the K-T extinction and ends with the sudden warming of the Palaeocene-Eocene Thermal Maximum, changes which reflect on plant-insects associations (Currano et al., 2010; Tanrattana et al., 2020). While Palaeocene plant-insect associations have already received a certain interest with the development of the wider discipline in the last 30 years, most of these studies have focused on North American floras (Wilf et al., 2006, Wilf, 2008), in no part due to the relative rarity of European Palaeocene sites in comparison (Kvaček, 2010). However, up to now, the only similar study on a European site, at Menat of Selandian (Middle Palaeocene) age (Tanrattana et al., 2020), has revealed some interesting dynamics in comparison to its American equivalents, in particular when it comes to the diversity of insect-mediated damages (Wappler et al., 2009), making the study of other European floras all the more interesting.

In such a context, this study aims at investigating the multiple traces of damages present in the Selandian flora of Gelinden, in Belgium (Saporta, 1873, Saporta & Marion, 1878), in particular from the point of view of damage diversity. The point is to provide a basis of data usable for comparison of sites of similar age and nature, and therefore lead to a better

understanding of the dynamics of plant-insect interactions during the Palaeocene of Europe, and in relation with the rest of the world.

References

- Currano, E.D., Labandeira, C.C. & Wilf, P., 2010. Fossil insect folivory tracks paleotemperature for six million years. *Ecological Monographs*, 80/4, 547-67.
- Kvaček, Z., 2010. Forest flora and vegetation of the European early Palaeogene – a review. *Bulletin of Geosciences*, 85/1, 63-76.
- Labandeira, C.C., 1998. Early history of arthropod and vascular plant associations. *Annual Review of Earth and Planetary Sciences*, 26, 329-77.
- Labandeira, C.C., 2005. Invasion of the continents: cyanobacterial crusts to tree-inhabiting arthropods. *Trends in Ecology & Evolution*, 20/5, 253-62.
- Labandeira, C.C., 2006. The four phases of plant-arthropod associations in deep time. *Geologica Acta*, 4/4, 409-38.
- Labandeira, C.C., 2007. Assessing the fossil record of plant-insect associations: Ichnodata versus body-fossil data. *SEPM Special Publications*, 88, 9-26.
- Liu, W.H., Dai, X.H. & Xu, J.S., 2015. Influences of leaf-mining insects on their host plants: A review. *Collectanea Botanica*, 34, e005.
- Misof, B., Liu, S., Meusemann, K., Peters, R.S., Donath, A., Mayer C, et al., 2014. Phylogenomics resolves the timing and pattern of insect evolution. *Science*, 346/6210, 763-7.
- Sanderson, M.J., Thorne, J.L., Wikström, N. & Bremer, K., 2004. Molecular evidence on plant divergence times. *American Journal of Botany*, 91/10, 1656-65.
- Saporta, G. de, 1873. *Essai sur l'état de la végétation à l'époque des marnes heersiennes de Gelinden*, 112 p.
- Saporta, G. de, Marion, A.F. 1878. *Révision de la flore heersienne de Gelinden: d'après une collection appartenant au comte G. de Looz. Académie royale des sciences, des lettres et des beaux-arts de Belgique*, 154 p.
- Tanrattana, M., Boura, A., Jacques, F.M.B., Villier, L., Fournier, F., Enguehard, A., Cardonnet, S., Volland, G., Garcia, A., Chaouch, S. & Franceschi, D.D., 2020. Climatic evolution in Western Europe during the Cenozoic: insights from historical collections using leaf physiognomy. *Geodiversitas*, 42/11, 151-74.
- Wappler, T., Currano, E.D., Wilf, P., Rust, J., Labandeira C.C., 2009. No post-Cretaceous ecosystem depression in European forests? Rich insect-feeding damage on diverse middle Palaeocene plants, Menat, France. *Proceedings of the Royal Society B: Biological Sciences*, 276(1677), 4271-7.
- Wilf, P. & Labandeira, C.C., 1999. Response of plant-insect associations to Paleocene-Eocene warming. *Science*, 284/5423, 2153-6.
- Wilf, P., Labandeira, C.C., Johnson, K.R. & Ellis, B., 2006. Decoupled Plant and Insect Diversity After the End-Cretaceous Extinction. *Science*, 313/5790, 1112-5.
- Wilf, P., 2008. Insect-damaged fossil leaves record food web response to ancient climate change and extinction. *New Phytologist*, 178/3, 486-502.

Session 7- Karsts Investigation and Subsurface Researches

Conveners:

Pascale Lahogue (RMCA), Vincent Hallet (UNamur), Michel Van Camp (ROB), Sophie Verheyden (RBINS)

Karstic regions face even more than other regions several societal challenges due to their specific characteristics, such as their secondary permeability, mid-to-long-term instability, detrital and chemical deposits as well as their strong anthropogenic interactions among which tourism. Karstic regions cover between 10 and 15% of the continental surface (with exception of Antarctica), and 25% of the world population is dependent of karstic water. Recently karst research gain interest on the international agenda since the discovery of new antibiotics in caves and the identification of potential karst systems on planet Mars, a pledge of successful human colonization since sheltered from cosmic rays. Karstic deposits, detrital or chemical provide since several decennia a window on earth history, through information on local and regional karstological, geological, tectonic, geomorphological, environmental and climatic evolution. Recently, Belgium was the driver of a change in paradigm of speleogenesis. The recent new perspectives ask for a better comprehension of karstic processes, still too much considered as a black box in its relationship with large geological processes, such as ore mineralization. These karst regions which are full of enchantment and legends are since long visited by humans that left their traces. The richness of these areas is the core of the geoheritage interest of several touristic areas. It is therefore no surprise that 2021 is the international year of karst



Radon gas in karstic environments, the case of the *Noû Bleû Cave, Belgium*

Boris DEHANDSCHUTTER ¹, Gauthier ROBA ²

1. federal Agency for Nuclear Control, Brussels, Brussels, Belgium

(Boris.dehandschutter@fanc.fgov.be)

2. Speleological research club Ourthe Amblève CRSOA, Awans, Belgium

(robbygees@hotmail.com)

Exposure to radon gas represents a significant health risk in certain situations and environments. Indoor exposure to radon in dwellings is one of the most important sources of radiological exposure of the Belgian population. Radon in workplaces can also be an important source of exposure and is therefore addressed in the radiological protection regulations. Karstic systems play a special role in the management of radon since they can lead to very local and very high radon concentrations. Therefore, a better understanding of the behaviour of radon in such systems is needed. The present study investigates the dynamics of radon gas and external gamma dose rate in the specific settings of the Grotte du Noû Bleû karstic system in Chanxhe (Sprimont). The radon concentrations vary highly depending of the ventilation and air exchange rate with outdoor air of the specific gallery location. The radon concentrations increase in summer, a phenomenon commonly observed in caves and controlled by the temperature differences between the cave and the outdoor air. The measurements also allow to evaluate the health risk and dose to the speleologist active in this specific cave, which seems to be moderate for ‘normal’ speleological activities of less than 100 hours per year.

Tracer tests in La Lembrée karstic system: the crucial importance of a good geological map

Romain DELEU¹, Laurent BARCHY², Paul DE BIE³, Jean-Marc MARION⁴, Amaël POULAIN⁵, Gaëtan ROCHEZ¹, Vincent HALLET¹

1. *Université de Namur, Département de Géologie, Namur, Belgium* (romain.deleu@unamur.be)

2. *Carmeuse SA, Seilles, Belgium*

3. *Speleo Club Avalon, Edegem, Belgium*

4. *Université de Liège, Département de Géologie, Liège, Belgium*

5. *Traqua, Namur, Belgium* (ap@traqua.be)

La Lembrée is a river of Belgium, located 25km south of Liège. Its watershed makes up to 52 km² from its outlet into the nearby Ourthe river on the west side, to the A26 highway on the East. Most of its surface is composed of Cambrian, Ordovician and Devonian shales, sandstones and conglomerates. However, a significant portion of the basin is composed of Givetian and Frasnian limestones on the west side, which are known to be subject to karstification, as many caves have been discovered in the region (De Bie & Van Houtte, 2020). Many occurrences of water infiltration points are listed over the calcareous aquifers (CWEPPS, 2020). This includes point infiltrations of 3 small streams (Bressine, Fermine and Izier sinkholes), as well as point and diffuse infiltrations in the thalweg of the Lembrée river (figure 1). The latter allow for the river to completely lose through those infiltration points during dry season, it is then common to mention the existence of a subsurface Lembrée which has been explored partially (De Bie & Van Houtte, 2020). A perennial resurgence, “Le Moulin”, is located 1km upstream the outlet of the basin. It is the only strongly active resurgence in the basin and is suspected to drain out a major portion of the limestones aquifers as well as the subsurface Lembrée stream. The objective of this study is to characterize those karstic flows in the Devonian limestones by the use of tracer tests.

A tracer tests campaign has been performed from May 2019 to January 2020. It consists of four tracer injections and 6 measurement points. The injections have been done using variable quantities of uranine tracer at the Bressine, Fermine and Izier sinkholes and in the Lembrée river, a few meters downstream the Moulin resurgence. The tracer concentration has been measured by the use of 6 fluorimeters Fluo-G (Poulain et al., 2017), which have been placed in the Moulin resurgence and a close-by small resurgence, in the Illusions cave and in 3 other nearby resurgences, just outside the basin in the nearby valley of the Ourthe river (figure 1). For each injection, restitution curves have been assessed on each fluorimeters to characterize the existing links between the sinkholes and the resurgences.

Results show that all three Bressine, Fermine and Izier sinkholes are in direct connection with the strongly active Moulin resurgence down the valley. Restitution curves have complex shapes spread throughout up to 16 days after the injection. First arrival times (FAT) and maximum travel speeds (MTS) are strongly variable. Bressine sinkhole connection with the Moulin resurgence shows low FAT and high MTS (128 m/h) compared to both Fermine and Izier sinkholes (15 and 13 m/h respectively). Additionally, the injection in the Lembrée river downstream the Moulin resurgence showed a link with a minor resurgence outside the basin (Etang resurgence).

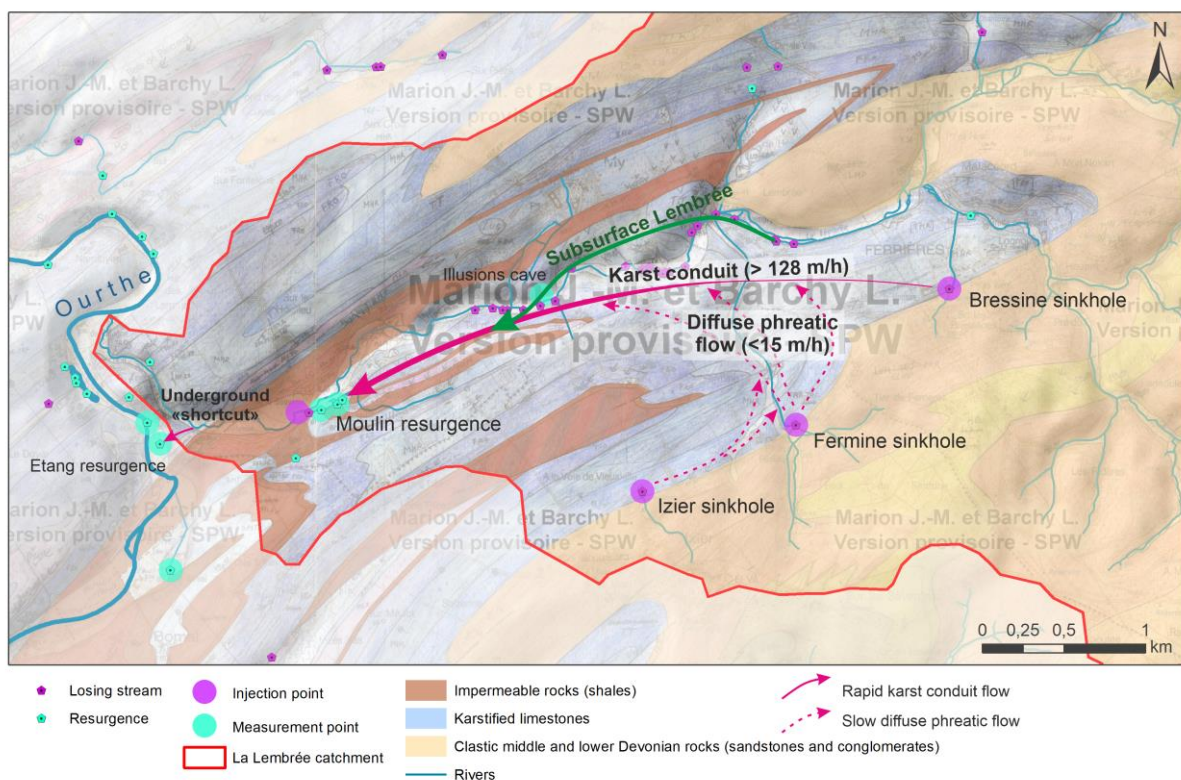
Based on the varied calculated MTS, two types of karstic flow can be proposed in the Devonian limestones: a well-developed karst conduit flow with fast travel speed (>128 m/h), and a slow diffuse flow throughout the saturated fissured limestone aquifers (<15 m/h). The two types of connections are drawn on the map (figure 1) based on the tracer tests results. The well-developed conduit spreads from the Bressine sinkhole to the Moulin resurgence, allowing the low MTS. The slow diffuse flow is observed for both Fermine and Izier sinkholes with low MTS. The previously

mentioned karstic network probably collects these waters, as it acts as a collector for the side limestone aquifers. This collector eventually mixes with the subsurface Lembrée, which is observed in many caves in the valley (De Bie & Van Houtte, 2020), before the Moulin resurgence. Those flows are consistent with the new geological map (Marion & Barchy, 2021) in terms of sinkholes location, links with the resurgences and flow directions.

These conclusions could not be made based on the previous version of the geological maps (Lohest & Fourmarier, 1902) and no clear interpretation could have been made without the recent map (Marion & Barchy, in press). This highlights the crucial importance of a good knowledge of the geology in terms of rock types and the structures they draw. A well-established geological map is of crucial importance for any hydrogeological characterization study.

Références

- CWEPPS, 2020. Atlas du Karst Wallon, Bassin de l'Ourthe Caestienne.
 De Bie P. & Van Houtte A., 2020. Recherches spéléologiques dans le vallon de la Lembrée. Atlas du Karst Wallon, Bassin de l'Ourthe Caestienne 43-52.
 Lohest M. & Fourmarier P., 1902. Carte Géologique de la Belgique, planche n°158 Hamoir - Ferrières.
 Marion J.M. & Barchy L., (in press). Carte Géologique de la Wallonie, Hamoir – Ferrières n°49/5-6 et sa notice explicative. SPW/Éditions, Cartes. <https://orbi.uliege.be/handle/2268/214331> (version provisoire).
 Poulain A., Rochez G., Van Roy J., Dewaide L., Hallet V., De Sadelaer G., 2017. A compact field fluorometer and its application to dye tracing in karst environments. Hydrogeology Journal 25(5):1517-1524.



Sources : Atlas du Karst Wallon (CWEPPS, 2020) ; Geological Map 49/5-6 (Marion & Barchy, 2021 - provisional version SPW)

Figure 7. Subsurface flows and flow speeds for Bressine, Fermine and Izier sinkholes.

Karstification and associated processes of the Waulsort Formation (Furfooz, Belgium)

Lorraine DEWAIDE¹, Jean-Marc BAELE², Vincent HALLET³ & Rudy SWENNEN⁴

1. UNAMUR, Namur, Belgium & ISSeP, Colfontaine, Belgium (lorraine.dewaide@unamur.be)
2. UMONS, Mons, Belgium (jean-marc.baele@umons.be)
3. UNAMUR, Namur, Belgium (vincent.hallet@unamur.be)
4. KUL, Leuven, Belgium (rudy.swennen@kuleuven.be)

The present study focuses on observations that were made on the dolostones of the Waulsort Formation outcropping in South of Belgium. The lenticular deposits of this Formation are made of massive limestones containing mainly bryozoans and stromatoporoids. Dolomitization affects some parts of those buildups in a very heterogeneous way.

At first, the research focused on karst developed in the dolomitized sections of the buildups (Dewaide et al., 2014). Distinctive field features associated to these karsts were defined: limited extension of the karst cavities, development along fracture planes, presence of different calcite facies underlying cavities. Micro-observations and cathodoluminescence (CL) conducted in this study highlighted dedolomitization processes. Petrographic and geochemical gradients (fig.1, fig.2) were observed and interpreted as the consequence of complex fluid flow history. A first paragenesis was proposed to explain the origin of the observed petrographic textures.

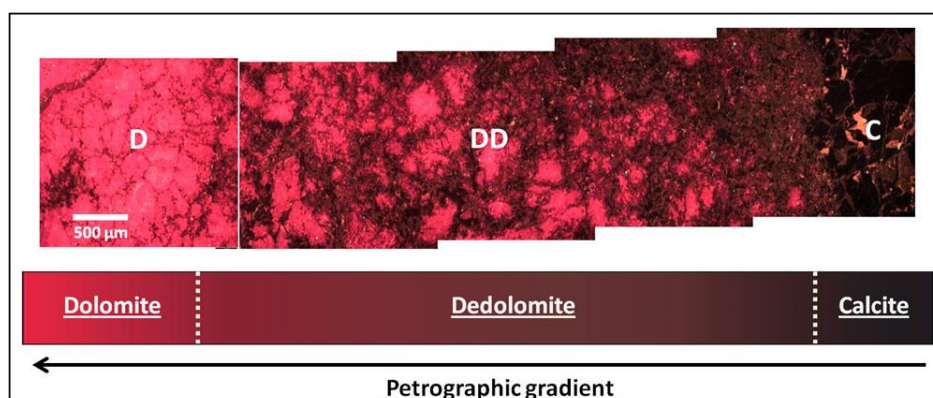


Figure 1. Sequence of cathodoluminescence photomicrographs showing a petrographic gradient from calcite to dolomite. [D] dolomite, [DD] dedolomite, [C] calcite cement in a micro-cavity.

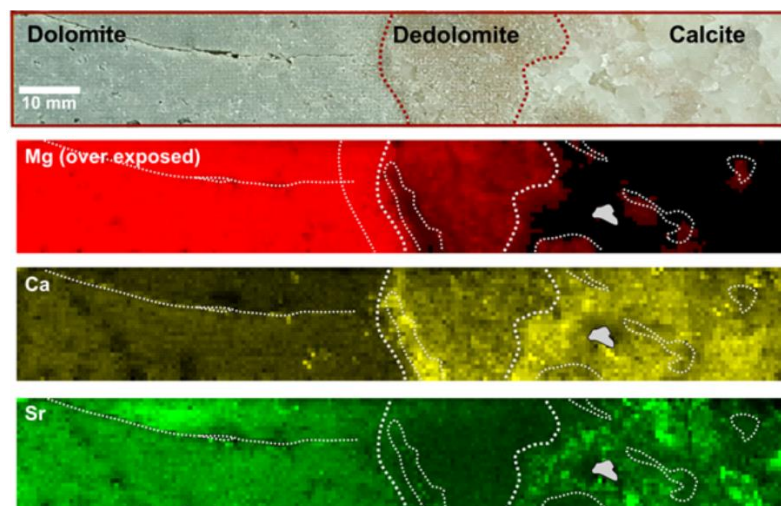


Figure 2. LIBS images illustrating geo-chemical variation through a rock sample (Mg, Ca and Sr content).

In 2015 and 2018, oxygen and carbon isotopes analysis were collected. The data show that the Waulsortian dolostone has a deep burial origin while dedolomitization and subsequent calcite cementation seem to be linked to meteoric water. Further investigations (2018, 2019) used LIBS (Laser-Induced Breakdown Spectroscopy) analysis in order to gather some clues regarding the geochemical evolution of samples from dedolomitized zones and the associated paragenesis. The results point out to oxidizing conditions and near-surface environments, as it would be consistent with an open karst system. Porosity development within dolomite was also questioned through these investigations.

Recently (2020-2021), LIBS, CL and Plasma-Induced Luminescence (PIL) analyses have focused on non-dolomitized limestones of the same study area. The presence of REE (Rare Earth Element) was evidenced by CL and in earlier calcite phases. Further investigations are undertaken in order to i) investigate in more detail the REE-bearing calcite, ii) understand the origin and the role of REE-enriched fluids in the Waulsortian rocks evolution and karst formation history.

References

- Dewaide L., Baele J-M., Collon-Drouaillet P., Quinif Y., Rochez G., Vandycke S. & Hallet V., 2013. «Karstification in dolomitized Waulsortian mudmounds (Belgium)». *Geologica Belgica*, volume 17 (2014) : 43-51.

RISSC: Towards a better management of cavity-related ground movements in Wallonia and Hauts-de-France Regions

Lorraine DEWAIDE¹, Fanny DESCAMPS², Cédric LEFEBVRE³, Catherine PINON⁴ & Jean-Marc WATELET⁵

1. ISSEP, Colfontaine, Belgium (l.dewaide@issep.be)
2. UMONS, Mons, Belgium (fanny.descamps@umons.ac.be)
3. CEREMA, Sequedin, France (cedric.lefebvre@cerema.fr)
4. Ineris, Verneuil-en-Halatte, France (catherine.pinon@ineris.fr)
5. Ineris, Verneuil-en-Halatte, France (jean-marc.watelet@ineris.fr)

Avec le soutien du Fonds Européen de Développement Régional

The RISSC project (<https://www.rissc-interreg.eu/>) is supported by the European “Interreg” program which develops social and economic cooperation between European regions. In this framework, Wallonia and Hauts-de-France Regions cooperate to improve risk management related to ground movements due to underground cavities. Due to similar geologic context and industrial history, both territories host similar cavities (natural or anthropic). These cavities induce a potential threat for the population or the infrastructures in terms of ground stability. However, the risk management is different in the two border regions because of distinct national or regional politic strategies. Furthermore, the tools that are used on both sides of the border need to be upgraded. For these reasons, the RISSC project has emerged in order to provide common and better tools for the prevention and the management of cavity-related ground movement issues.

Thanks to the cooperative work of several cross-border experts, RISSC achieves concrete results through three main work actions:

- 1) Inventory of the cavities and the threats, and characterization of the possible consequences at the surface;
- 2) Development of local solutions to monitor or even reduce the risk;
- 3) Supply of technical assistance for local actors and population through the creation of useful tools and sources of information.

Inventory and characterization

Inventories of underground cavities have been established on both sides of the border. Cross-check of these information allows to propose common typology and description of the cavity types. The possible threats they represent need to be assessed, namely through physical data. Several test sites were chosen and works have been conducted on site and in laboratory by actors of the RISSC project. Investigations lead to effective characterization of rock masses. Figure 1 illustrates a geo-mechanical map established on the site of La Malogne quarry (Wallonia). This analysis feeds the numerical models that are developed to assess the stability of cavities.

This work axis also aims to compare and improve existing methodologies for the evaluation of ground movement hazard (Kheffi and Pacyna, 2018; Ineris, 2012). The methods are applied on different sites across the border where ground movements represent a risk., and hazard mapping are built. Furthermore, compared accidents (collapse) analysis on both territories can be carried out in order to understand the mechanisms and the context that favour collapsing events. This approach is very important for the improvement of risk management politics.

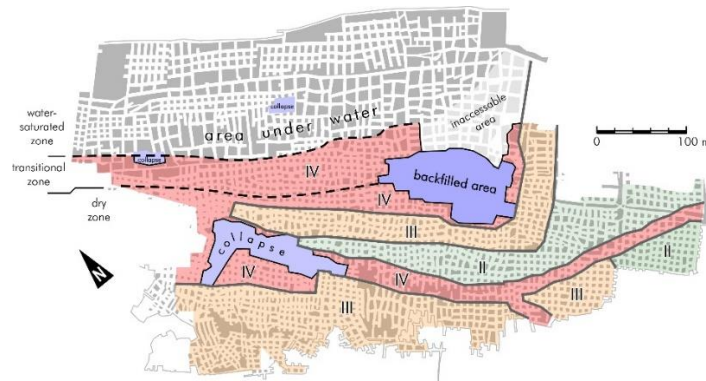


Figure 1. Definition of geo-mechanical zones on the test-site of La Malogne, ancient quarry (Belgium): II - Good rock mass quality; III – Fair rock mass quality, IV – Poor rock mass quality; and collapsed areas (Georgevia et al., 2020).

Local solutions for monitoring and reducing the risk

In this part of the project, the different techniques used for risk management (monitoring and securing) are addressed. Some of them are tested on pilot sites. This axis of the research aims to provide suitable solutions for specific contexts in terms of geology, type of cavity (shape and size), etc. Alternative solutions, as touristic valorisation, are also explored.

Technical support

This part of the project has, as main objective, to create an effective cross-border interaction between public services, local authorities and actors, experts and population. Through the lessons learned from the various technical works driven by the RISSC project, useful tools ought to be created (geo-portal, methodology guides, practical information, ...). Those tools will support the work of all the actors implied in the cavity risk management who should be included in a cross-border network created on the initiative of the RISSC project.

Acknowledgements

The authors thank the European Found for Regional Development (FEDER), through the Interreg V FWVI program, and Wallonia for funding the research.

References

- Georgieva, T., Descamps, F., Vandycke, S., Ajdanlijsky, G., Tshibangu, JP. (2020). Caractérisation géomécanique d'une carrière souterraine abandonnée par des méthodes in-situ. Journées Nationales de Géotechnique et Géologie de l'Ingénieur, Lyon, 2020.
- Kheffi A., Pacyna D. (2018). Elaboration de cartographies de zones d'aléas de mouvement de terrain engendrés par les objets souterrains connus de Wallonie – Rapport méthodologique, Département de l'Environnement et de l'Eau (DGO3), 0326/2018.
- Ineris, DGPR (Ministère de l'Ecologie, du Développement durable et de l'Energie), 2012. Plan de Prévention des Risques Naturels. Guide méthodologique : cavités souterraines abandonnées.

Sedimentary processes inside the Han-sur-Lesse Cave (Belgium)

Olivier FONTAINE¹, Sabine BLOCKMANS², Romain DELEU², Vincent HALLET², Amaël POULAIN³, Gaëtan ROCHEZ², Jean VAN CAMPENHOUT⁴, Geoffrey HOUBRECHTS⁴.

1. *Université Libre de Bruxelles, Bruxelles, Belgium (olivier.fontaine @ulb.be)*

2. *Université de Namur, Namur, Belgium (sabine.blockmans@unamur.be, romain.deleu@unamur.be, vincent.hallet@unamur.be, gaetan.rochez@unamur.be)*

3. *Traqua, Namur, Belgium (ap@traqua.be)*

4 *Université de Liège, Liège, Belgium (g.houbrechts@uliege.be, jean.vancampenhout@uliege.be)*

Located in Global UNESCO Geopark “Famenne-Ardenne”, the Han-sur-Lesse cave has been investigated for many years for its scientific interests in terms of karstic processes, speleothem growths, vault collapsing in link with earthquakes, Holocene deposits, ... but no research, that concern the current sedimentation, was done inside the cave.

However, during floods, huge quantities of sediments are depositing in some karstic chambers and covers long sections of the touristic footpaths that have to be cleaned several times per year. Despite the huge investment in footpath floor washing operations, no investigation was done to try to quantify and understand the current sedimentation processes inside the cave.

From the Belvaux sinkhole to the Trou de Han resurgence, the underground Lesse river is a complex network consisting of several subterranean rivers stretches that connect flooded areas. Inside the cave, three different flow paths can be, successively, activated according to the Lesse’s yields; over 25 m³/s the Belvaux sinkhole is saturated and the Lesse overflows in its open-air meander (Bonniver, 2011).

According to Van Campenhout & al. (in press), the annual solid discharge of suspended sediment, that enters the cave, may be estimated around 10,000 T/year.

As sedimentation is very fluctuant through the karst, going from large growing dunes in chambers to no sedimentation in narrow and siphoning zones, observations were conducted inside the main cave chambers that are (from upstream to downstream): “Daniel Ameye”, “Synanthrope”, “Armes”, “Draperie” and “Embarquement” chambers (figure 1).

In order to identify sediment sources and sediment path, sedimentological characterizations are done combining macroscopic observations, grain-size analyses, calcimetry and organic matter loss of ignition. First results show that: carbonate minerals are less than 1.5 %; organic matters (branches and leaves) can reach close to 100 %; several sedimentary sequences, due to organic matter variations, are observed on a yearly basis (figure 2); stygophile worms are very frequent and can disturb the sediment deposits; and clayey boulders are observed at several places probably in link with desiccation cracks.

Recent observations seem to indicate, on a long-term basis, an accumulation of sediments inside the cave. Together with sedimentation plates, they indicate that sediment accumulation is an ongoing process in certain places of the cave.

References

- Bonniver I., 2011. Caractérisation hydrogéologique et dimensionnement de systèmes karstiques par modélisation d’essais de traçage. Application au massif de Boine à Han-sur-Lesse. PhD Thesis. UNamur. Department of geology. 349 p.
- Van Campenhout J., Petit F., Peeters A., Houbrechts G., in press. Estimation of the area-specific suspended sediment yield from discrete samples in different regions of Belgium. *Journal of Soils and Sediments*.

Figures

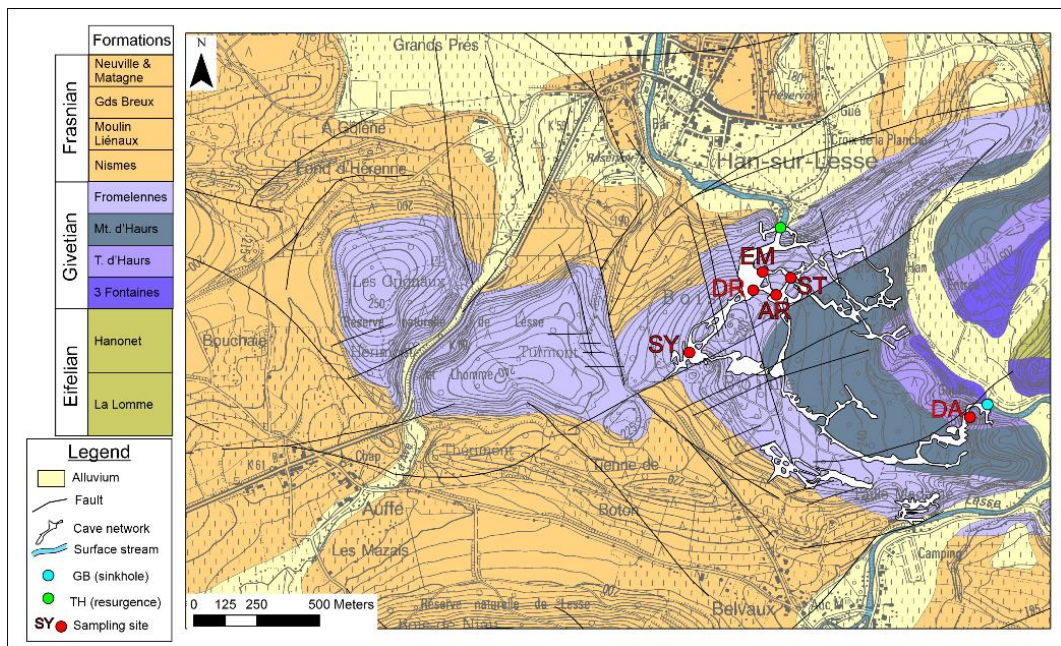


Fig 1 : Location map of the Han-sur-Lesse cave (modified from Bonniver, 2011).

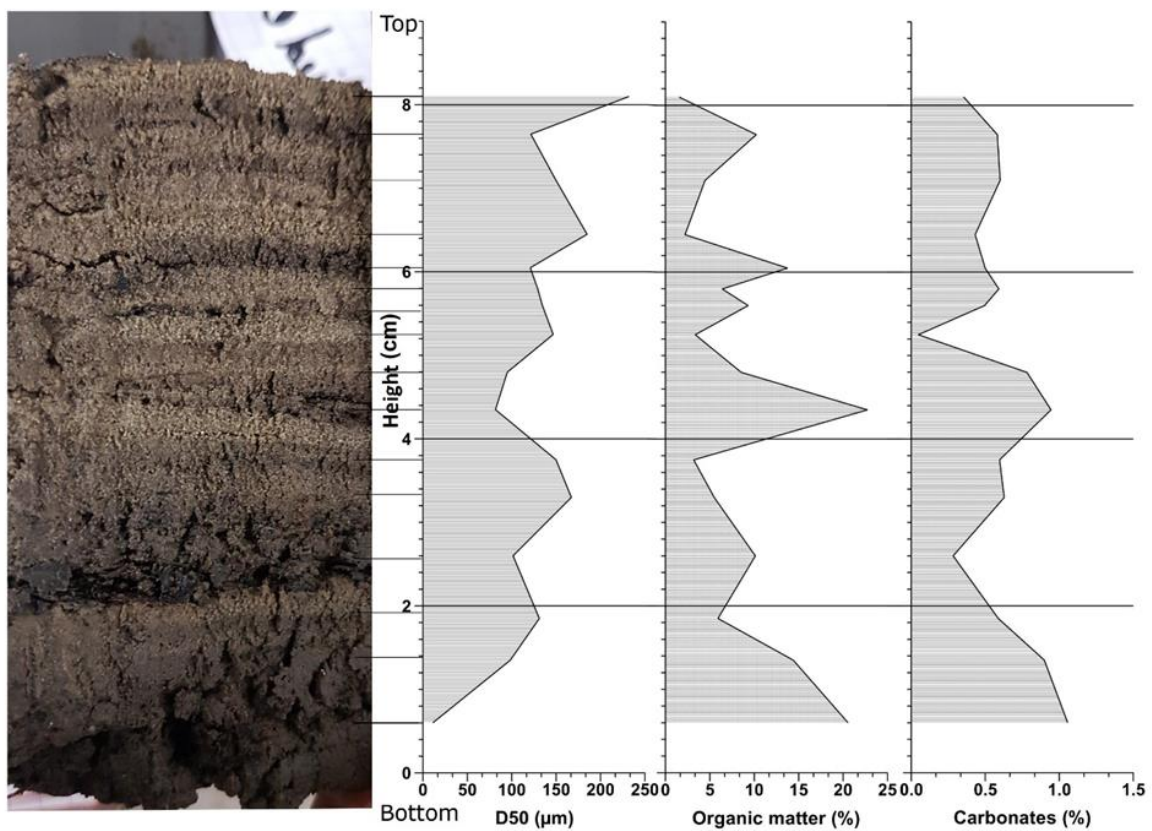


Fig 2: Sediment caractérisation of the Draperie cave's deposit

State of knowledge on Kongo Central karst, DRC

Pascale LAHOUE¹, Ange THIJENIRA²

1: *Royal Museum for Central Africa, Tervuren, Belgium*

2: *University of Kinshasa, Kinshasa, DRC*

Although knowledge of karst is of great importance both in terms of water resources and the risks it can generate for populations and infrastructures, it is currently little studied in the DRC from a geoscientific point of view. The GeoRes4Dev project, funded by Belgian cooperation, notably made it possible to award DEA and doctoral scholarships to geologists from the DRC and the Republic of Congo with the aim of increasing their capacities in the study of the Karst. This work is currently being carried out within the framework of this project. Karst *sensus stricto* develops in carbonate rocks. These are present in certain regions of the DRC, including in particular the urbanized areas of Lubumbashi (Haut-Katanga), Kisangani (Tshopo), Mbuji-Mayi (Kasai oriental), Kimpese and Mbanza-Ngungu (Kongo-Central). Our Karst study began in the latter region, the most accessible in a country where travel is often slow and expensive. In Kongo-Central, carbonate rocks are part of the Neoproterozoic Schisto-Calcaire subgroup that extends from southwest Gabon to northwest Angola over 1400 km. In the DRC, they cross the province from north to south over a width of up to 150 km. The different layers of this system are subhorizontal, the total thickness of carbonate rocks can reach more than 1000 m. The caves of this region have been widely described by biologists and archaeologists as the living environment of endemic species or ancient populations which have left vestiges of life there, but the study of karst as such has been generally limited to the exploration of a few speleologists or occasional visits from geoscientists. The most recent inventory of karst cavities in the DRC was published by Shaw in 2013 on the basis of a bibliographic review. It is fairly complete, but the location and description of the sites by the various authors, often old, are not very precise and the data have not been checked in the field. Indeed, in addition to the imprecision of location and description, a cave may have received different names and the same name has sometimes been assigned to different cave, which makes the unique identification of a cave is quite difficult.

As part of our work, following the compilation of data from bibliographic sources, information's obtained from local scientists, observations on satellite images and new field work, we have today arrived at a compilation of 150 caves in the Kongo-Central, some of which may however still be redundant. Only about 90 of them could be located with varying degrees of precision and of these, 11 were topographed. These figures are obviously provisional as the work is currently continuing. The longest known cave has nearly 10 km of galleries. Caves generally develop in a subhorizontal way, on 2 or 3 levels. The passages can be narrow but some caves have large multi-decametric rooms with speleothems beautiful enough to be of touristic interest. The observation of satellite images greatly contributed to the location of the sites but it also made it possible to highlight the presence of numerous geomorphological forms (sinkholes, losses, resurgences, etc.) which could be potential accesses to the endokarst. This region, still very partially explored, has great potential for discovering caves and a more exhaustive inventory, coupled with a more systematic underground topography, should serve as a basis for understanding both their development and the hydrogeological networks that use them and which constitute the region's water resources. It can also serve as a base for finding sites of interest to biologists and archaeologists working in the area

Shaw J.G., 2013. Caves of the Democratic Republic of the Congo: Exploration, science and history. Berliner Höhlenkundliche Berichte Band 53, 152p.

Origin of the collapse sinkholes of the Boukadir region (Chelif-Algeria)

Meriem Lina MOULANA^{1&2}, Aurélie HUBERT¹, Mostefa GUENDOZ², Camille EK¹ & Bernard COLLIGNON³

- 1. Department of Geography, University of Liege, Quartier Village 4, clos Mercator 3, 4000 Liège, Belgium, ml.moulana@student.ulg.ac.be (corresponding author), aurelia.ferrari@uliege.be & camille.ek@uliege.be*
- 2. Faculty of Earth Sciences, Geographical and Territorial Planning, University of Science and Technology Houari Boumediene, (USTHB), El Alia, BP 32, Bab Ezzouar, 16111 Algiers, Algeria, mguendouzdz@yahoo.fr*
- 3. Hydroconseil, 198, chemin d'Avignon - 84 470 Chateauneuf de Gadagne – France, collignon@hydroconseil.com*

Algeria offers a large variation of karstic landscapes (Collignon, 1991). This study focuses on the Messinian carbonate platform outcropping in the northern piedmont of Ouarsenis mountains and extending below the Chelif plain. Boukadir has not been classified as an Algerian karstic area. In June, 1988, in the region of Boukadir, northwestern Algeria, a large collapse sinkhole of 60 m in diameter and 35 m deep in the Chelif plain and it broke the national road RN4. This collapse sinkhole suggests that there were large underground cavities under the Quaternary alluvium, at an altitude near or lower than the present sea level. In the piedmont, there is another large collapse sinkhole perched high up called "Bir el Djeneb". Our aim, is to analyse the processes that lead to the formation of these sinkholes, using geological, speleological, and geomorphological data.

The Ouarsenis piedmont is made up of 3 main geological units. The basal Tortonian to Messinian blue marls are overlain by a 70 m thick bioclastic carbonate unit, and thereupon by 80 m of homogeneous Lithothamnium carbonate packstones (Neurdin- Trescartes, 1992; Moulana et al., 2021). A drill hole S1 was made in the Chelif plain, and it reveals that the same carbonates outcrop at 61 m depth under the plain. The cross-section based on 6 mechanical drill cores (Scet-Argi, 1985) parallel to the piedmont (Fig.1.a), highlight a 70 m deep incision in the carbonate at the level of the present river Oued Taflout, filled by a basal 35 m thick light brown clay unit with some gravels, then by a 30 m thick alluvium composed pebbles and gravels. The speleological analyses are based on Birebent (1947) evidenced five caves. The most considerable karstic feature is Bir Djeneb, a cylindrical pit about 20 m in diameter and 63 m deep, located 5.5 km SW of Boukadir. It is dug mostly in unconsolidated sediments with carbonates outcropping at its base (Fig. 1. b). Geomorphological analyses show a well-developed hydrological network on the carbonate piedmont, the lack of sinkholes and poljes, an important fracture/fault network and the occurrence of shelter caves at different levels attesting from the progressive incision of the drainage network.

The results show that an atypical karst with very minimal present-day surface weathering and deep active karstification. The development of a surface calcrete enhanced surface flow and the development of the hydrological network. The carbonate facies and pervasive vertical fractures still favours a diffuse infiltration, which reduced localized

dissolution and flow, and prevents the development of large caves. The endokarst is poorly developed whereas the epikarst is prevalent and characterized by shelter caves. The large voids deep below the present-day base-level are inferred to be a paleokarst related to the Messinian Salinity Crisis who lowered the Mediterranean Sea level. However, the link of Bir Djeneb with the MSC, is not evident. The genetic relation of the two holes thus remains problematic.

References

- Birebent, J. 1947. Spéléologie de l'Algérie : Inventaire. Agence National des Ressources Hydraulique. Alger, le 1er Décembre 1947. Rapport.
- Collignon, B. 1991. Les principaux karsts d'Algérie. Quelques éléments de synthèse, actes du 9ème Congrès National de la SSS., Akten des, 9.
- Moulana, M. L, Hubert-Ferrari, A. Guendouz, M. El Ouahabi, M. Boutaleb, A. & Boulvain, F. 2021. Contribution to the sedimentology of the Messinian Limestones of Boukadir (Chelif 2 Basin-Algeria). *Geologica Belgica*.
- Neurdin-Trescartes, J. 1992. Le remplissage sédimentaire du bassin néogène du Chelif, modèle de référence de bassins intramontagneux (Doctoral dissertation, Pau).
- Scet – Argi. 1985. Hydrologie – Hydrogéologie et bilan des ressources, Etude du réaménagement et de l'extension du périmètre du moyen Chélif : Rap A1.1. 2. Pub. Ministère de l'Hydraulique. 72 p.

Figures

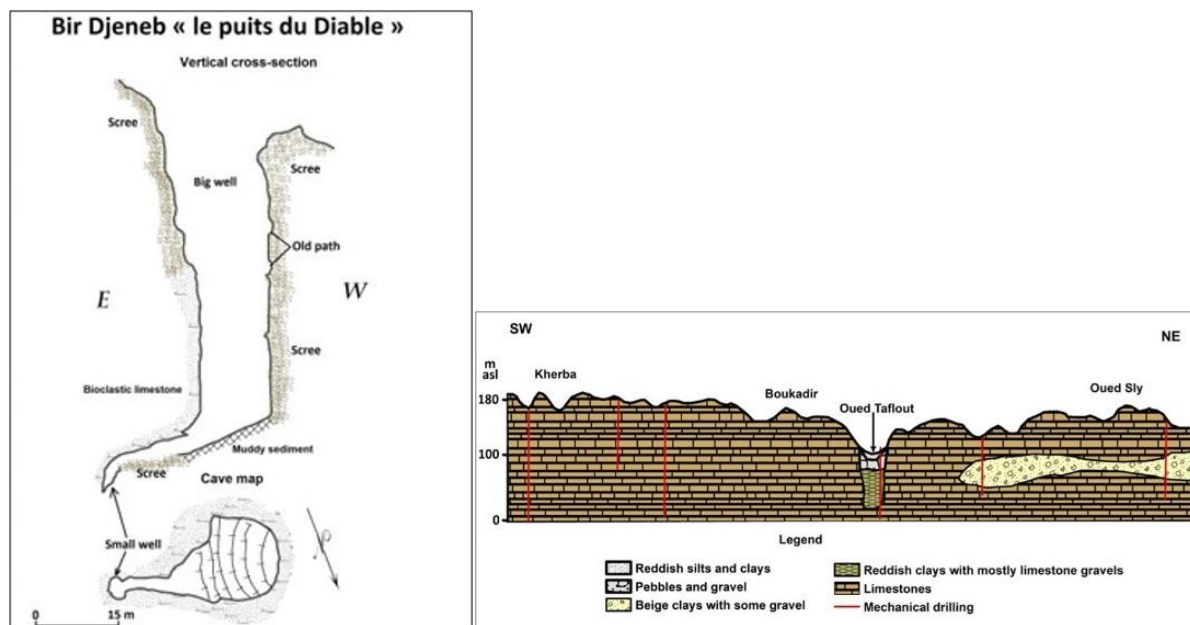


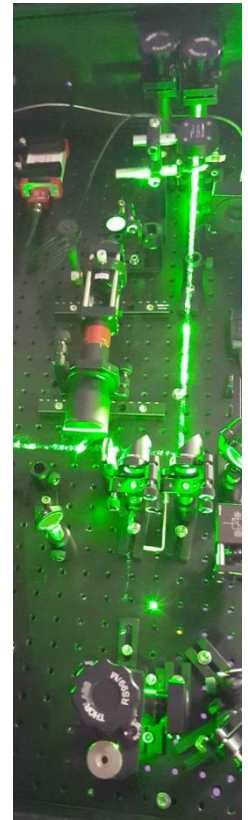
Figure 1. a. Map and cross-section of Bir Djeneb cave, northern Ouarsenis piedmont; after BIREBENT, 1947, modified. b. Reinterpreted geological cross-section based on 6 mechanical drill cores parallel to the piedmont and across Oued Tafkout (Scet-Argi, 1985). The section shows a ~ 70 m deep Messinian incision at the location of Oued Tafkout filled first by ~40 m of clay and then by coarser alluvial deposits.

Session 8- New Spectroscopic Methods in Geosciences

Conveners:

Jean-Marc Baele (UMons), Sophie Decrée (RBINS-GSB)

The technological advances of the last decades open new opportunities for geoscientists to solve a wide range of geological problems. Besides the emergence of new techniques such as LIBS (Laser-Induced Breakdown Spectroscopy), LAMIS (Laser-Ablation Molecular Isotopic Spectroscopy), PIL (Plasma-Induced Luminescence) and THz (Terahertz) spectroscopy, the increased availability and improved performance of radiation sources, detectors and spectrometers have brought more traditional techniques such as electron microscopy, X-ray and Raman spectroscopy to the next level. With these techniques, large geochemical and mineralogical datasets can be quickly acquired and with minimal efforts, which fosters the development of imaging and screening applications. In this session, we encourage any contribution on the application of new spectroscopic methods in geosciences, emphasizing their benefits, complementarity with other well-established techniques, but also their limitations.



High-resolution Raman mapping: using micro-analyses to reveal geological processes

Fernando P. ARAUJO^{1*}, Niels HULSBOSCH^{1,2}, Philippe MUCHEZ¹

1. *KU Leuven, Department of Earth and Environmental Sciences, Division of Geology. Celestijnenlaan 200E - Box 2410, 3001 Leuven, Belgium (*corresponding author: fernando.pradoaraujo@kuleuven.be)*

2. *Wetenschappelijk en Technisch Centrum voor het Bouwbedrijf. Avenue Pierre Holoffe 21, 1342 Limelette, Belgium*

Pegmatite deposits are an exploration frontier for some of the elements required to a transition towards greener and digital technologies. Critical raw materials such as lithium, niobium, and tantalum are commonly associated with pegmatites (Linnen et al., 2012). However, these deposits are frequently hosted by complex mineral assemblages (Galliski et al., 2019; Hulsbosch and Muchez, 2020; Kaeter et al., 2021), and some minerals within these assemblages cannot be straightforwardly analyzed by conventional analytical methods (e.g. XRD, XRF, EPMA, LA-ICP-MS).

Conventional methods are not ideal to analyze complex assemblages due to their lack of spatial resolution (i.e. bulk analyses), their difficulty to detect light elements (e.g. lithium and/or hydrogen) or elements with variable oxidation state (e.g. Fe and Mn) in the mineral structures, or because of problems with matrix matching and standardization. Conversely, Raman spectroscopy overcomes many of those problems allowing the direct analysis of complex minerals (Rondeau et al., 2006; Watenphul et al., 2016) with little to no previous sample preparation. Recent developments of hard- and software capacities have improved the potential of confocal Raman spectroscopy, allowing the fast measurement of Raman spectra (< 1s) with high spectral and spatial resolutions. Due to these technical advancements, we are now able to collect Raman images in realistic acquisition times at low user costs. Therefore, a new set of tools is available to obtain high-quality analyses of textural and molecular data and to investigate complex mineral assemblages in situ (Araujo et al., 2021).

The crystallization of the Buranga pegmatite will be used to show how Raman mapping can illustrate complex geological processes. The Buranga pegmatite is a phosphorus-rich and Nb-Ta-Sn-mineralized magmatic dike from western Rwanda, mostly known for its intricate phosphate mineralogy (Daltry and von Knorring, 1998; Fransolet, 1975). High-resolution Raman mapping is used to (1) highlight different members in solid solutions (amblygonite [LiAlPO₄F] - montebrasite [LiAlPO₄OH], Figure 8A); (2) investigate the textural relations in complex mineral assemblages showing multiple phosphate minerals; and (3) support the characterization of Nb-Ta oxide minerals within these complex assemblages (Figure 8B). Raman mapping can accurately detect textures and mineralogical changes in complex mineral assemblages with high spatial resolution. Moreover, Raman images can be used to spatially constrain chemical variations within some mineral phases. Most of the minerals determined could not be unambiguously identified by other methods (optical microscopy and EPMA), and could not be separated for bulk analyses (XRD or XRF), highlighting the strong potential of Raman spectroscopy for this type of study.

The recognition of complex mineral phases formed during the crystallization of pegmatitic melts is essential to unravel the petro-metallogenesis of pegmatites and to identify the geological processes taking place. This brings us closer to understanding some of the natural processes occurring on Earth and elucidates the way that some critical raw materials ore deposits have formed.

References

- Araujo, F.P., Hulsbosch, N. & Muchez, P., 2021. High spatial resolution Raman mapping of complex mineral assemblages: Application on phosphate mineral sequences in pegmatites. *J. Raman Spectrosc.* 52, 690–708. <https://doi.org/10.1002/jrs.6040>
- Daltry, V.D.C. & von Knorring, O., 1998. Type-mineralogy of Rwanda with particular reference to the Buranga pegmatite. *Geol. Belg.* 1, 9–15.
- Fransolet, A.-M., 1975. Etude minéralogique et pétrologique des phosphates de pegmatites granitiques. Fascicule I: Texte. PhD Thesis. University of Liège.
- Galliski, M.Á., Márquez-Zavalía, M.F., Škoda, R., Novák, M., Čopjaková, R. & Pagano, D.S., 2019. A Ta,Ti-rich oxide mineral assemblage from the Nancy beryl–columbite–phosphate granitic pegmatite, San Luis, Argentina. *Mineral. Petrol.* <https://doi.org/10.1007/s00710-019-00673-z>
- Hulsbosch, N. & Muchez, P., 2020. Tracing fluid saturation during pegmatite differentiation by studying the fluid inclusion evolution and multiphase cassiterite mineralisation of the Gatumba pegmatite dyke system (NW Rwanda). *Lithos* 354–355, 105285. <https://doi.org/10.1016/j.lithos.2019.105285>
- Kaeter, D., Barros, R. & Menuge, J.F., 2021. Metasomatic High Field Strength Element, Tin, and Base Metal Enrichment Processes in Lithium Pegmatites from Southeast Ireland. *Econ. Geol.* 116, 169–198. <https://doi.org/10.5382/econgeo.4784>
- Linnen, R.L., Van Lichtervelde, M. & Černý, P., 2012. Granitic pegmatites as sources of strategic metals. *Elements* 8, 275–280. <https://doi.org/10.2113/gselements.8.4.275>
- Rondeau, B., Fritsch, E., Lefèvre, P., Guiraud, M., Fransolet, A.-M. & Lulzac, Y., 2006. A Raman investigation of the amblygonite-montebbrasite series. *Can. Mineral.* 44, 1109–1117. <https://doi.org/10.2113/gscanmin.44.5.1109>
- Watenphul, A., Burgdorf, M., Schlüter, J., Horn, I., Malcherek, T. & Mihailova, B., 2016. Exploring the potential of Raman spectroscopy for crystallochemical analyses of complex hydrous silicates: II. Tourmalines. *Am. Mineral.* 101, 970–985. <https://doi.org/10.2138/am-2016-5530>

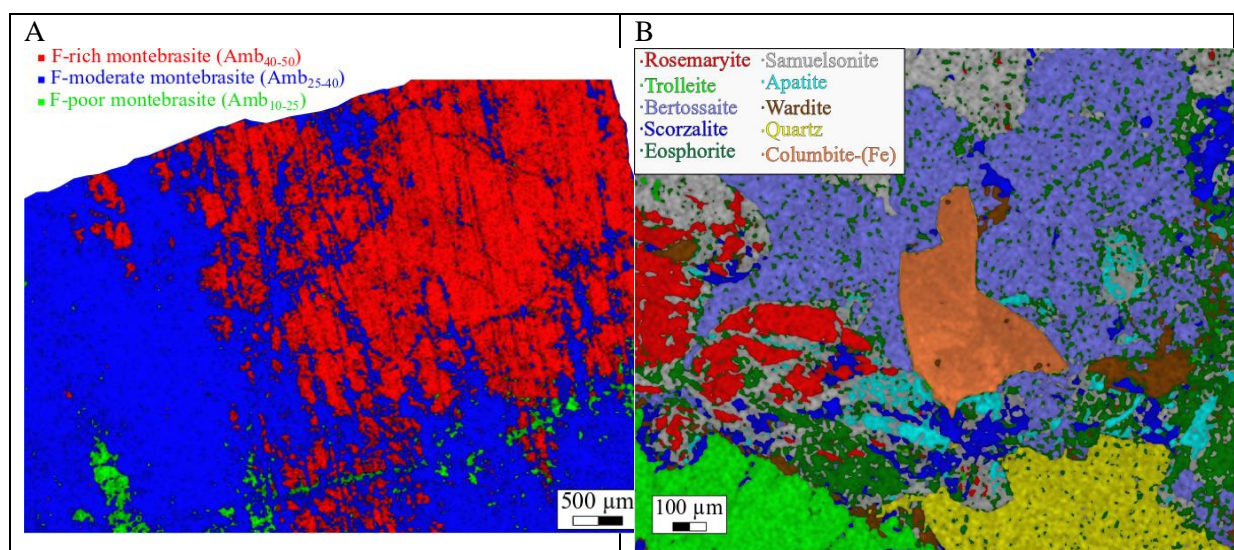


Figure 8. Raman maps of phosphate mineral assemblages from the Buranga pegmatite, Rwanda. (A) Raman map showing the alteration of primary F-rich montebbrasite by secondary F-moderate and F-poor montebbrasite. Modified from Araujo et al. (2021). (B) Raman map showing a columbite grain associated with secondary phosphates in an alteration pod within rosemaryite, a primary phosphate.

Combined Laser-Induced Breakdown Spectroscopy (LIBS) and Plasma-Induced Luminescence (PIL) for geochemical mapping and profiling of geological samples

Jean-Marc BAELE¹, Séverine PAPIER¹, Lorraine DEWAIDE², Joris CORON¹, Anne-Christine DA SILVA³, Vincent HALLET², Rudy SWENNEN⁴ and Vincent MOTTO-ROS⁵

1. *Geology and Applied Geology - Faculty of Engineering, University of Mons, Mons, Belgium (jean-marc.baele@umons.ac.be)*
2. *Geology, University of Namur, Namur, Belgium & ISSeP, Colfontaine, Belgium (lorraine.dewaide@unamur.be)*
3. *Geology, Faculty of Sciences, University of Liège, Liège, Belgium (ac.dasilva@uliege.be)*
4. *Geology, KU Leuven, Leuven, Belgium (rudy.swennen@kuleuven.be)*
5. *Institut Lumière Matière, University Claude Bernard Lyon 1, Lyon, France (vincent.motto-ros@univ-lyon1.fr)*

Laser-Induced Breakdown Spectroscopy (LIBS) allows to obtain elemental composition of a variety of materials through the interaction of high-power laser light with matter. Several physical processes take place when a laser pulse with sufficient energy to induce a breakdown and ignite a plasma is focused on the surface of a solid sample. First, radiative de-excitation of the plasma species (ions, atoms and molecules) results in a series of optical emissions combined into a spectrum which allows to obtain the elemental composition of the sample. Second, de-excitation of the luminescence centres in the material influenced by plasma radiation produces an optical emission recently recognized as Plasma-Induced Luminescence (PIL; Gaft et al., 2011). Both LIBS and PIL emissions coexist but the weaker PIL is masked by the intense LIBS emission, so only longer-lived PIL emissions are detectable when plasma has cooled down to ambient (i.e., ~ 100 µs after the laser has been fired).

Combining PIL with LIBS just requires a dedicated detector set to a specific delay and integration times, which are usually longer than for LIBS, and operates in parallel with the LIBS detector. A first advantage is that luminescence provides additional information to the elemental/molecular data collected by LIBS, including the detection of elements below the detection limit of LIBS (Gaft et al., 2019). A second advantage is that luminescence activators (similar to the well-known activators in e.g., cathodoluminescence) can be investigated as simultaneous LIBS analysis can be performed. So far, Mn²⁺ and rare-earth elements have been identified as PIL activators in an orange-luminescent calcite from Lompret Quarry, Frasnian (Figure 1) and a green-luminescent calcite from Furfooz, Waulsortian, respectively. In both cases, the images obtained with cathodoluminescence and PIL are comparable, except that PIL also includes some photoluminescence. As photons with a variety of wavelengths and possibly X-rays (and electrons?) from the plasma contribute together to the excitation of luminescence centres, laser-induced plasmas are a broader, but less selective excitation source. The possibility of gating PIL could improve selectivity of luminescence centres based on their specific decay time, though.

Just as importantly, with the ability of laser sources to fire at high repetition rates (Hz to kHz), PIL emission can be recorded along with elemental data across large surfaces or on a large number of hand samples for a period of time that is significantly reduced compared to other techniques (XRF, EDS, etc.) This allows to obtain elemental and luminescence images of large samples that could not fit within typical cathodoluminescence or SEM chambers and with minimal preparation (no polishing, no coating required). In addition, luminescence and geochemical profiles can be obtained from sample sets collected along geological sections for correlation or cyclostratigraphic applications. Preliminary results from Cretaceous chalk

(Mons Basin, Belgium) and Devonian carbonate/siliciclastic records (New York State, U.S.A.) show good consistency between LIBS and XRF profiles, and between PIL and Mn or Ca composition (Figure).

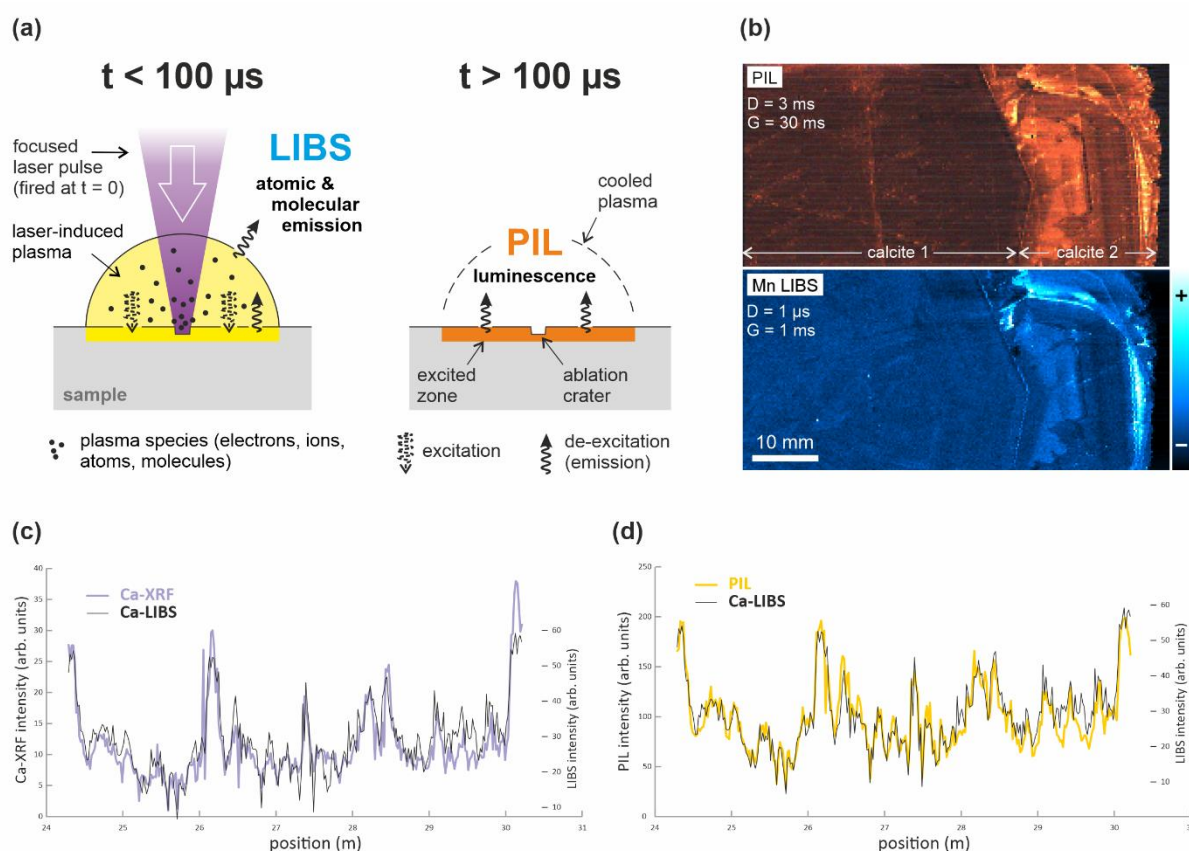


Figure 1. (a) principle of LIBS and PIL. Both optical emissions result from the same laser pulse but are recorded with a different timing. (b) 250 μm -resolution PIL image in real colours of a large calcite monocrystal with two syntaxial generations, and corresponding LIBS map in false colours for Mn (Lompret, Belgium). The similarity between the PIL image and Mn distribution suggests Mn^{2+} as a luminescence activator. D : integration delay, G : integration (gate) time. (c) comparison between Ca signals as measured by XRF and LIBS for a 6 m-thick Devonian carbonate/siliciclastic section. (d) same as (c) with PIL and Ca-LIBS.

References

- Gaft, M., Nagli, L. & Groisman, Y., 2011. Plasma induced luminescence (PIL). *Optical Materials*, 34, 368-375.
- Gaft, M., Raichlin, Y., Pelascini, F., Panczer, G. & Motto-Ros, V., 2019. Imaging rare-earth elements in minerals by laser-induced plasma spectroscopy: Molecular emission and plasma-induced luminescence. *Spectrochimica Acta Part B*, 151, 12-19.

The ROBOMINERS LIBS spectrometer: a mining sensor prototype for autonomous in-stream, in-slurry geochemical diagnostics

Christian BURLET¹, Giorgia STASI¹, Tobias PINKSE², Claudio ROSSI³

1. *Royal Belgian Institute of Natural Sciences – RBINS, Belgium.*
(cburlet@naturalsciences.be, gstasi@naturalsciences.be),
2. *K-UTEC AG Salt technologies -Sondershausen, Germany* (tobias.pinkse@k-utec.de)
3. *Escuela Técnica Superior de Ingenieros Industriales de Madrid-UPM, Centre for Automation and Robotics (CSIC), Madrid, Spain* (claudio.rossi@upm.es)

The ROBOMINERS project

ROBOMINERS (Bio-Inspired, Modular and Reconfigurable Robot Miners, Grant Agreement No. 820971, <http://www.robominers.eu>) is a European project funded by the European Commission's Horizon 2020 Framework Programme. The project brings roboticists and geoscientists together to explore new mining and sensing technologies and demonstrate a small robot-miner prototype designed to exploit unconventional and uneconomical mineral deposits (technology readiness level 4 to 5). This approach could change the current mining paradigms dictated by larger existing machines, while reducing mining waste and environmental footprint (Lopez and al. 2020).

ROBOMINERS selective mining ability

One of the key functions of ROBOMINERS is “selective real-time” mining, in other words the ability for the miner to choose an optimal progression path while mining in a particular orebody geometry (inspired by the petroleum industry geo-steering technique). This will be done by a continuous monitoring of the surrounding rock properties (hardness, abrasivity, electrochemistry, thermal conductivity, 3D electrical/induced polarization tomography), and by a “digestive mineralogy” unit, performing on-board mineralogical/geochemical diagnostics of the extracted material.

After an extensive review and tests on existing geochemical sensing techniques, the consortium selected a few sensing methods, based on the considered environment (underground gallery drilling, mud/slurry-filled environment with very limited to no visibility) and the opportunity to test proven techniques as well as original methods that can be distributed on and in the miner body. Amongst these are X-Ray fluorescence spectrometry, Laser-induced fluorescence spectrometry, near and mid-infrared reflectance spectrometry and laser-induced breakdown spectrometry.

ROBOMINERS LIBS spectrometer and preliminary lab results

Laser-induced breakdown spectrometry (LIBS) is a very interesting atomic emission technique for real-time monitoring of slurries. The technique uses a high-energy pulsed laser beam on the surface of a sample to produce a plasma. The plasma emission is then collected and coupled into a spectrometer for analysis to identify and quantify the chemical elements in the sample (Fabre, 2020). LIBS have many attractive features, such as fast multi-element detection, simple or no sample preparation, and low detection limits, even on light elements. It has been already used as a competitive approach to monitor slurries using flow cells in mining (Khajehzadeh et al., 2017) and inside molten metals in metallurgy applications (Moreau et al., 2018). While true quantitative measurements remain a challenge outside a

controlled lab environment, qualitative and semi-quantitative measurements are possible and is very relevant for ROBOMINERS selective mining application.

The work presented here deals with the conceptualization and prototyping of a slurry LIBS spectrometer, optimized for robotized and in-stream, in-slurry operation. We compare the performances of two candidate designs, one based on a fast-repetition, mid-energy fiber laser (1mJ/pulse@1064nm, 10KHz) and the other on a high energy compact diode pumped laser (50mJ/pulse@1064nm, 20Hz), both associated with simple, compact, and ruggedized optics and spectrometers. Tested slurry analogs include mixtures of lead-zinc sulfides, copper-cobalt oxides, phosphorites and oil shales. First results show very good characterisation capacity of both setups, with detection limits below 0.1% on most target elements, with an advantage of the high energy pulse setup for deep UV emissions (ex: Phosphorus detection) at the expense of ruggedness and flexibility.

Once an instrumental setup is selected, the next development steps include retrofitting for testing in an industrial scale slurry circulation system at the K-UTEC facilities (Sondershausen, Germany) and, after validation of all components, integration on the ROBOMINERS prototype for the field demonstrations planned in 2023.

References

- L. Lopes, B. Bodo, C. Rossi, S. Henley, G. Žibret, A. Kot-Niewiadomska, V. Correia, ROBOMINERS – Developing a bio-inspired modular robot-miner for difficult to access mineral deposits, *Advances in Geosciences*, Volume 54, 2020, 99–108
- C. Fabre, *Advances in Laser-Induced Breakdown Spectroscopy analysis for geology: A critical review*, *Spectrochimica Acta Part B: Atomic Spectroscopy*, Volume 166, 2020, 105799
- N. Khajehzadeh, O. Haavisto, L. Koresaar, On-stream mineral identification of tailing slurries of an iron ore concentrator using data fusion of LIBS, reflectance spectroscopy and XRF measurement techniques, *Minerals Engineering*, Volume 113, 2017, pp 83-94
- A. Moreau, A. Hamel, P. Bouchard, and M. Sabsabi, Laser-induced breakdown spectroscopy of molten matte, *CIM Journal*, Volume 9, No. 2, 2018

Unravelling the genesis of critical mineral resources by employing advanced imaging techniques

Florian BUYSE^{1,4}, Stijn DEWAELE², Matthieu BOONE^{3,4}, Frederic VAN ASSCHE^{3,4}, Veerle CNUUDE^{1,4,5}

- 1. Pore-Scale Processes in Geomaterials Research group (PProGress), Department of Geology, Ghent University, Krijgslaan 281/S8, B-9000 Ghent, Belgium (florian.buysse@ugent.be)*
- 2. Laboratory for Mineralogy and Petrology, Department of Geology, Ghent University, Krijgslaan 281/S8, B-9000 Ghent, Belgium*
- 3. Radiation Physics Research Group, Department of Physics and Astronomy, Ghent University, Proeftuinstraat 86/N12, B-9000 Ghent, Belgium*
- 4. Centre for X-ray Tomography (UGCT), Ghent University, Proeftuinstraat 86, B-9000 Ghent, Belgium*
- 5. Environmental Hydrogeology, Department of Earth Sciences, Utrecht University, Princetonlaan 8a, 3584 CB Utrecht, The Netherlands*

Ore deposit research conventionally relies on macroscopic and microscopic two dimensional (2D) observations of hand specimens and thin/polished sections. Microanalytical techniques are used to characterize the chemical and structural variations of millimeter- to centimeter-sized samples with a spatial resolution down to micrometer scales (Pearce et al., 2018). Microscopic observations are hereby often limited to 2D techniques, such as optical microscopy and scanning electron microscopy (SEM), assisted by mineralogical and chemical analyses (e.g. X-ray diffraction (XRD) and X-ray fluorescence (XRF)). Although these 2D techniques are well-known and commonly used for the characterization of geological samples, they are not capable of reproducing the real three-dimensional (3D) interior (Wang & Miller, 2020). As a consequence, estimations based on these 2D analyses are not sufficiently informative to characterize complex mineral resources.

This urges the need for the development of new and innovative technologies for adequate ore characterization (Gessner et al., 2018; Sittner et al. 2020). Additionally, 3D characterization is crucial for improving the understanding of ore genesis (Godel, 2013). This is particularly applicable to petrological and genetic investigations of low-grade fine-grained ore deposits (Kyle & Ketcham, 2015).

We developed a methodology to investigate in 3D both detailed structural and chemical information of ores, which are almost impossible to collect by only using traditional microscopic techniques. Using lab-based non-destructive X-ray micro-computed tomography (μ CT) within a comprehensive methodology, we enable the 3D chemical and mineralogical characterization of ore samples.

We present a methodology to investigate the mineralogy of a pegmatite-hosted Sn-Nb-Ta-(W) mineralization of Gatumba (Rwanda) (Dewaele et al. 2011), where we address the spatial and temporal position of the ore minerals with respect to the gangue minerals. We demonstrate the acquisition of novel hyperspectral μ CT data to complement high resolution μ CT data. Hyperspectral μ CT enables us to chemically differentiate between cassiterite, columbite-tantalite and ferberite-hübnerite in 3D.

This methodology combines 2D traditional techniques and advanced 3D techniques to allow for a thorough understanding of the geology and genesis of ore deposits. These results will enable us to acquire important 3D microscopic insights into the formation history of

economically relevant ore deposits and positioning of the elements of value in the mineralization, having direct implications for their exploration.

References

- Dewaele, S., Henjes-Kunst, F., Melcher, F., Sitnikova, M., Burgess, R., Gerdes, A., Fernandez, M., De Clercq, F., Muchez, P. & Lehmann, B., 2011. Late Neoproterozoic overprinting of the cassiterite and columbite-tantalite bearing pegmatites of the Gatumba area, Rwanda (Central Africa). *Journal of African Earth Sciences*, 61(1), 10-26.
- Gessner, K., Blenkinsop, T. & Sorjonen-Ward, P., 2018. Characterization of ore-forming systems – advances and challenges. In Gessner, K., Blenkinsop, T. G. & Sorjonen-Ward, P. (eds), Geological Society, London, Special Publications, 453, 1-6.
- Godel, B., 2013. High-Resolution X-Ray Computed Tomography and Its Application to Ore Deposits: From Data Acquisition to Quantitative Three-Dimensional Measurements with Case Studies from Ni-Cu-PGE Deposits. *Economic Geology*, 108(8), 2005-2019.
- Kyle, J.R. & Ketcham, R.A., 2015. Application of high resolution X-ray computed tomography to mineral deposit origin, evaluation, and processing. *Ore Geology Reviews*, 65(4), 821-839.
- Pearce, M.A., Godel, B.M., Fisher, L.A., Schoneveld, L.E., Cleverley, J.S., Oliver, N.H.S. & Nugus, M., 2018. Microscale data to macroscale processes: a review of microcharacterization applied to mineral systems. In Gessner, K., Blenkinsop, T. G. & Sorjonen-Ward, P. (eds), Geological Society, London, Special Publications, 453, 7-39.
- Sittner, J., Godinho, J., Renno, A., Cnudde, V., Boone, M., De Schryver, T., Van Loo, D., Merkulova, M., Roine, A. & Liipo, J., 2020. Spectral X-ray computed microtomography: 3-dimensional chemical imaging. *X-ray Spectrom*, 50, 92-105.
- Wang, Y. & Miller, J.D., 2020. Current developments and applications of micro-CT for the 3D analysis of multiphase mineral systems in geometallurgy. *Earth-Science Reviews*, 211, 103406, 26 p.

New thermal data for the Rocroi inlier, France and Belgium, based on Raman Spectroscopy of Carbonaceous Material (RSCM)

Corentin COBERT¹, Jean-Marc BAELE¹ and Abdeltif LAHFID²

1. *Department of Geology and Applied Geology – University of Mons, B-7000 Mons, Belgium (corentin.cobert@umons.ac.be)*
2. *BRGM, 45060 Orléans, France*

The Rocroi inlier is composed of two main groups of Cambrian to Ordovician rocks. The sedimentary rocks of the Deville Group (Lower Cambrian, about 400 to 600 m thick) have a rather light color and were deposited in a shallow platform environment with numerous sandstone beds interlayered. The sedimentary rocks of the Revin Group (Middle to Upper Cambrian and Lower Ordovician, >1000 m thick) are dominated by dark schists and quartzites that were deposited in a deeper environment, with common turbiditic sequences.

The overall structure of the eastern part of the Rocroi inlier may be summarized as a wide syncline in its central part (Revin Group) bounded by two anticlines (Deville Group). Folds are E-W-trending, N-verging and sometimes overturned. Cleavage is dipping to the south in both the Lower Paleozoic rocks from the inlier and unconformably overlying Upper-Silurian/Devono-Carboniferous formations.

144 magmatic veins up to 10 m thick and with a strike of N60° occur in a 8 x 20 km area in the south half of the inlier (Goffette, 1991). This vein swarm has a clear bimodal affinity, with diabase and/or microgranite fillings.

In the Rocroi inlier, metamorphism and cleavage affect both the Cambro-Ordovician basement and the Devonian cover as well as magmatic veins. This metamorphism, prograde from north to south, is characterized by a deep cleavage in slates, the presence of porphyroblasts (e.g., magnetite, pyrite, chlorite group, ilmenite) and color change of the Deville group rocks (north: red and green; south: purple-grey). Maximum metamorphic conditions known in the Rocroi inlier were defined in the range of 378 to 500°C and 300 MPa by Beugnies (1986), Potdevin and Goffette (1991b), Potdevin et al. (1993) and Robion et al. (1995) (Fig. 1). These data were mainly derived from mineral paragenesis and illite crystallinity of samples collected along the Meuse river, and represent a good N-S trend representative of the eastern part of the inlier. However, data is still lacking in most areas elsewhere and the techniques used to define peak metamorphic conditions can be impacted by retrograde metamorphism, which has been recognized in the Rocroi inlier.

To complete the dataset, we used Raman Spectroscopy of Carbonaceous Material (RSCM) approach to obtain the maximum (peak) metamorphic temperature reached by the rocks. From the 16 analyzed samples, 6 were collected in the Meuse valley to compare our results with previous data and 9 others were collected in other locations across the inlier to investigate lateral variation of peak temperature. Finally, one sample was collected in the Devonian cover at Mont de Vireux in the North of the Rocroi inlier (Fig. 1).

The results yielded three temperature groups: 1) the Devonian shale from Mont de Vireux, with 247.41 ± 18 °C, 2) the northern part of the Rocroi inlier, a group of 11 samples with a mean value of 361.58 ± 14 °C and 3) south of the Grande Commune fault, with a group of 3 samples with a mean value of 510.22 ± 8 °C. These results show that peak metamorphism temperature is homogeneous in a W-E trend and is not smoothly but abruptly changing along the N-S direction, with an overall decrease from south to north.

Two scenarios are currently investigated to explain the obtained peak metamorphism temperature. In the first scenario, the Rocroi inlier consists of two distinct blocks separated by the Grande-Commune fault. During the Silurian-Devonian back-arc extension event, the associated burial metamorphism (Fielitz, 1997; Fielitz and Mansy, 1999) was stronger in the south block due to a deeper burial depth associated to a normal (listric) fault (tilted blocks system). The Variscan

shortening subsequently uplifted the south block by inverting the Grande-Commune normal fault into a thrust fault. In a second scenario, contact metamorphism was induced by magma at depth. This scenario is supported by the fact that 2 out of the 3 samples that exhibit $>500^{\circ}\text{C}$ peak metamorphism are close to magmatic veins. However, the third sample was collected far from any known magmatic body. In addition, data from Robion et al. (1995) in the southernmost Rocroi inlier, where no magmatism is observed, also show a minimum metamorphism temperature of 500°C based on the breakdown of pyrrhotite into magnetite.

References

- Beugnies, A., 1986. Le métamorphisme de l'aire anticlinale de l'Ardenne. *Hercynica*, 2(1), 17-33.
- Fielitz, W., 1997. Inversion tectoniques and diastathermal metamorphism in the Serpont Massif area of the Variscan Ardenne (Belgium). *Aardkd. Meded*, 8, 79-82.
- Fielitz, W., & Mansy, J. L., 1999. Pre-and synorogenic burial metamorphism in the Ardenne and neighbouring areas (Renohercynian zone, central European Variscides). *Tectonophysics*, 309(1-4), 227-256.
- Goffette, O., 1991. Le magmatisme varisque en Ardenne méridionale : un marqueur de l'évolution géodynamique d'une paléomarge (Doctoral dissertation, Lille 1).
- Potdevin, J. L., & Goffette, O., 1991. Les assemblages métamorphiques du filon de diabase de la Grande Commune (Massif de Rocroi) ; des témoins d'une évolution rétrograde varisque en Ardenne. *CR Acad. Sci. Paris*, 312(2), 1545-1550.
- Potdevin, J. L., Goffette, O., & Lefevre, C., 1993. Découverte de grenats spessartine-almandin dans l'encaissant du filon de diabase de la Grande Commune (Massif de Rocroi). Origine et implications pour le métamorphisme de l'Ardenne. *Comptes rendus de l'Académie des sciences. Série 2, Mécanique, Physique, Chimie, Sciences de l'univers, Sciences de la Terre*, 316(12), 1763-1770.
- Robion, P., Frizon de Lamotte, D., Kissel, C., & Aubourg, C., 1995. Tectonic versus mineralogical contribution to the magnetic fabrics of epimetamorphic slaty rocks: an example from the Ardennes Massif (France-Belgium). *Journal of Structural Geology*, 17(8), 1111-1124.

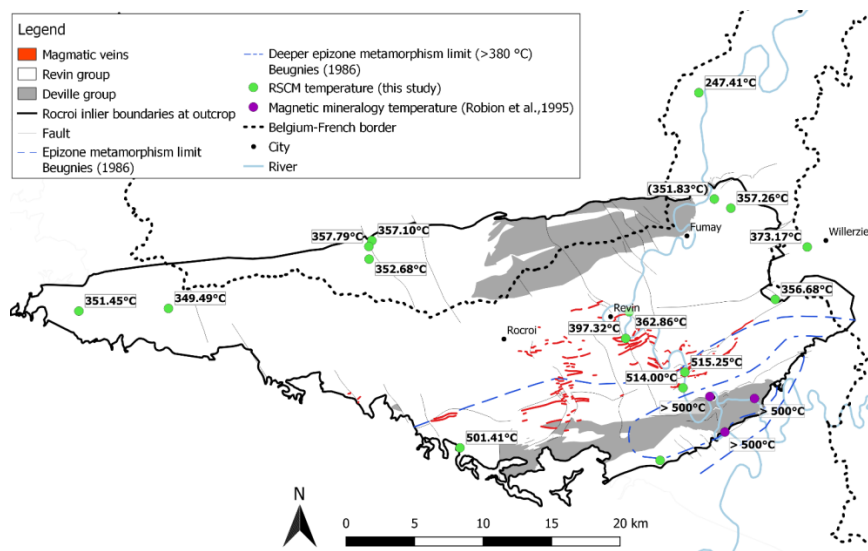


Figure 1: Geological map of the Rocroi inlier with RSCM sample temperatures (green dots), sample temperatures (purple dots, after Robion et al., 1995) and metamorphic zones (after Beugnies, 1986).

Phase identification and mapping of melt inclusions in complex mineral hosts by confocal Raman spectroscopy and multivariate data analysis

Niels HULSBOSCH¹ and Mona SIRBESCU²

¹*KU Leuven, Leuven - Belgium (niels.hulsbosch@kuleuven.be)*

²*Central Michigan University, Mount Pleasant, USA (sirbelmc@cmich.edu)*

Identification and mapping of mineral and volatile phases inside crystalline melt inclusions hosted in minerals is a particularly challenging analytical problem, especially for traditional micro-analyses based on electron-microbeams. Confocal Raman spectroscopy can provide a solution as the technique is able to target phases with high spatial resolution inside mineral hosts. However, the acquisition of normal Raman modes of a daughter mineral or volatile (e.g. H₂O, CO₂ etc.) phase inside a crystalline melt inclusion is complicated by the superposition of the Raman signal of the mineral phase hosting the inclusion. Consequently, these experiments de facto result in mixture spectra composed of the Raman vibrations of, on the one hand, the host phase and, on the other hand, the daughter mineral or volatile phase. Spectral analysis of mixtures in this type of Raman data is a particularly challenging task.

Traditionally, the Raman identification of phases in inclusions has been performed by manual separation of spectral components (e.g. Frezzotti et al., 2012). Actions can involve visually and qualitatively assigning individual peaks to either the host or daughter mineral based on reference spectra or by subtracting the host mineral spectrum from the mixture spectrum. These univariate procedures can be particularly prone to user-subjectivity and often lead to ambiguous phase identification, for example due to overlapping peaks in both host and daughter mineral spectra. In general, Raman spectroscopic identification of daughter minerals is a rather qualitative, time-consuming and challenging procedure. This is especially the case for mineral hosts with a complex Raman signature.

In order to overcome the above-mentioned analytical difficulties associated to univariate identification, we propose a novel methodology based multivariate spectral mixture analysis to generate and rank numerous calculated mixture spectra composed of two weighted components: (1) the measured host mineral spectrum and (2) a mineral reference spectrum from a spectral library. Mixture analysis is performed by convolution to create calculated mixture spectra composed of the measured pure host mineral spectrum and a mineral reference spectrum from a database. Multivariate spectra matching algorithms (correlation and first derivative Euclidean distance) have been applied to quantitatively evaluate similarities between the measured mixture spectrum and myriad calculated mixture spectra (i.e. combinations of spectra from database with the host spectrum). For the purpose of this study, the RRUFF database has been chosen, containing 2239 IMA approved minerals, supplemented with the Horiba and in-house spectral database for additional mineral and volatile spectra. The degree of similarity between the measured mixture spectrum and calculated mixture spectra is subsequently ranked based on the Hit Quality Index (HQI) parameter which is also used as a certainty indicator for daughter mineral identification.

The identification method is further extended to Raman mapping experiments of minerals and volatiles in melt inclusions. Here, the different spectral components imbedded in the hyperspectral Raman image have been initially resolved by two standard postprocessing multivariate algorithms for Raman mapping: (1) Multivariate Curve Resolution Alternating Least Squares (MCR-ALS) and (2) Classical Least Squares (CLS).

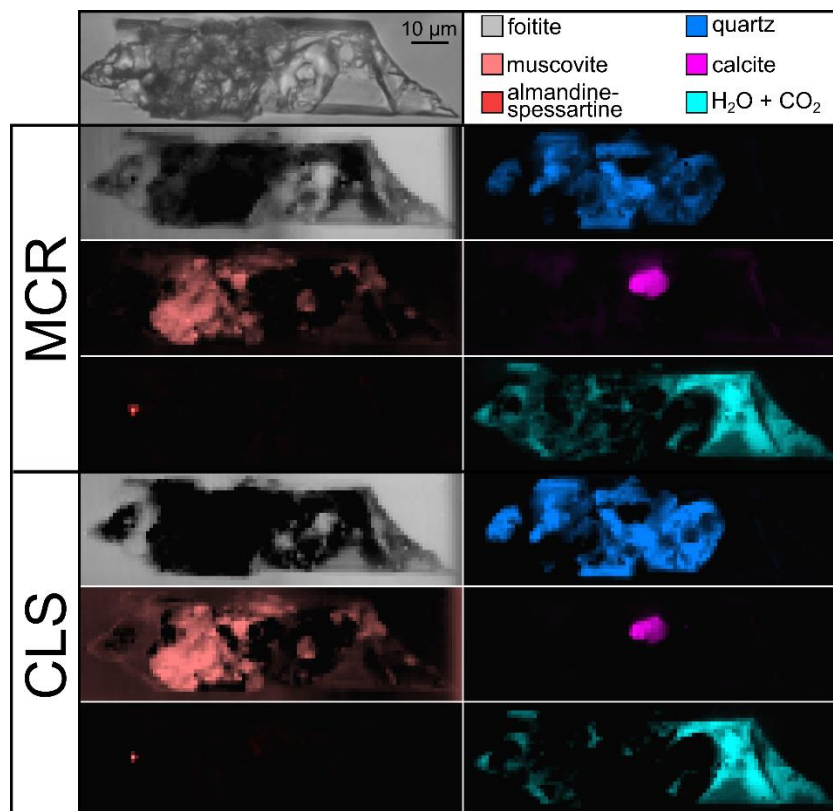


Figure 9. Raman mapping experiment of a crystalline melt inclusion in tourmaline from the Emmons Pegmatite. Phase identification is performed by spectra matching algorithms and the mapping data is resolved by both (1) Multivariate Curve Resolution Alternating Least Squares (MCR-ALS) and (2) Classical Least Squares (CLS) multivariate statistics.

The new procedure is ultimately applied to crystalline melt inclusions in foititic tourmaline from the Emmons Pegmatite (Maine, USA) using the Raman hardware described in Prado Araujo et al. (2020). Multivariate data analyses by spectra matching algorithms and subsequent MCR-ALS and CLS mapping routines resulted in high-spatial resolution ($\sim 1\mu\text{m}$) mineralogical maps of the felsic and volatile melt inclusions hosted inside foitite (i.e. muscovite, garnet, quartz, calcite and volatiles; Fig. 1). The proposed procedures enable user-independent, quantitative phase identification and mapping of crystalline melt inclusions hosted in complex minerals by confocal Raman spectroscopy.

References

- Prado Araujo, F, Hulsbosch, N & Muchez Ph, 2020. Raman mapping of complex mineral assemblages: Application on phosphate mineral sequences in pegmatites. *Journal of Raman Spectroscopy*;1–19.
- Frezzotti, M L, Tecce, F & Casagli A., 2012. Raman spectroscopy for fluid inclusion analysis. *Journal of Geochemical Exploration* 112, 1-20.

Latest developments in micro-X-ray fluorescence (μ XRF) analysis in geosciences: high-resolution element mapping, digital image analysis, and quantifications

Pim KASKES^{1,2}, Thomas DÉHAIS^{1,2}, Sietze J. DE GRAAFF^{1,2}, Steven GODERIS¹, Philippe CLAEYS¹

¹ *Analytical, Environmental & Geo-Chemistry Research Unit, Vrije Universiteit Brussel, Pleinlaan 2, Brussels, Belgium*

² *Laboratoire G-Time, Université Libre de Bruxelles, Avenue F.D. Roosevelt 50, 1050 Brussels, Belgium*

Quantitative insights into the geochemistry and petrography of sedimentary, igneous, and metamorphic rocks are fundamental to understand their formational processes. Traditional analytical techniques used to obtain major- and trace-element data sets focus predominantly on either destructive whole-rock analysis or laboratory-intensive phase-specific micro-analysis. Here, we present micro-X-ray fluorescence (μ XRF) as a state-of-the-art, time-efficient, and nondestructive alternative for major- and trace-element analysis for both small and large rock samples (up to 20 cm wide). This technique uses the principles of classical bulk X-ray fluorescence while being able to document the heterogeneous nature of a sample by applying multiple spot analyses, line scans, and high-resolution mapping of a flat sample surface. For the last five years, μ XRF has been used for geological applications but on a relatively small scale in predominantly invertebrate palaeontology and carbonate sedimentology (e.g., de Winter & Claeys, 2016). New developments in for instance experimenting with spatial resolution and measurement time, the use of specific X-ray tube filters, and the incorporation of certified reference materials have opened a wide array of applications in different geoscientific fields due to the rapidly produced geochemical data sets by μ XRF combined with petrographic and sedimentological data sets, that can be derived from μ XRF maps.

We demonstrate the potential of μ XRF analysis in geology by applying element mapping on 44 samples from the Chicxulub, Popigai, and Ries impact craters, including shocked crystalline basement, impact melt rocks, and impact melt-bearing polymict breccias (suevites). These samples were mapped under near-vacuum condition (20 mbar) using a Bruker M4 Tornado benchtop μ XRF instrument at the Vrije Universiteit Brussel, by using a rhodium X-ray source with maximized energy settings, two silicon-drift detectors, and a polycapillary lens focusing the X-ray beam down to 25 μ m. The μ XRF mapping required limited to no sample preparation and generated high-resolution major- and trace-element maps in a matter of hours (\sim 1 h for 8 cm², using an integration time of 1 ms for each 25- μ m-diameter-pixel at a 25 μ m spatial resolution). These chemical distribution maps can be used as qualitative multi-element maps, as semiquantitative single-element heat maps, and as a basis for a novel image analysis workflow. This workflow allows segmentation of clasts based on their geochemical composition rather than visual characteristics such as color. This way the modal abundance of major lithological components is quantified (Fig. 1), and an extensive data set of the size and shape of each clast is produced that aids in quantifying the degree of sorting of the sample (Kaskes et al., 2021). When thin sections are mapped with μ XRF, a direct petrographic verification of clast and matrix types is also possible. However, one should take into account that elements heavier than Fe are not fully attenuated due to the limited thickness of the thin section (30 μ m) and the corresponding μ XRF maps are therefore less reliable. This image analysis method is a powerful tool to characterize impact breccias and other relatively coarse-grained lithologies, such as plutonic rocks, volcanic breccias, conglomerates, and meteorites.

Both whole-rock and clast-specific compositional data can be derived from μ XRF mapping based on a manual selection of regions of interests. The quantification of the impact rocks from this study was based on the Standardless Fundamental Parameter method due to their strong heterogeneous nature. This technique is accurate for most major elements (with Na_2O – CaO being accurate within 10% compared to the results based on bulk powder techniques) but tends to overestimate most trace-element concentrations for samples thicker than 1 mm. To improve these results, matrix-specific calibration curves can be constructed using international reference materials in combination with the use of X-ray tube filters and a longer measurement time. Overall, we demonstrate that μ XRF is more than only a screening tool for heterogeneous impact rocks, because it rapidly produces bulk and phase-specific geochemical data sets that are suitable for various applications within the earth sciences.

References

- de Winter, N.J., and Claeys, Ph., 2017, Micro X-ray fluorescence (μ XRF) line scanning on Cretaceous rudist bivalves: A new method for reproducible trace element profiles in bivalve calcite: *Sedimentology* 64(1), 231–251, <https://doi.org/10.1111/sed.12299>.
- Kaskes, P., Déhais, T., de Graaff, S.J., Goderis, S., and Claeys, P., 2021, Micro-X-ray fluorescence (μ XRF) analysis of proximal impactites: High-resolution element mapping, digital image analysis, and quantifications, in Reimold, W.U., and Koeberl, C., eds., *Large Meteorite Impacts and Planetary Evolution VI: Geological Society of America Special Paper 550*, p. 1–36, [https://doi.org/10.1130/2021.2550\(07\)](https://doi.org/10.1130/2021.2550(07))

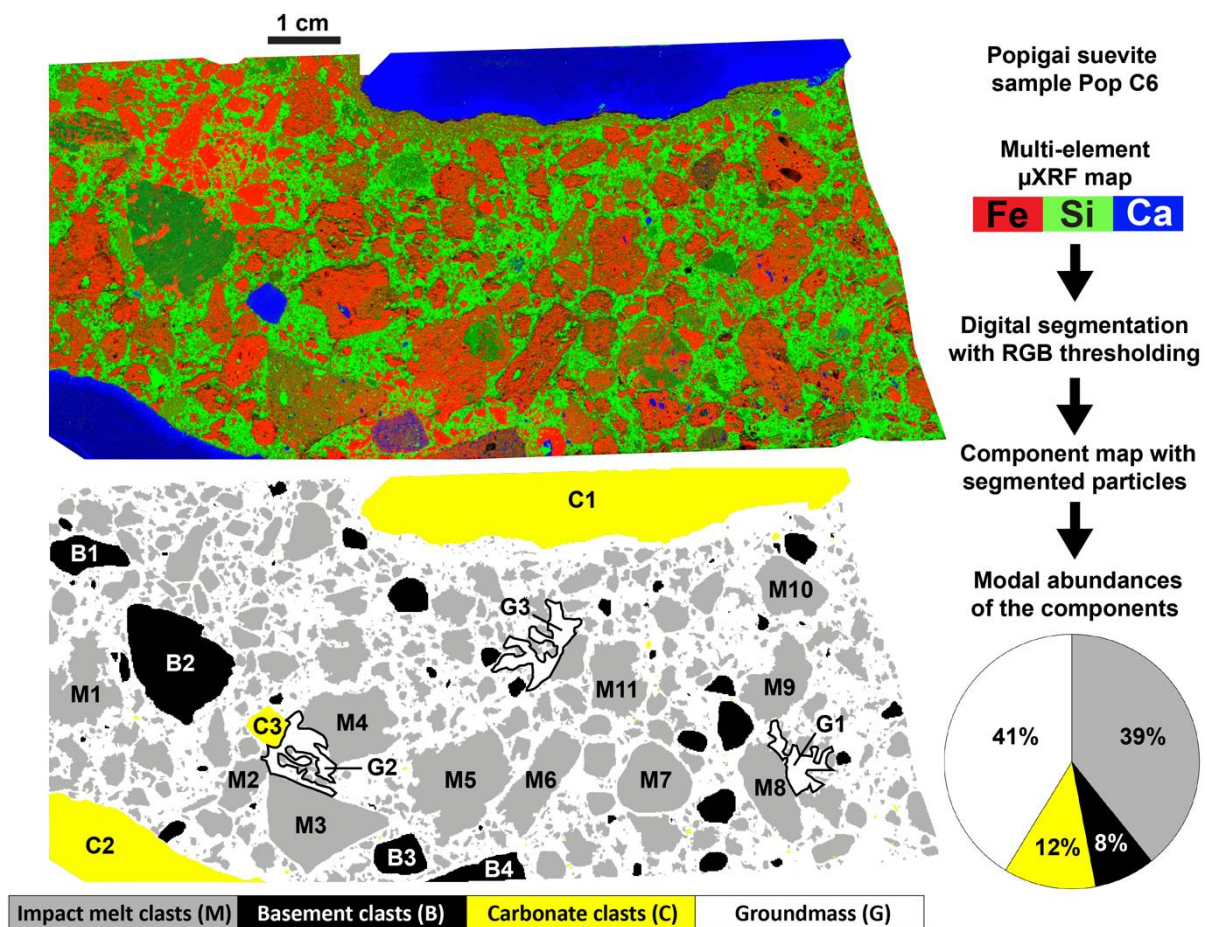


Figure 1. Image analysis results derived from digital segmentation based on an Fe-Si-Ca μ XRF map from Popigai suevite sample Pop C6 (modified from Kaskes et al., 2021).

Recent advances in infrared spectroscopy applied to single specimen dinoflagellate cysts: methodological framework and applications

Pjotr MEYVISCH^{1*}, Pieter Roger GURDEBEKE¹, Henk VRIELINCK², Kenneth Neil MERTENS³, Gerard VERSTEEGH⁴, Katarzyna SLIWINSKA⁵, Stephen LOUWYE¹

¹ Department of Geology, Ghent University, 9000 Ghent, Belgium

² Department of Solid State Sciences, Ghent University, 9000 Ghent, Belgium

³ Ifremer, LITTORAL, F- 29900 Concarneau, France

⁴ Marine Biochemistry section, Alfred-Wegener-Institute, 27570 Bremerhaven, Germany

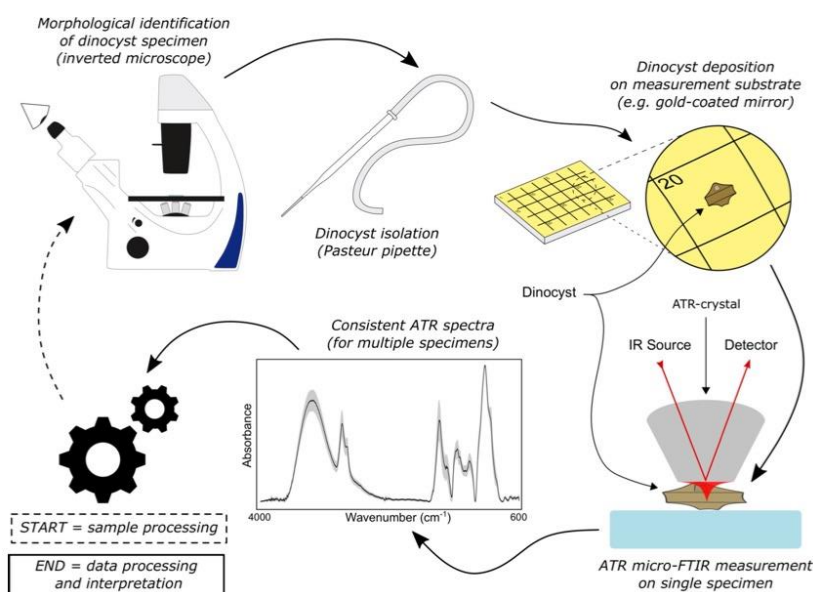
⁵ Department of Stratigraphy, GEUS, 1350 Copenhagen, Denmark

*Corresponding author: pjotr.meyvisch@ugent.be

Fourier-transformed infrared (FTIR) spectroscopy is a spectrochemical technique able to retrieve macromolecular information from organic materials. When combined with a microscope (micro-FTIR), the (geo)chemical composition of single specimen dinoflagellate cysts (dinocysts) can be determined. Over the last decades a small number of dinocyst micro-FTIR studies booked often inconsistent results by overlooking important methodological aspects during analysis.

This study takes into account variables like sample preparation, specimen morphology and size and spectral data processing steps and presents a standardized method based on attenuated total reflectance (ATR) micro-FTIR spectroscopy which is able to collect robust spectral datasets. These datasets are largely devoid of nonchemical artifacts inherent to other infrared spectrochemical methods which have typically been used in similar studies in the past (i.e. transmission and transflection spectroscopy). Several guidelines are proposed which facilitate the collection and qualitative interpretation of highly reproducible and repeatable spectrochemical dinocyst data. These, in turn, pave the way for a systematic exploration of dinocyst chemistry and its assessment as a chemotaxonomical tool or proxy.

An ATR micro-FTIR case study on morphologically similar late Paleogene to early Neogene dinocysts *Palaeocystodinium golzowense*, *Svalbardella clausii* and *Svalbardella cooksoniae* is also presented, which highlights the chemotaxonomical potential of the method.



Geochemical imaging at hand-sample scale of Belgian Zn-Pb ores using Laser-Induced Breakdown Spectroscopy (LIBS)

Séverine PAPIER¹, Jean-Marc BAELE¹, Hassan BOUZAHZAH², Sophie VERHEYDEN³, Christian BURLET³, Eric PIRARD², Anca CROITOR⁴, Sophie DECRÉE³, Guy FRANCESCHI⁵ and Léon DEJONGHE³

1. *Geology and Applied Geology - Faculty of Engineering, University of Mons, Mons, Belgium (jean-marc.baele@umons.ac.be)*
2. *GeMMe, University of Liège, Liège, Belgium (Hassan.Bouzahzah@uliege.be)*
3. *Royal Belgian Institute of Natural Sciences, Geological Survey of Belgium, Brussels, Belgium (sdecree@naturalsciences.be)*
4. *Center for Artificial Intelligence, KULeuven, Leuven, Belgium (anca.croitor@kuleuven.be)*
5. *GF-Consult bvba, Gent, Belgium (gfranceschi@gfconsult.be)*

Within the framework of the ongoing LIBS-SCReeN (Brain-be) project, strategies are being developed for screening trace-elements in Zn-Pb ores, waste products and contaminated soils from east Belgium using Laser-Induced Breakdown Spectroscopy (LIBS) technology (see also Verheyden et al., 2021). Here we address geochemical screening of hand samples of ores with the aim of rapid mineral and geochemical mapping. Several samples of Zn-Pb ores were selected from university and Royal Belgian Institute of Natural Sciences collections for LIBS mapping using a system developed at UMONS. With this system, the LIBS signal is recorded as the sample is moved in synchronization with the laser. Laser spot size can be selected from 50 to 500 μm and repetition rate up to 20 Hz. With these settings, a surface of several tens of cm^2 can be scanned in less than one hour depending on the chosen spatial resolution. A 100 Hz laser source is currently implemented to speed-up the acquisition process and obtain usable geochemical maps in minutes. The LIBS dataset consists of a hyperspectral datacube from which the elemental images are extracted. LIBS spectra are complex and computer-assisted methods for fast and efficient data retrieving and analysis are currently investigated in collaboration with KULeuven. At the moment, the analysis is qualitative but produces very informative images of relative concentration of major and trace-elements in the material. Comparison of LIBS data with EDS and XRF analyses performed on the same samples yielded very consistent results (Baele et al., in press). Besides its capability of high-speed measurement, LIBS offers several analytical advantages compared to other methods such as reduced matrix effect in high-z minerals (e.g., galena), which absorb much of the X-rays, and excellent detectability of trace-elements such as germanium, silver, cadmium, copper, antimony, arsenic, thallium and possibly gallium. The LIBS images obtained so far show that trace-element distribution is very heterogeneous and follows particular patterns in the investigated Zn-Pb ore samples (Fig. 1). This information is useful for the design of a point-and-shoot screening strategy of raw samples (for example, how many random spots are needed or which shooting pattern is best to have a chance to hit a zone with high trace-element concentration? Are there visual guides for pointing these particular zones on the samples?). LIBS images can also be used for selecting the most interesting areas on the sample to be further investigated with more conventional but quantitative microscopic techniques. Finally, LIBS imaging of Zn-Pb ores provides information of petrogenetical importance (Baele et al., in press). For example, trace-elements in sphalerite show contrasting relations, with common co-occurrence of Fe and Ge, which has only been reported in very few Zn deposits worldwide (Cook et al., 2009), and anti-correlation of Ge with Ag-Cd-Sb-Cu.

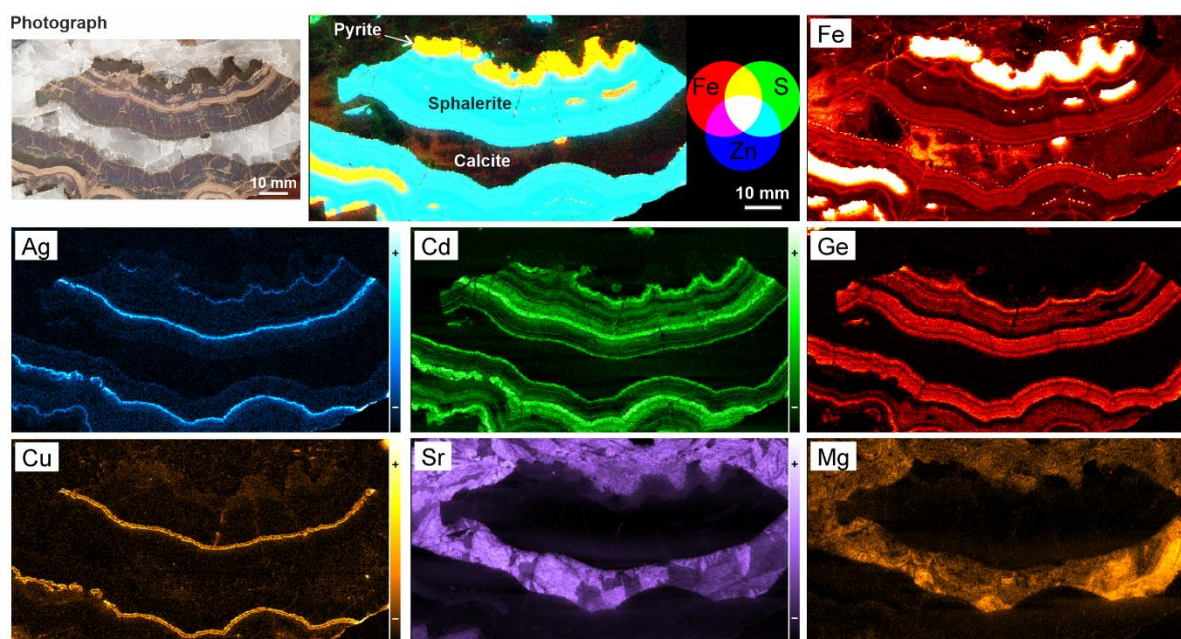


Figure 1. Example of elemental imaging by LIBS of a sphalerite-pyrite-calcite sample from Andenne, Belgium. The distribution of both major and trace-elements can be visualized in the images extracted from a single hyperspectral dataset (pixel size: 250 μm). Note the similar distribution pattern for Fe and Ge in sphalerite.

References

- Baele, J.M., Bouzahzah H., Papier, S., Decrée, S., Verheyden, S., Burlet, C., Pirard, E., Franceschi, G. & Dejonghe, L., in press. Trace-element imaging at macroscopic scale in a Belgian sphalerite-galena ore using Laser-Induced Breakdown Spectroscopy (LIBS). *Geologica Belgica*.
- Cook, N.J., Ciobanu, C.L., Pring, A., Skinner, W., Shimizu, M., Danyushevsky, L., Saini-Eidukat, B. & Melcher, F., 2009. Trace and minor elements in sphalerite: a LA-ICPMS study. *Geochimica et Cosmochimica Acta*, 73, 4761-4791.
- Verheyden, S., Burlet, C., Croitor, A., Baele, J.M., Papier, S., Pirard, E. & Bouzahzah H., 2021. Development of a Laser-Induced Breakdown spectrometry (LIBS) instrumentation and protocols for rapid screening of soils. *This issue*.

ROBOMINERS: changing the ground rules

Giorgia STASI^{1,15}, Christian BURLET^{1,15}, Luis LOPES², Claudio ROSSI³, Stephen HENLEY⁴, Tobias PINKSE⁵, Asko RISTOLAINEN⁶, Vitor CORREIA⁷, Alicja KOT-NIEWIADOMSKA⁸, Jussi AALTONEN⁹, Michael BERNER¹⁰, Nelson CRISTO¹¹, Eva HARTAI¹², Gorazd ZIBRET¹³, Janos HORVATH¹⁴

1. *Royal Belgian Institute of Natural Sciences – RBINS, Belgium.*
(gstasi@naturalsciences.be, cburlet@naturalsciences.be),
2. *La Palma Research Centre for Future Studies SL, Isla de La Palma, Canarias, Spain*
3. *CAR UPM-CSIC, Madrid, Spain*
4. *Resources Computing International Ltd, Matlock, UK*
5. *K-UTEC AG Salt technologies -Sondershausen, Germany*
6. *Center for Biorobotics, Tallinn University of Technology, Tallinn, Estonia*
7. *European Federation of Geologists, Brussels, Belgium*
8. *Mineral and Energy Economy Research Institute, Polish Academy of Science, Krakow, Poland*
9. *Tampere University, Faculty of Engineering and Natural Sciences, Tampere, Finland*
10. *Department Mineral Resources Engineering, University of Leoben, Leoben, Austria*
11. *Associação dos Recursos Minerais de Portugal, Lisboa, Portugal*
12. *University of Miskolc, Faculty of Earth Science and Engineering, Miskolc, Hungary*
13. *Geological Survey of Slovenia, Ljubljana, Slovenia*
14. *Geo-Montan Kft, Budapest, Hungary*
15. *University of Liège, Liège, Belgium*

Nowadays we are faced with several challenges regarding mineral exploration and exploitation in Europe. The biggest accessible deposits have already been discovered and exploited, with some of those mines dating back of thousands of years. What remains now are the small and difficult to access deposits, leading to the needs of new and more sustainable mining methods. In the last years several projects like ROBOMINERS were started with the expectation to have relevant impact in social, technological, environmental and economical areas and aiming to help in (i) reducing EU dependency on import of raw materials, (ii) pushing the EU to the forefront in sustainable minerals surveying and exploration technologies and to (iii) improve resource efficiency and responsible sourcing.

The main objective of the ROBOMINERS project is to develop a Bio-Inspired, Modular and Reconfigurable Robot Miner, equipped with selective mining perception and mining tools for small and difficult to access deposits. A consortium that includes geoscientists, roboticists and engineers is working to build a modular robot prototype (Technology Readiness Level 4 to 5), design a new mining system via simulation and modelling and to use the prototype to study and advance future research on different areas of robotics and raw materials alike (Lopez et al. 2020).

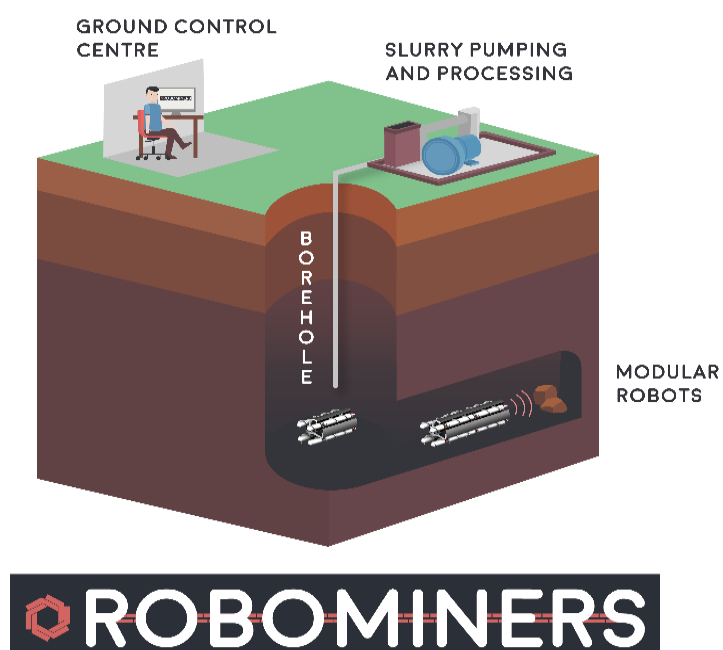
ROBOMINERS will not reach its end-state by the end of the project. Therefore, it already prepares future development with visions for 2030 and 2050, coinciding with important EU targets (2030: reduce GHG emissions, more renewable energy; 2050: climate neutrality). These visions will impact the developments of robotics, selective mining and mining ecosystem. The considered methods and tools, although innovative at this point, will be continuously assessed, and compared to new technology developments in the relevant fields.

The ROBOMINERS project has received funding from the European Union's Horizon 2020 research and innovation programme under grant agreement No. 820971.

References

L. Lopes, B. Bodo, C. Rossi, S. Henley, G. Žibret, A. Kot-Niewiadomska, V. Correia, 2020. ROBOMINERS – Developing a bio-inspired modular robot-miner for difficult to access mineral deposits, *Advances in Geosciences*, Volume 54, 2020, 99–108

Figure



Development of a Laser-Induced Breakdown spectrometry (LIBS) instrumentation and protocols for rapid screening of soils

Sophie VERHEYDEN¹, Christian BURLET¹, Anca CROITOR², Jean-Marc BAELE³, Severine PAPIER³, Eric PIRARD⁴, Hassan BOUZAHZAH⁴ and Matic PUSOVNIK⁵

1. *Royal Belgian Institute of Natural Sciences – RBINS, Belgium.*
(*sophie.verheyden@naturalsciences.be; cburlet@naturalsciences.be*),
2. *Institute for Artificial Intelligence, University of Leuven, KUL, Belgium.*
(*anca.croitor@kuleuven.be*)
3. *Geology and Applied Geology - Faculty of Engineering, University of Mons, Belgium*
(*Jean-Marc.baele@umons.ac.be; severine.papier@umons.ac.be*)
4. *ArGEnCo, University of Liège, Belgium* (*eric.pirard@uliege.be;*
hassan.bouzahzah@uliege.be)
5. *Biomedical MRI, KU Leuven, O&N1 Herestraat 49 Box 505, 3000 Leuven*
(*m.pusovnik@gmail.com*).

LIBS

LIBS or Laser-Induced Breakdown Spectroscopy is a trending technique for rapid and flexible elemental analyses of solids, liquids or gases (e.g., Fabre, 2020). High-energy laser pulses ablate materials and induce a plasma, which emits light that is analysed by a spectrometer. The produced wavelengths or spectral lines are related to the elements present in the target material. LIBS can analyse a broad range of elements, with the important challenge of producing quantitative or semi-quantitative analyses on materials with a variable matrix, such as soils.

The LIBS-SCReeN project

The LIBS-SCReeN project is dedicated to the development of LIBS instrumentation and rapid screening protocols for mineral exploration. The aim is to rapidly detect elements considered as economically interesting (especially linked to Critical Raw Materials) or economically and environmentally damaging. The chosen pilot study in LIBS-SCReeN focuses on Belgian lead-zinc ores and associated elements such as germanium, indium, gallium or silver. In addition, rapid soil monitoring LIBS tools designed to detect lead, cadmium or arsenic are also evaluated in the framework of post-industrial revalorisation of mining sites.

LIBS analysis of soils

Soil moisture, grain size and density influence laser/matter interactions, plasma temperature and lifetime, which, in turn have an impact on the intensity of the spectral lines and their distribution, i.e. the relative intensity of the spectral lines of a single element. To mitigate these effects and obtain reliable LIBS measurements, dried soil material sieved at 75 micrometers and compressed in pellets is usually used (Kim et al., 2013). The complex and high spectral resolution of LIBS signals (hundreds to thousands spectral lines are visible) combined with the variety of soil compositions may highly benefit from automated systems based on computer learning techniques.

Materials and methods

To start the experimental setup for soils in the LIBS-SCReeN project, two different soils are sampled from the Parc Leopold (Brussels) and from the Sclaigaux reserve (Liège), a

former industrial site known for its soils containing up to tens to hundreds ppm of zinc, lead, copper, or cadmium. The aim is to investigate whether major, minor and trace-elements can be identified, and which type of corrections and algorithms are best applied to automatically i) distinguish the different soils and ii) identify the target elements.

We analysed soil pellets from both sites 30 times by a small in-house LIBS instrument based on miniature DPSS laser producing 90 μ J, 1.2 ns, energy pulses at 1029 nm with a repetition rate of 2.5 kHz. The light is collected by two fiber optics and a benchtop two-channels CMOS spectrometer without time gating (i.e. the spectrometer records the light emitted during the entire plasma lifetime). This rather original setup allows a continuous ablation by thousands of laser shots and an accumulation of the produced light in a single spectrum with a relatively low background signal. The analysis is performed while slowly moving the sample during laser ablation, which allows to continuously renew the laser induced plasma sparks and produce an averaged spectral signature of the surface of the pellet. The 200 to 400 nm spectrum is given after subtraction of the dark signal, i.e. background light conditions before ablation.

Mathematical techniques are used to enhance the spectral information, compare different soils, discriminate between soil samples and detect target elements. Firstly, to correct for fluctuations in background light intensity, baseline correction was applied using statistics-sensitive Non-linear Iterative Peak-clipping method (SNIP). The obtained spectra are normalised and multivariate principal component analysis (PCA) is applied for comparing the two soils samples and identify the spectral lines that contribute the most to their discrimination.

Preliminary results and perspectives

The in-house low-energy, high-repetition miniature LIBS instrumentation recently developed at RBINS with a slow sample movement protocol succeeded to produce specific spectral lines of major and minor elements. Si, Ca, C, Al, Mg, Fe, Ti and Mn were easily identified. Na and K could not be identified since their lines fall outside the spectrometer range or overlap with Zn lines. Zn and Pb and maybe some Cu were identified in the Sclaigieux soil and small peaks of Zn were identified in the spectra of the soil from Brussels. Cd, As and Ni were not detected while these elements are probably present in the Sclaigieux soil.

PCA analysis shows we can clearly discriminate between the two soils (Brussels and Sclaigieux) based on their LIBS spectral profile. The spectral lines that showed to be retaining most variability and thus are most relevant in differentiating between the soils were corresponding to both major and minor elements as listed above. Trace elements, present at ppm-levels, are still difficult to identify. Another drawback in the analysis is the problem of overlapping peaks. We are continuing our efforts for optimizing the analytical protocol to increase sensitivity towards trace elements or elements with strongly overlapping spectral profile.

The rather original, easy-to-use, and relatively portable instrumentation and protocol needs to be further tested with soils with known composition (ground-truth measurements) and compared to results obtained with the bench LIBS instrumentation developed at UMONS to develop semi-quantitative analyses.

References

- Fabre C. 2020. *Spectrochimica Acta Part B* 166: 105799.
- Kim G., et al., 2013. *Journal of hazardous materials* 263: 754-760.
- Chatterjee, S., et al. 2019. *Anal Bioanal Chem* 411: 2855–2866.

Session 9- Polar Sciences and Ice-sheets

9.1. Polar Sciences and Ice-sheets

Conveners:

Xavier Fettweis (ULiège), François Fripiat (ULB), Frank Pattyn (ULB)

This sub-session will explore our understanding and quantification of past, present, and future interactions in the Polar Regions and the consequences for the earth system and society. We particularly invite contributions presenting the recent advances in future ice sheets and sea-level changes, atmosphere-sea ice-ocean processes, and biogeochemical cycling in the Polar Regions.



Finally, this session will be an opportunity to bring together modelers and observational scientists to share information, identify common problems, and seek collective vision and endeavors for Belgian research in Polar Regions.

9.2: Permafrost

Conveners:

Sandra Arndt (ULB), Sophie Opfergelt (UCLouvain), Bjorn Tytgat (UGent)

Permafrost, the ground that remains at or below 0°C for more than two consecutive years, underlines about one quarter of the exposed land surface in the Northern Hemisphere. In addition, the wide Arctic shelf hosts a large, yet poorly quantified reservoir of subsea permafrost- a terrestrial relict that mainly formed during glacial periods when the shelf was exposed during low sea level. The Earth's high latitude regions are warming twice as fast as the global average. As a



consequence, permafrost thaw unlocks previously frozen material which becomes available for biogeochemical reactions, with cascading, yet poorly known effects on the terrestrial and aquatic ecosystems, carbon and nutrient cycling, as well as Arctic greenhouse gas budgets and thus climate. In this session, we welcome contributions related permafrost-climate feedbacks, the impacts of permafrost degradation on Arctic biogeochemical cycling, ecosystems and hydrology, past permafrost dynamics as a key to future projections, Alpine permafrost systems, permafrost microbial ecology, remote sensing of permafrost dynamics, subsea permafrost, and thermokarst processes.

Modelling benthic methane efflux triggered by hydrate dissociation and its potential impact on ocean acidification

Maria DE LA FUENTE ¹, Sandra ARNDT ², Tim MINSHULL ³, Héctor MARIN-MORENO ⁴

1. *BGeosys, Department Geoscience, Environment & Society, Université Libre de Bruxelles, Brussels, Belgium* (maria.de.la.fuente.ruiz@ulb.be)
2. *BGeosys, Department Geoscience, Environment & Society, Université Libre de Bruxelles, Brussels, Belgium*
3. *Ocean and Earth Science, University of Southampton, European Way, Southampton, UK*
4. *Norwegian Geotechnical Institute, PB 3930 Ullevål Stadion, Oslo, Norway*

Methane hydrates located in upper continental slopes and associated with subsea permafrost are highly susceptible to dissociate (break apart and release methane) as the ocean continues to warm (Ruppel & Kessler, 2017). The dynamics and timescales of benthic methane seepage triggered by hydrate dissociation are critical in understanding the impact of methane hydrates on the ocean–atmosphere carbon system, and yet, remain poorly constrained. Previous modelling efforts show that ocean bottom warming over the next centuries will result in a decrease in the methane hydrate deposits, leading to methane seepage to the seafloor and an increase in ocean acidification, with the Arctic, being one of the most affected regions (Boudreau et al., 2015; Kretschmer et al., 2015; Biastoch et al., 2014; Marin-Moreno et al., 2013).

On a global scale, methane released from hydrates can be consumed at several stages during its transport through the sediment and the overlying water column. In particular, more than 80% of the methane migrating within the sediment can be microbially consumed via oxidation before it escapes into the water column (Hinrichs & Boetius, 2002; Reeburgh, 2007). However, active supplies of methane gas at shallow depths (Wallmann et al., 2006), slow microbial growth (Regnier et al. 2011) or insufficient intrusion of sulfate in recent sediments (Ruppel & Kessler, 2017) may lead to methane seepage at the seafloor before benthic sink processes can have a large mitigating impact. The DIC outflux through the SMTZ contributes to alkalinity or carbon dioxide in different proportions to the water column, depending on the rates of authigenic carbonate precipitation and sulfide oxidation and will significantly impact ocean chemistry and potentially atmospheric dioxide (Akam et al., 2020).

Here, we present a 1D thermo-hydro-(micro)biogeochemical hydrate model developed to improve the quantitative understanding of the benthic methane sink and assess the potential impact of hydrate-related methane fluxes on ocean acidification. The thermo-hydraulic formulation accounts for multi-phase transport of methane and allows capturing the dynamics of hydrate formation and dissociation in the pores media. The (micro)biogeochemical reaction network accounts for the main redox and equilibrium reactions (including, aerobic degradation of organic matter, denitrification, organoclastic sulphate reduction (OSR), methanogenesis, nitrification, sulfide re-oxidation and aerobic/anaerobic oxidation of methane (AeOM/AOM)) that drive methane, total alkalinity, total sulfide and dissolved inorganic carbon production/consumption in oxic and anoxic marine settings. In particular, the AOM rate can be expressed as a bioenergetic rate law, which explicitly resolves the dynamics of the microbial community to represent transient changes in the biofilter efficiency and thus capture windows of opportunity for methane to escape to the water column.

References

- Ruppel, C. D., and J. D. Kessler (2017), The interaction of climate change and methane hydrates, *Rev. Geophys.*
- Boudreau, B. P., Luo, Y., Meysman, F. J. R., Middelburg, J. J., and Dickens, G. R. (2015), Gas hydrate dissociation prolongs acidification of the Anthropocene oceans, *Geophys. Res. Lett.*
- Kretschmer, K., Biastoch, A., Rüpke, L., and Burwicz, E. (2015), Modeling the fate of methane hydrates under global warming. *Global Biogeochem. Cycles*, 29, 610– 625.
- Biastoch, A., et al. (2011), Rising Arctic Ocean temperatures cause gas hydrate destabilization and ocean acidification, *Geophys. Res. Lett.*, 38, L08602
- Marín-Moreno, H., Minshull, T. A., Westbrook, G. K., Sinha, B., and Sarkar, S. (2013), The response of methane hydrate beneath the seabed offshore Svalbard to ocean warming during the next three centuries, *Geophys. Res. Lett.*, 40, 5159– 5163
- Hinrichs, K. & Boetius, A. *The Anaerobic Oxidation of Methane: New Insights in Microbial Ecology and Biogeochemistry* (2002).
- Reeburgh, W. S. Oceanic methane biogeochemistry. *Chem. Rev.* 107, 486–513 (2007).
- Wallmann, K., Drews, M., Aloisi, G. & Bohrmann, G. Methane discharge into the Black Sea and the global ocean via fluid flow through submarine mud volcanoes. *Earth Planet. Sci. Lett.* 248, 545–560 (2006).
- Regnier, P., Andy W. D., Arndt, S., DE LaRowe, Mogollón J., and Van Cappellen, P (2011). Quantitative analysis of anaerobic oxidation of methane (AOM) in marine sediments: a modeling perspective. *Earth-Science Reviews* 106.1-2, pp. 105–13
- Akam S., Coffin R., Abdulla H., Lyons, T. (2020) Dissolved Inorganic Carbon Pump in Methane-Charged Shallow Marine Sediments: State of the Art and New Model Perspectives. *Front. Mar. Sci.* 7:206.

Greenland mass balance by 2200 using coupled atmospheric (MAR) and ice sheet (PISM) models

Alison DELHASSE¹, Johanna BECKMANN² and Xavier FETTWEIS³

1. *University of Liège, Department of Geography, Laboratory of climatology, Liège, Belgium (alison.delhasse@uliege.be)*

2. *Potsdam Institute for Climate Impact Research, Potsdam, Germany (beckmann@pik-potsdam.de)*

3. *University of Liège, Department of Geography, Laboratory of climatology, Liège, Belgium (xavier.fettweis@uliege.be)*

The Greenland ice sheet (GrIS) is a key contributor to sea level rise (Oppenheimer et al., 2019). By melting in surface, ice sheet is thinning and reaches higher temperature which accelerate the melting processes coming from Global Warming. The main goal of our research is to improve the representation of this melt-elevation feedback, which is crucial to determine how and when GrIS will melt and will involve in a near future, by coupling different kind of numerical models.

The difficulty to model this feedback relies on the fact that ice sheet models (ISMs) can reproduce the dynamic of the ice sheet and thus provide an evolution of the surface elevation, whereas (regional) climate models (RCMs) can represent the ice/snow and atmosphere interactions through the surface mass balance (SMB) and its components. A coupling between these two kind of models appears as a solution and has already been accomplished (Le clec'h et al., 2019). However, responses of ISMs to a same forcing field may be quite different, while SMB from different RCMs are relatively more similar with the same forcing (Goelzer et al., 2018; Fettweis et al., 2020). Coupling could therefore be dependent of which ISMs are used.

To avoid a coupling, costly in computing time, SMB vertical gradient as a function of local elevation variations could be used by ISMs to correct SMB forcing fields (Franco et al., 2012; Helsen et al., 2012). Nonetheless, these SMB gradients are computed with a RCM using a fixed topography, which could introduce biases if the surface topography vary significantly.

Here we decide to full couple the regional climate model MAR (Modèle Atmosphérique Régional, developed in Uliège, Fettweis et al., 2017) specifically developed to run polar climate and forced at his lateral boundaries by CESM2 (a CMIP6 Earth System Model, scenario ssp585), with the ISM PISM (Parallel Ice Sheet Model, developed in Postdam Institute for climate change research, PIK, Germany and in University of Alaska Fairbanks, UAF, USA, Winkelmann et al., 2011). The coupling means that, each year, we exchange ice thickness from PISM to update the topography and ice mask of MAR, and SMB fields from MAR to update forcing fields of PISM.

First of all the aim is to analyze what became the GrIS in 2200 with this extreme scenario. By comparing our coupled simulation with an uncoupled simulation, we have assessed the extent to which changes in surface elevation require the use of a coupling. This comparison also allows us to highlight the physical processes that are impacted by this change in surface topography.

References

Fettweis, X. et al., 2017. Reconstructions of the 1900-2015 Greenland ice sheet surface mass balance using the regional climate MAR model. *Cryosphere*, 11, 1015–1033.

- Fettweis, X. et al., 2020. GrSMBMIP: Intercomparison of the modelled 1980–2012 surface mass balance over the Greenland Ice sheet. *Cryosphere*, 2020, 1–35.
- Franco, B., et al., 2012. Impact of spatial resolution on the modelling of the Greenland ice sheet surface mass balance between 1990-2010, using the regional climate model MAR. *Cryosphere*, 6(3), 695–711.
- Goelzer, H., et al., 2018. Design and results of the ice sheet model initialisation initMIP-Greenland: An ISMIP6 intercomparison, *Cryosphere*, 12(4), 1433-1460.
- Helsen, M. M., et al., 2012. Coupling of climate models and ice sheet models by surface mass balance gradients: Application to the Greenland Ice Sheet. *Cryosphere*, 6(2), 255–272.
- Le clec'h, S., et al., 2019. Assessment of the Greenland ice sheet-atmosphere feedbacks for the next century with a regional atmospheric model fully coupled to an ice sheet model. *Cryosphere*, 13, 373–395.
- Oppenheimer et al., 2019. Sea Level Rise and Implications for Low-Lying Islands, Coasts and Communities. In: IPCC Special Report on the Ocean and Cryosphere in a Changing Climate [H.-O. Pörtner, et al. (eds.)]
- Winkelmann, R., et al., 2011. The Potsdam Parallel Ice Sheet Model (PISM-PIK) – Part 1: Model description. *Cryosphere*, 5, 715–726.

Reduction of the future Greenland ice sheet surface melt with the help of solar geoengineering

Xavier FETTWEIS¹, Stefan HOFER^{1,2}, Roland SÉFÉRIAN³, Charles AMORY^{1,4}, Alison DELHASSE¹, Sébastien DOUTRELOUP¹, Christoph KITTEL¹, Charlotte LANG¹, Joris VAN BEVER^{1,5}, Florent VEILLON¹, Peter IRVINE⁶

¹SPHERES research units, Geography Department, University of Liège, Liège, Belgium

²Department of Geosciences, University of Oslo, Oslo, Norway

³CNRM, Université de Toulouse, Météo-France, CNRS, Toulouse, France

⁴Univ. Grenoble Alpes, CNRS, Institut des Géosciences de l'Environnement, Grenoble, France

⁵Earth System Science, Departement Geografie, Vrije Universiteit Brussel, Brussels, Belgium

⁶Earth Sciences, University College London, London, UK

Correspondence to: Xavier Fettweis (xavier.fettweis@uliege.be)

The Greenland Ice Sheet (GrIS) will be losing mass at an accelerating pace throughout the 21st century, with a direct link between anthropogenic greenhouse gas emissions and the magnitude of Greenland mass loss. Currently, approximately 60 % of the mass loss contribution comes from surface melt and subsequent meltwater runoff, while 40 % are due to ice calving. In the ablation zone covered by bare ice in summer, most of the surface melt energy is provided by absorbed shortwave fluxes, which could be reduced by solar geoengineering measures. However, so far very little is known about the potential impacts of an artificial reduction of the incoming solar radiation on the GrIS surface energy budget and the subsequent change in meltwater production. By forcing the regional climate model MAR with the latest CMIP6 shared socioeconomic pathways (ssp) future emission scenarios (ssp245, ssp585) and associated G6solar experiment from the CNRM-ESM2-1 Earth System Model, we estimate the local impact of a reduced solar constant on the projected GrIS surface mass balance (SMB) decrease. Overall, our results show that even in case of low mitigation greenhouse gas emissions scenario (ssp585), the Greenland surface mass loss can be brought in line with the medium mitigation emissions scenario (ssp245) by reducing the solar downward flux at the top of the atmosphere by ~40 W/m² or ~1.5 % (using the G6solar experiment). In addition to reducing global warming in line with ssp245, G6solar also decreases the efficiency of surface meltwater production over the Greenland ice sheet by damping the well-known positive melt-albedo feedback. With respect to a MAR simulation where the solar constant remains unchanged, decreasing the solar constant according to G6solar in the MAR radiative scheme mitigates the projected Greenland ice sheet surface melt increase by 6 %. However, only more constraining geoengineering experiments than G6solar would allow to maintain positive SMB until the end of this century without any reduction in our greenhouse gas emissions.

Quantifying carbon transformations and fluxes at active methane seeps on the East Siberian Arctic Shelf

Alexis GEELS ¹, Sandra ARNDT ², Pierre REGNIER ³, Volker BRÜCHERT ⁴

1. BGeoSys (DGES, ULB), Brussels, Belgium (alexis.geels@ulb.be)
2. BGeoSys (DGES, ULB), Brussels, Belgium (sandra.arndt@ulb.be)
3. BGeoSys (DGES, ULB), Brussels, Belgium (pierre.regnier@ulb.ac.be)
4. Department of Geological Sciences (SU), Stockholm, Sweden (volker.bruchert@geo.su.se)

The Arctic shelf is the largest shelf on Earth and hosts vast amounts of subsea permafrost and associated gas hydrates buried in its sediments (Sloan and Koh, 2007). These large carbon reservoirs have been slowly destabilised by the immersion of the shelf in response to sea level rise since the Last Glacial Maximum. Projected anthropogenically induced climate change and ocean warming will accelerate this destabilization, increasing the risk of vast amounts of methane (CH₄) release from the shelf to the ocean-atmosphere system with important implications for global warming. However, in general, not all CH₄ that is produced in marine sediments escapes to the water column, let alone the atmosphere. Efficient CH₄ sinks generally consume a large fraction of the flux. In particular, the benthic CH₄ sink - the complex interplay of multiphase methane transport and microbial oxidation processes - acts as an efficient biofilter that can completely consume CH₄ fluxes anaerobically before they reach the seafloor. Nonetheless, the efficiency of this microbial filter is highly variable (0-100%) and depends on a complex interplay between fluid flow and microbial dynamics, as well as on the presence of CH₄(g) and dissolved sulfate. In addition, under certain circumstances, the benthic CH₄ sink also supports enhanced benthic alkalinity (ALK) effluxes with important, yet largely overlooked implications for ocean pH and CO₂ emissions. Therefore, the full environmental impact of Arctic CH₄ release to the ocean-atmosphere system, as well as its feedbacks on Arctic biogeochemical cycles and climate, still remains poorly quantified.

Here, we use an integrated model-data approach to quantitatively assess the full biogeochemical impact of deep CH₄ fluxes at active seep sites on the Eastern Siberian Arctic Shelf sampled during the SWERUS project (Brüchert et al., 2018). We quantify the efficiency of the benthic Anaerobic Oxidation of Methane (AOM) barrier, as well as its impact on benthic CH₄, Dissolved Inorganic Carbon (DIC), and ALK effluxes. Results reveal that AOM is generally a very efficient barrier that consumes almost 100% of the deep CH₄ flux, although the efficiency at seep sites can be significantly reduced. In addition, AOM produces DIC and ALK that locally increase the porewater pH, resulting in a porewater saturation with respect to calcium carbonate minerals (Ω_{Cal}). The quantitative assessment of the AOM process on the Arctic Ocean pH thus needs to include the potential effects of sedimentary carbonate precipitation on the DIC to ALK ratio of the benthic effluxes.

References

- E. Dendy Sloan Jr., & Carolyn A. Koh. (2008). *Clathrate Hydrates of Natural Gases*: Vol. 3rd ed. E. Dendy Sloan, Carolyn A. Koh. CRC Press.
- Brüchert, V., Bröder, L., Sawicka, J. E., Tesi, T., Joye, S. P., Sun, X., Semiletov, I. P., & Samarkin, V. A. (2018). Carbon mineralization in Laptev and East Siberian sea shelf and slope sediment. *Biogeosciences*, 15(2), 471–490. <https://doi.org/10.5194/bg-2017-119>

Evolution of iron-organic carbon interactions during abrupt thaw in ice-rich permafrost: case study in Siberia

Alexia GILLIOT¹, Arthur MONHONVAL¹, Justin LOUIS¹, Benoît PEREIRA¹, Aubry VANDEUREN¹, Loeka JONGEJANS², Jens STRAUSS², Sophie OPFERGELT¹

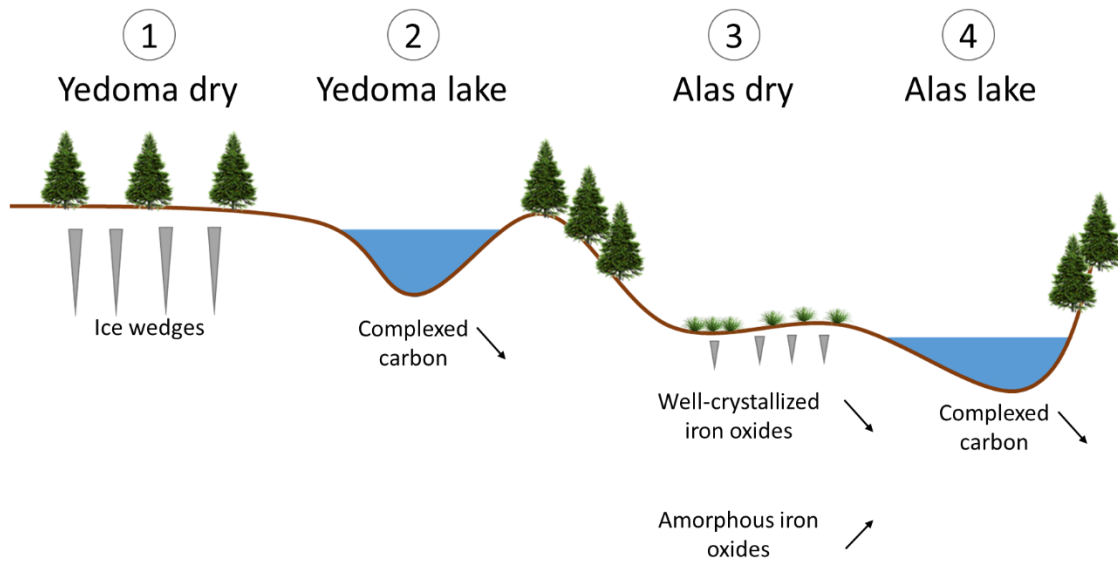
1. *Earth and Life Institute, Université catholique de Louvain, Louvain-la-Neuve, Belgium* (alexia.gilliot@student.uclouvain.be; arthur.monhonval@uclouvain.be; justin.louis@student.uclouvain.be; benoit.pereira@uclouvain.be; aubry.vandeuren@uclouvain.be; sophie.opfergelt@uclouvain.be)
2. *Permafrost Research Section, Alfred Wegener Institute Helmholtz Centre for Polar and Marine Research, Potsdam, Germany* (loeka.jongejans@awi.de; jens.strauss@awi.de)

Permafrost are permanently frozen ground found in northern latitudes. Deposits in permafrost regions store significant amounts of carbon, estimated at 1400 - 1600 GtC. Yedoma deposits, defined as ice-rich permafrost, contribute significantly to this carbon stock. With global warming, Yedoma deposits are likely to undergo abrupt thaw leading to thermokarst collapse, resulting in the formation of Alas deposits. The organic carbon stored in these frozen deposits could be exposed to microbial mineralization upon thaw, be released as CO₂ or CH₄ in the atmosphere and amplify global warming. However, many uncertainties remain on the subject, including the role of mineral elements on the mineralization rate of this carbon.

This study focuses on the evolution of the different forms of iron (i.e., crystalline, amorphous or complexed forms) during abrupt thaw of an ice-rich permafrost profile and its impact on organic carbon release. We analyzed four sediment cores from central Yakutia (Siberia) representative for progressive stages of thermokarst processes (i.e., Yedoma dry, Yedoma lake, Alas dry and Alas lake). The concentrations of total iron and iron selectively extracted using dithionite-citrate-bicarbonate (DCB), ammonium oxalate, and Na-pyrophosphate were measured. The organic carbon bound to these iron pools was also selectively extracted. We found i) a lower concentration of well-crystallized iron in Yedoma deposits that have already undergone abrupt thawing during the Holocene, and ii) a lower concentration of complexed carbon in samples underneath lakes, under anoxic conditions, compared to samples from drier areas (Figure 1).

References

Windirsch, T., Grosse, G., Ulrich, M., Schirrmeister, L., Fedorov, A. N., Konstantinov, P. Y., Fuchs, M., Jongejans, L. L., Wolter, J., Opel, T., & Strauss, J. (2020). Organic carbon characteristics in ice-rich permafrost in alas and Yedoma deposits, central Yakutia, Siberia. *Biogeosciences*, 17, 3797–3814. <https://doi.org/10.5194/bg-17-3797-2020>.



Modified from Windirsch et al., 2020

Figure 1. Schematic of the evolution of iron and carbon within the deposits from the four sampling site (Yukechi, Siberia): 1) Yedoma dry, 2) Yedoma lake, 3) Alas dry and 4) Alas lake.

Towards a Coupled Hydrological-Biogeochemical Model of Subglacial Environments

Nick HAYES, Ankit PRAMANIK, Sandra ARNDT

Université Libre de Bruxelles, BGeoSys, Avenue F.D. Roosevelt 50, Brussels 1050, Belgium

Subglacial environments are dynamic environments that support active ecosystems and complex biogeochemical reactions driven by a range of physical processes, challenging previously held notions that subglacial environments are inactive, lifeless regions (e.g. Sharp and Tranter, 2017). These ecosystems and processes have impacts on other earth systems with implications for biodiversity and economic considerations (Wadham et al, 2013, Hawkings et al, 2014). Another pressing concern is how climate change may also affect subglacial processes. Our understanding of these processes however is hampered by the difficulty of directly observing the subglacial environment in any comprehensive manner.

In the absence of direct observations, creating computer models of the subglacial environment is an attractive solution. Hydrological models of glacial environments have been in use for decades, while biogeochemical modelling has long been used by the geochemical community, although combining these approaches in one model has not yet been applied to the study of subglacial environments. To that end, we are developing a coupled hydrological-biogeochemical to investigate processes in subglacial environments, with particular focus on large ice sheets such as those in Greenland and Antarctica. We are also aiming towards an eventual goal of creating a modelling tool open for use and modification by the subglacial community.

Our preliminary efforts have focused on using data from a glacial hydrological model and applying that to a basic geochemical framework to model potential processes at the Leverett Glacier, Greenland. We present preliminary results of modelled chemical weathering processes and CH₄ production and compare these to known outflow data from Leverett. We also identify key directions for future development and highlight potential applications for the model to investigate other subglacial processes.

Sharp, M, and Tranter, M., 2017. Glacier biogeochemistry, *Geochemical Perspectives* 6, pp. 173-174

Wadham, J.L., De'Ath, R., Monteiro, F.M., Tranter, M., Ridgwell, A., Raiswell, R. and Tulaczyk, S., 2013. The potential role of the Antarctic Ice Sheet in global biogeochemical cycles. *Earth and Environmental Science Transactions of the Royal Society of Edinburgh*, 104(1), pp.55-67.

Hawkings, J.R., Wadham, J.L., Tranter, M., Raiswell, R., Benning, L.G., Statham, P.J., Tedstone, A., Nienow, P., Lee, K. and Telling, J., 2014. Ice Sheets as a significant source of highly reactive nanoparticulate iron to the oceans. *Nature communications*, 5(1), pp.1-8.

Assessing the production and efflux of methane gas from thawing subsea permafrost on the warming Arctic shelf

Constance LEFEBVRE¹, Emilia RIDOLFI², Maria DE LA FUENTE RUIZ³, Sandra ARNDT⁴

¹BGeoSys, Université Libre de Bruxelles, Brussels, Belgium, (Constance.Lefebvre@ulb.be)

²*Idem*, (Emilia.Ridolfi@ulb.be)

³*Idem*, (Maria.De.La.Fuente.Ruiz@ulb.be)

⁴*Idem*, (Sandra.Arndt@ulb.be)

As the world's oceans warm in the coming centuries, the temperature rise in the Arctic Ocean is expected to be even more pronounced because of Arctic amplification. As bottom water temperatures rise, the thawing of the subsea permafrost, believed to contain ~560 PgC of potential reactive organic matter (OM; Sayedi et al., 2020), is likely to accelerate. The projected thawing of the subsea permafrost will lead to a “reactivation” of this previously frozen and inaccessible OM. Bacterial degradation will resume, converting OM into methane (CH₄). The amount of CH₄ ultimately released into the Arctic Ocean is currently uncertain and the subject of debate, as a yet poorly understood portion of the CH₄ is consumed before it reaches the water column. In particular, the benthic CH₄ sink – the complex interplay of multiphase CH₄ transport and microbial oxidation processes – acts as an efficient biofilter that can completely consume permafrost-derived CH₄ fluxes before they reach the seafloor. Yet, the efficiency of this microbial filter is highly variable (0-100%) and can be significantly weaker if a large fraction of the produced CH₄ is transported in gaseous form (phase inaccessible to the microbial community).

The production of CH₄ gas on the Arctic shelf will vary between hundredths and tens of PgC by 2100, and it seems anaerobic oxidation will only consume part of the dissolved CH₄ (Ridolfi et al., *in preparation*). The rest will accumulate in porewaters, facilitating the formation of free gas when saturation is reached. Therefore, we aim to provide a quantification of potential gaseous CH₄ escape from projected permafrost thaw on the warming Arctic shelf by using a pseudo-3D reaction-transport model. The model is used to quantify multiphase CH₄ production and transport for different warming scenarios over the entire Arctic shelf. Darcy's law is used to describe the migration of the free CH₄ gas phase. Then, we evaluate the sensitivity of the model to the variability and uncertainty in the key controls on benthic CH₄ cycling: the quantity and reactivity of subsea permafrost organic matter, and the permeability of the sediments through which CH₄ is transported.

References

Ridolfi, E., et al. (in preparation).

Sayedi, S. S., Abbott, B. W., Thornton, B. F., Frederick, J. M., Vonk, J. E., Overduin, P., Schädel, C., Schuur, E. A. G., Bourbonnais, A., Demidov, N., Gavrillov, A., He, S., Hugelius, G., Jakobsson, M., Jones, M. C., Joug, D., Kraev, G., Macdonald, R. W., McGuire, A. D., Frei, R. J., 2020. Subsea permafrost carbon stocks and climate change sensitivity estimated by expert assessment. *Environmental Research Letters*, 15(12), 124075. <https://doi.org/10.1088/1748-9326/abcc29>

Influence of thermokarst formation on manganese-organic carbon interactions in ice-rich permafrost

Justin LOUIS¹, Arthur MONHONVAL¹, Alexia GILLIOT¹, Aubry VANDEUREN¹, Benoît PEREIRA¹, Loeka JONGEJANS², Jens STRAUSS², Sophie OPFERGELT¹

1. *Earth and Life Institute, Université catholique de Louvain, Louvain-la-Neuve, Belgium* (justin.louis@student.uclouvain.be; arthur.monhonval@uclouvain.be; alexia.gilliot@student.uclouvain.be; aubry.vandeuren@uclouvain.be; benoit.pereira@uclouvain.be; sophie.opfergelt@uclouvain.be)
2. *Permafrost Research Section, Alfred Wegener Institute Helmholtz Centre for Polar and Marine Research, Potsdam, Germany* (loeka.jongejans@awi.de; jens.strauss@awi.de)

Abrupt permafrost thaw leads to changing redox conditions (Figure 1), thereby affecting manganese forms and their potential role in organic carbon stabilization. We analyzed four sediment cores from Central Yakutia (Russia) representing progressive thermokarst processes, from continuously frozen Yedoma deposits (Windirsch et al., 2020) to an Alas lake in a Holocene thermokarst basin that underwent multiple lake generations (Jongejans et al, 2021). We analyzed total manganese concentrations and manganese selectively extracted with dithionite-citrate-bicarbonate (DCB), oxalate and pyrophosphate. In addition, we analyzed organic carbon selectively extracted by oxalate and pyrophosphate. We also determined the main crystalline minerals by X-ray diffraction analyses.

We found that i) selective extractions by DCB, oxalate and pyrophosphate are valid for quantifying manganese phases, and ii) thermokarst processes influence interactions between manganese and organic carbon in ice-rich permafrost.

References

Jongejans, L. L., Liebner, S., Knoblauch, C., Mangelsdorf, K., Ulrich, M., Grosse, G., Tanski, G., Fedorov, A. N., Konstantinov, P. Y., Windirsch, T., Wiedmann, J., & Strauss, J. (2021). Greenhouse gas production and lipid biomarker distribution in Yedoma and Alas thermokarst lake sediments in Eastern Siberia. *Global Change Biology*, 27, 2822-2839. <https://doi.org/10.1111/gcb.15566>.

Windirsch, T., Grosse, G., Ulrich, M., Schirrmeister, L., Fedorov, A. N., Konstantinov, P. Y., Fuchs, M., Jongejans, L. L., Wolter, J., Opel, T., & Strauss, J. (2020). Organic carbon characteristics in ice-rich permafrost in alas and Yedoma deposits, central Yakutia, Siberia. *Biogeosciences*, 17, 3797–3814. <https://doi.org/10.5194/bg-17-3797-2020>.

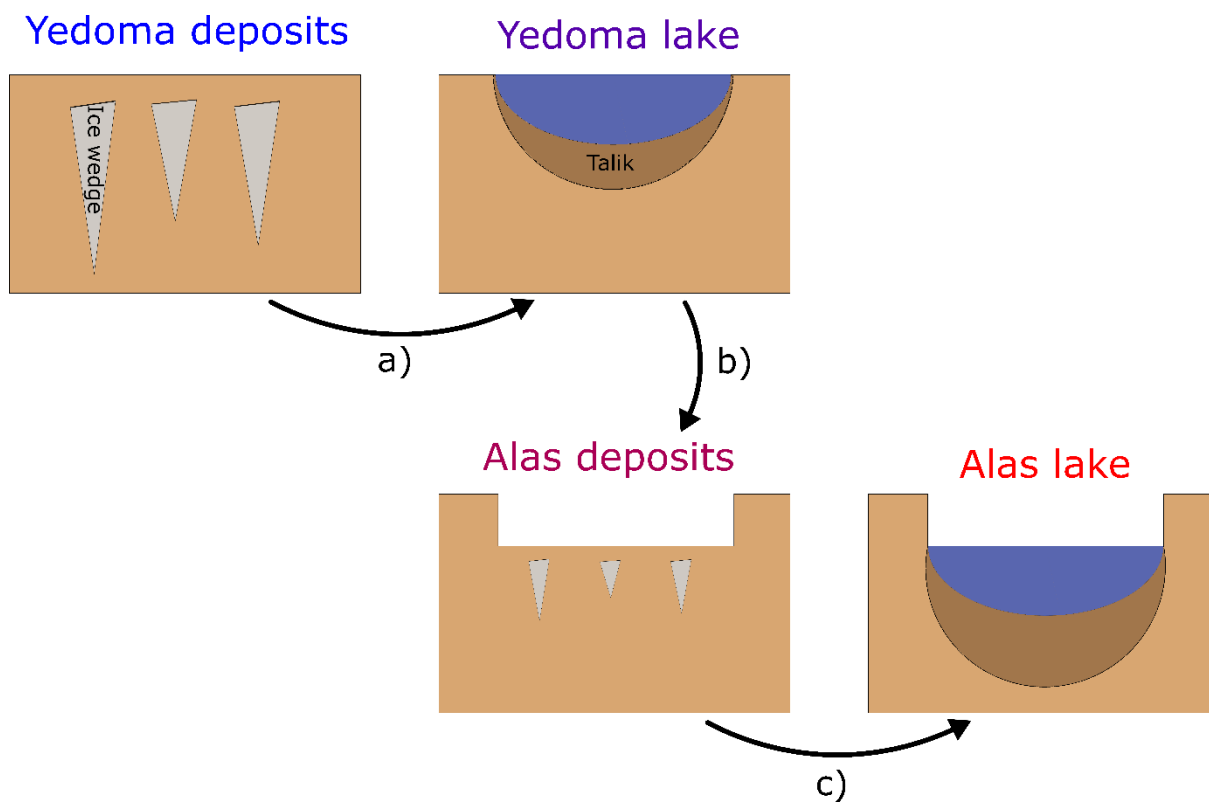


Figure 1: Evolution of redox conditions in response to progressive thermokarst processes: a) Surface subsidence and thaw lake development b) Lake drainage and sediment refreezing c) Second generation surface subsidence and thaw lake development.

Influence of permafrost degradation on foliar mineral element cycling upon changing subarctic tundra vegetation

Elisabeth MAUCLET¹, Yannick AGNAN¹, Catherine HIRST¹, Arthur MONHONVAL¹, Justin LEDMAN², Meghan TAYLOR², Edward A. G. SCHUUR², Sophie OPFERGELT¹

1. *Earth and Life Institute, Université catholique de Louvain, Louvain-la-Neuve, Belgium*

(elisabeth.mauclet@uclouvain.be, yannick.agnan@uclouvain.be, catherine.hirst@uclouvain.be, arthur.monhonval@uclouvain.be, sophie.opfergelt@uclouvain.be)

2. *Center for Ecosystem Society and Science, Northern Arizona University, Flagstaff, AZ, USA*

(justin.ledman@gmail.com, meghan.taylor@yale.edu, ted.schuur@nau.edu)

Climate warming strongly affects the Arctic region by creating soil subsidence, increasing thaw depth and modifying water table depth. Thawing permafrost unlocks deeper soil mineral nutrients that may boost plant growth, and generates microtopography that may induce contrasted local soil moisture conditions. According to soil subsidence and drainage capacity, shift in vegetation through the Arctic and sub-Arctic region may vary, with sedges (as part of graminoids) expanding through wetter lowlands and shrubs expanding through drier uplands. Consequently, changes in the composition of Arctic tundra vegetation may influence local mineral element cycling through litter production, but this remains poorly constrained. In order to evaluate the influence of permafrost degradation on litter composition, we determined foliar mineral element stocks and annual litterfall fluxes from a typical Arctic tundra. We measured foliar elemental composition (Al, Ca, Fe, K, Mn, P, S, Si, and Zn) of leaf samples from 7 vascular species and 6 non-vascular species (mosses and lichens) from two contrasted Alaskan sites, i.e., under experimental (CiPEHR) and natural (Gradient) warming. We found that foliar composition is specific to the species and independent of the permafrost degradation. Therefore, the shift in the tundra vegetation related to climate change is expected to mostly influence the change in litter mineral element composition.

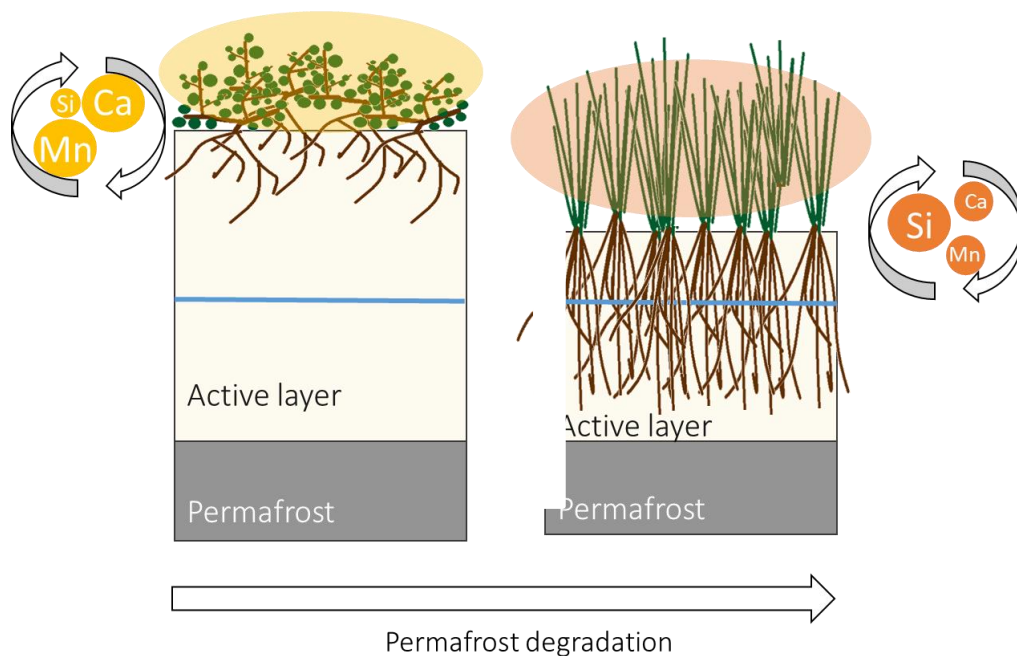
Upon sedge expansion, foliar mineral element stocks largely increased for elements highly concentrated into sedge leaves, such as Si (i.e., Si foliar stock increased ~4 times over 8 years of warming experiment and related sedge expansion). Upon shrub expansion, foliar mineral element stocks increased for elements highly concentrated into shrub leaves, such as Ca and Mn (i.e., Ca and Mn foliar stocks were ~1.5 times higher upon shrub- than sedge-land). As a cascade reaction, changes in foliar mineral element stocks related to the shift in vegetation led to changes in their annual litterfall fluxes, with an increase in Si annual foliar fluxes upon sedge annual litterfall, and an increase in Ca and Mn annual foliar flux upon shrub annual litterfall (Figure 1). Consequently, sedge and shrub expansion led to contrasted litter elemental composition, and thereby contrasted nutrient cycling, with implications for further vegetation succession across the Arctic tundra.

References

Schuur, E.A.G., Crummer, K.G., Vogel, J.G., Mack, M.C., 2007. Plant species composition and productivity following permafrost thaw and thermokarst in Alaskan tundra. *Ecosystems* 10, 280–292. <https://doi.org/10.1007/s10021-007-9024-0>

Schuur, E.A.G., Mack, M.C., 2018. Ecological response to permafrost thaw and consequences for local and global ecosystem services. *Annu. Rev. Ecol. Evol. Syst.* 49, 279–301. <https://doi.org/10.1146/annurev-ecolsys-121415-032349>

Figure: Changing element cycling upon shift in subarctic tundra vegetation from shrub to sedge upon permafrost degradation.



Seasonal dynamics of nitrous oxide in sea ice in the Central Arctic: insights from the MOSAiC Expedition

Sofia MULLER¹, Katarina ABRAHAMSSON², Michael ANGELOPOULOS³, Odile CRABECK¹, Ellen DAMM³, Alessandra D'ANGELO⁴, François FRIPIAT⁵, Daiki NOMURA⁶, Jonathan VAN HANJA¹, Liyang ZHAN⁷, Bruno DELILLE¹

1. *Université de Liège, Liège, Belgium*
(sofia.muller@uliege.be; ocrabeck@uliege.be; jonathan.vanhanja@student.uliege.be; bruno.delille@uliege.be)
2. *University of Gothenburg, Gothenburg, Sweden* (katarina.abrahamsson@gu.se)
3. *Alfred Wegener Institute, Potsdam, Germany* (michael.angelopoulos@awi.de; ellen.damm@awi.de)
4. *University of Rhode Island, Kingston, USA* (a_dangelo@uri.edu)
5. *Université Libre de Bruxelles, Brussels, Belgium* (Francois.Fripiat@ulb.be)
6. *Hokkaido University, Hakodate, Japan* (daiki.nomura@fish.hokudai.ac.jp)
7. *Third Institute of Oceanography, Xiamen, China* (zhanliyang@tio.org.cn)

Nitrous oxide (N₂O) is a potent greenhouse gas (GHG), and a major stratospheric ozone depleter with impacts comparable to CFCs. The recent growth in N₂O emissions to the atmosphere exceeds the worst scenarios of the IPCC, which highlights the importance to limit N₂O emissions but also to better constrain the underlying sources and sinks. There is a lack of data regarding natural sources, especially in polar regions. In addition, sea ice is still considered as an impermeable inert layer in most climate models.

MOSAiC, the largest survey of the Arctic Ocean, aimed to gain fundamental insights that are key to better understand global climate change at the epicentre of global warming. *R.V. Polarstern* drifted with the ice for one year, from 2019 to 2020 in the Central Arctic. MOSAiC provided a unique opportunity to monitor N₂O concentrations within sea ice over the complete sea ice life cycle. We observed that the imprint of sea ice growth processes on N₂O concentrations lasts until summer, with limited seasonal changes. The decoupling between N₂O and salinity patterns within sea ice suggests that N₂O is mainly stored in the gaseous phase (i.e., bubbles) in the sea ice matrix, which has consequences for N₂O transport and air-ice exchanges. Sea ice is N₂O oversaturated with respect to atmospheric concentrations from Fall to Spring, but undersaturated in the Summer. Therefore, assessing if sea ice acts as a source or a sink for atmospheric N₂O requires a careful budget calculation of N₂O in sea ice to account for the observed shift in N₂O saturation.

Further investigations on oxygen and nitrogen (N) isotopes of fixed nitrogen (i.e., nitrate, NO₃⁻, ammonium, NH₄⁺, dissolved organic N, DON, and particulate organic N, PON), will evaluate the biological contributions to N₂O dynamics, and provide a mechanistic understanding of the microbial processes at play.

Quantifying Fe-OC associations in sediment using Na-dithionite in Flow-Through Reactors (FTR)

Silvia PLACITU¹, Sandra ARNDT¹, Steeve BONNEVILLE¹

¹ Biogéochimie et Modélisation du Système Terre, Département Géosciences, Environnement et Société, Université Libre de Bruxelles, Belgium

(silvia.placitu@ulb.be; Sandra.Arndt@ulb.be; Steeve.Bonneville@ulb.be)

Fjord systems show an estimated burial of 18 Mt of C yr⁻¹, which corresponds to approximately 11 % of the C globally buried in marine sediments. Fjord system areas only represent the 0.12 % of the marine surface, which makes them the greatest carbon burial per unit area in the world, and a pivotal hotspot for the global carbon cycle. Thawing of ice sheets and glaciers caused by climate change which is known to be amplified in polar regions, releases additional dissolved organic matter and iron to fjord environments and polar coastal waters.

In sediments, the carbon and iron cycles are tightly interconnected. Organic molecules can be adsorbed onto Fe(III) oxyhydroxides surface but also co-precipitate with dissolved Fe to forms organo-mineral associations (Fe-OM). These processes are believed to participate into the preservation of OM from mineralization and facilitate organic carbon burial in sediments.

Globally, based on the so-called ‘citrate-bicarbonate-dithionite’ (CBD) extraction, approximately 21.5 ± 8.6% of total organic carbon in marine sediments from different depositional settings is believed to be bound within Fe-OM, in a process so called “rusty carbon sink” [1]. However, the CBD method may present some limitations. Chief among those is the need to run a “blank” extraction to evaluate the innocuity of high ionic strength used in the CBD method on the stability of loosely bound OC in sediment, that may actually lead to an underestimation of up to 33% of the Fe-OC association [2]. Here, we propose to use Flow-Through Reactor [3] to quantify Fe-OM in sediment. With respect to the CBD extraction, a slow but constant flux of Na-Dithionite is injected in the reactor, which result in a long time-course extraction that presents several advantages: (i) it allows to use a much lower concentration of Na-dithionite than in the CBD methods, hence limiting the destabilizing ‘salt-effect’ on loosely bound OC (ii) and it avoids the use of citrate as Fe(II)-ligand thus reducing the risk of artefacts. Further benefits are the possibility to work at a circumneutral pH, room temperature and with intact sediment. Overall, the Na-dithionite extraction that we are developing will mimic much better microbial Fe reduction, the metabolic pathways by which Fe-OM could be destabilized in sediment. The FTR setup could also be used to explore the fate of Fe-OM under changing environmental conditions (e.g. pH, salinity, redox conditions).

This new FTR-Na-dithionite method was applied on synthetic Fe-OM with different crystallinity levels, Ferrihydrite 2 Line-C, Ferrihydrite 6 Line-C, Goethite-C. The organic compound used to synthesize these mineral association was xylan, a compound commonly found in green algae and thus naturally present marine organic matter. Quartz sand coated with Fe-OM minerals previously synthesized, was used to fill a 1 cm sediment plug, deployed inside the FTR. The FTR is connected to a peristaltic pump, that allows to have a constant flow of the solution. The extractions were performed with different concentrations of Na-Dithionite (50 g/L, 20 g/L, 10 g/L), for a length of approximately 2 hours. Output solution was analyzed for DOC, Fe(II) and total Fe to follow the kinetic of the extraction. Further investigations will be conducted in Fe-OM from fresh sediment collected in the Scheldt Estuary (Belgium) and, in the future, in Fe-OM from three fjord sediments from Sweden: The

Hake fjord, the Gullmar fjord and the By fjord, that present different redox conditions, and will allow to evaluate the stability of Fe-OM associations in different environmental conditions.

References

- [1] K. Lalonde, A. Mucci, 2012, Preservation of organic matter in sediments promoted by iron. *Nature* 483,198-200. DOI: 10.1038/nature10855.
- [2] B. Fisher, Moore, 2020. Experimental evaluation of the extractability of iron bound organic carbon in sediments as a function of carboxyl content. *Chemical Geology*. 119853. 10.1016/j.chemgeo.2020.119853.
- [3] C. Pallud, C. Meile, 2007, The use of flow-through sediment reactors in biogeochemical kinetics: Methodology and examples of applications. *Marine Chemistry*, Volume 106, Issues 1–2, Pages 256-271, ISSN 0304-4203, DOI: 10.1016/j.marchem.2006.12.01

Figure 1: FTR setup

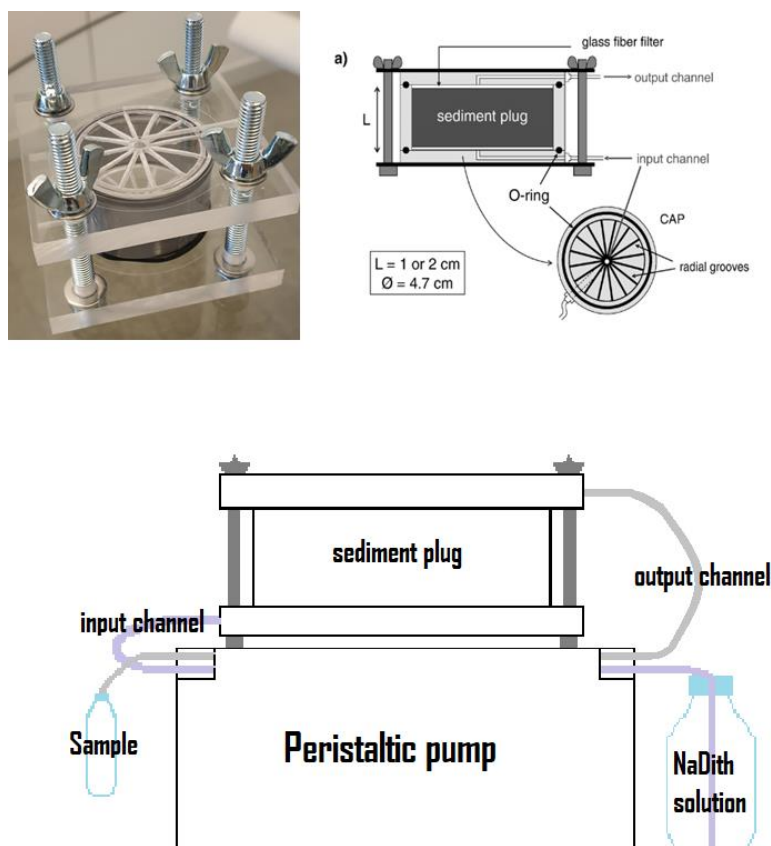


Figure 10: FTR setup

Modeling methane production and emission from thawing sub-sea permafrost on the warming Arctic Shelf

E. Ridolfi¹, S. Wikenskjeld², F. Miesner³, V. Brovkin^{2,4}, P. Overduin³, S. Arndt¹

¹ *Universite Libre de Bruxelles, Bruxelles, Belgium*

² *Max-Planck Institute for Meteorology, Hamburg, Germany*

³ *Alfred Wegener Institut, Potsdam, Germany*

⁴ *Center for Earth System Research and Sustainability, University of Hamburg, Germany*

Corresponding author email: emilia.ridolfi@gmail.com

The Arctic shelf hosts a large, yet poorly quantified reservoir of relic permafrost. It has been suggested that global warming, which is amplified in polar regions, will accelerate the thawing of this subsea permafrost, thus potentially unlocking large stocks of comparably reactive organic matter (OM). The microbial degradation of OM in the thawing and generally anoxic permafrost layer has the potential of producing and, ultimately, releasing important fluxes of CH₄ to the atmosphere. Because CH₄ is a potent greenhouse gas, such a release would further intensify global warming. However, the potential role of subsea permafrost thaw on microbial CH₄ production and CH₄ emissions from Arctic sediments currently remains unconstrained.

Here, we use a nested model approach to address this critical knowledge gap. We developed a pseudo-three-dimensional reaction-transport model for permafrost bearing sediments on the Arctic shelf to estimate the production, consumption, and, efflux of CH₄ on the Arctic shelf in response to projected subsea permafrost thaw. The model accounts for the most pertinent biogeochemical processes affecting methane and sulfur cycling in permafrost bearing marine sediments.

It is initialized based on an existing submarine permafrost map (SuPerMap, [1]) and forced by a range of projected thawing rate scenarios derived from the Max Planck Institute Earth System Model (MPI-ESM) simulation results for the period 1850-2100. Critical model parameters, such as permafrost OM content and its apparent reactivity are chosen based on a comprehensive analysis of published experimental data. Here, we present the output of this environmental scenario ensemble.

Simulation results reveal that CH₄ production rates are highly sensitive to changes in the apparent reactivity of permafrost OM. Although simulated CH₄ production rates vary over a large range (0.02-46 PgC produced over 250 years; 0.05-64 PgC produced over 250 years), they generally highlight the potential for producing and, thus releasing large amounts of methane from thawing subsea permafrost on the warming Arctic Shelf.

References

[1] Overduin, P. P., et al. (2019) - Submarine permafrost map in the Arctic modeled using 1-D transient heat flux (SuPerMAP). *Journal of Geophysical Research: Oceans*, 124, 3490–3507. <https://doi.org/10.1029/2018JC014675>

Influence of permafrost degradation and shift in vegetation on litter and soil properties: case study in Central Alaska

Maëlle VILLANI¹, Elisabeth MAUCLET¹, Yannick AGNAN¹, Edward A. G. SCHUUR², Sophie OPFERGELT¹

1. *Earth and Life Institute, Université catholique de Louvain, Louvain-la-Neuve, Belgium*

(maelle.villani@student.uclouvain.be, elisabeth.mauclet@uclouvain.be,
yannick.agnan@uclouvain.be, sophie.opfergelt@uclouvain.be)

2. *Center for Ecosystem Society and Science, Northern Arizona University, Flagstaff, AZ, USA*

(ted.schuur@nau.edu)

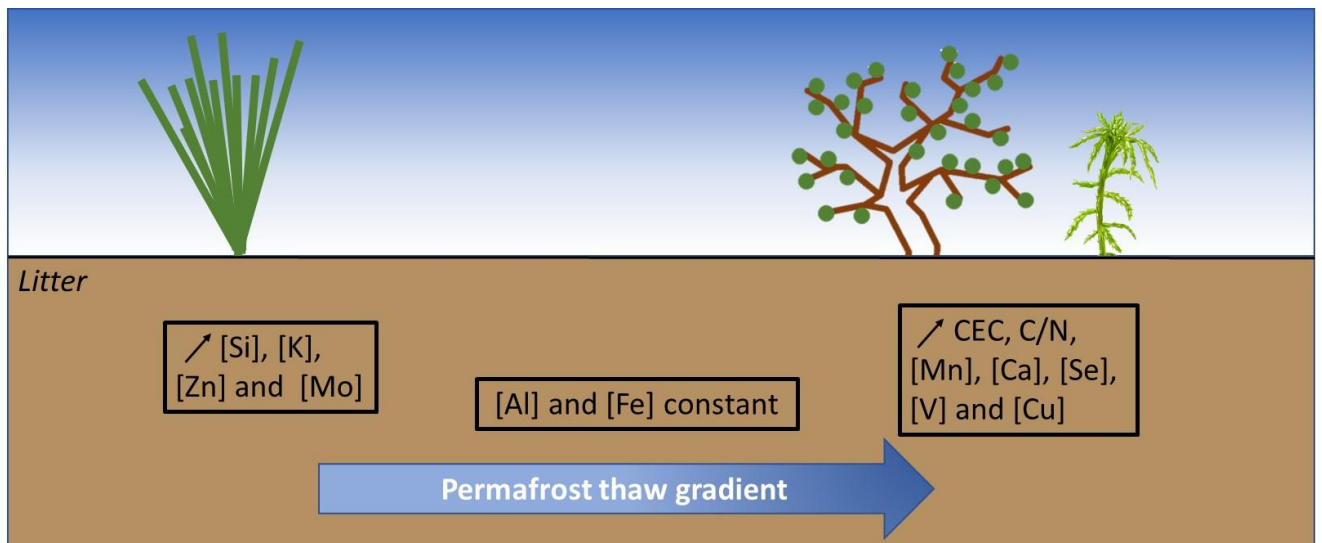
Global warming affects the Arctic and sub-Arctic regions by exposing previously frozen permafrost to thaw, unlocking mineral nutrients, stimulating microbial activity, and boosting plant growth. Initially composed of graminoids, forbs, deciduous and evergreen shrubs, mosses and lichens, Arctic tundra is subject to a shrub, forb and moss expansion, at the expense of graminoid species. For now, little is known about the intrinsic foliar properties of these plant species and how they may influence properties of the underlying litter. Therefore, we investigated vegetation foliar properties and litter properties (organic carbon, C/N ratio, cation exchange capacity (CEC), pH, and concentrations of major and trace elements), from a typical Arctic tundra across a natural gradient of permafrost degradation.

Results show that vegetation foliar properties are intrinsic to plant species and do not depend on the permafrost degradation stage. Furthermore, the natural gradient of permafrost degradation showed contrasts in litter mineral element concentrations, related to the occurring shift in vegetation. For example, we found a decrease in silicon concentrations in the litter between the least and the most degraded permafrost site, which is concurrent with the decrease in graminoids (Si-rich plant species) and the increase in shrubs biomass (Si-poor plant species), upon permafrost degradation. Therefore, changes in vegetation composition may influence litter properties, such as C/N ratio, CEC and mineral element concentrations (Figure 1), which could in turn influence C dynamics with the change of nutrient availability for plant cover.

References

- Chapin F. S., Sturm M., Serreze M. C., McFadden J. P., Key J. R., Lloyd A. H., McGuire A. D., Rupp T. S., Lynch A. H., Schimel J. P., Beringer J., Chapman W. L., Epstein H. E., Euskirchen E. S., Hinzman L. D., Jia G., Ping C-L., Tape K. D., Thompson C. D. C., Walker D. A., Welker J. M., 2005. Role of land-surface changes in Arctic summer warming. *Science*, 310(5748), 657-660.
- Hobbie, S. E., 1996. Temperature and plant species control over litter decomposition in Alaskan tundra. *Ecological monographs*, 66(4), 503-522.
- Schuur E. A. G., McGuire A. D., Schädel C., Grosse G., Harden J. W., Hayes D. J., Hugelius G., Koven C. D., Kuhry P., Lawrence D. M., Natali S. M., Olefeldt D., Romanovsky V. E., Schaefer K., Turetsky M. R., Treat C. C., Vonk J. E., 2015. Climate change and the permafrost carbon feedback. *Nature*, 520(7546), 171-179.

Figure: Changing litter elemental composition and properties upon shift in subarctic tundra vegetation from sedges (left) to forbs and mosses (right) upon permafrost degradation.



Session 10 - Quaternary and Anthropocene (BELQUA)

Convener:

Nathalie Fagel (ULiège)

This session, organized by the BELQUA National Committee, aims to review ongoing Quaternary research in Belgium and abroad. The Quaternary has been redefined in 2009 by the International Union of Geological Sciences (IUGS) and the International Commission of Stratigraphy (ICS) after decades of debates (Keer 2008). The Quaternary is now considered as the youngest system within the Cenozoic erathem, it is composed by the Pleistocene and the Holocene series and its base is fixed at 2.6 Ma. The Quaternary is characterized by a high climate variability, with a succession of cold (glacial) and warm (interglacial) periods. These environmental changes influence all the compartments of the Earth system (i.e., atmosphere, hydrosphere, cryosphere, lithosphere, and biosphere). The Quaternary also corresponds to a major evolution of the Hominids with the appearance of the earliest Homo genus. The human induced environmental changes will progressively exceed the natural changes, leading to the definition of the Anthropocene. We invite any contributions dealing with any field of the Quaternary, from field campaign to climate modelling.



Preliminary results from palynological and diatoms analyses from three sites of the Medieval harbour network in the Zwin area in North of Belgium and the Netherlands: Hoeke, Mude and Aardenburg

Coralie ANDRE¹, Wim DE CLERCQ², Dante DE RUIJSSCHER², Vanessa M.A. HEYVAERT^{1,3}, Frieda BOGEMANS³, Stephen LOUWYE¹

¹Ghent University, Department of Geology, Gent, Belgium.

²Ghent University, Department of Archaeology, Gent, Belgium.

³Royal Belgian Institute of Natural Sciences, Geological Survey of Belgium, Brussels, Belgium

Bruges late medieval harbour in northern Belgium is considered as a gateway society where goods, people and thoughts were exchanged. The landscape was earlier subject to an extreme flooding event leading to a natural large tidal inlet. Thereafter, interactions between man and nature in the Zwin area, via hydraulic interventions such as construction of canals and dikes, transformed the landscape into a major artery of connectivity. In the north-east, a network of outer ports arose: Damme, Monnikerede, Hoeke and Mude near the sea-mouth at Sluis. However, after its medieval heyday, Bruges' economy collapsed and the city and its outport network fell in disuse. This area has been covered by a thin layer of clay and spared from human activities, thus providing a huge potential for interdisciplinary paleoenvironmental studies.

Microfossils such as diatoms and palynological proxies (pollen, spores and non-pollen palynomorphs) are used to reconstruct the past landscapes of the greater Zwin area during the Roman/Medieval Age periods. Diatoms allow to visualize the evolution of the aquatic environment while pollen, spores and non-pollen palynomorphs allow a reconstruction of the evolution of the vegetation.

At Hoeke, a total of 28 regularly spaced subsamples were taken for palynological and diatom analyses below the embankment. The three lower subsamples belong to a peat layer and the 11 upper subsamples are part of a silty clay/clayey silt layer. The total pollen record shows several origins of the palynomorphs with the presence of eutrophic wetland (e.i. *Alnus*) and oligotrophic wetland (e.i. *Sphagnum*) but also dryland forest (e.i. *Corylus avellana* and *Quercus robur*). In the upper layer, saltmarshes taxa (e.i. *Chenopodiaceae* and *Senecio-type*), marine (dinoflagellate cysts) and freshwater (*Pediastrum*) occur next to the palynomorphs previously cited. The diatoms were however only present in the subsamples of the upper layer and in one subsample from the peat layer, and the assemblages are dominated by marine/brackish species (e.i. *Paralia sulcata* and *Rhaphoneis amphiceros*), typical from coastal deposits in Belgium and in the Netherlands. In conclusion, at Hoeke a natural coastal environment is recorded with the presence of an increased peat layer.

At Mude, 24 subsamples for palynological and diatoms analyses were taken from silty/clayey deposits. The main upper layer is an embankment structure consisting of a lower clay layer and an upper shell layer deposited by human as a waste layer. The pollen record contains a mixture of palynomorphs similar to those found in Hoeke. The diatom record shows mixed signals with on the one hand a natural coastal environment represented by the continuous presence of the marine/brackish diatoms (e.i. *Paralia sulcata* and *Rhaphoneis amphiceros*). On the other hand the high abundance of terrestrial diatoms (e.i. *Hantzschia amphioxys*) in the shell layer confirm the presence of an embankment. Further research is ongoing below the embankment in order to visualize the natural coastal environment evolution.

The palynological analysis at the Aardenburg site was carried out in three deposits: the Pleistocene sand, the Roman layer and the marine sediments. A total of 16 palynological subsamples were analysed and only 5 subsamples from the Pleistocene sand and the Roman layer held sufficient and well-preserved diatoms. The results indicate that the Romans were living in an occasionally flooded saltmarsh area that could have evolved into a mudflat environment by ever increasing flooding. This evolution ultimately would have led to an uninhabitable area during Roman times. In the upper marine sediment layer, we observe a lithological transition from clay to slightly clayey silt. At this depth, the saltmarshes taxa decrease while Poaceae and Cerealia-type sharply increase. Humans could have used the area as grassland for sheep in a passive agriculture or they could have actively used the land as arable fields for agriculture.

Has hydrologic connectivity been taken into account in the Lake Tana Basin (Ethiopia): a literature review on climate, hydrology and geomorphology

Anik Juli Dwi ASTUTI¹, Sofie ANNYS¹, Jan NYSSSEN¹, Stefaan DONDEYNE¹

1. Department of Geography, Ghent University, Krijgslaan 281 (S8), B-9000 Ghent, Gent, Belgium (AnikJuliDwi.Astuti@ugent.be; Sofie.Annys@ugent.be; Jan.Nyssen@ugent.be; Stefaan.Dondeyne@ugent.be)

Knowledge on hydrologic connectivity is important to grasp the hydrologic response at basin scales as changes in connectivity can lead to soil erosion, floods and land degradation. The Lake Tana Basin in Ethiopia constitutes the headwaters of the Blue Nile River and is undergoing rapid developments and environmental changes. Given the numerous studies on climate, hydrology and geomorphology conducted in the area, we analysed to what extent hydrologic connectivity has been taken into account. Doing so, we aimed at identifying research gaps relevant for land and water management.

Following a systematic quantitative approach (Pickering and Byrne 2014), publications available in the Web of Science and Scopus databases were identified by searching for “Lake Tana” in combination with terms relating to climate, hydrology, land use/land cover and geomorphology. The search yielded about 400 publications from which 135 publications were retained after removing duplicates and screening for relevance. Drawing on the conceptual framework for a “systems approach in sediment and water transfer” studies (Keesstra et al. 2018), we analysed to what extent changing drivers of connectivity, and their structural and functional relations have been taken into account. We further investigated the spatial scales at which these aspects have been studied, and the kind of models used as analytical tools (descriptive, empirical, statistical or process-based).

Amongst the drivers of changing connectivity, climate was covered in the majority of the publications (64%), land use and land cover in about half (52%) and specific land or water management issues, including soil and water conservation measures, only in a minority (17%) of the publications. Aspects of structural hydrologic connectivity were accounted for by considering geomorphology (54%) and soils (47%), and to a lesser extent by hydrography (16%) and geology (12%). Aspects of functional connectivity were covered by looking at surface water fluxes (61%), sediment fluxes (18%) and subsurface water fluxes (13%) (Figure 1). More than half (54%) of the publications reported on research conducted in one, or several, of the sub-basins of the Lake Tana Basin. About one third (34%) looked at the whole basin, or considered it as part of the wider Upper Blue Nile Basin, while a few (7%) were concerned with Lake Tana itself, and even fewer (4%) reported on studies conducted at field or plot level. Process-based models – with SWAT as the most popular – often combined with statistical models, were the most used tools of analysis (43%), directly followed by statistical models (36%). Some of the publications (19%) were solely descriptive and very few publications (3%) relied on empirical models such as the RUSLE equation.

Most striking is that none of the publications took hydrologic connectivity explicitly into account, but covered connectivity only implicitly. The implicit connectivity has been best accounted for by using semi-distributed process-based models. As changes in rainfall and evapotranspiration directly affect hydrologic connectivity, it is encouraging that this topic has already been extensively studied. However, more attention has been given to future projections of climate while little attention has been paid to the interaction between past changes in climate and land uses. Also, the variation in the water infiltration capacity in relation to geology, geomorphology and soils has received little attention. At the basin level, the impact of soil and water conservation measures has hardly been studied nor has the contribution of gully erosion been well taken into account in hydrologic and sediment modelling. We argue that by taking hydrologic connectivity explicitly into account in future research, better insights into the effects on hydrologic processes of changing climate and land uses could be obtained.

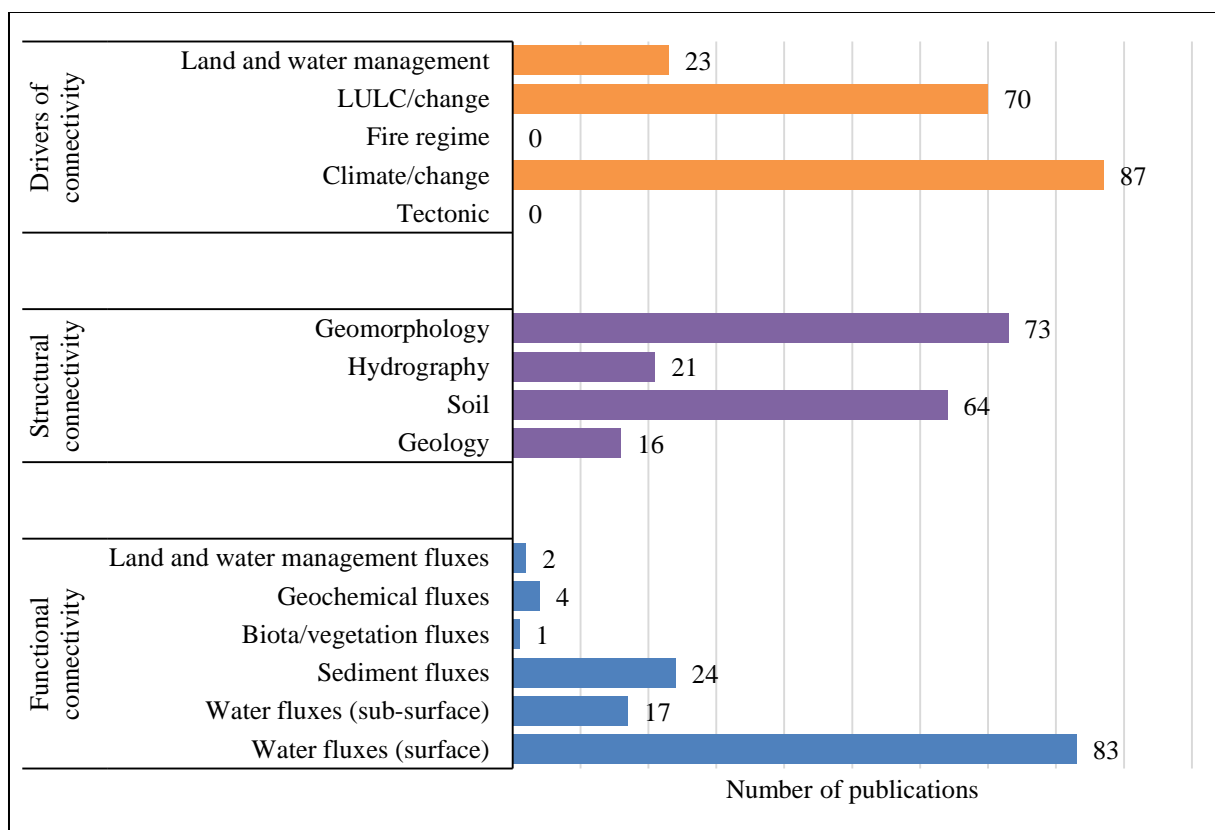


Figure 11 – Number of publications covering aspects of changing drivers of hydrologic connectivity, besides aspects of structural and functional connectivity, following the concepts proposed by Keesstra et al. (2018). One publication can cover multiple (sub)aspects.

References

- Keesstra S, Nunes JP, Saco P, et al (2018) The way forward: Can connectivity be useful to design better measuring and modelling schemes for water and sediment dynamics? *Science of The Total Environment* 644:1557–1572. <https://doi.org/10.1016/j.scitotenv.2018.06.342>
- Pickering C, Byrne J (2014) The benefits of publishing systematic quantitative literature reviews for PhD candidates and other early-career researchers. *Higher Education Research & Development* 33:534–548. <https://doi.org/10.1080/07294360.2013.841651>

Lacustrine record of last millennia precipitation from Lake Esponja and Lake Bertrand of Northern Chilean Patagonia (72°W)

Jeanne AUBOIRON¹, Denisse ALVAREZ², Alberto ARANEDA², Pablo PEDREROS², Roberto URRUTIA² and Nathalie FAGEL³

1. *University of Rouen, Rouen, France, jeanne.auboiron@univ-rouen.fr*
2. *Centre of Environmental Sciences EULA-Chile and CHRIAM Water Research Centre, Department of Aquatic Systems, Faculty of Environmental Sciences, Universidad de Concepción, P.O. Box 160-C Concepción, Chile, dealvarez@udec.cl, aaaranaeda.ec@gmail.com, papedrer@udec.cl, rurrutia@udec.cl*
3. *Departement of Geology, AGEs, University of Liège, 4000 Liège, Belgium, nathalie.fagel@uliege.be*

The aim of this study is to reconstruct climatic variability and its impact on the environment in Northern Chilean Patagonia during the last millennium, using a multi-proxy analysis of sediment cores from Lake Esponja (45°09'S, 72°08'W) and Lake Bertrand (46°55'S 72°50'W). The lakes are located in the Aysen del General Carlos Ibanez del Campo region of north-western Patagonia. Core LEs14 (150 cm) was collected in Lake Esponja in 2014 at a depth of 40 m and core LBb11A (161 cm) was collected in a sub-basin of Bertrand Lake in 2011 at a depth of 21 m.

XRF core scanner geochemistry and SCOPIX X-radiography were conducted at 1 mm sampling resolution. The lake sediments are mainly composed of clayey silts with some organic-rich layers. The XRF core scanner geochemistry indicates dominant detrital supplies (> 80%) into the Lake Bertrand. The organic matter mainly comes from the watershed. Correlations between sedimentological and geochemical parameters as well as instrumental data allowed the identification of precipitation proxies. A multivariate analysis was used to reconstruct the precipitation for the last 2200 years through the sedimentary sequences of the lake. Both the Little Ice Age and the Medieval Warming events are identified within these reconstructions.

The obtained reconstruction was compared with each other and with paleoclimatic information obtained from lake sediments and other climate archives. The application of similar methodology to other Patagonian lake sequences would bring a more global vision of the evolution of the climate in Patagonia over the last millennia.

Keywords

Holocene, Patagonia, Precipitation, Lake sediment, XRF core scanner geochemistry, Little Ice Age, Medieval warm period

Vegetation history in the Ethiopian Highlands for the past 18000 years: a multi-proxy analysis of high altitude wetlands

Femke AUGUSTIJNS ^{1,2}, Nils BROOThAERTS ², Gert VERSTRAETEN ²

1. *Research Foundation Flanders - FWO, Brussels, Belgium (femke.augustijns@kuleuven.be)*
2. *KU Leuven, Department of Earth and Environmental Sciences, Division of Geography and Tourism, Leuven, Belgium*

The Ethiopian landscape is characterized by a steep topography, resulting in an altitudinal zonation of climate and vegetation. Archeological evidence suggests that the relatively cool and wet highland environments might have served as human refugia during times of increased aridity in the warm and dry rift valley (Foerster et al. 2015). Long term human presence at high altitudes in SW Ethiopia is also shown by occupied rock shelters (Ossendorf et al. 2019) and sedimentological evidence of agriculture (Coltorti et al. 2019). The Ethiopian Highlands are even identified as a potential center of plant domestication for several crops including coffee and teff (Diamond 2002).

A good insight into Ethiopia's past vegetation would allow to shed light on vertical shifts of vegetation zones as a response to humidity fluctuations over time and could contribute to reconstruct Ethiopia's agricultural history, which is still largely unknown. A dozen pollen studies have been conducted in Ethiopia, but almost exclusively using single-proxy and single-location approaches, limiting the understanding of the past dynamics of a complex and zoned vegetation. This research aims to contribute to filling these research gaps by reconstructing the vegetation of the Gamo Highlands in SW Ethiopia, using a multi-proxy and multi-site approach. For this, several swamps and lakes were selected at different altitudes near the city of Arba Minch and sediment cores were collected for proxy analysis.

The pollen data obtained from a peat core from the wetland at Gelba (2300 m asl) will be presented. At this site, the Late Glacial is characterized by elevated values of afroalpine and ericaceous taxa, as well as podocarp and juniper pollen and high charcoal values. Around 13 ka BP the percentage of afroalpine pollen starts to increase. This vegetation change can be linked to the wet and warm conditions of the African Humid Period. A shift to more arid conditions is observed around 6.5 ka BP, shown by an increasing abundance of taxa from the wooded grassland zone. A final sudden shift in the vegetation composition is observed around two thousand years ago, simultaneously with a rise of charcoal and coprophilous fungi. This zone can be interpreted as a reflection of significant human impact on the vegetation, confirmed by an increase of disturbance taxa in the pollen record. The proxy records created in this study will be used to create a long-term reconstruction of the landscape in the study area and to identify the natural or anthropogenic driving forces of the observed landscape changes.

Coltorti, M., Pieruccini, P., Arthur, K. J., Arthur, J., & Curtis, M. 2019. Geomorphology, soils and palaeosols of the Chencha area (Gamo Gofa, south western Ethiopian Highlands). *Journal of African Earth Sciences*, 151, 225-240.

Diamond, J. 2002. Evolution, consequences and future of plant and animal domestication. *Nature*, 418(6898), 700-707.

Foerster, V., Vogelsang, R., Junginger, A., Asrat, A., Lamb, H. F., Schaebitz, F., & Trauth, M. H. 2015. Environmental change and human occupation of southern Ethiopia and northern Kenya during the last 20,000 years. *Quaternary Science Reviews*, 129, 333-340.

Ossendorf, G., Groos, A. R., Bromm, T., Tekelemariam, M. G., Glaser, B., Lesur, J. & Mieke, G. 2019. Middle Stone Age foragers resided in high elevations of the glaciated Bale Mountains, Ethiopia. *Science*, 365(6453), 583-587.

Reconstructing the late Holocene sedimentary landscape of the Zwin area nearby Bruges late-medieval outpost Hoeke

Frieda BOGEMANS¹, Vanessa HEYVAERT^{1,2}, Coralie ANDRÉ², Stephen LOUWYE², Jan TRANCHET³, Wim DE CLERCQ³

1. Geological Survey of Belgium, RBINS, Belgium (Vautierstraat 29, 1000 Brussels)
2. Department of Geology, Ghent University, Belgium (Krijgslaan 281, 9000 Ghent)
3. Department of Archaeology, Ghent University, Belgium (St.-Pietersnieuwstraat 35, Ghent)

This interdisciplinary research fits within the GOA project ‘High-tide, Low-tide’, studying the connectivity of the local and global maritime trade networks during the late-medieval heyday of Bruges, the transactions in commodities as well as the impact of residing foreigners on material culture. To understand this connectivity a geological approach is included, as Bruges’ development as the capital of the maritime cultural landscape, is inextricably associated with the existence of a Zwin tidal channel, connecting Bruges itself with the seashore. Along the Zwin waterway several harbours, so called outposts, got a piece of the pie and flourished.

Special attention is paid to the reconstruction of the late Holocene sedimentary landscapes in the Zwin area and more in particular the surroundings of the outpost Hoeke. The geological research is based on the analysis and correlation of 2 types of subsurface data a) cores: undisturbed continuous mechanically-drilled cores made for this research and all sorts of archived cores, and b) electrical cone penetration tests (CPT-e). In the preparation of infrastructural works, a series of CPT-e’s were made in the vicinity of Hoeke by the Flemish department of mobility and public works (DOV-GEO-18/057). Specifically for this project a series of new probes was carried out in 2019, a second one is planned for the summer of 2021. Five undisturbed cores were executed nearby Hoeke and described in detail, paying attention to primary and post-depositional sedimentological characteristics. Based on the observed properties, a series of lithofacies have been introduced and associated into architectural elements (sub-environments), specific for the tidal environment in the area.

In the current phase of the study it is clear that the Zwin area hides below its surface a complex late Holocene history. The late medieval “Zwin” mentioned in all historical texts, is not the only waterway that came into being. Larger and deeper tidal channels, predating the late medieval one, are observed, indicating different hydraulics and infilling histories.

Changes in vegetation and sediment transfers over the last 3000 years in the catchment of Lake Alaotra, Madagascar

Nils BROOThAERTS¹, Liesa BROSENS^{1,2}, Vao Fenotiana RAZANAMAHANDRY¹, Benjamin CAMPFORTS³, Liesbet JACOBS^{1,4}, Tantely RAZAFIMBELO⁵, Tovonarivo RAFOLISY⁵, Gert VERSTRAETEN¹, Steven BOUILLON¹, Gerard GOVERS¹

¹ *KU Leuven, Department of Earth and Environmental Sciences, Leuven, Belgium (nils.broothaerts@kuleuven.be)*

² *Research Foundation Flanders (FWO), Brussels, Belgium*

³ *Institute for Arctic and Alpine Research, University of Colorado at Boulder, Boulder, CO*

⁴ *Ecosystem & Landscape Dynamics, Institute for Biodiversity and Ecosystem Dynamics, University of Amsterdam, Amsterdam, Netherlands*

⁵ *Laboratoire des Radio Isotopes, Université d'Antananarivo, Antananarivo, Madagascar*

To understand the driving processes for changes in tropical ecosystems and related problems such as soil degradation, it is crucial to gain insight in the relative importance of human disturbance and climate change. Madagascar is known for its particularly high erosion rates in the central highlands, yet the role of human disturbance versus natural processes are not well understood and is a topic of ongoing debate. Recent studies have challenged the traditional view that the currently observed intense erosion processes and sediment fluxes in Madagascar are mainly driven by recent large-scale deforestation. However, at present almost no quantitative data is available to couple vegetation dynamics and sediment fluxes over time in Madagascar. This study aims to provide more insight in landscape changes (vegetation changes, sediment mobilization and deposition) in central Madagascar over the past 3000 years, and in the specific role of man and climate. The study focuses on the 1800 km² catchment of Lake Alaotra, located ca 200 km northeast of Antananarivo. Lake Alaotra is formed in a graben system in the highlands of Madagascar, and is the largest freshwater lake of the country (400 km²). The lake is surrounded by a wetland area, which is partly converted to irrigated rice fields. Two pollen records from Lake Alaotra were used to reconstruct regional vegetation changes. Radiocarbon dates of extracted pollen provide a detailed chronostratigraphic framework. Sediment accumulation rates were calculated based on corings in floodplains, wetlands and lake. The vegetation reconstructions show an early opening in the landscape, between 2000 and 1700 cal yr BP, with a change from a wooded grassland or woodland/grassland mosaic towards open grassland (Figure 1). Floodplain sedimentation rates only increase in the last 1000 years and peak in the last 400 years (Figure 1). This increased sedimentation can be linked to both the onset of a climatic drying trend since 950 cal yr BP and increased anthropogenic pressure (grazing and farming activities) upon the arrival of humans and cattle in the catchment dated between 1000 and 600 cal yr BP. No changes in sedimentation rate are observed in the downstream wetlands and lake, indicating that most sediments are buffered in the floodplains. Overall, this study provides a spatio-temporal integrated reconstruction of vegetation changes in the Lake Alaotra catchment and the link with sediment mobilization and deposition, thereby providing a better understanding of environmental changes in central Madagascar and its driving forces.

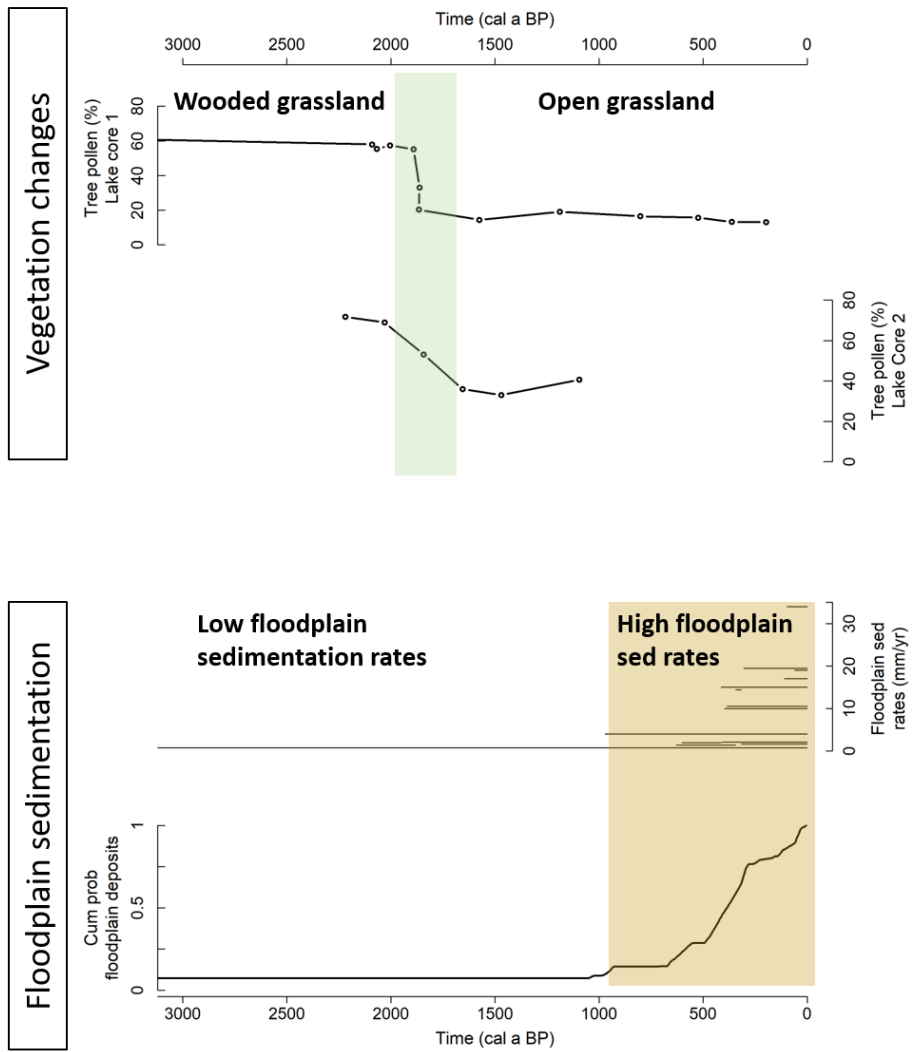


Figure 12. (Top) Vegetation changes in the Lake Alaotra Region, based on two pollen cores in Lake Alaotra. (Bottom) Floodplain sedimentation in the catchment of Lake Alaotra, showing floodplain sedimentation rates and the relative cumulative probability function of all available radiocarbon ages of floodplain deposits ($n=17$).

Metagenomics of tsunami deposits: developments and challenges from a case study on the Shetland Islands (UK)

Max ENGEL^{1,2}, Tasnim PATEL³, Anna PINT⁴, Sue DAWSON⁵, Isa SCHÖN^{3,6} & Vanessa M. A. HEYVAERT^{2,7}

1. *Heidelberg University, Institute of Geography, Im Neuenheimer Feld 348, 69120 Heidelberg, Germany (max.engel@uni-heidelberg.de)*
2. *Royal Belgian Institute of Natural Sciences, OD Earth and History of Life, Geological Survey of Belgium, Jennerstraat 10, 1000 Brussels, Belgium (mengel@naturalsciences.be; vanessa.heyvaert@naturalsciences.be)*
3. *Royal Belgian Institute of Natural Sciences, OD Nature, ATECO, Freshwater Biology, Vautierstraat 29, 1000 Brussels, Belgium (tpatel@naturalsciences.be; ischoen@naturalsciences.be)*
4. *University of Dundee, Department of Geography, Tower Building, Nethergate, Dundee DD1, UK (s.dawson@dundee.ac.uk)*
5. *University of Jena, Institute of Geosciences, Burgweg 11, 07749 Jena, Germany (anna.pint@uni-jena.de)*
6. *University of Hasselt, Research Group Zoology, Campus Diepenbeek, 3590 Diepenbeek, Belgium*
7. *Ghent University, Department of Geology, Krijgslaan 281, 9000 Ghent, Belgium*

Onshore tsunami deposits provide important information on long-term tsunami recurrence patterns in coastal areas. Their composition is mainly a function of the wave characteristics as well as the site-specific sediment system, bathymetry, onshore topography and flow conditions. Microfossils (e.g. foraminifera, ostracods, diatoms) are often used to identify tsunami deposits and differentiate them from other deposits. Foraminifera found within tsunami deposits mostly comprise allochthonous associations dominated by benthic intertidal to inner shelf taxa. Specimens may also originate from outer shelf to bathyal depths; even planktonic forms may occur. Furthermore, changes in test numbers, taphonomy, size or adult/juvenile ratios compared to background sedimentation are common (e.g. Hawkes et al., 2020). However, post-depositional degradation (e.g. dissolution) of carbonate tests often prevents identification, thereby reducing their value as a proxy.

This study aimed at developing high-throughput, metagenomic sequencing techniques to identify foraminifera assemblages in onshore extreme wave deposits from their environmental DNA (eDNA) signature (Engel et al., 2020). The project has sampled tsunami deposits from coastal peat sections at three sites on the Shetland Islands, UK, dated to approximately 1.5, 5.5 and 8.15 cal kyrs BP, respectively (Bondevik et al., 2005).

Tsunami deposits were identified by using high-resolution grain-size analysis, CT scanning, multi-sensor core logging and geochemical analyses. So far, no foraminiferal tests were found in any of the tsunami deposits, whilst inter- to subtidal offshore source deposits show moderate to high foraminiferal concentrations. This contrast indicates severe post-depositional dissolution of foraminifera in the onshore tsunami deposits, which are bracketed in between massive dystrophic peats.

Building on the protocol outlined in Pawłowska et al. (2014), different DNA extraction methods for the different sample types were optimised. Subsequently, polymerase chain reaction (PCR) primers and protocols which would amplify the target 18S rRNA regions of the foraminifera DNA were tested. Using the S14 F3 and S14 F1 ribosomal PCR primers we were able to amplify DNA and identify several foraminiferal taxa from modern

offshore samples to species level. However, this approach was less successful for the palaeo-samples which likely contained degraded DNA. Interestingly, when these primers were applied to tsunami deposits from the sites of Maggie Kettle's and Dury Voe (cf. Bondevik et al., 2005), we were able to obtain DNA sequence data, which unequivocally originates from fish and shrimp, testifying to the marine origin of the deposit.

Next, a modified protocol was developed using ribosomal PCR primers which would target shorter DNA fragments (i.e. 200 base pairs of length), and be more suitable for these deposits of high age. This new protocol, which also circumnavigated the a-specific amplification of DNA fragments of other organisms and possible time-associated DNA degradation, was finally successful for the PCR amplification of modern individual foraminifera, modern sediment and palaeo-tsunami sediment from a secondary study site. The first sequencing results of this palaeo-tsunami sediment were successful and the modified protocol will now be applied to the remainder of the Shetlands samples.

Acknowledgements: Funding by a BELSPO BRAIN-be pioneer grant (BR/175/PI/GEN-EX) is gratefully acknowledged.

References

- Bondevik, S., Mangerud, J., Dawson, S., Dawson, A. & Lohne, Ø., 2005. Evidence for three North Sea tsunamis at the Shetland Islands between 8000 and 1500 years ago. *Quaternary Science Reviews*, 24, 1757–1775.
- Engel, M., Schön, I., Patel, T., Pawłowski, J., Szczuciński, W., Dawson, S., Garrett, E. & Heyvaert, V.M.A., 2020. Paleogenetic approach in tsunami deposit studies. In Engel, M., Pilarczyk, J., May, S.M., Brill, D. & Garrett, E. (eds), *Geological records of tsunamis and other extreme waves*. Elsevier, Amsterdam, 427–442.
- Hawkes, A.D., 2020. Foraminifera in tsunami deposits. In Engel, M., Pilarczyk, J., May, S.M., Brill, D. & Garrett, E. (eds), *Geological records of tsunamis and other extreme waves*. Elsevier, Amsterdam, 239–259.
- Pawłowska, J., Lejzerowicz, F., Esling, P., Szczuciński, W., Zajączkowski, M. & Pawłowski, J., 2014. Ancient DNA sheds new light on the Svalbard foraminiferal fossil record of the last millennium. *Geobiology*, 12, 277–288.

The last millenia sedimentary record of Lago Esponja from Northern Chilean Patagonia

Nathalie FAGEL¹, Pablo PEDREROS², Denisse ALVAREZ², Isabel ISRADE ALCANTARA³, Alberto ARANEDA², Olivier NAMUR⁴, Sabine SCHMIDT⁵, Roberto URRUTIA²

1. AGEs, Department of Geology, Université de Liège, Liège, Belgique (Nathalie.fagel@uliege.be)
2. EULA, Faculty of Environmental Sciences, University of Concepcion, Concepcion, Chile (dealvarez@udec.cl; papedrер@udec.cl; aaraneda@udec.cl; rurrutia@udec.cl)
3. Instituto de Investigaciones en Ciencias de la Tierra, Universitaria Morelia, México (isabelisrade@gmail.com)
4. Department of Earth Sciences, KUL, Leuven, Belgique (olivier.namur@kuleuven.be)
5. UMR EPOC, Université de Bordeaux, France (sabine.schmidt@u-bordeaux.fr)

We evaluate the environmental variability of Northern Chilean Patagonia during the Last Millennia using a multi-proxy analysis of a sediment core from Lake Esponja (45°S 72°W). The lake is located in the region of Aysen del General Carlos Ibanez del Campo in NW Patagonia. The longest core (150 cm) was collected in 2014 at 40 m water depth. The sediment, which is composed of light brown organic-rich clayey silt, was analysed for sedimentology (grain size, magnetic susceptibility organic matter and biogenic silica content, diatom assemblages), mineralogy (X-ray diffraction), bulk geochemistry (C/N of organic matter, XRF core-scanner at 1 mm resolution) and glass shard composition (Microprobe, SEM-EDX).

The finely laminated sediments were interrupted by coarser and darker millimetric to centimetric layers that correspond to tephra deposition related to explosive Holocene eruptions of the regional volcanoes Mentolat (1710AD), Macá (550AD), and Hudson (2 and 3.6 kyr BP). The radiocarbon ages, measured on bulk sediment and macro-remains, suggest that the core covers the last ~4 kyr with a mean sedimentation rate of 0.1 to 0.4 mm/yr. The age of the bottom core is constrained by the presence of an Hudson-related tephra.

The laminations observed in Lake Esponja mainly reflect changes in the allochthonous detrital and volcanic inputs, also marked by changes in the chemical composition. The robust principal component analysis applied on the geochemical sedimentary composition of Lake Esponja evidences three groups of elements. The first group (Rb, K, Al, Si) indicates a control by fine detrital supplies enriched in clay minerals and K-feldspars. Within the same group, the high correlation between Al and Si evidences a dominant detrital origin for Si, consistent with both low abundance of diatoms in LEs14. The group (Zr, Ca, Sr, Ti) is related to coarse-grained fractions and/or to volcanic assemblages. The group 3 (Br, S, Zn) mainly represents the supplies of allochthonous organic matter by physical weathering and erosion in the watershed.

In complement to the geochemical signal, the diatom evolution indicates 3 main zonations, evidencing variable water column conditions over time in terms of pH, lake depth and turbidity. (1) The dominance of planktonic species *Aulacoseira* and *Staurosira* emphasizes turbid lake conditions over the first part of the lake evolution (150-80 cm, 2000-200BC). (2) The planktonic species are replaced by benthic species in an intermediate interval (55-80 cm, 200BC-200AD). The high abundance of *Surirella* marks a change to more stable conditions,

with calm and transparent water. The presence in sample 65-66 cm of *Aulacoseira* associated to only one benthic species (i.e., *Cymbella* spp.) records more turbid conditions due to sudden detrital inputs and nutrient availability in the lake. This interpretation is supported by the presence of coarse massive layers recording perturbation of the watershed. (3) Within the upper 55 cm (< 200AD), *Frustulia* and *Eunotia* are indicative of a closed and more acidic basin. The closure of the basin may record a rejuvenation of the local Rio Mañihuales fault during a major historical earthquake along the Liquiñe-Ofqui Fault Zone (LOFZ) recorded by massive deposit in the Aysén fjord sedimentation ~2 kyr ago.

The highest latitude waters of the Southern Ocean and glacial-interglacial change in atmospheric CO₂

François FRIPIAT^{1,2}, Alfredo MARTÍNEZ-GARCÍA², Frank LAMY⁴, Daniel M. SIGMAN³, and Gerald H. HAUG²

¹*Department of Geosciences, Environment and Society, Université Libre de Bruxelles, Brussels, Belgium*

²*Max Planck Institute for Chemistry, Mainz, Germany*

³*Department of Geosciences, Princeton University, Princeton, New Jersey, USA*

⁴*Alfred-Wegener-Institut, Helmholtz-Zentrum für Polar- und Meeresforschung, Bremerhaven, Germany*

Corresponding author: francois.fripiat@ulb.be

The Southern Ocean is the focus of most hypotheses for glacial-interglacial atmospheric CO₂ change. Today, most of the deep ocean is ventilated in this region, and the rapid surface-deep communication and the incomplete consumption of surface nutrients by phytoplankton in this region lead to the outgassing of deeply sequestered CO₂ to the atmosphere. Fossil-bound nitrogen isotope measurements in the Southern Ocean suggest more complete nitrate consumption in its surface waters, supporting a key role for the Southern Ocean in ice age reductions in atmospheric CO₂^[1,2]. In the Antarctic Zone, the more polar region of the Southern Ocean, the rise in the completeness of nitrate consumption coincides with evidence from proxies for a lower rate of export production. These two changes together point to lower gross nitrate supply to the surface and thus an apparent ice age reduction in the exchange of water between the surface and the underlying ocean^[3,4]. However, these records are confined to the more northern waters of the Antarctic Zone (i.e., near the Polar Front), where surface waters are transported northward and enter the interior ocean mostly as intermediate waters, not southward and into the deep ocean. Here, we present new diatom-bound nitrogen isotope measurements from a site in the more southern Antarctic Zone, a region that ventilates most of the deep ocean but from which few high-quality Pleistocene sediment records have been recovered. Preliminary results are promising, supporting a reduction in the exchange of water between the surface and the underlying ocean at the glacial inception, when most of the decrease in Antarctic air temperature is recorded. This process may explain the first drop in atmospheric CO₂ leading into the last ice age. In contrast, the record does not show a change at the next major transition to full ice age conditions. The finding is consistent with previous suggestions that this second drop in atmospheric CO₂ does not derive from Antarctic changes but is rather the result of iron fertilization further north in the Subantarctic Zone of the Southern Ocean^[5]. Thus, combining the new polar Antarctic Zone record with other records from the Southern Ocean leads to a remarkably complete explanation for glacial-interglacial CO₂ change.

References

- [1] Studer, A.S., Sigman, D.M., Martinez-Garcia, A.M., Benz, V., Winckler, G., Kuhn, G., Esper, O., Lamy, F., Jaccard, S.L., Wacker, L., Oleynik, S., Gersonde, R. & Haug, G.H., 2015. Antarctic Zone nutrient conditions during the last two glacial cycles. *Paleoceanogr.* 30, 845-862.
- [2] Ai, X.E., Studer, A.S., Sigman, D.M., Martinez-Garcia, A., Fripiat, F., Thöle, L.M., Michel, E., Gottschalk, J., Arnold, L., Moretti, S., Schmitt, M., Oleynik, S., Jaccard,

- S.L. & Haug, G.H., 2020. Southern Ocean upwelling, Earth's obliquity, and glacial-interglacial atmospheric CO₂ change. *Science* 370, 1348-1352.
- [3] Sigman, D.M., Fripiat, F., Studer, A.S., Kemeny, P.C., Martinez-Garcia, A., Hain, M.P., Ai, X., Wang, X., Ren, H. & Haug, G.H., 2021. The Southern Ocean during the ice ages: A review of the Antarctic surface isolation hypothesis, with comparison to the North Pacific. *Quaternary Sci. Rev.* 254, 106732, doi:10.1016/j.quascirev.2020.106732.
- [4] Kemeny, P.C., Kast, E.R., Hain, M.P., Fawcett, S.E., Fripiat, F., Studer, A.S., Martinez-Garcia, A., Haug, G.H. & Sigman, D.M., 2018. A seasonal model of nitrogen isotopes in the ice age Antarctic Zone: Support for weakening of the Southern Ocean upper overturning cell. *Paleoceanogr. Paleoclim.* 33, 1453-1471.
- [5] Martínez-García, A., Sigman, D.M., Ren, H., Anderson, R.F., Straub, M., Hodell, D.A., Jaccard, S.L., Eglinton, T.I., Haug, G.H., 2014. Iron Fertilization of the Subantarctic Ocean during the last ice age. *Science* 343, 1347-1350.

Spatio-temporal variation of the Omo Delta (1990-2018): what remote sensing data reveal and models explain

Gladys KANGI¹, Fritz KLEINSCHROTH², Jos VAN ORSHOVEN¹, Stefaan DONDEYNE³

1. *Department of Earth and Environmental Sciences, KU Leuven, Celestijnenlaan 200E, B-3001 Leuven, Belgium (gladys.kangi@kuleuven.be)*
2. *Department of Environmental Systems Science, ETH Zurich, Universitätstrasse 16, 8092 Zürich, Switzerland (fritz.kleinschroth@usys.ethz.ch)*
3. *Department of Geography, Ghent University, Krijgslaan 281 (S8), B-9000 Ghent, Gent, Belgium (stefaan.dondeyne@ugent.be)*

Formed where the Omo River discharges into Lake Turkana in north-western Kenya and south-western Ethiopia, the Omo Delta is a very dynamic landform as it is subjected to a variable climate, changing land-uses and fluctuating lake levels. We investigated the delta's spatio-temporal variation, based on freely available remote sensing data and attempted to explain these changes in terms of variation in rainfall, changes in land cover and irrigation perimeters, fluctuations in river discharges and lake levels. Distinguishing the impact of changes in climate from changes in land-use is particularly important in the light of climate change.

We derived the extent and shape of the delta from Landsat imagery for the dry season of each year between 1990 and 2018, then classified the images into land and water categories using a Random Forest classification algorithm (Fig. 1). Data driven statistical models including ordinary least square linear regression, multiple linear regression and Random Forest (RF) regression were used, with the delta extent as the response variable and annual rainfall (TAMSAT), forest cover (Global Forest Change datasets), river discharge (derived empirically from lake levels), lake levels, as well as irrigated perimeters delineated through visual interpretation from Google Earth Pro, as explanatory variables. The analysis was first carried out for the entire period and subsequently split into two distinct periods: 1990-2003 and 2004-2018, since the drivers of delta changes were markedly different for these two periods.

High overall accuracies (>98%) were obtained with the Random Forest classification algorithm for distinguishing land/water in the delta. The extent of the Omo Delta fluctuated between 949.3 km² in 1993 and 651.3 km² in 2000. Lake level, which is directly dependent on rainfall variability and river discharge, was the single best predictor explaining delta extent fluctuations. Multiple linear regression analysis and Random Forest regression brings to light that the expansion of irrigated perimeters coincides with changes in delta extent. The data do not allow to establish any causal relations between development of irrigated perimeters and changes in the delta but nevertheless supports the hypothesis that besides natural drivers such as rainfall variability, anthropogenic activities affect the delta area.

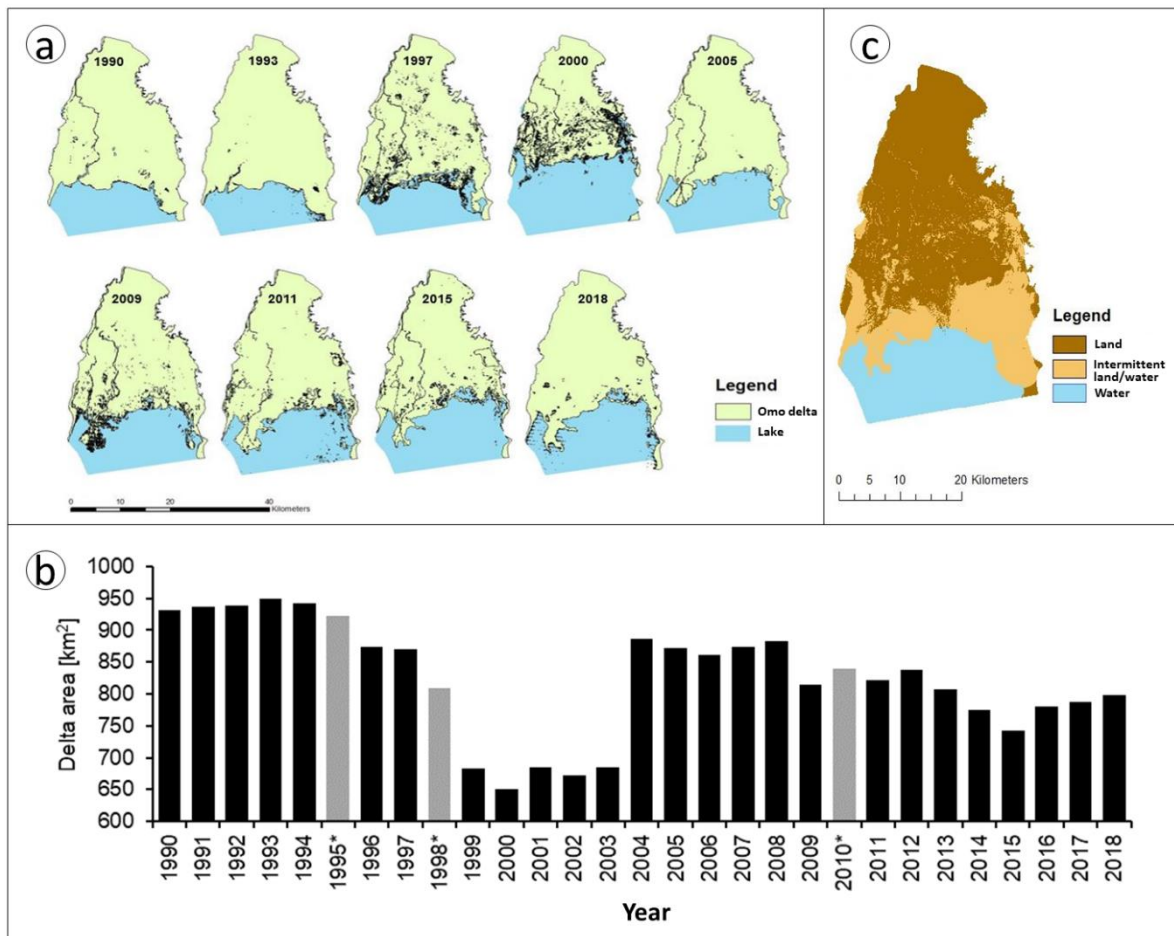


Figure 13 - Variation in the area of the Omo Delta for the period 1990-2018. (a) Extent of the area based on Landsat images and determined by a Random Forest classification; (b) Area of the delta for the dry season of each year between 1990 and 2018. Since there were no cloud free dry season images for the years 1995, 1998 and 2010, the delta area for these years was imputed using the mean of the three adjacent years. (c) Extent of the areas that was persistently either water or land, next to area which was intermittently either land or water.

Regional sensitivity of East Asian summer monsoon to ice sheet and orbital forcing

Anqi LYU¹, Qiuzhen YIN¹, Michel CRUCIFIX¹, Youbin SUN^{2,3}

1. *Georges Lemaître Center for Earth and Climate Research, Earth and Life Institute, Université Catholique de Louvain, Louvain-la-Neuve, Belgium (anqi.lyu@uclouvain.be)*
2. *State Key Laboratory of Loess and Quaternary Geology, Institute of Earth Environment, Chinese Academy of Sciences, Xian, China*
3. *CAS Center for Excellence in Quaternary Science and Global Change, Chinese Academy of Sciences, Xian, China*

The East Asian summer monsoon (EASM) is an important component of the climate system, and it influences the economy and life of a large population. Numerous paleoclimate records have been used to reconstruct the long-term evolution of the EASM. The strong regional dependence of the EASM variation as recorded in various proxy records questions the relative role of ice sheets and insolation on the EASM precipitation in different sub-regions in East Asia. In this study, we used a Gaussian emulator based on simulations with HadCM3 to investigate the relative importance of the orbital forcing and ice sheets on the summer precipitation in different latitudes of the EASM domain over the last 800 ky. Sensitivity analyses are performed to quantitatively assess the role of different factors. Our results show that a strong precessional signal exists in the long-term variation of the summer precipitation in all latitudes, while precipitation shows a different degree of response to ice volume between the northern and southern part of the EASM domain. In the north of 25°N, the ice sheets only modulate the effect of insolation by influencing the land-sea pressure gradient. Reduced land-sea pressure contrasts lead to a weakening of the EASM. Accordingly, the water vapor flux from the Northwest Pacific, one of the major moisture sources for the EASM precipitation, is also reduced. In the southern part, EASM is more sensitive to the glaciation level. A southward shift of the Intertropical Convergence Zone and the Hadley cell in response to the ice sheet forcing explains the stronger drought in southern China than in northern China. The relationship between precipitation and glaciation level varies for different astronomical configurations, showing the necessity of considering the background astronomical forcing when discussing the effect of ice sheets on the EASM.

Reference

Lyu, A. Q., Yin, Q. Z., Crucifix, M., & Sun, Y. B. (2021). Diverse Regional Sensitivity of Summer Precipitation in East Asia to Ice Volume, CO₂ and Astronomical Forcing. *Geophysical Research Letters*, 48(7), e2020GL092005.

Paleoclimatic evolutions during the Holocene: A stalagmite $\delta^{18}\text{O}$ record from Majiaping Cave, Guizhou, China

Ming-Qiang LIANG^{1,2}, Hong-Chun LI^{1*}, Qiu-Zhen YIN², Horng-Sheng MII³, Zhi-Bang MA⁴, Ting-Yong LI⁵, Ludvig LÖWEMARK¹

1. Department of Geosciences, National Taiwan University, Taipei 106, China
2. Georges Lemaître Center for Earth and Climate Research, Earth and Life Institute, Université Catholique de Louvain, Louvain-la-Neuve 1348, Belgium.
3. Department of Earth Sciences, National Taiwan Normal University, Taipei 106, China
4. Key laboratory of Cenozoic Geology and Environment Institute of Geology and Geophysics, Chinese Academy of Science, Beijing 100029, China
5. Yunnan Key Laboratory of Plateau Geographical Processes & Environmental Changes, Faculty of Geography, Yunnan Normal University, Kunming, 650500, China

*Corresponding author: Hong-Chun LI, E-mail: hcli1960@ntu.edu.tw

The speleothem oxygen isotope records from East Asia have been utilized to reconstruct Asian summer monsoon (ASM) variability over the last several hundred thousand years. However, what the isotope variation represents on orbital to annual timescales remains greatly debated. The high-resolution speleothem records combined with modern meteorological observation is essential for better understanding this problem. Here, we report a stalagmite $\delta^{18}\text{O}$ ($\delta^{18}\text{Oc}$) record of the highest resolution (average of $\sim 1\text{yr}$) between 1730 to 8590 yr BP from the Majiaping (MJP) cave, Guizhou province, southwest China. This record is precisely dated based on the ^{14}C dating method combined with $^{230}\text{Th}/\text{U}$, ^{210}Pb , and lamination counting dating methods. The result shows that the ^{14}C dating method can establish a reliable chronology for stalagmites that cannot be dated by $^{230}\text{Th}/\text{U}$. The comparisons of the precipitation $\delta^{18}\text{O}$ with the local temperature, rainfall amount, and moisture sources show that the $\delta^{18}\text{Oc}$ record from southwest China is mainly controlled by the “amount effect” on annual to decadal timescale modified by ENSO. The consistent long-term $\delta^{18}\text{Oc}$ trends among all monsoonal regions in the low latitudes of the northern hemisphere indicate that on the orbital timescale the $\delta^{18}\text{Oc}$ trend reflects changes in the large-scale spatial circulation of the atmosphere, which is controlled by the changes of northern hemisphere summer insolation. Ensemble Empirical Mode Decomposition (EEMD) and Bernaola-Galvan Segmentation Algorithm (BGSA) analyses real that on the semi-millennium timescale, the $\delta^{18}\text{Oc}$ of MJP stalagmite showed 8 weak East Asian summer monsoon events during 8.2ka BP, 7.3 ka BP, 5.9 ka BP, 5.5 ka BP, 4.2 ka BP, 3.1 ka BP, 2.4 ka BP, 1.9 ka BP. The comparisons of the structural and forcing of the first 7 events with the last event show that the first 7 events correspond to the total solar irradiance and the 1.9 ka event could be related to the internal fluctuation of the Earth system controlled by the ENSO. On the interannual-multidecadal timescale, the $\delta^{18}\text{Oc}$ shows the high-frequency cyclicities of 3-7y and 30-70y which are related to ENSO and PDO according to modern instrumental weather records. However, the relationships among ENSO, PDO, and the $\delta^{18}\text{Oc}$ are not constant during the Holocene.

Topoclimate and spatio-temporal distribution of summer rain over the Ethiopian highlands

Emnet NEGASH^{1,2}, Bert VAN SCHAEYBROECK^{3,4}, Piet TERMONIA^{3,4}, Michiel VAN GINDERACHTER^{3,4}, Jan NYSSSEN¹

¹ *Department of Geography, Ghent University, Ghent, Belgium (emnet.negash@ugent.be)*

² *Institute of Climate and Society, Mekelle University, Mekelle, Ethiopia*

³ *Royal Meteorological Institute of Belgium, Ukkel, Brussels, Belgium*

⁴ *Department of Physics and Astronomy, Ghent University, Ghent, Belgium*

Ethiopia is a mountainous country known for its distinct topography ranging from alpine environment to desert-like conditions along the rift valley. Topoclimate, orographic rains on windward slopes and leeward rain shadow control rainfall variability in tropical mountains (Van den Hende et al., 2021). Such variability has a substantial societal impact. For instance they can cause differences in susceptibility to geohazards and wealth of rain-fed agriculture farmers among the windward and leeward sides of the mountain. However, due to lack of detailed scientific knowledge, a one-size-fits-all approach has so far been used, without considering the inter-event rainfall variability. This study aims at characterizing and understanding the spatio-temporal characteristics of the summer rain climatology over the Ethiopian highlands using regional climate model ALARO-0 at 4 km resolution. Multiple determining factors are explored including: wind (windward or leeward), rain (wet or dry day) categories, and elevation. These are used to categorize the diurnal cycles of different meteorological variables including wind, temperature, humidity and rainfall frequency and intensity. Ethiopia's summer rain exhibits a clear diurnal and semi-diurnal pattern with the highest rainfall during the afternoon hours 1100–1800 EAT and the minimum values identified in the morning hours 0200–0900 EAT. During these peak hours, the mountain peaks receive up to 1.5mm hr⁻¹ for as long as seven hours a day, while lowlands receive little to no rainfall at most of the times. Besides, windward events are found to have extended spatial and diurnal range of rainfall with respect to shorter duration on leeward events. The predominant afternoon maximum rainfall, as well as the prevalence of windward over leeward events and high orographic rainfall suggest terrain-induced ascent owing to thermal rather than wind-induced forcing (Kirshbaum et al., 2018).

Moreover, the ALARO-0 model is found to reproduce well rainfall extremes. The recurrent flood hazard in lowland settlements such as Dire Dawa and Awash (Erena et al., 2018), an area of little or no rain, comes after heavy rainfall in the Ahmar mountains. Similarly, flash flood in catchment headwaters and hydrological deficit in the flood-plains (Negash et al., 2020), show higher rainfall with increasing elevation; where highland farmers mainly depend on rainfed agriculture while lowlanders could not harvest almost any crop unless supplemented by spate irrigation. This suggests the need for an alternative approach replacing the one-size-fits-all management approach with a site-specific approach taking into account topoclimatic differences.

References

Erena, S.H., Worku, H., De Paola, F., 2018. Flood hazard mapping using FLO-2D and local management strategies of Dire Dawa city, Ethiopia. *J. Hydrol. Reg. Stud.* 19, 224–239.

- Kirshbaum, D.J., Adler, B., Kalthoff, N., Barthlott, C., Serafin, S., 2018. Moist orographic convection: Physical mechanisms and links to surface-exchange processes. *Atmosphere* 9, 1–26.
- Negash, E., Gebresamuel, G., Embaye, T.-A., Nguvulu, A., Meaza, H., Gebrehiwot, M., Demissie, B., Gebreyohannes, T., Nyssen, J., Zenebe, A., 2020. Impact of headwater hydrological deficit on the downstream flood-based farming system in northern Ethiopia. *Irrig. Drain.* 69, 342–351.
- Van den Hende, C., Van Schaeybroeck, B., Nyssen, J., Van Vooren, S., Van Ginderachter, M., Termonia, P., 2021. Analysis of rain-shadows in the Ethiopian Mountains using climatological model data. *Clim. Dyn.* 56, 1663–1679.

A question of time: dating Quaternary fluvial archives and landscapes

Gilles RIXHON

Université de Strasbourg (gilles.rixhon@live-cnrs.unistra.fr)

A key topic in geomorphology, and more generally in all disciplines dealing with the shaping of the Earth surface (“surface geosciences”), addresses the study of processes and rates of landscape evolution. Quantifying these processes has increasingly become a central task in fluvial geomorphology, either on short timescales (i.e. 1-10² years; e.g. rates of bedload transport) or spanning the Quaternary (i.e. 10³-10⁶ years; e.g. fluvial incision rates in bedrock/valley formation). As for the second, dating fluvial landforms and associated material formed by river sediments from floodplains or terraces sequences has represented a recurring scientific challenge. Therefore, some of the main advances in fluvial geomorphology were closely intertwined with methodological developments achieved in Quaternary geochronology, the research field committed to generating chronologies of Earth’s history over the last 2.6 Ma. Importantly, it allowed gaining valuable new insights into the drivers of landscape evolution: “*Continuing advances in Quaternary geochronology have enhanced our ability to determine when events occurred, and thus to understand interactions between landscapes and potential controlling factors such as climate [, tectonics] and land use*” (Wohl, 2013). This lecture will tackle some tight relationships between fluvial geomorphology and Quaternary geochronology by taking advantage of some case studies recently carried out in Belgium. It will also integrate the dating of fluvial archives and/or landforms closely associated to key Belgian archaeological sites as well.

Spatial variation and factors controlling sediment fluxes along the western slopes of the Peruvian Andes

Miluska A. ROSAS^{1,2}; Veerle VANACKER¹

1 Earth and Life Institute, Georges Lemaître Centre for Earth and Climate Research, Université catholique de Louvain. Louvain la Neuve, Belgium

2 Departamento de Ingeniería, Pontificia Universidad Católica del Perú. Lima, Peru
(miluska.rosas@uclouvain.be/miluska.rosas@pucp.pe, Veerle.vanacker@uclouvain.be)

Knowledge of sediment production mechanisms and their potential controlling factors contributes to our understanding of geomorphological processes. Previous studies highlighted the link between sediment yield and anthropogenic, e.g. agricultural practices, and natural factors, e.g. climate, topography, river runoff, lithology and vegetation cover (Milliman & Farnsworth, 2011). The steep western slopes of the Peruvian Andes shows different climate regimes (Poveda et al. 2020). The southern region presents arid climates and deserted vegetation, in contrast with the north region where tropical climates and abundant vegetation are observed. Likewise, a large number of agricultural and water regulation projects characterizes this area.

However, the number of studies on sediment yield and its controlling factors are limited along the Peruvian Andes. The storm events rapidly mobilized the accumulated sediments in the mountain and piedmont areas during dry normal years. Most studies on the western slopes have focused on the Northern part of Peru and showed a three to 60 times increase of sediment yield during El Niño (ENSO) events compared to normal years (Morera et al., 2017). In the central part of Peru where the main reservoirs, irrigation systems, and water supply plants are located, few studies were realized (Morera et al., 2017; Rosas et al., 2020). They identified a lack of knowledge of the main environmental and anthropogenic controlling factors involve in the sediment production and transport.

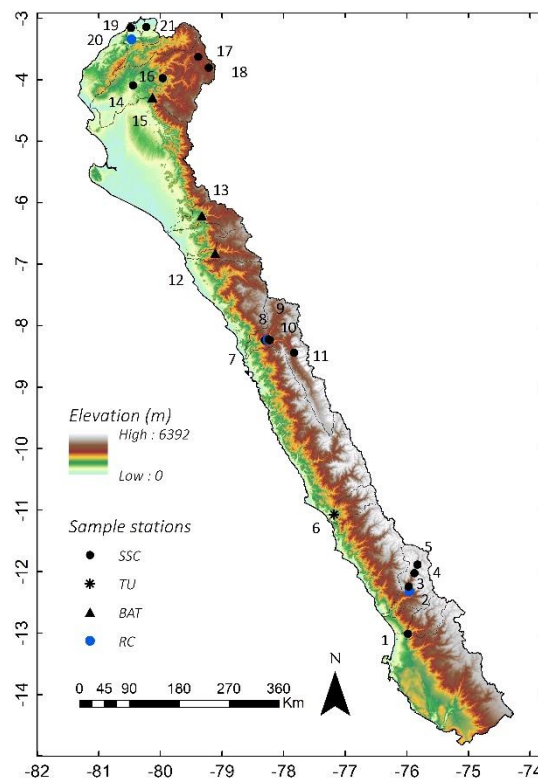
In this study, we identify the spatial patterns of sediment yield along the western slopes of the Peruvian Andes and analyze the main environmental controlling factors. Our study presents data on sediment yield of 21 sample sites (Figure 1). The data contains information on suspended sediment load from gauging stations, reservoir sedimentation and water turbidity. We used satellite-based data to derive topographic information: HydroSHEDS void-filled DEM (Lehner et al., 2008), daily precipitation data: PISCO product by Senamhi (Aybar et al., 2017), daily discharge: GloFAS-ERA5 global river dataset (Harrigan et al., 2020), lithological strength: global lithological map GLiM (Hartmann and Moosdorf, 2012), and vegetative cover: MODIS Land cover type product (Friedl and Sulla-Menashe, 2019). Our first results show a significant influence of the runoff and relief on sediment yield. Likewise, an important influence of percentage of cropland areas was observed. However these factors just explain the ~50% of the sediment yield in the region indicating that further studies are needed.

References

Aybar, C., Lavado-Casimiro, W., Huerta, A., Fernández, C., Vega, F., Sabino, E. and Felipe-Obando, O., 2017. Uso del Producto Grillado “PISCO” de precipitación en Estudios, Investigaciones y Sistemas Operacionales de Monitoreo y Pronóstico Hidrometeorológico. Nota Técnica 001 SENAMHI-DHI-2017, Lima-Peru.

- Friedl, M. and Sulla-Menashe, D., 2019. MCD12Q1 MODIS/Terra+Aqua Land Cover Type Yearly L3 Global 500m SIN Grid V006 [Data set]. NASA EOSDIS Land Processes DAAC.
- Harrigan, S., Zsoter, E., Alfieri, L., Prudhomme, C., Salamon, P., Wetterhall, F., Barnard, C., Cloke, H., and Pappenberger, F., 2020. GloFAS-ERA5 operational global river discharge reanalysis 1979–present, *Earth Syst. Sci. Data*, 12, 2043–2060.
- Hartmann, J., and Moosdorf, N., 2012. The new global lithological map database GLiM: A representation of rock properties at the Earth surface. *Geochem. Geophys. Geosyst.*, 13, Q12004.
- Lehner, B., Verdin, K., Jarvis, A., 2008. New global hydrography derived from spaceborne elevation data. *Eos, Transactions, AGU*, 89(10): 93-94.
- Milliman, J., and Farnsworth, K., 2011. In *River Discharge to the Coastal Ocean: A Global Synthesis*. Cambridge: Cambridge University Press.
- Morera, S.B., Condom, T., Crave, A., Steer, P. and Guyot, J.L., 2017. The impact of extreme El Niño events on modern sediment transport along the western Peruvian Andes (1968–2012). *Sci. Rep.* 7, 11947.
- Poveda, G., Espinoza, J.C., Zuluaga, M.D., Solman, S.A., Garreaud, R. and van Oevelen, P.J. 2020. High Impact Weather Events in the Andes. *Front. Earth Sci.* 8:162.
- Rosas, M.A., Vanacker, V., Viveen, W., Gutierrez, R. R., Huggel, C., 2020. The potential impact of climate variability on siltation of Andean reservoirs. *Journal of Hydrology*, 581, 124396.

Figure 1: Spatial distribution of the measurement stations (1-21 dots) studied in the Peruvian western Andes. SSC: sediment concentration, TU: turbidity, BAT: reservoir bathymetric.



Atmospheric beryllium-10 (^{10}Be), a versatile cosmogenic nuclide to reconstruct geomagnetic strength variations, quantify paleoenvironmental processes, provide chronostratigraphic markers and date sedimentary sequences

Quentin SIMON, Nicolas THOUVENY, Didier L. BOURLÈS

CEREGE UM34, Aix Marseille Univ, CNRS, IRD, INRAE, Coll France, 13545 Aix en Provence, France. (simon@cerege.fr; quentin.simon@gmx.com)

Paleo-studies require robust proxies and chronostratigraphic tools to understand and time geophysical processes. Both are sometimes intermingled mixed and difficult to assess. Chronological uncertainties further hinder accurate correlation of paleoclimatic series, limiting their interpretations. The use of an independent tool capable of 1) controlling accuracy of paleomagnetic records, 2) providing global chronostratigraphic constraints, 3) radiometrically dating sediments or other objects and 4) quantifying rates and dynamics of surface processes is therefore of significant interest.

One such a tool exists: atmospheric cosmogenic radionuclide ^{10}Be (see pioneering works by Didier L. Bourlès and others sum up in Braucher et al., 2021). However, the use of ^{10}Be in different settings and for various purposes need to be carefully evaluated before being applied. The atmospheric ^{10}Be production results from spallation reactions when highly energetic galactic cosmic rays collide with oxygen and nitrogen atoms. Once produced, ^{10}Be bounded to particles and is rapidly deposited/incorporated in sediments, snow, soils or ferromanganese nodules/crusts. Because ^{10}Be and its stable isotope counterpart ^9Be have independent origins, their ratio (i.e. authigenic $^{10}\text{Be}/^9\text{Be}$ ratio) can be use to estimate denudation rates or freshwater inputs changes (Simon et al., 2016a). Because ^{10}Be decays ($T_{1/2}=1.39$ Ma), it can be used to radiometrically date Mio-Plio-Pleistocene sedimentary archives (Simon et al., 2020a). At centennial to millennial time scales, reconstruction of ^{10}Be production rates using the authigenic $^{10}\text{Be}/^9\text{Be}$ ratio clues on geomagnetic intensity variations (Simon et al., 2016b, 2018a, 2018b, 2020b). This permits to test and improve the reliability, resolution and precision of paleomagnetic records. It also offers chronostratigraphic markers to synchronize sedimentary and ice records at global scale, particularly during geomagnetic excursions and reversals (Simon et al., 2017, 2019).

Here, I will present new authigenic $^{10}\text{Be}/^9\text{Be}$ ratio records obtained from several Plio-Quaternary marine sedimentary sequences and discuss how using ^{10}Be can help improving magnetic and oxygen isotope stratigraphies; and reconstruct precise dynamics of geomagnetic excursions and reversals. I will show examples where $^{10}\text{Be}/^9\text{Be}$ ratio helped establishing radiometric chronologies in very different settings (marine and lacustrine sediments, nodule) and provide a reliable stratigraphic marker for the Global Boundary Stratotype Section and Point (GSSP) of the Middle Pleistocene Subseries. Along with these applications, I will show how the large dataset obtained within the frame of the ANR MAGORB and ERC EDIFICE research projects reveals new challenges on geochemical interpretation of ^{10}Be records.

References

Braucher, R., Blard, PH., Brown, E.T., Carcaillet, J., Lebatard, A.E., Siame, L., Simon, Q., Thouveny, N., Aumaître, G., Bard, E., Carretier, S., Cornu, S., Fink, D., Finkel, R., German, C., Godard, V., Gosse, J., Hamelin, B., Hofmann, F.M., Jomelli, V., Keddadouche, K., Kurz, M.D., Matman, A., Palacios, D., Measures, C., Merchel, S., Regard, V., Schimmepfennig, I., von Blanckenburg, F., 2021. Didier L. Bourlès (1955-2021), the 5 MV cosmogenic rock star. *Quat. Geochronol.* 65, 101186.

- Simon, Q., Thouveny, N., Bourlès, D.L., Nuttin, L., St-Onge, G., Hillaire-Marcel, C., 2016a. Authigenic $^{10}\text{Be}/^9\text{Be}$ ratios and ^{10}Be -fluxes ($^{230}\text{Th}_{\text{xs}}$ -normalized) in central Baffin Bay during the last glacial cycle: Paleoenvironmental implications. *Quat. Sci. Rev.* 140, 142-162.
- Simon, Q., Thouveny, N., Bourlès, D.L., Valet, J.-P., Bassinot, F., Ménabréaz, L., Guillou, V., Choy, S., Beaufort, L., 2016b. Authigenic $^{10}\text{Be}/^9\text{Be}$ ratio signatures of the cosmogenic nuclide production linked to geomagnetic dipole moment variation since the Brunhes/Matuyama boundary. *J. Geophys. Res.* 121, 7716–7741.
- Simon, Q., Bourlès, D.L., Bassinot, F., Nomade, S., Marino, M., Cirafo, N., Girone, A., Maiorano, P., Choy, S., Dewilde, F., Scao, V., ASTER Team, 2017. Authigenic $^{10}\text{Be}/^9\text{Be}$ ratio signature of the Matuyama- Brunhes boundary in the Montalbano Jonico marine succession. *Earth Planet. Sci. Lett.* 460, 255-267.
- Simon, Q., Bourlès, D. L., Thouveny, N., Horng, C.-S., Valet, J.-P., Bassinot, F., Choy, S., 2018a. Cosmogenic signature of geomagnetic reversals and excursions from the Réunion event to the Matuyama–Brunhes transition (0.7–2.14 Ma interval). *Earth Planet. Sci. Lett.* 482, 510–524.
- Simon, Q., Thouveny, N., Bourlès, D. L., Bassinot, F., Savranskaia, T., Valet, J.-P., 2018b. Increased production of cosmogenic ^{10}Be recorded in oceanic sediment sequences: Information on the age, duration, and amplitude of the geomagnetic dipole moment minimum over the Matuyama–Brunhes transition. *Earth Planet. Sci. Lett.* 489, 191–202.
- Simon, Q., Suganuma, Y., Okada, M., Haneda, Y., ASTER Team, 2019. High-resolution ^{10}Be and paleomagnetic recording of the last polarity reversal in the Chiba composite section: Dynamics of the Matuyama-Brunhes transition. *Earth Planet. Sci. Lett.* 519, 92-100.
- Simon, Q., Ledru, M.P., Sawakuchi, A., Favier, C., Mineli, T.D., Bard, E., Thouveny, N., Garcia, M., Tachikawa, K., Guedes, M., Grohman, C., Rodriguez-Zorro, P.A., ASTER Team, 2020a. Chronostratigraphy of a 1.5 ± 0.1 Ma composite sedimentary record from Colônia basin (SE Brazil): Bayesian modeling based on paleomagnetic, authigenic $^{10}\text{Be}/^9\text{Be}$, radiocarbon and luminescence dating. *Quat. Geochronol.* 58, 101081.
- Simon, Q., Thouveny, N., Bourlès, D.L., Valet, J.-P., Bassinot, F., 2020b. Cosmogenic ^{10}Be production records reveal dynamics of geomagnetic dipole moment (GDM) over the Laschamp excursion (20–60 ka). *Earth Planet. Sci. Lett.* 550, 116

The response of global terrestrial vegetation to orbital forcing and CO₂ during MIS 11 and MIS 13

Qianqian SU ¹, Qiuzhen YIN ², Anqi LYU ³, Zhipeng WU ⁴

1. *Georges Lemaître Centre for Earth and Climate Research, Earth and Life Institute, Université Catholique de Louvain, Louvain-La-Neuve, Belgium (qianqian.su@uclouvain.be)*
2. *idem (qiuzhen.yin@uclouvain.be)*
3. *idem (anqi.lyu@uclouvain.be)*
4. *idem (zhipeng.wu@uclouvain.be)*

Despite significant progress in paleoclimate reconstructions and modelling of different aspects of the past interglacial cycles, the mechanisms which transform the impact of solar insolation variations into long-term and global-scale terrestrial vegetation changes are still not fully understood.

Here using the Earth system model of intermediate complexity LOVECLIM, we performed simulations of the coevolution of climate and vegetation during MIS 11 and MIS 13 setting the orbital forcing alone or both orbital forcing and GHGs as external forcings.

Through simple and multilinear regression analysis, the results indicate the response of climate variables and vegetation cover to orbital forcing mainly controlled by precession during MIS 13 while by obliquity during MIS 11. On the other hand, the CO₂ contribution show more important role during MIS 13. GHGs largely enhanced the impact of orbital forcing especially eccentricity during MIS 13 while reverse the effect phase of eccentricity during MIS 11. The effect of CO₂ on climate variables and vegetation cover is of similar size to that of precession on these variables.

Anthropogenic legacy effects control sediment and organic carbon storage in temperate river floodplains

Ward SWINNEN¹, Nils BROOThAERTS¹, Gert VERSTRAETEN¹

Department of Earth and Environmental Sciences, KU Leuven, Leuven, Belgium

ward.swinnen@kuleuven.be

Rivers convey mineral sediment and organic carbon through the landscape but also store a significant part in floodplains for varying amounts of time. Reliable quantifications of this storage component is necessary to understand the cascades and land-ocean transfers of sediment and organic carbon at longer timescales. In this study, the Holocene floodplain sediment and organic carbon storage was quantified for four medium-sized rivers in Belgium, located in the European loess (Dijle and Mombeek rivers) and sand belts (Grote Nete and Zwarte Beek rivers).

The Holocene stratigraphy was reconstructed using 630 soil corings across 53 river valley cross-sections. Combining the stratigraphic reconstructions with measured sediment properties and 126 radiocarbon dates allowed to quantify the total mineral sediment and organic carbon storage and reconstruct the Holocene storage trajectories. The results indicate that floodplains in the loess belt underwent a marked shift from peat-forming wetlands to a meandering river channel with overbank deposition of mineral sediment. The river floodplains in the sand belt show a more variable floodplain stratigraphy with alternating phases of peat formation and mineral overbank sedimentation. For each cross-section location, the total mineral sediment and organic carbon storage was calculated. Overall, the area-specific mineral sediment storage ranges between 3,097 and 63,350 Mg ha⁻¹, while the area-specific organic carbon storage ranges from 121 to 3,930 Mg ha⁻¹. The area-specific mineral sediment storage is the highest for the river Dijle, with a mean storage of 43,090 Mg ha⁻¹ floodplain area. Floodplain sediment storage is on average 4.4 times larger in the river catchments located in the loess belt compared to those in the sandy region. Similar differences, although less pronounced, can also be observed for organic carbon storage, with floodplains in loess catchments storing 2.6 times more organic carbon than floodplains in the sand belt. The organic carbon storage values for the Dijle and Mombeek rivers obtained in this study are higher than previously reported in other studies across the globe.

In general, the reconstructed stratigraphies demonstrate that alluvial peatlands were quite common in the studied river systems throughout the Holocene. As a result, although active peat growth is limited in recent time periods, especially in the loess belt, a large fraction of the total Holocene organic carbon stock is stored in (buried) peat layers, ranging from 45.21% of the total organic carbon stock for the river Grote Nete to 75.03% for the river Zwarte Beek. The observed regional variability in floodplain storage shows to be controlled by river basin characteristics such as soil erodibility and long-term anthropogenic impact (land cover change). The marked shift from peat-forming wetlands to a meandering river system with mineral sedimentation can be related to an opening of the landscape and increased hillslope erosion since the Bronze Age, which accelerated during the Roman period and Middle Ages. Even more, the historic human impact trajectory has a strong impact on the position of the organic-rich peat layers relative to the floodplain water table. The relatively thick layer of overbank sediments in the loess belt protects the Early and Middle Holocene peat from oxic conditions and thus decomposition. As such the past floodplain development has a profound impact on the stability of the organic carbon stock to external factors in current times.

Reconstructing the spatial redox structure of anoxic oceans using a 3D ocean-based Earth system model

Sebastiaan J. VAN DE VELDE ^{1,2}, Dominik HÜLSE ³, Christopher T. REINHARD ⁴, Andy RIDGWELL ³

1. Department of Geoscience, Environment and Society, Université Libre de Bruxelles, Brussels, Belgium (sebastiaan.van.de.velde@ulb.be)

2. OD Nature, Royal Belgian Institute of Natural Sciences, Brussel, Belgium

3. Department of Earth and Planetary Sciences, University of California, Riverside, USA

4. School of Earth and Atmospheric Sciences, Georgia Institute of Technology, Atlanta, USA

Today, oxygen-depleted marine environments are limited to oxygen minimum zones, restricted basins and sedimentary pore waters. Prior to the Phanerozoic Eon (more than 542 million years ago) however, the global ocean hosted extensive anoxic regions. In the absence of oxygen, seawater should become either buffered by dissolved ferrous iron (ferruginous) or buffered by dissolved sulphide (euxinic). The development of redox proxies in the 1980s allowed, based on the geological record, to infer whether a water column was oxic or euxinic. Further refinements of these redox-proxies in the early 2000s extended this to ferruginous water-column conditions. Today, decades of research has generated a complex picture of spatial and temporal patterns in ancient ocean redox conditions.

Unfortunately, none of the current suite of ocean models is capable of explicitly simulating anoxic water-column iron cycling. Consequently, there is no numerical model available that is capable of reproducing (and thus testing) the spatial and temporal redox patterns proposed in the literature. We have recently updated a 3-dimensional ocean-based Earth system model (cGENIE.muffin) with a water-column Fe-S cycle (van de Velde et al., 2021). This model is capable of reproducing complex spatial patterns of oxic, ferruginous and euxinic conditions. We illustrate the applicability and versatility of the cGENIE model using example model runs of a hypothetical Proterozoic ‘shelf-world’ and for the end-Permian mass extinction (~251 Ma). We believe that our model description of the anoxic Fe-S cycle in cGENIE presents a valuable tool to explore spatial patterns in Precambrian redox chemistry, but also during ocean anoxic event in the Phanerozoic, and on hypothetical (extra-terrestrial) worlds

References

Van de Velde, S., Hülse, D., Reinhard C.T. & Ridgwell, A., 2021. Iron and sulfur cycling in the cGENIE.muffin Earth system model (v0.9.21). *Geoscientific Model Development*. 14, 2713-2745.

Constraining the depositional history of Quaternary fluvial deposits based on grain size, geochemistry and cosmogenic radionuclides

Nathan VANDERMAELEN¹, Veerle VANACKER¹, Marcus CHRISTL² Koen BEERTEN³

1. *Georges Lemaitre Centre for Earth and Climate Research, Earth and Life institute, University of Louvain, Place Louis Pasteur 3, 1348 Louvain-la-Neuve, Belgium*

2. *Laboratory of Ion Beam Physics, ETH Zurich, Department of Physics, Zurich, Switzerland*

3. *Engineered and Geosystems Analysis, Waste and Disposal, Belgian Nuclear Research Centre SCK CEN, Boeretang 200, 2400 Mol, Belgium*

Nathan.vandermaelen@uclouvain.be

Fluvial sediment sequences can preserve relevant information on paleo-climatic and physiographic conditions under which the sediments were deposited, and their source areas. However, the geochronology of braided river deposits remains challenging due to their variable deposition mode. In this research, we evaluated the potential of combining information from grain size analyses, elemental geochemistry and cosmogenic radionuclides (¹⁰Be) to better constrain the duration of sedimentary sequences and hiatuses. The study was realised on pebbly braided river deposits of the river Meuse. The Zutendaal gravels belong to Main Terrace deposits, and are considered to be deposited between 0.5 and 1.0 Ma under periglacial conditions. The 7 m high exposure at the geosite in As was described and sampled. Thirty-five samples were analyzed for grain size and eighteen for major and minor element composition on ICP-AES after metaborate fusion. From the elemental composition, we derived the indices: Chemical Index of Alteration, Al_2O_3/SiO_2 , $\frac{Fe_2O_3+MnO}{Al_2O_3}$ for weathering and Ti/Zr, Cr/Zr, Ba/Sr for provenance study. Fifteen samples were processed at the cosmogenic laboratory at UCLouvain for in-situ ¹⁰Be analyses, and were measured at the 500kV Tandy at ETH-Zurich.

After integrating the datasets, we identified in the profile three units that show significant differences in grain size, weathering extent and that show distinct ¹⁰Be accumulation phases. Based on weathering indices only, two subunits could be identified in the upper unit. When the top of a fining upward sequence shows a particular increase in ¹⁰Be concentration in comparison with deeper samples, there is evidence for a hiatus that lasted > 5000 yrs. In the As quarry, this is observed in two of the three units only, and indicates that longer hiatuses were alternating with shorter (< 1000 yrs) phases of non-deposition. Throughout the profile, there is an absence of a correlation between provenance and weathering extent indicating that weathering is essentially intraformational or post-depositional. This study also illustrates the added value of contrasting ¹⁰Be cosmogenic data with provenance and weathering indices: it allowed us to identify variation in ¹⁰Be concentration that was associated to a particular deviation in provenance. As such, based on the elemental geochemistry, we could flag the aberrant isotopic data. In summary, we can conclude that evaluating co-variations between different types of data such as weathering, provenance, granulometry indices and ¹⁰Be concentration is a promising technique to constrain the (depositional history of sediments, and their aggradation mode. A next step is to quantify the effect of hiatuses on CRN accumulation using forward modeling of cosmogenic nuclide accumulation.

Mineralogical and geochemical signal of the crater lake *La Alberca de Tacámbaro* in Central Mexico as an archive of precipitation over the last millennia

Gaëlle WANLIN¹, Isabel ISRADE², Nathalie FAGEL¹

1. AGEs, Département de Géologie, Université de Liège, 4000 Liège, Belgium (gaëlle.wanlin@student.uliege.be)(nathalie.fagel@ulg.ac.be)
2. Estratigrafía y Paleoambientes, Instituto de Investigaciones en Ciencias de la Tierra, Universidad Michoacana de San Nicolas de Hidalgo, 58030 Morelia, Mexico (isabelisrade@gmail.com)

This study investigates the sedimentary sequences of Mexican crater lakes as climate-sensitive archive of past environments. Crater lakes are closed hydrological systems, highly sensitive to weathering and climate conditions (Newton *et al.*, 2005). Here we focus on the sedimentation record of one maar lake situated in the State of Michoacán, in Central Mexico (101° 27.5' W, 19° 12.7' N, 1480 m asl). La Alberca de Tacámbaro is a crater located in the western Trans-Mexican Volcanic Belt, in the Michoacán-Guanajuato Quaternary Volcanic Field (Ortega-Guerrero *et al.*, 2021). The basaltic crater is filled with a warm monomictic lake, slightly alkaline, with an early stratification starting in February (Ortega-Guerrero *et al.*, 2021). Central Mexico is highly sensitive to climate variability (Holmes *et al.*, 2016). The site of Tacámbaro is characterized by all year-round warm temperature (average 18°C) and a pronounced dry season from November to April (tropical sub-humid climate) with 1140 mm of annual precipitation (Ortega-Guerrero *et al.*, 2021). At present the tropical climate of Mexico is dominated by the North American Monsoon (NAM), with a rainy season linked to the northward migration of the Intertropical Convergence Zone (ITCZ) (Caballero *et al.*, 2016). The strength of the summer monsoon is affected by the El Niño-Southern Oscillation (ENSO). ENSO is a pseudo-periodic climate pattern involving variations in sea surface temperatures and winds over the eastern Tropical Pacific but with worldwide consequences on multi-annual climate variability (Caballero *et al.*, 2016).

According to its key location, the mechanisms which control interannual variability in Mexican precipitation are complex but interesting to reconstruct. For this purpose, a short lacustrine sediment core (LTa19, 94 cm) was retrieved in spring 2019 with a manual Uwitec© coring system. The sediments have been described by macroscopic and smear slide observation and analyzed for physical (magnetic susceptibility, grain size distribution by laser diffraction, loss-on-ignition for water content and organic matter abundance), mineralogical (X-ray diffraction on bulk and clay fraction) and geochemical (X-Ray fluorescence, C/N for organic matter origin) parameters with variable resolution. Sedimentation rate and dating of the short core will be done by the measurement of the geochronometers ²¹⁰Pb and ¹³⁷Cs.

Continuous SCOPIX X-ray imaging system and XRF core scanner performed at 2 mm resolution evidence a finely laminated sediment with a few coarser and darker layers (see Figure 1). A robust PCA will be applied to SCOPIX and XRF core scanner data to identify the different sedimentary components (detrital, volcanic or biogenic) and to link the sedimentary grey-scale levels with specific geochemical elements (e.g., Ti) or element ratios.

Mineralogical assemblages and geochemical composition of the sediments will be used to reconstruct the type (physical or chemical) and intensity of the weathering processes, both controlled by precipitation abundance. By applying the age model of recent sediments, the XRF elemental data or elemental ratios will be compared with regional meteorological data to validate any geochemical proxy for rainfall intensity in complement to XRF-Ti signal that was already used in former paleo-ENSO studies (Newton *et al.*, 2005, Ortega-Guerrero *et al.*, 2021,...). Any validation of the sedimentary proxies would request a calibration with instrumental data retrieved from local meteorological station. The approach will be further applied to several crater lake sequences within the framework of the FNRS-funded HolMeCl project.

References

Caballero, M. Vázquez, G. Ortega, B. Favila, M. E. & Lozano-García, S., 2016. Responses to a warming trend and “El Niño” events in a tropical lake in western Mexico. *Aquatic Sciences*, 78(3), 591–604.

<https://doi.org/10.1007/s00027-015-0444-1>

Holmes, J. A. Metcalfe, S. E. Jones, H. L. & Marshall, J. D., 2016. Climatic variability over the last 30 000 years recorded in La Piscina de Yuriria, a Central Mexican crater lake. *Journal of Quaternary Science*, 31(4), 310–324.

<https://doi.org/10.1002/jqs.2846>

Newton, A. J. Metcalfe, S. E. Davies, S. J. Cook, G. Barker, P. & Telford, R. J., 2005. Late Quaternary volcanic record from lakes of Michoacán, central Mexico. *Quaternary Science Reviews*, 24(1-2), 91–104.

<https://doi.org/10.1016/j.quascirev.2004.07.008>

Ortega-Guerrero, B. Caballero, M. & Israde-Alcántara, I., 2021. The Holocene record of Alberca de Tacámbaro, a tropical lake in western Mexico: evidence of orbital and millennial-scale climatic variability. *Journal of Quaternary Science*, 36(4), 649–663. <https://doi.org/10.1002/jqs.3316>

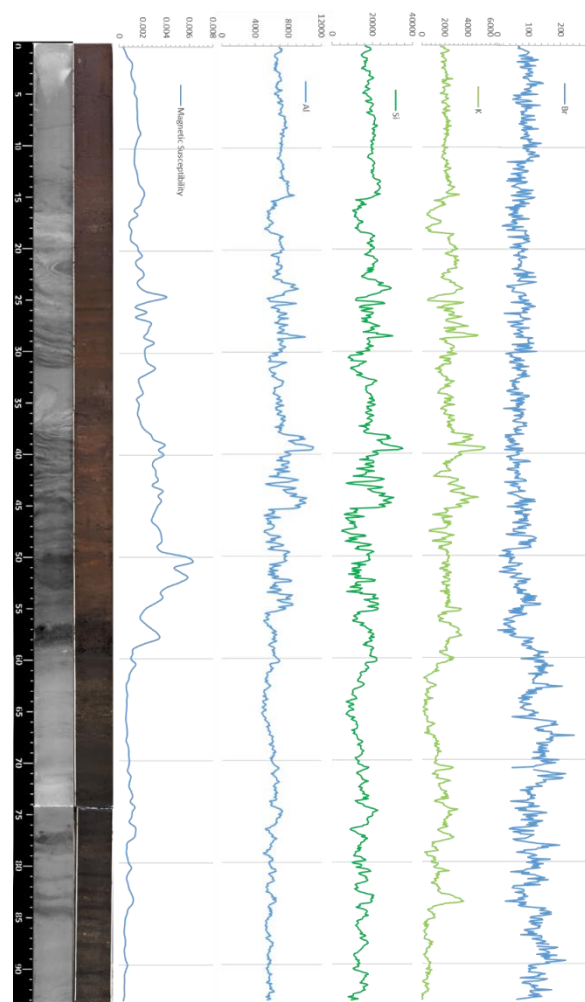


Figure 1. Sediment characteristics (SCOPIX X-ray image, color photograph, magnetic susceptibility) and a selection of XRF core scanner geochemical profiles (i.e., Al, Si, K, Br) of core LTa19, retrieved from the crater maar lake “la Alberca de Tacámbaro” in central

Session 11-Geophysics and Seismology

Conveners:

Thomas Lecocq (ROB), Frédéric Nguyen (ULiège), Adrien Oth (ECGS, Luxembourg)

Geophysical techniques are widely used to characterise structures and dynamic processes in the subsurface. While numerous advances in experimental design, instrumentation, data acquisition and processing, numerical modeling, and inversion constantly push the limits of spatial and temporal resolution, the interpretation of the results often remains ambiguous. We invite contributions covering



(but not limited to): Geophysical imaging or monitoring approaches such as seismic, electrical resistivity, electromagnetic or ground-penetrating radar. Seismological studies using ambient noise to characterise subsurface structures and dynamic processes are welcome including volcano- and induced seismicity aspects; earthquake source studies; or groundwater related studies.

CO₂ gas discharge in Laacher See: visualization and mapping of accumulated gas in the water column and sedimentary infill of a caldera lake in western Germany

Stijn ALBERS¹, Anouk VERWIMP¹, Corentin CAUDRON², Thomas VANDORPE³, and Marc DE BATIST¹

1. *Renard Centre of Marine Geology (RCMG), Ghent University, Ghent, Belgium* (stijn.albers@ugent.be; anouk.verwimp@ugent.be; marc.debatist@ugent.be)
2. *Institut des Sciences de la Terre (ISTerre), Université Grenoble-Alpes, Grenoble, France* (corentin.caudron@univ-smb.fr)
3. *Flanders Marine Institute (VLIZ), Ostend, Belgium* (thomas.vandorpe@vliz.be)

Volcanic activity has shaped the Eifel region in western Germany during the Quaternary, as evidenced by the presence of numerous volcanic features, such as maars and volcanic domes. The region is generally subdivided in a West and East Eifel Volcanic Field, with the latter remaining dormant ever since the eruption of the Laacher See Volcano 12,900 years BP. This event featured several phreatomagmatic and Plinian eruption phases and included volcanic vent migration and magma chamber collapse, resulting in the formation of a caldera subsequently filled with groundwater to form a lake, the present-day Laacher See. Magmatic recharge of crustal reservoirs beneath Laacher See and plume-induced deformation in the Eifel has recently been evidenced by deep microearthquake activity (Hensch et al., 2019) and ground uplift (Kreemer et al., 2020), respectively, resulting in an increased scientific attention towards the region. Furthermore, investigating indications of volcanic activity in the Eifel is of great importance, since the related hazards could pose a significant risk in this densely populated region.

Current volcanic activity in Laacher See is most notably evidenced by several gas seeps (i.e. mofettes) in the lake and its surrounding shore, emitting CO₂ of magmatic origin. During a survey in August 2019, several geophysical techniques were used to localize and image the CO₂ seepage in the water column, as well as gas accumulation in the sedimentary infill of the lake. A Norbit 400 kHz multibeam echosounder was used to locate gas seeps in the water column, visible by their high backscatter intensity. The resulting map with the distribution of gas seeps is comparable to that of a previous study (Goepel et al., 2014) showing high concentrations of gas seeps along the old crater rims of the 12,900 years BP eruption. High-resolution sub-bottom data, acquired with an Innomar SES-2000 quattro parametric sub-bottom profiler (10 kHz), show the presence of free gas in the subsurface, as evidenced by enhanced seismic reflections and acoustic blanking. Accumulated gas is present at different depths (5 to > 25 m) in the lake sediments, making it possible to map areas with high concentrations of free gas at different levels. Our results show that the subsurface gas accumulation often coincides with gas seep locations in the water column, with an especially large area of acoustic blanking in the center of the lake.

Our preliminary data confirm that volcanic gas is actively migrating through the sedimentary infill and water column of Laacher See and illustrate the need for monitoring these gas migration processes. The upward migration of free gas through the lake sediments towards the surface still needs further investigation (i.e. what drives this migration processes, what determines its natural temporal and spatial variability, how much of the gas is of volcanic origin, etc.), but our results show that the use of high-resolution sub-bottom profiler data can help in precisely localizing free gas in the lake subsurface. The monitoring of gas seeps at Laacher See and a further understanding of its gas-laden sedimentary infill can ultimately contribute to a better volcanic hazard assessment in the Eifel region.

References

- Goepel, A., Lonschinski, M., Viereck, L., Büchel, G. & Kukowski, N., 2014. Volcano-tectonic structures and CO₂-degassing patterns in the Laacher See basin, Germany. *Int. J. Earth Sci.*, 104(5), 1483–1495.
- Hensch, M., Dahm, T., Ritter, J., Heimann, S., Schmidt, B., Stange, S. & Lehmann, K., 2019. Deep low-frequency earthquakes reveal ongoing magmatic recharge beneath Laacher See Volcano (Eifel, Germany). *Geophys. J. Int.*, 216, 2025–2036.
- Kremer, C., Blewitt, G. & Davis, P.M., 2020. Geodetic evidence for a buoyant mantle plume beneath the Eifel volcanic area, NW Europe. *Geophys. J. Int.*, 222, 1316–1332.

A new Hainaut coal area earthquake intensity attenuation model using 19th - 20th century shallow seismicity data

Thierry CAMELBEECK¹, Koen VAN NOTEN^{1,*}, Thomas LECOCQ¹, Marc HENDRICKX¹

1. Royal Observatory of Belgium, Uccle, Belgium (koen.vannoten@seismology.be)

**presenting author*

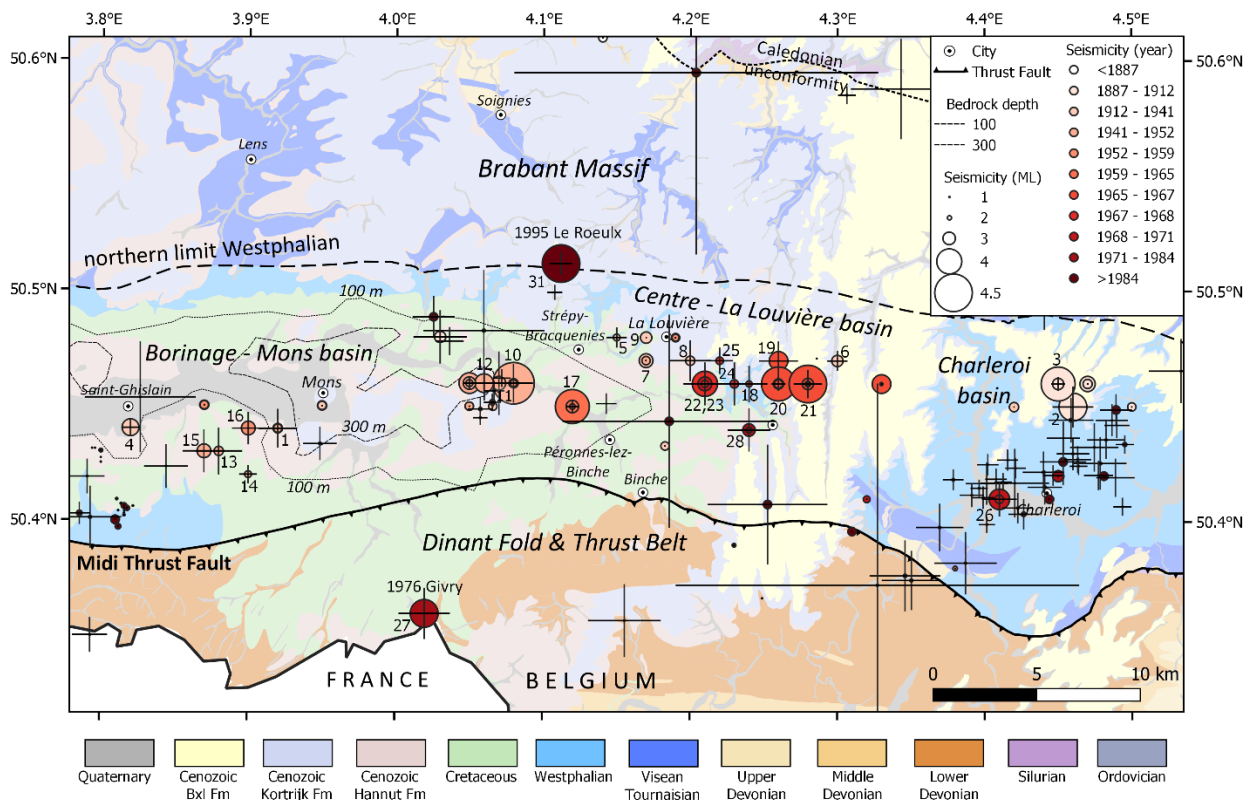
In the Carboniferous coal area of the Hainaut province in Belgium, a century of shallow seismic activity occurred from the end of the 19th century until the late 20th century. This seismicity is the second largest source of seismic hazard in NW Europe. In this sequence, five seismic events (M_w~4.0), that occurred on 3 June 1911, 3 April 1949, 15 December 1965, 16 January 1966, and 28 March 1967, locally caused moderate damage to buildings to maximum intensity VII on the EMS-98 scale. For decades, the natural causality of this seismicity and its potential link with coal extraction is disputed due to uncertainties in earthquake location and depth. To tackle this discussion in the near future, we reviewed a century of intensity data collected by official macroseismic surveys held by the Royal Observatory of Belgium, press reports, and contemporary scientific studies.

In this contribution, we present methodological advances on how we updated the magnitude, epicentral intensity and location, and depth of 123 Hainaut seismic events only using macroseismic data. We discuss the impact and damage of this unique seismicity on the building infrastructure and people. Our study highlights the capability of shallow (< ~6km), small-magnitude earthquakes to generate damage. The intensity dataset shows that inside the Carboniferous coal basin (that extends from Mons to Liège) intensity attenuates much faster than in the surrounding Paleozoic Brabant and Ardenne basements due to unique characteristics of the coal basin. Using the improved intensity dataset, we modelled a new Hainaut intensity attenuation law and created relationships linking magnitude, epicentral intensity and focal depth. The new attenuation model suggests that current (international) hazard maps overestimated ground motion levels in the Hainaut area due to the use of inadequate ground motion prediction equations. Hence, the model should be used to evaluate the potential impact of current and future, e.g. geothermal energy, projects in the Hainaut area and other regions with a similar geological configuration.

References:

Camelbeeck, T., Van Noten, K., Lecocq, T., and Hendrickx, M. 2021. The damaging character of shallow 20th century earthquakes in the Hainaut coal area (Belgium). *Solid Earth Discussions*. <https://se.copernicus.org/preprints/>

Figure



Past seismicity in the coal mining area of the Hainaut province in Belgium. Seismicity (up to 2020) colored in function of time and sized to magnitude. Black error bars show location uncertainty. Location, depth and magnitude and uncertainties of the seismicity between 1887 and 1982 was reviewed using only macroseismic intensity data. Source: Camelbeeck et al. 2021.

Insights from the new 3D fault model for eastern Flanders (northern Belgium)

Jef DECKERS¹, Bernd ROMBAUT¹, Katrijn DIRIX¹, Matsen BROOThAERS¹, Timothy N. DEBACKER²

1. VITO, Boeretang 200, Mol, Belgium (jef.deckers@vito.be)
2. TiBa ScConsulting / Geognostics; Hofmeierstraat 7, 9000 Gent, Belgium (tibadebacker@gmail.com)

1. Introduction

Eastern Flanders (northeastern Belgium) comprises two main Meso- and Cenozoic geological entities, called the Campine Basin in the west and the Roer Valley Graben (RVG) in the east. These entities contain successions of Upper Paleozoic, Mesozoic and Cenozoic strata and experienced faulting during several tectonic phases of both compression and extension, which resulted in a complex fault system.

Based on mainly 2D seismic data and coal-mine information, fault-maps of the Paleozoic and Mesozoic strata of eastern Flanders were created by Langenaeker (2000). These fault-maps were used by Matthijs et al. (2013) to create a 3D fault model from the surface up to the Paleozoic, as part of the G3Dv2-model of Flanders. In the latter model, Paleozoic and Mesozoic fault traces of Langenaeker (2000) were extended into the shallow subsurface (Upper Cretaceous and Cenozoic) when indications for fault reactivations were found in the set of - generally widely spaced - deep boreholes. This approach makes it difficult to estimate the exact location, orientation and lateral extent of reactivated faults. In order to get a better image of Cenozoic fault activity, an updated set of 2D seismic data was re-interpreted from the Lower Carboniferous upwards in the context of the follow-up 3D model of the Flemish subsurface, called the G3Dv3-model (Deckers et al., 2019). The G3Dv3-model was constructed from 2014 to 2019 by VITO for the Bureau for Environment and Spatial Development of the Flemish Government (VPO). For this model, faults were for the first time modelled and interpreted in 3D from the Lower Carboniferous upwards. In addition, a large number of stratigraphic layers were interpreted on both seismic and borehole data and modelled into 3D-layers. These layers enabled us to make estimates on the timing and amounts of vertical throws along the newly modelled faults. The new fault and horizon models thereby provide the opportunity to study the kinematics of faulting and fault reactivation in the southern North Sea area.

2. Dataset and methodology

The G3Dv3-model comprises the geological units (groups, formations and members) and faults in the subsurface of Flanders, from the surface down to the Lower Paleozoic basement. The model was largely based on borehole data from the DOV database (“Database subsoil Flanders”; <https://www.dov.vlaanderen.be/>). In the western part of Flanders, the model represents a modification and refinement of the previous G3Dv2-model by Matthijs et al. (2013). In the structurally more complex eastern part of Flanders (Campine Block and RVG) however, the G3Dv3-model is an entirely new model. In the latter area, horizon and fault modelling - besides boreholes - also strongly relied on seismic data. Additional data such as gravimetric data, coal-mine information and topographic maps were used as secondary inputs. In parts of the border areas with the Netherlands, the Cenozoic 3D (hydro)geological layer and fault models of cross-boundary projects (so-called H3O-projects) were integrated in the

G3Dv3-model. These border areas include the RVG (H3O-Roer Valley Graben; Deckers et al., 2014) and the northeastern part of the Campine Block alongside the RVG (H3O - Campine area; Vernes et al., 2018).

The output of the G3Dv3-model consists of depth and thickness maps, geographic extents of units, fault lines, fault surfaces, etc.. The geological model is available at <https://www.dov.vlaanderen.be/page/geologisch-3d-model-g3dv3>.

3. Results

The G3Dv3-model provides interesting insights into the evolution of two major rifting phases and an inversion phase in eastern Flanders. The first rifting phase took place during the Jurassic (Cimmerian phase), or when the RVG possibly developed. This phase was succeeded by a Late Cretaceous inversion phase of the RVG. The second rifting phase occurred during the Cenozoic when the RVG was reactivated as part of the larger Roer Valley Rift System. The insights that the G3Dv3-model provides on the expression of the Late Cretaceous inversion phase of the RVG are yet discussed by Deckers et al. (2021), so this paragraph will focus on the two rifting phases.

The G3Dv3-model shows that both the Cimmerian (Jurassic) and Cenozoic phases were dominated by WNW-ESE and (N)NW-(S)SE fault populations. Seismic data illustrate that most of the Cenozoic faults (including all those with the largest throw) are rooted in the Cimmerian faults, indicating major Cenozoic reactivation of Cimmerian faults. The Cimmerian faults were probably also inherited, as the WNW-ESE Cimmerian faults become dominant in the southwest close to the Lower Paleozoic Brabant Massif, which is characterized by WNW-ESE striking features on gravimetric maps. The (N)NW-(S)SE Cimmerian faults become dominant further to the northeast, where they were active already during the Early Carboniferous (Muech and Langenaeker, 1993). Cimmerian fault reactivation explains the presence of populations with different fault orientations as well as the linkage of these faults into long (> 10 km) systems, despite having generally relatively small vertical throws (< 500 m). In addition to the general trends, pre-existing zones of weakness, such as the latest Carboniferous/early Permian transpressional Donderslag and Gruitrode Lineaments, caused segmentation of the Cimmerian faults into structural domains that are characterized by their own typical fault patterns and kinematics.

Although the Cenozoic faults were mostly inherited Cimmerian faults, we identified several differences between these faults or phases:

- The Cimmerian phase was markedly stronger than the Cenozoic phase: more faults were active and throws were consistently larger during the Cimmerian phase.
- During the Cimmerian phase, faulting was also more widespread, albeit with relative high concentrations at the southwestern margin of the Campine Basin, and the boundary between the Campine Basin and the RVG. In comparison, during the Cenozoic, strain was focused on the pre-existing RVG border fault system and re-utilised Cimmerian faults in further development of the RVG.
- Cimmerian faulting in the border fault system of the RVG frequently caused rotation of hangingwall blocks, whereas Cenozoic faulting generally caused little or no hangingwall block rotation

References

- Deckers, J., De Koninck, R., Bos, S., Broothaers, M., Dirix, K., Hambsch, L., Lagrou, D., Lanckacker, T., Matthijs, J., Rombaut, B., Van Baelen, K. & Van Haren, T., 2019. Geologisch (G3Dv3) en hydrogeologisch (H3D) 3D-lagenmodel van Vlaanderen. Studie uitgevoerd in opdracht van het Vlaams Planbureau voor Omgeving, departement Omgeving en de Vlaamse Milieumaatschappij. VITO, Mol, VITO-rapport, 2018/RMA/R/1569.
- Deckers, J. Rombaut, B., Vannoten K. & Vanneste, K., 2021. Influence of inherited structural domains and their particular strain distributions on the Roer Valley graben evolution from inversion to extension. *Solid Earth*, 12, 345–361.
- Deckers, J., Vernes, R., Dabekaussen, W., Den Dulk, M., Doornenbal, H., Duser, M., Matthijs, J., Menkovic, A., Reindersma, R., Walstra, J., Westerhoff, W. & Witmans, N.: Geologisch en hydrogeologisch 3D model van het Cenozoïcum van de Roerdalslenk in Zuidoost-Nederland en Vlaanderen (H3O-Roerdalslenk). VITO-rapport, 2014/ETE/R/1, 200 pp, 2014.
- Langenaeker, V., 2000. The Campine Basin: stratigraphy, structural geology, coalification and hydrocarbon potential for the Devonian to Jurassic. *Aardkundige Mededelingen*, 10, 1-142.
- Matthijs, J., Lanckacker, T., De Koninck, R., Deckers, J., Lagrou, D. & Broothaers, M., 2013. Geologisch 3D lagenmodel van Vlaanderen en het Brussels Hoofdstedelijk Gewest - versie 2, G3Dv2. Studie uitgevoerd door VITO in opdracht van de Vlaamse overheid, Departement Leefmilieu, Natuur en Energie, Afdeling Land en Bodembescherming, Ondergrond, Natuurlijke Rijkdommen, VITO-rapport, 2013/R/ETE/43.
- Muchez, P. & Langenaeker, V., 1993. Middle Devonian to Dinantian sedimentation in the Campine Basin (northern Belgium): its relation to Variscan tectonism. *Special Publication of the International Association of Sedimentologists*, 20, 171-181.
- Vernes, R.W., Deckers, J., Bakker, M.A.J., Bogemans, F., De Ceukelaire, M., Doornenbal, J.C., den Dulk, M., Duser, M., Van Haren, T.F.M., Heyvaert, V.M.A., Kiden, P., Kruisselbrink, A.F., Lanckacker, T., Menkovic, A., Meyvis, B., Munsterman, D.K., Reindersma, R., ten Veen, J.H., van de Ven, T.J.M., Walstra, J. & Witmans, N., 2018. Geologisch en hydrogeologisch 3D model van het Cenozoïcum van de Belgisch-Nederlandse grensstreek van Midden-Brabant / De Kempen (H3O – De Kempen). Studie uitgevoerd door VITO, TNO-Geologische Dienst Nederland en de Belgische Geologische Dienst in opdracht van Vlaams Planbureau voor Omgeving, Vlaamse Milieumaatschappij, TNO, Geologische Dienst Nederland, Nederlandse Provincie Noord-Brabant, Brabant Water, Programmabureau KRW/DHZ Maasregio.

BarrosRedefinition of the structural units of the Variscan Front based on the results of the Mons2012 and Hainaut2019 seismic surveys in the Hainaut (SW Belgium)

Nicolas DUPONT ¹, Olivier KAUFMANN ², Jean-Marc BAELE ³

1. *University of Mons, Faculty of Engineering, Geology and Applied Geology, Place du Parc, 20, 7000 Mons, Belgium (nicolas.dupont@umons.ac.be)*
2. *Idem (olivier.kaufmann@umons.ac.be)*
3. *Idem (jean-marc-baele@umons.ac.be)*

In order to investigate the structure and the properties of the Dinantian deep geothermal reservoir in the Hainaut, new 2D seismic surveys have been carried out in this area in the last decade (Mons2012 and Hainaut2019). The previous seismic surveys (e.g. Hainaut1979, Belcorp1986) resulted in heterogenous data, due to the combined presence of many coal mines and dense urbanization in the central part of the surveyed area (Dejonghe et al., 1992). Moreover, the complexity of the geological context makes seismic imaging difficult, especially due to a thick Meso-Cenozoic cover, leading to a high impedance contrast at its base, and thick deformed thrust sheets along the Variscan Front. Thus, the design of the new surveys has been optimized to enhance the quality of the seismic imaging. The acquisition was conducted along 7 lines long of about 20 km each. The N-S direction of the lines was defined to cross perpendicularly the Variscan Front from the outcrop of the reservoir's top to the French border.

The interpretation of the new seismic reflection data has allowed, for the first time, to clarify the structure of the basement in the study area. In particular, the structures of the Variscan Front in the Hainaut were revisited in the light of new seismic reflection data completed by reprocessed sections from previous surveys (Hainaut1979, Belcorp1986). According to the interpretation of these data, the Variscan Front is structured in an autochthonous unit (Brabant Autochthon), overlain by a set of thrust sheets (Haine-Sambre-Meuse Thrust Sheets) and by an allochthonous unit (Ardenne Allochthon). The lower part of the Brabant Parautochthon of Belanger et al. (2012) would be therefore included in the autochthonous unit, whereas its upper part would be included in the Haine-Sambre-Meuse Thrust Sheets. The thrust sheets that have been identified in the new seismic sections correspond to different degrees of deformation and allochthony. From bottom to top, they would be an early duplex (i.e. parautochthon sensu stricto), a duplex, partially overturned thrust sheets and finally overturned thrust sheets. The duplex would correspond to a set of units formerly recognized in the coal mines of the West of Mons and the Centre district including the imbricated structure ("*massifs imbriqués*"), the Grisœil unit, the "Faulted Ground" ("*Nappe faillée*") and the units that could be considered as its less deformed lateral variation (Placard et Centre units).

The Variscan Front would be much shallower than previously assumed since the deep geothermal reservoirs would be located within the autochthonous unit and, therefore, would not have been deformed during the Variscan shortening. Nevertheless, a set of subvertical structures (faults and folds), mainly dipping northwards, have been identified within the autochthonous unit and thus at the level of the deep geothermal reservoirs.

Acknowledgments

This research is carried out under the MORE-GEO project, supported by ERDF funds (Wallon Region + UE).

References

Belanger, I., Delaby, S., Delcambre, B., Ghysel, P., Hennebert, M., Laloux, M., Marion, J.-M., Mottequin, B. & Pingot, J.-L., 2012. Redéfinition des unités structurales du front varisque utilisées dans le cadre de la nouvelle Carte géologique de Wallonie (Belgique). *Geologica Belgica*, 15, 169–175.

Dejonghe, L., Delmer, A. & Hance, L., 1992. Les enseignements d'une campagne sismique conduite en Belgique dans le Hainaut, selon l'axe Erquelines - Saint-Ghislain. *Annales de la Société Géologique du Nord*, 1, 135–142.

Figure

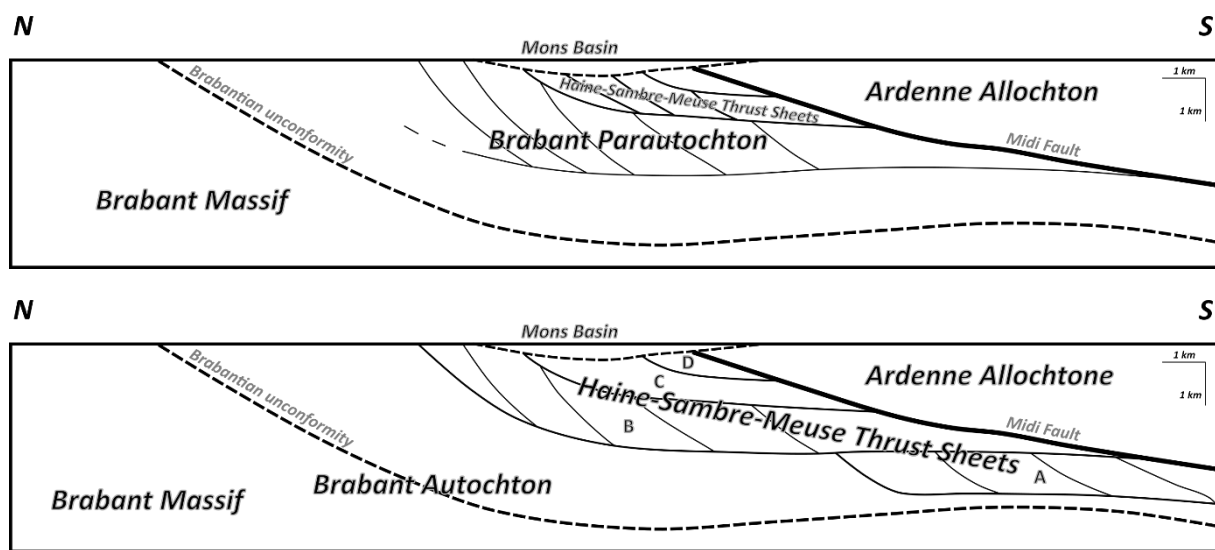


Figure 1: Synthetic N-S cross-section across the Variscan Front. Top: after Belanger et al. (2012), modified. Bottom: after the interpretation of the Mons2012 et Hainaut2019 seismic surveys. A: early duplex; B: duplex; C: partly overturned thrust sheets (e.g. Masse-Borinage unit); D: overturned thrust sheets (e.g. Boussu unit).

Statistical imaging of the deformation over Belgium using multiple geodetic techniques

Kevin GOBRON¹, Pierre-Yves DECLERCQ², Xavier DEVLEESCHOUWER², Michel VAN CAMP¹

1. *Royal Observatory of Belgium, Avenue Circulaire, 3, 1180 Brussels, Belgium* (michel.vancamp@seismologie.be ; kevin.gobron@oma.be)
2. *Royal Belgian Institute of Natural Sciences, Geological Survey of Belgium, Rue Vautier 29, 1000 Brussels, Belgium* (xdevleeschouwer@naturalsciences.be; pydeclercq@naturalsciences.be)

One of the challenges of geodesy is to characterize at the sub-millimeter level the vertical deformation of the ground in response to tectonic, anthropogenic, and climatic forcing. Reaching this level of accuracy is crucial to understand the deformation mechanisms acting in Belgium and it contributes to the mitigation of geo-hazards and the operational management of the territory. To address this challenge, the LASUGEO project, aiming at identifying ground deformation caused by groundwater exploitation, makes use of the observations of three independent geodetic techniques, namely: Global Navigation Satellite System (GNSS), Permanent Scatterers Interferometry Synthetic Aperture Radar (PS-InSAR), and repeated Absolute Gravity measurements (AG). Because GNSS, PS-InSAR, and AG provide independent measurements with different spatial and temporal resolutions, they are highly complementary. However, considering that each technique also comes with its own reference frames, accuracy, and source of biases, the optimal combination of these observations requires an appropriate statistical methodology.

To estimate the deformation over Belgium, we performed a joint analysis of the GNSS position time series provided by the Nevada Geodetic Laboratory (Blewitt et al., 2018), the PS-InSAR time series processed at Geological Survey of Belgium (Declercq et al., 2021), and the AG measurement carried out by the Royal Observatory of Belgium (Van Camp et al., 2011). Our statistical analysis is divided in three steps: (1) trajectory modelling of each geodetic time series, that is, the model of the predictable motion (e.g., linear trend, periodic deformation, and instrumental discontinuities), (2) surface reconstruction of the subsidence/uplift rates from each technique, and (3) the comparison of the result of the different techniques. For each step, attention is paid to the realistic estimation of the model uncertainties, by accounting for the influence of the time correlated stochastic variability in the geodetic time series (Williams et al. 2003). We propose to describe the algorithms used and results obtained from the trajectory modelling and surface reconstruction of the subsidence/uplift rates. We show that, by combining a large number of observation, we are able to image vertical deformation at the 1.0 mm/yr level over Belgium (see Figure 1 for the GNSS imaging). We also discuss differences between GNSS, AG and PS-InSAR that could highlight the need to calibrate PS-InSAR relative estimates with GNSS and AG geocentric velocities.

References

- Blewitt, G., Hammond, W. C., & Kreemer, C. 2018. Harnessing the GPS data explosion for interdisciplinary science. *Eos*, 99(10.1029).
- Declercq, P.-Y. Gérard, P. Pirard, E. Walstra, J. & Devleeschouwer, X., 2021. Long-Term Subsidence Monitoring of the Alluvial Plain of the Scheldt River in Antwerp (Belgium) Using Radar Interferometry. *Remote Sensing* 13/6: 1160.
- Van Camp, M., de Viron, O., Scherneck, H. G., Hinzen, K. G., Williams, S. D., Lecocq, T., ... & Camelbeeck, T. 2011. Repeated absolute gravity measurements for monitoring slow intraplate vertical deformation in western Europe. *Journal of Geophysical Research: Solid Earth*, 116(B8).
- Williams, S. D. P. 2003. The effect of coloured noise on the uncertainties of rates estimated from geodetic time series. *Journal of Geodesy*, 76(9-10), 483-494.

Figure

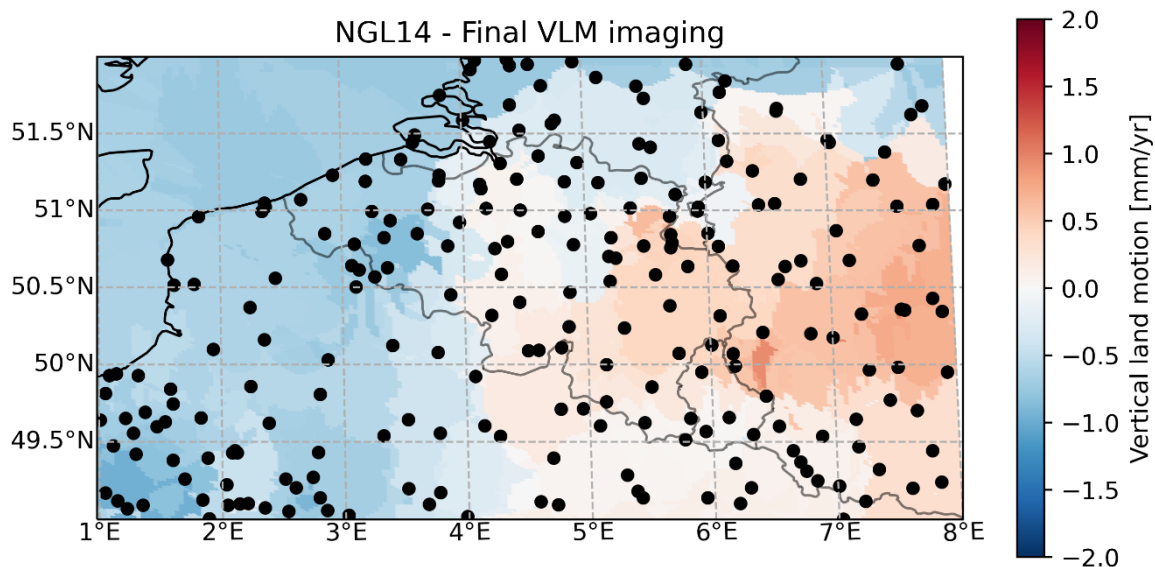


Figure 14 Imaging of the vertical land motion (VLM) over Belgium using a dense network of GNSS position time series computed by the Nevada Geodetic Laboratory.

Study of the eigenfrequencies of stalagmites to better understand paleoseismicity

Aurélien MARTIN^{1,2}, Thomas LECOCQ¹, Ari LANNOY³, Yves QUINIF⁴, Sophie VERHEYDEN⁵, Serge DELABY⁶, Thierry CAMELBEECK¹, Nathalie FAGEL²

1. Royal Observatory of Belgium, Brussels, Belgium (aurelie.martin@oma.be)
2. University of Liège - Department of Geology - AGEs, Liège, Belgium
3. Domaine des Grottes de Han-sur-Lesse, Han-sur-Lesse, Belgium
4. University of Mons, Faculty of Engineering Geology and Applied Geology, Mons, Belgium
5. Royal Belgian Institute of Natural Sciences, Brussels, Belgium
6. Geopark Famenne-Ardenne, Han-sur-Lesse, Belgium

The frequency-band of regional earthquake ground motions generally does not exceed 20 Hz. In this frequency band, structures (such as candlestick stalagmites) can resonate and break at a lower acceleration than expected during an earthquake, if the ground movement is strong enough. Therefore, the absence of breakage in these structures would indicate that a certain level of ground movement has not been exceeded since they existed. The existence of intact candlestick stalagmites in the caves is therefore an indicator of the upper limit of ground movements (e.g., Gribovszki *et al.* 2017) that a specific site may have encountered, and the natural frequency is a fundamental parameter in the study of the response of these stalagmites to seismic movement.

In this context, field surveys were carried out in the Han-sur-Lesse Cave (Belgian Ardennes) to identify the stalagmites for which an analytical approach (based on cantilever beam theory for free vibration, a specific case of the Euler–Bernoulli theory) gives an eigenfrequency less than 20 Hz. In this formula, the stalagmite is considered as a perfect cylinder and therefore depends only on the mechanical properties of the stalagmite and their height and diameter. These two parameters were measured in the cave. This study identified 27 stalagmites distributed in different areas of the cave (Synanthropes and Cornet room; Vervietois Gallery) and on different substratum (stalagmitic floor, fallen rocks, ...).

Thanks to a three-component seismic sensor placed on the stalagmite itself, the eigenfrequencies of these eligible stalagmites are then obtained by the direct measurement of the ambient seismic noise caused by human activities, microseisms, etc. This acquisition campaign is underway and already gives an idea of the frequency of 6 stalagmites thanks to acquisitions of 15 to 30 minutes each.

To explore the reactions of these structures to external events such as quarry blasts or earthquakes, seismic measurements will be carried out over a longer period (weeks) as was the case for the Minaret studies (Martin *et al.* 2020). With sensors located at the base of the stalagmites, in the middle of the cave room and at the surface outside the cave, this will allow to compare the results and identify a possible amplification of movement at eigenfrequencies as was shown for the Minaret (Martin *et al.* 2020).

References

- Gribovszki, K., Kovács, K., Mónus, P., Bokelmann, G., Konecny, P., Lednická, M., Moseley, G., Spötl, C., Edwards, R. L., Bednárík, M., Brimich, L., & Toth, L., 2017. Estimating the upper limit of prehistoric peak ground acceleration using an in situ, intact and vulnerable stalagmite from Plavecká priepast cave (Detrekői-zsomboly), Little Carpathians, Slovakia - first results. *Journal of Seismology*, 21, 1111-1130. <https://doi.org/10.1007/s10950-017-9655-3>
- Martin, A., Lecocq, T., Hinzen, K.-G., Camelbeeck, T., Quinif, Y., & Fagel, N. (2020). Characterizing Stalagmites' Eigenfrequencies by Combining In Situ Vibration Measurements and Finite Element Modeling Based on 3D Scans. *Geosciences*, 10(10), 418. <https://doi.org/10.3390/geosciences10100418>

The effects of Belgian crustal geology and its sedimentary cover on macroseismic intensity attenuation

Ben NEEFS ¹, Koen VAN NOTEN ¹, Thierry CAMELBEECK ¹

1. Royal Observatory of Belgium, Uccle, Belgium (ben.neefs@oma.be)

To quickly assess the impact of earthquakes, many countries make use of earthquake intensity prediction equations (IPEs). These empirical equations describe the decay of ground motion in terms of macroseismic intensity and consequently can simulate the damage distribution and damage degree in near real-time. Intensity attenuation is region-specific and is dependent on seismic wave propagation in the crust and its sedimentary cover.

To develop IPEs suitable for modelling the impact of Belgian earthquakes, local macroseismic data is thus required. The Royal Observatory of Belgium (ROB) has a rich heritage in collecting felt earthquake and damage reports. This database was extended by intensity data from neighboring countries and is used to develop Belgian IPEs. However, the traditional methodology, i.e. constructing a single intensity attenuation law for large areas, is not fit for the complex geological situation in Belgium. Macroseismic intensity distribution patterns of past Belgian earthquakes do not cohere to the common assumption of an isotropic intensity decrease with increasing epicentral distance. Intensity attenuation is strongly influenced by crustal and cover geological features that heavily control and limit seismic wave propagation and cause an anisotropic display of intensity decay.

Geological features that have influenced past intensity distribution patterns and attenuation in Belgium are:

- The strongly compacted and deformed Lower Palaeozoic Anglo-Brabant Massif, which easily transfers ground motion along its core axis in a WNW-ESE direction.
- The increasing thickness of soft sedimentary Cenozoic strata covering the Anglo-Brabant massif towards the Belgium-Dutch border, effectively filtering high-frequency ground motions.
- The Lower Rhine Embayment boundary faults, impeding effective ground motion transfer and serving as seismic mirrors.
- The Midi-Eifel Fault which separates the Ardenne allochthon from its foreland and acts as a seismic barrier.
- The shallow Walloon Carboniferous coal basins along a thin band across the country with a fast intensity attenuation.

The quantitative effects of these geological regions on macroseismic intensity are best to be modelled separately, with different IPEs for each characteristic region in Belgium. But given the small size of both Belgium and these regions, local earthquakes are prone to hit multiple areas with different attenuation properties at once. This urges the necessity to subselect macroseismic data out of different earthquakes to be able to model IPEs independently. Furthermore, modelling anisotropic intensity decay requires an additional dimension, e.g. such as bedrock depth, to be added to the prediction equation, which is uncommon in literature and further complicates this goal. The complex Belgian geology thus requires an entire new methodology to be developed to be able to construct Belgian IPEs, which will be elaborated in detail in this presentation.

Slip tendency apply to faults systems in the Congo Basin and its surroundings: A clue to explain western central African passive margin seismicity

Hardy Medry Dieu-Veill NKODIA ^{1,*}, Timothée MIYOUNA ¹, Florent BOUDZOUYOU ^{1,2}, Folarin KOLAWOLE ^{3,4}, Damien, DELVAUX ⁵

¹ Marien Ngouabi University, Faculty of Sciences and Technics, Department of Geology, Brazzaville, Republic of Congo.

² National Research Institute in Exact and Natural Sciences of Brazzaville, Republic of Congo

³University of Oklahoma

⁴United States, 5BP (United States), United States

⁵ Department of Geology, Royal Museum for Central Africa, Tervuren, Belgium.

* Corresponding author: nkodiahardy@gmail.com

The Congo basin and its surrounding orogens in the western Central African region had been experiencing several earthquakes, even though quite few studies had attempted to explain their occurrences. The link between the recent seismicity and known faults does not look straightforward. The analysis of seismic history of the onshore and offshore areas revealed that the earthquakes are occurring on pre-existing fault systems of the Congo Basin, its surroundings units, and along near-shore extensions of the oceanic transform faults. In addition, the western Central African passive margin is undergoing two principal stress regime, one which is a ENE-NE trending horizontal compression in a thrust regime, and the other which is a normal faulting regime. Using the slip tendency method, the application of these present stress regimes on the mapped pre-existing fault systems which are mostly high-angle strike-slip faults systems, suggest that it is difficult to reactivate these faults under a thrust faulting stress regime, but more easily in a normal faulting stress regime. As most of the earthquakes occur at upper-crustal depths, we propose three hypotheses: 1.) there might be a brittle shear zone at depth that is accommodating tectonic reactivation leading to seismogenic rupture, which could be achieved by landward stress transmission by oceanic transform faults; 2.) these earthquakes might be generated by plate uplift and gravitational collapse; 3.) some of the events may have been triggered by local anthropogenic stress perturbation. The second hypothesis is quite probable as the western Central African margin has experienced repeated episodes of tectonic uplift in the Cenozoic as recorded in the Congo Basin. A thorough seismic analysis of the western Central African margin would provide more insight into the most probable causative mechanism for the earthquakes.

Analyzing seismic anomalies in Carboniferous strata in the surroundings of three wells in Mol (Campine Basin, northern Belgium) by means of Amplitude Variation with Offset (AVO) analysis shows potential for deep geothermal exploration

Bernd ROMBAUT, Jef DECKERS, Katrijn DIRIX, Matsen BROOTHAERS, Ben LAENEN

VITO, Mol, Boeretang 200 (bernd.rombaut@vito.be)

Introduction and methodology

Anomalies in the seismic reflection pattern (e.g. high amplitude anomaly, polarity reversal), hereafter referred to as seismic anomalies, were observed in Carboniferous strata during interpretation of seismic reflection data in northern Belgium. Seismic anomalies can be the expression of several geological and non-geological features or processes. One of the more interesting geological features from a geothermal point of view are fluid reservoirs in the subsurface. The GeoConnect^{3d} European research project, which is part of the bigger GeoERA research program, gave us the opportunity to study these geomanifestations and their possible link to fluid reservoirs within the context of the structural framework that has been developed in this project (Barros et al., this volume). For this purpose we applied an Amplitude Variation with Offset (AVO) analysis. This analysis studies the variability in seismic reflection amplitude with changing distance between shotpoint and receiver, which indicates differences in lithology and fluid content in rocks above and below a certain reflector. Therefore this sort of analysis is ideal to analyze observed seismic anomalies, but also to detect additional seismic anomalies which do not show up or remained unnoticed on the seismic image. Previous research from Vandenberghe et al. (1986) already showed the potential of this technique to detect zones with increased secondary porosity in Lower Carboniferous limestone of the Campine Basin.

In order to carry out reliable AVO analyses, first, a specific pre-stack processing sequence was applied by TEEC on the data acquired from the Mol-Herentals 2D seismic survey in 2010. Next, AVO analysis was performed on the Upper Carboniferous strata (Lower Westphalian and Namurian) consisting of an alternation of claystone, siltstone, sandstone and coal layers. Thereafter, the same analysis was performed on the Lower Carboniferous limestone (Dinantian), which constitute the geothermal reservoir targeted by the Balmatt project in Mol (Bos & Laenen, 2017). The well trajectories from this project are situated near the seismic lines of the Mol-Herentals survey.

For the AVO analysis intercept and gradient attributes have been derived by applying Shuey's 2-term approximation (Shuey, 1985) using the Probe software from Paradigm. The intercept hereby represents the reflectivity at normal incidence angle or zero offset, while the gradient is the trend of changing reflectivity with changing incidence angle or offset distance. The classification scheme of Rutherford & Willams (1989), later on updated by Castagna & Swan (1997) was used to interpret the observed anomalies on intercept-gradient crossplots.

Results

In the upper part of the Lower Westphalian strata, just below the unconformable contact with the overlying Upper Cretaceous cover, class IV type anomalies have been identified according to the abovementioned classification schemes. Class IV anomalies can be typical for coal bed methane gas (Chen et al., 2013). Dry gas was indeed detected in strata of the Lower Westphalian Charleroi Formation in three nearby geothermal wells. The highest spikes in methane gas coincide with the abundant coal layers in this formation.

In the underlying Lower Westphalian and Namurian strata, class I anomalies were detected. Class I anomalies are typical for gas- or water filled strongly compacted sandstone units within claystone sequences (Rutherford & Willams, 1989). In the study area, the class I anomalies can be correlated with the thickest, often coal bearing and/or by coal-rich claystone surrounded, sandstone units of the Lower Westphalian and Namurian strata in the three nearby wells. The methane-rich coal layers within or just on top or below the sandstone units could therefore constitute the source for the gas-related anomalies in the sandstone units themselves. Additionally, in well MOL-GT-02, besides methane gas at the coal layers, also relatively high concentrations of dense gas / condensate were - almost continuously - measured along the claystone dominated sequence of the Lower Westphalian Châtelet Formation. Capping claystone sequences could therefore also have been a source for the anomalies in the sandstone units.

The strongest cluster of class I anomalies is situated within a large graben structure. Due to the large throw, the sandstone units were put in lateral contact with sealing claystone units, thereby creating a fault bounded reservoir. Also the other anomalies are often delimited by faults. Most of these faults were active during the Mesozoic and are dormant now, but some still show minor activity in the Cenozoic.

The reservoir potential of the underlying Dinantian limestone (Lower Carboniferous) is determined by open fractures/faults and dissolution features. In this type of setting, the AVO response is not as straightforward as in common siliciclastic reservoirs. Therefore, initially, the synthetic AVO response was derived from the reservoir intervals in well MOL-GT-01 in order to understand the type of response to look for. Thereafter, the AVO analysis was performed for the Dinantian interval on the seismic lines, which lead to the detection of several small, generally clustered, anomalous zones. One of the strongest anomalies (class I type) is located in the direct proximity of well MOL-GT-01 and correlates with a gas rich productive reservoir interval in this well. The strength of the anomaly is probably related to the high gas concentrations measured within this interval, as gas is known to enhance the AVO response.

Conclusions

AVO analyses were performed on different types of deeply buried sediments in northern Belgium. Across the entire Carboniferous, numerous anomalies were detected, which can be grouped in different types and are related to different intervals. Despite these

differences, the zones with observed anomalies were generally at least partly bounded by faults.

Correlations with nearby geothermal wells enabled reliable interpretations of the anomalies.

- Class IV type anomalies detected in the Lower Westphalian strata are related to gas-rich coal layers.
- Class I type anomalies in the claystone-dominated Lower Westphalian and Namurian strata can be correlated with thick sandstone units, which are possibly gas / fluid filled along these anomalous zones. The source of the gas could be coal layers or capping claystone.
- Class I type anomalies in the Dinantian limestone correlate with a gas rich reservoir interval.

This study confirms the potential of AVO analyses for the detection of gas rich pockets with corresponding reservoir potential, even in the deep subsurface (> 3 km). Well MOL-GT-01 proves that gas rich intervals in the Dinantian limestone can constitute interesting geothermal targets. Therefore, AVO analysis forms an important tool to increase the success of geothermal projects by highlighting some of the most interesting targets along seismic lines.

This project has received funding from the European Union's Horizon 2020 research and innovation programme under grant agreement No 731166.

References

- Barros, R., Piessens, K., Dirix, K., 2021. Structural framework as the new fundament for geoscientific communication and international scientific cooperation, *Geologica Belgica Conference, 2021*
- Bos, S., & Laenen, B., 2017. Development of the first deep geothermal doublet in the Campine Basin of Belgium. *European Geologist*, 43, 16-20.
- Castagna, J.P. & Swan, H.W., 1997, Principles of AVO crossplotting: *The Leading Edge*, 16, p. 337-342.
- Chen, X. P., Huo, Q., Lin, J., Wang, Y., Sun, F., Li, W. & Li, G., 2014. Theory of CBM AVO: I. Characteristics of anomaly and why it is so. *Geophysics*, vol. 79, no. 2, p. 55-65.
- Rutherford, S. R. & R. H. Williams, 1989. Amplitude versus-offset variations in gas sands: *Geophysics*, 54, p. 680-688.
- Shuey, R.T., 1985. A simplification of the Zoeppritz equations: *Geophysics*, 50, p. 609-614.
- Vandenberghe, N., Poggiagliomi, E., Watts, G., 1986. Offset-dependent seismic amplitudes from karst limestone in northern Belgium. *First Break* 4, 9-27.

Geophysical well log correlations in the Quaternary deposits of the Campine area, northern Belgium

Jan WALSTRA¹, Frieda BOGEMANS¹, Marleen DE CEUKELAIRE^{1,2}, Michiel DUSAR¹, Vanessa M.A. HEYVAERT^{1,3}, Bruno MEYVIS¹ & Kris WELKENHUYSEN¹

1. *Royal Belgian Institute of Natural Sciences – Geological Survey of Belgium, Brussels, Belgium (Jan.Walstra@naturalsciences.be)*

2. *Royal Belgian Institute of Natural Sciences – Scientific Heritage, Brussels, Belgium*

3. *Ghent University – Department of Geology, Ghent, Belgium*

The examination of natural gamma ray (GR) and resistivity (SN, LN) borehole logs distributed over the Campine area in northern Belgium shows systematic variations within the Quaternary deposits. These variations can be attributed to alternating clay and sand layers of the Lower Pleistocene Weelde and Malle Formations. The logs can be correlated rather well between neighbouring wells, whilst correlations over larger distance are more doubtful due to lateral changes in lithology and sedimentary characteristics.

In previous research the sedimentary characteristics of these deposits have been studied in great detail in temporary outcrops and undisturbed cores (Kasse, 1988; Bogemans, 1999). In the present study, borehole log signatures are correlated to well-defined lithostratigraphic units recorded in these undisturbed cores. In this way, a framework is created that allows for higher confidence correlation and mapping of the lithostratigraphic units in areas with sparse data from high-quality cores.

References

Bogemans, F., 1999. The Campine Clays and Sands in northern Belgium: a depositional model related to sea level fluctuations. *Contributions to Tertiary and Quaternary Geology*, 36 (1-4), pp. 59-72.

Kasse, K., 1988. Early-Pleistocene tidal and fluvial environments in the southern Netherlands and northern Belgium. PhD thesis. Free University Press, Amsterdam, 190 pp.

Towards a site-characteristic database for the Belgian permanent seismic network

Martin ZECKRA¹, Koen VAN NOTEN¹, Thomas LECOCQ¹

¹ Royal Observatory of Belgium, Uccle, Belgium (martin.zeckra@seismology.be)

The Belgian network of seismological stations is a permanently recording scientific entity. It allows the monitoring of seismic activity from tectonic and non-tectonic origin within the political boundaries of the country and neighboring foreign regions. The network consists of 25 sensor locations, from which 12 are instrumented with broadband sensors and 13 are recording with short-period instruments. In addition, three broadband sensors are managed in Luxembourg. As the Belgian contribution to the international EPOS initiative, the ROB is gradually renewing those sensors with outdated equipment in favor to borehole instruments. This enhances the inherent data quality by increasing the signal-to-noise ratio, as the distance between sensor and anthropogenic noise sources is enlarged, and site-effects of the shallow surface are suppressed, enabling the recording of the original wavefield close to the bedrock. Further it is planned to make their data publicly available through the ORFEUS EIDA waveform data access node¹.

ORFEUS also provides the STATION BOOK portal². It serves as a platform that distributes additional station meta information with large focus on site-specific subsurface parameters that are usually not allocated in seismological standard inventory file formats. For each station in the Belgian seismic network, site characteristics of the subsurface are not yet available. The availability of such knowledge for external users of the permanent recordings is crucial for an adequate processing and separation of instrument and site effects from the seismic source and path signal. Especially, the substantial North to South contrast in subsurface geology in Belgium (see Figure 1) strongly influences the feasibility to obtain seismological recordings. The stations in the south are located in the vicinity of the seismically most active regions and placed in areas where the metamorphic basement rock is situated close to the surface. That leads to high average seismic velocities and fairly isotropic radiation of seismic waves with a low attenuation that barely alters the frequency content of the seismic signals. The propagation abilities of seismic waves in the northern part of Belgium are influenced by the bedrock depth and the orientation of the Brabant Massif that shows a highly anisotropic characteristic. Especially the thickness of the sedimentary cover introduces scattering of the wavefield and thus a loss of energy of the wavefield over short distances. In addition, the damping in sediments is frequency dependent. First, this complicates the extraction of original source parameters of the seismic source. Second, shifting the energy amplitudes into certain bands of frequencies has major implications for engineering and safety building codes.

Main site-effect parameters to resolve for each site are shear-wave velocity of the first 30 m (v_{s30}), fundamental frequency (f_0), groundwater- and bedrock depth, and, at best, a local, shallow 1D velocity model. In our site characterization, we use a set of 24 SmartSolo three-component geophone sensors (5 Hz, also known as “nodes”), that enable easy deployment for short term array installations using ambient noise sources. These low-cost instruments in an autarkic casing, that includes GPS, digitizer and internal storage, surpass conventional seismic sensors in reduced weight and size. A variety of well-established processing methods is then further applied on the passive seismic array recordings, e.g., frequency-wavenumber analysis, H/V ratio, MSPAC. External geological information from geological maps and the national borehole database provide boundary parameters to restrain the

1 <http://orfeus-eu.org/data/eida/>

2 <https://orfeus-eu.org/stationbook/networks/BE/1980/>

velocity inversion into a realistic subsurface 1D velocity model. During the array measurement processing, signals from active sources, such as quarry blasts, are included to further narrow expected velocity values.

The use of the industrial SmartSolo nodes in a scientific context is a novelty. Thus, special attention was given to the quality of the recorded data. Besides different polarity conventions of these industrial sensors, their overall sensitivity is astonishing such that they could record events of large epicentral distance far below their natural frequency. Also, the transfer function given by the manufacturer is suitable to reconstitute the signals comparable to standard instruments, presenting them as appropriate tools for seismological surveys.

Due to the subsurface variability of all seismological sensor sites throughout Belgium, this study will contribute steadily to a potent database of lithological site parametrization. That results in a handy reference for under-investigated study areas in various fields of geosciences. Especially, the quality of future hazard and risk modeling will be enhanced strongly through such a not yet existing regionally adapted input.

Figure

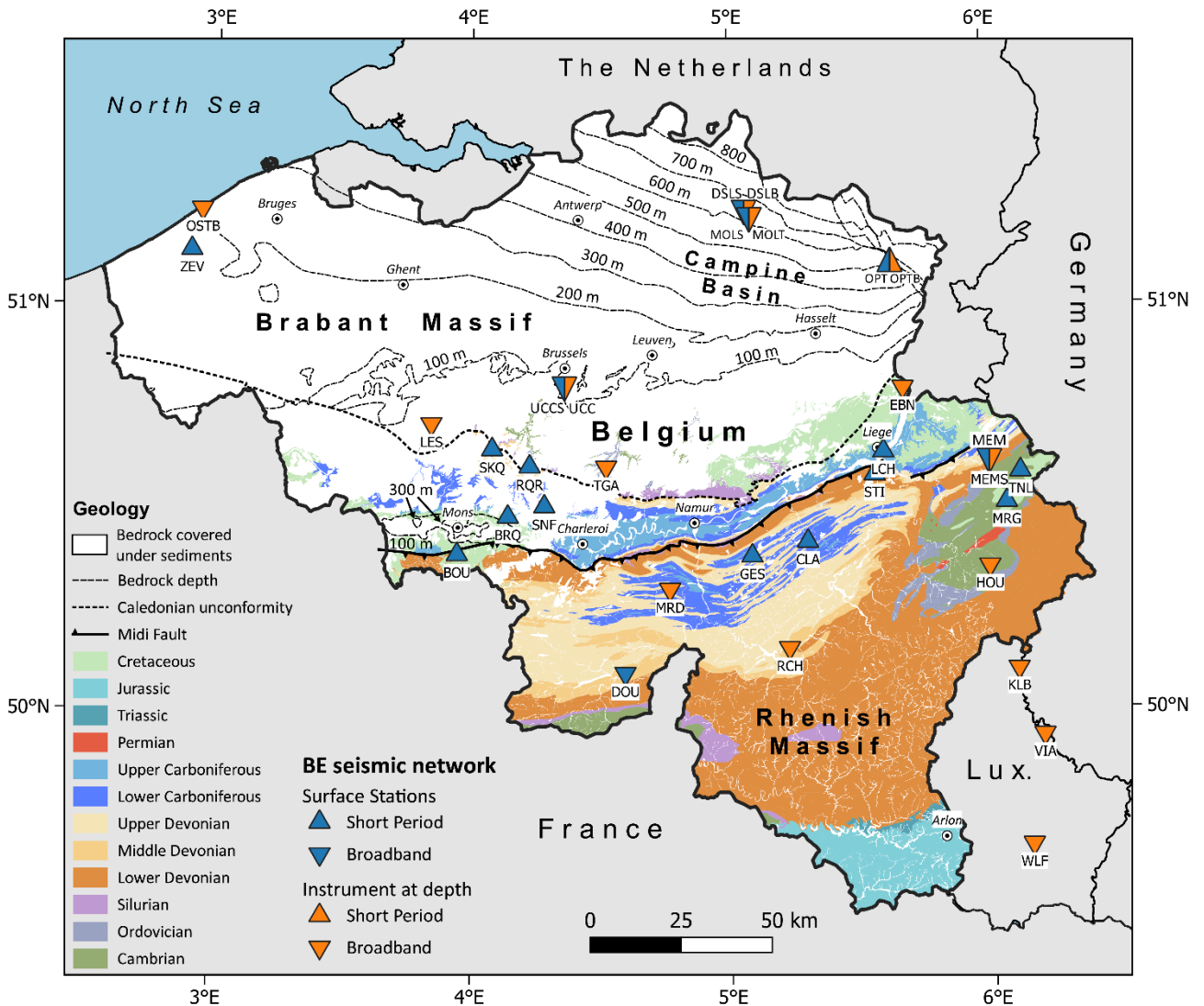
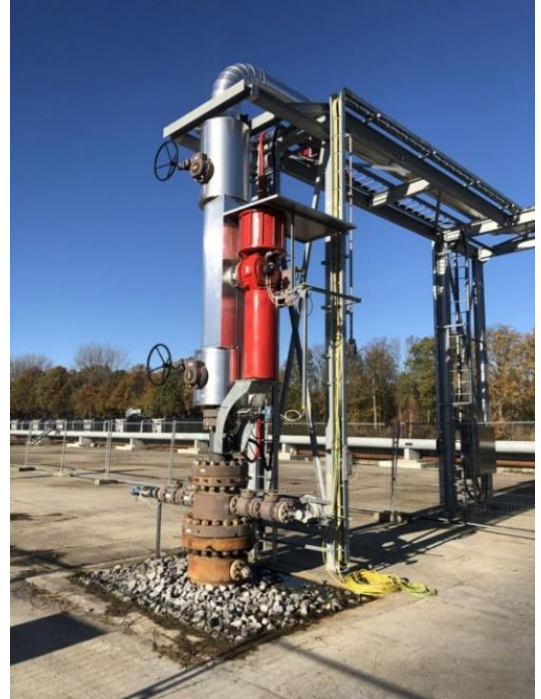


Figure 1: Overview of the Belgian permanent seismic network in relation to the Belgian subsurface geology. Primary purpose of this study is to provide site characteristic parameters for each of these stations.

Session 12- Geo-energy

The subsurface of our planet Earth has provided fossil fuels as the main energy source for many decades. In the fight against climate change, fossil fuel consumption must decrease, but our planet's subsurface remains an important source of solutions. Geothermal energy, both shallow and deep, plays a substantial role in the sustainable energy mix of the future as it is a local, sustainable, reliable, and affordable source of energy below our feet. Underground energy storage can be used to accommodate the seasonal difference in heat supply and demand. CO₂ Capture and Storage, CCS) consist in capturing the CO₂ contained in the emissions of industrial plants, then injecting it deep underground. This technology can play an important role in the transition from fossil to sustainable energy sources and reduce unavoidable process emissions. From these various applications linked to the use of the (deep) subsurface, synergies can emerge but also conflicts of use; to avoid the latter while offering realistic, safe, economical and sustainable solutions, a new level of subsoil planning and assessment methods is needed.



[12.1. Geo-energy: Opportunities and Constraints for Subsurface Uses](#)

Conveners:

Virginie Harcouët-Menou (VITO), Olivier Kaufmann (UMons), David Lagrou (VITO)

This session will cover the specific themes (not exclusive): geothermal energy (shallow, deep and ultra-deep), energy storage, CO₂-storage, geological economics, synergies and conflicts of use.

Delineation of inferred high-transmissivity zones in the Dinantian geothermal reservoir of Hainaut (SW Belgium)

Nicolas DUPONT ¹, Olivier KAUFMANN ², Jean-Marc BAELE ³

1. University of Mons, Faculty of Engineering, Geology and Applied Geology, Place du Parc, 20, 7000 Mons, Belgium (nicolas.dupont@umons.ac.be)

2. University of Mons, Faculty of Engineering, Geology and Applied Geology, Place du Parc, 20, 7000 Mons, Belgium (olivier.kaufmann@umons.ac.be)

3. University of Mons, Faculty of Engineering, Geology and Applied Geology, Place du Parc, 20, 7000 Mons, Belgium (jean-marc-baele@umons.ac.be)

The Dinantian aquifer is currently the only reservoir used for deep geothermal applications in Belgium, especially in the Hainaut (SW Belgium). In this area, 3 deep wells drilled in the 1970-80s produce hot water (typically 67-73°C @ 100-150 m³/h) from breccia and/or dissolution levels located in the upper part of the reservoir. Despite the presumed high potential of this reservoir, the development of the resource is currently limited by significant geological uncertainties. These uncertainties are mainly related to the lack of knowledge about its structure and the heterogeneity of its properties (e.g., temperature and transmissivity). To mitigate these uncertainties, several sources of data were considered, especially 2D seismic imaging and mining maps from the coal industry.

The integrated results of the Mons2012 and Hainaut2019 seismic surveys provided a crucial updated imaging of the Palaeozoic basement and its structures. Among these, an E-W synsedimentary structure including an *en-echelon* margin seems to accommodate most of the difference in sedimentary thickness between the northern part (cf. Saint-Ghislain) and the southern part (cf. Jeumont-Marpent) of the reservoir.

The analysis of many coal mining maps contributed to highlight and to map some features linked to the dissolution and/or the migration of evaporites into the underlying Dinantian reservoir. Among these features, domes and centroclines including radial structures have been considered as linked to diapirs with various states of dissolution. Based on these results, the northern part of the Dinantian reservoir has been subdivided into several categories, in agreement with deep borehole data. These categories were defined according to the intensity of the deformations identified in the coal deposit, the presence of sinkholes and indications of halokinesis.

Finally, some characteristics of the Dinantian reservoir were clarified. Its geometry has been modeled based on different hypotheses supported by deep borehole data, the structural framework derived from the interpretation of the seismic sections and the characterization of the deformation in the overlying coal deposit. The spatial distribution of high-transmissivity zones related to dissolved horizons such as breccias was mapped based on the degree of dissolution of the evaporites as suggested by both the structure of the coal measures and the spatial distribution of sinkholes.

Acknowledgments

This research is carried out under the MORE-GEO and the DESIGNATE projects. MORE-GEO is supported by ERDF funds (Walloon Region + UE). DESIGNATE receives

funding from the BELSPO BRAIN-be 2.0 research programme under contract nr B2/191/P1/DESIGNATE.

Figure

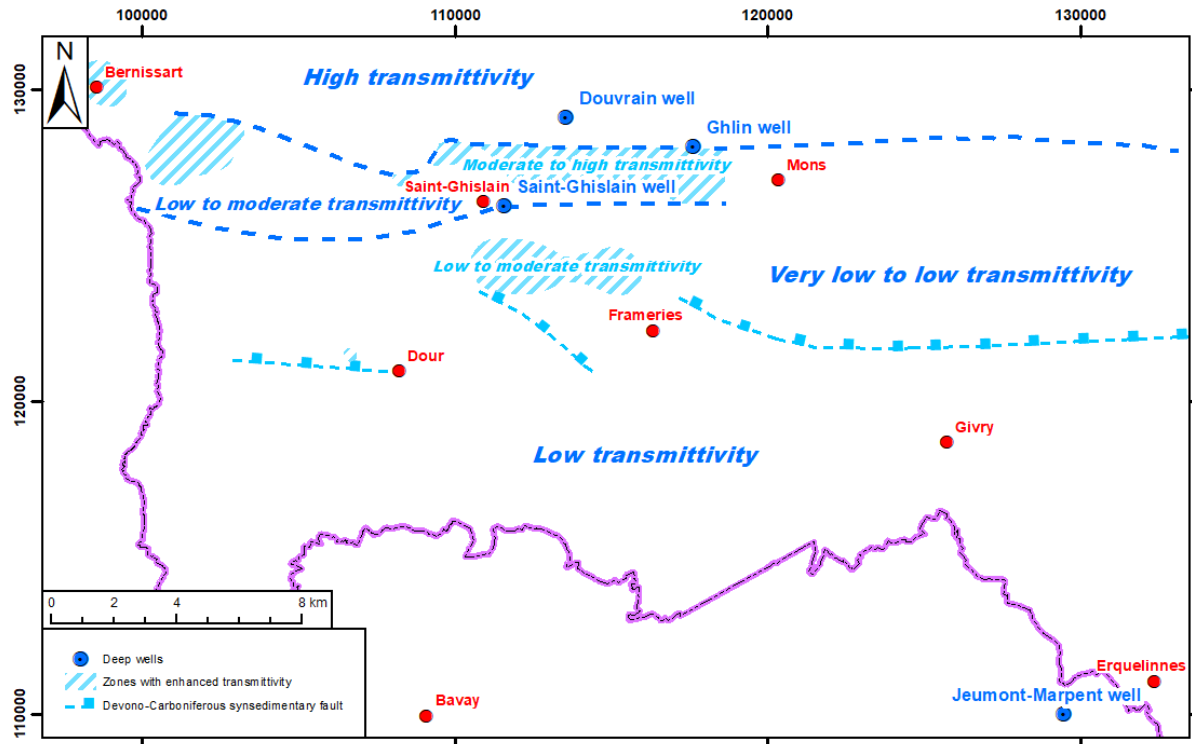


Figure 1. Delineation of inferred high-transmittivity zones in the Dinantian geothermal reservoir of Hainaut (SW Belgium).

How geomanifestations can help in policy challenges

Helga FERKET 1, Johanna VAN DAELE 1

¹ *Vlaams Planbureau voor Omgeving (VPO), Departement Omgeving van de Vlaamse Overheid, Koning Albert II-laan 20, bus 8, 1000 Brussel, Belgium (helga.ferket@vlaanderen.be)*

Our subsurface will increasingly play a vital role in both economical and societal aspects of everyday life in the future. Early prognosis studies show that Flanders could achieve about half of the renewable energy targets from green heat. This underlines the need to explore in more detail the potential for geothermal energy and subsurface heat storage. In the deeper subsurface of Flanders, good geological reservoirs suitable for various applications are only found in a relatively small sedimentary basin. This forces policymakers to develop a long-term vision in order to make smart and sustainable regulatory choices. On the one hand, georesources should be exploited efficiently and safely and, on the other hand, the fundamental functions of the subsurface should be safeguarded for the future. The biggest barrier that impedes data-driven decision-making relates to the fact that data on the subsurface is limited and often sparsely distributed. Conventional techniques to investigate the deep subsurface (e.g. boreholes, seismic surveys, ...) are expensive and strongly linked to actual projects. This selective data collection challenges policymakers in building a solid vision, while lacking insights on both the real potential for subsurface applications and on geohazards that may interfere with certain developments.

In the context of the European GeoConnect³d project, VPO focused on geological anomalies —“geomanifestations”— in a wide cross-border area covering parts of Belgium, the Netherlands, Germany, France and Luxembourg, looking to data that might reveal geological processes and give insight in aspects that are hard to unravel in our local Flemish setting. Two policy challenges and how geomanifestations bring up guidance to them are discussed in this contribution: i) predicting geothermal potential by identifying “sweet spots” and ii) understanding the migration of gases through the subsurface.

When comparing the distribution of thermal anomalies in the whole study area to a topographic map, a strong relationship between these two appears, showing high concentrations in the Upper Rhine Graben, the Roer Valley Graben, and the Rhine and Mosel river valleys. Not surprisingly, this points to the key role of a strong hydraulic gradient in forcing topography-driven flow. The height difference between the highest topography and the base of the sediments determines the deepest groundwater circulation cells. For the Upper Rhine Graben, the east shoulder formed by the Black Forest is more elevated than the west shoulder formed by the Vosges, resulting in asymmetric flow cells with the strongest thermal anomalies at the west side of the graben (Stober & Bucher, 2015). Combined with high transmissivities along fracture networks, an efficient upward flow of hot water is created in the area between Soultz (France) and Landau (Germany), where a series of successful deep geothermal projects has been developed over the past decades.

At a more local scale, linear trends in thermal anomalies can often be recognized, such as in Wiesbaden and Aachen (Germany). Again, topography-driven flow seems to be a motor for transport of large volumes of fluid through permeable layers in Variscan thrust sheets. In the case of Wiesbaden, the thermal anomaly weakens in the direction of a crosscutting graben-related fault (Mittelbach & Siebert, 2014). In the case of Aachen, both thermal and geochemical anomalies increase in the direction of a crosscutting graben-related fault (Hersch, 2000). Intersection of fault sets seems to be interesting in creating high permeability areas, but also deep-seated faults can either bring upflow of warmer water or downflow of

cooler water. Understanding the data and local hydrogeology is needed to interpret the findings and use them for predictions. The Aachen example shows the presence of 50-70 °C springs at the Variscan front faults, at and close to the intersection with a Roer Valley Graben fault. Following the latter fault to the north leads to another thermal anomaly in Heerlen (the Netherlands). During coal mining, a breakthrough of 50 °C hot saline water was encountered at a depth of 250 m (Kimpe, 1963), in an area otherwise not regarded as showing geothermal potential. Again, the interplay between topography-driven flow towards a fractured Variscan anticline and a crosscutting deep-seated fault bringing up the anomaly determines the location of this geomanifestation. Going away from this graben fault to the west, a series of weak thermal anomalies (e.g. surface springs at a constant 14 °C) was found in the past. Making use of the key elements from this geothermal play, several locations of high prospective interest can be identified to the east. Without the mining activity, which revealed the presence of this thermal anomaly by accident, this sweet spot of high geothermal potential would probably have remained hidden. Where the warm upflow along the fault crosses an overlying aquifer, the signature gets easily diluted and weak anomalies don't attract attention. Therefore, it could pay off to follow anomalies through the aquifer and drill deeper at the location of a suspected fault.

Secondly, looking into the CO₂ and He data in the study area, mainly reported in the volcanic Eifel area, different migration mechanisms could be identified at varying scales. On the regional scale, an obvious correlation with the Quaternary volcanic activity pops up. At a smaller scale, linear trends indicate the role of faults in bringing up the mantle gases. Zooming in to the local level reveals the strong correlation of gas seepage with groundwater discharge zones (Weyer et al., 2012). All three mechanisms, volcanic sourced upflow, preferential migration along faults and migration of dissolved gases through aquifers play a role and can be studied in the natural analogue of the Eifel.

The acquired insights, although gathered in a remote study area, give support for various policy challenges that Flanders is confronted with. Sharing geomanifestations and lessons learnt for policy between countries also helps reflecting on subsurface management.

This project has received funding from the European Union's Horizon 2020 research and innovation programme under grant agreement No 731166.

References

- Herch, A., 2000. The thermal springs of Aachen/Germany – what Charlemagne didn't know. *Environmental Geology* 39, 437-447.
- Kimpe, W.F.M., 1963. Geochimie des eaux dans le houiller du Limbourg (Pays-Bas). *Verhandelingen van het Koninklijk Nederlands Geologisch Mijnbouwkundig Genootschap* 21, 25-46.
- Mittelbach, G., Siebert, S., 2014. Gutachten zur Festsetzung eines Heilquellenschutzgebietes für die Heilquellen (Große und Kleine Adlerquelle, Schützenhofquelle, Kochbrunnen, Salmquelle und Faulbrunnen) von Wiesbaden, Stadt Wiesbaden (WSG-ID 414-005), Wiesbaden, pp. 1-52.
- Stober, I. and Bucher, K., 2015. Hydraulic and hydrochemical properties of deep sedimentary reservoirs of the Upper Rhine Graben, Europe. *Geofluids* 15, p. 464–482.
- Weyer, U., May, F. and Ellis, J., 2012. Association between discharge areas of groundwater and volcanic CO₂. Third EAGE CO₂ Geological Storage Workshop, Edinburgh, United Kingdom, 26 - 27 March 2012, poster.

Deep Geothermal Energy Extraction, a Review on Environmental Hotspots with Focus on Geo-technical Site Conditions

Spiros GKOUSIS¹, Tine COMPERNOLLE^{1,2}, Kris WELKENHUYSEN²

*1. Department of Engineering Management, University of Antwerp, Antwerp, Belgium
(Spiros.Gousis@uantwerpen.be), (Tine.Compernelle@uantwerpen.be)*

2. Royal Belgian Institute of Natural Sciences – Geological Survey of Belgium, Jennerstraat 13, 1000 Brussels, Belgium (kris.welkenhuysen@naturalsciences.be)

Knowledge on the environmental impacts of geothermal energy is of major importance to understand the role this technology could play in the transition towards sustainable energy systems. Life cycle analysis (LCA) methodology is a widely used tool for assessing the environmental impacts of products and systems, which has been implemented numerous times on geothermal systems. Previous reviews on geothermal LCA studies identify large variability on the reported environmental impacts. In this work we aim to provide a more in-depth analysis to explain the variability across the different LCAs. We review 28 LCA studies on geothermal energy published between 2005 and 2020, following a four step reviewing sequence; in step 1 we identify the LCA methodological choices and the plant geo-technical characteristics, in step 2 we identify the LCA results and the LCI inputs, in step 3 we perform contribution analysis based on the reported results and in step 4 we investigate the sensitivity and scenario analysis performed in the studies. If the data is available we triangularly evaluate the reported impacts considering a) the plants' geo-technical characteristics, b) the hotspot analyses results and c) the Life cycle inventory (LCI) inputs. We focus our analysis on the six most frequently assessed impact indicators (GWP, AP, HTP, FETP, CED, ADP)* and distinguish between the different energy conversion technologies used for geothermal energy exploitation. This way we aim to provide a more transparent picture on the variability of environmental impacts across the LCAs by focusing on the environmental hotspots and on the cause-effect relationships between geo-technical parameters and the environmental impacts. We also aim for drawing LCA guidelines for future LCA studies on geothermal systems and proposing methods for impact mitigation.

The variability on the LCA results is caused by differences on the choices of the LCA practitioners, on the energy conversion technologies used, on geological parameters and on plant design parameters. Most studies focus on the GWP and AP impacts, while information for the rest of the impacts is much more limited. For flash and dry steam power plants the direct emissions of non-condensable gases (NCGs) emerging can cause high GWP, AP, FETP and HTP impacts depending on the geofluid's composition. The CED and ADP impacts are dominated by the steel and diesel consumption during the development of the wells. Thus differences on the geo-technical parameters determining the power output and the total material and energy consumption cause the variability on the reported results. Direct emissions of NCGs do not emerge in plants utilizing binary technology. In these plants the development of the wells dominates the impacts and this phenomenon is more intense when EGS-binary plants are investigated due to the large depth drilled. Also the production of the working fluid used in the ORC and its annual leakage can highly affect the GWP impact in these plants depending on the type of working fluid used. In heating plants high amounts of grid-electricity are needed for the plant operation as no power is produced. Therefore differences in the fossil-fuel-intensity of the electricity mix supplying the plant can result in large variability. The choice of the LCA practitioner to include or not the heat

distribution network in the boundaries of the system also affects the results, while a significant portion of the impacts is caused during the development of the wells. Combined heat and power plants using flash or binary technology present similar results. However the co-production of heat and power is expected to lead to some benefits.

A direct correlation between the GHGs and the NH₃/H₂S direct emissions with the GWP and AC impacts, respectively, is observed for flash and dry steam power plants. Direct emissions are determined by the geofluid composition which highly varies between different reservoirs. For mitigating these impacts the installation of abatement systems shall be considered, while the identification of the geofluid composition and of the natural emissions emerging prior to the plant development is suggested for estimating the actual anthropogenic emissions. For plants utilizing binary technology and heating plants it is observed that higher capacity generally leads to lower GWP and AP impacts per functional unit. The capacity is a product function of the temperature and production flow. Similar observation can be extracted for the temperature while this is not the case for the flow. No clear correlation can be seen between the impacts and the depth. This is because larger depths lead –on the one hand– to higher impacts because of higher material and energy consumption which are compensated –on the other hand– to the increase on the fluid temperature and flow. For mitigating impacts caused during the construction phase the use of renewable energy sources for supplying the machinery used is suggested, while proper fluid re-injection should be designed for keeping the capacity constant during the operation. Also for binary plants the working fluid shall be selected such that its GWP impact is low, while for heating plants the installation of a small ORC unit shall be considered if the conditions are appropriate for meeting the pumping needs of the plant. The reviewed studies show that geothermal energy exploitation can lead to significant environmental benefits compared to fossil sources, as most of the times the impacts caused by geothermal plants are in the range of other renewable sources.

Further research is needed on deep geothermal energy exploitation to better understand its environmental impacts. A significant portion of the impacts is caused during the operation of the plants regardless of the technology used (direct emissions, electricity consumption, working fluid losses, make-up well drilling). All of the LCA studies reviewed are static LCAs. Thus a dynamic LCA framework considering the time aspect is needed for better estimations of the environmental impacts. Also consequential LCAs on geothermal energy plants need to be conducted in order to assess how the global environmental impacts may change by the wider implementation of geothermal energy. In addition, future LCA studies shall also focus on environmental impacts other than the GWP as information regarding them is limited. Finally the sustainability of geothermal investments is to be further explored by investigating the social impacts of geothermal development and comparing them to other energy sources but also the financial aspect of such investments.

Acknowledgments

This research is carried out under the DESIGNATE project, which receives funding from the BELSPO BRAIN-be 2.0 research program under contract nr B2/191/P1/DESIGNATE.

* *GWP: Global Warming Potential, AP: Acidification Potential, HTP: Human Toxicity Potential, FETP: Freshwater EcoToxicity Potential, CED: Cumulative Energy Demand, ADP: Abiotic resources Depletion Potential*

Influence of the heat network rollout time on the risk and profitability of a deep geothermal plant

Bruno MEYVIS¹, Virginie HARCOUET-MENOU², Kris WELKENHUYSEN¹

1. *Royal Belgian Institute of Natural Sciences – Geological Survey of Belgium, Jennerstraat 13, 1000 Brussels, Belgium (bruno.meyvis@naturalsciences.be)*

2. *VITO*

The development of geothermal energy is below the European National Renewable Energy Action Plans' anticipated trajectory. For deep geothermal energy projects in particular, multiple sources of uncertainty in combination with high upfront investment costs result in a major investment risk, hampering the mobilization of required capital (Compernelle et al., 2019). The uncertainty sources include market uncertainty, uncertainty regarding new technologies and uncertainty inherent to working with subsurface data.

The objectives of the DESIGNATE project for deep geothermal systems in Belgium, including applications in abandoned mines are two folds. First, to create tools for integrated forecasts under uncertainty and second to set-up a methodological framework for territorial Life Cycle Analysis (LCA) considering surface and subsurface impacts. To do so, analytical reservoir models will be developed to assess the effect of uncertainties about geological data and concepts on the performance and impact of the geothermal applications. These will be coupled with a techno-economic analysis in combination with a territorial, environmental life cycle analysis. To evaluate the impact of different policy measures, the techno-economic analysis consists of a Monte Carlo simulation model that integrates both market and geological uncertainties and a project developers' option to wait or abandon the geothermal project development at different steps in the development of the project (Welkenhuysen et al., this conference).

As a preliminary step, the influence of the rollout time of a heat network on the risk and on the profitability is investigated. At the start often only a part of the district heating network is in place at the time of commissioning and the geothermal plant operates at much lower capacity. Part of the capacity is foreseen for district heating networks linked to residential districts expected to be built or renovated in the near future. In this research, the change in income of a project considering a stepwise rollout of a district heating network compared to a full load from the start, in combination with a reduced maximum capacity of the geothermal plant compared to the expected output is calculated. This is done with a simplified spreadsheet techno-economic model, limiting variability to the rollout scenarios. For the calculation, data provided by the project developer HITA of the Turnhout NW geothermal project is used. In the next section the four cases used to evaluate the risk and profitability linked to the changes in the rollout time of a heat network are described.

In the first case, the base case, the production plant is assumed to work at full capacity once the construction of the geothermal plant is achieved. Full capacity means that the production plant will be working at 100% during the heating season. Additional production for cooling or for heat storage in summertime are not taken into account. The second case considers that the maximum production capacity is 20% lower than in the first case due to lower-than-expected reservoir temperature or flow rate. In the third case, the full capacity is equal to the one of the base case but will be reached in three steps, simulating a growing demand by adding new district heating networks. The demand is expressed as a percentage of

the expected maximum production capacity of the geothermal plant. At the start of production, the geothermal plant runs at 50%. After 5 years this is increased to 75% and after 10 years full capacity is reached. The fourth and last case is similar to the third case, with a stepwise increase of the demand, but the maximum production capacity is, as in second case, 20% lower. Because the demand is lower than the total capacity in the first 10 years, the production plant will however be able to supply the required energy. Only after 10 years when the demand rises to the expected maximum production capacity, only 80% of the required energy can be delivered without additional investments. As such, the income of the project will be the same the first 10 years compared to the third case.

In a best-case scenario, demand and rollout of a district heating network will be fast and the production plant will run at full capacity during the heating season from the start (case 1). This is however unlikely and assuming this to be the base case will result in many projects not reaching predetermined targets, as the income of the project will be lower during the first years of production. In this respect, the third case or a similar scenario is a better option to use as a base case. This will put more stringent conditions on the expected output parameters of the production well to ensure an economic viable project, and hence provide a more realistic outlook. When using case 3 as the base case this also has the complementary benefit of reducing the risk related to the maximum production capacity. If the real maximum production capacity is lower than expected, the reduction of income will be lower than the decrease in the maximum production capacity. In other words, a reduction of 20% of the maximum production capacity will not lead to a reduction of 20% of the income, but will be between 0 and 20%, depending on the interest rate and on the time frame to reach full capacity.

Acknowledgments

This research is carried out under the DESIGNATE project, which receives funding from the BELSPO BRAIN-be 2.0 research programme under contract nr B2/191/P1/DESIGNATE. HITA kindly provided input for the development for this case study.

References

- Compernelle, T., Welkenhuysen, K., Petitclerc, E., Maes, D. & Piessens, K., 2019. The impact of policy measures on geothermal energy investments. *Energy Economics*, 84, 104524. <https://doi.org/10.1016/j.eneco.2019.104524>
- Welkenhuysen, K., Compernelle, T., Kaufmann, O., Laenen, B., Meyvis, B., Piessens, K., Gousis, S., Dupont, N., Harcouet-Menou, V. & Pogacnik, J., this conference. Decision support under uncertainty for geothermal applications: case selection and concept development.

New geological information of the Cambrian basement obtained from geothermal exploration projects in Brussels and Walloon- and Flemish-Brabant

Estelle PETITCLERC 1, Pabitra GURUNG 1, Pierre GERARD 2, Marc VAN CAMP 3, Jeroen VAN DER VEKEN 4, Gust VAN LYSEBETTEN 4, Koen VAN NOTEN 5, Kristine WALRAEVEN 3

1. *Geological Survey of Belgium, Royal Belgian Institute of Natural Sciences, Brussels, Belgium (pgurung@naturalsciences.be, epetitclerc@naturalsciences.be)*
2. *Université Libre de Bruxelles, Brussels, Belgium (gerard.pierre@ulb.ac.be)*
3. *Laboratory for Applied Geology and Hydrogeology, Ghent University, Ghent, Belgium (marc.vancamp@ugent.be, kristine.walraevens@ugent.be)*
4. *Belgian Building Research Institute, Limelette, Belgium (jeroen.van.der.veken@bbri.be, gust.van.lysebetten@bbri.be)*
5. *Royal Observatory of Belgium, Uccle, Belgium (koen.vannoten@seismology.be)*

During the past years, research has been conducted on shallow geothermal energy (SGE) with projects such as SmartGeotherm (VLAIO) and Brugeo (EFRD). Although the Belgian SGE market is steadily growing (Lagrou et al., 2019), some main barriers such as better knowledge of the underground and economic potential, investment costs, financial support, policy measures and public awareness must be tackled to further develop the market. Most of the existing geothermal systems are traditionally installed in the soft, sedimentary Mesozoic-Cenozoic cover, however, the exploration drilling at Anderlecht (2017) and the operational open geothermal system at Gare Maritime (2020) have demonstrated the higher potential and efficiency of the Cambrian core of the Brabant Massif. Although this has also led to more feasibility studies for the exploitation of the Cambrian basement during the past years, more research must be conducted if extensive use is envisaged to significantly contribute the renewable share of the total energy production and to enhance the geothermal sector development.

With the GeoCamb (Belspo) project, not only the geothermal potential of the Cambrian bedrock will be evaluated and demonstrated, the energy demand of specific, public buildings will be incorporated to maximise the efficiency of the system. Therefore, geological, hydrogeological and geophysical exploration will be performed. To have a full understanding of the sustainability of geothermal installations, the economic and environmental impacts will also be investigated.

Eight different sites with a total of 22 destructive boreholes (up to 252 m below ground level) have been analysed. 6 sites are located in the Brussels Capital Region and one in both Walloon- and Flemish-Brabant. In this article, the lithology, mineralogy, geophysical and thermal characteristics of the encountered Cambrian basement and its weathered/eroded top will be presented. Before encountering siltstones and (quartzitic) sandstones with some quartz-rich layers of the Tubize Formation (Verniers et al., 2001), a few meters up to more than 20 meters of weathered layer is observed in almost all sites. This weathering zone consists of clay, silt, sand, weathered siltstone and sandstone, (large) quartz veins, faults and cavities which can have serious implications on the design, budget and risks of exploration drillings. To have a better understanding of the Cambrian basement and to de-risk geothermal feasibility studies in the future, not only the top of the basement should be investigated but

also the thickness and lithology of the weathered zone, which is not considered as a separate layer in existing geological models (Brugeo, DOV).

References

Lagrou, D., Petitclerc, E., Hoes, H., Dupont, N. & Laenen, B., 2019. Geothermal energy use, country update for Belgium. European Geothermal Congress 2019, 7p.

Verniers, J., Herbosch, A., Vanguestaine, M., Geukens, F., Delcambre, B., Pingot, J.-L., Belanger, I., Hennebert, M., Debacker, T.N., Sintubin, M. & De Vos, W., 2001. Cambrian Ordovician-Silurian lithostratigraphic units (Belgium). In Bultynck, P. & Dejonghe, L. (eds), Guide to a revised lithostratigraphic scale of Belgium. *Geologica Belgica*, 4, 5–38.

Early Carboniferous limestones of southern and central Britain: preliminary assessment of deep geothermal prospectivity

Tim PHARAOH¹, Darren JONES², Tim KEARSEY², Andrew NEWELL³, Corinna ABESSER³, Tom RANDES², Ashley PATTON⁴ and Rhian KENDALL⁴

1. British Geological Survey, Keyworth, UK (tcp@bgs.ac.uk)

2. British Geological Survey, Edinburgh, UK (darjones, timk1, tar@bgs.ac.uk)

3. British Geological Survey, Wallingford, UK (ajn, cabe@bgs.ac.uk)

4. British Geological Survey, Cardiff, UK (ashleyp, rhnd1@bgs.ac.uk)

In Britain, thick limestones of early Carboniferous (Mississippian: 359-323 Ma) age are present in two provinces to south and north of the Wales-Anglo-Brabant landmass (Holliday et al., 1986). In the southern province, early Carboniferous limestones (ECL) were deposited upon a southward-deepening shelf, laterally continuous from Ireland to the Rhineland. They now occupy a number of discrete minibasins as a consequence of Variscan orogenic thrusting and significant post-Carboniferous erosion. In the northern province, local tectonic controls led to the development of a mosaic of deep-water basins, ramps and platforms in response to Mississippian extensional stress. The interaction with glacioeustatic sea-level change led to the development of more complex carbonate depositional systems in these northern basins.

Given favourable conditions of palaeokarst development and fracturing, hydraulic transmissivity could be sufficient to allow development of the ECL as a geothermal resource (Narayan et al., 2018), as recently demonstrated in Belgium and The Netherlands. Deep geothermal prospectivity is controlled by a hierarchy of factors, operating on scales ranging from provincial (1000 – 100 km) down to outcrop (1000 – 10 m), reflecting processes operating on the lithospheric down to sub-basinal scale respectively (Pharaoh et al., 2021). On the scale of the individual prospect, these factors include the mode of carbonate deposition, particularly depth of water and angle of depositional slope, which are tectonically controlled; the history of synsedimentary exposure, erosion and karstification, strongly influenced by sea-level change; by the diagenetic history and subsequent basin evolution; by deformation, fracturing, dolomitisation and mineralisation during Variscan basin inversion; and by the post Carboniferous history of subsidence, uplift and karstification.

The contrasting impact of these various processes upon hydraulic transmissivity in the two provinces is reviewed, and a preliminary assessment of the geothermal prospectivity of each is presented. The most prospective areas for deep geothermal exploitation are considered to be basins, shelves and platforms lying at depths of 2 to 5 km below sea-level. Deepwater basins are considered less prospective because of the lack of thick limestones, except in the hangingwall at fault-bounded margins, where Waulsortian mud-mounds with good residual porosity and fault-zones with polyphase history are likely present (Pharaoh et al., 2021). Granite underpinned highs in Northern England, where ECL are typically at crop, and shallow basins of Carboniferous age lying on the Wales-Anglo-Brabant Massif, are considered less prospective in the deep geothermal context.

References

Holliday, D.W., 1986. Devonian and Carboniferous basins. In: Downing, R.A. & Gray, R.A. (eds.) Geothermal Energy – the Potential in the United Kingdom. British Geological Survey: 84-110.

Narayan, N., Gluyas, J. & Adams, C., 2018. Is the UK in Hot Water? *Geoscientist*, 28, 10-15.
<https://doi.org/10.1144/geosci2018-014>

Pharaoh, T.C., Jones, D., Kearsy, T., Newell, A., Abesser, C., Randles, T., Patton, A. & Kendall, R., 2021 (in press). Early Carboniferous limestones of southern and central Britain: characterisation and preliminary assessment of deep geothermal prospectivity. *Zeitschrift der Deutschen Gesellschaft für Geowissenschaften*.

Figure

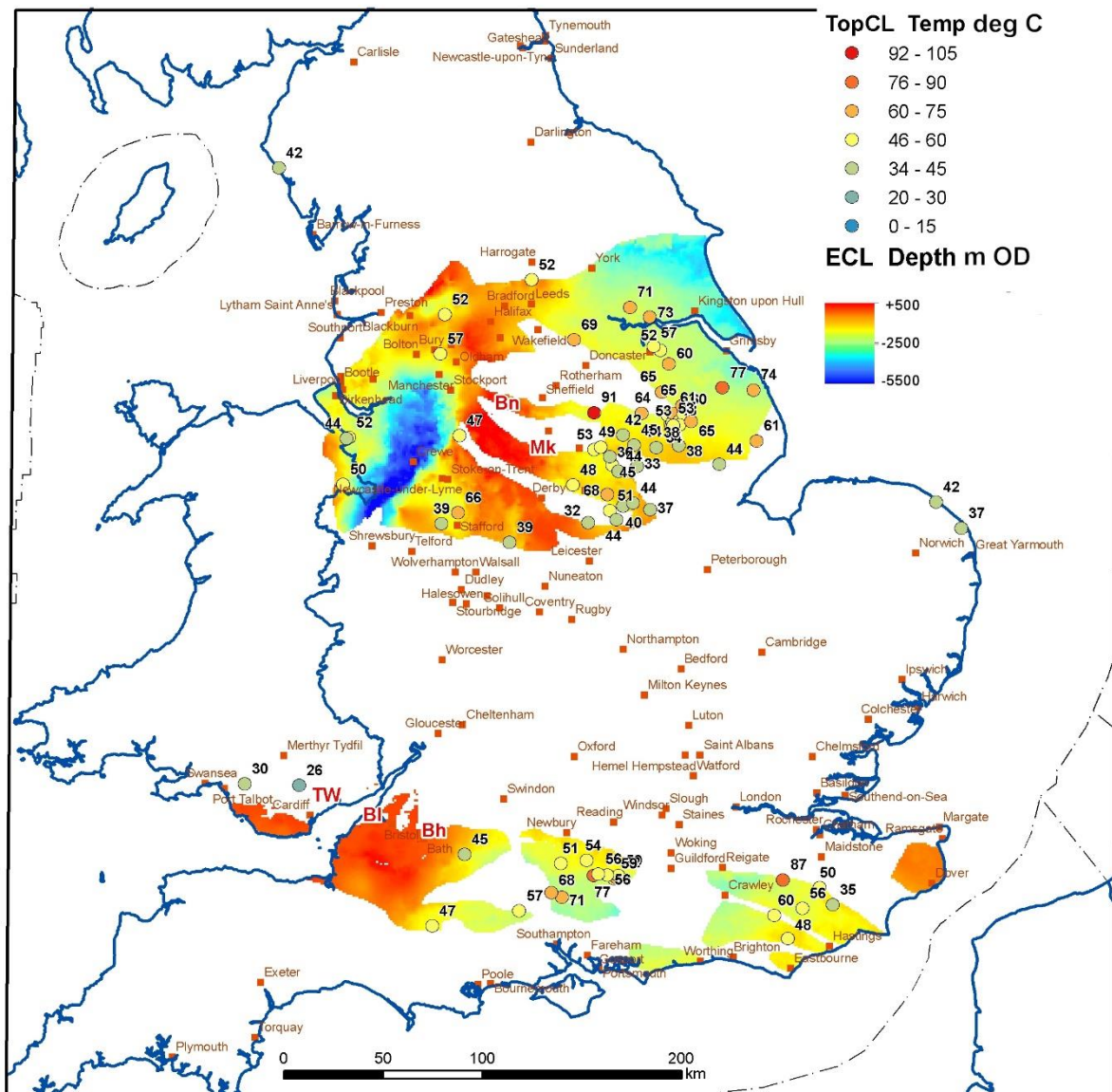


Figure Calculated temperature at the top of the ECL plotted on a map of depth relative to mean sea-level (OD, Ordnance Datum) in southern Britain.

Fractured Lower Carboniferous carbonates of the Campine Basin (NE-Belgium) as potential geothermal reservoirs: age and origin of open carbonate veins

Rudy SWENNEN¹, Eva VAN DER VOET^{1, 2}, Wei WEI¹ and Philippe MUCHEZ¹

1. KU Leuven, Department of Earth & Environmental Sciences, Geology, Celestijnenlaan 200E, B-3001 Heverlee, Belgium (Rudy.Swennen@kuleuven.be; Eva.Vandervoet@kuleuven.be; Wei.Wei@kuleuven.be; Philippe.Muchez@kuleuven.be)
2. Vlaamse Instelling voor Technologisch Onderzoek (VITO NV), Boeretang 200, BE-2400, Mol, Belgium

Lower Carboniferous carbonates form an interesting target for deep geothermal energy in the Campine Basin (NE-Belgium), as recently demonstrated in the Balmatt (Mol) and Janssen Pharmaceutica (Beerse) projects. But also past projects, such as the underground gas storage site in Loenhout (Heibaart structure) and the Merksplas semi-doublet project testify of this potential. The limestones, however, are mostly non-porous and most fractures are cemented. Consequently, the open fracture network and the potential development of meteogene and/or hypogene karstification is important. We therefore studied the partially open veins of the Lower Carboniferous limestones in the Turnhout, Heibaart (DZH1) and Poederlee boreholes. First classical petrographic analysis and stable oxygen and carbon isotope analysis were performed. Subsequently clumped Δ_{47} isotope analysis and U/Pb age dating were conducted aiming to unravel the formation conditions of these veins as well as to reconstruct the geodynamic evolution of this sedimentary basin. These analyses revealed that the host rock limestones are recrystallized, and that the open carbonate vein cements often possess a similar depleted $\delta^{18}\text{O}_{\text{PDB}}$ signature as the host rock. The latter is interpreted in terms of vein cement precipitation in a rock-buffered system. The host rock $\delta^{13}\text{C}$ signature often displays a marine signature. In contrast, two carbon isotopic clusters can be differentiated in the veins. Veins with cleavage twins and characterized by slightly to moderately depleted $\delta^{13}\text{C}$ signature make up the first cluster. They reflect a mixture of marine carbon with carbon derived from organic matter. This group predominantly occurs in the open veins from the microbially dominated Poederlee and Heibaart buildups that are characterized by on-lapping organic-rich Namurian black shales. Most of these veins formed at temperatures varying between 110 and 130°C as deduced from clumped isotopes, indicating that they could have been formed during the late Carboniferous burial stage or after the Sudetic – Asturian deformation and uplift. The second cluster which displays host-rock buffered $\delta^{13}\text{C}$ signatures, groups veins that may, but often do not, contain cleavage twins. U/Pb age dating of some of these veins indicate a Cretaceous (late Aptian/early Albian) and/or Paleocene age while formation temperatures dominantly vary between 50 and 80°C based on clumped isotopes. This age dating confirms that for exploration and production for geothermal energy with respect to Lower Carboniferous carbonates in the Campine Basin (Belgium) one needs to take the Cretaceous – Paleocene tectonic stress field into account to predict which fractures might still be open.

Ranking CO₂ storage capacities and identifying their technical, economic and regulatory constraints: A review of methods and screening criteria

Alejandra TOVAR, Kris WELKENHUYSEN, Kris PIESENS

*Geological Survey of Belgium – Royal Belgian Institute of Natural Sciences, Brussels,
Belgium (atovar@naturalsciences.be)*

One of the greatest challenges of the last decades in the fight against climate change has been to achieve net-zero emissions by mid-century. According to the US EPA (2016), in 2014, global anthropogenic emissions of carbon dioxide (CO₂) accounted for ~64% of the greenhouse effect. Carbon dioxide capture and storage (CCS) plays an irreplaceable part as a mitigation technology that avoids CO₂ emissions at their source and bridges the transition into a non-carbon-based energy future. The International Energy Agency (IEA) estimates that the need to store CO₂ will grow from 40 Mt/y at present to more than 5000 Mt/y by 2050. Additionally, in the IEA's Sustainable Development Scenario, which aims for global net-zero CO₂ emissions from the energy sector by 2070, CCS needs to become a global industry supporting emissions reductions across the overall energy system.

CCS technologies essentially consist of capturing and compressing the CO₂ at the source and then transport it towards deep suitable rock formations where it is injected to be permanently stored. The key to successful and permanent CO₂ storage is the proper analysis and characterization of the reservoir and seal formation. Among the types of reservoir suitable for CO₂ storage are unmined coal beds, depleted oil and gas fields, EOR/EGR, saline aquifers, man-made caverns, and basaltic formations (IPCC, 2005).

The storage capacity of any of these reservoirs is the subsurface commodity whose quantities and properties are assessed when existing data is provided. Capacity estimations bring their own level of uncertainty and complexity according to the scale at which they are addressed and the nature of the geological conditions of the reservoir. This degree of uncertainty should be accounted for in every estimation (Bradshaw et al., 2007)

Resource classification systems (RCS) are frameworks that establish the principles and boundaries for each level of capacity assessment. By making use of these frameworks, it is possible to properly allocate the stage of development of a resource (United Nations, 2020). For every level of assessment, the principles of the estimation change and so do the scale and purpose. As the analysis moves forward, a prospective site develops and exhaustive information is acquired, initial estimations are adjusted, and uncertainty is likely to reduce. Additionally, different economic, technical, regulatory, environmental and societal factors are integrated into the assessment to bring the estimations under present conditions. For instance, if the storage capacity is to be matched with a CO₂ source, detailed simulations and analyses regarding injectivity, supply rate, potential routes and economic distances must be performed to achieve a realistic estimation. However, an assessment where the main goal is to merely quantify the space available to store CO₂ in a reservoir, does not consider the aforementioned limitations and will carry higher risk and uncertainty in its estimation (Bradshaw et al., 2007).

Even though resource classification systems provide a solid foundation for CCS projects, they do not provide the input parameters and analyses needed to reach every level of assessment. This is why storage capacity estimation methodologies go hand in hand with RCS given that the former can

give information related to the parameters and constraints considered in the estimation. No standard process has been proposed that can be followed from the starting level of a CO₂ storage capacity assessment until a fully developed carbon storage resource; that is, a CO₂ storage site ready to become fully operational. This paper aims to develop a methodology where the fundamental steps needed to go through every level of the resource classification systems are standardized. This methodology intends to serve as a general baseline that, regardless of the geological settings and techno-socio-economic conditions, can be adopted for any CCS assessment.

The proposed methodology is built by reviewing the available capacity estimation methods for every level of assessment and identifying social, technical and economic aspects that come into play as the resource is being developed. Considering that capacity estimation methodologies can vary their approach even for the same level of assessment, the rationales behind them are expected to be determined. Such rationales can be related to in-place policy restrictions, geographical economic behavior, or the nature of the parameters contemplated.

Additionally, PSS, an in-house developed tool that can assess CO₂ storage reservoirs at different levels, will be proposed within the methodology. This tool is a bottom-up geotechnical and economic forecasting simulator that can generate source-sink matching for CCS projects, where technical, economic, and geological uncertainties are handled through a Monte Carlo approach for limited foresight (Welkenhuysen et al., 2016).

Acknowledgments

This research is carried out under the LEILAC2 project, which receives funding from the European Union's Horizon 2020 research and innovation program under grant agreement number 884170. *The LEILAC2 consortium consists of: Calix Europe SARL, HeidelbergCement AG, Ingenieurbüro Kühlerbau Neustad GmbH (IKN), Centre for Research and Technology Hellas (CERTH), Bundesanstalt für Geowissenschaften und Rohstoffe (BGR), Politecnico di Milano (POLIMI), Geological Survey of Belgium (RBINS-GSB), ENGIE Laborelec, Port of Rotterdam, Calix Limited, CIMPOR-Indústria de Cimentos SA and Lhoist Recherche et Development SA.*

References

- Bradshaw, J., Bachu, S., Bonijoly, D., Burruss, R., Holloway, S., Christensen, N. P., & Mathiassen, O. M. (2007). CO₂ storage capacity estimation: Issues and development of standards. *International Journal of Greenhouse Gas Control*, 1(1), 62–68. [https://doi.org/10.1016/S1750-5836\(07\)00027-8](https://doi.org/10.1016/S1750-5836(07)00027-8)
- IPCC. (2005). *Carbon Dioxide Capture and Storage*. <https://www.ipcc.ch/report/carbon-dioxide-capture-and-storage/>
- United Nations. (2020). *United Nations Framework Classification for Resources: Update 2019*. UN. <https://doi.org/10.18356/44105e2b-en>
- US EPA. (2016). *Global Greenhouse Gas Emissions Data*. US EPA. <https://www.epa.gov/ghgemissions/global-greenhouse-gas-emissions-data>
- Welkenhuysen, K., Brüstle, A.-K., Bottig, M., Ramírez, A., Swennen, R., & Piessens, K. (2016). A techno-economic approach for capacity assessment and ranking of potential options for geological storage of CO₂ in Austria. *Geologica Belgica*. <http://dx.doi.org/10.20341/gb.2016.012>

Optimal geodata centralization and disclosure as support for subsurface exploration

Johanna VAN DAELE ¹, Helga FERKET ¹, Renata BARROS ²

1. *Vlaams Planbureau voor Omgeving (VPO), Departement Omgeving van de Vlaamse Overheid, Koning Albert II-laan 20 (bus 8), 1000 Brussel, Belgium*
(johanna.vandaele@vlaanderen.be)

2. *Royal Belgian Institute of Natural Sciences - Geological Survey of Belgium, Jennerstraat 13, 1000 Brussels, Belgium*

It is widely known that the subsurface will play a crucial role in the transition towards a carbon-neutral society, with the aid of technologies like geothermal energy, CO₂-storage, Nevertheless, still a lot of aspects concerning the subsurface, its structure and characteristics remain to be investigated to facilitate the use of underground space in an efficient and safe way. In-depth investigation of the subsurface with conventional techniques such as seismic campaigns or drillings requires high investments, and it is not always straightforward to determine the success-rate upfront. This leads to geodata collections typically displaying a large variety and scatter, both concerning data (type) availability and in spatial distribution. Additionally, incorporating subsurface knowledge from neighboring countries often is challenging, but at the same time indispensable to increase understanding of the own subsurface, not least because some projects may display cross-border influences.

It is clear that subsurface exploration benefits from a cross-border and cross-thematic data collection and interpretation approach. One way to organize such data centralization was explored in the framework of the European Horizon2020-project GeoConnect^{3d}, by means of constructing a Structural Framework (SF) and a database of Geomanifestations (GM) for several pilot study areas. The Structural Framework defines geological units by its limits (e.g., faults, terrane boundaries, ...). All known limits and associated parameters are structured in a uniform and inter-connected way. Furthermore, the SF is designed on multiple zoom-levels, hence it can serve as a real backbone to integrate multiple other subsurface models of various scale and resolution together. Geomanifestations are anomalous observations covering a wide range of geo-disciplines, including —but not limited to— temperature, geochemistry, mineralogy and even geophysics data. Such irregularities are too often excluded or ignored in view of the larger cloud of ‘normal’ datapoints. Nevertheless, precisely these anomalies can be of great value for identifying subsurface processes and serve as an excellent pathway for communication to non-experts, and also as guideline for further research. In addition to GIS- and attribute-information, Factsheets summarize the relations between individual geomanifestations, and, if applicable, their connection to the Structural Framework.

Especially the latter, the combination of the (independent) elements SF and GM, gives a powerful tool that allows exploring the subsurface in an original and cost-efficient way. The newly gained insights can be directly linked and are extremely relevant to the use of the subsurface, either as storage space or as renewable/green energy-source. But it goes further than that. The overall usability of the SF and GM database is far more fundamental, as it gives innovative clues about characteristics and processes at play in the subsurface, such as fault permeability and connectivity, the presence of advection cells in the upper crust, or gas origin and migration pathways. To quote just one example; in the area of Spa, Belgium, elevated ³He/⁴He-ratios were analyzed (Griesshaber et al., 1992), a parameter that can highlight mantle gas contribution in gas seeps (White, 2013). This observation was unexpected given the far

distance from any volcanic activity, but suggests the presence of deep-seated, transcrustal faults and/or a large-distance connectivity till the Eifel area where mantle-derived magma was involved in recent volcanism. When indirect indications like this are not considered further, such valuable subsurface knowledge is easily overlooked and not at all taken into account for investigating in more detail in the future.

Even when limited resources or funding is available, the above-illustrated SF+GM approach can shed new light on properties and processes of the subsurface, given its novel and multidisciplinary approach. An inherent drawback, however, is that such a database is never complete and includes information from a variety of sources. Not only does this demands careful consideration on which data is included (or not), it also has to be taken into account for future database expansion as well as for data interpretation. Simple visualizations on a map without further (geological) background, e.g., combining both surface and at depth data as is the case for Wiesbaden, Germany (Mittelbach & Siebert, 2014), may lead to false conclusions. However, the provided Factsheets and metadata can help in this. Furthermore, at this moment, a large proportion of the entries depends on the availability of literature data, which implies some data source bias is unavoidable. For example, CO₂-data typically is measured for springs and streams, while dry CO₂-seeps easier remain unnoticed and therefore are reported less consistently. New data collection campaigns, possibly including bio-indicators like plants or ants (e.g., Berberich & Schreiber, 2013), can provide a good starting point for this. The uniform and well-designed structure of the database allows very easy expansion, be it for newly discovered faults, additional geomanifestation types, or parameter updates of either part. In addition, as demonstrated in the GeoConnect^{3d} project, the SF+GM approach is fully transferable to other study areas. This clears the way for a cost-efficient cross-border exploration of the subsurface with wins for both the academic world and common public (geoheritage, education, ...), and significantly contributes to a more data-supported outline for subsurface management.

This project has received funding from the European Union's Horizon 2020 research and innovation programme under grant agreement No 731166.

References

- Berberich, G., & Schreiber, U., 2013. GeoBioScience: Red Wood Ants as Bioindicators for Active Tectonic Fault Systems in the West Eifel (Germany). *Animals*, 3, 475-498.
- Griesshaber, E., O'Nions, R.K. & Oxburg, E.R., 1992. Helium and carbon isotope systematics in crustal fluids from the Eifel, the Rhine Graben and Black Forest, F.R.G. *Chemical Geology*, 99, 213-235.
- Mittelbach, G. & Siebert, S., 2014. Gutachten zur Festsetzung eines Heilquellenschutzgebietes für die Heilquellen (Große und Kleine Adlerquelle, Schützenhofquelle, Kochbrunnen, Salmquelle und Faulbrunnen) von Wiesbaden, Stadt Wiesbaden (WSG-ID 414-005), Wiesbaden, pp. 1-52.
- White, W.M., 2013. Chapter 12: Noble Gas Isotope Geochemistry, *Isotope Geochemistry course notes*. Cornell University.

Analysing CO₂ capture, transport, and storage chain options for cement industry in the LEILAC2 project

Kris WELKENHUYSEN, Alejandra TOVAR GAVIRIA, Kris PIESENS

Geological Survey of Belgium – Royal Belgian Institute of Natural Sciences, Brussels, Belgium (kris.welkenhuysen@naturalsciences.be)

In order to reach greenhouse gas emission reduction targets, atmospheric CO₂ emissions from all industrial sectors need to be avoided. Globally, the cement production industry emits 2.4 Gt CO₂ per year, or 7% of all CO₂ emissions (IEA). While about a third of this could be reduced by using renewable energy sources, the remainder are process emissions from the calcination process. Lime or CaO is produced by heating limestone (CaCO₃), emitting CO₂. The Australian company Calix has developed a direct separation technology for capturing these process emissions; a pilot-scale installation is operational at the Lixhe cement plant in Belgium (Figure 1).

The EU H2020-funded LEILAC2 project (Low Emission Intensity Lime and Cement 2: Demonstration Scale) upscaling and integrating a novel type of carbon capture technology. This technology aims to capture, at low cost, unavoidable process emissions from cement and lime plant. This large-scale capture plant will be installed at the Heidelberg Cement's plant in Hannover, Germany, capturing 20% of a typical cement plant's CO₂ emission.

Apart from the physical installation and operation of the capture unit, a business case will be developed for the downstream components of transport, use and geological storage for the captured CO₂. In order to develop a business case, a very large number of options, combinations and scenarios for each these components need to be evaluated, taking into account the intricacies of for example dealing with geological data in economic calculations. The PSS suite of geo-techno-economic simulators has been developed by the Geological Survey of Belgium, specifically for creating forecasts on the deployment of CO₂ capture and geological storage (CCS) technologies (Welkenhuysen et al., 2013). In PSS, investment decisions for the full CCS chain are simulated as a forecast in a non-deterministic way, considering uncertainty and flexibility. Especially for matching storage, these elements are essential.

While capture in this demonstration project is a given, several scenarios will be analyzed: the current demo-scale, full-scale capture, and CO₂-network integration. Due to its location, several CO₂ transport options can be considered at the Hannover plant: from low-volume truck, railway or barge transport, up to ships and pipelines. Special attention is given to possible connections with ongoing and planned initiatives for infrastructure and hub development such as the Porthos project in the port of Rotterdam or the Northern Lights project offshore Norway.

In the wider area around the capture location, North-Western Europe including the North Sea offshore area, there are many potential storage options available. Offshore storage options will be the primary targets for assessment, with many (nearly) depleted hydrocarbon fields and saline aquifers that are present in the southern North Sea. Storage aspects are treated as stochastic parameters, with for example storage capacity and injectivity of the reservoirs represented by probability density functions.

In order to compare storage options, the degree of knowledge, uncertainty and economic and practical development feasibility of such a storage location needs to be assessed. An analysis of such storage classification systems is created by Tovar et al. (this conference).

With the above-mentioned PSS method and CCS project development options, source-sink matching is performed to create forecasts on project and network development. Results

will provide insight in the probability of preferred storage option development for steering exploration and development efforts, preferred transport modes and routes, the optimal timing of investments, and the influence of market parameters, such as the ETS price of CO₂ emissions.

Acknowledgments

This research is carried out under the LEILAC2 project, which receives funding by the European Union's Horizon 2020 research and innovation program under grant agreement number 884170. The LEILAC2 consortium consists of: Calix Europe SARL, HeidelbergCement AG, Ingenieurbüro Kühlerbau Neustad GmbH (IKN), Centre for Research and Technology Hellas (CERTH), Bundesanstalt für Geowissenschaften und Rohstoffe (BGR), Politecnico di Milano (POLIMI), Geological Survey of Belgium (RBINS-GSB), ENGIE Laborelec, Port of Rotterdam, Calix Limited, CIMPOR-Indústria de Cimentos SA and Lhoist Recherche et Development SA.

References

- IEA, 2020. Energy Technology Perspectives 2020. <https://www.iea.org/reports/energy-technology-perspectives-2020>
- Tovar, A., Piessens, K. & Welkenhuysen, K., this conference. Ranking CO₂ storage capacities and identifying their technical, economic and regulatory constraints: A review of methods and screening criteria.
- Welkenhuysen K., Ramírez A., Swennen R. & Piessens K., 2013. Strategy for ranking potential CO₂ storage reservoirs: A case study for Belgium. *International Journal of Greenhouse Gas Control*, 17, 431-449. <http://dx.doi.org/10.1016/j.ijggc.2013.05.025>

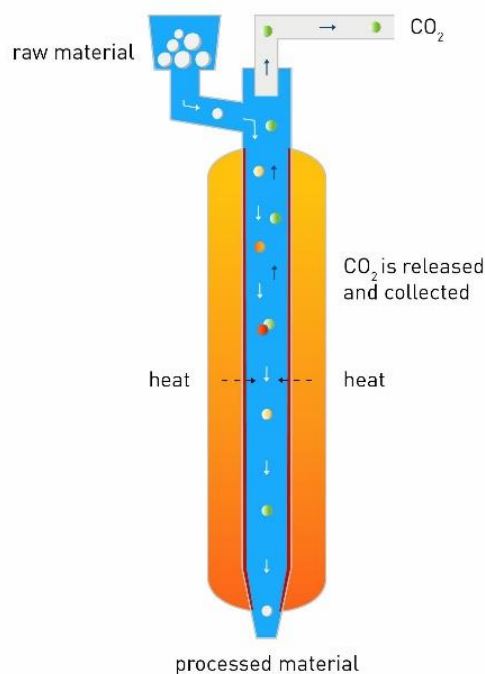


Figure 1. Left: schematic section of the LEILAC1 capture plant. Right: LEILAC1 capture plant at the Lixhe cement factory.

Decision support under uncertainty for geothermal applications: case selection and concept development

Kris WELKENHUYSEN¹, Tine COMPERNOLLE^{1,2}, Olivier KAUFMANN³, Ben LAENEN⁴, Bruno MEYVIS¹, Kris PIESSENS¹, Spiros GOUSIS², Nicolas DUPONT³, Virginie HARCOUET-MENOU⁴, Justin POGACNIK⁴

1. Royal Belgian Institute of Natural Sciences – Geological Survey of Belgium, Jennerstraat 13, 1000 Brussels, Belgium (kris.welkenhuysen@naturalsciences.be)

2. University of Antwerp – Faculty of Business and Economics, Prinsstraat 13, 2000 Antwerp, Belgium

3. University of Mons – Faculty of Engineering, Rue de Houdain 9, 7000 Mons, Belgium

4. VITO – Sustainable Land Use, Boeretang 200, 2400 Mol, Belgium

In order to meet climate goals and provide energy security, geothermal energy can play an important part in Belgium's energy production portfolio. The current implementation of geothermal energy in Belgium is very limited, making accurate forecasts about the economic potential difficult. In the DESIGNATE project, tools and workflows are developed to investigate the potential of deep geothermal energy and geothermal applications in abandoned mines in Belgium, considering uncertainties at reservoir, technology and economic level.

The goal of this project is to make forecasts about the role of these geothermal applications in the Belgian energy portfolio and provide support for strategic planning of subsurface activities by: explicitly considering uncertainties in modelling non-standard geothermal resources; creating tools for integrated forecasts under uncertainty; setting up a methodological framework for territorial LCAs considering surface and subsurface impacts; and analysing interferences and their consequences for geothermal energy deployment in Belgium.

These workflows will be developed for and applied to five real and theoretical case studies throughout Belgium, in different geological settings. A first case is the Balmatt deep geothermal project, a deep geothermal research project led by VITO in Mol, of which two wells are operational as a doublet. To allow for a realistic economic assessment, this case takes the basic structure and development of the Balmatt project, but as if it would be a commercial doublet project at the same location and in the same Carboniferous strata. A second case is a deep doublet system in NW Turnhout, currently under development by the geothermal development company HITA. This project allows supplying heat to part of the city of Turnhout's residential and tertiary sector's buildings. A third case involves the application of a novel single-well technology for geothermal heat extraction. To compensate for the unknowns of the new technology, a more uniform and predictable reservoir type was chosen for this application: the Cretaceous deposits in the Campine Basin. The fourth case will investigate a new deep geothermal doublet in the Mons Basin, the Deep Mons project. At Porte de Nimy, close to a hospital, two wells of about 2.5km depth are planned to reach the Carboniferous. A fifth and last case is the application of an open geothermal system in former coal mine galleries. Preliminary, the Péronnes-lez-Binche coal mines were selected, as the structural separation of the galleries in a shallower colder part and a deeper warmer part allows for several applications such as seasonal use of heat and cold.

Because a portfolio of methods will be developed to analyse different aspects of these projects, a solid common base is needed across all methods. These "project concepts" start

from a decision tree, listing the major decision steps for each case, such as seismic exploration, well drilling, and the potential use cases. Additionally, options for waiting and abandoning the project are also included. Other data such as duration and cost are tied to this framework. Figure 1 shows a flow chart of such a decision tree for the Balmatt case.

Because of their flexibility and speed, analytical solutions will be developed from numerical models for simulating the reservoir behavior and predict the evolution of temperature and pressure. The project uses an innovative approach by stepping away from simple well designs and homogeneous reservoirs, and introducing uncertainty. These analytical models will provide direct input for a geological techno-economic assessment (G-TEA), a territorial life cycle assessment (LCA), and a new version of the PSS simulator. Project development is simulated considering the analytical reservoir models as resource, the technical and economic aspects of project development, heat transport, energy demand, environmental impact, energy market and the policy framework.

Acknowledgements

This research is carried out under the DESIGNATE project, which receives funding from the BELSPO BRAIN-be 2.0 research programme under contract nr B2/191/P1/DESIGNATE.

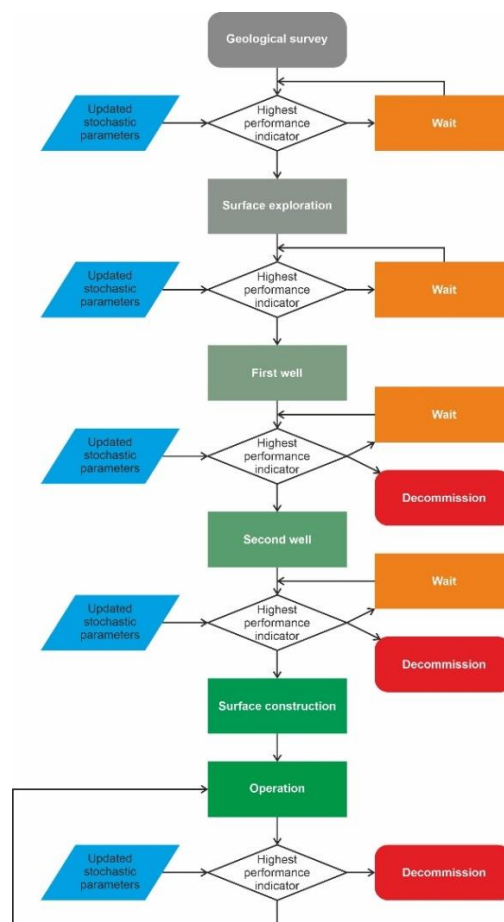


Figure 1. Decision tree for the Balmatt case. Only one use case is listed (“Operation”), as the heat network is already existing.

[12.2. DGE Rollout, Roll-out of Deep Geothermal Energy in NW-Europe](#)

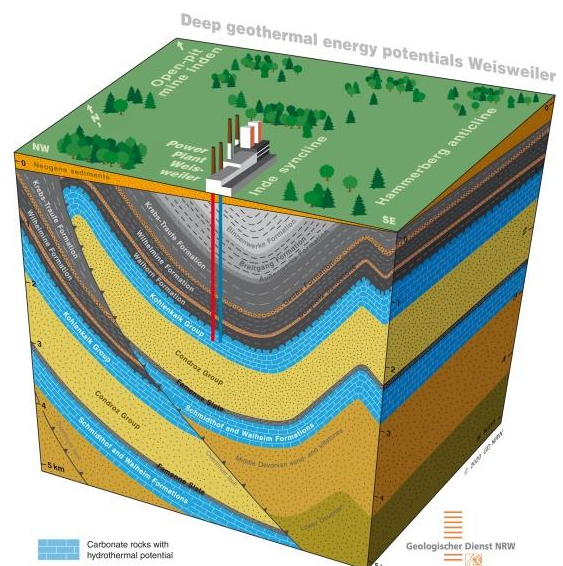
Conveners:

Matsen Broothaers (VITO), Tobias Fritschle (GD-NRW), Estelle Petitclerc (RBINS-GSB), Kris Welkenhuysen (RBINS-GSB)



The transnational EU-Interreg funded project “Roll-out of Deep Geothermal Energy in North-West Europe” (DGE-ROLLOUT; www.nweurope.eu/DGE-Rollout) aims to foster the use of deep geothermal energy as a climate- and environmentally-friendly resource in North-West Europe (NWE). Following a multi-disciplinary geoscientific approach, DGE-ROLLOUT investigates one of the most promising carbonate reservoirs in NWE, the Lower Carboniferous Kohlenkalk-Group situated within the Rhenohercynian Basin. The exploitation of such reservoirs using hydrothermal techniques provides the potential to generate climate-neutral heat and power, and therefore helps reduce CO₂ emissions.

This session aims to present the different aspects implemented through and within DGE-ROLLOUT. Presenters from Belgium, France, Germany and the Netherlands will provide insight to current projects, such as cross-border acquisition of 2D-seismic surveys, 3D-modelling of the Kohlenkalk-Group in the subsurface of the transnational area, as well as the development and optimisation of new and existing deep geothermal power plants. A major focus of this session is to contribute to the dissemination of the state of the art on deep geothermal energy, and to establish transnational collaboration to promote the use of this sustainable and widely available energy resource.



The Lower Carboniferous geothermal reservoir of the deep subsurface of North Rhine-Westphalia and its border regions: New insights from 3D mapping

Martin ARNDT ¹, Tobias FRITSCHLE ¹ & Martin SALAMON ¹

Geological Survey of North Rhine-Westphalia, Krefeld, Germany (martin.arndt@gd.nrw.de, tobias.fritschle@gd.nrw.de, martin.salamon@gd.nrw.de)

Within the scope of the EU-Interreg-funded project Roll-out of Deep Geothermal Energy in North-West Europe (DGE-ROLLOUT) (www.nweurope.eu/DGE-ROLLOUT, Fritschle et al. 2021), the Geological Survey of North Rhine-Westphalia has produced a depth and thickness map of the Lower Carboniferous (Dinantian) geothermal reservoir occurring in the subsurface of the German federal state of North Rhine-Westphalia (Arndt 2021).

The largely karstified limestone deposits of the Dinantian Kohlenkalk Group, which are well known from outcrops in north-eastern Belgium and the Aachen area in North Rhine-Westphalia, are expected to serve as a suitable aquifer for geothermal energy production. Information from well data and outcrop analogues suggest more than 400 m thick deposits of karstified and dolomitised platform carbonates in the deep subsurface from the border triangle of Belgium, Germany, and the Netherlands towards the eastern extents of the Lower Rhine embayment. These subsurface carbonate occurrences have been constructed using the commercial 3D modelling software MOVE (Petroleum Experts, Version 2019.1) in order to better characterise the geothermal potential of this region.

Further east of the Lower Rhine embayment, the platform carbonates translate into the basinal Kulm facies, which is dominated by starved siliciclastic sedimentation with turbiditic interruptions. Some of these turbiditic sequences reach thicknesses of more than 150 m in the Remscheid-Altena anticline, indicating the presence of another carbonate source likely situated in the deep subsurface of the Münsterland area. This hidden platform or intra-basinal swell may also provide significant potential for geothermal exploitation.

The border region between Belgium, Germany and the Netherlands is of particular interest for geothermal prospecting considering current projects in Mol (BE) and Venlo (NE). However, geological ambiguities in the Aachen area emphasise the need for more comprehensive geothermal investigation. New data from seismic exploration campaigns obtained within DGE-ROLLOUT and through the Dutch SCAN programme (<https://www.nlog.nl/en/scan>) will further improve the cross-border correlation of the Dinantian between the countries.

References

- Arndt, M., 2021. 3D modelling of the Lower Carboniferous (Dinantian) as an indicator for the deep geothermal potential in North Rhine-Westphalia (NRW, Germany). *Zeitschrift der Deutschen Gesellschaft für Geowissenschaften (ZDGG)*.
- Fritschle, T., Petitclerc, E., van Melle, T., Broothaers, M., Passamonti, A., Arndt, M., Tasdemir, B., Pederson, C., Salamon, M., 2021. DGE-ROLLOUT: Promoting Deep Geothermal Energy in North-West Europe, *Proceedings World Geothermal Congress, 2021, Reykjavik*.

Deep geothermal energy in the Lower Carboniferous carbonates in the Belgian Campine Basin: current status of the Balmatt project in Mol

Matsen BROOThAERS^{1*}, Virginie HARCOUËT-MENOU¹, Ben LAENEN¹, David LAGROU¹, Justin POGACNIK¹

1. VITO, Boeretang 200, 2400, Mol, Belgium (matsen.broothaers@vito.be)*

The recent developments in deep geothermal in the Campine Basin (Northern Belgium) focus on the Lower Carboniferous Limestone Group (LCLG). However, deep geothermal energy in the Belgian Campine Basin is not a new development. In fact, the first steps were already taken in the 1950's when the Turnhout well was drilled, revealing the presence of a geothermal reservoir at depth. Nevertheless, it took until the late 1970's for a new project to materialize, leading to the Merksplas-Beerse well in 1983. It provided a wealth of information, including hydraulic, chemical and radiological data. However, it did not result in the development of a geothermal site providing heat to consumers. Renewed interest from 2009 onwards eventually led to the Balmatt project in Mol, with the aim of demonstrating the technical and economic feasibility of a geothermal site in the LCLG at a depth of more than 3000 m.

The first well (Mol-GT-01) was spudded in 2015 and drilled vertically. The top of the LCLG was found at a depth of 3175 m (Bos & Laenen, 2017). Well TD was reached at 3609 m depth. As the geological setting was considered different from previously drilled wells, extensive karst levels were not expected. Instead, the well aimed at finding zones of increased permeability along faults and fractures. Total mud losses were encountered while drilling in the reservoir section, indicating the presence of increased transmissivity at least in the immediate vicinity of the well. A second well (Mol-GT-02) was spudded in 2016 and deviated towards the northeast. The top of the LCLG was encountered at 3300 m TVD (Bos & Laenen, 2017) and well TD was reached at 4341 m MD (or 3830 m TVD).

Following the completion of both wells, work started on the construction of the surface installations of the geothermal plant and on the connection to the heating network of VITO (and adjacent companies), already in place. Connecting low temperature heating networks, that could go as low as 30°C, would double the thermal output. As the two wells did not reach the base of the LCLG, VITO planned to drill a third well that would cover the entire limestone sequence and would explore the underlying Devonian sandstones.

Mol-GT-03 was spudded in December 2017, targeting the same faulted and fractured zone as Mol-GT-01-S1, although now in southeastern direction at 1,6 km distance to Mol-GT-01-S1 (Broothaers et al., 2019). The top of the LCLG was reached at a depth of 3142 m TVD. Mol-GT-03 became the third well in the Belgian part of the Campine Basin to reach the base of the limestone sequence, which was found at 3992 m TVD (base Vesdre Formation). TD was called at 4905 m MD (4235 m TVD) in July 2018. Initial well tests pointed to productivity far lower than anticipated. As a consequence, Mol-GT-03 was classified as a dry well.

The start-up phase was initiated in November 2018 and continued until June 2019. During this time fourteen periods of test operation were carried out comprising injection in the well Mol-GT-02 and production from Mol-GT-01. Each period covered between 0.5 and 240 operational hours. In total, 50.000 m³ of geothermal brine was produced and 3.200 MWh of heat was extracted. The energy was used for heating purposes or for the production of power by means of an organic rankine cycle (ORC).

The results and observations made during the start-up phase revealed several challenges related to the characteristics of the brine, such as the presence of gas, the occurrence of Natural Occurring Radioactive Materials (NORM), corrosion and scaling. The observations showed that free gas was present in the installations. Considering the nature of the gas (mainly CO₂), separation of gas from the fluid would have an impact on the chemical composition of the brine and on its potential for scaling. The proper functioning of the scaling inhibitor was evaluated through the amount and type of material in the filter elements. Analysis of the material captured in the filter elements revealed the presence of Galena (PbS). The start-up phase also confirmed the occurrence of induced seismicity in the vicinity of the injection well, culminating in a M_L 2.2 event on June 23rd 2019. The initial start-up phase was stopped, and seismic events were analyzed in order to understand the mechanisms leading to induced seismicity. This led to a substantial extension of the existing seismic monitoring network. At the same time, changes were made to the geothermal installations to better meet with the challenges encountered and to optimize production. These include an increase in system pressure, the installation of an injection tubing, changes in the mesh size of the filters, and the use of different inhibitors.

In February 2021 the Board of Directors of VITO approved a restart of the geothermal site in the framework of a research program. Test activities were started from mid April 2021 on, after communication to authorities, inhabitants of Mol and Dessel, and neighboring companies. The test program will run for one year and aims to achieve a better understanding of the seismological behavior of the LCLG and of the seismic risk when operating a geothermal doublet. In addition, the test phase will allow to evaluate the hydraulic characteristics of the reservoir and efficiency of the changes implemented in the geothermal installations.

References

- Bos, S. & Laenen, B., 2017. Development of the first deep geothermal doublet in the Campine Basin of Belgium. *European Geologist*, 43, 16-20.
- Broothaers, M., Bos, S., Lagrou, D., Harcouët-Menou, V. & Laenen, B., 2019. Lower Carboniferous limestone reservoir in northern Belgium: structural insights from the Balmatt project in Mol. *European Geothermal Congress 2019*, Den Haag, the Netherlands, 7p.

DGE-ROLLOUT - Promoting Deep Geothermal Energy in North-West Europe

Tobias FRITSCHLE¹, Estelle PETITCLERC², Timme VAN MELLE³, Matsen BROOThAERS⁴, Arianna PASSAMONTI⁵, Martin ARNDT¹, Burcu TAŞDEMİR¹, Chelsea PEDERSON⁶ and Martin SALAMON¹

- 1. Geological Survey of North Rhine-Westphalia, De-Greiff-Straße 195, 47803 Krefeld, Germany (Tobias.Fritschle@gd.nrw.de)*
- 2. Royal Belgian Institute for Natural Sciences, Geological Survey of Belgium, Rue Jenner, 13, 1000-Brussels, Belgium*
- 3. Energie Beheer Nederland B.V., Daalsesingel 1, 3511 SV Utrecht, The Netherlands*
- 4. Flemish Institute for Technological Research, Boeretang 200, 2400 Mol, Belgium*
- 5. Fraunhofer Institution for Energy Infrastructures and Geothermal Systems IEG, Am Hochschulcampus 1, 44801 Bochum, Germany*
- 6. Ruhr-University Bochum, Institute for Geology, Mineralogy and Geophysics, Universitätsstraße 150, 44801 Bochum, Germany*

The transnational EU-Interreg funded project “Roll-out of Deep Geothermal Energy in North-West Europe” (DGE-ROLLOUT; www.nweurope.eu/DGE-Rollout) aims to foster the use of deep geothermal energy as a climate- and environmentally-friendly resource in North-West Europe (NWE), and therefore aims to reduce CO₂ emissions.

Besides the Geological Survey of North Rhine-Westphalia as the lead partner, the DGE-ROLLOUT project partners include the national geological surveys of Belgium, France, and the Netherlands, as well as industry partners (DMT GmbH & co. KG, EBN B.V., RWE Power AG) and research institutions (Fraunhofer Institution for Energy Infrastructures and Geothermal Systems IEG, Technical University Darmstadt, Flemish Institute for Technological Research).

One major aim of the DGE-ROLLOUT project involves the geothermal characterisation of the Lower Carboniferous Kohlenkalk Group situated within the Rhenohercynian Basin. Using lithostratigraphic and structural data obtained from drilling operations, geological mapping, and seismic campaigns, the project intends to provide a comprehensive 3D subsurface model of the Kohlenkalk geothermal reservoir within NWE.

Further challenges addressed in the DGE-ROLLOUT project include: the storage of heat in a decommissioned hard-coal mine as well as in crystalline rocks, the optimisation of production outputs through the installation of high-temperature heat pumps and new cascading schemes in several geothermal installations, and the development of innovative decision and exploration strategies promoting the establishment of renewable and sustainable deep geothermal energy.

Similar to the VITO Balmatt Energy Plant (www.vito.be/en/deep-geothermal/balmatt-energy-plant), the conventional lignite-fired power plant Weisweiler (RWE) is aimed to utilise the Kohlenkalk aquifer in its subsurface to introduce geothermal energy into the regional district-heating network following the forthcoming fossil fuel phase-out. First investigations in this instance are undertaken within the DGE-ROLLOUT project.

Exploration for Deep Geothermal Energy at the RWE Power Plant Weisweiler, Germany

Thomas OSWALD ¹, Frank STROZYK ², Tobias FRITSCHLE ³, Martin SALAMON ³

1. RWE Power AG, Cologne site, Stüttgenweg 2, 50935 Köln, Germany (thomas.oswald@rwe.com)
2. Fraunhofer Research Institution for Energy Infrastructures and Geothermal Systems IEG, Kockerellstraße 17, 52062 Aachen, Germany (frank.strozyk@ieg.fraunhofer.de)
3. Geological Survey of North Rhine-Westphalia, De-Greiff-Straße 195, 47803 Krefeld, Germany (tobias.fritschle@gd.nrw.de, martin.salamon@gd.nrw.de)

Carboniferous and Devonian carbonate rocks in the deeper subsurface below the Weisweiler lignite-fired power plant near Aachen, Germany, will be explored and exploited for the purpose of deep geothermal energy extraction using hydrothermal techniques. First steps are undertaken as green field exploration in the course of the transnational EU-Interreg-funded “Roll-out of Deep Geothermal Energy in North-West Europe” (DGE-ROLLOUT) project, which aims to provide solutions to reduce carbon-dioxide emissions using a variety of geoscientific approaches.

Although multiphase deformation and faulting during both Variscan and Alpine (post-) orogenic processes formed a complex geological setting in the area, it appears to exhibit favourable conditions for deep geothermal exploitation at several depth levels. A preliminary geological 3D model of the subsurface of the Weisweiler area has been constructed on the basis of which a first c. 1,500 m deep drilling operation and additional exploration campaigns such as a seismic survey and other deeper exploration wells are currently being planned. The preparatory work for the construction of the first exploratory well and the required approval procedures are underway.

A Fraunhofer demonstrator on high temperature heat pump coupled with high temperature mine thermal energy storage

Arianna PASSAMONTI ¹, Matthias UTRI ¹, Florian HAHN ¹

1. Fraunhofer Research Institution for Energy Infrastructures and Geothermal Systems IEG, Am Hochschulcampus 1, 44801 Bochum, Germany (arianna.passamonti@ieg.fraunhofer.de)

In order to achieve the European and German CO₂ reduction targets, sustainable and renewable solutions for the heating sector, especially in the populated regions of North-West Europe (NWE) are required. With this motivation, the two coherent projects Geothermica HeatStore and NWE-Interreg DGE-ROLLOUT work on the development of a high temperature mine thermal energy storage (HT-MTES) pilot plant utilised as a heat source for a high temperature heat pump (HTHP), connected to the local district heating grid (DH).

During the summer, solar thermal energy will heat up the water present in a small flooded mine located in the subsurface of the Fraunhofer IEG campus in Bochum. Flow and heat transport simulations on the mine water were carried out in order to choose the best locations for production, injection and monitoring wells, which have already been drilled by Fraunhofer IEG in 2020.

Major results include new insights on large scale HTHP, the requirements for the complex cascading technology, and the modelling of the mine water as a geothermal reservoir. Next steps will involve pumping and tracer tests, the first injection of heat into the mine water in summer 2021, and HTHP installation and testing in winter 2021/22. The development of these projects will demonstrate how the usage of abandoned mines as subsurface heat storage facilities, and their coupling with innovative heat pump systems covering a significant range of temperature sources and output parameters, can support the energy conversion towards the European and German CO₂ reduction goals.

Sustainability and renewability of Geothermal Energy

Timme VAN MELLE ¹, Hester DIJKSTRA ², Dorien DINKELMAN ³

*1. Energie Beheer Nederland B.V., Daalsesingel 1, 3511 SV Utrecht, The Netherlands
(timme.melle-van@ebn.nl)*

2. Netherlands Organization for Applied Scientific Research, Princetonlaan 6, 3584 CB Utrecht, The Netherlands (hester.dijkstra@tno.nl)

3. Netherlands Organization for Applied Scientific Research, Princetonlaan 6, 3584 CB Utrecht, The Netherlands (dorien.dinkelman@tno.nl)

The main driver for the DGE-Rollout project is to reduce CO₂ emissions. Geothermal energy is generally accepted as a technology that can help reduce CO₂ eq-emissions by replacing fossil fuel in the heating of buildings, and provide energy to current as well as many future generations. However, it should be acknowledged that, like any energy technology, there are, directly and indirectly, emissions related to the production of geothermal energy.

We will look into the overall emissions related to geothermal energy, taking into account the whole lifetime (construction, use phase and abandonment) of a geothermal project. We will firstly discuss DGE in isolation, and compare it to other (non-fossil) sources of heat. Secondly, we will look at DGE as part of a portfolio of sources for a district heating network and how it helps to reduce emissions for the system overall. Finally, we will investigate how emissions can be further reduced.

High-Temperature Medium Deep Borehole Thermal Energy Storage Pilot Plant

Bastian WELSCH^{1,2}, Julian FORMHALS^{1,2}, Kristian BÄR¹, Lukas SEIB¹, Ingo SASS^{1,2}

*1. Technische Universität Darmstadt, Geothermal Science and Technology,
Schnittspahnstraße 9, 64287 Darmstadt, Germany (welsch@geo.tu-darmstadt.de)*

*2. Darmstadt Graduate School of Excellence Energy Science and Engineering, Otto-Berndt-
Straße 3, 64287 Darmstadt, Germany*

Borehole thermal energy storage (BTES) is eminently suitable for seasonal storage of large amounts of excess heat. However, water authorities regard the associated thermal impact on shallow aquifers as critical. Medium deep borehole heat exchangers (BHE) tap into larger depth and allow for the use of thermal insulation in the topmost section of the boreholes. As a result, the thermal load on topmost aquifers is significantly reduced and shifted to the rock volume below, where heat can be stored at high temperature (up to 90°C). Numerical simulations have shown that these medium deep BTES systems can store heat on a large scale and effectively protect critical drinking water reservoirs. However, large BTES system sizes are required for an efficient operation, which also entails high investment costs. Moreover, to efficiently integrate such systems into district heating grids, low-temperature grids of the fourth generation are required, which are still rather an exception in many countries. As a result of both high investment costs and the lack of suitable heating grids, medium deep BTES systems have not been put into practice so far.

Within the framework of the Interreg Project “DGE-ROLLOUT – Roll-out of Deep Geothermal Energy in North-West Europe” the concept of the first pilot plant for a medium deep BTES system built on the campus of Technische Universität Darmstadt is developed. The storage array consists of four coaxial BHEs, which tap into a crystalline reservoir rock underneath a sedimentary cover of approximately 50 m thickness. All BHEs are equipped with flowmeters and fiber optic cables for depth-dependent temperature measurements during operation. In close vicinity, groundwater monitoring wells with multi-parameter probes complete the extensive monitoring setup. Experiments run using mobile heating and cooling units, which simulate charging at up to 90°C and discharging at down to 10°C cycles and allow for full control of the storage operation. Together with geophysical exploration data from the construction phase we expect the pilot plant to provide a comprehensive dataset for the validation of our numerical experiments and to proof the concept of medium deep BTES. Based on these validated simulations a prognosis of the performance and efficiency of even larger scale systems will be possible.